Strathclyde Institute of Pharmacy and Biomedical Sciences
GlaxoSmithKline

Development Towards Prospective Modelling of In Vivo Rabbit QTc Prolongation

Gareth John Lewis

Postdoctoral PhD

2017

DECLARATION OF AUTHENTICITY AND AUTHOR'S RIGHTS

This thesis is the result of the author's original research. It has been composed by the author and has not been previously submitted for examination which has led to the award of a degree.

Signed: Date:

ABSTRACT

This thesis describes a series of experimental studies (in vitro, ex vivo, in vivo) conducted and integrated using modelling/scaling approaches to develop compartmental and physiologically based models from early cardiovascular screening and pharmacokinetic data to predict measured in vivo rabbit QTc PKPD data. A terminally anaesthetised rabbit model was set-up and evaluated to measure the in vivo PKPD QTc response with a set of marketed test compounds (cisapride, sparfloxacin, moxifloxacin) known to prolong the QT interval and a negative control (verapamil).

Using pharmacodynamic data generated in the ex vivo rabbit ventricular wedge model, a concentration-response relationship for QT interval changes was determined. This was combined with rat pharmacokinetic parameters scaled using two single species allometry methods and cross-species protein binding data (rat, dog, rabbit, guinea-pig and human) in plasma, blood and heart tissue, investigated using the rapid equilibrium dialysis device, to develop a physiologically-based mechanistic model along with a semi-compartmental model to predict the rabbit response to the marketed tool compounds.

A whole-body physiologically-based pharmacokinetic (PBPK) model suitably described the rat intravenous plasma concentration-time profile of each test compound and was translated to the rabbit using GastroPlus™ software. From the scaled approach, resultant simulated plasma and subsequent predicted heart concentration data successfully informed the PD model of the related QTc change. To demonstrate the functionality of the mechanistic model this was assessed against observed clearance and heart:plasma Kp ratio in the anaesthetised rabbit. The semi-PBPK compartmental model of the heart further supported the physiologically relevant heart compartment.

This work is the first description of using PBPK modelling translation towards rabbit cardiovascular QT prolongation and demonstrates the potential for preclinical translation.

ACKNOWLEDGEMENTS

Firstly, I would like to take this opportunity to acknowledge the support and guidance I have received from my industrial supervisor Paul Scott-Stevens and my academic supervisor Edward Rowan. Thank you for your time, input, review and objective discussion which has been extremely valuable in enabling the completion of this thesis.

I would also like to acknowledge the following colleagues who assisted in some of the logistical and practical aspects in this report:

Ali Robinson and Brian Mardell (Animal Sciences Delivery Team) for their assistance during in vivo work in the study; including rabbit handling, anaesthesia monitoring and training and learning off each other.

Marcello Tontodonati and Hugh Edgar (Laboratory Animal Sciences) for their advice of anaesthesia and veterinary input. In particular, Marcello for his assistance in electrocardiograph limb-lead placement and optimisation of the anaesthetised model.

James Louttit, Bethan Gibson and Sam Turner (Safety Pharmacology) for their assistance with all matters associated with generating the cardiovascular data. In particular, James provided initial support for this investigation and anaesthetised rabbit model set up including training in Ponemah and loan of equipment. Bethan provided invaluable assistance in EMKA training to allow interpretation and processing of the data, and troubleshooting any software issues. Sam kindly helped with conducting the rabbit ventricular wedge preparations, interpretation, obtaining data and discussion.

Anna Williams (Drug Metabolism and Pharmacokinetics) for her time training and support in mass spectrometry and associated software to enable me to develop the skills for sample analysis.

Neil Miller (Systems Modelling and Translational Biology) for his tuition in GastroPlus software, his attention to detail and modelling discussions to assist me in data integration.

Finally, I would like to acknowledge and thank my family for their loving support throughout and that anything is possible through perseverance and hard work even in challenging times.

ABBREVIATIONS

$5HT_4$	5-hydroxytryptamine serotonin receptors, G-protein coupled subfamily 4.
ADC	Analogue to digital converter
ADME	Absorption, distribution, metabolism and excretion
AE	Adverse Event
AGP	α-1-acid glycoprotein
AMS	Accelerated mass spectrometry
AP	Action potential
APD	Action potential duration
AUC	Area under the curve
BP	Blood pressure
B:P	Blood-to-plasma ratio
CA	Carotid artery
Ca^{2+}	Calcium ion
CAST	Cardiac Arrhythmia Suppression Trial
CAVB	Chronic atrio-ventricular block
CDER	Center for Drug Evaluation and Research
CF	Contractile force
CHO	Chinese Hamster ovarian cells
CL_p	Total clearance in plasma
CM	Cardiomyocytes
C_{max}	Concentration maximum
CNS	Central nervous system
CO	Cardiac Output
CPMP	Committee for Proprietary Medicinal Products
CPP	Coronary perfusion pressure
CS	Candidate Selection
CV	Cardiovascular
CYP450	Cytochrome P450 enzyme e.g. 3A4
DBP	Diastolic blood pressure
DIAMOND	Danish Investigations of Arrhythmia and Mortality on Dofetilide trial
DDI	Drug-drug interaction
dp/dt_{max}	Change in blood pressure with time
DMPK	Drug Metabolism and Pharmacokinetics
DMSO	dimethyl sulfoxide
EAD	Early after depolarisation
dQTc	Delta (Δ) change in QT corrected interval (vehicle or baseline)
ddQTc	Double delta (ΔΔ) change in QT corrected interval (vehicle and baseline)
EC_{50}	The drug concentration which produces 50% of the maximum stimulation
ECG	Electrocardiogram or electrocardiograph

ED	Equilibrium dialysis
E_{max}	The maximum effect attributed to the drug
EMA	European Medicines Agency
EMLA	Eutectic Mixture of Local Anaesthetics (lidocaine and prilocaine)
ESP	Early safety prediction
eXP	Enhanced cross screen panel
F	Bioavailability
FDA	U.S. Food and Drug Agency
FSA	Foetal serum albumin
FTiH	First time in human
Fu_b	Fraction unbound in blood
Fu_p	Fraction unbound in plasma
Fu_t	Fraction unbound in tissue
GC	Gas chromatography
GLP	Good Laboratory Practice
GSK	GlaxoSmithKline
H&E	Hematoxylin and Eosin stain
Hct	Haematocrit
HEK	Human embryonic kidney cells
hERG	Human ether-a-go-go related gene
hiPSC	Human induced pluripotent stem cells
HLQ	Higher limit of quantification
HPLC	High performance liquid chromatography
HR	Heart rate
HSA	Human serum albumin
GI	Gastro-intestinal
GLP	Good Laboratory Practice
IC_{50}	half maximal inhibitory concentration (IC50) value measures
iCEB	index of Cardiac Electrophysiological Balance
ICF	Isometric contractile force
ICH	International Conference on Harmonisation
ID	Identification
I.D.	Internal diameter
I_{Kr}	Inward potassium (K^+) rapid delayed rectifier current
I_{Ks}	Inward potassium (K^+) slow delayed rectifier current
IM	Intramuscular
IMI	Innovative Medicine Initiative
IMS	Imaging mass spectrometry
I.S.	Internal standard
IV	Intravenous
JV	Jugular vein

K^+	Potassium ion
KCl	Potassium chloride
Kd	Dissociation rate constant
K_3EDTA	Potassium Ethylenediaminetetraacetic acid anticoagulant
LA	Left atrium
LBF	Liver blood flow
LC	Liquid Chromatography
LLQ	Lower limit of quantification
LQTS	Long QT syndrome
LV	Left ventricle
LVP	Left ventricular pressure
MAP	Mean arterial pressure
MAP	Monophasic action potential
MALDI	Matrix-assisted laser desorption ionisation
MBP	Mean blood pressure
MEA	Multi-electrode assay
MeOH	Methanol
MHW	Ministry of Health and Welfare
MRM	Multiple reaction monitoring
ms	millisecond unit of time
MS	Mass spectrometry
MS/MS	Tandem mass spectrometry
MW	Molecular Weight
m/z	Mass to charge ratio
Na^+	Sodium ion
NaCl	Sodium chloride
NaOH	Sodium hydroxide
Na_v	Sodium voltage-gated ion channel
NCA	Non compartmental analysis
NCE	New Chemical Entity
NHP	Non-human primate
NSA	Non-specific adsorption
NZW	New Zealand White rabbit
O.D.	Outer diameter
PB	Protein binding
PBPK	Physiologically-based Pharmacokinetics
PBS	Phosphate buffered saline
PD	Pharmacodynamic
PEG200	Polyethylene glycol (mean molecular weight 200)
pIC_{50}	Logarithmic value of the half maximal inhibitory concentration measured
PK	Pharmacokinetics

PK/PD	Pharmacokinetic / Pharmacodynamic
PO	Oral
PPB	Plasma protein binding
PR	Interval between start of P wave and peak of R wave
QA	Interval between start of Q wave and subsequent rise in systolic blood pressure
QC	Quality control
QRS	Interval between start of Q wave and end of S wave
QSAR	Quantitative Structural Activity Relationship
QT	Interval between start of Q wave and end of T wave
QTc	Interval between QT wave corrected for HR by appropriate method
QTcB	Interval between QT wave corrected for HR by Bazett's method
RA	Right atrium
RED	Rapid Equilibrium Dialysis
RR	Interval between one R wave peak to the next R wave peak
RV	Right ventricle
RVW	Rabbit ventricular wedge
SBP	Systolic blood pressure
SC	Subcutaneous
S.D.	Standard deviation
S.E.M.	Standard error of the mean
SoC	Start of Chemistry
Soc2CS	Start of Chemistry to Candidate Selection
SPME	Solid Phase Microfibre Extraction
SWORD	Survival With Oral D-sotalol trial
$t_{1/2}$	Terminal half-life
TdP	*Torsades de pointes*
TDR	Transmural dispersion of repolarisation
T_{max}	Time to maximum concentration or effect
Tp-e	T-peak to T-end
TQT	Thorough QT study
TRIaD	Triangulation, Reverse-use dependence, Instability and Dispersion
UC	Ultracentrifugation
UF	Ultrafiltration
UGT	UDP-glucuronyltransferase2
UPLC	Ultra performance liquid chromatography
UV	Ultra violet
V_d	Volume of distribution
VF	Ventricular fibrillation
V_{ss}	Volume of distribution at steady-state
VT	Ventricular tachycardia

Contents

Strathclyde Institute of Pharmacy and Biomedical Sciences
GlaxoSmithKline

CHAPTER 1

Introduction

1. INTRODUCTION

This project is concerned with the potential application of combining pharmacokinetic (PK) and pharmacodynamic (PD) generated information to support safety sciences. More specifically the project aims to establish the potential of utilising data from early preclinical species and safety screens to provide a translational link to predict between models and the potential implementation of physiologically-based (PB)PK/PD modelling to aid the therapeutic development of new drugs.

In the following sections an introduction to safety pharmacology, specifically relating to the cardiovascular system will be given, along with the study designs, data utilised and compounds investigated. PBPK/PD modelling, cross-species scaling and their current use in industry and academia will also be discussed. Methods and approaches used in this project will be presented individually as chapters, with information regarding the background and results included. An outcome and review will be addressed in the discussion and conclusion of this project.

1.1. Safety Pharmacology

Pharmacology studies are traditionally associated with the discovery of properties related to therapeutic use i.e. efficacy. The concept of safety pharmacology however, is concerned with the adverse pharmacodynamic effects of a drug on organ functions that standard toxicological testing methods do not easily detect (Bass et al., 2004).

1.1.1. Evolution of the Discipline

The first mention of organ function testing appeared in Japanese regulatory documentation as early as 1975 (MHW-Japan, 1975). The concept of safety pharmacology formally came into existence in the 1990's as a result of a number of marketed drugs being withdrawn due to cardiovascular adverse safety events. It became a public concern that non-cardiovascular agents, such as terfenadine, terolidine, and cisapride, could cause the rare but potentially life threatening arrhythmia *Torsades de pointes* (TdP). Up until this time, it had been believed such a pre-disposition would only have been limited to cardiovascular drugs (Pugsley et al., 2008). In addition it would not have been identified by the toxicity study methodology employed at that time. Therefore industry and regulatory authorities began to recognise that

further specific safety studies were required to help protect patients receiving new chemical entities (NCEs) from adverse effects related to systems pharmacology.

This awareness was highlighted through a 'Points to Consider' document drafted by the Committee for Proprietary Medicinal Products (CPMP and EMEA, 1997) in 1997 based on the Japanese guidelines (MHW-Japan, 1995), which were the most advanced at the time, giving specific guidance on the non-clinical study requirements (Kinter and Valentin, 2002). In 1998, the EU, US and Japanese regulators (EMEA, FDA and MHW) each produced draft concept papers on "safety pharmacology". An international survey was conducted in 1999 to assess the current practices in the pharmaceutical industry for methods of collecting and evaluating non-clinical cardiac electrophysiology data (Hammond et al., 2001). These practices and papers were debated at the inaugural Safety Pharmacology Society (Bass et al., 2004) and later that year implementation of global safety pharmacology guidelines were proposed to the steering committee of the International Conference on Harmonisation (ICH) of technical requirements for registration of pharmaceuticals for human use. This was accepted and in 2000 led to a harmonised defined set of safety pharmacology studies (S7A, 2000), which was accepted by global regulators.

The ICH S7A guidelines define safety pharmacology as "those studies that investigate the potential undesirable effects of a substance on physiological functions in relation to exposure in the therapeutic range and above." The ICH S7A documentation provides a framework for pharmaceutical companies to conduct a series of preclinical safety studies, denoted as a 'core battery of tests' based on three functional areas considered vital to life; the central nervous, cardiovascular, and respiratory systems, which must be performed prior to human administration. So this distinguished a separate arm to safety testing, where toxicological assessment focuses on the adverse action on clinical chemistry, histopathology and survival relative to dose or exposure.

1.1.2. Cardiovascular Safety Pharmacology

Drug attrition in pharmaceutical development remains high with 9 out of 10 compounds failing in clinical development, with drug safety and toxicity being the leading cause, accounting for ~30%, at all stages of the drug development process (Kola, 2008). Adverse effects of drugs on the cardiovascular system is one of the main reasons for attrition in drug

development and post-marketing, with 45% of drugs withdrawn from the market between 1975 and 2007 due to cardiovascular toxicities (Stevens and Baker, 2009). Currently a third of withdrawals are a result of cardiovascular issues and this remains the leading cause of attrition with cardiovascular toxicity resulting from modification of structural and/or functional components of the heart which is also observed within GSK (Figure 1.1)(Ferri et al., 2013). Cardiovascular adverse events (AE's) are diverse and may not be a direct result of the primary pharmacology, therapeutic class or chemical class. However most AE's are dose related and, therefore, predictable from a number of primary, secondary and safety pharmacology screening models (Valentin et al., 2010).

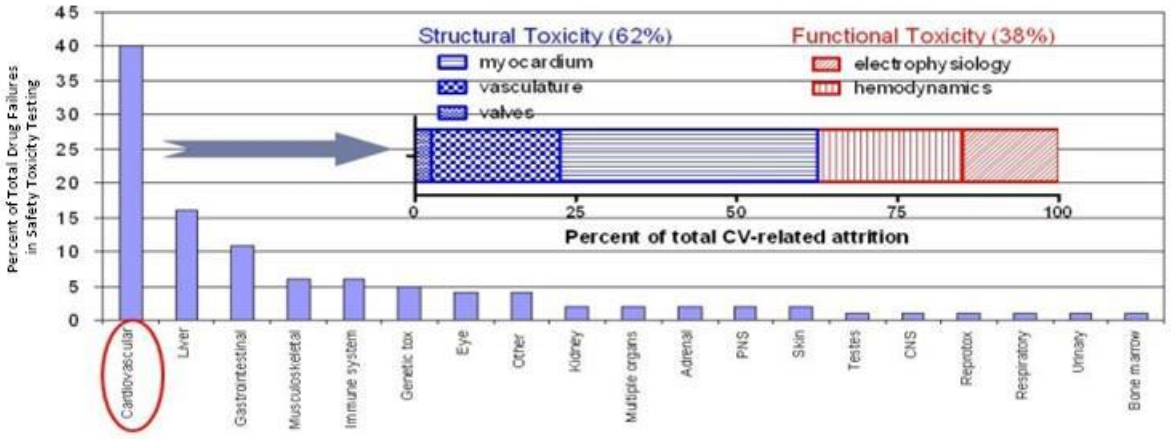

Figure 1.1: Leading causes of safety drug attrition within GSK and inset the relevant breakdown of contributing factors of cardiovascular toxicity under structural and functional descriptors.

According to the ICH S7A guidance, the cardiovascular system function should be assessed by measurements of blood pressure (BP), heart rate (HR) and the electrocardiogram (ECG). In addition, if an adverse effect is identified and follow-up studies are required, then cardiac output (CO), ventricular contractility, vascular resistance and the effect of the substance on the cardiovascular system may also be evaluated. However, these studies are not specifically designed to assess TdP risk, which is the main cause of drug withdrawal (Stevens and Baker, 2009). A further extension of ICH S7A was published with a greater focus on evaluation of delayed ventricular repolarisation potential (QT prolongation) by human pharmaceuticals using a non-clinical testing strategy prior to clinical administrations (S7B, 2005). In parallel, a guidance document outlined the recommendations for conducting early clinical trials evaluation of proarrhythmic risk in a "*thorough QT study*" (TQT) investigation (E14, 2005).

1.1.3. Cardiac Action Potential

Most cells maintain an electrical potential difference across their plasma membranes, with the inside negative to the resting outside. Excitable cells, such as nerve and muscle cells, have a resting potential around -70 to -90mV compared to non-excitable cells, such as hepatocytes, at -10 to -30mV. In excitable cells it is this negative resting potential that goes through transient changes known as an action potential during its activity to transmit the electrical signal as sodium and calcium ions flow through gap junctions to trigger depolarisation from cell-to-cell. It is considered that the cardiac action potential is similar in many properties to that found in nerve and skeletal muscle cells but also differs on some important points. The cardiac action potential cycle is shown in Figure 1.2.

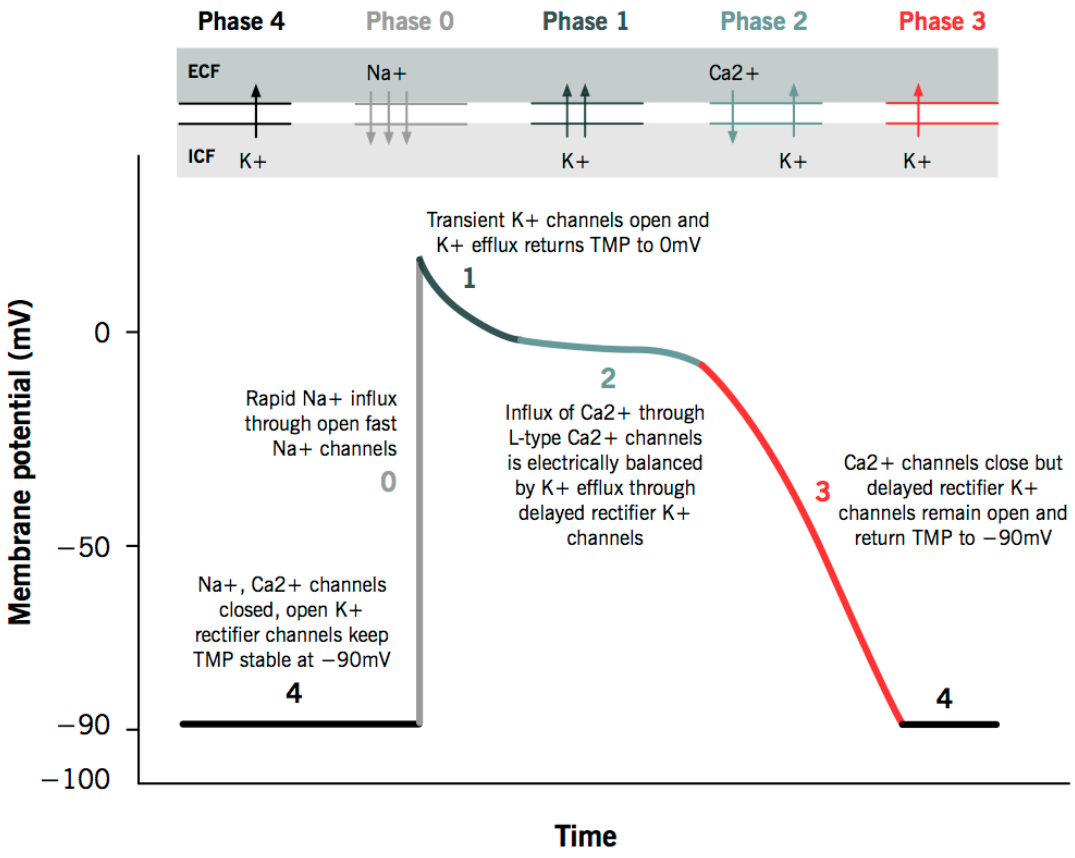

Figure 1.2: Schematic diagram of the phases within the cardiac action potential duration (APD) identifying the changes in transmembrane potential, TMP, (mV, Y axis) with time (ms, X-axis). The APD is approximately 200 ms long and is a result of the influx of ions such as sodium (Na^+) and calcium (Ca^{2+}) from the extracellular fluid (ECF) into the cardiomyocyte and efflux of potassium (K^+) from the intracellular fluid (ICF) through specific channels propagating the electrical stimulus from cell to cell.

The upstroke of the cardiac potential (depolarisation) is caused by an increase in the sodium permeability across the membrane due to opening of sodium (Na^+) voltage-gated channels and influx of Na^+ ions into the cardiac cell resulting in a shift towards a positive electrical potential. This rapid transient change (fast depolarisation, Phase 0) that occurs in the plasma membrane leads to inactivation of the Na^+ channel due to approaching the sodium resting potential (+30mV) and produces an 'overshoot' in positive membrane potential. This is similar to what happens in skeletal muscle.

The down stroke of the cardiac potential (repolarisation) is caused by the opening of potassium (K^+) channels (transiently open at Phase 1) and efflux of K^+ ions out of the cardiac cell, as the action potential is driven back towards the cell's resting potential. This is also similar to what occurs in skeletal muscle. However in cardiac cells repolarisation is a relatively slow process due to delayed-rectifier voltage-gated K^+ channels (Phase 2 and 3). As the cardiac cell returns to its resting potential (Phase 4), Na^+ leak channels and K^+ leak channels allow some diffusion into and out of the cell, respectively, making the membrane potential slightly less negative and slows the repolarisation process further as these excitable cells reset. At rest, the equilibrium potential for K^+ (E_K ~-100mV) is more negative than that of Na^+ (E_{Na} ~+50mV) and so the resting potential lies toward that of potassium. This ion concentration gradient is maintained during Phase 3 and 4 of the action potential by Na^+ and K^+ ATPase pumps. Between depolarisation and repolarisation, the potential stays about 0 mV for a relatively long time (100-300 ms). This period is called the "plateau" and is characterised by the flat region of the action potential caused by L-type voltage-gated calcium (Ca^{2+}) channels that are opened (Phase 2). This allows an influx of Ca^{2+} ions into the cell, which triggers calcium-induced calcium release from the sarcoplasmic reticulum (SR) via ryanodine receptors. These Ca^{2+} ions are used to bind the myosin cross-bridges to the actin molecules in the subsequent contraction of the muscle. As with skeletal muscle, the action potential in a heart cell will initiate contraction of that cell. One important consequence of a plateau in the heart action potential is its duration. These action potentials last up to eight milliseconds in nerve and muscle cells compared to a few hundred milliseconds in heart muscle. The contraction in the heart occurs during the action potential, whilst in skeletal muscles the contraction occurs after the action potential.

1.1.4. Regional Differences in Cardiac Action Potentials

It has been established that there is a significant difference between the electrical properties of cardiomyocytes isolated from different regions of the heart from isolated canine and human hearts (Durrer and Netter 1971). There are three types of cardiomyocytes that have been identified and give rise to the different regional characteristics of the cardiac action potential (shape and duration) depending on where in the heart the action potential was generated. Differences in ion channel composition determine the difference between myocytes from atria, ventricle, and conduction system (Figure 1.3). Contractile lineage myocytes make up the atria and ventricles which provide the classic normal cardiac APD curve with extended plateau. Pacemaker lineage myocytes consist of the SA node and AV node which exhibit a slow changing pacemaker potential. Whilst conduction lineage myocytes, which include the Purkinje system, Bundle of His and AV node, exhibit a normal cardiac action potential with a shortened plateau phase. Different regional expression levels of ion channels from cardiomyocytes across the heart tissue have also been demonstrated (Gaborit 2007). Furthermore the characteristics of the action potential also change across the myocardial wall from endocardium (inner), mid-myocardium, to epicardium (outer). Epicardial cells have the shortest action potential and mid-myocardium the longest. The average duration of the ventricular action potential can be interpreted as the QT interval on the ECG.

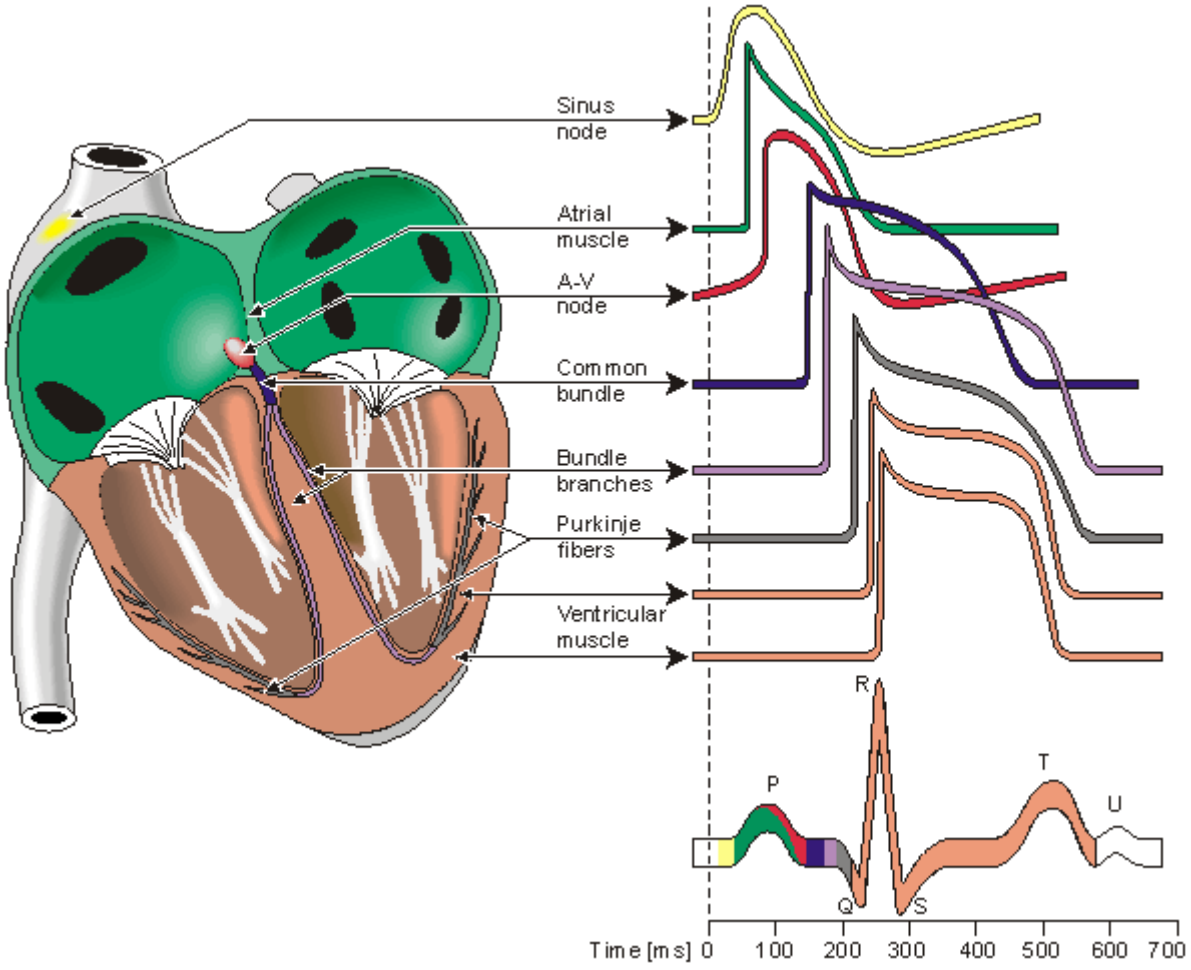

Figure 1.3: Diagram of the regional differences in cardiac action potential (AP) shape and duration from cardiomyocytes from across the heart and the corresponding changes observed on the surface electrocardiogram (ECG). The sino-atrial (SA) node (yellow) and atrio-ventricular (AV) node (red) are pacemaker cells that initiate the electrical stimulation for the cardiac cycle. The atrial cardiomyocytes are responsible for contraction of the atria, observed as the P-wave on the ECG, whilst the bundle of His and Purkinje fibres are responsible for signal propagation and transduction to the ventricular cardiomyocytes, and contraction of the ventricle, observed as the QRS and QT interval on the ECG.

1.1.5. Regulatory Guidance for Cardiovascular Safety

The ICH S7B guidelines recommend an integrated assessment to evaluate the overall cardiovascular risk. There are no mandatory studies defined except that a minimum of an in vitro I_{Kr} assay and an in vivo QT assay is required in a suitable non-clinical species to assess the delayed ventricular repolarisation (QT prolongation) risk. I_{Kr} stands for the rapid delayed rectifier potassium current, crucial for the repolarisation of the cardiac action potential (Phase 2 and 3), through potassium channels which are encoded by the *human ether-a-go-go related* (hERG) gene (Sanguinetti and Jurkiewicz, 1990). Inhibition of hERG is the most common mechanism of drug-induced QT prolongation for many non-cardiovascular drugs (Redfern et al., 2003). Further studies on other ion channels may also be undertaken, however this is much less common (Lindgren et al., 2008). As a result, pharmaceutical companies have tailored drug programmes to avoid development of compounds with dangerous I_{Kr}-blocking properties potentially at the expense of other electro-physical disturbances that may lead to arrhythmias (Picard et al., 2011).

There has been a call for a greater focus on more integrated cardiovascular safety assessment (Pettit et al., 2010; Berridge et al., 2013) and numerous recent pharmaceutical perspectives to approaching this through the drug discovery and progression paradigm (Guth et al., 2004; Cavero and Kaplan, 2008; Pollard et al., 2008; Valentin and Hammond, 2008; Stevens and Baker, 2009; Cavero, 2011). Pharmaceutical companies have adopted a tiered integrated approach within cardiovascular safety pharmacology to utilise decision making based on the collective information generated from a variety of studies which is central to the proposed non-clinical safety pharmacology testing strategy in ICH S7B.

1.2. Tiered Approach to QT Assessment

Delayed ventricular repolarisation is the major drug-related risk factor associated with ventricular arrhythmias such as TdP (Redfern et al., 2003). Ventricular repolarisation is determined by cardiac action potential duration (APD) and is a complex regulated process governed by sets of ion channels, pumps and exchangers as well as autonomic nervous system modulators. A substance's ability to prolong the APD can be observed in the ECG recording as a prolongation of the QT interval (from the beginning of the QRS complex to the

end of the T wave on an ECG trace), which covers the ventricular depolarisation and subsequent repolarisation (Figure 3).

QT is a key parameter in cardiovascular safety pharmacology and it has an inverse relationship with heart rate (S7A, 2000). Each heart beat is recorded on the ECG trace as the R-R interval. Thus the faster the heart rate, the shorter the R-R interval and the shorter the QT interval (Piotrovsky, 2005). Correction of QT interval for changes in heart rate (denoted QTc) is important for accurately detecting drug-induced QT changes, since HR is one of the major sources of QT variability (Ollerstam et al., 2007). The HR-QT relationship varies between and within species. Various correction formulas (e.g. Bazett, Fredericia, Van der Water) have been proposed and often used to correct human data; however these assume the same correction for all individuals, which may be inconsistent with actual observations (Piotrovsky, 2005). It has been shown that individual corrections are superior, particularly in dogs, which exhibit large variations in heart rate (Ollerstam et al., 2007). Large, rapid intra-individual variations are also common in many non-clinical species due to emotional and physical response and variability is further complicated by the presence of respiratory sinus arrhythmia (differences in heart rate on inhalation and exhalation). In addition to the correction method used, it must be recognised that there may be a delay in QT changes following abrupt changes in HR between species. In human, it takes approximately 2-3 minutes for QT interval to adapt to HR changes, whereas in dogs it has been shown that 90% adaptation occurs within 1.5 minutes (Ollerstam et al., 2007; Pueyo et al., 2010). However, unambiguous evidence from a consortium has recently indicated that the implementation of standardized QTc data presentation, QTc reference cycle lengths, and rate-correction coefficients across all preclinical in vivo repolarisation assays, when accurately modelled and evaluated, can markedly improve the concordance of preclinical and clinical outcomes in most preclinical species (Holzgrefe et al., 2014).

1.2.1. In Vitro

At the earliest stages of drug discovery pharmaceutical companies now employ a phenotypic screen which is designed to the main human target classes or liabilities, including the core functional systems (Kleinstreuer et al., 2014; Schirle and Jenkins, 2015). The screen panel consists of high-throughput functional in vitro assays which measure the effect of test compounds on receptor sites, ion channels, transporters, enzymes and phenotypic assays. It is

a minimal selectivity panel required to cover relevant biological space, a scaled approach similar to that described as network pharmacology using chemo-genomics for off-target activity and selectivity screening (Hopkins, 2008). Further specific in vitro cellular or membrane assays are required for confirmatory and targeted assessment to define the risk assessment or therapeutic target profile (Hamon et al., 2009).

Assessment of cardiac ion-channel activity of NCEs is now an integral component of drug discovery programmes to assess potential for cardiovascular side effects (Lawrence et al., 2008). Electrophysiological techniques are particularly useful for voltage-gated channels, as the activation of these channels can be precisely controlled. Traditionally, electrophysiologists have relied upon patch-clamp electrophysiology in mammalian cells, which is considered the gold standard assay. Recent advances in automated platforms for both single-channel (PatchXpress) and multi-channel systems for conventional and perforated patch-clamp (IonWorks) electrophysiology in mammalian or oocyte cells have aided this discovery screening (Dunlop et al., 2008).

Implementation of hERG assays into early drug discovery is aimed to limit the potential interaction with the potassium channel without compromising the drug's target efficiency due to the ion channel's promiscuity, binding to a broad range of drug-like molecules (Sanguinetti and Tristani-Firouzi, 2006). There are generally three main hERG assays available; i) binding assay, ii) rubidium efflux and iii) automated voltage clamp-based assays, in order of relative cost, ease and throughput to more expensive, technically challenging and time consuming (Rampe and Brown, 2013). A review of the merits of each assay and their relative correlation to IonWorks pIC_{50} values, demonstrating that the advent of high-throughput voltage clamp electrophysiology confers the greatest concordance and offers the option of a two-tiered in vitro screening process (Pollard et al., 2010).

A combination of screening assays with physicochemical properties, measured activity at therapeutic and any selectivity/orthologue targets, allow prioritisation and progression as well as identify potential safety concerns to further define cardiovascular liabilities (Laverty et al., 2011).

1.2.2. Ex Vivo

In addition to the ICH S7B minimum requirements, specific assays measuring action potential duration (APD), QT/TdP liability, conductivity and contractility are often employed in vitro or ex vivo (Lindgren et al., 2008). These can be specific regional models such as Purkinje fibre, papillary muscle and ventricular wedge, or whole tissue (Langendorff-heart), from dog, rabbit and guinea pig (Lawrence et al., 2008; Pugsley et al., 2014).

The Langendorff-perfused model consists of a paced female rabbit heart, known as the Screenit assay, designed to test the potential to prolong cardiac repolarisation and arrhythmias, including TdP (Hondeghem, 1994). It has also been assessed using isolated guinea pig hearts (Testai et al., 2007; Guo et al., 2009b) or contractility in rat hearts (Henderson et al., 2013). Largely due to practical considerations, experimental studies of the mechanisms of arrhythmogenesis in the whole heart often examine the epicardial surface in isolation and thereby disregard differing AP's across the ventricle wall (transmural electrophysiology). This is addressed by the arterially (coronary) perfused ventricular wedge preparation, first developed to study the electrical heterogeneity of canine left ventricular myocardium (Yan and Antzelevitch, 1996).

As with all screens there are limitations such as protein-free buffer, potential lack of metabolism, insufficient equilibration/tissue distribution and variability in associated concentration effects. However this ex vivo model does provide detailed information on the overall profile of drug-induced electrophysiological effects and is considered a valuable tool to establish an integrated cardiovascular risk assessment of pharmaceutical compounds (Valentin et al., 2004; Steidl-Nichols et al., 2008; Beattie et al., 2013).

Female tissues are often utilised as it has been demonstrated that there is a difference in the action potential duration. Females have a longer action potential, as a result of a prolonged plateau phase due to L-type calcium channels and reduced I_{Ks}, combined with a reduced repolarisation reserve increasing the tendency for TdP (Lu et al., 2000; Sims et al., 2008; Gonzalez et al., 2010). This has also been linked with age and sex differences in humans (Vicente et al., 2014).

1.2.3. Anaesthetised Models

The draft guideline ICH S7B Step 2 Revision (2004) allows the use of anaesthetised models to be used for QT measurements, and the Japanese guidelines (MHW-Japan, 1995) advises the use of anaesthetised animals. As a result of the Japan Manufacturers' Association PRODACT Initiative many pharmaceutical companies reliably use anaesthetised models of guinea pigs, rabbits and dogs as a predictive screening tool for cardiac electrophysiology and QT prolongation (Hammond et al., 2001; Hashimoto, 2008). The PRODACT Initiative confirmed that the anaesthetised dog is a sensitive model for detecting drug-induced effects on QT interval (Tashibu et al., 2005). However this model is less favourable today primarily due to ethical reasons and the ease of telemetered (jacketed/implanted) dogs.

The overall use of anaesthetised preparations is generally limited in number as many anaesthetics can affect the normal function of the cardiovascular system or produce drug interactions (Mitchell et al., 2010), and the study duration is restricted. However there are benefits in that higher dose levels via the intravenous route can be administered in a controlled manner in an early discovery environment where drug availability may be limited. As with all experimental studies it is important that consistency and reproducibility is achieved and maintained in a control baseline group for comparison. Therefore with the accepted caveats associated with the anaesthetised model set up, results or changes can be measured and interpreted accordingly. Anaesthetised preparations are considered an acceptable adjunct to conscious studies, though the choice of anaesthetic is important (Hammond et al., 2001; Vincze et al., 2008).

1.2.4. In Vivo

The in vivo QT assay as the names suggests is generally designed to measure QT interval from an ECG, which is the most common endpoint for ventricular repolarisation. The recommendation is to design the assay to also meet the objectives of the S7A guidance, to help reduce the number of animals used. A recent survey of safety pharmacology practices showed that the most common species used for the in vivo assay was the dog (Cavero, 2011). This is likely due to the fact that the electrophysiology of the dog heart and the functionality of the canine I_{Kr} channel (cERG) are similar to human (Wang et al., 2003).

Since the S7A guidance indicates a preference for animals to be in a conscious, unrestrained state, radio-telemetry is often used to simultaneously collect ECG and hemodynamic parameters, as the 'gold standard' (Sivarajah et al., 2010). Animals are generally chronically instrumented with telemetry transmitters, consisting of an intra-arterial catheter to measure blood pressure and a Lead II ECG. Once implanted, the telemetry devices cause negligible stress to the animals, and enable high quality data to be routinely monitored and collected, providing an extended time course (e.g. onset and duration of response typically over a 24 hour period) of any effect on the physiological parameters being measured. The benefits of the model include the ability to dose via the oral route (typically the intended clinical route of administration), administer increasing single doses on separate occasions (typically via a Latin-square design), reducing variability caused by the use of different animals, reuse and thus reducing the number of animals required to provide statistical validity (Ollerstam et al., 2007). The main limitation appears to be the potential for higher doses to induce side-effects such as emesis or sedation/excitation in the dog (De Clerck et al., 2002; Sivarajah et al., 2010). This may cause difficulty in reaching the expected exposure, which ideally includes and exceeds the therapeutic range, and also increases the variability between concentration-effect for interpretation. It is becoming more acceptable and common place for non-invasive telemetry jacketed animals to be used to facilitate earlier data acquisition (Prior et al., 2009; Klein and Redfern, 2015).

Other species may also be used in the in vivo QT assay; the most common species after dogs are non-human primates (NHP) (Lindgren et al., 2008). Increasing use of NHPs in toxicological studies has led to the need for a cardiovascular safety model in this species (Guth and Rast, 2010) and models using invasive (Authier et al., 2007) and non-invasive (Mitchell et al., 2010) telemetry techniques have been validated. Due to problems with primate availability and the associated ethical concerns, the mini-pig is another species that has been suggested as an alternative. A mini-pig model which simultaneously measures cardiovascular and respiratory safety endpoints has been proposed (Authier et al., 2011). This approach to combine the different aspects of the core-battery requirements has also been proposed in the monkey (Ingram-Ross et al., 2012) and in dogs where cardiovascular and neurological endpoints were obtained (Moscardo et al., 2009).

In vivo QT models do not include mice or rats since the ion channels involved in repolarisation differ in these rodent species (S7B, 2005), however telemetered rats are

commonly used for hemodynamic (heart rate, blood pressure and contractility) assessment (Adeyemi et al., 2009; Tontodonati et al., 2011). Other species used less frequently as conscious telemetered models are guinea-pigs (Hess et al., 2007) and rabbits (Kijtawornrat et al., 2006b) due to the difficulties in reliable recovery from anaesthesia, manual handling and animal training. These species are often utilised as an intermediary model in terminally anaesthetised or ex vivo preparations prior to full regulatory assessment (Hammond et al., 2001).

1.3. Protein Binding

Protein binding measurement is an important factor that needs to be considered as part of drug discovery. It is necessary for the scaling of pharmacokinetic and pharmacodynamic parameters from animal models to human for new drugs and differences in interspecies protein binding (PB) need to be considered. The fraction unbound (f_u) parameter supports various in vitro-to-in vivo correlations and preclinical-to-clinical predictions, including microsomal and allometric clearance projections, metabolism and transport drug interactions. It is also important to define safety margins (such as QT prolongation liability) and understanding of in vivo pharmacodynamics (such as receptor occupancy) as it is the free drug concentration that drives the efficacy and pharmacological response. Likewise, f_u must be incorporated into the estimated First Time in Human (FTiH) dose as calculated from in vitro measures of target concentrations. Protein binding in plasma (PPB), hepatic microsomes and relevant target tissues (e.g. brain homogenate) is often routinely assessed in drug discovery to determine the fraction unbound, (f_{up} or f_{ut}).

1.3.1. Free Drug Hypothesis

The free drug hypothesis states that "*only unbound drug is available for clearance and drug-drug interactions with metabolising enzymes and transporters, equilibration into tissues, and pharmacological activity*". This statement of free drug hypothesis has been further defined that "*in the absence of transporters, the free drug concentration is the same on both sides of the biological membrane at steady state and the free drug concentration at the site of action is the species that exerts pharmacological activity*" (Smith, et al., 2010). As such, unbound drug concentrations drive pharmacokinetics, pharmacodynamics, and drug-drug interactions. For most organs there are no barriers between blood and the organ to restrict diffusion between them, and as a result, the unbound drug concentration is the same as the unbound drug concentration at the drug target site. Exceptions to this are organs such as the brain and

testes which have both an anatomical and biochemical barrier to restrict the molecular exchange between the blood and tissue. However, understanding the unbound fraction and tissue specific binding may provide insight into the CNS penetration and drug efficacy (Summerfield, et al., 2006).

1.3.2. Regulatory Assessment

In drug development of the past, the goal of the definitive PB studies was characterization of the extent of binding in plasma, and not necessarily a quantitative determination of the f_u and its impact on pharmacokinetics and drug interactions. As such, reporting plasma binding as greater than the radiochemical purity (i.e. high binding) was sufficient to support drug development and registration, as shown by submissions for Lipitor [Pfizer 2009], Singulair [Merck 2010] and Voltaren [Novartis 2009]. The FDA drug interaction draft guidance in 2006 indicated that the decision whether a drug interaction study is necessary for a drug that inhibits a metabolic pathway is based on the total systemic concentration [FDA, CDER, 2006]. However, European regulators in 2010 have amended this long-standing approach in favour of simulations driven by unbound concentrations. Regulatory guidance continually evolves, and there is now the expectation for the quantitative determination of the unbound drug concentration and f_u value, even for highly-bound drugs, to make key development recommendations (ICH (M3)R2, 2009;CDER FDA, 2012). This has been reflected in the bioanalytical arenas; in which white papers address the unbound concentrations (Fluhler, et al., 2014;Timmerman, et al., 2015). Given the importance being placed on unbound drug concentration and f_u values, there is no harmonised regulatory guidance on the conduct and validation of such studies. There are examples of validated protocol suggestions and tiered discovery design approaches (Zhang, et al., 2012;Buscher, et al., 2014;Lambrinidis, et al., 2015).

1.3.3. Protein Binding Methodologies

There are a number of in vitro assays that can be utilised to determine the extent of protein binding in drug discovery from chromatography based methodologies to in vivo microdialysis. For example, such techniques include equilibrium dialysis (ED), ultrafiltration (UF), ultracentrifugation (UC), albumin-column chromatographic methods, fluorescence spectroscopy, ultraviolet spectroscopy, circular dichroism, nuclear magnetic resonance spectroscopy, and capillary electrophoresis (Pacifici and Viani, 1992). Some techniques are very labour intensive, whilst others have been adapted to higher throughput to 96 and 384

well formats (Hartmann, et al., 2006). Protein binding in plasma (or blood) is the most common, to determine free concentrations of drug exposure. There have also been a wide variety of tissues matrices investigated (brain, liver, lung and bone) (Mariappan, et al., 2013).

Table 1.1 Comparison of Standard Protein Binding Methods

Technique	Advantages	Disadvantages
Rapid Equilibrium Dialysis (RED)	Standardised methodology; widely used; 96-well format	Time to reach equilibrium; drug stability; dilution of plasma proteins
Ultrafiltration (Centri-free)	Technically simple; inexpensive; suitable for unstable drugs	Adsorption of drugs onto filter; disassociation of bound drug; limited filtrate
Ultracentrifugation	No non-specific binding to membrane	Time consuming; expensive equipment; back diffusion

For protein binding the most common techniques within industry are those that are most reproducible, simple and allow greater throughput, as shown in Table 1.1. Equilibrium dialysis is the most commonly employed technique and considered to be the 'gold standard', followed by ultrafiltration, ultracentrifugation and gel filtration. An extensive review by Zhang et al. provided a critical evaluation of techniques for the largest (n=222 cpds) collection of protein binding data to date (Zhang, et al., 2012).

Previously definitive protein binding used to be assessed with radiolabelled drug material where the radiochemical purity limits quantitative PB measurement. Dilution of plasma or matrix has been an approach previously for highly protein bound drugs (Kalvass and Maurer, 2002). In a recent study, plasma binding was determined by equilibrium dialysis using non-radiolabeled compound and was validated against the respective definitive values obtained by accepted radiolabeled protocols. The methodology reported enabled reliable quantification of f_u values for highly-bound drugs that was not limited by the radiochemical purity (Zamek-Gliszczynski, et al., 2011). An alternative approach – opposite to commonly used methods - is equilibrium gel filtration, which measures the amount bound at set-free concentrations as a method for measuring very highly plasma protein bound drugs (Weiss and Gatlik, 2014). This addresses the more difficult experimental bias for highly bound drugs, and is not

restricted by assay sensitivity. This challenge is being investigated as part of an IMI collaborative initiative, and one such example is the very high binding itraconazole, an important marketed compound used for clinical drug-drug interaction studies (Riccardi, et al., 2015). The bioanalytical challenge is measuring unbound fraction for many techniques along with a robust experimental design has been discussed (Nilsson, 2013).

1.3.4. Cross-Species Protein Binding

The above methods are suitable for measuring the total plasma protein binding using plasma samples from different species, while they can also be applied for binding to the individual plasma proteins and potential different tissues (matrices).

It is suggested that inter-species comparisons, and comparisons across compounds or concentrations, should ideally be based on unbound values (Smith, 2010). It is recommended that unbound fractions should be only compared between species for the calculation of safety margins using the same method and device (Nilsson, 2013). Comparisons based on total concentrations will be confounded by the fact that the total plasma concentration is the ratio of the unbound concentration and the unbound fraction, which may differ. The aspects of concentration-dependent PPB and inter-species differences in PPB are possible and if there are inter-species differences in the unbound fraction then there will be subsequent changes with concentration, as demonstrated across 7 species for a given compound (Nilsson, 2013). This makes it difficult to assess the safety margin or the concentration–response relationship across species. Therefore a protein binding assessment will be made using ED as a common technique, in a 96-well block format across a range of species and in plasma, blood and heart tissue to aid interpretation of PK and PD.

1.4. Pharmacokinetics and Pharmacodynamics

Pharmacokinetics (PK) and pharmacodynamics (PD) are the two disciplines that determine the relationship between concentration and effect, and the mechanisms that characterise it. Pharmacokinetics is defined as “what the body does to the drug” and pharmacodynamics is “what the drug does to the body” in their most simplest of terms (Holford and Sheiner, 1982).

In more specific terms, the field of pharmacokinetics is concerned with quantifying the relationship between an administered dose and the resulting concentrations in the body

(Machado et al., 1999). The literal meaning of pharmacokinetics is "drug movement" within a biological system and is governed by the characteristic interactions of a drug and the body in terms of its absorption, distribution, metabolism, and excretion (ADME) and it is through the drug's quantification that an understanding of the relationship between dose and concentration can be obtained.

Pharmacokinetic data is comprised of drug concentrations measured over a time-course following dosing. Concentrations are usually in plasma/blood (as an easy accessible body fluid) representative of systemic exposure and act as a surrogate indicator as drug concentrations at the site of action are rarely measured, although target/specific tissue may also be determined (Aarons, 2005). The resulting concentration-time profile(s) are analysed to derive parameters that explain the ADME processes in mathematical terms, such as clearance (CL), volume of distribution (V), and half-life ($t_{1/2}$). This analysis can be performed using a non-compartmental analysis or through fitting of a model to the data.

Pharmacodynamics is the study of the biochemical and physiological effects of drugs on the body, the mechanisms of drug action and the relationship between drug concentration and effect (Machado et al., 1999). This pharmacological effect can include both adverse and beneficial responses and can be a result of direct or indirect measure of efficacy/safety (Derendorf et al., 2000). Effects can be measured as biomarkers, surrogate end points or clinical outcome. Clinical outcome is a direct result of the drug treatment such as survival, prevention and cure, as well as subjective endpoints like wellbeing and pain relief. Biomarkers are defined as "cellular, biochemical or molecular alterations that are measurable in biological media such as human tissues, cells, or fluids" (Naylor, 2003). More recently, the definition has been broadened to include biological characteristics that can be objectively measured and evaluated as an indicator of normal biochemical processes (e.g. cytokines), pathogenic processes (e.g. cardiac troponin), or physiological (e.g. blood pressure) responses to a therapeutic intervention (Mayeux, 2004). However if a biomarker is strongly predictive of the clinical outcome then it is classed as a surrogate end point (Lesko and Atkinson, 2001). Although clinical outcome is the ideal PD measure, it is often difficult to quantify and may require large numbers of samples due to its categorical nature. Therefore biomarkers or surrogate end points are often used as they can be measured in a shorter time frame (Colburn and Lee, 2003).

PD data may also be recorded in a number of different forms, such as continuous, categorical, count, or time to an event. Similar to PK data, quantification of the relationship between dose administered and effect is obtained by applying a mathematical model. Continuous PD data is the most informative describing a pharmacological response over time and so is typically modelled in conjunction with a PK model (via PKPD model) to fully characterise the dose-concentration-effect relationship.

1.4.1. Modelling

PKPD models are often described as a simplified description of reality (Holford and Sheiner, 1982). The complexity of the model depends on the amount and quality of the data available and what it will be used for. Models can be descriptive i.e. for a given set of conditions or predictive, where variables are included that allow the model to predict different outcomes dependent on the values of those variables used (Rajman, 2008). Models can also be described mechanistically, where parameters related to physical entities such as physiological and biological aspects are incorporated, or empirically where such parameters are absent. In general those models that are more mechanistic will prove to be more predictive and representative (Birtwistle et al., 2013). Where models take a step further and incorporate physiological and biochemical mechanisms into pharmacokinetic-pharmacodynamic models, it is referred to as systems pharmacology (Eissing et al., 2011; van der Graaf and Benson, 2011).

1.4.2. PKPD Modelling in Industry

It has been noted that PKPD modelling could aid safety pharmacology studies in many ways (e.g. with respect to interpretation of exposure and time-response data, minimising animal usage, maximising study designs) for selection of drug candidates (Cavero, 2007). A recent analysis has shown that both PKPD relationships and model translation are popular themes at the safety pharmacology society (Redfern and Valentin, 2011), and there is a growing momentum of literature publications demonstrating examples and influencing regulatory submissions (Rowland et al., 2015).

Successful prediction of early clinical trials is vital to ensure that the risk of adverse effects in humans is sufficiently low, to both protect the participants (healthy volunteers and patients) and to prevent further costly development of unsafe medicines. Prediction of adverse effects in patient populations, where underlying conditions may affect their response, is the ultimate

aim. It has been recognised that the use of PKPD modelling may help in this area (Bass et al., 2011), yet problems may still exist, particularly with QT as the primary biomarker of TdP. Additional biomarkers are the focus of interest not only for predictivity of TdP (Lu et al., 2013) but also other areas of cardiotoxicity (Berridge et al., 2013; Klein and Redfern, 2015). With more studies now performed in the discovery stage with a variety of animal models (Fryer et al., 2012), it is hoped that adverse effects can be predicted early on and a greater translational-link be built between models (Caruso et al., 2014).

1.5. Non-Clinical Translation of Safety Pharmacology

Cardiovascular adverse events (AEs) are diverse and may not be a direct result of the primary pharmacology, therapeutic class or chemical class. However most AEs are dose related and, therefore, predictable from a number of primary, secondary and safety pharmacology screening models (Valentin, 2010). However, the cardiovascular toxicity may also result from modification of structural and/or functional components within the cardiovascular system which may not manifest in acute dosing (Ferri et al., 2013) (Figure 1.1).

The S7A guidance indicates that the choice of non-clinical experimental models, endpoints and study designs *"should be relevant to the prediction of the potential human response"*. Although careful consideration is given to the design of such studies, translational aspects have been limited to determining firstly whether the models have the statistical power to detect a response (Sivarajah et al., 2010) and secondly if they have the appropriate sensitivity, specificity and predictive capacity determined qualitatively by comparing rates of true and false negative and positive signals (Valentin, 2010). Quantitatively, the current best practice for the magnitudes of effect remain with QT translation due to the more comprehensive study of the area compared to assumptions between non-clinical and man for HR and BP (Leishman et al., 2012). The reliability of the predictions from non-clinical studies is indeed vital, as the result is often used for decision making and may impact upon clinical progression. The S7A guidelines make reference to defining the dose (concentration)-response relationship of any observed adverse effect and the majority of companies will test doses that give multiples of (most commonly 10, 30 and 100 times) the expected clinical concentration (Lindgren et al., 2008). Interpretation of the concentration-response relationship is not always straightforward though and techniques such as PKPD modelling may be required to truly uncover the potential risk.

1.5.1. Cross-Species Scaling

Modelling at the early discovery non-clinical stage is often used to aid selection of the candidate drug for progression into the clinic, aid dose selection and assess safety aspects (Wishart, 2007; Wang et al., 2015b). Prediction of the human dose-response relationship is essential for such decisions and requires techniques for accurate scaling of animal data. Data from compounds of the same class can be used as comparators, with the relative difference between the comparator's efficacy and potency in animals compared to man applied to the new drug of interest. Confidence can be gained from predictive models scaling between other non-clinical species (Riviere et al., 1997). For example PK parameters are usually scaled allometrically and this has been a successful approach. However, for PD in the absence of comparator data then this type of empirical scaling would not be feasible and a mechanistic approach would be required (Huang and Riviere, 2014).

1.6. Bioanalytical Methods

Bioanalytical approaches have been employed within this project to enable the generation of data from different compounds and biological study designs. Provided is a background to bioanalysis, the regulatory landscape applied to pharmaceuticals and the currently most utilised analytical technique, along with detailed sections of the methodological approach undertaken to support the work within this thesis. Bioanalytical assay methods utilised were qualified based upon existing validated assays that have been adapted from regulated studies or from literature, such that high quality bioanalytical peak-area-ratios or concentration data was produced to support study interpretation and integration. Further specific analytical details are given in appendices for each respective compound (Appendix 1).

1.6.1. Background to Bioanalysis

In the context of analytical chemistry, this is the intentional separation of a substance into one or more constituents (e.g. elements, compounds or ingredients), usually by chemical means, to ascertain the kind, composition or quantity of component parts whether obtained in separate intact form or not. Bioanalysis is a sub-discipline of analytical chemistry covering the identification or measurement of xenobiotic substances (such as drugs and/or their metabolites) or biotics (such as macromolecules, proteins, DNA, large molecule drugs, metabolites) in a biological system (such as blood plasma, urine, or tissue).

Bioanalysis is an important facet to the measurement of physico-chemical and metabolic properties that are crucial to the discovery and development of new drug candidates. If these properties fit the target therapeutic profile required of a commercial drug, they are considered to have "drug-like properties" which may be exhibited by good absorption after oral dosing, bioavailability, pharmacokinetics and stability. Biological profiling of drug candidates may be achieved through qualitative or quantitative assessment and by a combination of analytical separation techniques using chromatographic resolution (e.g. TLC, GC or HPLC) and detection techniques (e.g. UV, fluorescence, radioactivity, MS) (Ding et al., 2013).

Quantitative bioanalysis involves determining the concentration of drugs and/or metabolites in a biological matrix such as plasma or blood. Methodologies must generate reproducible and reliable data to allow valid interpretation, especially when attempting to develop appropriate dosing regimens, therapeutic strategies and safety exposure in patients. Therefore regulatory guidance has been an equally important component which has accompanied bioanalytical methodologies to ensure high quality and integrity (Shah and Bansal, 2011).

1.6.2. Bioanalytical Regulatory Landscape

Prior to 1990, there were only regulations requiring bioanalytical methods to be sensitive, specific, accurate and precise (US 21 Code of Federal Regulations, 2002) where bioanalysts provided their own interpretations of procedures and specifications to meet the regulatory requirements. As a result there was a lack of uniformity to the approaches to validation of bioanalytical methods, submission of data to the regulatory agencies and evaluation of the data submitted.

At a workshop, subsequently known as "Crystal City Bioanalytical Workshops", dedicated to the bioanalytical method validation (BMV) the first concept 'white paper' of a harmonised approach was made (Shah et al., 1992) The conference focussed on defining the essential parameters (accuracy, precision, selectivity etc) and addressed a 'how to' evaluate approach as well as defining the standard curve, recovery and replicate analysis for BMV. However it was not until 10 years later that a draft regulatory guidance was issued (FDA, 1999). A second workshop reported on the progress made within the decade and formed the basis of the first formal FDA Guidance on BMV (FDA, 2001). At the time the EMA produced a brief directive in 2003 and then comprehensive guidance in 2009 with minor differences highlighted as result of field progression (Smith, 2010). Numerous workshops since the

inaugural Crystal City meeting have lead to white papers which recognise the continual advancement in methods and techniques (Savoie et al., 2009; Savoie et al., 2010; Fluhler et al., 2014). The need for a 'global' harmonisation from constituent bioanalytical bodies, such as European Bioanalytical Forum (EBF) and Japanese Bioanalysis Forum (JBF), was recognised in the formation of the Global Bioanlytical Consortium (GBC). The GBC is currently working towards a harmonised document between various global regulatory agencies and bioanalytical groups (van Amsterdam et al., 2010; Imazato, 2013).

With regulatory guidance documents in place, a considered best practice approach as part of the bioanalytical toolbox can be applied to appropriate studies within early discovery (Timmerman et al., 2015). Quantitative drug bioanalysis measures drug concentrations in biological specimens for different purposes. It can be divided into non-regulated (non-GLP) and regulated (GLP) bioanalysis. In the pharmaceutical industry, regulated studies refer to bioavailability/ bioequivalence, GLP toxicokinetic and human PK studies that are used for clinical drug toxicology and therapeutic monitoring. Non-regulated studies refer to early discovery and development pharmacokinetics, investigative and preliminary safety toxicology studies that are not critical in a regulatory submission (Huang et al., 2012).

Within discovery sample bioanalysis there is the need to balance data quality with speed for 'fast turnaround' decision making. This is not simplified regulated bioanalysis with relaxed acceptance criteria, but a more pragmatic approach to balance the level of assessment of BMV reporting and generic method suitability to deliver sample analysis (Ho, 2014).

1.6.3. Bioanalysis

The most robust and abundant bioanalytical tool used in the pharmaceutical industry currently is reverse-phase ultra high performance liquid chromatography (UHPLC) coupled with mass spectrometry (MS) (Ramanathan et al., 2011). Referred to as LC-MS/MS, it meets all the prerequisite requirements for analysing drug concentrations in biological fluid samples in-line with current standard approaches (Ding et al., 2013; Zhang et al., 2013).

1.6.4. Ultra High Performance Liquid Chromatography (UHPLC)

Chromatographic methods in the pharmaceutical industry fall into three categories; high throughput, high productivity, and high resolution. These are defined by the objective of the separation and application area, which include run time, efficiency and resolution (Chesnut and Salisbury, 2007). HPLC is a common versatile technique that has a wide range of

applications and compatible with numerous detection techniques for determining the assay or impurity/ metabolic profiles of drugs. There are two variants of HPLC dependent on the relative polarity of the solvent and the stationary phase (silica column packing material). Normal phase chromatography is similar to thin layer chromatography or column chromatography, where polar compounds in the mixture pass through a column and 'stick' longer to the polar silica phase than non-polar compounds. The non-polar compounds therefore pass more quickly through the column. Reverse phase (RP) is the opposite, where a polar solvent is used and polar molecules elute more rapidly due to the non-polar components forming interactions with the hydrocarbon column residues, and this is the most common technique deployed in the pharmaceutical industry (Dejaegher et al., 2010; Pieters et al., 2010).

RP-UHPLC utilised in quantitative or qualitative bioanalysis falls into the category of high productivity where reduced run time and efficiency is the most important factor. Traditional isocratic or gradient methods can be developed and applied with specific column phase chemistries and mobile phases to further aid efficiencies (Molnar, 2002; Krisko et al., 2006). These traditional methods can simply be applied to UPLC for improved productivity by systems now utilising columns that are smaller in length, packed with smaller diameter particle sizes (<2 µm), results in higher backpressure, and termed "ultra" HPLC (Chesnut and Salisbury, 2007). As a result, UHPLC chromatography greatly enhances MS sensitivity through reduced dispersion at lower flow rates and increased source ionisation as shown by a diverse application in quantitative studies (Gosetti et al., 2013; Wang et al., 2015a).

1.6.5. Mass Spectrometry (MS)

Mass spectrometry (MS) is an analytical chemistry technique that helps identify the amount and type of chemicals (analytes) present in a sample by measuring the mass-to-charge (m/z) ratio and abundance of gas-phase ions under vacuum. MS is now a fundamental application to pharmaceutical analysis (Kerns and Di, 2006).

There are three basic components to a mass spectrometer; firstly under atmospheric conditions there is the in-let, which receives the sample either directly or from a separation system (such as gas or liquid chromatography (GC or LC)), and ionisation source, where the analytes become negatively or positively charged as a result of source method used, such as electrospray ionisation (ESI) or atmospheric chemical ionisation (APCI). The second is the mass analyser quadrupole, which separates and focuses gas ions based on m/z using 4

electro-magnetic rods under vacuum (for example instruments such as TOF, IonTrap and Orbitrap). The final component is the detector and recorder, which can be in the form of counts per second (CPS), continuous electron multiplier (CEM) with or without deflection. A mass spectrum plot is generated of the ion signals detected as a function of the m/z ratio, which for example is achieved when analysing full scan spectra for potential metabolites.

Quantitative MS analysis is highly selective as it can be optimised to 'filter' the molecule of interest based on its m/z ratio and input parameters for the mass spectrometer components. Further specificity is achieved by fragmenting the parent molecule in the MS to its 'daughter ions' that give a characteristic product ion profile which can be further focussed for multiple reaction monitoring (MRM) in MS/MS mode (tandem). Sensitivity for each individual analyte of interest can be achieved by optimising a range of custom parameters within the MS, such as temperature, curtain gas, collision energy, declustering potential, and cell exit potential (Higton, 2001). An internal standard (I.S.) is used as a reference point to calculate peak area ratios of drug-related material of interest and determine its relative ratio or concentration (based on a calibration line). An internal standard is also used to correct any inter-sample variability in signal response, extraction and identify issues. In combination with sample preparation (extraction solvents) and chromatographic resolution (column chemistry, gradient and solvents) a highly selective, sensitive and reliable bioanalytical method is achieved (Kerns and Di, 2006; Plumb, 2008; King et al., 2014).

Therefore UPLC-MS/MS was employed for the analysis of biological samples (plasma, blood and heart tissue) from studies conducted within this thesis to deliver fast, sensitive, reproducible qualitative and quantitative data in line with current practices for bioanalytical methods in the pharmaceutical industry.

1.7. Investigational Compounds

Many compounds over the past 20 years have been identified with QT-prolongation from pre-clinical development screening studies to incidence in clinical TQT studies and post-marketing frequencies from such clinical trials as CAST, SWORD and DIAMOND (Greene et al., 1992; Pratt MD et al., 1998; Pedersen et al., 2001). Many of these compounds come from diverse structural and therapeutic backgrounds from the various classes (I-III) of proarrhythmia drugs designed to lengthen QT (e.g. quinidine, dofetilide, D-sotalol) to drugs where QT prolongation was unexpected, for example; quinolone anti-bacterials (e.g. moxifloxacin), anti-histamines (e.g. terfenadine), anti-psychotics (e.g. thioridazine) and anti-malarials (e.g. halofantrine) to name but a few. These drugs illustrate some aspects of the structural diversity of hERG blockers and have been shown to block hERG by binding to sites within the inner cavity of the channel. Many contain a positive central amine that's stabilised by cationic π bond interactions, with hydrophobic moieties either end, one of which contains hydrogen bond acceptors, to interact with hERG channel motifs (Perry et al., 2010) (Figure 1.4) This cannot be a diagnostic tool alone for hERG channel blockade but through an SAR model screening approach drug discovery can reduce unwanted combinations of moieties.

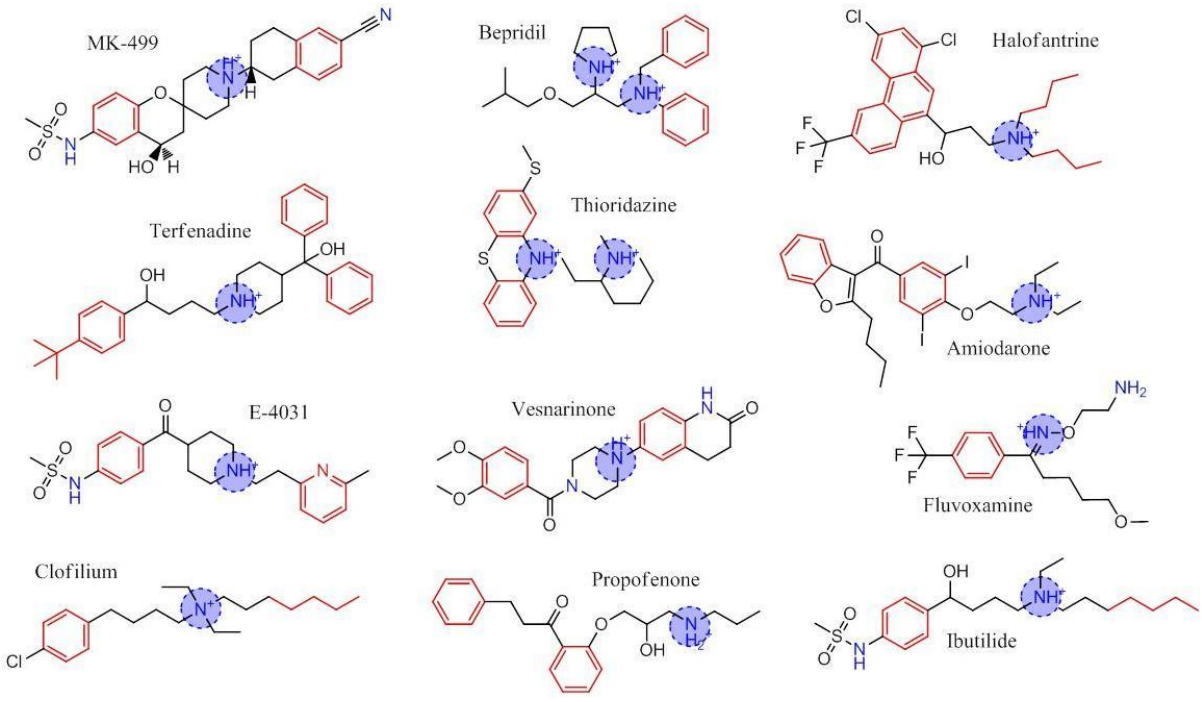

Figure 1.4: A diverse array of chemical structures of known hERG channel blockers. The central positive amine which interacts with the Tyr652 is indicated by the blue circle. The hydrophobic aromatic/alkyl moieties are highlighted in red which interact with the Phe656 or those with associated nearby hydrogen bond acceptor moieties with Thr623 and Ser624 within the hERG channel structural motifs.

In this investigation compounds were considered that affected QT prolongation as an undesired pharmacological side effect and where the heart was not their intended primary target organ. Using Redfern's categorisation (Redfern et al., 2003), based on Vaughan-Williams classification, this excluded the anti-arrhythmic drugs such as a dofetilide and sotalol considered as Category 1, even though there is a wealth of published data available across a variety of models. With this in mind Category 2 compounds are classified as drugs that have been withdrawn or suspended from the market due to an unacceptable risk of TdP for the condition being treated. Therefore these drugs would make possible positive tool compounds.

In the following section, background information for each of the selected investigational tool compounds will be given for cisapride, moxifloxacin, sparfloxacin and verapamil. More specifically, this includes PK, safety and bioanalytical details in support of this study.

Cisapride was selected as it was one of the earliest non-cardiovascular agents to be reported with QT prolongation and subsequent TdP, leading to its withdrawal, at the same time as Terfenadine. Its structural activity relationship (SAR) and mechanism of action led to the implementation of hERG screening in drug development, acting as a potent indicator of QT prolongation.

Two fluoroquinolones were chosen, moxifloxacin because this remains a marketed anti-bacterial agent with a known QT prolongation and is utilised as a positive marker against new chemical entities (NCE's) in clinical TQT studies. Whilst sparfloxacin is an earlier fourth generation fluroquinolone, with restricted licensing, and has a more potent hERG inhibition and QT prolongation. At the time of this work sparfloxacin in GSK was being investigated for metabolomic effects with QT prolongation as potential biomarkers in the rabbit.

Verapamil was chosen as a negative control compound, as it is often utilised in safety pharmacology studies. Verapamil has some hERG channel activity but is predominated by its action on the L-type calcium channel which manifests through observed contractility, heart rate and blood pressure changes, and thus has little or no effect on the observed QT.

1.8. Cisapride

Cisapride (R 51619; (±)-cis-4-amino-5-chloro-N-[1-(3-(4-fluoro-phenoxy)propyl)-3-methoxy -4-piperidinyl]-2-methoxybenzamide; Figure 1.5) was a novel gastro-intestinal prokinetic agent discovered by Janssen Pharmaceutica in 1980. It is devoid of anti-dopaminergic and direct muscarinic activity, and activates $5HT_4$ serotonin receptors in the intestinal wall exerting its effect through release of acetylcholine at myenteric plexus sites of the gut. Stimulation of the receptors increases acetylcholine release in the enteric nervous system and motility of the upper gastrointestinal tract without stimulating gastric, biliary, or pancreatic secretions (McCallum et al., 1988).

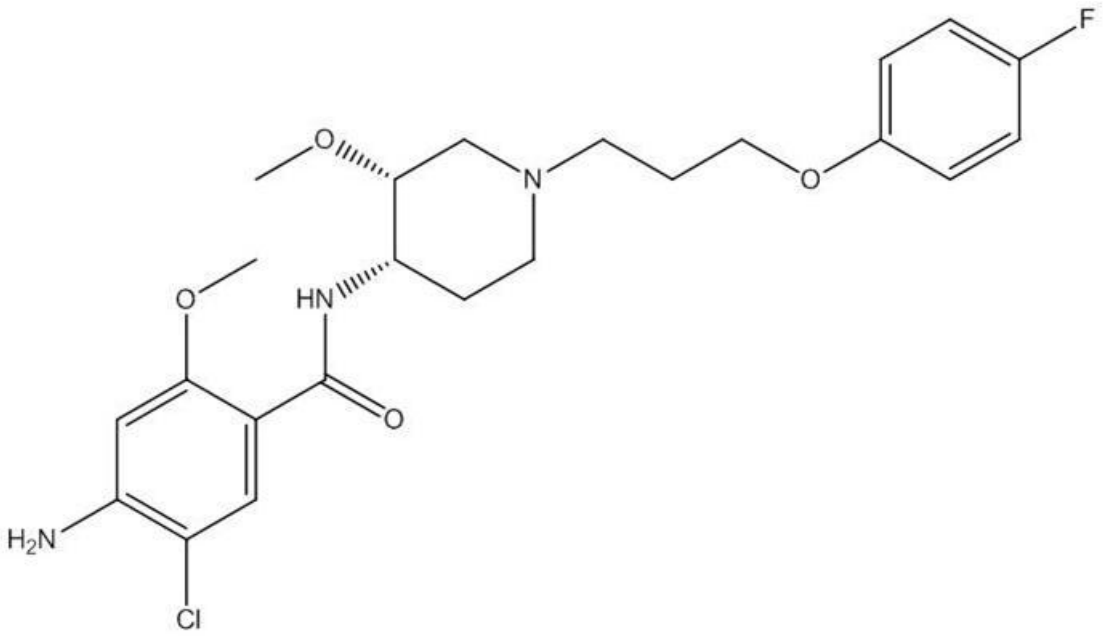

Figure 1.5: Chemical Structure of Cisapride

Clinically, cisapride is usually given orally but has also been administered intravenously, intramuscularly and rectally. It has been shown to be effective in treating gastro-oesophageal reflux diseases in adults, children and neonates, functional dyspepsia, and other disorders associated with impaired gastrointestinal motility. Cisapride was largely marketed under its trade name Propulsid or Prepulsid, in 1993 but it was withdrawn or had its indications limited because of reports of the side effect of long QT syndrome, which predisposes to arrhythmias such as *Torsades de pointe* (TdP). It was voluntarily removed in 2000 in the US following the FDA issuing a warning letter regarding this risk (Georgiadis et al., 2000).

1.8.1. Cisapride PK and Safety Information

The potential cardiac safety risk for cisapride was not identified until wider clinical trials which revealed a risk of TdP (Georgiadis et al., 2000) and subsequent post-market review (Wysowski et al., 2001). A systematic review of cardiovascular safety of $5HT_4$ agonists developed for gastrointestinal disorders revealed diverse chemical structures and selectivity as a route cause for potential hERG interactions (Tack et al., 2012).

Cisapride is one such example where it was demonstrated as a potent hERG channel blocker, 6-14 nM (Mohammad et al., 1997; Wang et al., 2003). Subsequently QT prolongation with cisapride has been characterised in a variety of in vitro and in vivo models (Carlsson et al., 1997; Sugiyama, 2008). The link between in vitro hERG (I_{Kr}) inhibition and in vivo QT were highlighted for cisapride in a benchmark safety review (Redfern et al., 2003).

Anaesthetised models have been used to assess the cardiovascular effects of cisapride using rats (Kii et al., 2001), guinea pigs (Kii et al., 2001; Testai et al., 2004; Hauser et al., 2005; Shiotani et al., 2005; Yao et al., 2008), rabbits (Carlsson et al., 1997; Wu et al., 2003), as well as conscious models in rabbits (Kijtawornrat et al., 2006b), cats (Kii et al., 2001) and monkeys (Ando et al., 2005). A variety of conscious and anaesthetised dog models have been assessed for the effects of QT prolongation (Webster et al., 2001; Al-Wabel, 2002; Toyoshima et al., 2005; Ollerstam et al., 2007) and attempts to link a translational gap (Chain et al., 2013).

Pharmacokinetics and tissue distribution studies have been described in the rat, rabbit and dog (Michiels, 1987), along with the excretion and biotransformation in dogs and humans (W, 1988). The absolute bioavailability and half-life ranged from 23% and 1-2h in the rat, with 53% and 4-10h in the rabbit and dog, and reported as 40-50% in man. The reported plasma protein binding is considered high at ~98% in man and 95% in dog (Limberis et al., 2007). Cisapride is primarily metabolised by P450 enzyme (3A4) in the liver to the N-dealkylated metabolite, norcisapride, which is renally and biliary excreted, with routes comparatively similar between species (W, 1988). This major metabolite has been shown to have some $1/6^{th}$ activity compared to the parent molecule (Gladziwa et al., 1991) and quantified in man (Cisternino et al., 1998). As such there is considered a potential for drug-drug interaction with other 3A4 metabolised co medications (Bedford and Rowbotham, 1996; Hennessy et al., 2008).

1.8.2. Cisapride Bioanalytical Background

In pharmaceutical preparations, numerous spectrophotometric methods have been reported by measuring the intrinsic fluorescence of cisapride. These methods are based on the fact that cisapride exhibits an emission spectrum with a maximum at a wavelength of 355.2 nm and excitation wavelength at 310 nm (Martin et al., 1994). Also described are extraction spectrophotometric methods using oxidative reactions, which are time consuming, with respect to processing and reconstitution of samples (Sastry et al., 1997; Hassan et al., 2001).

A simpler, faster and accurate method for determination of cisapride in pharmaceutical preparations using first- and second-derivative spectrophotometry with High Performance Liquid Chromatography (HPLC) has been reported (Argekar and Sawant, 1999; Hassan et al., 2001). These assays are typically used for quality control of commercial formulations and are still being applied (Shafi, 2011). These methods are not appropriate for drug concentrations over a dynamic range in vivo studies and biological matrices.

Several cisapride studies report analysis of biological samples such as plasma (Preechagoon and Charles, 1995; Campanero et al., 1998), serum (Lee et al., 1999) or animal tissues (Woestenborghs et al., 1988). For example, HPLC with UV detection and gas chromatography (GC) have been described (Woestenborghs et al., 1988), and initially over a relatively small range 10 to 150 ng/ml with an improved sample volume (150 µL) (Cisternino et al., 1998), and improved to 10 to 250 ng/mL for the simultaneous determination of cisapride and ranitidine in small volume paediatric plasma samples (Hare et al., 2004). A rapid and robust HPLC method utilizing fluorescence detection can provide relatively high sensitivity (Preechagoon and Charles, 1995) but also has disadvantages requiring a chemically synthetic internal standard (I.S.). For the quantitative analysis of cisapride in human plasma, more selective, sensitive and rapid procedure using reverse-phase HPLC technique, with fluorescence detection have been described with a range of 0.3 to 100 ng/mL using azelastine as an I.S. (Park et al., 2001), or a range of 5 to 200 ng/mL using a demethoxy analogue as an I.S. (Kiss et al., 2003) with 100 µL samples.

LC-MS/MS methods to determine the concentrations of cisapride have not been described. However, cisapride has been utilised as an internal reference standard in a number of studies (Lee et al., 2003; Ji et al., 2008; Lee et al., 2010).

1.9. Sparfloxacin

Sparfloxacin (RP 64206; AT-4140; cis-5-Amino-1-cyclopropyl-7-(3,5-dimethyl-1-piperazinyl)-6,8-difluoro-1,4-dihydro-4-oxo-3-quinolinecarboxylic acid; Figure 1.6) is an orally administered, synthetic, broad spectrum fluoroquinolone antibiotic that was discovered by Rhone Poulenc Rorer in 1990. It belongs to the class of organic compounds known as quinoline carboxylic acids, where the quinoline ring system is substituted by a carboxyl and fluorine group at one or more positions. Sparfloxacin is one of the 'fourth generation' fluroquinolones along with Levofloxacin and Grepafloxacin and was shown to be more potent than previous generations such as Ciprofloxacin (Andersson and MacGowan, 2003).

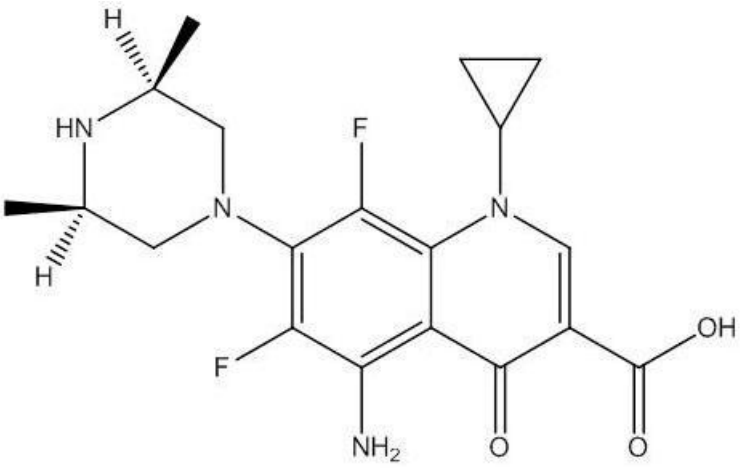

Figure 1.6: Chemical Structure of Sparfloxacin

Sparfloxacin, known as Zagam, is indicated for the treatment of community-acquired lower respiratory tract infections caused by bacterial infections. Sparfloxacin exerts its antibacterial activity by inhibiting bacterial enzymes topoisomerase II and topoisomerase IV (DNA gyrase). DNA gyrase is an essential enzyme which controls DNA topology and assists in DNA replication, repair, deactivation, and transcription in the bacterial growth cycle (Schentag, 2000).

It has better in vitro activity against both Gram-positive and Gram-negative bacteria than previously available quinolone antibiotics (Kojima et al., 1989; Nakamura et al., 1989). It is considered to have a controversial safety profile, including phototoxicity, CNS liabilities and potential serious adverse arrhythmias. Yet it was still marketed in 1995, to be later withdrawn in the US in 2000 and most markets by 2001 due to poor sales, although it is still available in Asia-Pacific.

1.9.1. Sparfloxacin PK and Safety Information

During preclinical development, sparfloxacin was noted to cause prolongation of QTc interval in dogs (Lipsky et al., 1999). This effect was confirmed in subsequent European and US Phase I and Phase II studies in human (Jaillon et al., 1996; Morganroth et al., 1999). Since, sparfloxacin has been shown to exert pure class III electrophysiological effects in rabbit Purkinje fibres (Adamantidis et al., 1998) and shown to correlate with other quinolone hERG / I_{Kr} activity (13-44 μM) with in vivo QTc prolongation, that might result in further arrhythmias in the presence of other predisposing factors to cause TdP (Anderson et al., 2001; Kang et al., 2001; Redfern et al., 2003). This includes anaesthetised models in guinea pigs (Yao et al., 2008; Park et al., 2013), sensitised-rabbits (Anderson et al., 2001; Akita et al., 2004; Chiba et al., 2004a; Chiba et al., 2004b) and dogs (Chiba et al., 2004a). This can explain the prolongation of QT interval observed clinically in some patients.

Pharmacokinetics, distribution and metabolism of sparfloxacin have been studied in a wide range of preclinical species from mice, rats, rabbits, dogs and monkeys (Nakamura et al., 1990; Matsunaga et al., 1991a; Matsunaga et al., 1991b; Yamaguchi et al., 1991; Naroa et al., 1992; Liu et al., 1998; Noh et al., 2010). Clinical assessment of human PK has been conducted in a number of trials (Shimada et al., 1993; Montay et al., 1994; Jaillon et al., 1996; Morganroth et al., 1999).

In man sparfloxacin is considered to be well absorbed following oral administration with an absolute oral bioavailability of 92%. Maximum concentrations in plasma are observed 3–5 h after oral administration (Schentag, 2000). Sparfloxacin shows a long elimination half-life of 16–20 h, moderate protein binding (45%), excellent tissue distribution, and effective penetration into extracellular fluids to allow a once-daily administration (Matsunaga et al., 1991b; Shimada et al., 1993). Primarily, sparfloxacin is hepatically metabolized by phase II glucuronidation to form a glucuronide conjugate. The only metabolite of sparfloxacin isolated in man is sparfloxacin glucuronide, which is excreted in urine by both glomerular filtration and tubular secretion (Montay et al., 1994). Unlike other fluoroquinolones, metabolism of sparfloxacin is not cytochrome P-450-dependent and will not result in any CYP mediated drug interactions (Mizuki et al., 1996). Instead, elimination of sparfloxacin is through a combination of renal, biliary, and trans-intestinal secretion (Schentag, 2000). It has been observed that plasma concentration-time profile decreases in a biphasic manner.

1.9.2. Sparfloxacin Analytical Background

Several analytical methods for sparfloxacin have been reported to date, including bioassay (Nakamura et al., 1990), high-performance thin-layer chromatography (Mody et al., 1998) and high-performance liquid chromatography with ultraviolet (Kamberi et al., 1999; Cho et al., 2006) or fluorescent detection (Borner et al., 1992).

Sparfloxacin has been quantitatively analysed in a range of preclinical biological samples such as plasma (Yamaguchi et al., 1991), serum and CSF (Naroa et al., 1992), vitreous humour (Liu et al., 1998) or animal tissues (Nakamura et al., 1990; Katoh and Kaneko, 1991). Radioactivity studies using ^{14}C and ^{3}H-labelled sparfloxacin (total and parent drug-related material) were conducted to identify plasma and tissue distribution information (Matsunaga et al., 1991a; Matsunaga et al., 1991b).

The initial bioassay was conducted using an agar well diffusion method with E.coli, and the measured inhibitory zone around a 60 µL sample well (plasma or tissue homogenate) and converted to concentrations against standard lines (Nakamura et al., 1990). A more specific bioanalytical assay was developed, for example, using reverse-phase HPLC with UV detection (240-280 nm) and fluorescence detector (280 nm, excitation emission 450 nm) and has been described with a range of 0.01 to 1.7 µg/mL in serum and detection limit of 0.005 µg/mL when using 1 mL of serum (Yamaguchi et al., 1991; Borner et al., 1992; Perkins et al., 1995). A more rapid and dynamic HPLC-UV assay with semi-automated solid phase-extraction method was applied to the clinical studies, using 0.5 mL sample, and range 25 to 2000 ng/mL in plasma and 500 to 10000 ng/mL in urine. The main metabolite, sparfloxacin glucuronide, was identified by alkaline hydrolysis of samples in relation to total sparfloxacin, as a metabolite reference standard was unavailable (Montay et al., 1994).

However, analytical methods using mass spectrometry for sparfloxacin quantification have been limited to animal tissue, such as chicken muscle and liver, and fish as part of a dietary assessment of quinolones in the food chain (Yue et al., 2007). Until more recently, a rapid and simple chromatographic method for the determination of sparfloxacin in rat plasma using liquid chromatography with tandem mass spectrometry (LC-MS/MS) has been described (Noh et al., 2010). This method, using 100 µL plasma, with a range of 10 to 1000 ng/mL was applied successfully to characterize the time course of plasma sparfloxacin concentrations following oral administration in rats and adapted in this thesis.

1.10. Moxifloxacin

Moxifloxacin is an 8-methoxyquinolone (BAY 12-8039; 1-cyclopropyl-7-[(S,S)-2,8-diaza-bicyclo-[4.3.0]non-8-yl]-6-fluoro-8-methoxy-4-oxo1, 4-dihydro-quinoline-3-carboxylic acid; Figure 1.7) belonging to the fourth-generation of synthetic fluoroquinolone antibacterial agents. It was developed by Bayer AG in 1989 and accepted onto the market as moxifloxacin-HCl in 1999. Similar to other fluoroquinolones of its generation, moxifloxacin shows potent antibacterial activity by inhibiting bacterial enzymes topoisomerase II and topoisomerase IV (DNA gyrase) both Gram-positive and Gram-negative bacteria (Lode and Schmidt-Ioanas, 2008).

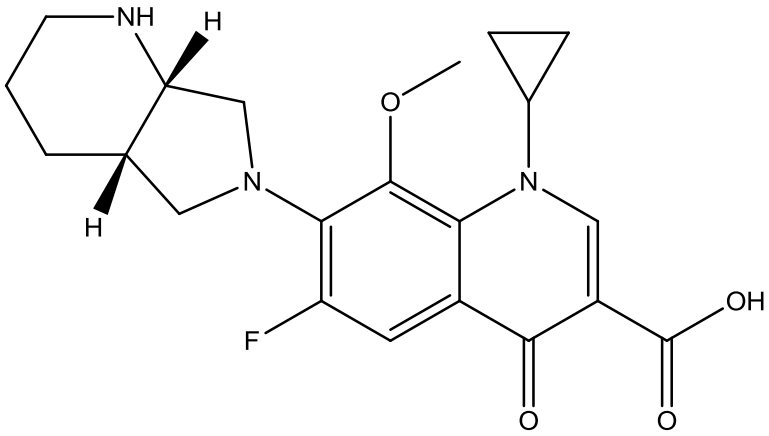

Figure 1.7: Chemical Structure of Moxifloxacin

It is marketed worldwide in conjunction with Merck (as the hydrochloride) in more than 80 countries under the brand names Avelox, Avalox, and Avelon for oral treatment of acute bacterial sinusitis, exacerbations of chronic bronchitis, community acquired pneumonia, complicated and uncomplicated skin infections, and complicated intra-abdominal infections. In most countries (but not EU), the drug is also available in parenteral form for intravenous infusion. Moxifloxacin is also sold in an ophthalmic solution (eye drops) as Vigamox, and Moxeza for the treatment of infections such as conjunctivitis (Keating and Scott, 2004). A review of the preclinical safety profile of moxifloxacin is considered more favourable in comparison to other fluorquinolones as it lacks phototoxicity and oculotoxicity, but still carries a risk of heptatotoxicity and cardiovascular liability (von Keutz and Schluter, 1999). According to the available case reports and clinical studies, moxifloxacin carries the greatest risk of QT prolongation from all quinolones (gemifloxacin, levofloxacin, ofloxacin and ciprofloxacin) still available in clinical practice and it should be used with caution in patients with predisposing factors for *Torsades de pointes* (TdP) (Briasoulis et al., 2011).

1.10.1. Moxifloxacin PK and Safety Information

Following previous fluoroquinolone antibacterial association with QT interval prolongation as a result of HERG/ I_{Kr} channel inhibition, moxifloxacin was similarly investigated (IC_{50} of 30-100 μM). It was identified that this is not a class effect of fluoroquinolones, but is highly dependent upon specific substitutions within this series of compounds (Kang et al., 2001).

Positive in vitro assessments were replicated in a variety of preclinical screening models detecting the drug-induced QT interval prolongation, showing a concordance of preclinical models in relation to clinical outcome with moxifloxacin (Chen et al., 2006), and within various dog models (Ollerstam et al., 2007). A sensitivity analysis of preclinical models revealed that isolated cardiomyocytes lacked the specificity to distinguish proarrhythmia (Nalos et al., 2012). Moxifloxacin induced QT prolongation and proarrhythmia has also been assessed in the anaesthetised sensitised-rabbit (Anderson et al., 2001), guinea pig (Yao et al., 2008; Marks et al., 2012), dog (Chiba et al., 2004a; Ollerstam et al., 2007), as well as telemetered dog (Sivarajah et al., 2010) and cynomolgus monkey (Watson et al., 2011).

As such, moxifloxacin, has been recommended as a positive control by regulatory authorities to evaluate the sensitivity of both clinical and preclinical studies to detect small but significant increases in QT interval measurements (Chen et al., 2005; Florian et al., 2011; Holzgrefe et al., 2014) with a tangible link between PK and QTc and inter-study variability (Chain et al., 2013; Parkinson et al., 2013; Gotta et al., 2015a).

Extensive PK and tissue distribution has been summarised in a variety of mammalian species (mice, rat, dogs, minipigs, monkey) and man (Siefert et al., 1999a; Siefert et al., 1999b) and additionally in rabbits (IV, IM, PO and SC) (Fernandez-Varon et al., 2005); (Carceles et al., 2006). Human PK and elimination after oral and IV administration has been determined (Stass and Kubitza, 1999) and absolute bioavailability given as 92% (Ballow et al., 1999), with maximum concentrations rapidly reached within 2 hours. Moxifloxacin shows a long elimination half-life of 12–16 h, moderate protein binding (~45%), with rapid and extensive tissue distribution into intra- and extracellular space to allow a once-daily administration (Siefert et al., 1999a; Siefert et al., 1999b). Moxifloxacin is primarily metabolized by phase II enzymes in the liver to form a glucuronide and N-sulfate conjugate. Both metabolites are observed in man and excreted via renal and biliary elimination (Moise et al., 2000). Neither renal nor hepatic impairment significantly affects the PK, and there are limited drug interactions in man (Stass and Kubitza, 2001).

1.10.2. Moxifloxacin Analytical Background

Moxifloxacin analysis was initially quantified using a bactericidal exclusion zone bioassay based on gel diffusion and compared to a reverse-phase HPLC separation assay with fluorescence detection (excitation 290 nm; emission at 500 nm) (Stass and Dalhoff, 1997). This has been applied to mammalian (mice, rat, dogs, minipigs, monkey and man) analysis using 0.2 mL sample and assay range 5 µg/mL to 1000 µg/mL (Siefert et al., 1999a; Siefert et al., 1999b).

Many HPLC chromatographic methods have been reported with UV and fluorescence detection biological fluids (plasma, urine and saliva) (Fernandez-Varon et al., 2005; Chan et al., 2006; Xu et al., 2010; Raju et al., 2012). Most of the modified methods involve the more sensitive fluorescence detector with unique requirements, such as special analytical columns with direct injection of plasma (Laban-Djurdjeviç et al., 2006), a gradient elution program with ion pairing agents (Nguyen et al., 2004) and tedious time and sample consuming liquid–liquid extraction (Srinivas et al., 2008).

Tissue distribution of moxifloxacin was investigated using radioalbelled [^{14}C]-BAY 12-8039 in a whole-body autoradioagraphy study as a qualitative assessment (Siefert et al., 1999b). Quantitative analysis of rat tissues (lung, muscle, fat and bone) was conducted by homogenisation with an assay range of 50 to 2000 ng/mL (Beckmann et al., 2007).

New, accurate, sensitive and reliable kinetic spectrophotometric methods are continuing to be developed, for assays in pharmaceutical tablet formulations, via oxidative coupling to measure the coloured product formed (Ashour and Bayram, 2015). Advances have also been made through chemiluminescence determination of moxifloxacin in pharmaceutical and biological samples based on its enhancing effect of the luminol-ferricyanide system using a microfluidic chip to determine concentrations from 0.14 to 55.0 ng/mL (Suh et al., 2014). However, analytical methods using industry standard LC-MS/MS methodology have somewhat been limited since the first report for human plasma (Vishwanathan et al., 2002). Currently, many preclinical and clinical studies with moxifloxacin are on-going in Asia-pacific as part of research into first-line therapy treatment of pulmonary Tuberculosis (Burman et al., 2006). As such, more sensitive and dynamic methods have recently been developed from 0.1 to 50 µg/mL (Wang et al., 2014) and 10 to 6000 ng/mL using rat plasma (Raju et al., 2012), or detection of the N-sulfate metabolite, 2 to 200 ng/mL, (Li et al., 2015) for application to pharmacokinetic studies.

1.11. Verapamil

Verapamil is a phenylalkylamine (enzeneacetronitrile, α[3-[[2-(3,4-dimethoxyphenyl) ethyl]methylamino]propyl]-3,4- dimethoxy-α-(1-methylethyl)) (Figure 1.8) voltage-dependent L-type calcium channel blocker belonging to the Class IV anti-arrhythmic drugs used extensively in the treatment of a wide range of cardiovascular disorders (Hamann et al., 1984).

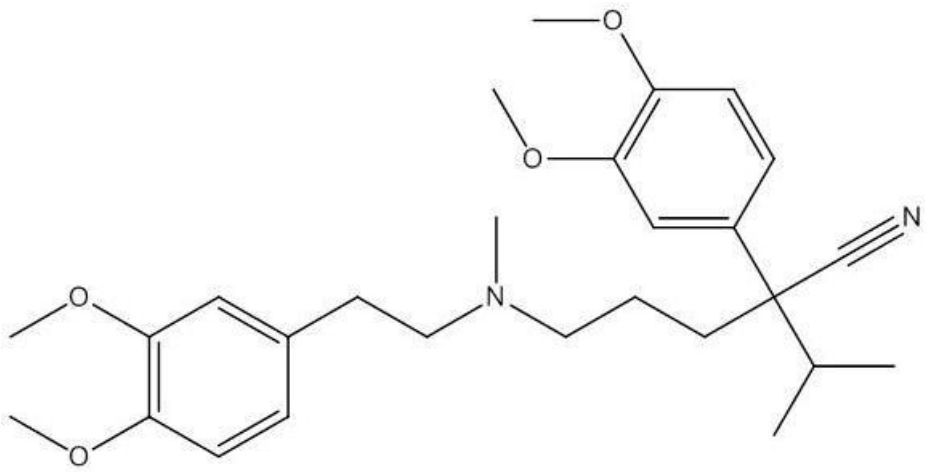

Figure 1.8: Chemical Structure of Verapamil

Verapamil hydrochloride was approved for medical use in the United States in 1981 from Genpharm Inc., a subsidiary of Merck, having been initially discovered in 1962 as Iproveratril. Today, it is marketed by many generic companies, such as Glenmark Generics, under various brand names Calan, Isoptin, Verelan and Covera with extended release formulations.

Its effects on cardiac and endothelial cells result in a relaxation of arterial smooth muscle and a decrease in cardiac contractility. Given these actions, verapamil is utilized therapeutically to treat most notably angina pectoris, essential hypertension, and cardiac arrhythmias. In general it is better tolerated than nitrates and beta blockers (Xiong and Sperelakis, 1995). Verapamil along with diltiazem, both non-dihydropyridones, and short-acting dihydropyridones such as nifedipine and amlodipine have been the most widely prescribed and important agents for hypertension (Opie et al., 2000; Basile, 2004).

1.11.1. PK and Safety Information

The safety record of verapamil is considered comparable to beta-blockers (Opie et al., 2000) and a close relationship between verapamil plasma concentration and effect on P-R interval has been established both after single IV and oral administration. Verapamil exists as a racemic isomer mixture of d- and dl-verapamil and has been shown that the dl—verapamil has a greater pharmacodynamic effect pre-clinically and clinically (Eichelbaum et al., 1980; Giacomini et al., 1985) and appears to have a slight preferential clearance which explains a greater plasma concentration required following oral administration (Eichelbaum et al., 1984). Studies have shown the potent anti-arrhythmic effects of verapamil from isolated tissue preparations to anaesthetised and conscious in vivo experiments (Yamaguchi et al., 1978). The class IV calcium channel blocker prevents sino-atrial node conduction (PR interval), reducing the contraction force and thus pressure (pulse or ventricle) as shown by the conscious rat model (Adeyemi et al., 2009) and does have hERG inhibition (1 μM).

Verapamil pharmacokinetics have been investigated in a number of preclinical species such as rat (Todd and Abernethy, 1987; Kataoka et al., 2016); dog (Chelly et al., 1986; Bai et al., 1993); rabbit (Giacomini et al., 1985; Mori et al., 2001) and man (Hamann et al., 1984), including metabolism in vitro (Kantharaj et al., 2003) and radiolabelled metabolism (McIlhenny, 1971; Eichelbaum et al., 1979). Verapamil has been shown to be more than 90% absorbed, but due to extensive first-pass metabolism, bioavailability is much lower (10–35%). It is ~90% bound to plasma proteins and has a volume of distribution of 3–5 L/kg. It takes 1 to 2 hours to reach peak plasma concentration after oral administration. Concentrations of verapamil (ranging from 50 to 250ng/mL) appear to correlate well with cardiac response, and are frequently monitored to ensure optimal concentrations are achieved to assess the potential toxic side effects. There is a nonlinear dependence between plasma concentration and dosage, with a half-life of 5–12 hours (Eichelbaum et al., 1984; Hamann et al., 1984; Manitpisitkul and Chiou, 1993). Verapamil is metabolized by CYP3A4 in the liver primarily by *N*-demethylation to an active metabolite, norverapamil and at least 12 inactive metabolites. Norverapamil retains 20% of the vasodilating activity of the parent drug and is usually found in similar concentrations to the parent drug after steady state is reached, with a known half life (~10 hr). As its metabolites, 70% is excreted in the urine and 16% in faeces; 3–4% is excreted unchanged in urine. Therefore, decreased clearance, and increased bioavailability, volume of distribution and half-life may be observed in patients with severe hepatic dysfunction (Eichelbaum et al., 1979; Pauli-Magnus et al., 2000).

1.11.2. Verapamil Bioanalytical Background

There is no immunoassay for therapeutic drug monitoring of verapamil, but both verapamil and its active metabolite norverapamil can be measured in serum or plasma using either gas chromatography or high-performance liquid chromatography. Initially, verapamil concentrations were measured in blood, urine, or tissue homogenates fluorometrically in the 0.1-10-ug/ml range (McAllister and Howell, 1976). This is a common approach adopted for quantification of verapamil in tablet formulations utilising the excitation bands 230 and 280nm, emission band at 312nm and between 609 and 615nm (Esteves da Silva et al., 2002).

The primary bioanalytical methods of verapamil describe the rapid chromatographic separation for the measurement of verapamil and its major metabolite norverapamil in biological matrices in the 1980's where fluorescence detection was made at 203nm (Cole et al., 1981; Watson and Kapur, 1981). Other methodologies describe the use of gas chromatography as an alternative assay but narrow analytical range of 5-30 ng/mL (Hege, 1979). This range later increased to 1 – 500 ng/mL as part of a comparison with high pressure liquid chromatography (Abernethy et al., 1984; Hynning et al., 1988). HPLC methods have been applied to plasma and tissue quantification in rats (Hanada et al., 1998). As part of understanding the tissue distribution of verapamil and influence of P-gp, radioligand binding assays have been developed and quantitative PET (Döppenschmitt et al., 1999; Bart et al., 2003).

As liquid chromatography improved numerous methods of bioanalysis are described in conjunction with mass spectrometry to provide simultaneous quantification and accurate measurement without potential fluorescent interference of endogenous materials or metabolites (von Richter et al., 2000; Hedeland et al., 2004; Singhal et al., 2012). Ultra-performance liquid chromatography (UPLC) resolution for quantification and identification of verapamil and its metabolites provided further benefit for in vitro metabolite and pharmacokinetic studies (Kantharaj et al., 2003; Pedraglio et al., 2007). Chytil et al. describe how this simple and rapid sample analysis methodology approach enabled the monitoring of patient non-compliance (Chytil et al., 2010). The combined use of radiolabel and accelerated mass spectrometry (AMS) were used to define low level dose human intravenous pharmacokinetics along with oral dosing as part of a microtracer study (Simpson et al., 2010). A similar bioanalytical method employed in this thesis was used to investigate verapamil drug-drug interactions induced by a CYP inhibitor in rodents (Kataoka et al., 2016).

1.12. Aims and Objectives

The aim of this project was to determine whether data obtained from early non-clinical cardiovascular safety screening models could be utilised towards a prospective predictive PBPK model of in vivo rabbit QTc prolongation.

The objectives were:

Obtain protein binding in plasma, blood and heart tissue and blood:plasma ratios for cisapride, sparfloxacin, moxifloxacin and verapamil across a range of species using one single methodology, RED device, to enable comparison. Protein binding values enable the free drug concentrations to be determined to interpret the drug concentration-time profiles and the pharmacological QTc response to be used in a PBPK model.

Develop suitable quantitative bioanalytical LC-MS/MS assays for cisapride, sparfloxacin, moxifloxacin and verapamil to support the protein binding studies to provide peak-area ratios for calculations and concentration-time course data for rat and rabbit studies.

Obtain and interpret QT prolongation information from the cardiovascular screening study using the ex vivo isolated rabbit left ventricular wedge (RVW) preparation for cisapride, sparfloxacin, moxifloxacin and verapamil to form a concentration-response model.

Develop an in vivo anaesthetised rabbit QTc model to investigate the effects of cisapride, sparfloxacin, moxifloxacin and verapamil on QT prolongation relative to plasma and heart tissue concentrations data.

Integrate physiological and physicochemical determinants for cisapride, sparfloxacin, moxifloxacin and verapamil incorporating the data generated from this thesis to develop towards translational in vivo rabbit QTc in a PBPK/PD model.

Strathclyde Institute of Pharmacy and Biomedical Sciences
GlaxoSmithKline

CHAPTER 2

Protein Binding and Blood Partitioning

2. IN VITRO PROTEIN BINDING & PARTITIONING

Many drugs bind with varying degrees of association to plasma proteins. Plasma protein binding (PPB) is the reversible association of a drug with the proteins of the plasma due to hydrophobic and electrostatic interactions such as van der Waals and hydrogen bonding. The bound drug exists in equilibrium with the free drug. The extent of protein binding and its reversible interaction can greatly influence the pharmacokinetic properties as well as the pharmacological effect of the drug. It is an important parameter used in many in vivo modelling calculations to estimate the volume of distribution, organ clearance, and for scale-up of pharmacokinetic and pharmacodynamic parameters from animal models to humans (Benet and Hoener, 2002; De Buck et al., 2007b). The significance of PPB in pharmacokinetics and pharmacodynamics is therefore of paramount importance in the characterisation of drugs in the assessment of human risk (Schmidt et al., 2010). The convergence of several trends in the pharmaceutical industry including high speed chemical synthesis technologies, the increasing use of in silico ADME modelling together with early in vivo evaluations of lead compounds has increased the demand for protein binding determinations (Kariv et al., 2001). However it is often difficult to obtain PPB values from literature reviews or product/prescribing information data sheets, and tissue binding is often not considered. It is also often unclear what protein binding (PB) technique has been used to make the assessment or whether species differences in PB have been considered. In addition blood:plasma ratios are another important parameter scarcely reported but used in modelling.

Therefore the aim of this investigation was to determine the PB of cisapride, moxifloxacin, sparfloxacin and verapamil using a single technique, the rapid equilibrium dialysis (RED) device in a 96-well format, across a range of species in plasma, blood and heart tissue homogenate. Sotalol and quinidine were also included in this analysis as these compounds demonstrate concentration-dependent protein binding to act as a positive control. Blood:plasma partitioning (ratio) was also evaluated to enable the inter-conversion of plasma or blood concentration time profiles along with the fraction unbound in each matrix, and be used in determination of in silico tissue partitioning coefficients (Kp) for modelling.

This work enables direct comparison of the rabbit protein binding and blood:plasma parameters to other species. It allows interpretation of concentration-time profiles in the rat and rabbit, and gives heart tissue exposure relative to pharmacological QT changes to develop towards translational PBPK/PD modelling in the rabbit.

2.1. Background Protein Binding by Equilibrium Dialysis

Initially, protein binding by equilibrium dialysis (ED) was first described by Davis in 1943 through the binding of sulphonamide drugs to plasma proteins. It was further developed by Klotz et al. using 'visking tubing' filled with albumin solution, in a beaker containing the dialysis medium (Klotz and Walker, 1947; Klotz and Urquhart, 1949; Rowland, 1980). This technique used to require large volumes of plasma/protein solution/buffer media and the 'visking' was prone to damage, but it remained largely unchanged until early 2000. Volumes were reduced through the use of 'Teflon' cells that became available using a clamped manifold. ED is regarded as the gold standard to determine PPB, which has served as a reference technique against other methods (ML et al., 2010; Bohnert and Gan, 2013). Originally, ED was known to be slow and laborious, but there are at least three different commercially available 96-well plates for ED, which makes the technique more convenient for early discovery higher throughput. In 2001, the ED PB method was transformed as devices based on a 96-well format were developed to enhance the throughput and became commercially available (Equilibrium Dialyzer-96 from Harvard Biosciences (Holliston, MA, USA), Rapid Equilibrium Device from Thermo Scientific/ Pierce (Rockford, IL, USA), Micro Equilibrium Dialysis Device from HT dialysis LLC (Gales Ferry, CT, USA)) (Banker et al., 2003). The Rapid Equilibrium Dialysis (RED) device has been developed for increased productivity and versatility (Waters et al., 2008).

The biggest advantage with ED is that non-specific adsorption (NSA) is believed to not affect the unbound fraction; a new equilibrium will be established although at a lower concentration than intended. A disadvantage is that at equilibrium the concentration is lower than the initial concentration as a part of the compound is now in the buffer chamber. There is also a small osmotic volume shift that occurs due to the protein in the plasma compartment becoming diluted with buffer and the volume on the buffer side of the semi-permeable membrane decreases (Tozer et al., 1983). One way to adjust for this is through the addition of 5% dextran to the buffer side (Kariv et al., 2001) or an adjustment of buffer compartment volumes to maintain membrane levels. It is believed that omotic shift has little effect on ED over a short period of time (Zhang et al., 2012; Nilsson, 2013).

Plasma or blood protein binding is the primary matrix for the assessment of protein binding such that circulating free unbound concentrations can be determined and correlated to pharmacologic effect. In vitro techniques allow measurement of drug binding to a particular

organ yet extrapolation to the whole body is difficult (Nilsson, 2013). Several techniques are available, such as isolated organ perfusion models, tissue slices, isolated cells, homogenates and subcellular particles. Tissue protein binding using homogenates in the RED device have been conducted and dilution factor taken into account, in a similar fashion for brain protein binding (Kalvass and Maurer, 2002; Summerfield et al., 2006; Kalvass et al., 2007; Summerfield et al., 2008). Each technique suits a particular problem but they are neither equivalent nor interchangeable, and each has advantages and disadvantages (Pacifici and Viani, 1992; Mariappan et al., 2013).

2.2. In Vitro Source of Biological Matrices

Control blank blood and plasma were ethically sourced from approved vendors and heart tissue from within GlaxoSmithKline (GSK), all in accordance with GSK's policy on the Care, Welfare and Treatment of laboratory animals in the UK and in accordance with the Animals (Scientific Procedures) Act, 1986.

Human biological samples (blood) were sourced ethically and their research was conducted in accordance with the terms of the informed consent. The relevant processes for collecting, obtaining, using, storing, transferring, tracking and disposing of human biological samples were in accordance with GSK's SOP (POL-GSKF-401) and the Human Tissue Act, 2004.

2.2.1. Blood

Fresh naïve control blood was obtained from Harlan Sera Labs, UK for male rats (Han Wistar), female guinea pigs (Dunkin-Harltey), female rabbits (New Zealand White, NZW), and male dogs (Beagle Marshall). Blood was pooled from at least three different animals. Human blood was obtained from at least three healthy male volunteers (GSK volunteers). EDTA was used as the anti-coagulant for all species. All blood was stored at $+4^0$ C and used as fresh as possible.

2.2.2. Plasma

Frozen naïve control plasma from male rats (Han Wistar), female guinea pigs (Dunkin-Harltey), female rabbits (New Zealand White, NZW), male dogs (Beagle Marshall), and pooled human plasma was obtained from B&K Universal, UK, for all species. EDTA was used as the anti-coagulant for all species. All plasma was allowed to defrost at room temperature unassisted.

2.2.3. Heart

Control heart tissue was obtained from male rats (Han Wistar), female rabbits (New Zealand White) and male dogs (Beagle Marshall) from naïve (control/sentinel) animals within GSK. Heart tissue was prepared as a homogenate following sectioning of the tissue using a cryostat microtome to generate very thin slices of tissue, which were weighed, collected and diluted with 5 volumes of physiological buffered saline (PBS), that easily formed a consistent pipettable homogenate on vortex mixing, suitable for use in a 96-well RED device.

2.3. Experimental RED Protein Binding Method

Protein binding of cisapride, moxifloxacin, sparfloxacin, verapamil, sotalol and quinidine was determined in vitro in the rat, guinea pig, rabbit, dog, and human by equilibrium dialysis using the Rapid Equilibrium Dialysis (RED) device. Stock working solutions were prepared for each compound at either 1 or 10 mg/mL in DMSO and subsequently diluted further with 50:50 acetontrile:water. Compounds were spiked into the matrix of interest (blood, plasma or heart tissue homogenate) from each species, where relevant, at target concentrations at approximate human therapeutic C_{max} and 10-fold orders of magnitude above/below or more as appropriate, such that the amount of organic solvent present was <1%. Each spiked matrix was mixed gently for at least 30 minutes at 37ºC prior to use. Three aliquots (300 µL) of each spiked matrix sample was dialysed against PBS (500 µL, isotonic phosphate buffered saline, pH7.4) at 37°C using a RED device with the two halves of each dialysis well separated by a dialysis membrane (molecular weight cut-off 8,000 Daltons). The dialysis was stopped at 4 hours when equilibrium was assumed to have been achieved, based on historical experience and standard protocol procedures. Aliquots of dialysed buffer and matrix (blood, plasma or heart tissue homogenate) from each well were taken and matrix-matched.

Protein binding was calculated by Equation 1.

$$\text{Protein Binding \%} = \frac{(\text{Peak Area ratio of Matrix} - \text{Peak Area ratio of Buffer})}{\text{Peak Area ratio of Matrix}} \times 100 \qquad \text{Equation 1}$$

For tissue protein binding, the peak area in the buffer to that in the heart tissue homogenate requires correction for dilution factor according to Equation 2 (Kalvass and Maurer, 2002).

$$Undiluted\ f_{ut} = \frac{(1/D)}{\left(\left(\frac{1}{f_{ut,apparent}}\right) - 1\right) + 1/D} \qquad \text{Equation 2}$$

2.4. Experimental Blood:Plasma Partitioning Method

The in vitro evaluation of blood:plasma partitioning was assessed using fresh control blood obtained from Harlan sera labs, UK for rat (pooled Han Wistar), female guinea pig (Dunkin-Hartley), female rabbit (NZW), dog (pooled Beagle). Human blood was obtained from three individual healthy male volunteers (GSK volunteers).

Briefly, fresh whole blood was pre-incubated at 37ºC for at least 5 minutes prior to use. Using stock solution of each test compound prepared in DMSO, compounds were spiked (n=3) into blood in 1.2 mL polypropylene alpha-numeric matrix tubes, at a ratio of 1:100 (v/v) such that the amount of organic solvent was <1%, to give a nominal 1 µg/ml final concentration and mixed by gentle inversion. Prepared blood standards were placed on a plate shaker for incubation at 37°C for 120 minutes. Following incubation, triplicate aliquots were taken for analysis (sample A). The remaining blood was centrifuged at 1,800 g (4000 rpm) for 15 minutes at 4°C to obtain plasma. With sufficient residual plasma available, duplicate aliquots for rat, dog, rabbit and guinea pig, and triplicate aliquots for human were taken for analysis (sample B).

Blood:plasma (Cb/Cp) ratio was by Equation 3.

$$\text{Blood: Plasma} = \frac{C_b}{C_p} \qquad \text{Equation 3}$$

Where,

C_b = concentration in blood (Peak area of analyte/peak area of internal standard) sample A;
C_p = concentration in plasma (Peak area of analyte/peak area of internal standard) sample B.

2.4.1. Bioanalysis of Protein Binding and Blood:plasma

All samples for bioanalysis were stored at -20ºC prior to determination of each respective compound in plasma, blood, heart tissue homogenate and PBS buffer from each species.

All protein binding samples (plasma, blood and heart homogenate) from both the incubated spiked matrix and PBS buffer were matrix-matched with blank dialysed plasma, blood, heart or PBS accordingly. This enabled a direct comparison to be made by determination of each respective compound from buffer and matrix dialysis compartments by peak-area ratio.

The amount (peak-area ratio) of each compound was determined from triplicate aliquots by appropriate LC-MS/MS analysis (Appendix 1). The original spiked (non-dialysed) sample was also analysed as a time zero stability control reference sample.

2.4.2. Statistical Analysis

All protein binding values have been assessed against rabbit as the comparator species and the effect of concentration was also considered, separately.

The data were analysed using a 2-way ANOVA approach, with Concentration and Species as treatment factors, by a Single Measures Parametric Analysis module using In Vivo Stat software. This was followed by planned comparisons of the predicted means to compare the levels of the Concentration * Species interaction using an all pair-wise comparison analysis without adjustment for multiplicity (LSD test). The response was Arcsine transformed prior to analysis to stabilise the variance.

Using an External Studentised residuals plot against predicted values, observations with a residual less than -3 or greater than 3 (SD) were considered as possible outliers and removed from the data set. The 2-way ANOVA approach was then repeated with the pair-wise comparison. The appropriate unadjusted p-values were selected and adjusted post-hoc using Bonferroni's multiple comparison procedure to remove the likelihood of false positives and identify statistical significance.

2.5. Protein Binding Results and Discussion

Protein binding was determined for cisapride, sparfloxacin, moxifloxacin, verapamil, sotalol and quinidine across a range of species (rat, dog, guinea pig and human) to compare against the rabbit. Blood to plasma ratios were also experimentally determined.

2.5.1. Cisapride Protein Binding Results and Discussion

Protein binding of cisapride was investigated at a range of concentrations, 100 ng/mL (low), 1,000 ng/mL (medium) and 10,000 ng/mL (high), representing parity, 10x and 100x above approximate clinical therapeutic concentration with respect to human plasma. Results have been represented graphically as box plots across species (rat, dog, rabbit, guinea pig and human) in plasma (A), blood (B) and heart tissue homogenate (C) (Section 2.5.2). Corresponding tabulated data of cisapride protein binding mean values (n=6 replicates) are given for plasma (A), blood (B) and heart homogenate (C), including overall mean and ±SEM, as well as blood:plasma ratios in Appendix 2.

2.5.1.1. Cisapride: Plasma Protein Binding Results

Plasma protein binding values experimentally derived from this study for rabbit were 96.9% ±0.169, 96.9% ±0.200, and 97.2% ±0.549, for low, medium and high concentrations, respectively. The overall mean for the rabbit was 98% and was shown not to be different to guinea-pig or dog at 98.0%, with the exception of dog plasma protein binding investigated at the low concentration (91.1% ±1.33, *p*-value <0.01). This group had significantly lower PB binding values, which appears not to be related to a concentration-dependent change but may be a result of experimental error in the wells investigated as shown by the greater variability in comparison across each group. Given the reproducibility across the other species including dog medium (98.2% ±0.20) and high (98.2% ±0.056) concentrations, a further repeat experiment in the dog at a low concentration would be required to confirm this group anomaly. Data from the plasma PB results for rat and human indicate that there was a significant difference compared to rabbit with rat low, 96.9% ±0.122 (*p*-value <0.01) and medium, 96.9% ±0.082 (*p*-value <0.05) were both lower than rabbit, and with human medium, 99.3% ±0.061 (*p*-value <0.01) and high, 98.7% ±0.117 (p-value <0.05), were both higher than rabbit. This observation has been highlighted as a result of the very reproducible results and low replicate variations (n=6) for each species in this experimental instance. The data for each species shows that there is no concentration dependent change in protein binding in any species or matrix (Figure 2.1A and Table 2.3A).

Plasma protein binding of cisapride was available from reported literature and regulatory documentation for rat, dog and human, as well as in silico. In this study, the overall mean plasma PB for rat, was 97.0%, which is higher than in comparison to literature for rat, 91.6% (Michiels, 1987), 69.2 to 94.4% for single and repeat dose radiolabelled [^{14}C]-cisapride (FDA approval package, p.28) and 84.2% from in silico software (Adamantis ACD).

In the dog, the overall mean was 95.8% binding derived experimentally which was in agreement with 95% binding reported (Michiels, 1987; W, 1988; Veereman-Wauters et al., 1991). The calculated human protein binding was determined as 98.5% for the overall mean, and the observed low concentration values determined (97.5%±0.419), were close or equivalent to the literature quoted values 97.5% from in vitro (Michiels, 1987; Hardman and Limbird, 2011) and 98% (McCallum et al., 1988; Redfern et al., 2003; Gertz et al., 2010). Ex vivo PB values from human samples have been reported to be lower at 88% (W, 1988) and 96-97% (FDA approval package p.32), respectively, and similarly for in silico predictions 90.4% (Adamantis ACD) and 91.6% (De Buck et al., 2007b).

Table 2.1 Referenced Cisapride Plasma Protein Binding Information

Species	PPB (%)	Fu_p	Reference
Rat (in silico)	84.2	0.158	Adamantis ACD software
Rats (in vitro)	91.6	0.084	Michiels et al. 1987
Rats (Single & repeat [^{14}C])	69.2 to 92.1 77.0 to 94.4	0.079 to 0.308 and 0.056 to 0.23	FDA Approval Package pg 28
Dog (in vitro)	95	0.05	Michiels et al. 1987
Dog	95	0.05	Veereman-Wauter et al. 1991
Human (in silico)	90.4; 91.6	0.084	Adamantis ACD software; De Buck et al. 2007
Human (in vitro)	97.5	0.025	Michiels et al. 1987
Human (ex vivo)	88	0.12	Meuldermans et al. 1988
Human (10; 20; 40mg)	96.8; 96.4; 96.1	0.0325; 0.036; 0.0395	FDA Approval Package pg 32
Human	97.5	0.025	Hardman and Limbird 2011
Human	98	0.02	McCallum et al. ; Redfern et al. 2003; Gertz et al.2010

PPB (Plasma Protein Binding); Fup (Fraction unbound plasma)

Overall the plasma protein binding values for cisapride are comparable to literature where appropriate comparisons can be made and give confidence in the derived values for rabbit and guinea-pig which do not have literature references. With the observed statistical

difference compared to rat and human the translation across species needs to be appreciated with respect to the free fraction and noted in physiological modelling.

2.5.1.2. Cisapride: Blood Protein Binding Results

Blood protein binding values across all species and most concentrations was deemed to be significantly different (p-value < 0.01) compared to rabbit, with 89.9% ±0.439, 88.9% ±0.324 and 87.3% ±0.171 at low, medium and high concentrations, and with an overall mean PB at 88.7%. The rat (medium, 91.4% ±0.452 and high, 91.8% ±0.429), all dog (96.7% ±0.251; 96.8% ±0.285; and 95.3% ±0.318) and all human (95.7% ±0.276; 94.9% ±0.211; 93.9% ±0.249) blood protein binding values were observed to be notably higher than rabbit at low, medium and high concentrations, respectively. The guinea-pig (medium, 86.3% ±0.511, and high, 81.6% ±0.442) were observed to be notably lower than rabbit. The exceptions were rat (90.4% ±0.976) and guinea-pig (88.1 ±0.439) blood binding at low concentrations, which were comparable to rabbit. Variability across replicates was increased in blood binding and the protein binding values were consistently lower in blood compared to plasma and consistent across concentrations within species.

The blood:plasma ratios determined showed minor differences across each species, with values which were generally less than 1, except for rat which was 1.08 ±0.08, indicating that cisapride does not have a preferential distribution into the erythrocyte cellular fraction. Values experimentally determined in this study were similar to those in the literature, where available. Rat B:P reported here was approximately 1.1, as identified by Michiels et al (1987) and Meulderman et al (1988), and dog B:P was determined to be 0.72 ±0.05 compared to 0.66 (W, 1988). Human B:P was experimentally calculated as 0.81 ±0.05 and in silico has been estimated to be 1.1 (De Buck et al., 2007a; De Buck et al., 2007b); and in vitro stated as 1 (Gertz et al., 2010) to 0.64 ex vivo (W, 1988).

Table 2.2 Referenced Cisapride Blood:Plasma Ratio Information

Species	Blood:Plasma ratio (B:P)	Reference
Rat (^{14}C)	1.1 – 1.2	Michiels et al. 1987
Rat	1.11	Meuldermans et al. 1988
Dog	0.657	Meuldermans et al. 1988
Human	0.644	Meuldermans et al. 1988
Human (in silico)	1.11	De Buck et al. 2007
Human	1.0	Gertz et al. 2010

2.5.1.3. Cisapride: Heart Protein Binding Results

Cisapride protein binding values in heart tissue have been determined in the rat, dog and rabbit. The mean values at low, medium and high concentrations investigated were 98.2% ±0.323, 98.8% ±0.142, 98.7% ±0.134 for the rat; 98.9% ±0.048, 98.8% ±0.070, 98.7% ±0.136 for the dog; in comparison to 98.8% ±0.184, 99.2% ±0.307, 99.0% ±0.210 for rabbit. These results show no statistical difference (*p*-value >0.05) compared to rabbit, and overall mean 99.0% for the rabbit was similar to rat (overall mean 98.6%) and dog (overall mean 98.7%).

2.5.2. Cisapride Protein Binding Data

Figure: 2.1A

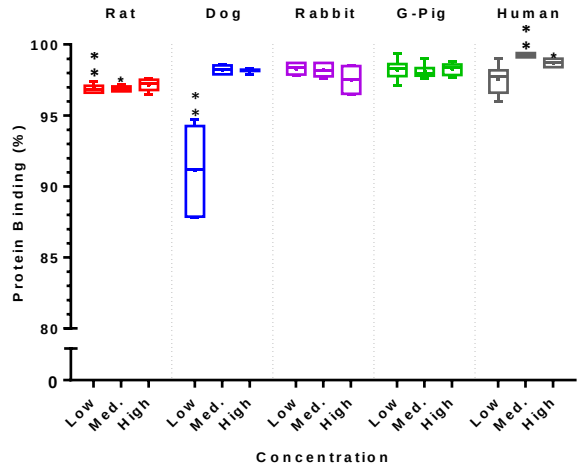

Figure: 2.1B

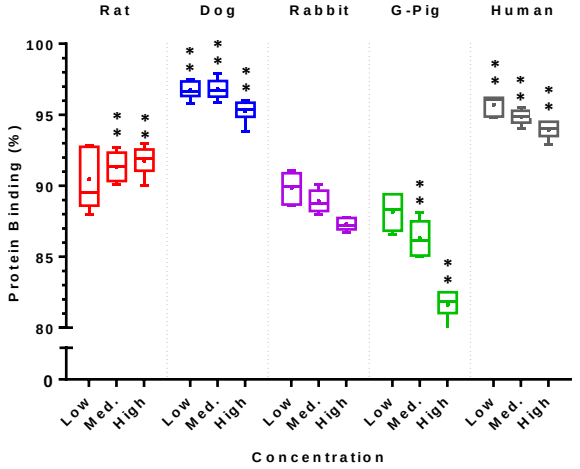

Figure: 2.1C

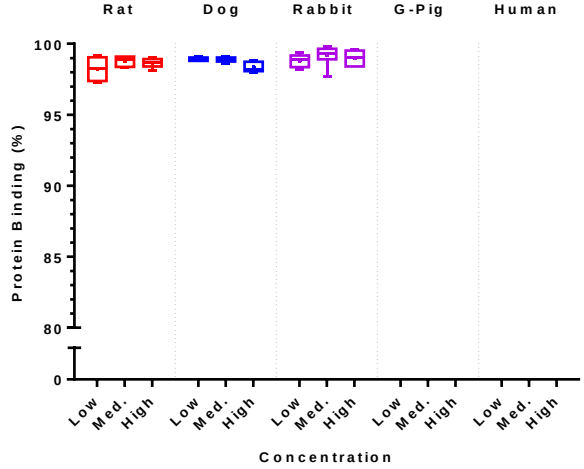

Table: 2.3A

Protein Binding (PB)	Mean Plasma				
	Rat	**Dog**	**Rabbit**	**G Pig**	**Human**
Low	96.9** ±0.122	91.1** ±1.33	98.3 ±0.169	98.2 ±0.170	97.5 ±0.419
Medium	96.9* ±0.082	98.2 ±0.120	98.2 ±0.200	98.1 ±0.126	99.3** ±0.061
High	97.2 ±0.178	98.2 ±0.056	97.5 ±0.549	98.3 ±0.114	98.7* ±0.117
Overall Mean	**97.0**	**95.8**	**98.0**	**98.2**	**98.5**

Table: 2.3B

Protein Binding (PB)	Mean Blood				
	Rat	**Dog**	**Rabbit**	**G Pig**	**Human**
Low	90.4 ±0.976	96.7** ±0.251	89.9 ±0.439	88.1 ±0.488	95.7** ±0.276
Medium	91.4** ±0.452	96.8** ±0.285	88.9 ±0.324	86.3** ±0.511	94.9** ±0.211
High	91.8** ±0.429	95.3** ±0.318	87.3 ±0.171	81.6** ±0.442	93.9** ±0.249
Overall Mean	**91.2**	**96.3**	**88.7**	**85.4**	**94.8**
B:P	**1.08** ±0.08	**0.72** ±0.05	**0.91** ±0.01	**0.87** ±0.06	**0.81** ±0.05

Table: 2.3C

Protein Binding (PB)	Mean Heart				
	Rat	**Dog**	**Rabbit**	**G Pig**	**Human**
Low	98.2 ±0.323	98.9 ±0.048	98.8 ±0.184	ND	ND
Medium	98.8 ±0.142	98.9 ±0.070	99.2 ±0.307	ND	ND
High	98.7 ±0.134	98.4 ±0.136	99.0 ±0.210	ND	ND
Overall Mean	**98.6**	**98.7**	**99.0**	**NC**	**NC**

Figure 2.1: Box plots illustrating the extent of protein binding (%) observed across species (rat, dog, rabbit, guinea pig and human) for cisapride in plasma (A), blood (B) and heart homogenate (C) are shown in the upper pane. Concentrations of cisapride investigated were: 100 ng/mL (low), 1,000 ng/mL (medium) and 10,000 ng/mL (high), representing parity, 10x and 100x approximate clinical therapeutic concentration with respect to plasma. Corresponding tabulated data of cisapride protein binding mean values (n=6 replicates) are given for plasma (A), blood (B) and heart homogenate (C), including overall mean and ± S.E.M. Blood:plasma (B:P) ratios were determined (n=3) and tabulated with the blood binding data. The individual data were analysed by a 2-way ANOVA approach, with concentration and species as treatment factors. This was followed by all pair-wise comparisons between the predicted means of the concentration*species interaction and adjusted post-hoc using Bonferroni's multiple comparisons procedure with respect to rabbit as a comparator; *p* value <0.05 *; <0.01 **.

2.5.3. Moxifloxacin Protein Binding Results and Discussion

Protein binding of moxifloxacin was investigated at a range of concentrations, 500 ng/mL (low), 5,000 ng/mL (medium) and 50,000 ng/mL (high), representing 10x below, parity and 10x above approximate clinical therapeutic concentration with respect to plasma (Section 2.5.4). Corresponding tabulated data of moxifloxacin protein binding mean values (n=6 replicates) are given for plasma (A), blood (B) and heart homogenate (C), including overall mean, as well as blood:plasma ratios are given in Appendix 2.

2.5.3.1. Moxifloxacin: Plasma Protein Binding Results

Plasma protein binding values experimentally derived from this study showed the overall mean for rabbit was 43.8%, with 43.9% ±5.38 for low, 41.0% ±1.59 medium and 46.4% ±1.50 for high concentrations, respectively. These results were similar to all species (range 36.0 to 46.4%), with the exception of human plasma protein binding investigated at the low concentration (26.1% ±2.69, p value <0.01). This human group had significantly lower PB binding values in comparison to the rabbit low concentration group 43.9% ±5.38, and other species, rat 37.1% ±4.54, dog 36.1% ±1.32 and guinea pig 40.9% ±2.20. This difference is not related to a concentration-dependent change but may be from a set of experimental results at the lower range skewing the distribution, given the greater variability also seen at human and guinea-pig high concentrations, and rat and rabbit low concentrations. The data for each species shows that there is no concentration dependent change in protein binding in any species or matrix (Figure 2.2A and Table 2.6A).

Plasma protein binding of moxifloxacin was available from reported literature and regulatory documentation for rat, dog and human, as well as mouse, mini-pig, monkey, and in silico. In this study, the overall mean plasma PB for rat was 42.6%, which was higher in comparison to literature values for rat. However the lower concentration investigated matched reported values of 37% (Siefert et al., 1999b); FDA Approval Package, p.30) from radiolabelled [^{14}C]-cisapride, whereas an in silico software prediction for rat indicated plasma protein binding of 84.2% from Adamantis ACD.

In the dog, the overall mean binding was 36.9% derived experimentally, with 36.1% ±1.32 (low), 38.7% ±2.19 (medium) and 45.0% ±2.41 (high), which were all higher than the 29% binding reported for radiolabelled moxifoxacin by ultrafiltration (Siefert et al., 1999a). The calculated overall mean human protein binding was determined as 37.2%, with 26.1% ±2.69 (low), 40.5% ±3.57 (medium) and 45.0% ±4.45 (high). The medium and high concentrations

investigated reflect literature quoted binding values 30-50% from in vitro (FDA Approval package, p.3) and 45% by radiolabelled ultrafiltration (Siefert et al., 1999a). This is also similar to ex vivo PB values from human samples reported at 39.4-48% (Stass and Dalhoff, 1997; Stass and Kubitza, 1999) and 50% (Andersson and MacGowan, 2003) and 50% (FDA approval package p.7), respectively. In addition reported literature values by ultrafiltration for mouse, mini-pig and monkey were 31%, 37% and 38%, respectively, which demonstrate for moxifloxacin the similarity across species in protein binding. In contrast in silico predictions 70.2% and 77.1% for human and rat, respectively, suggest much greater binding than observed in this study and previously reported (Adamantis ACD).

Table 2.4 Referenced Moxifloxacin Plasma Protein Binding Information

Species	PPB (%)	Fup	Reference
Mouse (M) (in vitro 14C UF)	31	0.69	Siefert et al. 1999a
Rat (in silico)	77.1	0.229	Adamantis ACD software
Rat	37	0.63	FDA Approval Package pg 30
Rat (M) (in vitro 14C UF)	37	0.63	Siefert et al. 1999b
Dog (F) (in vitro 14C UF)	29	0.71	Siefert et al. 1999a
Minipig (F) (in vitro 14C UF)	37	0.63	Siefert et al. 1999a
Monkey (F) (in vitro 14C UF)	38	0.62	Siefert et al. 1999a
Human (in silico)	70.2	0. 298	Adamantis ACD software
Human (M) (in vitro 14C UF)	45	0.55	Siefert et al. 1999a
Human (in vitro)	30-50	0.50-0.70	FDA Approval Package pg 3
Human (ex vivo)	39.4	0.606	Stass & Kubiza 1999
Human (ex vivo)	48	0.52	Stass & Dalhoff 1998
Human	50	0.50	Andersson & MacGowan 2003;
Human (400mg in vivo)	50	0.50	FDA Approval Package pg 7
Human	37	0.63	Hardman & Limbird, 2012

PPB (Plasma Protein Binding); Fup (Fraction unbound plasma)

Overall for moxifloxacin the plasma protein binding values are comparable to literature where appropriate comparisons can be made and give confidence in the derived values for rabbit and guinea-pig which do not have literature references. Therefore the translation across species appears consistent even with the observed statistical difference between rabbit compared to human at low concentration.

2.5.3.2. Moxifloxacin: Blood Protein Binding Results

Blood protein binding values across all species and concentrations appear to be a significantly different (p-value < 0.01) compared to rabbit, that had an overall mean protein binding of 68.0%, with 58.0% ±2.81 (low), 79.7% ±1.01 (medium) and 66.2% ±1.22 (high). The rat (low and mid), dog and human (low and high) were all significantly higher than the rabbit, whilst rat, dog and guinea pig medium concentration were significantly lower. The remainder, guinea-pig low concentration (54.4% ±1.57), human at the medium concentration (75.4% ±0.931), and rat (68.4% ±0.802) and guinea-pig (74.3% ±0.927) blood at high concentrations were comparable to rabbit. Variability across replicates was reduced in blood binding which may account for the statistical differences observed. The protein binding values were consistently higher in blood compared to plasma and consistent across concentrations within species (Figure 2.2B and Table 2.6B).

The blood:plasma ratios determined showed minor differences across each species, with values which were greater than 1 indicating that moxifloxacin has a preferential distribution into the erythrocyte cellular fraction. The rabbit B:P was calculated to be 1.22 ±0.02. Values experimentally determined in this study were similar but higher than those in the literature for species, where available. Rat and human B:P reported here was 1.45 ±0.01 and 1.19 ±0.01, respectively, in comparison to 1.25 and 1.09 as identified by (Siefert et al., 1999a; Siefert et al., 1999b) using [14C]-moxifloxacin. Both dog (1.63 ±0.01) and guinea-pig (1.34 ±0.02) B:P ratios were high like rat, but no comparable reference could be made.

Table 2.5 Referenced Moxifloxacin Blood:Plasma Ratio Information

Species	Blood:Plasma ratio (B:P)	Reference
Rat (M) (in vitro 14C)	1.25	Siefert et al. 1999b
Monkey (F) (in vitro 14C)	1.13	Siefert et al. 1999a
Human (M) (in vitro 14C)	1.09	Siefert et al. 1999a
Rat Heart (in silico)	3.76 Kp (heart)	(Zhu et al., 2015)
Rat Muscle (in vivo)	6 (muscle)	(Beckmann et al., 2007)

2.5.3.3. Moxifloxacin: Heart Protein Binding Results

Moxifloxacin protein binding values in heart tissue have been determined in the rat, dog and rabbit. The mean values determined at low, medium and high concentrations investigated

were 89.1% ±0.416, 85.4% ±0.969, 85.1% ±0.725 for the rat; 94.0% ±0.634, 94.3% ±0.578, 90.8% ±0.736 for the dog; in comparison to 88.6% ±1.53, 89.0% ±1.10, 86.4% ±0.998 for rabbit. These results show no statistical difference (*p*-value >0.05) comparing rat to rabbit, except with rat medium concentration being shown to be different (*p*-value < 0.05), with the overall mean protein binding values in heart tissue in the rat (86.5%) and rabbit (88.0%) being similar (Figure 2.2C and Table 2.6C). However there was a notable statistical difference in the dog (*p*-value <0.01) at each concentration, with an overall mean 93% compared to rabbit, 88.0%. The variability was low highlighting the difference observed with dog heart tissue homogenate binding (*p*-value <0.01). All tissue homogenate binding values were greater than those in plasma or blood.

2.5.4. Moxifloxacin Protein Binding Data

Figure: 2.2A

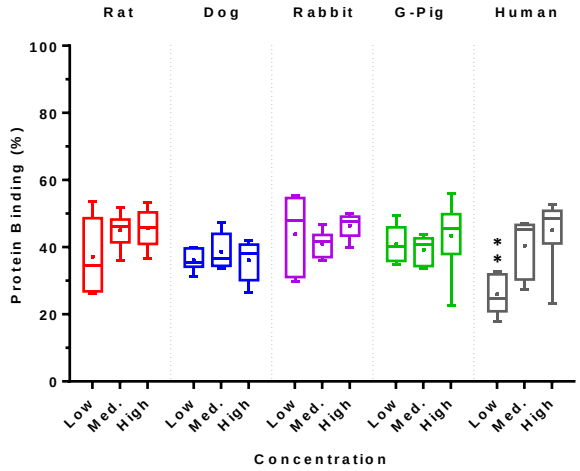

Figure: 2.2B

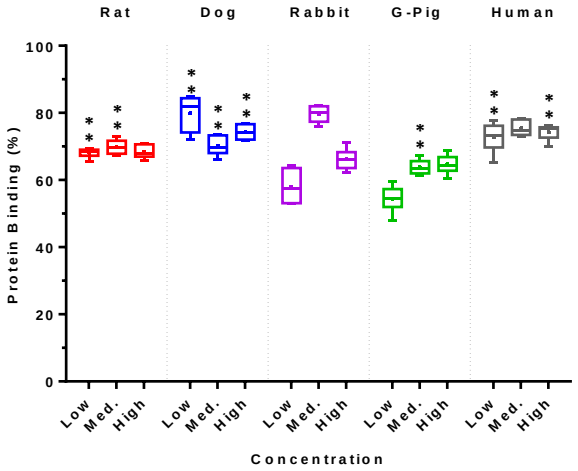

Figure: 2.2C

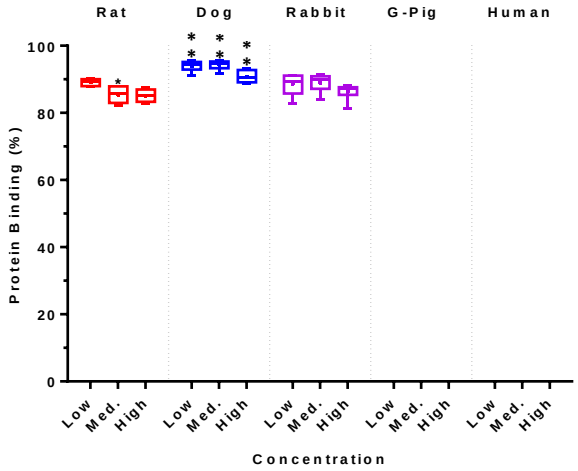

Table: 2.6A

Protein Binding (PB)	Mean Plasma				
	Rat	**Dog**	**Rabbit**	**G Pig**	**Human**
Low	37.1 ±4.54	36.1 ±1.32	43.9 ±5.38	40.9 ±2.20	26.1** ±2.69
Medium	45.1 ±2.13	38.7 ±2.19	41.0 ±1.59	39.3 ±1.71	40. 5 ±3.57
High	45.5 ±2.44	36.0 ±2.41	46.4 ±1.50	43.4 ±4.55	45.0 ±4.45
Overall Mean	**42.6**	**36.9**	**43.8**	**41.2**	**37.2**

Table: 2.6B

Protein Binding (PB)	Mean Blood				
	Rat	**Dog**	**Rabbit**	**G Pig**	**Human**
Low	68.1** ±0.573	76.3** ±2.17	58.0 ±2.81	54.4 ±1.57	72.7** ±1.81
Medium	69.8** ±0.873	70.5** ±1.15	79.7 ±1.01	63.8** ±0.851	75.4 ±0.931
High	68.4 ±0.802	74.3** ±0.892	66.2 ±1.22	64.6 ±1.14	74.3** ±0.927
Overall Mean	**68.8**	**73.7**	**68.0**	**61.0**	**74.1**
B:P	**1.45** ±0.01	**1.63** ±0.01	**1.22** ±0.02	**1.34** ±0.02	**1.19** ±0.01

Table: 2.6C

Protein Binding (PB)	Mean Heart				
	Rat	**Dog**	**Rabbit**	**G Pig**	**Human**
Low	89.1 ±0.416	94.0** ±0.634	88.6 ±1.53	ND	ND
Medium	85.4* ±0.969	94.3** ±0.578	89.0 ±1.10	ND	ND
High	85.1 ±0.725	90.8** ±0.746	86.4 ±0.998	ND	ND
Overall Mean	**86.5**	**93.0**	**88.0**	**NC**	**NC**

Figure 2.2: Box plots illustrating the extent of protein binding observed across species (rat, dog, rabbit, guinea pig and human) for moxifloxacin in plasma (A), blood (B) and heart homogenate (C) are shown in the upper pane. Concentrations of moxifloxacin investigated were: 500 ng/mL (low), 5,000 ng/mL (medium) and 50,000 ng/mL (high), representing 10x below, parity and 10x above approximate clinical therapeutic concentration with respect to plasma. Corresponding tabulated data of moxifloxacin protein binding mean values (n=6 replicates) are given for plasma (A), blood (B) and heart homogenate (C), including overall mean and ± S.E.M. Blood:plasma (B:P) ratios were determined (n=3) and tabulated with the blood binding data. The individual data were analysed by a 2-way ANOVA approach, with concentration and species as treatment factors. This was followed by all pair-wise comparisons between the predicted means of the concentration*species interaction and adjusted post-hoc using Bonferroni's multiple comparisons procedure with respect to rabbit as a comparator; *p* value <0.05 *; <0.01 **.

2.5.5. Sparfloxacin Protein Binding Results and Discussion

Protein binding of sparfloxacin was investigated at a range of concentrations, 100 ng/mL (low), 1,000 ng/mL (medium) and 10,000 ng/mL (high), representing 10x below, parity and 10x above approximate clinical therapeutic concentration with respect to plasma (Section 2.5.6). Corresponding tabulated data of sparfloxacin protein binding mean values (n=6 replicates) are given for plasma (A), blood (B) and heart homogenate (C), including overall mean, as well as blood:plasma ratios are given in Appendix 2.

2.5.5.1. Sparfloxacin: Plasma Protein Binding Results

Plasma protein binding values experimentally derived from this study for the rabbit were 55.7% ±1.79, 47.8% ±2.30 and 44.7% ±1.69, for low, medium and high concentrations, respectively. Generally the rabbit plasma protein binding values at each concentration were similar to each species, with the exception of guinea-pig plasma protein binding at the medium and high concentration (73.1% ±0.962 and 72.9% ±2.07, *p*-value <0.01) which was notably higher, and rat and dog at the low concentration 42.4% ±2.26 (*p*-value 0.05) and 23.5% ±2.19 (*p*-value <0.01), respectively, were significantly lower. Rabbit protein binding overall mean was 49.4% and comparable to rat, dog and human values. The data for each species shows that there is no concentration dependent change in protein binding in any species or matrix (Figure 2.3A and Table 2.9A).

Plasma protein binding of sparfloxacin was available from reported literature for rat, dog, rabbit, and human, as well as monkey and in silico predictions. The mean experimentally determined plasma PB in this study for rabbit was 49.4%, which was higher than the single reported literature value of 42% as determined by ultrafiltration (Liu et al., 1998).

In this study, the overall mean plasma PB for rat was 45.1%, which is comparable to literature values for rat, 44.6-44.9% (Matsunaga et al., 1991b; Yamaguchi et al., 1991) in vitro. Also the low concentration investigated resulted in 42.4%, similar to the radiolabelled [^{14}C]-sparfloxacin at 36.6% (Matsunaga et al., 1991a; Matsunaga et al., 1991b), and the medium concentration result of 48.7% equivalent to the reported ultrafiltration result, 50.4% (Naroa et al., 1992). However, other reported data appears to be significantly different at 5-14% (Nadai et al., 2001), in comparison to an in silico rat prediction of 76.1% (Adamantis ACD). In the dog, 35.3% binding was derived experimentally which was lower than the

43.6% binding reported for sparfloxacin (Yamaguchi et al., 1991), yet similar to rat using radiolabelled [^{14}C]-sparfloxacin at 36.6% (Matsunaga et al., 1991b).

The calculated mean human protein binding was determined as 56%, with 54.6% (low), 56.1% (med) and 57.1% (high). These PB values are greater than literature quoted binding values 46% from in vitro (Matsunaga et al., 1991b). This is similarly higher than ex vivo PB values from human samples reported at 37% (Shimada et al., 1993; Morganroth et al., 1999; Hardman and Limbird, 2011), 40% (Andersson and MacGowan, 2003) and 45% (Montay et al., 1994), respectively. In contrast reports of sparfloxacin human plasma PB at 25% have been quoted (Zlotos et al., 1998a; Zlotos et al., 1998b). In addition, reported in vitro literature values for monkey were 45.1% (Yamaguchi et al., 1991), which demonstrates for sparfloxacin the similarity across species in protein binding. In contrast human in silico prediction suggest much greater binding 79.3% than observed in this study and previously reported (Adamantis ACD).

Table 2.7 Referenced Sparfloxacin Plasma Protein Binding Information

Species	PPB (%)	Fup	References
Rat (in silico)	76.1	0.239	Adamantis ACD
Rat (ex vivo 14C)	36.6	0.634	Matsunaga et al. 1991
Rat (in vitro)	44.6	0.554	Matasunaga et al. 1991; Yamaguchi et al. 1991
Rat (ex vivo UF)	50.4	0.496	Naroa et al. 1992
Rat (ex vivo)	44.9	0.551	Yamaguchi et al. 1991
Rat (ex vivo)	5-14	0.05 – 0.14	Nadai, 2001
Rabbit (in vitro UF)	42	0.58	Liu et al. 1998
Dog (in vitro)	43.7	0.563	Yamaguchi et al. 1991
Monkey (in vitro)	45.1	0.549	Yamaguchi et al. 1991
Human (in silico)	79.3	0.207	Adamantis ACD
Human (in vitro)	46	0.54	Matsunaga et al. 1991
Human	25	0.75	Zlotos et al. 1998
Human	45	0.55	Montay 1994; Redfern et al. 2003
Human	40	0.60	Andersson & McGowan 2003
Human	37	0.63	Shimada et al. 1993; Morganroth et al. 1999; Hardman & Limbird, 2011

PPB (Plasma Protein Binding); Fup (Fraction unbound plasma)

Sparfloxacin plasma protein binding values are comparable to literature where appropriate comparisons can be made and give confidence in the derived values across species and may

highlight guinea-pig as being different. Therefore the translation across species appears consistent even with the observed statistical difference between rabbit compared to guinea pig.

2.5.5.2. Sparfloxacin: Blood Protein Binding Results

Blood protein binding values were determined at medium and high concentrations representing parity and 10x fold above human equivalent therapeutic concentrations. Lower concentrations (10x) could not be accurately reported due to assay sensitivity and reliability of data generated.

Rabbit blood protein binding values, 73.4% ±1.62 and 73.5% ±0.523, at medium and high concentrations, respectively, were consistent with rat at both medium (75.9% ±1.08) and high (74.6% ±0.453) concentration levels, respectively, and human at the medium (77.0% ±1.29) concentration. Compared to rabbit, both the dog (61.4% ±2.87 and 59.2% ±0.681) and guinea-pig (63.7% ±1.70 and 62.7% ±1.12) were significantly lower (p-value < 0.01) (Figure 2.3B and Table 2.9B).

The protein binding values were consistently higher in blood compared to plasma and consistent across concentrations within species, with the exception of guinea-pig blood binding which was lower.

The blood:plasma ratios determined showed minor differences across each species, with values approximately 2 indicating that sparfloxacin has a distinct distribution into the erythrocyte cellular fraction. The rabbit B:P ratio was calculated to be 1.80 ±0.10 and was closest to human which was lower at 1.6 ±0.05.

Table 2.8 Referenced Sparfloxacin Tissue:Plasma Ratio Information

Species	Tissue:Plasma ratio (T:P)	Reference
Dog Heart (oral at 4h)	0.8 (heart)	Yamaguchi et al.1991

2.5.5.3. Sparfloxacin: Heart Protein Binding Results

Sparfloxacin protein binding values in heart tissue have been determined in the rat, dog and rabbit. The mean binding values in the rabbit were 91.8% ±1.24, 93.9% ±0.664 and 89.9% ±1.52, for low, medium and high concentrations. Protein binding values in heart tissue were identified to be statistically different (p-value <0.01) at low and medium concentrations in the

rat (79.2% ±3.26 and 85.0% ±1.29), and with no statistical difference at high concentrations (85.7% ±0.725). The rat tissue homogenate binding had a greater range of values at the low and medium concentrations compared to either dog or rabbit. There was no notable difference at any concentration in dog, mean low 93.8% ±0.521, medium 94.6% ±0.305, and high 94.0% ±0.471, compared to rabbit. All tissue homogenate binding values were greater than those in plasma or blood (Figure 2.3C and Table 2.9C). A reported literature ex vivo blood:tissue or tissue binding ratio for dog heart at 4 hour post oral dosing has been reported as 0.8 (Table 2.8) (Yamaguchi et al., 1991).

2.5.6. Sparfloxacin Protein Binding Data

Figure: 2.3A

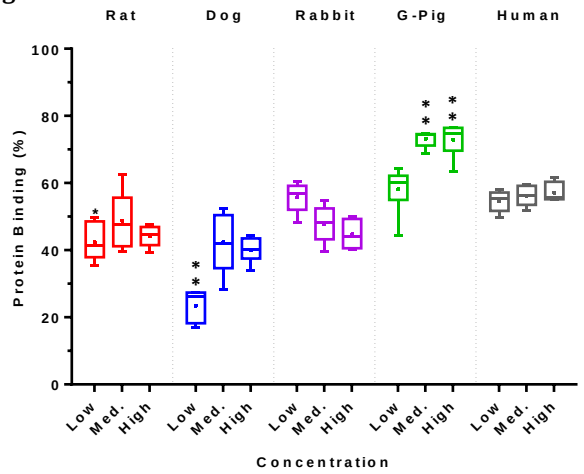

Figure: 2.3B

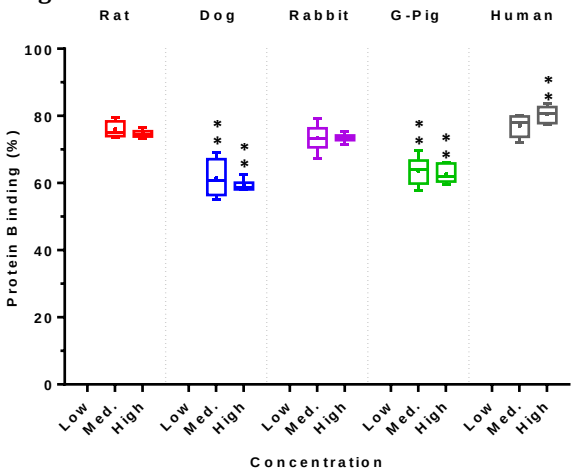

Figure: 2.3C

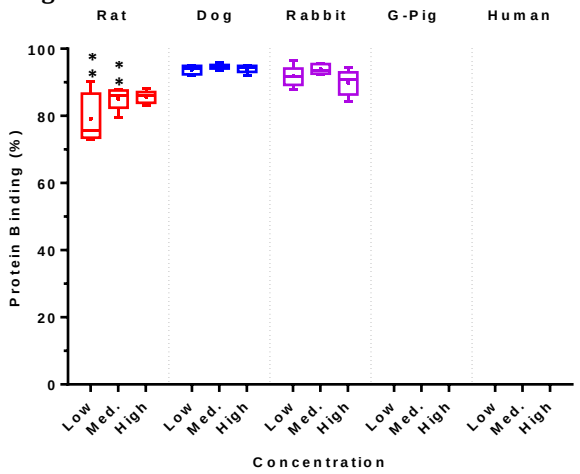

Table: 2.9A

Protein Binding (PB)	Mean Plasma				
	Rat	**Dog**	**Rabbit**	**G Pig**	**Human**
Low	42.4* ±2.26	23.5** ±2.19	55.7 ±1.79	58.2 ±2.91	54.6 ±1.26
Medium	48.7 ±3.42	42.4 ±4.10	47.8 ±2.30	73.1** ±0.962	56.1 ±1.27
High	44.2 ±1.32	40.0 ±1.50	44.7 ±1.69	72.9** ±2.07	57.1 ±1.16
Overall Mean	**45.1**	**35.3**	**49.4**	**68.1**	**56.0**

Table: 2.9B

Protein Binding (PB)	Mean Blood				
	Rat	**Dog**	**Rabbit**	**G Pig**	**Human**
Low	ND	ND	ND	ND	ND
Medium	75.9 ±1.08	61.4** ±2.87	73.4 ±1.62	63.7** ±1.70	77.0 ±1.29
High	74.6 ±0.453	59.2** ±0.681	73.5 ±0.523	62.7** ±1.12	80.5** ±0.993
Overall Mean	**75.3**	**60.3**	**73.4**	**63.2**	**78.7**
B:P	**2.14** ±0.15	**1.92** ±0.05	**1.80** ±0.10	**2.01** ±0.03	**1.60** ±0.05

Table: 2.9C

Protein Binding (PB)	Mean Heart				
	Rat	**Dog**	**Rabbit**	**G Pig**	**Human**
Low	79.2** ±3.26	93.8 ±0.521	91.8 ±1.24	ND	ND
Medium	85.0** ±1.29	94.6 ±0.305	93.9 ±0.664	ND	ND
High	85.7 ±0.725	94.0 ±0.471	89.9 ±1.52	ND	ND
Overall Mean	**83.3**	**94.1**	**91.9**	**NC**	**NC**

Figure 2.3: Box plots illustrating the extent of protein binding observed across species (rat, dog, rabbit, guinea pig and human) for sparfloxacin in plasma (A), blood (B) and heart homogenate (C) are shown in the upper pane. Concentrations of sparfloxacin investigated were: 100 ng/mL (low), 1,000 ng/mL (medium) and 10,000 ng/mL (high), representing 10x below, parity and 10x above approximate clinical therapeutic concentration with respect to plasma. Corresponding tabulated data of sparfloxacin protein binding mean values (n=6 replicates) are given for plasma (A), blood (B) and heart homogenate (C), including overall mean and ± S.E.M. Blood:plasma (B:P) ratios were determined (n=3) and tabulated with the blood binding data. The individual data were analysed by a 2-way ANOVA approach, with concentration and species as treatment factors. This was followed by all pair-wise comparisons between the predicted means of the concentration*species interaction and adjusted post-hoc using Bonferroni's multiple comparisons procedure with respect to rabbit as a comparator; *p* value <0.05 *; <0.01 **.

2.5.7. Verapamil Protein Binding Results and Discussion

Protein binding of verapamil was investigated at a range of concentrations, 100 ng/mL (low), 1,000 ng/mL (medium) and 10,000 ng/mL (high), representing parity, 10x and 100x above approximate clinical therapeutic concentration with respect to human plasma. Results have been represented graphically as box plots across species (rat, dog, rabbit, guinea pig and human) in plasma (A), blood (B) and heart tissue homogenate (C) (Section 2.5.8). Corresponding tabulated data of verapamil protein binding mean values (n=6 replicates) are given for plasma (A), blood (B) and heart homogenate (C), including overall mean, as well as blood:plasma ratios are given in Appendix 2.

2.5.7.1. Verapamil: Plasma Protein Binding Results

Verapamil plasma protein binding values experimentally derived from this study were shown to be similar comparing rabbit (low 92.8% ±0.541; medium 93.3% ±0.550; high 92.8% ±0.558) to any species except guinea-pig. The guinea-pig had significantly higher protein binding values (*p*-value <0.01), with very little variability at each low, medium and high concentration, 99.3% ±0.084, 99.4% ±0.014 and 99.2% ±0.025, respectively. Given the reproducibility across all the concentrations investigated in guinea-pig then the difference in results are deemed valid (Figure 2.4A and Table 2.12A).

Data from the mean plasma PB results for low, medium and high concentrations in rat (93.6% ±0.20, 93.3% ±0.536 and 91.7% ±0.334), dog (93.7% ±0.11, 94.6% ±0.066 and 94.1% ±0.182) and human (90.3% ±2.20, 90.6% ±2.11 and 90.0% ±1.95.) indicate that there is no significant difference compared to rabbit. Both rabbit and human experiments were n=12 replicates; rabbit was conducted twice in error, whereas human was repeated due to initially much lower than expected results across all concentrations (~80%). The repeated experiment (~95%) was greater than the reported 88-90%, and as a result the variability for human is notable. The RED device technique is known for its reliability and robustness, so this variability could be a result of distinctly different batches of human plasma used, even unknown co-medications present in the collected plasma, different experimental time period or different analytical MS instrumentation (switched MS machine, UPLC, MS response). Nevertheless the results span the reported literature values.

The data for each species shows that there is no concentration dependent change in protein binding in any species or matrix.

In this study, the overall mean plasma PB for rat was 92.9%, which is comparable to literature values for rat, 82-93% (Sattari et al., 2003; Kalvass et al., 2007) in vitro, and in-line with an in silico rat prediction of 93.1% (Adamantis ACD).

The calculated mean human protein binding was determined as 90.3% in this present study which is equivalent to a range of literature quoted binding values 88% (Hardman and Limbird, 2011), 90% (Redfern et al., 2003; Zhang et al., 2012), 90.7% (Gertz et al., 2010) and 93% (Vozeh et al., 1988). A human in silico prediction suggest greater plasma binding of 96.3% than observed in this study and previously reported (Adamantis ACD).

Table 2.10 Referenced Verapamil Plasma Protein Binding Information

Species	PPB%	Fup	Reference
Rat	89	0.11	Kalvass 2007
Rat	82-93	0.07 – 0.18	Sattari et al. 2003
Human	88	0.12	Hardman & Limbird, 2011
Human	90	0.10	Redfern et al. 2003; Zhang et al. 2012
Human?	90.7	0.093	Gertz et al.2010
Human	93	0.07	Vozeh et al. 1988

PPB (Plasma Protein Binding); Fup (Fraction unbound plasma)

Verapamil plasma protein binding values are comparable to literature where appropriate comparisons can be made and give confidence in the derived values across species and may highlight guinea-pig as being different. Therefore the translation across species appears consistent compared to rabbit but with guinea pig the observed statistical difference needs to be appreciated with respect to the free fraction and noted in physiological modelling.

2.5.7.2. Verapamil: Blood Protein Binding Results

Blood protein binding values across all species and concentrations were generally significantly different (*p*-value <0.01) compared to rabbit values 82.9% ±0.704, 84.2% ±0.295 and 83.7% ±0.877 at low, medium and high concentrations, respectively. The guinea-pig, was again notably the highest of all species with binding values (96.8% ±0.084, 97.2% ±0.099 and 95.9% ±0.168) and human (87.0% ±0.704, 90.0% ±0.572, and 89.5% ±0.759) were both significantly higher (*p*-value <0.01) in comparison to rabbit at all concentrations. The blood protein binding values at medium concentrations in the rat (87.4% ±0.294) and dog (87.3% ±0.309) were also significantly different to the rabbit medium concentrations, as a result of the tight grouping of data. However, the rat and dog binding at low (85.2% ±0.294

and 84.4% ±0.758) and high (85.1% ±0.911and 85.8% ±0.877) concentrations were similar to rabbit. The protein binding values were consistently lower in blood compared to plasma, and consistent across concentrations within species, except for human which was similar to human plasma binding given the wide experimental range observed (Figure 2.4B and Table 2.12B).

The blood:plasma ratios determined showed some differences across each species, with all values less than 1 indicating that verapamil does not have the propensity to distribute into the erythrocyte cellular fraction. The rabbit B:P ratio was calculated to be 0.81 ±0.01 and was the highest value observed followed by guinea-pig (0.74 ±0.03), then rat (0.68 ±0.04). Human was lower at 0.59 ±0.03 and the lowest ratio was dog at 0.4 ±0.03. A reported literature value of 0.89 has been stated for human B:P ratio (Gertz et al., 2010).

Table 2.11 Referenced Verapamil Blood:Plasma Ratio Information

Species	Blood:Plasma ratio (B:P)	Reference
Human	0.89	Gertz et al. 2010

2.5.7.3. Verapamil: Heart Protein Binding Results

Verapamil protein binding values in heart tissue have been determined in rat, dog and rabbit heart tissue homogenate. Binding values at low, medium and high concentrations for the rabbit were calculated at 98.1% ±0.114, 98.2% ±0.113 and 97.5% ±0.276, respectively. The rat values at all concentration (98.4% ±0.068, 98.0% ±0.146 and 97.2% ±0.246) and the dog at medium and high concentration (98.6% ±0.174 and 97.8% ±0.271), were not statistically different to the rabbit, except dog low value 98.8% ±0.143 (p-value <0.05). The variability observed was low for each species. All tissue homogenate binding values were greater than those in plasma or blood (Figure 2.4C and Table 2.12C)

2.5.8. Verapamil Protein Binding Data

Figure: 2.4A

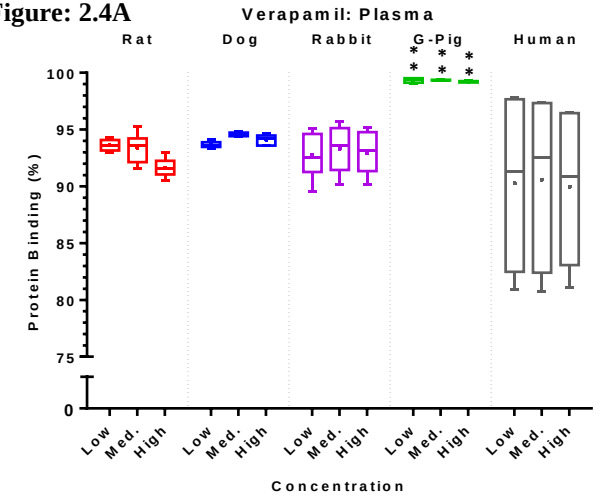

Figure: 2.4B

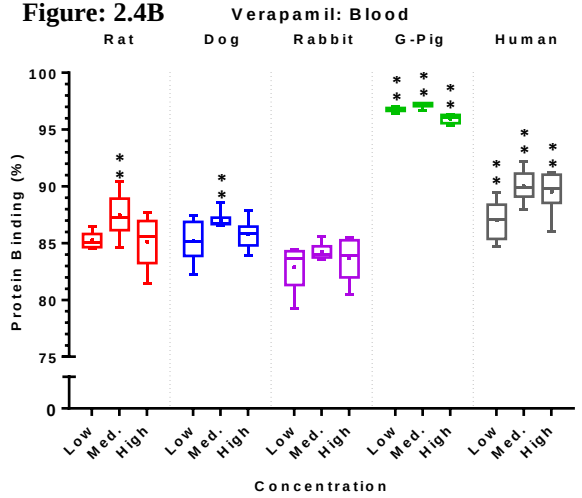

Figure: 2.4C

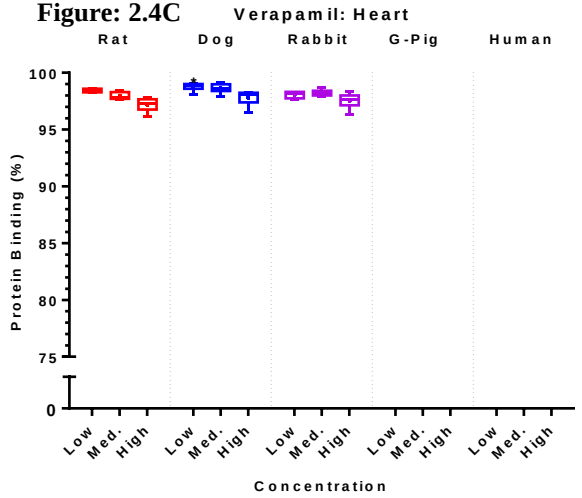

Table: 2.12A

Protein Binding (PB)	Mean Plasma				
	Rat	**Dog**	**Rabbit**	**G Pig**	**Human**
Low	93.6 ±0.200	93.7 ±0.110	92.8 ±0.541	99.3** ±0.084	90.3 ±2.20
Medium	93.4 ±0.536	94.6 ±0.066	93.3 ±0.550	99.4** ±0.014	90.6 ±2.11
High	91.7 ±0.334	94.1 ±0.182	92.8 ±0.558	99.2** ±0.025	90.0 ±1.95
Overall Mean	**92.9**	**94.1**	**93.0**	**99.3**	**90.3**

Table: 2.12B

Protein Binding (PB)	Mean Blood				
	Rat	**Dog**	**Rabbit**	**G Pig**	**Human**
Low	85.2 ±0.294	84.4 ±0.758	82.9 ±0.812	96.8** ±0.084	87.0** ±0.704
Medium	87.4** ±0.782	87.3** ±0.309	84.2 ±0.295	97.2** ±0.099	90.0** ±0.572
High	85.1 ±0.911	85.8 ±0.528	83.7 ±0.877	95.9** ±0.168	89.5** ±0.759
Overall Mean	**85.9**	**85.8**	**83.6**	**96.6**	**88.9**
B:P	**0.68** ±0.04	**0.40** ±0.03	**0.81** ±0.01	**0.74** ±0.03	**0.59** ±0.03

Table: 2.12C

Protein Binding (PB)	Mean Heart				
	Rat	**Dog**	**Rabbit**	**G Pig**	**Human**
Low	98.4 ±0.068	98.8* ±0.143	98.1 ±0.114	ND	ND
Medium	98.0 ±0.146	98.6 ±0.174	98.2 ±0.113	ND	ND
High	97.2 ±0.246	97.8 ±0.271	97.5 ±0.276	ND	ND
Overall Mean	**97.9**	**98.4**	**97.9**	**NC**	**NC**

Figure 2.4: Box plots illustrating the extent of protein binding observed across species (rat, dog, rabbit, guinea pig and human) for verapamil in plasma (A), blood (B) and heart homogenate (C) are shown in the upper pane. Concentrations of verapamil investigated were: 100 ng/mL (low), 1,000 ng/mL (medium) and 10,000 ng/mL (high), representing parity, 10x and 100x above approximate clinical therapeutic concentration with respect to plasma. Corresponding tabulated data of verapamil protein binding mean values (n=6 replicates) are given for plasma (A), blood (B) and heart homogenate (C), including overall mean and ± S.E.M. Blood:plasma (B:P) ratios were determined (n=3) and tabulated with the blood binding data. The individual data were analysed by a 2-way ANOVA approach, with concentration and species as treatment factors. This was followed by all pair-wise comparisons between the predicted means of the concentration*species interaction and adjusted post-hoc using Bonferroni's multiple comparisons procedure with respect to rabbit as a comparator; *p* value <0.05 *; <0.01 **.

2.5.9. Sotalol Protein Binding Results and Discussion

Protein binding of sotalol was investigated at a range of concentrations, 100 ng/mL (low), 1,000 ng/mL (medium) and 10,000 ng/mL (high), representing 10x below, parity and 10x above approximate clinical therapeutic concentration with respect to human plasma. Results have been represented graphically as box plots across species (rat, dog, rabbit, guinea pig and human) in plasma (A), blood (B) and heart tissue homogenate (C) (Section 2.5.10). Corresponding tabulated data of sotalol protein binding mean values (n=6 replicates) are given for plasma (A), blood (B) and heart homogenate (C), including overall mean, as well as blood:plasma ratios, as well as blood:plasma ratios are given in Appendix 2.

2.5.9.1. Sotalol: Plasma Protein Binding Results

Plasma protein binding values experimentally derived from this study were shown to be similar between rabbit at low, medium and high concentrations (14.0% ±1.14, 20.8% ±1.37 and 24.8% ±1.54, respectively) compared to dog, guinea-pig and human. The mean dog values were 24.9% ±3.88, 23.8% ±3.84 and 33.4% ±2.27, and guinea-pig were 8.9% ±1.92, 26.5% ±3.09 and 30.9% ±2.92, and human were 12.9% ±0.739, 23.5% ±2.25 and 31.1% ±1.62, at low, medium and high concentrations investigated, respectively. The rat had significantly higher plasma protein binding values at the low and high concentrations investigated, low, 37.4% ±4.72, (p-value <0.01) and high, 36.3% ±1.65, (p-value <0.05), whilst the mean medium concentration value was 30.0% ±2.78 (Figure 2.5A and Table 2.17A). The data indicated there was concentration dependent change with a clear trend for an increase in protein binding with an increase in concentration for each species, except for rat which may account for the difference compared to rabbit and the other species.

For sotalol protein binding values reported in the literature for plasma are predominantly for human and vary dramatically, with many authors suggesting sotalol has negligible or no protein binding (Anttila et al., 1976; Vozeh et al., 1988; Campbell and Williams, 1998; Redfern et al., 2003; Hardman and Limbird, 2011). Sotalol has also been reported to have low plasma binding with a range of values quoted from, 7% (Carr et al., 1995), 17.5% (Kratochwil et al., 2002; Zhang et al., 2012), up to 20-40% (Giudicelli et al., 1973; Sundquist, 1980; Fiset et al., 1993). In this study human plasma PB was observed from 12.9%, 23.5% and 31.1% which covers the range of literature values, but does not indicate zero binding.

Limited PB values have been reported for other species, such as rat 2.3% (Carr et al., 1995), 0% in the dog (Schnelle and Garrett, 1973) determined by ultrafiltration, neither of which are comparable to results calculated in this study. In silico prediction suggests plasma binding of 30.3% and 54.3% for rat and human, respectively, slightly greater than observed in this study and previously reported (Adamantis ACD).

Table 2.13 Referenced Sotalol Plasma Protein Binding Information

Species	PPB%	Fup	References
Rats (in vitro UF)	2.3	0.977	Carr et al. 1995
Dog (in vitro UF)	0	1	Schnelle & Garrett 1973
Guinea Pig (blood 96-well)	46.2	0.538	Osuna (Neurology CEDD, GSK)
Human (in vitro UF)	0	1	Antilla et al. 1976
Human (in vitro UF)	7	0.93	Carr et al. 1995
Human (in vitro)	40	0.60	Giudicelli et al. 1973
Human (ex vivo)	35-38	0.62-0.65	Fiset et al. 1993
Human (ex vivo)	22	0.78	Giudicelli et al. 1973
Human	0	1	Redfern et al. 2003; Hardman and Limbird, 2006
Human	17.5	0.825	Kratochwil et al. 2002; Zhang et al. 2012
Human	<1	>0.99	Vozeh et al. 1988; Campbell & Williams 1998
Human	20	0.80	Sundquist et al. 1980
Human (ex vivo)	22	0.78	Giudicelli et al. 1973

PPB (Plasma Protein Binding); Fup (Fraction unbound plasma)

Sotalol plasma protein binding values in this study are consistent compared to literature where appropriate comparisons can be made yet there are gross variations in the literature. This study uses a consistent technique for comparison, gives confidence in the derived values across species and highlights the trend of increasing binding with concentration. The rat has been shown not to exhibit this trend. Therefore the translation across species is consistent compared to rabbit but with rat the observed statistical difference needs to be appreciated in this study and also the literature disconnect with respect to the free fraction and noted in physiological modelling.

2.5.9.2. Sotalol: Blood Protein Binding Results

Sotalol blood protein binding values across all species and concentrations were similar to rabbit (20.8% ±2.59, 32.9% ±2.29 and 44.4% ±1.16), with the exception of human at all concentrations. The data indicate there was a significant concentration dependent change with an increase in concentration resulting in an increase in protein binding for each species. In this study the change was more pronounced for human, at low (11.8% ±3.25, *p*-value <0.05) which was lower than rabbit, and then at the medium and high (51.6% ±2.40 and 59.6% ±1.33, respectively; *p*-value <0.01), which led to the significant difference in protein binding values compared to rabbit (Figure 2.5B and Table 2.17B).

The protein binding values were approximately the same or greater in blood compared to plasma, and consistent across concentrations within species, except for human which was similar to human plasma binding with a wider experimental range observed. From a separate unpublished internal study, sotalol had been previously investigated at 2 µM (equivalent to 540 ng/mL) in guinea-pig blood using the RED device and reported a protein binding value of 46.2% (Osuna and unit, 2006) which is comparable to the high concentration value determined, 44.5% ±1.91.

Table 2.14 Referenced Sotalol Blood Protein Binding Information

Species	PPB%	Fup	References
Guinea Pig (blood 96-well)	46.2	0.538	Osuna (Neurology CEDD, GSK)

The blood:plasma ratios determined showed some differences across each species, with all values less than 1 indicating that sotalol does not have the propensity to distribute into the erythrocyte cellular fraction. The rabbit B:P ratio was calculated to be 0.93 ±0.02 and was similar value observed in dog (0.98 ±0.12) and human (0.90 ±0.09), which is line with reported literature value of 1.16 for dog (Schnelle and Garrett, 1973). Rat and guinea-pig were lower at 0.68 ±0.01 and 0.69 ±0.03, respectively.

Table 2.15 Referenced Sotalol Blood:Plasma Ratio Information

Species	Blood:Plasma ratio (B:P)	References
Dog plasma	1.16	Schnelle & Garrett 1973

2.5.9.3. Sotalol: Heart Protein Binding Results

Sotalol protein binding values in heart tissue have been determined in the rat, dog and rabbit. Binding values were shown to be similar between rabbit at low, medium and high concentrations, 73.0% ±1.67, 82.6% ±2.15 and 77.2% ±4.08, respectively, compared to binding values in the dog, 86.0% ±1.61, 86.8% ±1.69 and 84.4% ±1.52, respectively (Figure 2.5C and Table 2.17C).

The rat heart binding was deemed similar at the lowest concentration, with a mean value 65.9% ±9.99; however this showed the greatest variability across any species or even matrices investigated. The rat was also statistically different to rabbit at the medium (56.3% ±4.92, *p*-value <0.01) and high concentrations (60.5% ±4.90, *p*-value <0.05). The variability observed was notable for rat and less so for rabbit and dog. All tissue homogenate binding values were greater than those observed in plasma or blood, and did not show a concentration-dependence in protein binding. Additionally in the dog a value of 2-3 blood:heart ratio has been reported (Gomoll, 1990).

Table 2.16 Referenced Sotalol Blood:Tissue Ratio Information

Species	Blood:Tissue ratio (B:P)	References
Dog heart	2-3	Gomoll, 1990

2.5.10. Sotalol Protein Binding Data

Figure: 2.5A

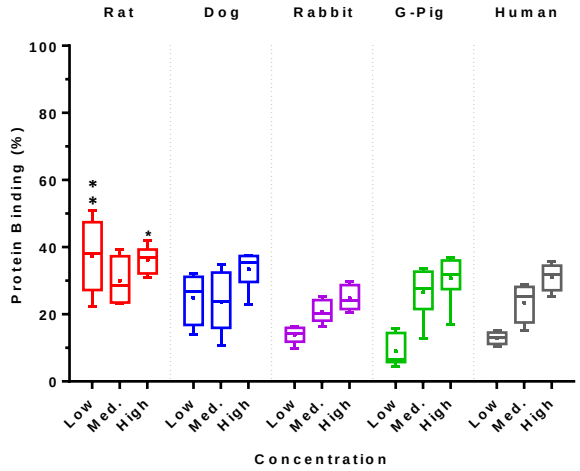

Figure: 2.5B

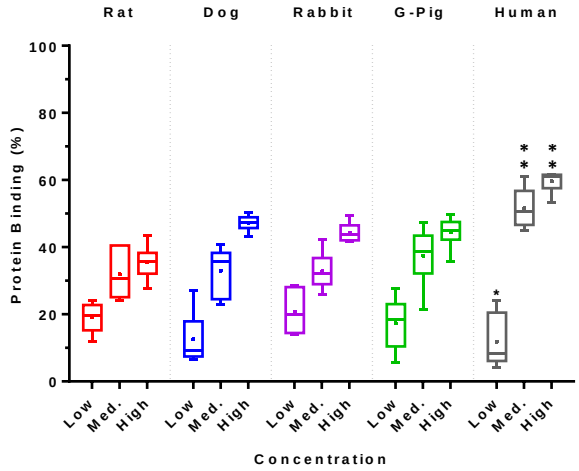

Figure: 2.5C

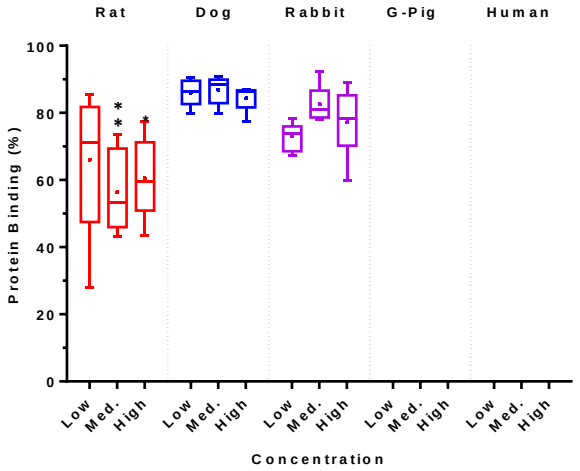

Table: 2.17A

Protein Binding (PB)	Mean Plasma				
	Rat	**Dog**	**Rabbit**	**G Pig**	**Human**
Low	37.4** ±4.72	24.9 ±3.88	14.0 ±1.14	8.9 ±1.93	12.9 ±0.739
Medium	30.0 ±2.78	23.8 ±3.84	20.8 ±1.37	26.5 ±3.09	23.5 ±2.25
High	36.3* ±1.65	33.4 ±2.27	24.8 ±1.54	30.7 ±2.92	31.1 ±1.62
Overall Mean	**33.2**	**28.6**	**22.8**	**28.6**	**27.3**

Table: 2.17B

Protein Binding (PB)	Mean Blood				
	Rat	**Dog**	**Rabbit**	**G Pig**	**Human**
Low	19.1 ±2.03	12.5 ±3.16	20.8 ±2.59	17.3 ±3.16	11.8* ±3.25
Medium	32.0 ±2.91	32.9 ±2.97	32.9 ±2.29	37.4 ±3.58	51.6** ±2.40
High	35.5 ±2.09	47.2 ±0.958	44.4 ±1.16	44.5 ±1.91	59.6** ±1.33
Overall Mean	**33.7**	**40.1**	**38.6**	**40.9**	**55.6**
B:P	**0.68** ±0.01	**0.98** ±0.12	**0.93** ±0.02	**0.69** ±0.03	**0.90** ±0.09

Table: 2.17C

Protein Binding (PB)	Mean Heart				
	Rat	**Dog**	**Rabbit**	**G Pig**	**Human**
Low	65.9 ±9.99	86.0 ±1.61	73.0 ±1.67	ND	ND
Medium	56.3** ±4.92	86.8 ±1.69	82.6 ±2.15	ND	ND
High	60.5* ±4.90	84.4 ±1.52	77.2 ±4.08	ND	ND
Overall Mean	**60.9**	**85.8**	**77.6**	**NC**	**NC**

Figure 2.5: Box plots illustrating the extent of protein binding observed across species (rat, dog, rabbit, guinea pig and human) for sotalol in plasma (A), blood (B) and heart homogenate (C) are shown in the upper pane. Concentrations of sotalol investigated were: 100 ng/mL (low), 1000 ng/mL (medium) and 10,000 ng/mL (high), representing 10x below, parity and 10x above approximate clinical therapeutic concentration with respect to plasma. Corresponding tabulated data of sotalol protein binding mean values (n=6 replicates) are given for plasma (A), blood (B) and heart homogenate (C), including overall mean and ± S.E.M. Blood:plasma (B:P) ratios were determined (n=3) and tabulated with the blood binding data. The individual data were analysed by a 2-way ANOVA approach, with concentration and species as treatment factors. This was followed by all pair-wise comparisons between the predicted means of the concentration*species interaction and adjusted using Bonferroni's multiple comparisons procedure with respect to rabbit as a comparator; *p* value <0.05 *; <0.01 **

2.5.11. Quinidine Protein Binding Results and Discussion

Protein binding of quinidine was investigated at a range of concentrations, 1000 ng/mL (low), 10,000 ng/mL (medium) and 100,000 ng/mL (high), representing 10x below, parity and 10x above approximate clinical therapeutic concentration with respect to human plasma. Results have been represented graphically as box plots across species (rat, dog, rabbit, guinea pig and human) in plasma (A), blood (B) and heart tissue homogenate (C) (Section 2.5.12). Corresponding tabulated data of quinidine protein binding mean values (n=6 replicates) are given for plasma (A), blood (B) and heart homogenate (C), including overall mean, as well as blood:plasma ratios are given in Appendix 2.

2.5.11.1. Quinidine: Plasma Protein Binding Results

Quinidine plasma protein binding values experimentally derived from this study were generally significantly different comparing rabbit to all other species. In the rabbit, mean protein binding at low, medium and high concentrations was 88.6% ±0.594, 90.1% ±0.365 and 87.0% ±0.131, respectively, and did not change with concentration. All other species exhibited a significant (*p*-value <0.01) concentration dependent change with a large decrease in protein binding with an increase in quinidine concentration for each species, unlike rabbit, accounting for the difference in values observed. The dog and guinea-pig were similar in protein binding and had the most significant decrease over the low, medium and high concentration range from 98.6% ±0.126, 90.2% ±0.282 down to 67.8% ±1.08, respectively in the dog, and from 99.0% ±0.123, 92.2% ±0.183 down to 83.5% ±0, respectively in the guinea-pig. Human plasma protein binding declined from 91.0% ±0.207, 87.1% ±0.303 down to 75.2% ±0.757 and rat reduced from 81.6% ±0.485, 7.8% ±1.09 to 69.7% ±1.18. This indicates that quinidine plasma protein binding is saturable in these species and less so in the rabbit (Figure 2.6A and Table 2.20A).

In one study, quinidine rabbit plasma protein binding ranged from 84-94% and only exhibited a small degree of concentration dependence (Guentert and Oie, 1980), and in another study by the same authors ranged from 77-94% (Guentert et al., 1982; Guentert and Oie, 1982). The values obtained for the rabbit in this study were similar and also comparable to 86% described by another author (Sawada et al., 1984). Protein binding and B:P of quinidine was described as nonlinear over the in vivo plasma concentration range with values between 60-75% in rats (Harashima et al., 1984), guinea-pigs (Minematsu et al., 2001) and dogs (Rakhit et al., 1984; Ikenoue et al., 2000). Although this was observed in rat plasma, it was not for

the blood cell association concentration-dependence by another author (Watari et al., 1989). The dissociation binding constant for quinidine at low concentrations reverses at high concentrations as binding sites become saturated. This is a result of alpha acid-1glycoprotein (AAG) being the major binding protein for quinidine. This observation was also made in human plasma ranging from 64% to 87% (Mihaly et al., 1987). For quinidine protein binding values reported in the literature for plasma are predominantly for human. The values determined in this study are consistent with the literature range of 80% (Vozeh et al., 1987), and 84-87% (Redfern et al., 2003; Brown et al., 2007; Hardman and Limbird, 2011; Zhang et al., 2012) and up to 90% (Drayer, 1984). In silico prediction suggests plasma binding of 69.7% and 82.4% for rat and human, respectively, slightly greater than observed in this study and previously reported (Adamantis ACD).

Table 2.18 Referenced Quinidine Plasma Protein Binding Information

Species	PPB%	Fup	Reference
Rat	60 - 75	0.25 – 0.40	Harashima et al. 1984
Rat	84	0.16	Kalvass 2007
Rat	67.5	0.325	Sawada et al. 1984
Rabbit	84-94	0.06-0.16	Guentert & Oie, 1980
Rabbit	77-94	0.06-0.23	Guentert & Oie, 1982; Guentert et al. 1982
Rabbit	86	0.14	Sawada et al. 1984
Monkey	97	0.03	Sawada et al. 1984
Human	77	0.23	Sawada et al. 1984
Human	89	0.11	Drayer 1984
Human (ex vivo)	80	0.20	Vozeh et al. 1987
Human	85	0.15	Redfern et al. 2003
Human	84	0.16	Hardman & Limbird, 2011
Human	87	13	Brown et al. 2007; Zhang et al. 2012

PPB (Plasma Protein Binding); Fup (Fraction unbound plasma)

Quinidine plasma protein binding values in this study are consistent compared to literature and generally replicate the dose dependent decrease in binding with increase in concentration across species, but not the rabbit. The extent of this decrease varies and combined with the known non-linear kinetics of quinidine make the effect of translation across species more uncertain in plasma. The rabbit difference needs to be appreciated in this study and although the blood binding appeared more appropriate between rabbit to rat and human as a viable connection in physiological modelling.

2.5.11.2. Quinidine: Blood Protein Binding Results

Blood protein binding values in the rabbit (86.4% ±0.514, 84.3% ±0.380 and 82.5% ±0.361) were similar to rat (84.2% ±0.511, 81.9% ±0.893 and 79.7% ±0.928). Rabbit binding values were near to human (88.1% ±0.517, 86.9% ±0.385 and 85.2% ±0.361), although the mean human medium and high concentrations did have a noted difference (*p*-value <0.05). Rabbit, rat and human species blood binding values did not statistically show a concentration dependent change in protein binding yet a decreasing trend was observed. Both the dog (98.0% ±0.125, 92.1% ±0.291 and 85.6% ±0.353) and guinea-pig (90.6% ±0.347, 79.0% ±0.970 and 75.0% ±0.797) showed a significant difference (*p*-value <0.01) to the rabbit and again showed the greatest decrease in protein binding values with an increasing sotalol concentration (Figure 2.6B and Table 2.20B).

The protein binding values were approximately the same in blood compared to plasma, and consistent across concentrations within species, except for human which was similar to human plasma binding given the wide experimental range observed.

The blood:plasma ratios determined were similar across each species, with all values approximately close to 1 indicating that quinidine does not have the propensity to distribute into the erythrocyte cellular fraction. The rabbit B:P ratio was calculated to be 1.02 and was similar value observed in rat (1.19), dog (1.05), guinea-pig (0.95) and human (0.94). Rabbit reported literature value of 0.97 (Guentert and Oie, 1980) and human 0.87 (Brown et al., 2007), respectively, were not too dissimilar to values calculated. Literature results have been shown to vary from 0.92-1.56 for quinidine based on animal and human data (Harashima et al., 1984; Sawada et al., 1984).

Table 2.19 Referenced Quinidine Blood:Plasma Ratio Information

Species	Blood:Plasma Ratio	Reference
Human	0.87	Brown et al. 2007
Rabbit	0.97	Guentert & Oie, 1980
Mouse	1.56	Sawada et al. 1984
Rat	1.40	Sawada et al. 1984
Rabbit	1.05	Sawada et al. 1984
Monkey	1.23	Sawada et al. 1984
Human	0.92	Sawada et al. 1984

2.5.11.3. Quinidine: Heart Protein Binding Results

Quinidine protein binding values were determined in rat, dog and rabbit heart tissue. Values calculated in the rabbit at low (99.0% ±0.069), medium (98.9% ±0.105) and high (98.7% ±0.117) concentrations were similar to rat at low (98.6% ±0.253) and medium (98.4% ±0.242), whilst the highest concentration binding value of 97.6% ±0.365 (*p*-value <0.01) was significantly different. All dog heart tissue binding values were statistically different (*p*-value <0.01) at low (97.7% ±0.221), medium (97.8% ±0.159) and high (97.5% ±0.188) concentrations (Figure 2.6C and Table 2.20C). Rat, dog and rabbit did not show any concentration-dependence in tissue binding. The variability observed was very tight for the rabbit which highlights the minimal differences compared to narrow data set of values for both rat and dog. All tissue homogenate binding values were greater than those observed in plasma or blood.

2.5.12. Quinidine Protein Binding Data

Figure: 2.6A

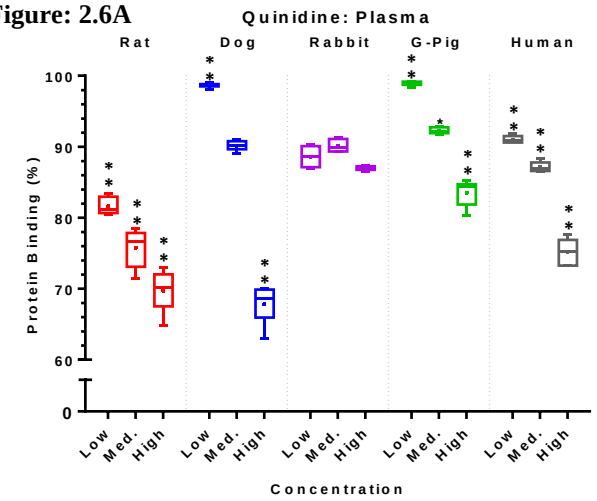

Figure: 2.6B

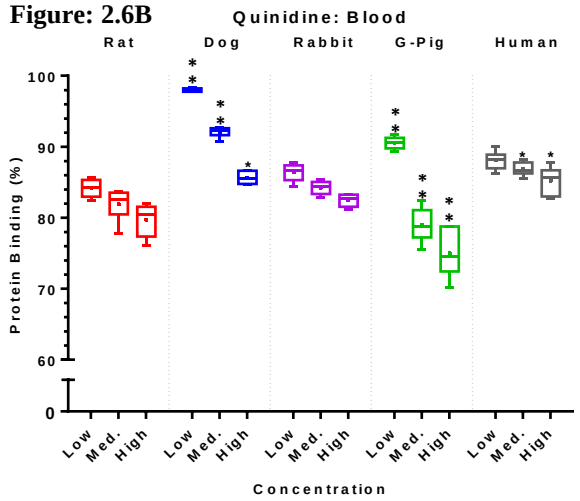

Figure: 2.6C

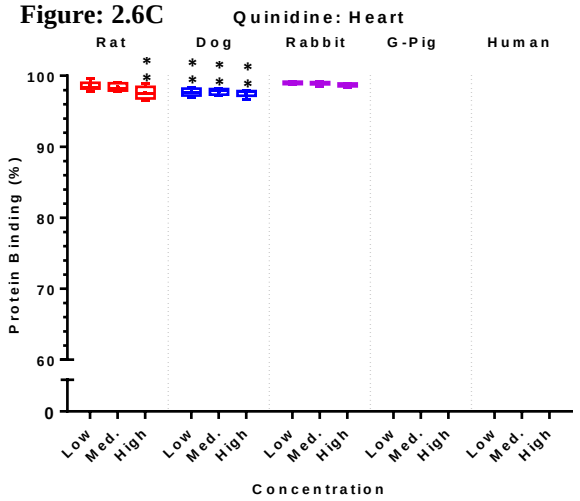

Table: 2.20A

Protein Binding (PB)	Mean Plasma				
	Rat	**Dog**	**Rabbit**	**G Pig**	**Human**
Low	81.6** ±0.485	98.6** ±0.126	88.6 ±0.594	99.0** ±0.123	91.0** ±0.207
Medium	75.8** ±1.09	90.2 ±0.282	90.1 ±0.365	92.2* ±0.183	87.1** ±0.303
High	69.7** ±1.18	67.8** ±1.08	87.0 ±0.131	83.5** ±0.755	75.2** ±0.757
Overall Mean	**75.7**	**85.5**	**88.6**	**91.6**	**84.5**

Table: 2.20B

Protein Binding (PB)	Mean Blood				
	Rat	**Dog**	**Rabbit**	**G Pig**	**Human**
Low	84.2 ±0.511	98.0** ±0.125	86.4 ±0.514	90.6** ±0.347	88.1 ±0.517
Medium	81.9 ±0.893	92.1** ±0.291	84.3 ±0.380	79.0** ±0.970	86.9* ±0.385
High	79.7 ±0.928	85.6* ±0.353	82.5 ±0.361	75.0** ±1.38	85.2* ±0.797
Overall Mean	**81.9**	**91.9**	**84.4**	**81.5**	**86.7**
B:P	**1.19** ±0.04	**1.05** ±0.06	**1.02** ±0.02	**0.95** ±0.01	**0.94** ±0.03

Table: 2.20C

Protein Binding (PB)	Mean Heart				
	Rat	**Dog**	**Rabbit**	**G Pig**	**Human**
Low	98.6 ±0.253	97.7** ±0.221	99.0 ±0.069	ND	ND
Medium	98.4 ±0.242	97.8** ±0.159	98.9 ±0.105	ND	ND
High	97.6** ±0.365	97.5** ±0.188	98.7 ±0.117	ND	ND
Overall Mean	**98.2**	**97.7**	**98.9**	**NC**	**NC**

Figure 2.6: Box plots illustrating the extent of protein binding observed across species (rat, dog, rabbit, guinea pig and human) for quinidine in plasma (A), blood (B) and heart homogenate (C) are shown in the upper pane. Concentrations of quinidine investigated were: 1,000 ng/mL (low), 10,000 ng/mL (medium) and 100,000 ng/mL (high), representing 10x below, parity and 10x above approximate clinical therapeutic concentration with respect to plasma. Corresponding tabulated data of quinidine protein binding mean values (n=6 replicates) are given for plasma (A), blood (B) and heart homogenate (C), including overall mean and ± S.E.M. Blood:plasma (B:P) ratios were determined (n=3) and tabulated with the blood binding data. The individual data were analysed by a 2-way ANOVA approach, with concentration and species as treatment factors. This was followed by all pair-wise comparisons between the predicted means of the concentration*species interaction and adjusted post-hoc using Bonferroni's multiple comparisons procedure with respect to rabbit as a comparator; *p* value <0.05 *; <0.01 **

2.6. Summary Conclusion

Protein binding values of cisapride, moxifloxacin, sparfloxacin, verapamil, sotalol and quinidine drugs were successfully investigated in rat, dog, rabbit, guinea-pig and human plasma and blood, as well as heart tissue homogenate for rat, dog and rabbit.

Following equilibrium dialysis, using the RED device, aliquots of incubated dialysed buffer and matrix (blood, plasma or heart tissue homogenate) were matrix-matched for analysis by appropriate LC-MS/MS methods (Wan and Rehngren, 2006; Banker and Clark, 2008). Protein binding values derived for particular species and compounds were in agreement to literature where comparisons could be made, adding to the validity of unknown species protein binding results for each compound (Nilsson, 2013). Replicate analysis of each compound tested with two independent preparations and consistent methodology conditions reduced analytical and experimental variability (Wang et al., 2014). Protein binding assessment using the rapid equilibrium dialysis (RED) device was shown to be a reliable, robust and reproducible method for protein binding analysis in this study, and in agreement with literature (Waters et al., 2008; Zhang et al., 2012).

In ED, two chambers are separated by a semi-permeable membrane. Plasma is placed in one chamber and a buffer in the other chamber. The buffer should be as similar to plasma water as possible and usually isotonic phosphate-buffered saline (PBS; pH 7.4) is used. This technique is usually carried out at body temperature, the extent of binding being temperature-dependent. Membranes of different thickness are available, with 12kDa being standard, and in the case of a drug that binds to the membrane, it is important to use a membrane that is as thin as possible. The molecular weight cut-off point also varies and as it decreases it may increase the length of time to reach the equilibrium. Time to equilibrium experiments can be conducted prior to ED for definitive optimised protein binding determination. Rapid dialysis systems use a membrane with high permeability. Protein binding occurs within milliseconds, and it is the diffusion equilibrium that varies (Smith et al., 2010). Using commercial membrane dialysis, 2 to 4 hours are required to reach equilibrium and a dialysis of 4 hours at 37°C has been found optimal for acidic and basic drugs (Banker et al., 2003). Under some circumstances, a longer dialysis period is required and the possible degradation of the binding proteins and/or of the drug must be taken into consideration through stability assessment.

2.6.1. Plasma Protein Binding

Regarding the data sets across species for each compound, the rabbit was generally statistically different to at least one species. This indicates the value of obtaining species specific protein binding information to determine the free fraction or free concentration relative to that species. Free concentration is important in the determination for species translation of pharmacokinetics and pharmacological effect (Nilsson, 2013).

The plasma protein binding data generated shows that the rabbit generally has the greatest similarity with human across the series of compounds tested in this study. Rat, dog and guinea-pig were equally similar and different (50:50) in comparison to rabbit as shown in summary Figure 2.7. This is too small a data set of compounds to draw conclusive interpretation for overall species similarities and would require a greater number of compounds grouped according to therapeutic target, effective concentration, and also native ionic species (acids, bases or zwitterions). Out of the 6 compounds investigated four were basic and two were zwitterions.

Figure 2.7: Summary Mean Comparison of Compound Plasma Protein Binding Across Species

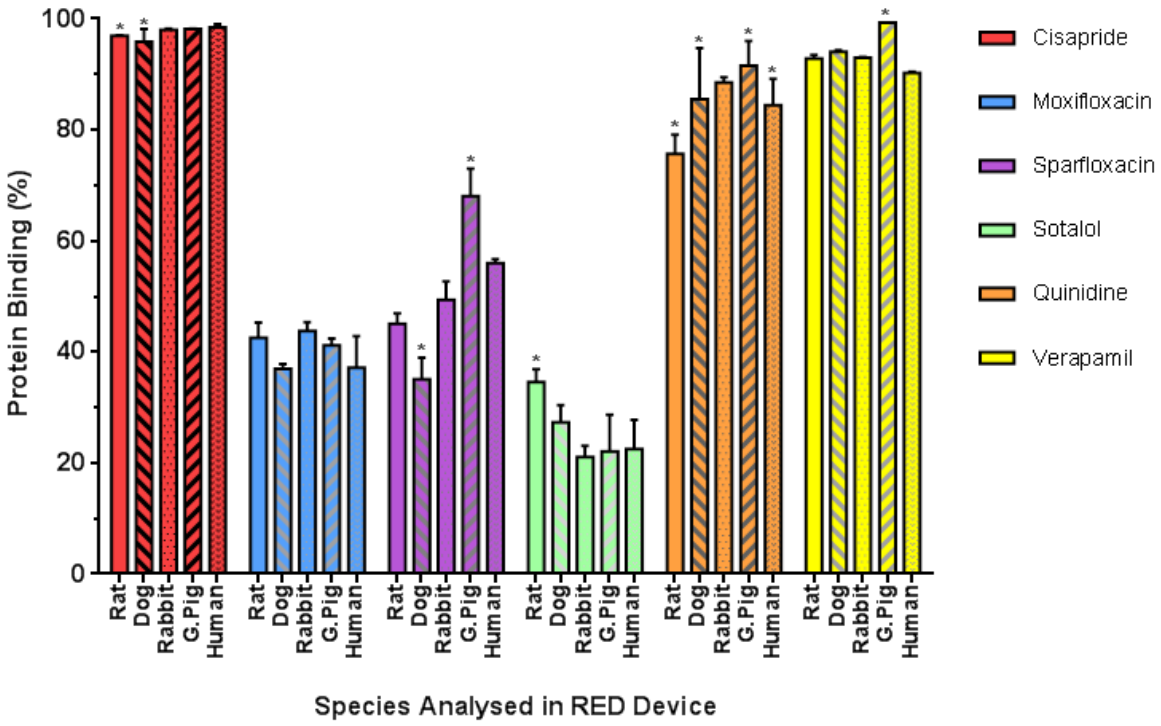

Figure 2.7: Summary mean comparison of the plasma protein binding investigated for cisapride (—), moxifloxacin (—), sparfloxacin (—), sotalol (—), quinidine (—) and verapamil (—) across a number of species (rat, dog, rabbit, guinea pig and human). The mean data were analysed by a 2-way ANOVA approach, with concentration and species as treatment factors, followed by all pair-wise comparisons between the predicted means of the concentration*species interaction and adjusted post-hoc using Bonferroni's multiple comparisons procedure with respect to rabbit as a comparator; *p* value <0.05 *

Alpha-1-acid glycoprotein (AGP, also known as AAG or orosomucoid) is an important plasma protein involved in the binding and transport of many drugs, especially basic compounds (Routledge, 1986). AGP has some unique drug-binding properties that differ from those of albumin. For example, the plasma concentration of AGP is relatively low and there is only one drug-binding site in each AGP molecule, thus binding to AGP is saturable and displaceable.(Huang and Ung, 2013).

Quinidine (Nilsen et al., 1978) and verapamil (McGowan et al., 1983) have been shown to bind significantly to AGP. A nonlinear change in protein binding was observed for quinidine compared to verapamil binding due to saturation of the binding sites on AGP (1:1) as the therapeutic concentration of quinidine was approximate to the endogenous protein level (Guentert and Oie, 1982; Mihaly et al., 1987). Within this study a 10-fold span above and below this, resulted in the reduction in protein binding of quinidine whereas verapamil concentrations were below this threshold and thus no change in binding with concentration observed. Similarly, the same statement is true for the protein binding observed for cisapride, which was assessed at the same concentrations as verapamil. For sotalol, which is a relatively small molecular weight molecule (M.wt. 272), positively ionised, logP near zero, the opposite trend was observed in comparison to quinidine. This potentially is a result of the increasing concentration of sotalol and increased electrostatic interactions. It has been noted in literature the sotalol protein binding is often quoted as negligible or <1% but then not assessed for contributing HSA or AGP binding (Belpaire et al., 1982). It has been shown that extended dialysis results in decreased concentrations of immunoreactive AGP and increased free fraction, such that these PPB experiments are from 24 hour incubations (Morse et al., 1985). Conversely a varied range of low binding has been quoted from 20-40% (Giudicelli et al., 1973; Fiset et al., 1993) where binding has been determined which may indicate the increased change in binding, and reflect the data observed in this study.

Altered plasma AGP levels affects pharmacokinetic parameters of basic antimicrobials (Kuroha et al., 2001). However in this study, both antimicrobial agents, moxifoxacin and sparfloxacin are fluoroquinolones, which exist as zwitterions at neutral pH and were similar across all the species. As a result the dual charge means it is largely buffered by its binding to serum albumin and not affected in the same way (Siefert et al., 1999a).

2.6.2. Blood Protein Binding

Blood protein binding was investigated in simultaneous fashion to plasma for each of the compounds and the blood:plasma ratios determined. Data generated in this study demonstrates that blood protein binding in the rabbit was generally statistically different for any given compound in comparison to other species. A greater variability in results was observed across each of the species, concentrations and compounds relative to plasma as shown by S.E.M. For the compound data set analysed the blood:plasma ratios were consistent across species and comparable to the limited species specific data reported in literature. The differences observed may result in part from the subtle changes in species haematocrit levels or species differences in protein levels. Observed haematocrit values were similar to industry accepted values, 0.36 for the rabbit compared to 0.42 in the dog, 0.44 for human and 0.46 for rat (Davies and Morris, 1993).

For moxifloxacin and sparfloxacin the percent bound was generally greater for each species compared to plasma protein binding. This is a reflection of the preferential distribution for these fluoroquinolones for red blood cells as indicated by the relatively higher blood:plasma ratios (Zlotos et al., 1998a; Zlotos et al., 1998b). Both sotalol and quinidine demonstrated similar blood binding to that of plasma as the blood:plasma ratios were approximately equivalent to 1, and these compounds again clearly demonstrated changes in binding with quinidine binding reduced and sotalol binding increased, respectively with increased concentrations. Whilst for cisapride and verapamil, with blood:plasma ratios less than 1, the blood protein binding was observed to be lower than that in plasma.

2.6.3. Heart Tissue Binding

Tissue protein binding investigated with heart homogenate was successfully completed for all compounds using rat, dog and rabbit heart tissue. Heart binding values calculated in the rabbit were generally similar to both rat and dog tissues. Statistical differences were observed but this appears to be a result from very limited variability in data at each concentration and species for each compound as shown in a summary comparison of the mean heart binding (Figure 2.8).

Figure 2.8: Summary Mean Comparison of Compound Heart Protein Binding Across Species

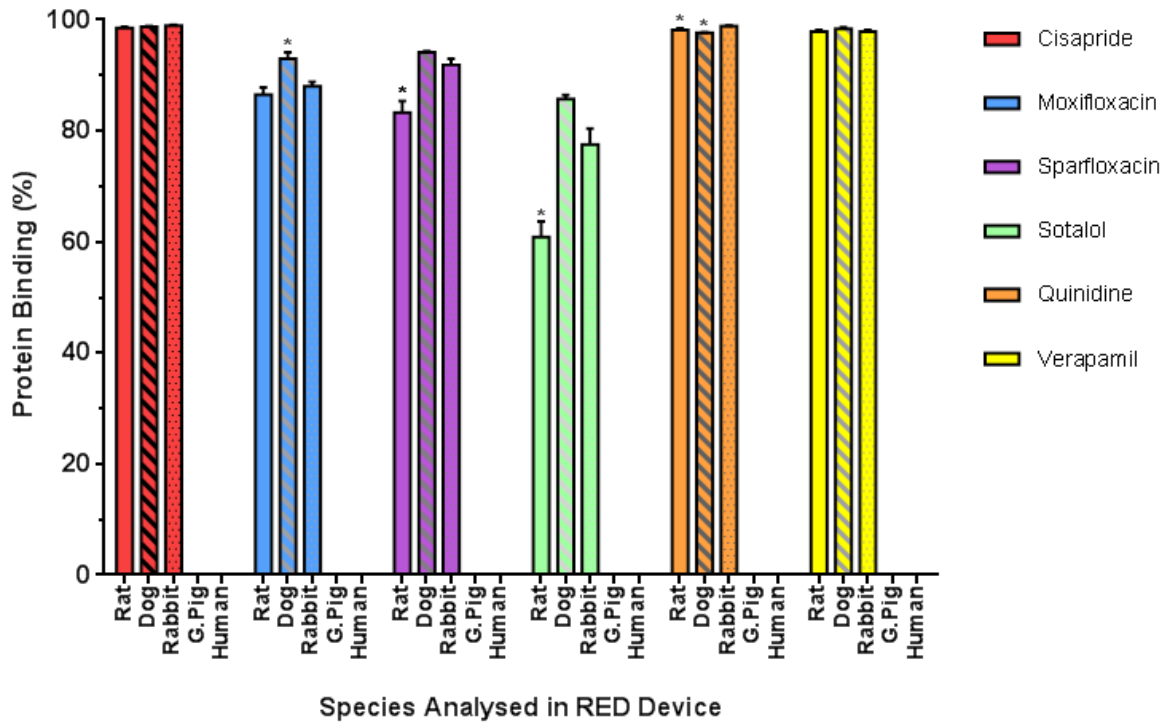

Figure 2.8: Summary mean comparison of the heart tissue protein binding investigated for cisapride (—), moxifloxacin (—), sparfloxacin (—), sotalol (—), quinidine (—) and verapamil (—) across a number of species (rat, dog and rabbit). The mean data were analysed by a 2-way ANOVA approach, with concentration and species as treatment factors, followed by all pair-wise comparisons between the predicted means of the concentration*species interaction and adjusted post-hoc using Bonferroni's multiple comparisons procedure with respect to rabbit as a comparator; *p* value <0.05 *

The variability and range was less in heart tissue homogenate than in either plasma or blood. This reduced variability was unexpected given the nature of the matrix being investigated compared to plasma and blood. It has been reported that the density and viscosity of the homogenate can prevent feasible dialysis, such that the membrane becomes blocked during ultrafiltration (Pacifici and Viani, 1992). In this study this was overcome by having homogenates that were easily and accurately dispensed with a pipette, good agitation in the incubator and porous breathable membrane to prevent homogenate gelling whilst incubated at 37°C. Homogenates were prepared following tissue section slicing (combining 50x 12 µm slices in replicates) and homogenised (1:5 w/v) with physiological buffered saline (pH 7.4). Using microtome prepared tissue allowed for simple vortex mixing of sample tissue tubes containing silica beads to obtain suitable matrices for dialysis with the RED device. From this study it is unclear if this tissue homogenate are too dilute (1:5) and give misleading results (Pacifici and Viani, 1992) as this would require a range of buffer:tissue homogenate ratios to

be investigated. Therefore an assumption from this data is that the tissue binding reflects the true drug protein association. If the tissue content was too low for drug protein binding then either peak-area ratios would not be obtainable from the sampled homogenate or calculated binding values would be considered low/negligible as a result of essentially performing equilibrium dialysis between buffers, which was not the case in the tissue analysis. Tissue protein binding using homogenates in the RED device were reported and dilution factor taken into account, in a similar fashion for brain protein binding (Kalvass and Maurer, 2002; Summerfield et al., 2006; Kalvass et al., 2007; Summerfield et al., 2008). This study adopted a similar tissue preparation to that reported in literature methodologies either using saline, deionised/distilled water or PBS buffer. Protein binding using tissue homogenates in the RED device have been reported for brain (Kalvass and Maurer, 2002; Summerfield et al., 2006; Kalvass et al., 2007; Summerfield et al., 2008), liver and pancreas (Pfefferkorn et al., 2011).

There is limited literature discussing protein binding across species or different tissue assessments; one example describes a developmental drug that was shown to vary considerably between species (Nilsson, 2013); whilst another compared protein binding of propanolol and taxol across a range of tissues in rat (Xia et al., 2009). The latter made an assessment using a multi-compartmental 96-well *cRED* device where tissue homogenates are placed inside discrete membrane chambers immersed in a pool of drug spiked plasma. Both tissue homogenates and plasma are equally diluted. Tissue homogenates have been utilised to mirror the technique employed for the plasma/blood binding assessment. Its major advantage is the simplicity and application into the widely used 96-well rapid equilibrium device, but also this simplicity is disadvantage. Conversely, too dilute a homogenate will make the protein content too low for drug protein association, which may be misleading (Pacifici and Viani, 1992; Mariappan et al., 2013).

All compounds investigated had greater heart tissue protein binding values compared to plasma or blood. It is accepted that one main disadvantage of the homogenisation process is the destruction of tissue architecture and disruption of the cellular/subcellular components which may unmask additional binding sites not readily available in the intact tissue. A consideration to reduce the potential for unmasked binding sites or non-specific binding would be the addition of protease inhibitors to prevent structural protein degradation of tissue during preparation. For these compounds investigated all have cardiac tissue targets, namely ion channels. These transverse the cardiomyocyte membrane and with cellular disruption

may expose greater access to the intracellular side of the channels for occupancy, and possibly in addition to any extracellular ion channel binding. Also tissue binding will be dependent on each compounds affinity or specificity (IC_{50}) for the target ion channels, such as hERG K^+ channel for compounds like cisapride, moxifloxacin, sparfloxacin and sotalol, or Ca^{2+} channel by verapamil, or Na^+ channel by quinidine as well as propensity to bind to other channels or cellular components at increasing concentrations.

2.6.4. Importance of Protein Binding

2.6.4.1. In silico

Plasma protein binding (PPB) is relevant in the pharmacokinetic modelling of drugs and specific pharmacokinetic parameters which may be affected by protein binding, such as volume of distribution, clearance and half-life. In early discovery and chemistry there is a need to understand the implications of the physical-chemical properties of drugs and the impact on such in vivo parameters. As a result many in silico prediction methods for protein binding are now available in software packages such as ACDLabs, ADMET Predictor, SimCYP. These packages incorporate various aspects of in silico predictions relevant to estimating binding and clearance from structural moieties and physico-chemical properties (Emoto et al., 2009). The in silico methods require the molecular structure and/or physicochemical parameters such as log *P*o:w (octanol:water) and log *D*o:w at pH 7.4, and *pK*a values as input, which themselves are not always experimentally measured at the early stages of discovery. Again, some commercially available software packages such as ACDLabs, ADMET Predictor, SimCyp and GastroPlus can be used for the prediction of these physico-chemical parameters based upon molecular structure (Rodgers et al., 2005; Rodgers and Rowland, 2006). Recently, there have been further advances in the predictive approaches using Quantitative-Structural Activity Relationships (QSAR) incorporating additional MOE and Symyx QSAR software packages, using data mining and regression analysis tools to accurately predict PPB for 794 structurally diverse compounds (Ghafourian and Amin, 2013), but did not contain any of the six compounds investigated in this thesis.

2.6.4.2. In vitro

Often in vitro cell assays require minimum protein content for viability and functionality, for example in the assessment of kinase and proteinase inhibitors, cell-based assays require 5-

20% foetal bovine serum as part of the discovery program. Foetal bovine serum is the most commonly used plasma protein, and although often at low concentrations a significant amount of drug may still bind, but give a perception of greater target potency due to the relative free amount of drug. It is common that potency in a cell based assay is worse than the potency in a protein based biochemical assay. The underlying mechanisms of the shift may include different PPB, cell membrane permeability, membrane drug transport, endogenous ligands and/or ligand concentrations. Therefore it is most appropriate to determine the free unbound fraction in the in vitro cell medium ($f_{u,\ medium}$), which will correct for any changes in protein concentration (Equation 4) (Liu et al., 2014). This has been demonstrated for a number of antiretroviral drugs such as lopinavir (Molla et al., 1998; Boffito et al., 2003).

$$f_{u,medium} = \frac{1}{(protein\ \%)\ x\ \left(\frac{1}{f_u} - 1\right) + 1} \qquad \text{Equation 4}$$

2.6.4.3. In vivo

Decreases in PPB leads to an increase in unbound concentration based on the definition of protein binding. This is true for in vitro systems, however for in vivo systems; the unbound concentration does not depend on PPB after oral administration. The relationship between dose and plasma concentration is given as follows;

$$AUC_{total} = \frac{F\ x\ Dose}{Cl_{total}} \qquad \text{Equation 5}$$

Where, F is the oral bioavailability, and Cl_{total} is the total clearance (hepatic, renal, metabolic). AUC_{total} is the area under the total plasma concentration-time curve, which represents the overall drug exposure.

If hepatic clearance is assumed to be the major clearance mechanism, then Cl_{total} may be determined by intrinsic clearance, PPB and hepatic blood flow rate. The relationship between total clearance and PPB can be described by a number of mathematical models (Pang and Rowland, 1977a; Pang and Rowland, 1977b; Roberts and Rowland, 1986); the most commonly used is the well-stirred model. This describes hepatic clearance as;

$$Cl_{total} = \frac{Q\ x\ f_u\ x\ Cl_{in}}{Q + f_u\ x\ Cl_{in}} \qquad \text{Equation 6}$$

Where, Q is the hepatic liver blood flow and Cl_{in} is the hepatic intrinsic clearance. This demonstrates that the lower the PPB is, the higher f_u is, and the higher Cl_{total} becomes. This

concept is important in drug design as an increase in clearance is often ascribed to an increase in metabolic rate.

For orally administered drugs, PPB also affects the oral bioavailability (*F*) in the same way using the theory behind the well-stirred model, making the assumption that absorption is complete and there is no gut metabolism.

$$F = \frac{Q}{Q + f_u \, x \, Cl_{in}} \qquad \text{Equation 7}$$

This demonstrates that the lower PPB is, the higher the f_u, the lower the oral bioavailability becomes. This concept is often neglected as low oral bioavailability is often associated with low solubility, permeability and metabolic stability.

$$AUC_u = \frac{Dose}{Cl_{in}} \qquad \text{Equation 8}$$

Therefore by insertion of Equations 6 and 7 into Equation 5 (above), this shows that a gain of unbound concentration in vivo by an increase of f_u is countered by an increase of the clearance and a decrease of the oral bioavailability. This demonstrates that there is no net gain for the in vivo unbound drug concentration, by just reducing PPB without reducing intrinsic clearance (Berezhkovskiy, 2010). This statement is true for all drugs orally administered and eliminated hepatically and to all low extraction drugs regardless of route. Total exposure is independent of protein binding, and results in no change in exposure or pharmacological effect – the total plasma drug concentration may change but seldom leads to a change in free plasma concentration, so it is free drug exposure that remains constant (Benet and Hoener, 2002).

The pharmaceutical industry has learnt that drug discovery should not optimise or limit protein binding but understand its implications with respect to pharmacokinetic drug disposition and pharmacological efficacy (Smith et al., 2010; Bohnert and Gan, 2013; Mariappan et al., 2013). Protein binding is important to inform and aid the increasing requirements for in silico PBPK modelling in support of drug development (Smith, 2012).

Data from this protein binding and blood:plasma investigation has been generated to demonstrate that there is value in obtaining species specific protein binding data and that the rabbit can be significantly different to ther species. This precludes the assumption that the protein binding or fraction unbound values are conserved across species.

In the following chapter, compounds are administered to the rabbit ventricular wedge (RVW) tissue preparation in a protein free buffer, and that it is assumed this equates to the free heart tissue concentration driving the QTc response. Therefore as it is the free drug concentrations that exert the PD response and used in the subsequent E_{max} model of QT.

The fraction unbound in rat and rabbit plasma along with the corresponding B:P ratios are key parameters that were used in Chapter 5 for the PBPK/PD in vivo modelling. These parameters were used in the allometric scaling approaches (single-species and liver blood flow, Equation 11 and 13), to convert the rat total clearance (CL_p) parameter obtained from the intravenous pharmacokinetic study to prospectively predict and simulate rabbit plasma concentration profiles. The plasma protein binding and B:P ratio were also utilised in the PBPK modelling software GastroPlus™ as an input parameter to determine the amount of drug eliminated from excretory tissues (liver and kidney, Equation 15) as well as in the determination of the individual tissue partition coefficients (Equation 19 and 20).

The subsequent simulated PBPK output and the actual pharmacokinetic plasma and heart concentration-time profiles of the in vivo rabbit model need to be put in context with the observed pharmacological QT response by using the fraction unbound in plasma and heart tissue generated from the protein binding studies to aid this interpretation.

CHAPTER 3

Rabbit Ventricular Wedge Model

3. RABBIT VENTRICULAR WEDGE

The ICH S7B guidelines recommend an integrated assessment to evaluate the overall cardiovascular risk. As a minimum, in support of any in vitro hERG assay screening an in vivo study should be conducted (S7B, 2005). However due to the relative expense and ethical considerations, the pharmaceutical industry adopt a tiered approach and therefore within GSK an interim ex vivo assessment of QT using the rabbit ventricular wedge is conducted (Pollard et al., 2010).

The rabbit ventricular wedge assay forms part of a core battery of assays within GSK's CV strategy to assess the arrhythmogenic potential of compounds prior to, or nearing candidate selection. This is aimed at identifying compounds with unwanted cardiovascular effects and reduces CV liabilities early in drug development. Specifically, the rabbit ventricular wedge preparation is a functional, multiple-ion channel assay that assesses parameters such as QT, QRS, contractility, action potentials and proarrhythmia (including ventricular tachycardia, ventricular fibrillation and *Torsade de pointes* (TdP)).

The purpose of this study was to generate change in QT interval data for several compounds, cisapride, moxifloxacin and sparfloxacin (and verapamil), known for their potential to prolong QT interval and assess in the rabbit isolated perfused ventricular wedge preparation. The aim was to generate a concentration-response model of QT change for each of these compounds in the ex vivo rabbit wedge to enable comparison across compounds based on relative potency of the hERG ion channel. This concentration-response model obtained was combined with the fraction unbound (plasma and heart) and B:P ratio information generated (Chapter 2) to enable prospective translational physiological-based pharmacokinetic and pharmacodynamic (PBPK/PD) modelling of the rabbit (Chapter 5) against the information generated in an anaesthetised rabbit preparation (Chapter 4).

3.1. Background to Rabbit Ventricular Wedge

The arterially (coronary) perfused ventricular wedge preparation was first developed to study the electrical heterogeneity of canine left ventricular myocardium (Yan and Antzelevitch, 1996). At the time of the implementation of the ICH guidance S7A, its use was limited in the pharmaceutical industry (Hammond et al., 2001; Joshi et al., 2004), but following several assessments the rabbit left ventricular wedge preparation appears to be a favoured ex vivo model to assess the electrophysiology across the endo-, mid- and epi-myocardium (Liu et al., 2006; Wang et al., 2008). As its name suggests a cross sectional 'wedge' (commonly left ventricle wall) is perfused via cannulation of subsidiary branches of the right coronary artery and submerged in an organ perfusion bath. There are a number of well recognised technical difficulties in making a successful preparation (Lawrence et al., 2005), but despite these it has been used to identify the mechanism underlying the generation of arrhythmias for some QT-prolonging agents (Chen et al., 2006). The rabbit left ventricular wedge preparation is highly sensitive to QT-prolonging drugs because the left ventricular endocardium has a very small I_{Ks} (Xu et al., 2002) component so that even weak QT-prolonging agents can prolong the QT interval substantially at a slower pacing rate. The most recent progression in this preparation is the use of optical and electrical mapping to visually follow the electrophysiological changes across the ventricular wall (Di Diego et al., 2013).

3.2. Rabbit Ventricular Wedge Experiments

All in vivo experiments were ethically reviewed and carried out in accordance with Animal (Scientific Procedure) Act 1986 and the GlaxoSmithKline (GSK) policy on the Care, Welfare and Treatment of laboratory animals and under the authority of Project Licence No PPL P265EEA6E 19b PR0 (in vitro/ex vivo). All personnel involved in the conduct of scientific procedures on animals did so under the authority of a Home Office Personal Licence issued under the Act.

3.2.1. Surgical preparation

Surgical preparation of the rabbit left ventricular wedge has been described in detail in previous publications (Yan et al., 2001). In brief, female rabbits (New Zealand White) weighing 2.5–3.0 kg were anti-coagulated with heparin (800 UI/kg) and sedated by intramuscular or subcutaneous injection of xylazine (5-6 mg/kg), then anesthetised by intravenous administration of ketamine hydrochloride (30–35 mg/kg) or pentobarbital (50 mg/kg). The chest was opened via a left thoracotomy, and the heart was excised and placed in cold (4°C) cardioplegic Tyrode's solution containing 24 mM potassium chloride (KCl), buffered with 95% O_2/5% CO_2. The left circumflex/descending branch of the coronary artery was cannulated and perfused with cold cardioplegic solution. A transmural wedge is dissected from the left ventricle (approximately 1.5cm x 3cm). Unperfused areas of the left ventricle were removed, which were easily identified by their reddish appearance due to the existence of residual erythrocytes (red blood cells). The preparation was then placed in a small tissue bath and arterially perfused with normal Tyrode's solution containing 4 mM KCl buffered with 95% O_2 and 5% CO_2 (temperature: 35.7 ± 0.1°C, mean perfusion pressure: 30–45 mmHg). The preparations were stimulated at a frequency of either, 0.5 Hz, 1 Hz, or 2 Hz using a stimulating electrode applied to the endocardial surface of the tissue. The tissue viability and signal response were maintained for 4 hours

3.2.2. Perfusion Media

3.2.2.1. Tyrode's Solution

Tyrode's solution (pH 7.38-7.42) was freshly prepared on each day of experimentation and contained (mM): NaCl (129), KCl (4), $CaCl_2$ (1.8), $MgSO_4$ (0.5), NaH_2PO_4 (0.9), $NaHCO_3$ (20), glucose (5.5). The solution was gassed with 95% O_2 / 5% CO_2 for at least 30 minutes prior to the addition of $CaCl_2$. The gassed Tyrode's was contained in a reservoir from where it was pumped to perfuse the preparation via the cannula.

3.2.2.2. Cardioplegic solution

The cardioplegic solution was formulated by adding additional potassium chloride (KCl) to 1000 mL of Tyrode's solution to give 24 mM KCl and the pH of the solution was adjusted to 7.38-7.42.

Figure 3.1: Freshly Excised Rabbit Heart

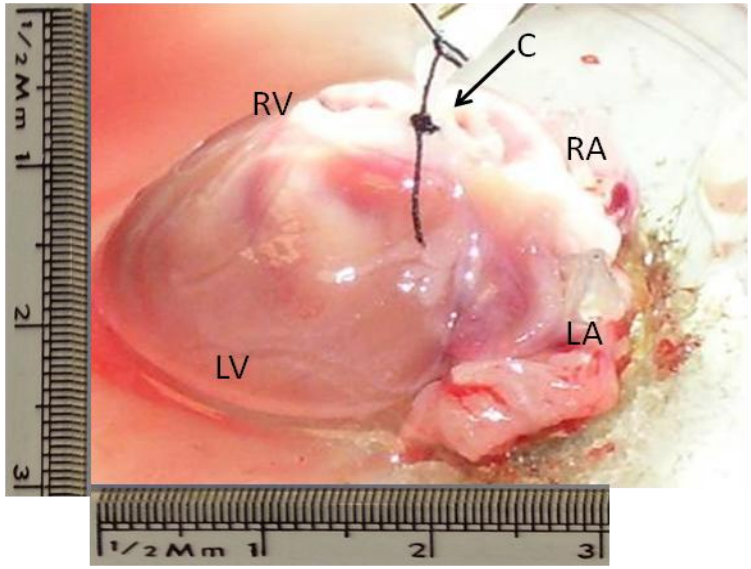

Figure 3.1: Freshly excised rabbit heart pictured bathed in normal Tyrode's cardioplegic solution at +4ºC. The tissue is arterially perfused with Tyrode's solution containing 24 mM potassium chloride (K^+), buffered with 95% O_2/5% CO_2, via a small branch of the left descending coronary artery accessed via the aorta (arrow C). The left ventricle becomes pale following perfusion and removal of red blood cells, any redness is indicative of ischemic areas. The atria (LA and RA) and the right ventricle (RV) are removed, with the left ventricle (LV) opened out exposing the papillary muscle and the endocardial surface. The left ventricle is further trimmed of any unperfused areas to leave a transmural "wedge" with dimensions of approximately 1.5 cm wide and 2-3 cm long ready for transfer.

Figure 3.2: Arterially perfused rabbit ventricular wedge preparation

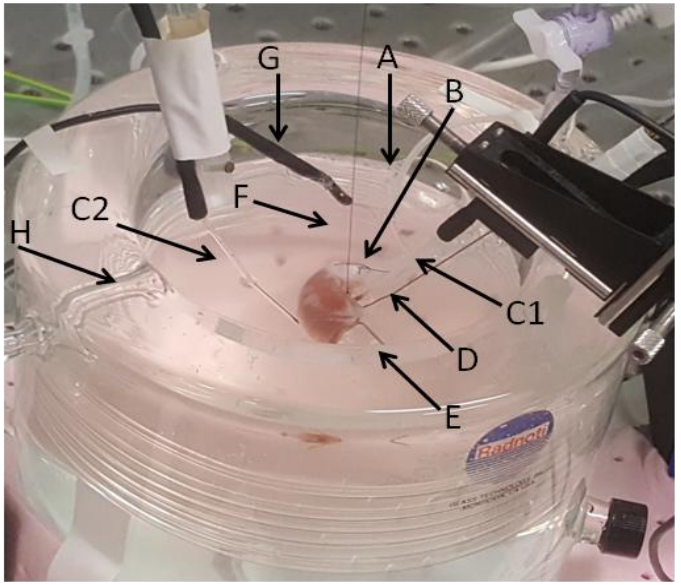

Figure 3.2: Arterially perfused rabbit left ventricular wedge preparation pictured in situ. The ventricular wedge is placed in a jacketed tissue bath (temperature: 35.7 ± 0.1°C) with Tyrode's solution containing 4 mM K^+ buffered and gassed with 95% O_2 and 5% CO_2 [**A**]. The tissue is perfused with same Tyrode's solution during equilibration, then containing vehicle and test article, at a mean perfusion pressure 30–45 mmHg, through the previously implanted cannula [**B**]. A transmural ECG signal is recorded using extracellular silver/silver chloride electrodes placed in the Tyrode's solution bathing the preparation 1.0 to 1.5 cm from endocardial ("-" pole) [**C1**] and the epicardial ("+" pole) [**C2**] surfaces following pacing stimulation probe [**D**] placed near the endocardial apex to propagate signal transduction and mimic contraction. The ventricle wedge is maintained in position with a suture pin [**E**], whilst a tension suture hook [**F**] connected to a force transducer which records contractility. Within the water bath a grounding earth /reference electrode is placed [**G**]. Excess perfusion media is drained via an overflow and pump [**H**].

Figure 3.3: Arterially Perfused Rabbit Ventricular Wedge Preparation Set Up

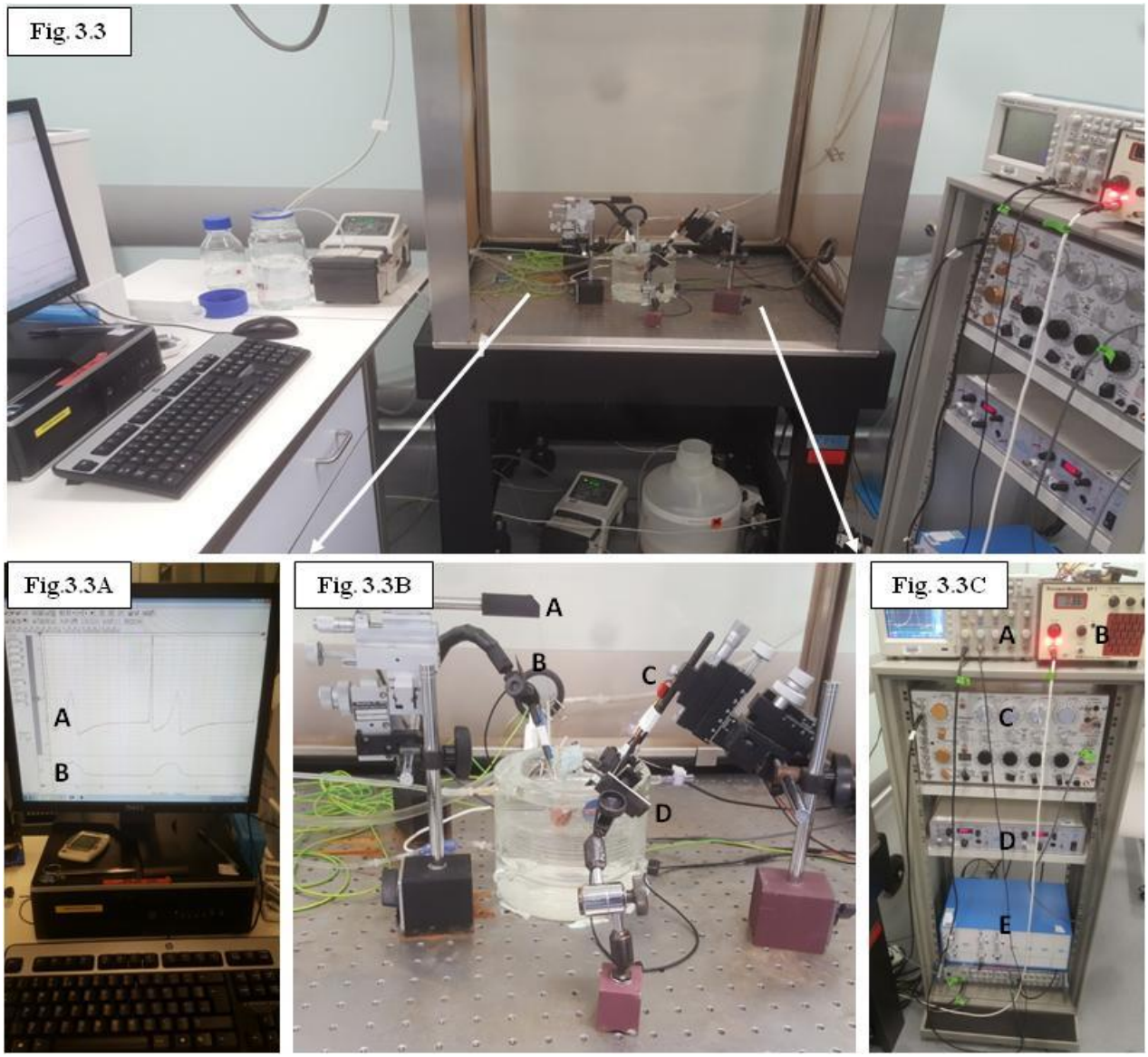

Figure 3.3A: The continuous recording of ECG waves [**A**] and contraction signals [**B**] is within pClamp software and analysed in Clampfit. Trace data is visually overlaid and captured data is stored for reference (Digidata 1440A, pCLAMP v10, Molecular Devices, MDS Analytical Technologies).

Figure 3.3B: Tissue water bath containing the arterially perfused left ventricular wedge with electrodes positioned around using stereotaxic clamps , with the force transducer [**A**], epicardial electrode [**B**], endocardial electrode [**C**] and stimulating electrode [**D**].

Figure 3.3C: Shows the equipment units containing Digital Storage Oscilloscope TDS-2014 (Tektronix) [**A**]; Blood Pressure Monitor BP-1, and BLPR2 fluid filled perfusion pressure transducer (World Precision Instruments, Inc.) [**B**]; Grass S88 Stimulator and SIU5 stimulus isolation unit (Grass Telefactor) [**C**]; Isometric force transducer, positioner/tensioner (World Precision Instruments, Inc.) [**D**]; Iso-DAM8A amplifier (World Precision Instruments, Inc.) [**E**].

3.2.3. Electrode Stimulation

A transmural ECG signal was recorded using extracellular silver/silver chloride electrodes placed in the Tyrode's solution bathing the preparation 1.0 to 1.5 cm from the epicardial ("+" pole) and endocardial ("-" pole) surfaces, along the same vector as the transmembrane recordings. Transmembrane action potentials can be recorded from epicardium (epi) and endocardium (endo) using floating glass microelectrodes but were not carried out. ECG and contraction signals were monitored at 1 kHz and digitally recorded using pClamp version 10.

The primary basic cycle length used to pace the preparation from the endocardial surface was 1 Hz (1 second), with two other pacing lengths of 0.5 Hz and 2 Hz also used for analysis of bradycardiac and tachycardiac effects.

Following one hour equilibration at 1 Hz frequency in the tissue bath, the ventricular wedge preparation has been shown to achieve electrical stability (Yan et al., 2001). Electrical recordings were made at 1 Hz, the maintenance pacing frequency, before the stimulation frequency was reduced to 0.5 Hz for a 5 minute period of stabilisation after which baseline ECG and contractile force (CF) were recorded. Then the stimulation frequency was increased to 2 Hz for a period of 30 seconds stabilisation only, after which baseline ECG was recorded. The preparations were then returned to 1 Hz at a maintenance pacing frequency and perfused with Tyrode's solution containing a test compound (Figure 3.4).

3.3. Rationale for Concentration Selection

Concentrations for each test compound were selected to bracket the hERG IC_{50} (or $Na_v1.5$) while aiming to provide at least a 100-fold safety margin above the estimated clinical free C_{max} at an efficacious dose. Four ascending concentrations were tested at Log or ½ Log units from at or around, the known clinical free C_{max} e.g. 0.1, 1, 30 and 100 µM.
Stock solutions were dissolved in DMSO, with the exception of sparfloxacin which was dissolved in 0.2 N NaOH, and these were diluted in Tyrode's solution to produce perfusion solutions. The vehicles were either 0.1% or 0.3% v/v DMSO in Tyrode's solution. The test substance perfusion solutions were freshly prepared on each day of experimentation. Solutions were gassed with 95% O_2 / 5% CO_2 and pH adjusted to 7.38-7.42 prior to use.

Four compounds were prepared as DMSO stock solutions at a concentration of 1000- fold (cisapride and verapamil) or 300-fold (sparfloxacin and moxifloxacin) greater than the

highest concentration administered in this study, such that cisapride, verapamil and sparfloxacin stocks were 10 mM and moxifloxacin was 3 mM.

Each rabbit wedge preparation acted as one treatment group and its own control as vehicle was administered first followed by 4 concentrations of each compound, in ascending order, at each concentration for approximately 30 minutes such that two concentrations were below and two concentrations were above reported hERG IC_{50} values. Each compound was tested in at least four rounds (total of 4 × 4 = 16 rabbits). All concentrations are nominal and expressed in terms of the parent compound.

3.4. Test Substance Addition

Following administration of Tyrode's during the equilibration period each preparation was exposed to each of the 4 drug concentrations for a period of 30 minutes prior to beginning of recorded data collection ("R") (Figure 3.4). For each test concentration, wedge preparations were perfused for 30 minutes and stimulated at a frequency of 1 Hz followed by 5 minutes at 0.5 Hz during which ECG and CF were recorded. The total drug perfusion time at each concentration was up to 40 minutes, and then the perfusion pump was switched to the next test compound concentration. At the maximum test concentration, ECG and CF were recorded for 30 seconds at 2 Hz following the 0.5 Hz recordings. The total time course for one experiment was approximately 5 hours for which the ventricular tissue was viable for.

Figure 3.4: Schematic protocol time course for perfused rabbit wedge.

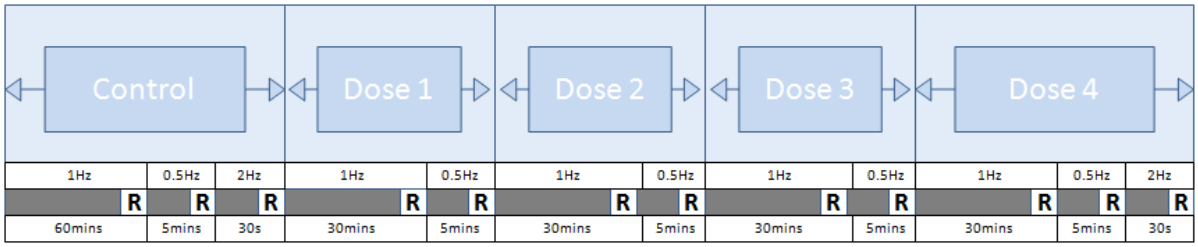

Figure 3.4: Schematic protocol time course for perfused rabbit wedge. The sequential steps of control/equilibration period for at least 60 minutes and subsequent increase in test compound concentration administration termed "Dose 1", "Dose 2", "Dose 3" and "Dose 4" for up to 35-40 minutes. The stimulation pacing frequency applied to the endocardial surface is indicated as 1 Hz as the primary basic cycle length used to pace the preparation, with two other pacing lengths of 0.5 Hz and 2 Hz also used for analysis of bradycardiac and tachycardiac effects. Data was continuously monitored in pClamp (version 10) at a capture rate of 1000 ms and at the end of each stimulation period ECG waves are recorded "R" for 30 seconds for analysis by Clampfit.

3.5. Electrophysiological Data Analysis

All electrophysiological data was captured within pClamp (Digidata 1440A, pCLAMP v.10, Molecular Devices, MDS Analytical Technologies) and analysed using Clampfit. From the 30 second recorded ("R") data at each step, only an average 4 sweeps/ECG traces in Clampfit were analysed to derive parameters.

The electrocardiogram (ECG) was recorded (Iso-DAM8A Amplifier, World Precision Instruments), to enable identification of the electrocardiogram parameters; QT interval, QRS interval, as well as transmural dispersion of repolarisation (TDR).

On the ECG, the QT interval was defined as the time from the onset of the QRS to the point at which the final downslope of the T-wave crossed the isoelectric line. The Tp-e interval, which closely approximates transmural dispersion of repolarisation (TDR), was defined as the time interval between the T-wave peak to the end of the T wave. The QT and Tp-e intervals were measured manually in four consecutive beats within the last minute of the recording and the values were then averaged.

The Isometric Contractile Force production (ICF) was recorded (World Precision Instrument isometric force transducer/ Radnoti 159901A Isometric force transducer) to determine the percent change in isometric contractile force. On the contractile force trace, the peak of contraction was measured and converted from force measurement with respect to baseline at each test compound concentration expressed as a percentage change (Appendix 3).

3.5.1. Statistics for QT Response

2-Way ANOVA was conducted on each variable and each frequency separately, for analysis of concentration-response compared to pre-treatment, as well as between tissue comparisons. This was followed by Dunnett's test for statistical significance, where if the p-value of the Dunnett's t-test was <0.05, the difference between the treatment and the control was considered statistically significant.

3.5.2. Non-Linear Fit for QT Response

Data for QT response generated following analysis of waveforms in Clampfit was imported into GraphPad PRISM® for plotting. Data was transformed for analysis fitting of a commonly used PD model, based on the sigmoidal E_{max} model, which describes non-linear concentration-effect relationships (Equation 9).

$$E = \frac{E_{max} \times {C_p}^n}{{EC_{50}}^n + {C_p}^n} \qquad \text{Equation 9}$$

Where E is the QT effect as a function of E_{max}, which is the maximum effect, C_p is the plasma drug concentration, EC_{50} is the concentration of drug producing half maximal effect and n is the Hill coefficient referred to as the shape factor.

All the vehicle control QT response (ms) values from n= 32 preps, (GSK RVW validation data sets, not shown) were used for a mean baseline QT response (ms) for each compound. This mean baseline was used to generate a 'surrogate' individual vehicle corrected delta QT to give some baseline experimental RVW preparation variability with each vehicle control. As a vehicle control correction should result in little or no change in QT interval. The vehicle control is '0 µM' of test compound, which cannot be log-transformed, so this has been set against an arbitrary small reference value 1.0 $x10^{-10}$µM (1.0 $x10^{-16}$M) to enable the data to be logged. Therefore against each compound data set a baseline best fit value was determined as the bottom minimum value which would be associated with some error.

If the maximum change in QT response from baseline is considered then there must be a physiological upper limit possible for the rabbit ventricular wedge. This would be equivalent to total K^+ channel blockade and independent of any other channels, such as Na^+, influencing the QT interval. From internal and literature review the maximum change in delta QT appears to 200% (Liu et al. 2006). Therefore in the sigmoidal response model an upper limit has been set to 700 ms which equates to approximately 200% delta QT from baseline which based on literature and in house GSK values is approximately 300 – 350ms.

3.6. Assumptions and Limitations of the RVW:

As with any in vitro/ex vivo experimental technique there are inherent limitations which are not just only pertinent to the rabbit ventricular wedge preparation which cannot completely mimic the in vivo conditions (Lawrence et al., 2008; Hamon et al., 2009). The aim was to use rabbit ventricular wedge QT response and generate a concentration-response model for each compound, which is subject to a number of assumptions and/or limitations with the ex vivo model.

1) The RVW is an ex vivo isolated wedge of ventricle tissue and not a whole organ perfusion system, that is devoid of any compensatory/stimulatory mechanism, or influencing factors from metabolism and hormones.

2) Each wedge preparation is replicated in the same way, from response to the premedication anaesthetics, euthanasia, the time to process tissue collection through to isolation of the tissue by cannulation and pacing stimulation.

3) Subsequent perfusion of the ventricular tissue yields the same viable mass to be investigated such that following equilibration periods of 1 hour the control baseline ECG parameters obtained are within acceptable ranges and stable wave form.

4) For each free drug concentration perfused, a 30 minute first-pass perfusion is sufficient for tissue equilibration of drug. Given that cardiac ventricular tissue is highly perfused, no accumulation of drug during infusion and subsequent doses is considered. With that there are a limited number of concentrations/data points from each RVW preparation.

5) A theoretical maximum QT threshold of 700 ms was imposed as a physiological upper limit that the delta QT interval could change, representing an approximate 200% increase from a baseline based on maximum literature values observed. Hill coefficient, n, should be approximately equal to representing unity of binding 1:1, and is rapid and reversible.

6) The QT interval is a parameter from multiple ion channel interplay, not only hERG K^+ channel activity, which is assumed, but also Ca^{2+} and Na^+ channel. It also assumes that the binding is both rapid and reversible. If additional ion channel interactions attenuate the maximal QT response then these have been excluded.

3.7. Rabbit Ventricular Wedge Results and Discussion

The rabbit isolated perfused ventricular wedge preparation was used to generate data for cisapride, moxifloxacin and sparfloxacin, known for their potential to prolong QT interval and generate a concentration-response model.

3.7.1. Control RVW Results and Discussion

Table 3.1 Control RVW: Individual Experimental delta QT Interval

Control Compound	Vehicle Control QT (Δ ms) for each RVW Preparation					
	A	B	C	D	E	Mean ±SEM
Cisapride	327	324	310	258	344	313 ±14.7
Moxifloxacin	332	304	313	328	-	319 ±6.5
Sparfloxacin	336	366	341	359	-	351 ±7.1
Verapamil	-	-	-	-	-	327.4 ±35

The observed results in the vehicle control cisapride, moxifloxacin, sparfloxacin and verapamil was 313 ±14.7ms, 319 ±6.5ms, 351 ±7.1ms and 327.4 ±35ms. The observed QT interval for each compound baseline vehicle control was consistent within preps and between vehicle controls and was not statistically different (p-value >0.05) compared to the other preps (Table 3.1). Sparfloxacin did have a higher baseline overall which may be a result of the different vehicle NaOH being used compared to DMSO for the other compounds. Using existing data from internal GSK validation compound preparations (n=32) the overall control baseline QT interval was 323.6 ±4.8ms and the current data sets are not statistically different (p-value >0.05). This is comparable to observed QT interval at 0.5 Hz stimulation from Chen et al., which was 308.6 ±6.9ms based on n=28 preparations (Chen et al. 2006).

3.7.2. Cisapride RVW Results and Discussion

As part of a validation protocol cisapride was investigated in the rabbit ventricular wedge (RVW) preparation (n=5, A-E experiments) at 0.01, 0.1, 1 and 10 µM free drug concentration. The data presented in Table 3.2, shows the baseline QT interval following administration of control vehicle after 1 hour equilibration time and then the subsequent change in QT measured after 30 minutes infusion at increasing dose concentrations of cisapride. Representative changes in the ECG are shown in Figure 3.5. Cisapride shows a positive effect on increasing the change in QT interval with an increasing dose administration of cisapride up to at least 1 µM. At 0.01 µM, the mean QT interval increased by 19.7± 9.57ms, which was not statistically significant (*p*-value >0.05). At 0.1 µM and 1 µM, the mean QT interval increased by 70.0 ±26.6ms and 282 ±28.5ms, respectively, which were both significantly different (*p*-value 0.0063 and <0.01) compared to control vehicle. The highest concentration investigated was 10 µM which increased the QT interval by 136 ±26.6ms, which was less than the change observed at 1 µM, yet still statistically significant (*p*-value <0.05). The full range of parameters obtained from the RVW, including QRS (ms), Tp-e (ms), ratio Tp-e/QT and contractility are presented in Appendix 3 and have not been used for further analysis.

Table 3.2 Cisapride RVW: Individual Experimental delta QT Interval

Concentration (µM)	Delta QT (Δ ms) for each RVW Preparation against Vehicle Control					
	A	B	C	D	E	Mean ±SEM
Control	327	324	310	258	344	313 ±14.7
0.01	10.0	32.8	0.50	4.50	50.8	19.7 ±9.6
0.10	31.0	147	61.8	40.0	259[b]	70.0* ±26.6
1.00	ND	322	227	93.5 [b]	298	282* ±28.5
10.00 [a]	*129*	*144*	*163*	*73.5*	*168*	136* ±17.0

a. Highest concentration excluded from further analysis due to Na^+ channel inhibition by cisapride
Values excluded as outliers ≥±3 standard deviations as determined by externally studentised residuals plot
* p-value <0.05 compared to vehicle control

Figure 3.5 Cisapride RVW: Representative Graph of the Change in ECG in the RVW Following Investigation with Different Cisapride Concentrations

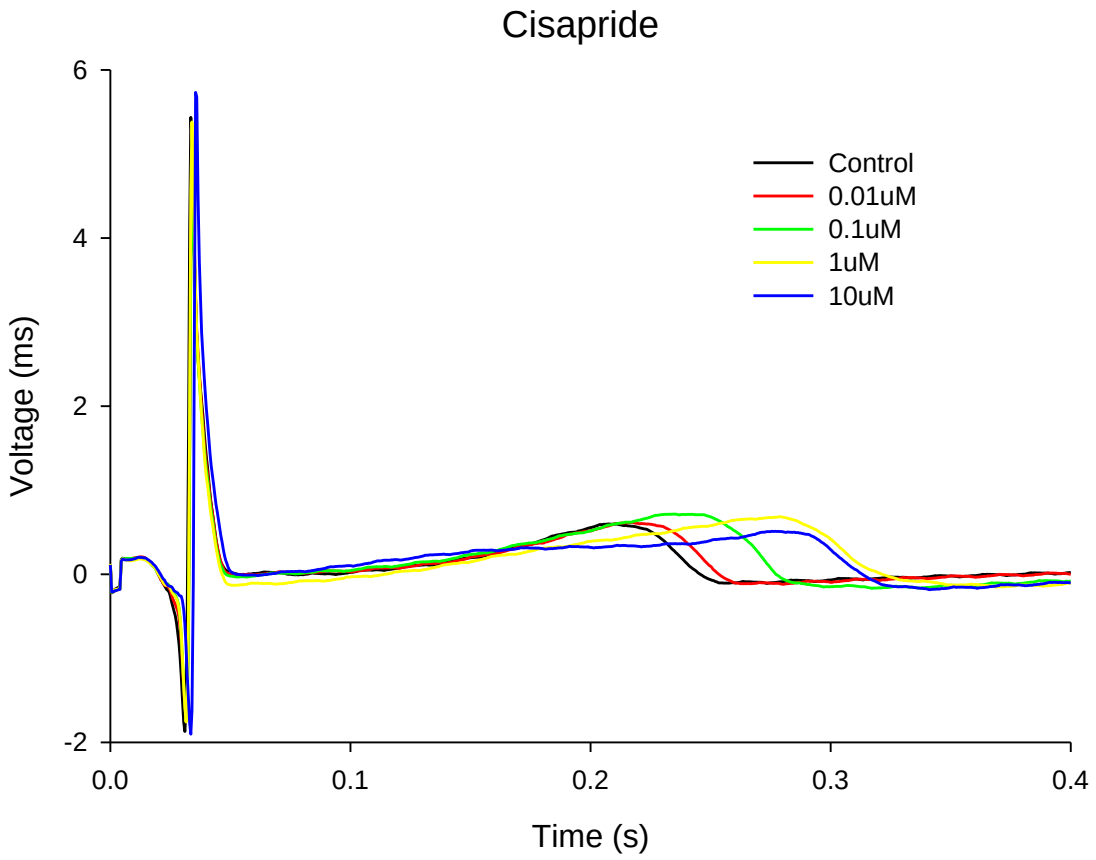

Figure 3.5: Representative plot of the change in ECG waveform generated in the rabbit ventricular wedge (RVW) preparation over a range of free cisapride drug concentrations, 0.01 (—), 0.1 (—), 1 (—) and 10 µM (—) prepared in Tyrode's perfusion media compared to vehicle control (—).

The RVW data generated in this study is comparable to reported literature data for cisapride (Chen et al., 2006; Liu et al., 2006) as shown in Table 3.3 and Figure 3.6. In an internal validation assessment conducted by GSK in the US (2009), cisapride was investigated at equivalent concentrations at 0.01, 0.1, 1 and 10 µM (n=4) and demonstrated a QT prolongation of 36.8ms, 123ms, 217ms and 120ms, respectively. Data was extracted from literature plots (Chen et al., 2006; Liu et al., 2006), and converted using graph-plot digitising software (Digit v1.0.4). Data shown gives the mean data point value and the estimated minimum and maximum based on the error bar plots. In the study by (Liu et al., 2006), 0.1, 1 and 10 µM concentrations were investigated and resulted in estimated increases in QT change of 35ms, 239ms and 244ms, respectively. The reported RVW data by (Chen et al., 2006) was conducted over 5 different concentrations, at 0.01, 0.03, 0.1, 0.3 and 1 µM. The indicated baseline vehicle control QT interval at 0.5 Hz stimulation, was 308.6 ±6.9ms based on n=28 preparations, which is comparable to the observed results in this study of 313 ±14.7ms. The extent of QT change across the dose concentrations was similar, except at 0.01 µM and 0.03 µM, where the mean QT interval did not increase by visual inspection of the plot (Chen et al., 2006), equating to approximately -2.0ms and 3.0ms, respectively. At 0.1, 0.3 and 1 µM, the mean QT interval increased by 34ms, 85ms and 308ms, respectively, which is similar to the observed increase of 70ms at 0.1 µM, and 282ms at 1 µM.

Table 3.3 Cisapride RVW: Table of Extracted Literature Data for Changes in QT Response (Δ ms) in the RVW Following Investigation with Cisapride

Expt.	Concentration (µM)	ΔQT (mean) (ms)	ΔQT (max.) (ms)	ΔQT (min.) (ms)
GSK, US (2009)	0.01	36.8	47.8	25.8
	0.10	123	154	92.0
	1.00	218	249	187
	10.00[a]	120	128	112
Liu et al. (2006)	0.10	35.2	42.0	24.3
	1.00	239	292	186
	10.00[a]	245	291	200
Chen et al. (2006)	0.01	-2.0	0.0	1.0
	0.03	3.0	7.0	6.0
	0.10	34.0	72.0	32.0
	0.30	85.0	138	85.0
	1.00	308	309	305

b. Highest concentration excluded from further analysis due to Na^+ channel inhibition by cisapride

Data was extracted from literature plots by Liu et al. (2006) and Chen et al. (2006) and converted using graph-plot digitising software (Digit v1.0.4). Data shown gives the mean data point value and the estimated minimum and maximum based on the error bar plots.

Figure 3.6 Cisapride RVW: Graph of Changes in QT Response (Δms) in the RVW Following Investigation with Cisapride and Comparison to Literature

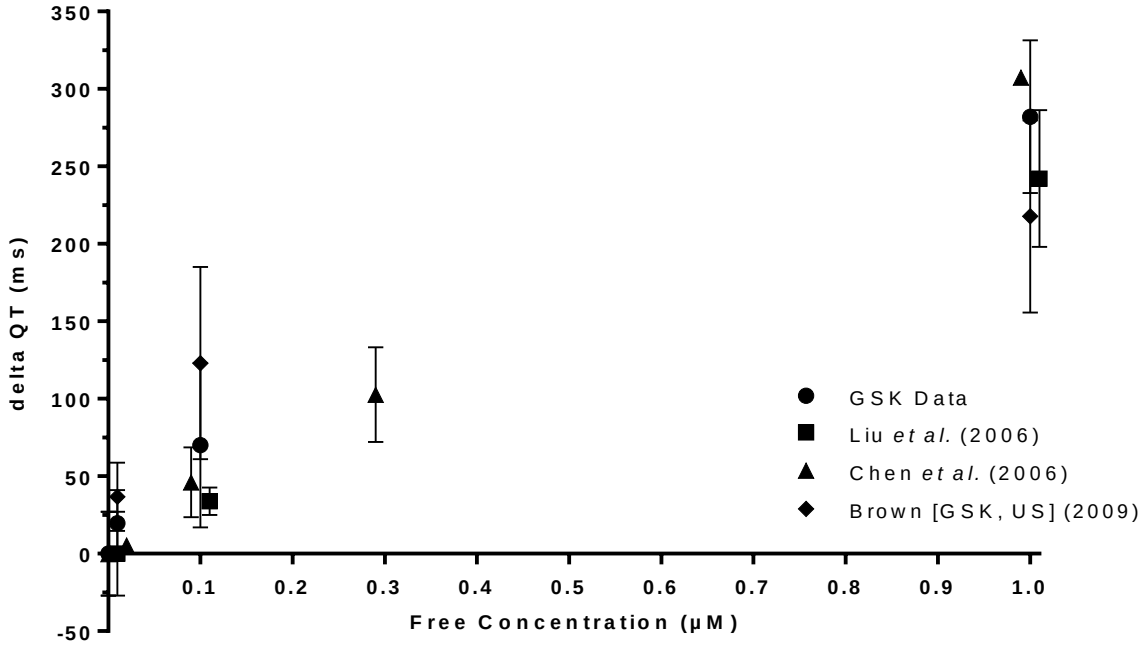

Figure 3.6: Graph of the delta change in QT response (ms) data generated in the rabbit ventricular wedge (RVW) preparation over a range of free cisapride drug concentrations, 0.01, 0.03, 0.1, 0.3, 1 µM prepared in Tyrode's perfusion media compared to vehicle control. Data from a GSK investigation, UK (●), and US (♦) is plotted with extracted data from literature plots by Liu et al. (2006, ■) and Chen et al. (2006, ▲) and converted using graph-plot digitising software (Digit v1.0.4). Data shown gives the mean data point value and the standard error bars.

3.7.3. Non-Linear Fit Analysis of Cisapride RVW Data

The cisapride data generated in the RVW was log-transformed in GraphPad PRISM® and fitted with a non-linear function based on the E_{max} response model to produce a sigmoidal curve. Each of the cisapride data sets were analysed this way, including literature extracted data, and the best-fit response output values with S.E.M. shown in Table 3.4. Each cisapride data set used was fitted against all the vehicle control QT response (ms) values from n= 32 preps, (GSK RVW validation data sets, not shown) to derive a bottom value and set with a top limit of 700 ms, as a theoretical maximum change in delta QT (approximately 200%).

From the four data sets analysed the bottom values were consistent and ranged from -0.389 to 0.581 ms with a standard error approximately ±5ms. This shows that there is a small variation in the baseline vehicle control between published RVW preps. Both the EC_{50} and Hill slope coefficient, *n*-value, were similar across the experimental RVW data sets, with the exception of the GSK, US data (2009) that had a higher EC_{50} value (7.2 ±1.6 µM) and lower Hill slope coefficient, *n*-value, 0.4 ±0.06, as a result of a shallower response curve. The EC_{50} values for GSK, UK was 1.7 ±1.2 µM compared to 1.9 ±1.2 µM and 1.2 ±1.1 µM for by (Liu et al., 2006) and (Chen et al., 2006), respectively. The Hill slope values for GSK, UK, *n*-value, 0.76 ±1.1, (Liu et al., 2006), *n*-value, 1.0 ±0.2 and (Chen et al., 2006), *n*-value, 1.2 ±0.1 were similar and approximately close to 1. The goodness of fit values, as denoted by R-squared, was reasonable for each data set between 0.85 and 0.91.

Table 3.4 Cisapride RVW: Non-Linear Fitted Parameters of Log Transformed delta QT Response (Δ ms) in the RVW Following Investigation with Cisapride and Extracted Literature Data

Best-fit values	GSK, UK	GSK, US (2009)	Liu et al. (2006)	Chen et al. (2006)
Bottom, ms	0.581 ±5.2	-0.389 ±4.8	0.00938 ±5.2	0.0938 ±4.0
Log[EC_{50}]	0.227 ±0.08	0.852 ±0.2	0.272 ±0.07	0.0934 ±0.03
EC_{50} (µM)	1.69 ±1.2	7.12 ±1.6	1.87 ±1.2	1.24 ±1.1
Hill Slope, *n*	0.765 ±1.1	0.392 ±0.06	1.02 ±0.2	1.20 ±0.1
Top (E_{max}), ms	700	700	700	700
R squared	0.858	0.851	0.901	0.914

Non-linear parameters presented as best-fit values with EC_{50} and Hill slope coefficient, n, and ±SEM. Top value upper limit (E_{max}) set as 700 ms as an estimated theoretical maximum delta QT response from baseline control following a range of free cisapride drug concentrations in the rabbit ventricular wedge (RVW) preparation. Bottom QT value response fitted against vehicle control data from n=32 preparations. Each data set including extracted literature from Liu et al. (2006) and Chen et al. (2006) was assessed independently along with R-square value for goodness of fit.

The line of best fit for GSK, UK cisapride data is shown in Figure 3.7, along with all mean cisapride data with ±S.E.M. bars. The plot shows the delta change in QT response (ms) data generated in the rabbit ventricular wedge (RVW) preparation over a range of cisapride log[free drug concentrations], 0.01, 0.03, 0.1, 0.3, 1 µM prepared in Tyrode's perfusion media compared to vehicle control. Data from a GSK investigation, UK (●), and US (2009, ♦) is plotted with extracted data from literature plots by Liu et al. (2006, ■) and Chen et al. (2006, ▲). Data shown gives the mean data point value and the standard error bars. GSK Data (UK) fitted (— red line) using a non-linear response model with 95% confidence interval range shaded (pink) within the dotted lines (····) with the parameters described in Table 26. The fitted curve of the GSK, UK data shows that the externally sourced experimental data generally fall within the bounds of the predicted line and confidence interval.

Figure 3.7 Cisapride RVW: Graph of Non-Linear Fit of Log Transformed delta QT Response (Δ ms) in the RVW Following Investigation with Cisapride and Comparison to Literature

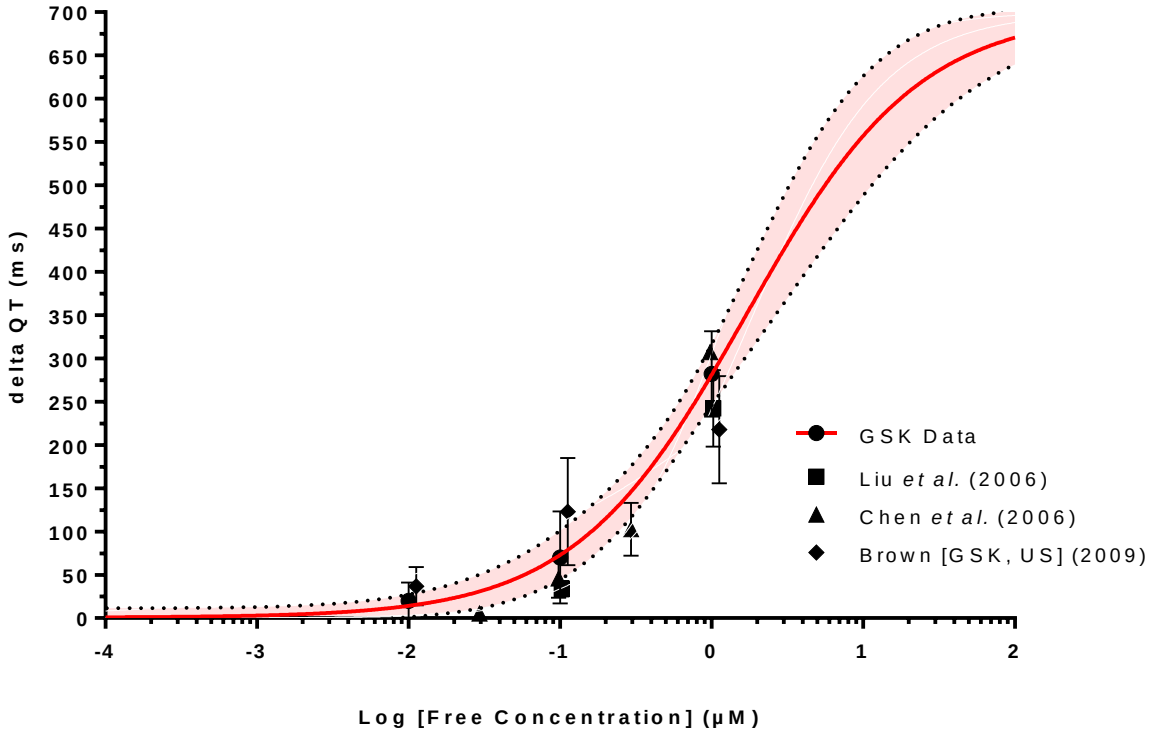

Figure 3.7: Graph of the delta change in QT response (ms) data generated in the rabbit ventricular wedge (RVW) preparation over a range of cisapride log [free drug concentrations], 0.01, 0.03, 0.1, 0.3, 1 µM prepared in Tyrode's perfusion media compared to vehicle control. Data from a GSK investigation, UK (●), and US (♦) is plotted with extracted data from literature plots by Liu et al. (2006, ■) and Chen et al. (2006, ▲). Data shown gives the mean data point value and the standard error bars. GSK Data (UK) is shown fitted (— red line) using a non-linear response model with 95% confidence interval range shaded (pink) within the dotted lines (····).

3.7.4. Moxifloxacin RVW Results and Discussion

Moxifloxacin was investigated in the rabbit ventricular wedge (RVW) preparation (n=4, A-D experiments) at 3, 10, 30 and 100 µM free drug concentration. The data presented in Table 3.5, shows the baseline QT interval following administration of control vehicle after 1 hour equilibration time and then the subsequent change in QT measured after 30 minutes infusion at increasing dose concentrations of moxifloxacin. Representative changes in the ECG are shown in Figure 3.8. Moxifloxacin showed a positive effect on increasing the change in QT interval with an increasing dose administration of moxifloxacin up to 100 µM. At 3 µM the mean QT interval increased by 6.1 ±5.15ms, which was not statistically significant (*p*-value >0.05). At 10, 30 and 100 µM, the mean QT intervals increased by 28.0 ±6.15ms, 68.2 ±8.27ms and 196 ±12.5ms, respectively, which were all significant different (*p*-value 0.0271 at 10 µM and <0.0001 at both 30 and 100 µM) compared to control vehicle. The full range of parameters obtained from the RVW, including QRS (ms), Tp-e (ms), ratio Tp-e/QT and contractility are presented in Appendix 3 and have not been used for further analysis.

The RVW data generated in this study is comparable to reported literature data for moxifloxacin as shown by (Liu et al., 2006) and (Chen et al., 2006), (Lu et al., 2006) (Eichenbaum et al., 2012) in Table 3.6 and Figure 3.9. These published data were investigated over a similar concentration range from 3 µM up 1000 µM. Data was extracted from literature plots and converted using graph-plot digitising software (Digit v1.0.4). Data shown gives the mean data point value and the estimated minimum and maximum based on the error bar plots.

Table 3.5 Moxifloxacin RVW: Individual Experimental delta QT Interval

Concentration (µM)	Delta QT (Δ ms) for each RVW Preparation against Vehicle Control				
	A	B	C	D	Mean ±SEM
Control	332	304	313	328	319 ±6.5
3	-8.00	13.0	5.00	14.5	6.10 ±5.2
10	33.0	15.8	ND	35.3	*28.0 ±6.2
30	60.3	84.3	48.8	79.3	*68.2 ±8.3
100	233 [a]	189	185	179	*196 ±12.5

a. Value excluded as outliers ≥±3 standard deviations as determined by externally studentised residuals plot
* p-value <0.05 compared to vehicle control

Figure 3.8 Moxifloxacin RVW: Representative Graph of the Change in ECG in the RVW Following Investigation with Different Moxifloxacin Concentrations

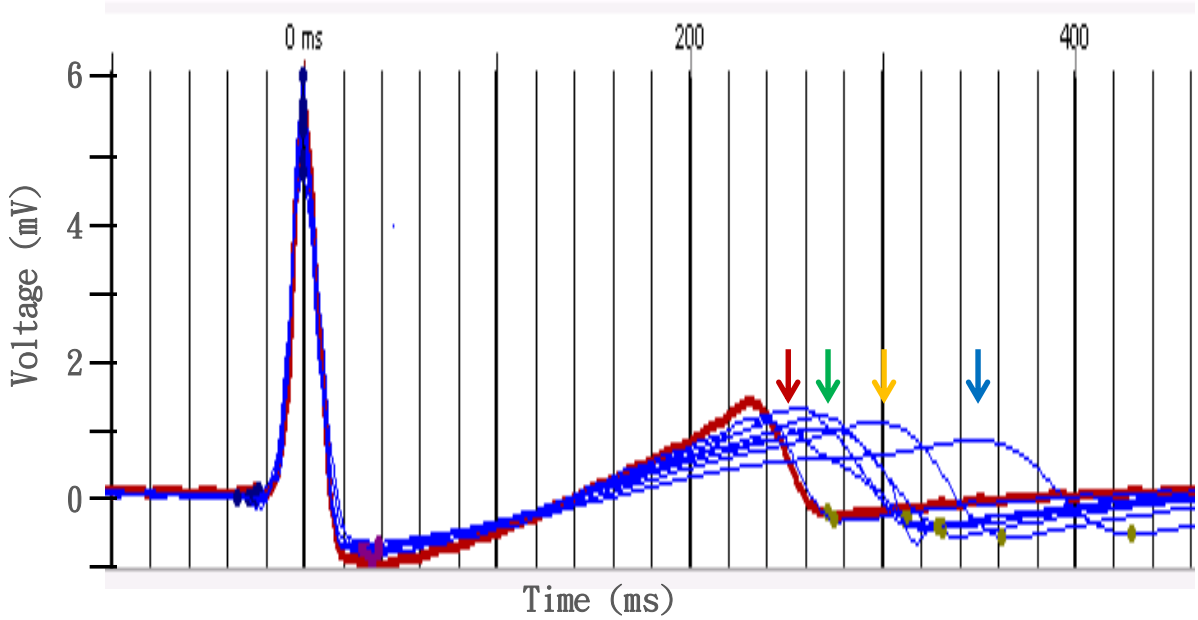

Figure 3.8: Representative plot of the change in ECG waveform generated in the rabbit ventricular wedge (RVW) preparation over a range of free moxifloxacin drug concentrations, 3 (↓), 10 (↓), 30 (↓) and 100 µM (↓) prepared in Tyrode's perfusion media compared to vehicle control (—).

The reported RVW data by (Chen et al., 2006) was conducted at the same 4 concentrations, as the GSK UK data, at 3, 10, 30 and 100 µM. The indicated baseline vehicle control QT interval at 0.5Hz stimulation, as previously stated was 308.6 ±6.9ms (n=28) and comparable to the observed results in this study of 312 ±4.8ms. The extent of QT change across the dose concentrations at 3, 10, 30 and 100 µM, increased by 27ms, 70ms, 144ms and 298ms (Chen et al., 2006). In comparison the QT change in response was lower at all concentration in the GSK study of 6.1ms (-8 to +15ms range), 28ms (16 to 35ms range), 68ms (49 to 84ms range) and 196ms (179 to 233ms range), at 3, 10, 30 and 100 µM, respectively. A similar response to QT response increasing between the two studies is observed but to a lesser extent.

Table 3.6 Moxifloxacin RVW: Table of Extracted Literature Data for Changes in QT Response (Δ ms) in the RVW Following Investigation with Moxifloxacin

Expt.	Concentration (µM)	ΔQT (mean) (ms)	ΔQT (max) (ms)	ΔQT (min) (ms)
Liu et al. (2006)	3	17.6	21.6	9.5
	30	100	109	92.1
	300	391	413	372
	1000	682	730	633
Chen et al. (2006) [a]	3	27.0	36.0	31.0
	10	70.0	86.0	61.0
	30	144	165	136
	100	298	318	288
Lu et al. (2006)	3	12.9	12.1	13.7
	30	86.5	99.8	85.4
	100	249	290	219
	300	454	520	400
Eichenbaum et al. (2012)	3	15.2	21.2	3.0
	30	81.9	94.1	69.8
	100	234	261	203
	300	428	483	373

a. 308.6±6.9ms (n=28) Overall mean QT baseline control (Chen et al.)

Data was extracted from literature plots by Liu et al. (2006), Chen et al. (2006), Lu et al. (2006) and Eichenbaum et al. (2012) and converted using graph-plot digitising software (Digit v1.0.4). Data shown gives the mean data point value and the estimated minimum and maximum based on the error bar plots.

In the study by (Liu et al., 2006), 3, 30, 300 and 1000 µM concentrations of moxifloxacin were investigated and resulted in estimated increases in QT change of 18ms, 100ms, 390ms and 682ms, respectively. At the two concentrations, 3 µM and 30 µM the change in delta QT response was approximately similar, with this study also conducted at two notably higher concentrations. (Lu et al., 2006) study demonstrated approximate QT increases of 13ms, 87ms, 249ms and 454ms, at 3, 30, 100 and 300 µM concentrations, respectively, which were in agreement with the 3 µM and 30 µM results observed in the GSK study, and with other authors (Chen et al., 2006) at 100 µM and with (Eichenbaum et al., 2012) at all the same concentrations. In the data set from (Eichenbaum et al., 2012) investigated the RVW at 3, 30, 100 and 300 µM with increased changes in QT interval observed with delta QT (ms) increasing by 15ms, 82ms, 234ms and 428ms which were similar to (Lu et al., 2006) at the same concentrations.

Figure 3.9 Moxifloxacin RVW: Graph of Changes in QT Response (Δ ms) in the RVW Following Investigation with Moxifloxacin and Comparison to Literature

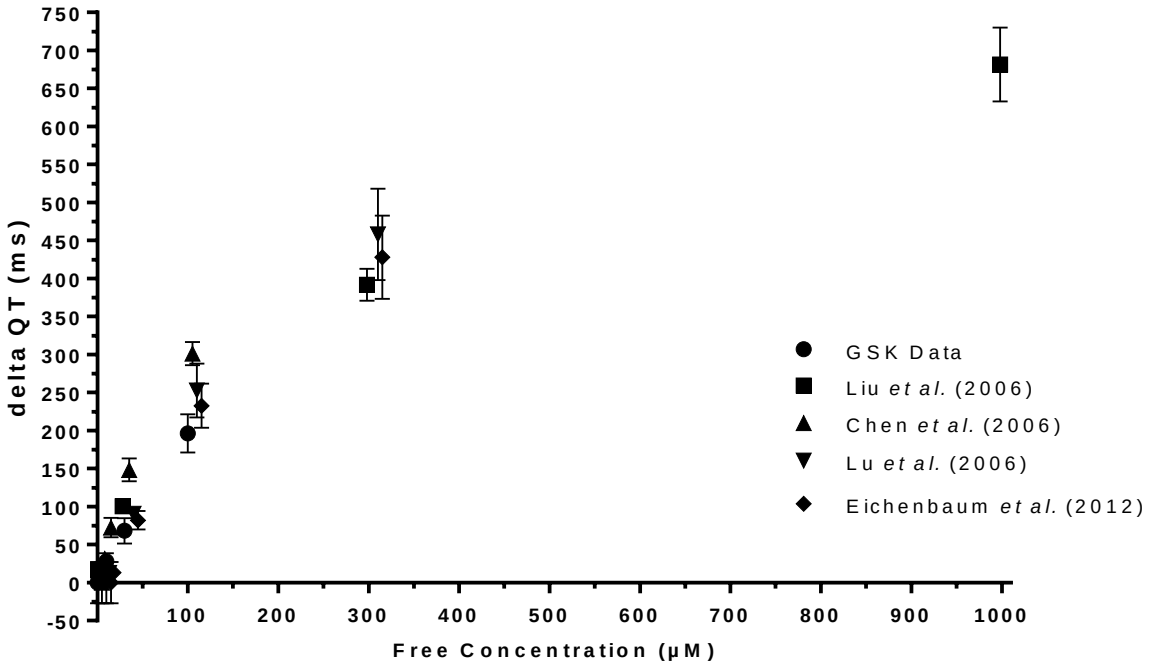

Figure 3.9: Graph of the delta change in QT response (ms) data generated in the rabbit ventricular wedge (RVW) preparation over a range of free moxifloxacin concentrations, 3, 10, 30, 100, 300 and 1000 µM prepared in Tyrode's perfusion media compared to vehicle control. Data from a GSK investigation, UK (●) and plotted with extracted data from literature plots by Liu et al. (2006, ■) and Chen et al. (2006, ▲), Lu et al. (2006, ▼) and Eichenbaum et al. (2012, ♦) and converted using graph-plot digitising software (Digit v1.0.4). Data shown gives the mean data point value and the standard error bars.

3.7.5. Non-Linear Fit Analysis of Moxifloxacin RVW Data

The moxifloxacin data generated in the RVW was log-transformed in GraphPad PRISM® and fitted with a non-linear function based on the E_{max} response model to produce a sigmoidal curve. Each moxifloxacin data set was analysed this way, including literature extracted data, and the best-fit response output values with S.E.M. shown in Table 3.7. Each moxifloxacin data set used was fitted against all the vehicle control QT response (ms) values from n= 32 preps, (GSK RVW validation data sets, not shown) to derive a bottom value and set with a top limit of 700 ms, as a theoretical maximum change in delta QT (approximately 200%).

From the five data sets analysed the bottom values were consistent and ranged from 0.085ms to 0.346ms with a standard error approximately ±5ms, except for Liu et al. (2006) which has a bottom baseline value at +4.33ms. This shows that there is a small variation in the baseline vehicle control between author RVW preps and that Liu et al. baseline threshold is higher. Both the EC_{50} and Hill slope coefficient, *n*-value, were similar across the five experimental RVW data sets. The EC_{50} value for GSK, UK was 248 ±1.2 µM which was highest out of the data sets in comparison to 212 ±1.1 µM, 142 ±1.1 µM, 168 ±1.1 µM and 195 ±1.1 µM for (Liu et al., 2006), (Chen et al., 2006), (Lu et al., 2006) and (Eichenbaum et al., 2012), respectively. The Hill slope *n*-values were similar and approximately close to 1, for GSK, UK, *n*-value, 1.0 ±0.15, (Liu et al., 2006), *n*-value, 1.3 ±0.16, (Chen et al., 2006), *n*-value, 0.8 ±0.08, (Lu et al., 2006), *n*-value, 1.1 ±0.09) and (Eichenbaum et al., 2012), *n*-value 1.1 ±0.09.

Table 3.7 Moxifloxacin RVW: Non-Linear Fitted Parameters of Log Transformed delta QT Response (Δ ms) in the RVW Following Investigation with Moxifloxacin and Extracted Literature Data

Best-fit values	Moxifloxacin	Liu et al. (2006)	Chen et al. (2006)	Lu et al. (2006)	Eichenbaum et al. (2012)
Bottom, ms	0.0852 ±4.2	4.33 ±6.0	0.242 ±4.2	0.346 ±4.8	0.299 ±4.7
Log[EC_{50}]	2.39 ±0.08	2.33 ±0.04	2.15 ±0.05	2.23 ±0.03	2.29 ±0.03
EC_{50} (µM)	248 ±1.2	212 ±1.1	142 ±1.1	168 ±1.1	195 ±1.1
Hill Slope, *n*	1.04 ±0.2	1.33 ±0.2	0.825 ±0.08	1.10 ±0.09	1.06 ±0.09
Top (E_{max}), ms	700	700	700	700	
Goodness of Fit					
R square	0.849	0.968	0.924	0.956	0.952

Non-linear parameters presented as best-fit values with EC_{50} and Hill slope coefficient, n, and ±SEM. Top value upper limit (E_{max}) set as 700 ms as an estimated theoretical maximum delta QT response from baseline control following a range of free moxifloxacin drug concentrations in the rabbit ventricular wedge (RVW) preparation. Bottom value response fitted against vehicle control data from n=32 preparations. Each data set including extracted literature from Liu et al. (2006), Chen et al. (2006), Lu et al. (2006) and Eichenbaum et al. (2012) was assessed independently along with R-square value for goodness of fit.

The line of best fit for GSK, UK moxifloxacin data is shown in Figure 3.10, along with all mean moxifloxacin data with ±S.E.M. bars. The plot shows the delta change in QT response (ms) data generated in the rabbit ventricular wedge (RVW) preparation over a range of moxifloxacin log[free drug concentrations], 3, 10, 30, 100, 300 and 1000 µM prepared in Tyrode's perfusion media compared to vehicle control. Data from a GSK investigation, UK (●), is plotted with extracted data from literature plots by Liu et al. (2006, ■) and Chen et al. (2006, ▲), Lu et al. (2006, ▼) and Eichenbaum et al. (2012, ♦). Data shown gives the mean data point value and the standard error bars. GSK Data (UK) is shown fitted (— red line) using a non-linear response model with 95% confidence interval range shaded (pink) within the dotted lines (····) with the parameters described in Table 29. The fitted curve of the GSK, UK data shows that the externally sourced experimental data generally fall within the bounds of the predicted line and confidence interval, except for (Chen et al., 2006) which has a greater dose response as indicated by the lower EC_{50} value.

Figure 3.10 Moxifloxacin RVW: Graph of Non-Linear Fit of Log Transformed delta QT Response (Δ ms) in the RVW Following Investigation with Moxifloxacin and Comparison to Literature

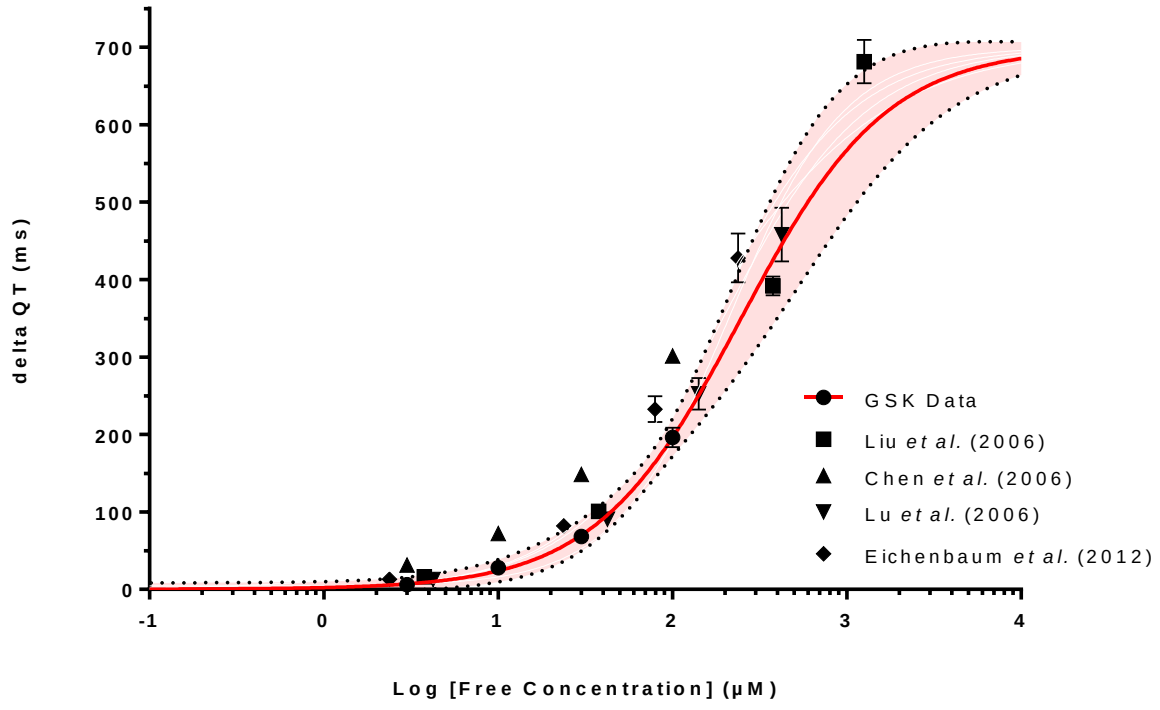

Figure 3.10: Graph of the delta change in QT response (ms) data generated in the rabbit ventricular wedge (RVW) preparation over a range of moxifloxacin log [free drug concentrations], 3, 10, 30, 100, 300 and 1000 µM prepared in Tyrode's perfusion media compared to vehicle control. Data from a GSK investigation, UK (●) is plotted with extracted data from literature plots by Liu et al. (2006, ■) and Chen et al. (2006, ▲), Lu et al. (2006, ▼) and Eichenbaum et al. (2012, ♦). Data shown gives the mean data point value and the standard error bars. GSK Data (UK) is shown fitted (— red line) using a non-linear response model with 95% confidence interval range shaded (pink) within the dotted lines (····).

3.7.6. Sparfloxacin RVW Results and Discussion

Sparfloxacin was investigated in the rabbit ventricular wedge (RVW) preparation (n=4, A-D experiments) at 1, 10, 100 and 333 µM free drug concentration. The data presented in Table 3.8, shows the baseline QT interval following administration of control vehicle after 1 hour equilibration time and then the subsequent change in QT measured after 30 minutes infusion at increasing dose concentrations of sparfloxacin. Representative changes in the ECG are shown in Figure 3.11. Sparfloxacin showed a positive effect on increasing the change in QT interval with an increasing dose administration of sparfloxacin up to 333 µM. At 1 µM, the mean QT interval increased by 22.8 ±9.3ms, which was not statistically significant (*p*-value >0.05). At 10, 100 and 333 µM, the mean QT interval increased by 152 ±29.0ms and 397 ±13.0ms and 466 ±14.1ms, respectively, which were all statistically significant (*p*-values <0.0001) compared to control vehicle. The full range of parameters obtained from the RVW, including QRS (ms), Tp-e (ms), ratio Tp-e/QT and contractility are presented in Appendix 3 and have not been used for further analysis.

The RVW data generated in this study is in accordance with reported literature data for sparfloxacin as shown by (Liu et al., 2006), (Liu et al., 2006) and (Eichenbaum et al., 2012) in Table 3.9 and Figure 3.12. These published data were investigated over a similar concentration range from 0.1 µM up 333 µM. Data was extracted from literature plots and converted using graph-plot digitising software (Digit v1.0.4). Data shown gives the mean data point value and the estimated minimum and maximum based on the error bar plots.

Table 3.8 Sparfloxacin RVW: Individual Experimental delta QT Interval

Concentration (μM)	Delta QT (Δ ms) for each RVW Preparation against Vehicle Control				
	A	B	C	D	Mean ±SEM
Control	336	366	341	359	351 ±7.1
1	3.0	11.0	37.0	40.0	22.8 ±9.3
10	112	98.5	175	224	*152 ±29.0
100	398	369	389	432	*397 ±13.0
333	505	448	443	469	*466 ±14.1

* *p*-value <0.05 compared to vehicle control

Figure 3.11 Sparfloxacin RVW: Representative Graph of the Change in ECG in the RVW Following Investigation with Different Sparfloxacin Concentrations

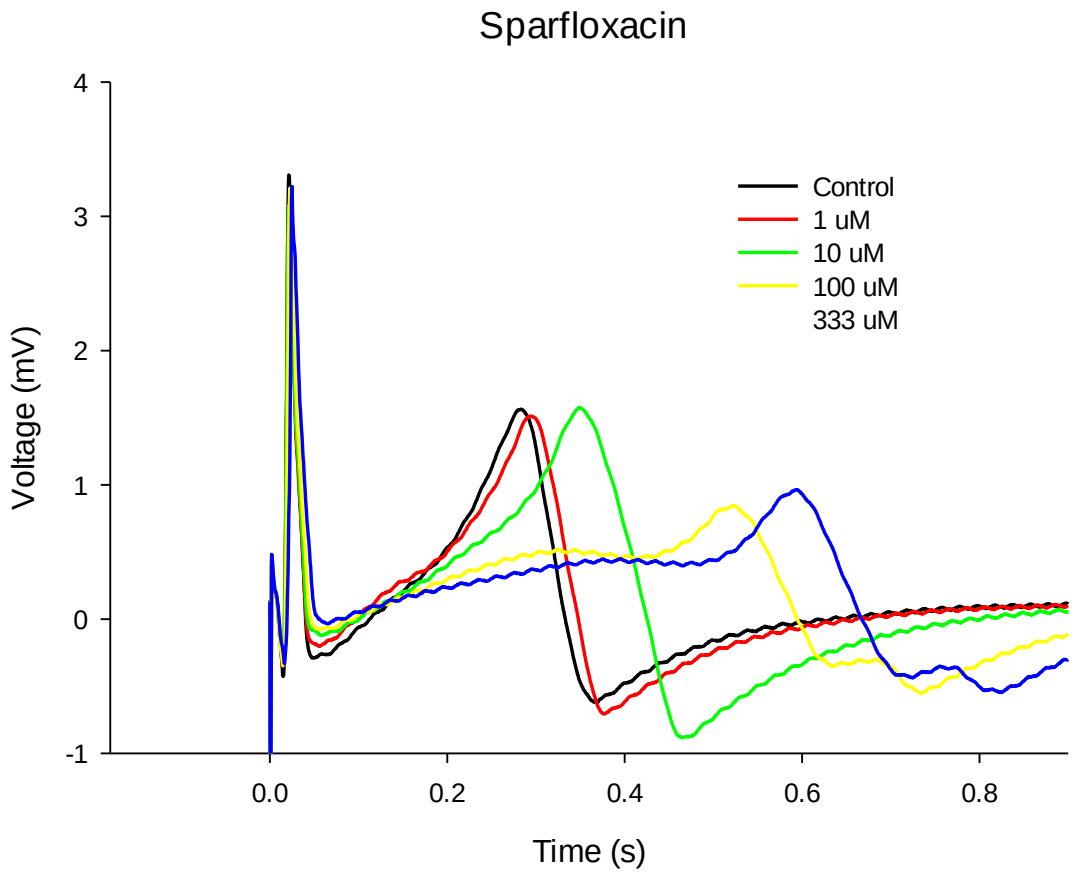

Figure 3.11: Representative plot of the change in ECG waveform generated in the rabbit ventricular wedge (RVW) preparation over a range of free sparfloxacin drug concentrations, 1 (—), 10 (—), 100 (—) and 333 μM (—) prepared in Tyrode's perfusion media compared to vehicle control (—)

Table 3.9 Sparfloxacin RVW: Table of Extracted Literature Data for Changes in QT Response (Δ ms) in the RVW Following Investigation with Sparfloxacin

Expt.	Concentration (μM)	ΔQT (mean) (ms)	ΔQT (max) (ms)	ΔQT (min) (ms)
Liu et al. (2006)	1	28.4	43.3	12.2
	10	158	182	132
	100	426	523	333
	333	481	565	397
Lu et al. (2006)	0.1	13.6	17.1	10.1
	1	77.6	96.5	58.7
	10	228	293	162
	100	397	435	360
Eichenbaum et al. (2012)	0.1	6.07	27.3	-8.19
	1	78.9	106	45.5
	10	228	304	152
	100	398	443	349

Data was extracted from literature plots by Liu et al. (2006), Lu et al. (2006) and Eichenbaum et al. (2012) and converted using graph-plot digitising software (Digit v1.0.4). Data shown gives the mean data point value and the estimated minimum and maximum based on the error bar plots.

The reported RVW data by (Liu et al., 2006) was conducted at the same 4 concentrations, as the GSK UK data, at 1, 10, 100 and 333 μM. The extent of QT changes across the dose concentrations were very similar, increasing by 28ms, 158ms, 426ms and 481ms (Liu et al., 2006) in comparison to 22.8 ±9.3ms, 152 ±29.0ms and 397 ±13.0ms and 466 ±14.1ms, from the GSK, UK data. RVW preparations from authors (Lu et al., 2006) and (Eichenbaum et al., 2012) were conducted are the same free sparfloxacin concentrations (0.1, 1, 10 and 100 μM). The results generated between authors were similar, such that QT interval increased at 0.1 μM by approximately 10ms; at 1 μM and 10 μM, an approximate 78ms and 228ms increase for both was observed respectively; at 100 μM an increase of nearly 400ms change in QT interval. All the data sets provide high concordance with GSK, UK data and between each extracted literature values, where comparable dose concentrations were investigated.

Figure 3.12 Sparfloxacin RVW: Graph of Changes in QT Response (Δ ms) in the RVW Following Investigation with Sparfloxacin and Comparison to Literature

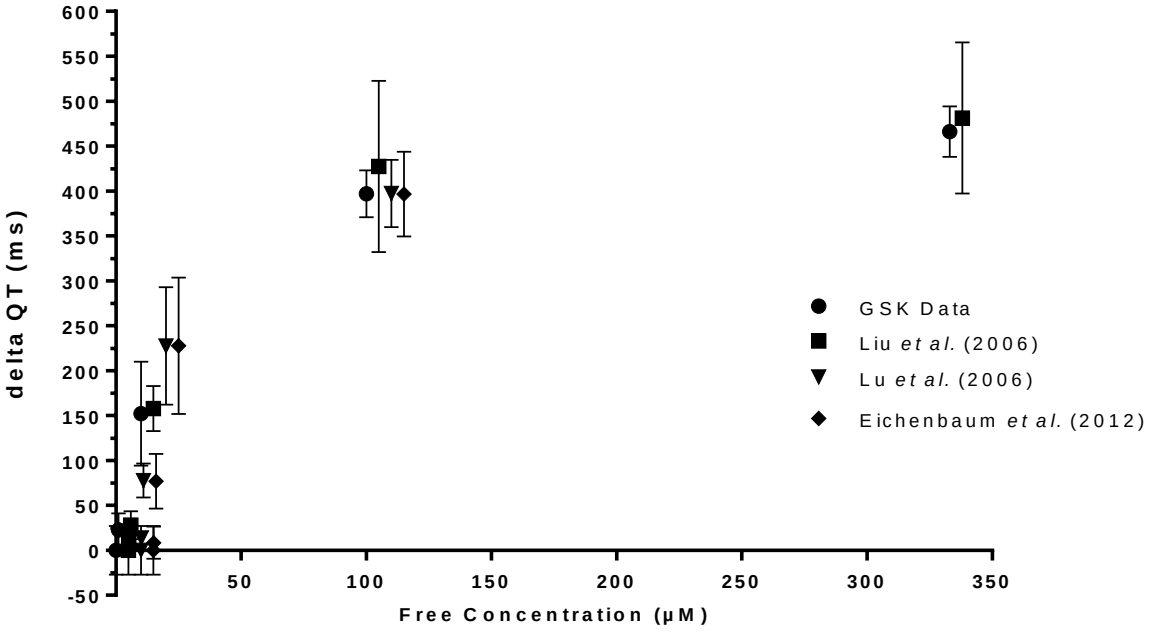

Figure 3.12: Graph of the delta change in QT response (ms) data generated in the rabbit ventricular wedge (RVW) preparation over a range of free sparfloxacin concentrations, 0.1, 1, 10, 100, and 333 µM prepared in Tyrode's perfusion media compared to vehicle control. Data from a GSK investigation, UK (●) and plotted with extracted data from literature plots by Liu et al. (2006, ■), Lu et al. (2006, ▼) and Eichenbaum et al. (2012, ♦) and converted using graph-plot digitising software (Digit v1.0.4). Data shown gives the mean data point value and the standard error bars.

3.7.7. Non-Linear Fit Analysis of Sparfloxacin RVW Data

The sparfloxacin data generated in the RVW was log-transformed in GraphPad PRISM® and fitted with a non-linear function based on the E_{max} response model to produce a sigmoidal curve. Each sparfloxacin data set was analysed this way, including literature extracted data, and the best-fit response output values with S.E.M. shown in Table 3.10. Each sparfloxacin data set used was fitted against all the vehicle control QT response (ms) values from n= 32 preps, (GSK RVW validation data sets, not shown) to derive a bottom value and set with a top limit of 700 ms, as a theoretical maximum change in delta QT (approximately 200%).

From the four data sets analysed the bottom values were consistent and ranged from -1.19 to -1.90ms with a standard error approximately ±6ms. The fitting is taking the value just below zero using baseline vehicle control from internal GSK preps, indicating that baselines author RVW preps are lower but within the error range. Both the EC_{50} and Hill slope coefficient, *n*-value, were similar across the four experimental RVW data sets. The EC_{50} value for GSK, UK was 81.3 ±1.1 µM which was highest out of the data sets in comparison to 66.4 ±1.2 µM for (Liu et al., 2006), and 52.6 ±1.2 µM, for both (Lu et al., 2006) and (Eichenbaum et al., 2012), respectively. The Hill slope values were similar and approximately 0.6, with data from GSK, UK, giving *n*-value 0.61 ±0.04, (Liu et al., 2006) *n*-value, 0.63 ±0.06, and an *n*-value of 0.5 ±0.04-0.05 for both (Lu et al., 2006) and (Eichenbaum et al., 2012), respectively.

Table 3.10 Sparfloxacin RVW: Non-Linear Fitted Parameters of Log Transformed delta QT Response (Δ ms) in the RVW Following Investigation with Sparfloxacin and Extracted Literature Data

Best-fit values	Sparfloxacin	Liu et al. (2006)	Lu et al. (2006)	Eichenbaum et al. (2012)
Bottom, ms	-1.90 ±5.5	-1.24 ±6.5	-1.19 ±5.2	-1.45 ±5.7
Log[EC_{50}]	1.91 ±0.05	1.82 ±0.06	1.72 ±0.07	1.72 ±0.08
EC_{50} (µM)	81.3 ±1.1	66.4 ±1.2	52.6 ±1.2	52.6 ±1.2
Hill Slope, *n*	0.605 ±0.04	0.625 ±0.06	0.498 ±0.04	0.502 ±0.05
Top (E_{max}), ms	700	700	700	700
Goodness of Fit				
R square	0.965	0.944	0.937	0.925

Non-linear parameters presented as best-fit values with EC_{50} and Hill slope coefficient, n, and ±SEM. Top value upper limit (E_{max}) set as 700 ms as an estimated theoretical maximum delta QT response from baseline control following a range of free sparfloxacin drug concentrations in the rabbit ventricular wedge (RVW) preparation. Bottom value response fitted against vehicle control data from n=32 preparations. Each data set including extracted literature from Liu et al. (2006), Lu et al. (2006) and Eichenbaum et al. (2012) was assessed independently along with R-square value for goodness of fit.

The line of best fit for GSK, UK sparfloxacin data is shown in Figure 3.13, along with all mean sparfloxacin data with ±S.E.M. bars. The plot shows the delta change in QT response (ms) data generated in the rabbit ventricular wedge (RVW) preparation over a range of moxifloxacin log[free drug concentrations], 1, 10, 100 and 333 µM prepared in Tyrode's perfusion media compared to vehicle control. Data from a GSK investigation, UK (●), is plotted with extracted data from literature plots by Liu et al. (2006, ■), Lu et al. (2006, ▼) and Eichenbaum et al. (2012, ♦). Data shown gives the mean data point value and the standard error bars. GSK Data (UK) is shown fitted (— red line) using a non-linear response model with 95% confidence interval range shaded (pink) within the dotted lines (····) with the parameters described in Table 32. The fitted curve of the GSK, UK data shows that the externally sourced experimental data generally fall on the outer bounds of the 95% confidence interval of the predicted line.

Figure 3.13 Sparfloxacin RVW: Graph of Non-Linear Fit of Log Transformed delta QT Response (Δ ms) in the RVW Following Investigation with Cisapride and Comparison to Literature

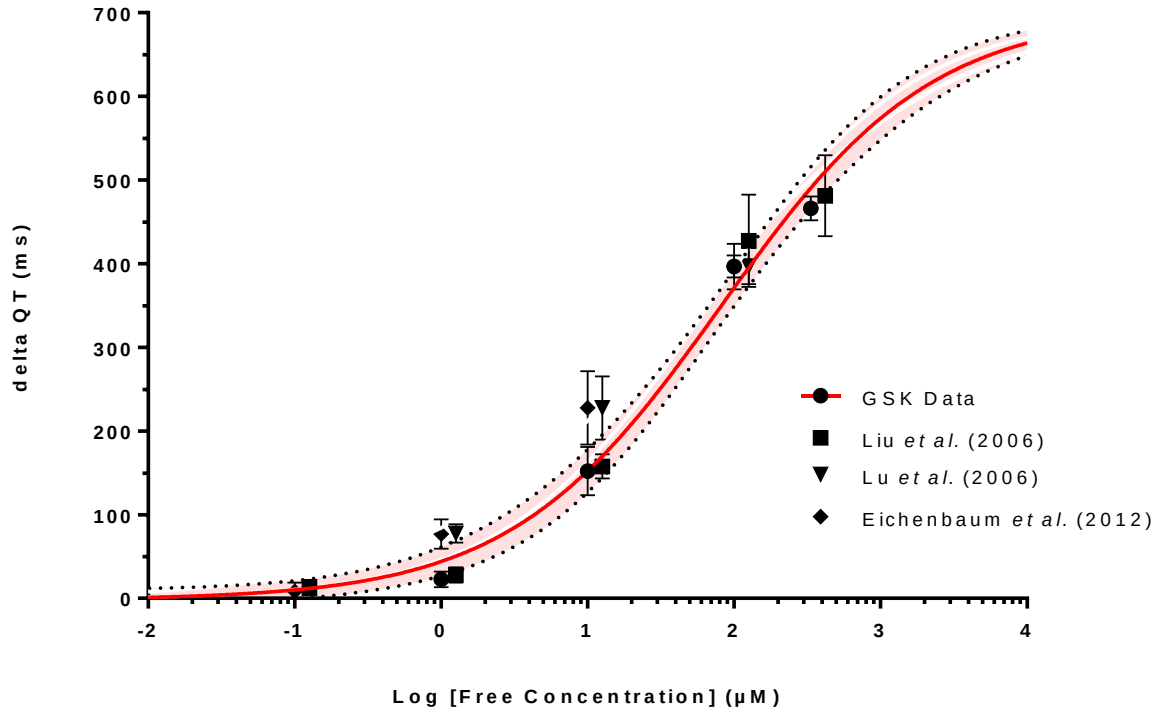

Figure 3.13: Graph of the delta change in QT response (ms) data generated in the rabbit ventricular wedge (RVW) preparation over a range of sparfloxacin log [free drug concentrations], 0.1, 1, 10, 100, and 333 µM prepared in Tyrode's perfusion media compared to vehicle control. Data from a GSK investigation, UK (●) is plotted with extracted data from literature plots by Liu et al. (2006, ■) and Chen et al. (2006, ▲), Lu et al. (2006, ▼) and Eichenbaum et al. (2012, ♦). Data shown gives the mean data point value and the standard error bars. GSK Data (UK) is shown fitted (— red line) using a non-linear response model with 95% confidence interval range shaded (pink) within the dotted lines (····).

3.7.8. Verapamil RVW Results and Discussion

Verapamil was investigated in the rabbit ventricular wedge (RVW) preparation and the data generated was from GSK, US (n=4, individual data was not supplied) at 0.01, 0.1, 1 and 10 µM free drug concentration. The data presented in Table 3.11, shows the mean and S.E.M. baseline QT interval following administration of control vehicle after 1 hour equilibration time and then the subsequent change in QT measured after 30 minutes infusion at increasing dose concentrations of verapamil. Representative changes in the ECG are shown in Figure 3.14. Verapamil showed no effect on the change in QT interval with an increasing dose administration of verapamil, except at the top dose of 10 µM which reduced the observed QT but was not statistically significant (*p*-value >0.05). At each of the dose concentrations investigated there was variable response and overlap between each concentration. At 0.01, 0.1, 1 and 10 µM, the mean QT interval changed from vehicle baseline control by 23.2 ±27.0ms, 13.5 ±31.0ms and 14.0 ±18.0ms and -12.6 ±13.0ms, respectively, which were all not statistically significant (*p*-values >0.05) compared to control vehicle. The full range of parameters obtained from the RVW, including QRS (ms), Tp-e (ms), ratio Tp-e/QT and contractility are presented in Appendix 3 and have not been used for further analysis.

The RVW data generated in this study is in accordance with reported literature data for verapamil as shown by Liu et al. (Liu et al., 2006), in Table 3.11 and Figure 3.15. These published data were investigated over a similar concentration range from 0.1 µM up 100 µM. Data was extracted from literature plots and converted using graph-plot digitising software (Digit v1.0.4). Data shown gives the estimated mean data point value, the minimum and maximum based on the error bar plots could not be determined. Liu et al. also demonstrated that no change in QT was observed for verapamil at 0.1, 1 and 10 µM, and a decrease at 100 µM, such that changes in QT interval from vehicle control were 15.0, 16.9, 17.4 and -22.7ms, respectively.

Table 3.11 Verapamil RVW Mean Experimental delta QT Interval

Concentration (μM)	Delta QT (Δ ms) for each RVW Preparation against Vehicle Control					
	Mean ±SEM		ΔQT (mean) (ms)	ΔQT (max.) (ms)	ΔQT (min.) (ms)	Liu et al. (2006)
Control	327.4±35		0.0	35.0	-35.0	
0.01	350.6±27		23.2	15.2	31.2	-
0.1	340.9±31		13.5	9.5	17.5	15.0
1.0	341.4±18		14.0	-3.0	31.0	16.9
10.0	314.8±13		-12.6	-34.6	9.4	17.4
100	ND		ND	ND	ND	-22.7

* *p*-value <0.05 compared to vehicle control

Data was extracted from literature plots by Liu et al. (2006) and converted using graph-plot digitising software (Digit v1.0.4). Data shown gives the mean data point value but no estimated minimum and maximum as it was not possible to observe the error bars.

Figure 3.14 Verapamil RVW: Representative Graph of the Change in ECG in the RVW Following Investigation with Different Verapamil Concentrations

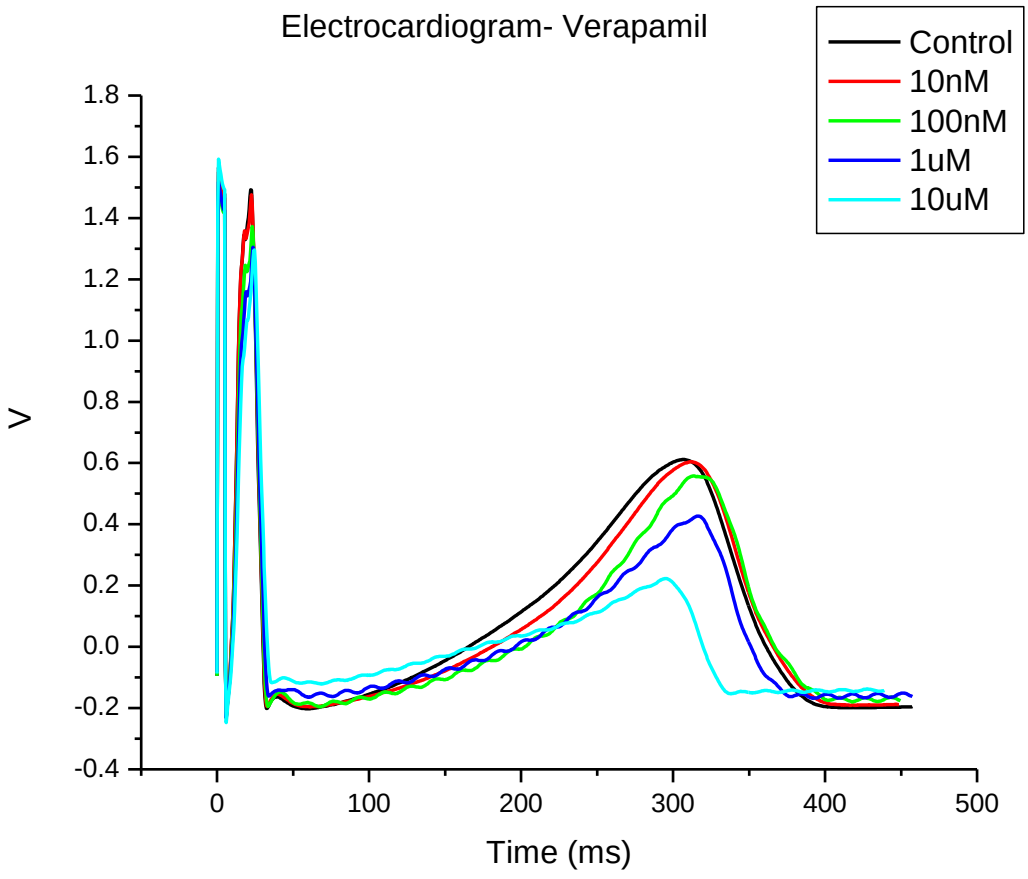

Figure 3.14: Representative plot of the change in ECG waveform generated in the rabbit ventricular wedge (RVW) preparation over a range of free verapamil drug concentrations, 0.01 (—), 0.1 (—), 1.0 (—) and 10 μM (—) prepared in Tyrode's perfusion media compared to vehicle control (—)

Figure 3.15 Verapamil RVW: Graph of Changes in QT Response (Δ ms) in the RVW Following Investigation with Verapamil and Comparison to Literature

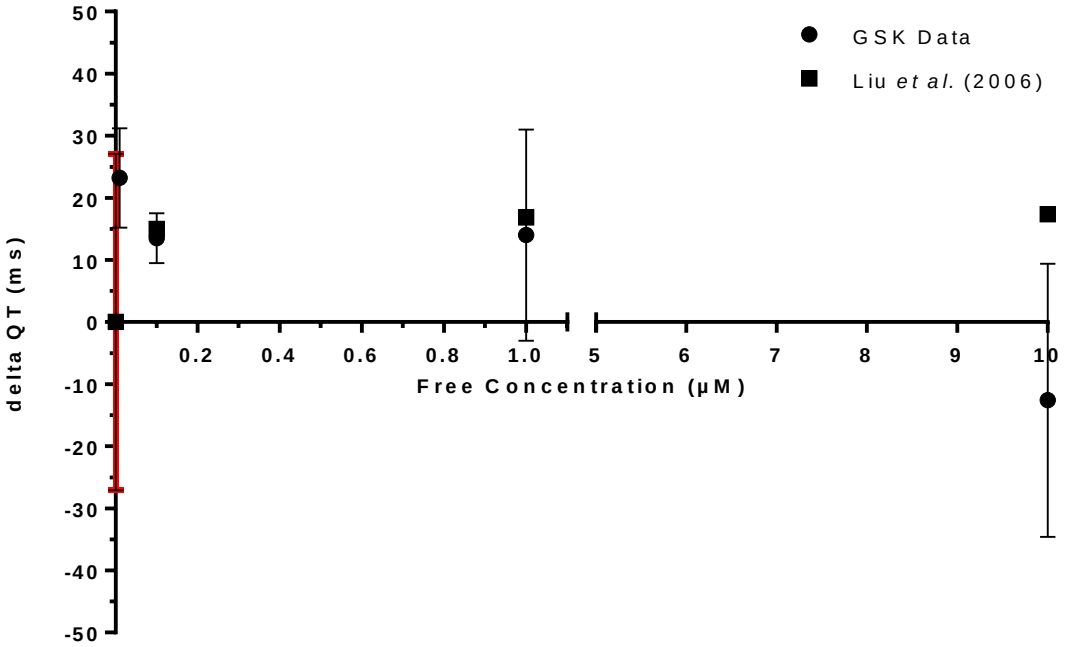

Figure 3.15: Graph of the delta change in QT response (ms) data generated in the rabbit ventricular wedge (RVW) preparation over a range of free verapamil concentrations, 0.01, 0.1, 1, and 10 µM prepared in Tyrode's perfusion media compared to vehicle control. Data shown gives the mean data point value and the standard error bars from a GSK investigation, US (●) and plotted with extracted data from literature plots by Liu et al. (2006, ■) and converted using graph-plot digitising software (Digit v1.0.4) to estimate the mean delta change in QT but it was not possible to observe the error bars.

3.8. Rabbit Ventricular Wedge Summary Conclusion

The purpose of this study was to generate ex vivo PD data for cisapride, moxifloxacin and sparfloxacin, known for their potential to prolong QT interval, and verapamil to act as a control, in the isolated perfused rabbit ventricular wedge (RVW) preparation.

The RVW model is utilised as a CV preclinical model in Safety Pharmacology studies. It exhibits both sensitivity and specificity to detect drug-induced proarrhythmias as part of the pharmaceutical drug development and patient safety which forms part of the integrated risk assessment (Lawrence et al., 2008; Wang et al., 2008; Picard et al., 2011). It has been validated in a blinded investigation with the ability to differentiate proarrhythmic drugs from non-arrhythmic drugs (Liu et al., 2006). The tissue preparation is considered intact with cellular coupling preserved through the coronary arterial perfusion and viability maintained for 4 to 5 hours. The electrophysiological stability has been reported up to 7 hours (Yan and Antzelevitch, 1996; Yan et al., 2001; Chen et al., 2006; Liu et al., 2006), an advantage over the Langendorff-perfused rabbit heart (Screenit assay) which deteriorates over a 1 hour perfusion as shown by a 3.5% QT interval abbreviation (Hondeghem, 1994; Hondeghem et al., 2003; Valentin et al., 2004). The increased viability is a result of using a section of tissue with greater perfusion, shortened preparation time, rather than the more complex whole-heart. This extended viability allows for repeated drug concentration assessment, combinations and even delayed time-course of action.

GSK experiments for the rabbit left ventricular wedge preparation treated with less than 0.5% DMSO as part of the vehicle control formulation (n = 6, not shown) have demonstrated that the QT and Tp-e intervals change within 2% and 5%, respectively, over a period of 4 hours. This is equivalent to approximately 6 ms increase over time if the baseline stimulated QT interval is 300ms. This is comparable to the simulated baseline S.E.M. value in each concentration-response model across each compound data set. Similar data have been obtained in other laboratories for baseline changes in QT following vehicle administration (Chen et al., 2006).

The RVW model uses a simple pacing protocol with preparations stimulated at 0.5, 1, or 2 Hz stimulation frequency to detect frequency-dependent changes on QT/QRS. Even though rates may be physiologically low, in isolated tissue this allows membrane recovery and a standardised protocol for comparison of species APD, with the rabbit most similar to human (Franz 1988). It has been shown that pacing at 1 Hz gives the maximal area of APD across

ventricular tissue, with steady state APD shorter at higher frequency (Gibbs and Johnson, 1961; Carmeliet, 2006). ECG parameters are routinely measured at 0.5 Hz following a 30 min equilibration period with compound at 1 Hz. Many I_{Kr} (hERG) blockers have typically been shown to cause a reverse-use dependent prolongation of QT interval (i.e. a more pronounced effect at lower stimulation frequencies). Therefore a 0.5 Hz stimulation frequency is used to detect changes in QT that are not detectable at 1 Hz, with a more prolonged plateau phase. A stimulation frequency of 2 Hz can be used to detect changes in QRS. QRS prolongation is indicative of conduction slowing caused by sodium channel block (Yan and Antzelevitch, 1996; Xu et al., 2002; Varro and Baczko, 2011).

It has been found that the surface density of I_{Kr} in rabbit hearts and human (hERG) channel in human cell lines are under direct control of extracellular K^+ concentration, and reduction results in accelerated internalization and degradation of the channel within hours, and associated with QT prolongation (Guo et al., 2009a). The cardioplegic Tyrode's solution containing 24 mM KCl used in the RVW is an excessive concentration to maintain the extracellular K^+ concentration whilst the tissue is being dissected and is unperfused. The 4 mM Tyrode's solution perfused through the RVW tissue provides the correct physiological K^+ concentration, and together maintain greater viability of the ventricular tissue. These mechanisms may play important roles in changes in repolarisation reserve following electrolyte disturbances. I_{Kr} may play a positive feedback role contributing to repolarisation lengthening when repolarisation is already prolonged due to its very fast inactivation and recovery from inactivation, (Virag et al., 2009).

Although the rabbit heart is similar to the human heart in many electrophysiological attributes, such as cardiac action potential properties, intracellular ion concentrations I_{Kr} reverse rate dependence and electrophysiological responses (Odening and Kohl, 2016), the interspecies differences, such as cardiac rate may account for discrepancies in translation to human (O'Hara and Rudy 2012). It is well established that there is a significant difference between the electrical properties of myocytes and ion channel composition isolated from different regions of the heart from canines and humans (Szabo et al., 2005; Gaborit et al., 2007). The rabbit left ventricle provides an improved model compared to canine and guinea pig because rabbit hearts are more prone to the occurrence of EADs and susceptibility to TdP due to low expression of slow delayed rectifier current (I_{Ks}) and repolarisation reserve (Zicha et al., 2003; Guo et al., 2009a; Jost et al., 2013).

The rabbit ventricular wedge preparation has been shown to be a highly predictive model for clinical QT prolongation and TdP (Liu et al., 2006). Similarly Lu et al, (2006) reported the direct comparison of four in vitro models to predict the TdP liability of five different antibiotics, with the RVW being the most sensitive to correctly rank clinical liability (Lu et al., 2006). In a separate assessment the same conclusions were drawn for 13 compounds around the prospective role of the arterially perfused rabbit left ventricular wedge (Wang et al., 2008). Recent development in the RVW has been through an index of Cardiac Electrophysiological Balance (iCEB) (TdP scoring and QT assessment incorporating beat-to-beat instability) as a biomarker for predicting potential risks for drug-induced non-TdP-like VT/VF (Lu et al., 2013).

3.8.1. Review of Assumptions and Limitations of the RVW:

The rabbit ventricular wedge QT response to generate a concentration-response model for each compound, which was subject to a number of assumptions and/or limitations previously described (Section 3.6).

1) The RVW examines the isolated tissue response devoid of external influences which is an advantage like many other isolated organ preparations (liver and lung perfusions) and it has greater viability compared to the whole Langendorff-heart (Lawrence 2008).

2) The ventricular wedge preparation has become an established ex vivo methodology with consistent and reproducible tissue preparations through standard protocols and consistent experimenter. Through consistent protocols and experimenter, the viable mass of tissue is consistent to provide a good signal response devoid of ischemic tissue interference (Chen 2006; Picard 2011).

3) Given that cardiac ventricular tissue is highly perfused, an assumption is no accumulation of drug during infusion and subsequent doses is considered, and that a 30 minute first-pass perfusion is sufficient for tissue equilibration of free drug at steady state. ECG parameters obtained and stable wave forms used are captured at the end of equilibration or dosing periods to reflect the steady state response. Potential biopsy/microdialysis/SPME of tissue samples could be used to show tissue concentrations equivalent to the perfusion media concentrations infused and demonstrate

equilibrium or accumulation, if no adverse effects on ECG signal capture (Abrahamsson et al., 2011).

4) Limited number of concentrations/data points from each RVW preparation. This could be addressed by increasing preparation number, increasing the number of concentrations per experiment or varying a range of different concentrations to fully define a response curve (Meibohm and Derendorf, 1997). Furthermore, the RVW is an ex vivo preparation that uses cardiac tissue from rabbits, so it is limited in terms of ethical use of large numbers of animals.

5) A theoretical maximum QT threshold of 700ms was imposed as a physiological upper limit that the delta QT interval could change, representing an approximate 200% increase from a baseline based on maximum values observed (Liu et al. 2006). This maximal response may be restricted in vivo due to other compensatory mechanisms or adverse cardiovascular effects resulting from blood pressure or heart rate changes which may invoke drug-induced arrhythmias (Cherry et al., 2012). The fitted Hill coefficient ranged from 0.5 to 1.2 which indicates that the binding was approximately 1:1. The E_{max} model assumes that receptor binding is rapid and reversible. This statement is true for many cardiac ion channel inhibitors and the reversibility is dependent on the affinity, dissociation rate constant (K_d). A limitation is that some compounds are voltage-dependent, which means preferential binding relative to the open or closed states of the ion channel. (Dumotier et al., 2001; Milnes et al., 2010; Kamiya et al., 2015).

6) The QT interval measured is a parameter consisting of multiple ion channel interplay, not only hERG K^+ channel activity, which is assumed, but also Ca^{2+} and Na^+ channel. Additional ion channel interactions attenuate the maximal QT response, then these have been excluded, for example with cisapride at 10 μM as identified in this study but also previously described (Liu et al., 2006; Wang et al., 2008).

The aforementioned assumptions support comparison of the RVW data to data obtained in an anaesthetised rabbit preparation. These assumptions and limitations are indeed also similar to those postulated by Beattie et al., in an in silico model using ion channel screening data to predict QT interval changes in the rabbit ventricular wedge (Beattie et al., 2013). It has been

shown that the hERG block alone causes concentration-dependent QT prolongation (Rampe and Brown, 2013), whereas when multichannel block is regarded, the effect could be reduced or even shortened. For that reason, the multichannel interaction of tested compounds should be taken into consideration, in order to make the proarrhythmic risk assessment more reliable (Wisniowska et al., 2012). Therefore a developmental progression would be the translational step from in silico to whole-body in vivo response incorporating the multichannel effects for predictive thorough QT clinical results from simulated AP's and utilising an open-source web portal. (Mirams et al., 2014; Williams and Mirams, 2015). Alternatively, the utilisation of a promising in vitro screening assay using human-induced pluripotent stem cell cardiomyocytes (hiPSC-CMs) on multielectrode arrays (MEA) may bridge the translational gap. This assay has shown good correlation with the RVW and other in vivo cardiovascular models (Harris et al., 2013; Harris, 2015).

3.8.2. Non-linear QT Response Model in the RVW

From the data generated for each compound in the RVW, a sigmoidal concentration-response curve was shown to be present when integrating data from GSK and published literature. Drug responses are often measured as a change from a baseline state (E_0) which may be incorporated and allow for potential variability to be included. In the RVW preparations there was some variability in baseline QT interval (ms), and vehicle corrected delta (Δ) change in QT (ms) used in the sigmoidal E_{max} model. The E_{max} model is based on receptor theory, where the E_{max} reflects the efficacy of the drug, or maximal response (e.g. QT change, ms), which in this study was set to a theoretical maximum ΔQT based on reported data at 700ms (~200%) in the RVW. The EC_{50} or IC_{50} reflects the potency of a given compound, the concentration which evokes a 50% change or inhibition. In this instance, the maximal response possible in the RVW model was 200%, therefore when compared to an in vitro hERG IC_{50} is plotted at the 50% change (175ms) observed in the RVW.

The Hill coefficient parameter, *n*-value, can be thought of as the number of molecules binding but in practice it is simply used to give a better fit to the data (Derendorf and Meibohm, 1999). From the data generated, *n* ranged from 0.5 to 1.2, which is an acceptable range from limited data points and representative of 1:1 drug-channel binding. This is similar to the acceptance criteria applied by Beattie et al. and Mirams et al. using a predictive in silico model of QT response in the RVW (Beattie et al., 2013; Mirams et al., 2014). There are other simpler PD models that are related to the sigmoidal E_{max} model, such as the simple E_{max}

model (where, the Hill coefficient, *n*=1), the linear model, log-linear model and the fixed-effect model (Holford and Sheiner, 1982). However these models are less commonly used as they are generally only valid over a limited concentration range (Csajka and Verotta, 2006).

Figure 3.16 Comparison of Non-Linear QT Response Model in the RVW between Cisapride, Moxifloxacin and Sparfloxacin

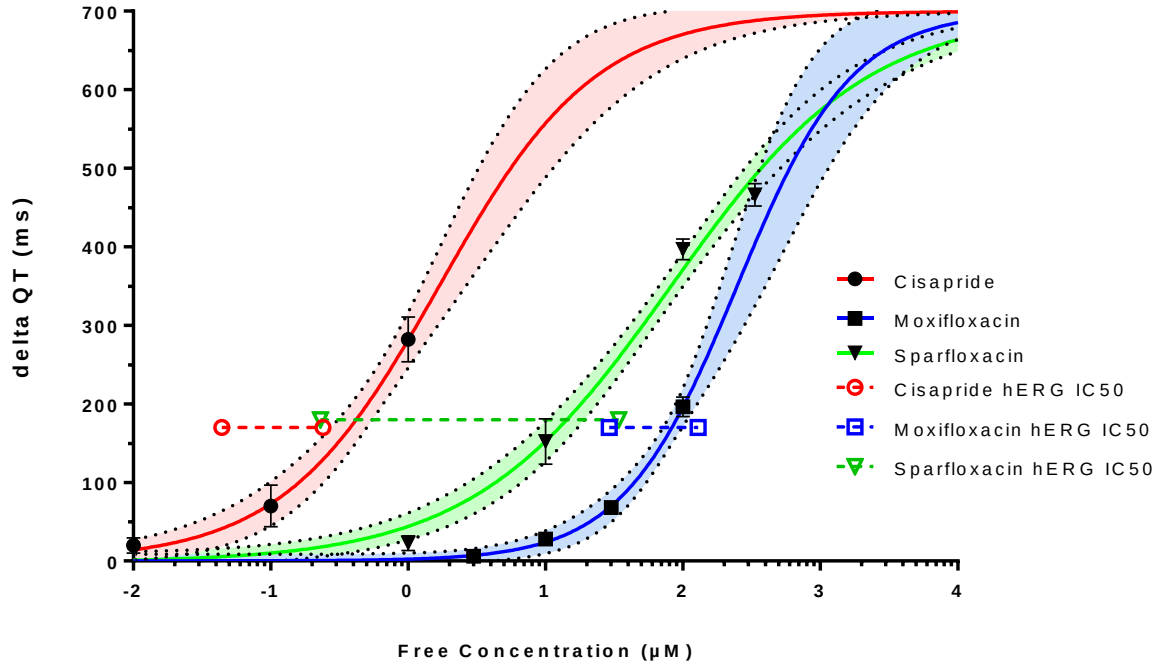

Figure 3.16: Graph comparing the delta change in QT response (ms) data generated in the rabbit ventricular wedge (RVW) preparation over a range of log [free drug concentrations] between cisapride (●), moxifloxacin (■) and sparfloxacin (▼) which has been fitted using a non-linear response model shown for cisapride (— red line), moxifloxacin (— blue line) and sparfloxacin (— green line) with 95% confidence interval range shaded within the dotted lines (····). Literature ranges of reported hERG IC_{50} data is plotted for reference against cisapride from Milnes et al., (2010, ○), moxifloxacin from Kang et al. and Alexandrou et al. (2001 and 2006, □) and sparfloxacin from Redfern et al. (2003, Δ) is shown.

Table 3.12 Literature Ranges of hERG IC_{50} for each compound Investigated in the RVW

Compound	hERG IC_{50} (µM)	Reference
Cisapride	0.04 – 0.24	Milnes et al. 2010
Moxifloxacin	29 – 114; 129	Alexandrou et al. 2006; Kang et al.2001
Sparfloxacin	0.23 - 34	Redfern et al. 2003

Table 3.12 shows the literature reported range of hERG IC_{50} values, where each reference has collected data from multiple sources and techniques for comparison.

In summary, the relative sigmoidal concentration-QT response curves for cisapride, moxifloxacin and sparfloxacin generated, show the difference in potency of each compound (cisapride > sparfloxacin > moxifloxacin) (Figure 3.16). Each non-linear QT response modelled (with 95% confidence interval) in the RVW is in the range of the hERG IC_{50} values as shown in Table 3.12. The range of literature in vitro IC_{50} values reported are a result of different experimental set ups, such as model (patch-clamp, whole cell), cell type (HEK, CHO), temperature, and voltage protocols (Polak et al., 2009). A further adaptation of the modelled RVW concentration-response is to incorporate potential tissue binding as the RVW assumes free drug concentrations in the perfusion media but not any cardiac binding.

For each compound, the concentration-QT response sigmoidal E_{max} model parameters from this RVW investigation were then used as the mathematical PD model to predict the QT response following the simulated PBPK modelling of the in vivo rabbit (Chapter 5) against the observed change in QTc following investigation in the anaeasthetised rabbit (Chapter 4). The free heart tissue concentrations in the anaesthetised rabbit model and the PBPK simulation model were derived from the tissue binding data generated from protein binding experiments (Chapter 2) and each used the RVW E_{max} model determined in this chapter.

Strathclyde Institute of Pharmacy and Biomedical Sciences
GlaxoSmithKline

CHAPTER 4

Anaesthetised Rabbit QTc Model

4. ANAESTHETISED RABBIT PKPD MODEL

Cardiovascular toxicity is a primary cause of compound attrition during drug development (Ferri et al., 2013; Pugsley et al., 2015). To specifically address the cost of attrition due to functional CV effects e.g. QT interval prolongation, a core set of assays are performed to provide an integrated risk assessment to project/program teams (Pollard et al., 2010). The ex vivo rabbit ventricular wedge (RVW), previously described (Chapter 3), forms part of the screening process. The next minimum requirement as part of the ICH S7B guidance is an in vivo QT assessment in a non-clinical species, such as the dog or monkey. However the use of conscious animals needs to be considered carefully, therefore an in vivo rabbit model was developed in an anaesthetised preparation to support in vivo translation utilising the protein binding and RVW data. The anaesthetised rabbit model is considered an acceptable adjunct to conscious studies, though the choice of anaesthetic is important (Hammond et al., 2001; Vincze et al., 2008). From a cross-pharma survey (Hammond, et al., 2001; Hammond et al 2011) and the PRODACT Initiative, many pharmaceutical companies reliably use anaesthetised models such as the rabbit, as a predictive screening tool for cardiac electrophysiology and QT prolongation (Hammond et al., 2001; Hashimoto, 2008).

The purpose of this study was to generate data for several compounds, cisapride, moxifloxacin and sparfloxacin and verapamil, known for their potential for QT interval prolongation and assess in the terminally anaesthetised rabbit model preparation. The aim was to generate a concentration-response model of the in vivo rabbit to enable comparison to an ex vivo rabbit ventricular wedge preparation and other PK sources by translational physiological-based pharmacokinetic modelling (PBPK).

4.1. Background to the Anaesthetised Rabbit Model

A broad review of the literature on in vivo models that use anaesthetised preparations to assess cardiovascular parameters in support of safety pharmacology is mainly represented by three models; the anaesthetised guinea-pig, the methoxamine-sensitised rabbit and the halothane-sensitised dog / Chronic Atrio-Ventricular Block (CAVB). The halothane-sensitised / CAVB dog model is an infrequently used model today, primarily due to ethical reasons and use of the conscious telemetered dog as the gold standard for GLP cardiovascular assessment in drug development prior to FTIH (Sivarajah *et al.*, 2010). The anaesthetised guinea pig is a common model for QT prolongation assessment, albeit with inherent anaesthesia difficulties, has been previously investigated within the GSK cardiovascular

screening strategy (Yao *et al.*, 2008). The anaesthetised methoxamine-sensitised rabbit equally remains a model of choice for early preclinical screening for TdP liability and not only to scrutinize for proarrhythmic biomarkers such as QT interval prolongation or TRIaD-related cofactors (Picard *et al.*, 2011).

The anaesthetised rabbit model was first developed in 1990 following unexpected mortalities in a rabbit melanin-binding study of Almokalant due to TdP (Carlsson et al., 1990). The anaesthetised animal was shown to be less sensitive than the conscious state, with TdP induced at much higher doses with known I_{Kr} – blockers (Carlsson et al., 1993). QT prolongation occurs in a normal anaesthetised model but without TdP (White et al., 1999). The difference observed is postulated to be a result of factors influencing the repolarisation reserve on extracellular K^+ and intracellular Ca^{2+} being less affected in the anaesthetised state (Varro and Baczko, 2011). Hypokalaemia has been shown to increase susceptibility of TdP (White et al., 1999; Farkas et al., 2002). Alpha1-adrenergic stimulation and mechanical load are considered crucial for the expression of sarcolemmal Na^+/Ca^{2+} exchanger (NCX1) and intracellular Ca^{2+} concentrations (Schillinger et al., 2007). Pre-treatment with an α1-adrenergic blocker, prazosin, in the anaesthetised model has been shown to abolish TdP incidence (Carlsson et al., 1990). The rabbit also exhibits a greater density of α1-adrenoreceptors compared to most other species, including man, (Mukherjee et al., 1983). As a result, the requirement of a sensitising agent, in the rabbit influences Ca^{2+} and K^+ concentrations repolarisation reserve and incidence of TdP in the anaesthetised state (Mukherjee et al., 1983; Carlsson et al., 1996). Additional sensitising factors include reflex bradycardia following blood pressure elevation, increased ventricular stretch, action potential prolongation and increases in intracellular calcium concentrations (Carlsson, 2008; Farkas et al., 2009). Consequently pre-treatment with selective α1-adrenoreceptor agonists, such as methoxamine or phenylephrine, via concomitant administration with I_{Kr} blocking agents increase TdP occurrence at doses similar to conscious rabbits (Farkas et al., 2002; Vincze et al., 2008). The anaesthetised α1-sensitised rabbit model often remains the choice for screening new compounds directly for their TdP liability for some companies (Picard et al., 2011), with the use of sling trained conscious rabbits limited (Kijtawornrat et al., 2006b). This has led to the sensitised model as good indicator of TdP liability (Carlsson, 2008) with electrical stability and beat-to-beat variability recently assessed as preceding markers of TdP (Farkas et al., 2010; Jacobson et al., 2011).

4.2. Anaesthetised Rabbit Method

The terminally anaesthetised rabbit model used within this project was based on methodologies described in detail in previous publications (Carlsson et al., 1993; Carlsson et al., 1997; Batey and Coker, 2002; Farkas et al., 2004) and differs in that no sensitising agents (methoxamine or phenylephrine) were used to induce TdP. Initial pilot and baseline experiments were important to determine the optimal induction and anaesthetic regimen without excessive use of animals. The anaesthesia protocol was adapted from other model set up using propofol induction and isoflurane to meet internal best practices (Wu et al., 2005; Vincze et al., 2008; Nalos et al., 2012).

All in vivo experiments were ethically reviewed and carried out in accordance with Animal (Scientific Procedure) Act 1986 and the GlaxoSmithKline (GSK) policy on the Care, Welfare and Treatment of laboratory animals and under the authority of Project Licence No PPL 80/2588 19b PR03 (terminally anaesthetised models). All personnel involved in the conduct of scientific procedures on animals did so under the authority of a Home Office Personal Licence issued under the Act.

4.2.1. Surgical Model Preparation

In brief, female (New Zealand White) rabbits weighing between 2.3 kg to 4.6 kg, aged at least 12 weeks old, were utilised in this study. Rabbits were pre-medicated with local anaesthetic to the ears (EMLA cream, lidocaine/prilocaine), at least 30 minutes prior and administered a sedative via subcutaneous injection (medetomidine, Domitor Janssen, Orion Pharma, 10 mg/kg) 15 minutes prior to induction. Anaesthesia was carried out by administration of propofol (Propoflo, Abbott Pharmaceuticals, 10 mg/kg), via the marginal ear vein as a slow bolus for induction and maintained by Isoflurane/O_2 via a face mask (3-4%) in a recumbent dorsal position on a heat mat (37°C). A tracheotomy was performed with an endotracheal tube (3.5mm diameter) inserted 1-2 cm into the trachea to allow direct delivery of anaesthetic to the animal and self-maintained ventilation with observations (respiration, heart rate and temperature) recorded every 10 minutes. The left carotid artery (CA) was cannulated with cut-down polypropylene tubing (Cat catheter with female luer mount, AS96, Arnolds; 1.3 mm O.D. (4F) x 30.5cm) filled with heparinised saline (10UI). The CA cannula was connected to a manometer probe via the opening of a three-way tap to record arterial blood pressure and facilitated blood sampling. The jugular vein (JV) was cannulated with polypropylene tubing (I.D. 0.58 mm x O.D. 0.96 mm, Smith Medical tubing)

connected to 5-French silastic, silicone catheter (I.D. 0,25mm x O.D. 0,51mm, BC-5S; Royem Scientific Limited) filled with heparinised saline (10UI). The JV cannula was connected to a syringe infusion pump (Cole-Parmer, 115 VAC, Linton Scientific) to enable drug dose administration. Total time taken from induction and maintenance of anaesthesia (10-15 minutes) to completion of surgical preparation (25 minutes) was approximately 40 minutes. Post surgery, the animal was allowed to equilibrate for at least 20 minutes to allow collection of baseline predose data.

4.2.2. Electrophysiological Data Analysis

Electrophysiological data for cardiovascular endpoints and haemodynamics were captured as part of the experimental set up. Standard cardiovascular parameters (PR, RR, QRS and QT intervals and HR) were continuously recorded at a sampling rate of 1kHz data acquisition system software (Ponemah, St Paul, MN, USA) in Lead II configuration from surface ECG via skin clips. Haemodynamic parameters (mean arterial blood pressure (MBP), systolic blood pressure (SBP), diastolic blood pressure (DBP), heart rate (HR)) were obtained from the manometer connected to carotid artery, which was discontinuous due to blood sampling via a three-way valve. Electrophysiological data was recorded, using separate channels on a Gould multi-channel detector via an Analogue to Digital converter (ADC, Gould 6615-65). Raw data from Ponemah was transferred to EMKA ECG Auto (EMKA Technologies) for analysis. On screen markers of intervals were positioned manually on selected ECG waves for measurement and data characterised by the software's pattern recognition for optimal integration to be placed into 5 or 10 minute bins of data with mean, standard deviation and standard error of the mean (S.E.M.) reported. Rate-corrected QT intervals were calculated in EMKA ECG Auto (EMKA Technologies), using the widely accepted Bazett's correction method based on the mean individual animal data from the pre-treatment equilibration period (DeClerk 2002).

Bazett Correction formula: $$QT_c = {QT}/{\sqrt{RR}}$$ Equation 10

QT = interval from start of the deflection point Q from the isoelectric line to the end of the T wave, return to isolectric point (ms); RR = R to R peak interval (ms); QT_c = heart rate corrected QT interval (ms);

All cardiovascular parameters were summarized as 'baseline-corrected', which was defined as the delta change (Δ) or percent change (Δ%) in mean, for example QTc, from baseline (pre-infusion) to post-infusion for any given individual and subsequently 'double delta corrected' changes (ΔΔ) for any mean vehicle effects.

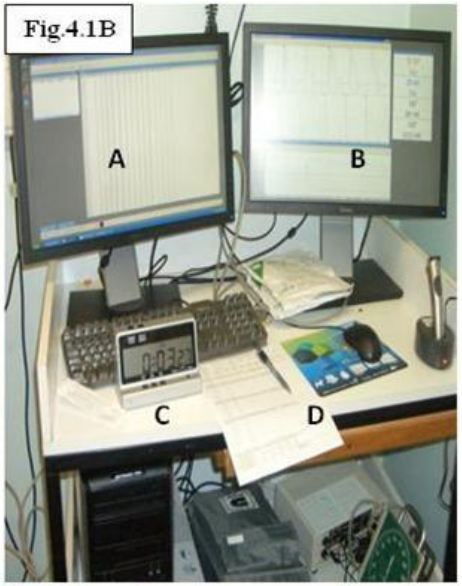

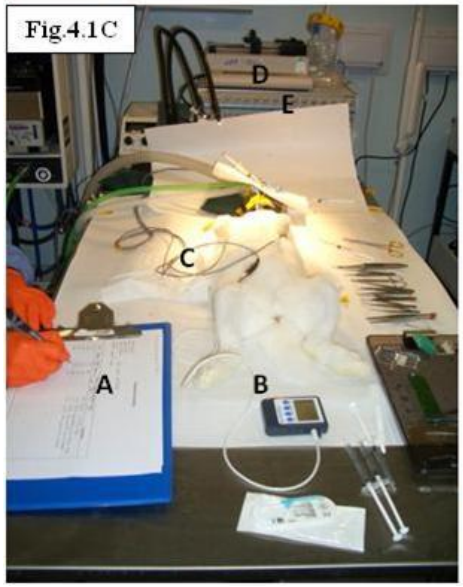

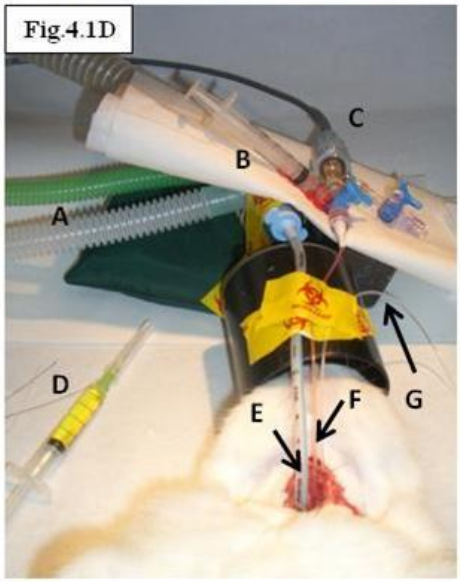

Figure 4.1A: The anaesthetic system set up used for the induction and maintenance of the anaesthetised rabbit preparation. Anaesthesia rig (Ohmeda excel prodigy) [**A**], with vet-scavenger exhaust extraction via a facemask [**B**]. Isoflurane/O_2 delivery system post tracheotomy [**C**] and scavenger system [**D**].

Figure 4.1B: Shows the computer station equipment providing continuous monitoring of cardiovascular parameters via Ponemah data collection, with raw data stream [**A**] and graphical output [**B**] screens. Digital stop-clock [**C**] used to check equilibration and dosing/sampling times, along with hardcopy data log used at each blood time point for back up [**D**].

Figure 4.1C: The anaesthetised rabbit preparation set up. Hardcopy data recording was used for anaesthesia monitoring (respiration rate, heart rate, isoflurane %) at each time point for back up [**A**] and included temperature monitoring via a rectal probe [**B**]. The pictures shows the ECG leads in a Lead II configuration connected to forelimbs and hind leg via crocodile skin clips [**C**]. A syringe infusion pump (Cole-Parmer, 115 VAC, Linton Scientific) was used for delivery of vehicle or test article via a jugular vein cannula [**D**] and cardiovascular parameters captured through a Gould multi-channel detector and an Analogue to Digital converter (ADC, Gould 6615-65) [**E**].

Figure 4.1D: Isoflurane/O_2 delivery system post tracheotomy (green tube) and scavenger system (opaque white tube) [**A**]. Blood sampling syringe inserted [**B**] via a three-way tap to access carotid artery which was also connected to the manometer probe (Gould) [**C**]. Sodium pentobarbitone (10 mg/kg, Euthatal, Merial Animal Health Ltd) was used for termination administered via the jugular cannula [**D**]. An indwelling intubation endotracheal tube (3.5mm diameter) was inserted 1-2cm into the trachea for direct delivery of gaseous anaesthetic following a tracheotomy [**E**]. Catheters were implanted in the left carotid artery and jugular vein for recording of arterial blood pressure/blood sampling and infusion of drugs, respectively. The carotid artery (CA) was isolated, ligated and cannulated with a cut-down polypropylene tubing (Cat catheter with female luer mount, AS96, Arnolds; 1.3 mm O.D. (4F) x 30.5cm) filled with heparinised saline (10UI, diluted from 5000UI stock heparin) previously connected to the pressure probe [**F**]. The jugular vein (JV) was isolated, ligated and cannulated with polypropylene tubing (I.D. 0.58 mm x O.D. 0.96 mm, Smith Medical tubing) connected to 5-French silastic, silicone catheter (I.D. 0.25mm x O.D. 0.51mm, BC-5S; Royem Scientific Limited) filled with heparinised saline (10UI) [**G**].

4.3. Assumptions and Limitations of the Anaesthetised Rabbit Model

There are inherent limitations with any in vitro/ex vivo experimental technique which are not just only pertinent to the anaesthetised rabbit model preparation, which may not be able to completely mimic the conscious in vivo conditions (Lawrence et al., 2008; Hamon et al., 2009). The aim was to use the anaesthetised rabbit model to generate a concentration-response model for QTc for each compound, which is subject to a number of assumptions and/or limitations with the model, that should be considered;

1) The effects of premedication administered to the rabbit as part of the surgical procedure may affect the variability not only during sedation, induction and maintenance of anaesthesia but also the response to the drug (cisapride, sparfloxacin, moxifloxacin or verapamil).
2) The selection of the anaesthetic agent utilised is important with regards to the potential cardiovascular effect in this model and species as a direct result of the agent used (Hammond et al., 2001; Vincze et al., 2008). With any given selection of anaesthesia there may also be variability in the response of each individual animal to the anaesthesia administered which may also impact upon the physiological response.
3) The duration of the anaesthetised surgical preparation, whether this is the animal's physical viable limit post surgery and time maintained under anaesthesia, and/or the combination impact of the insult of the test article.
4) Reproducibility / response in each rabbit model preparation is replicated in the same way, from response to the premedication analgesics, anaesthetics (induction and maintenance), the surgery time to process tissue collection through to isolation of the tissue by cannulation and pacing stimulation.
5) The magnitude of QT prolongation response in the anaesthetised state is unaffected and translatable, as the model described is a non-sensitised model such that it differs to the literature standard α-1 sensitised model which uses agents (methoxamine or phenylephrine) to induce a TdP response at a drug threshold.
6) The number of anaesthetised preparations required is limited to one animal one dose concentration, which means increased animal numbers to generate concentration-QT data and with an increased time/resource burden.
7) The suitability of the test article compound's solubility is a factor required for the intravenous infusion and may limit the upper dose or adapt the infusion rate / volume.

8) The complex nature of the interplay between the cardiovascular system and the autonomic parasympathetic nervous system may evoke other compensatory mechanisms which may mask changes or complicate interpretation.

4.4. Dose Selection and Formulation

Concentrations for each test compound were selected to primarily evoke a range of changes in QT prolongation which may also be associated with other cardiovascular responses. Generally at least two doses of each test compound were investigated in the anaesthetised model. Cisapride monohydrate, moxifloxacin hydrochloride, sparfloxacin and verapamil hydrochloride, were purchased from Sigma Aldrich, UK and formulations were prepared as below (Table 4.1).

Table 4.1 Compound and Dose Formulation Details used in the Anaesthetised Rabbit Prpearations

Compound	M. Wt	Compound Form	Salt M. Wt	Chemical Purity (%)	Adjusted Purity (%)	Formulation
Cisapride	483.9	Cisapride Monohydrate (Batch 080M4751V)	465.9	99	95.3	5% dimethylsulfoxide in polyethylene glycol 200
Sparfloxacin	392.4	Sparfloxacin (Batch BCBF4939)	n/a	98	98	α-gluconolactone in water
Moxifloxacin	401.4	Moxifloxacin Hydrochloride (GW646803A) (Batch VBOG/5504/8/4)	437.9	98	89.8	5% DMSO–10% SBE–cyclodextrin in 5 mM methanesulphonic acid
Verapamil	454.6	Verapamil Hydrochloride (Batch 047206 L75939)	454.6	100	92.6	0.9% (w/v) aqueous sodium chloride

4.4.1. Cisapride:

Cisapride monohydrate (Batch C4740; Lot 080m4751) was purchased from Sigma Aldrich, UK. Cisapride was administered at doses of 0.3, 1 and 3 mg/kg with n=7, 3 and 8, respectively, at each dose level. Cisapride was formulated as a solution using dimethylsulfoxide (DMSO) and polyethylene glycol with an average molecular weight of 200 (PEG200) as the vehicle. The DMSO was initially added and then PEG200 added which was

sonicated, vortex mixed and protected from light to provide a solution of cisapride at nominal concentrations of 0.5 and 5 mg/mL This formulation was a stable solution and did not require constant stirring.

4.4.2. Sparfloxacin:

Sparfloxacin (Batch 56968-10G-F; Lot BCBF4939V) was purchased from Sigma Aldrich, UK. Sparfloxacin was administered at doses of 16.7, 33.3 and 100 mg/kg (free base) with n=5 at each dose level. Sparfloxacin was prepared as an *in situ* salt formulation by the addition of α-gluconolactone in a ratio of 0.8:1 to weighed sparfloxacin, such that upon the addition of water provided a solution of sparfloxacin at nominal concentrations of 4.2, 8.3, and 25 mg/mL (Conrath 1995). The resultant formulation was bright yellow in colour, which was protected from light and required constant stirring, and was approximately pH 3.8.

4.4.3. Moxifloxacin:

Moxifloxacin hydrochloride (Batch VBOG/5504/8/4) was purchased from Sigma Aldrich, UK. Moxifloxacin was administered at doses of 5 and 20 mg/kg (free base) with n=4 at each dose level. Moxifloxacin was formulated by the addition of DMSO initially to solubilise the material and subsequent addition of 5% DMSO–10% SBE–cyclodextrin in 5 mM methanesulphonic acid to the weighed moxifloxacin, to provide a solution of moxifloxacin at 8.3 and 33.3 mg/mL. This was sonicated for 5 minutes in a water bath at 37°C and vortex mixed to maintain a solution. The resultant formulation was yellow in colour, which was protected from light and required constant stirring.

4.4.4. Verapamil:

Verapamil hydrochloride (Batch 047206; Lot L75939) was purchased from Sigma Aldrich, UK. Verapamil was administered at doses of 0.1, 0.3 and 1 mg/kg with n=2 at each dose level. Verapamil was prepared as a solution using sterile saline (0.9% sodium chloride) as the vehicle. This was sonicated, vortex mixed and protected from light. This formulation was a stable solution and did not require constant stirring.

4.5. Drug Administration to the Anaesthetised Rabbit

A single intravenous dose infusion of drug or control vehicle over a 30 minute period (unless stated) was administered to an anaesthetised rabbit model to assess the PK/PD response. Drug or vehicle was infused at a constant rate corrected for bodyweight, such that over the infusion period the correct dose volume was delivered to administer the appropriate dose level (mg/kg). Following the infusion, a blood sample was taken immediately before the infusion pump was switched off, then the jugular cannula was clamped and disconnected. Cardiovascular PD parameters were measured continuously as previously described and the PK sampling continued to the designated end of experiment.

Figure 4.2 Schematic of Protocol Time course for the Anaesthetised Rabbit Model

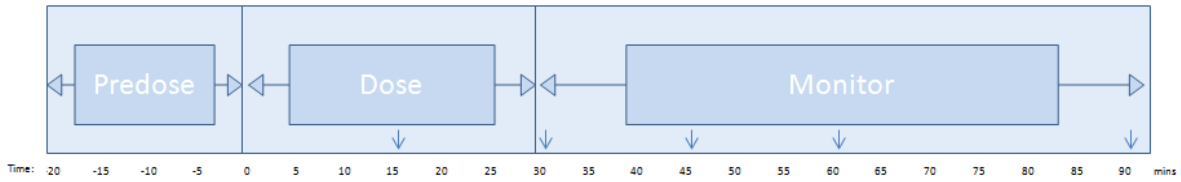

Figure 4.2: Schematic protocol time course for the anaesthetised rabbit model. The sequential steps of control/equilibration predose period for at least 20 minutes post surgical preparation (carotid and jugular cannulations); followed by a typical 30 minute infusion of test compound "Dose" and subsequent monitoring for up to 60 minutes during which blood samples were taken. Cardiovascular data was continuously monitored using Ponemah (St Paul, MN, USA) in Lead II configuration from surface ECG via skin clips at a capture rate of 1000 ms via a Gould multi-channel detector using an Analogue to Digital converter (ADC, Gould 6615-65). Raw data from PoneMah was transferred to EMKA ECG Auto (EMKA Technologies) for analysis. Blood samples were taken every 5 minutes via a three-way tap connected to the carotid artery to enable PK sample analysis.

4.5.1. Administration for Control Baseline Assessment

Following the surgical preparation of the initial anaesthetised rabbit experiments, the effects of anaesthesia following surgical preparation, animal induction and maintaining anaesthesia were determined. Animals (n=4) were not administered vehicle or test article, but were maintained for the 90 minute experiment, with blood sampling and cardiovascular data collected for evaluation.

4.5.2. Administration of Cisapride

A single intravenous dose infusion of cisapride was administered to each animal at the rate of 0.6 mL/kg over a 30 minute period via the jugular vein at an infusion rate of approximately 0.06 mL/min, to achieve a 0.3 mg/kg, and 3 mg/kg with a dose formulation of 0.5 and 5 mg/mL. Each dose volume/rate was adjusted per individual bodyweight. A 1mg/kg dose was

achieved through an infusion rate of 0.02 mL/min using a 5 mg/mL solution. Cardiovascular monitoring and PK sampling continued for a further 60 minutes and a total experiment time of 90 minutes. Cisapride vehicle control animals were administered 5% dimethylsulfoxide in PEG 200 vehicle in the same manner for comparison.

4.5.3. Administration of Sparfloxacin

A single intravenous dose infusion of sparfloxacin was administered to each animal at the rate of 4 mL/kg over a 60 minute period via the jugular vein at an infusion rate of approximately 0.2 mL/min, to achieve a 16.7, 33 and 100 mg/kg with a dose formulation of 4.2, 8.3 and 25 mg/mL. Each dose volume/rate was adjusted per individual bodyweight. Cardiovascular monitoring and PK sampling continued for a further 120 minutes and a total experiment time of 180 minutes. The extended dose in fusion and experimental period was required for a separate metabolomic assessment and mimic a study in guinea pigs (Park et al., 2013). Sparfloxacin vehicle control animals were administered α-gluconolactone in water vehicle in the same manner for comparison.

4.5.4. Administration of Moxifloxacin

A single intravenous dose infusion of moxifloxacin was administered to each animal at the rate of 0.6 mL/kg over a 30 minute period via the jugular vein at an infusion rate of approximately 0.06 mL/min, to achieve a 5 mg/kg and 20 mg/kg with a dose formulation of 8.3 and 33.3 mg/mL. Each dose volume/rate was adjusted per individual bodyweight. Cardiovascular monitoring and PK sampling continued for a further 60 minutes and a total experiment time of 90 minutes. Moxifloxacin vehicle control animals were administered 5% DMSO–10% SBE–cyclodextrin in 5 mM methanesulphonic acid in water vehicle in the same manner for comparison.

4.5.5. Administration of Verapamil

A single intravenous dose infusion of verapamil was administered to each animal at the rate of 0.6 mL/kg over a 30 minute period via the jugular vein at an infusion rate of approximately 0.06 mL/min, to achieve a 0.1 mg/kg, 0.3 mg/kg and 1 mg/kg with a dose formulation of 0.167, 0.5 and 1.67 mg/mL. Each dose volume/rate was adjusted per individual bodyweight. Cardiovascular monitoring and PK sampling continued for a further 60 minutes and a total experiment time of 90 minutes. Verapamil vehicle control animals were administered 0.9% (w/v) aqueous sodium chloride (saline) vehicle in the same manner for comparison.

4.6. Blood Sampling

Blood samples were collected predose at -10 minute (to mimic sample effect and recovery) and 0 minute immediately before dosing and then post dose subsequently every 5 minutes (or every 10 minutes for Sparfloxacin) until the end of the experiment. Approximately 0.5 mL of blood was sampled via the carotid artery cannula 3-way tap and collected into 1 mL micro-container tubes containing anticoagulant (heparin during baseline experimental studies (Fisher Scientific) and K_3EDTA during all other study investigations); roller mixed and place on crushed wet ice.

4.6.1. Blood Clinical Chemistry

Blood clinical chemistry parameters such as Na, K, Cl, pH, glucose and spO_2, were obtained for diagnostic assessment of the anaesthetised model during the baseline experimental set up. From blood samples acquired into heparinised micro-containers at the specified time intervals, glass capillary tubes were used to draw triplicate aliquots for analysis using blood-gas analyser (ABL-77, Radiometer).

4.6.2. Blood Sample Processing

At the end of the experiment blood samples were centrifuged at 3,000 g for 5 minutes, refrigerated at +4°C (Hettitch micro-centrifuge or Jouan A14 micro-centrifuge) to yield plasma which was removed and placed into individual tubes in a 96-well matrix block (Alphanumeric Matrix Block, Nunc).

Plasma samples were stored at -20°C prior to quantitative bioanalysis by appropriate LC-MS/MS analysis (Appendix 1). This was conducted for all experiments at all time points whether baseline, control vehicle or test article post start of dose infusion.

4.7. Cardiac Tissue Sampling

At the end of the experimental period or selected terminal time points, the rabbit was euthanased by an overdose of anaesthetic (sodium pentobarbitone, Euthatal, Merial Animal Health Ltd, 10 mg/kg) via the jugular cannula. Immediately upon confirmation of death (respiratory cessation and diminished ECG signal), the thoracic cavity was opened and the heart was removed (< 2minutes). The heart was briefly rinsed in cold saline, the pericardial sac removed, pat dried and frozen at -20°C. Hearts were collected to obtain tissue drug concentrations determined by appropriate quantitative LC-MS/MS bioanalysis (Appendix 1).

4.7.1. Cisapride Heart Tissue

Heart tissue was obtained at selected terminal time points of; 15, 30 (end of infusion), 45 and 60 minutes post dose start (n=1 per time point) and at 90 minutes (n=4) at 0.3 mg/kg and 3 mg/kg. No cardiac tissue was obtained at 1 mg/kg as this dose infusion was part of an experimental ramped infusion (not reported).

4.7.2. Sparfloxacin Heart Tissue

Heart tissue was obtained at selected terminal time points of; 60 minutes end of infusion for 16 and 100 mg/kg (n=5 per time point) and 33.3 mg/kg (n=2 per time point); and 120 and 180 minutes (n=1) for 33.3 mg/kg.

4.7.3. Moxifloxacin Heart Tissue

Heart tissue was obtained at selected terminal time points of; 30 minutes (end of infusion), 60 minutes (n=1 per time point) and at 90 minutes (n=3) at 5 mg/kg and 20 mg/kg for moxifloxacin.

4.7.4. Verapamil Heart Tissue

Heart tissue was obtained at selected terminal time points of; 30 minutes (end of infusion) and 90 minutes (n=1 per time point) at 0.1, 0.3 and 1 mg/kg for verapamil, respectively.

4.7.5. Heart Tissue Processing

4.7.5.1. Heart Dissection for Homogenisation

Sample processing of heart tissue for cisapride was conducted by dissection, to obtain samples suitable for homogenisation and extraction for quantitative bioanalytical analysis.

Briefly, following collection of the heart tissue (as described previously section 4.8, cardiac tissue sampling), the tissue was allowed to defrost at room temperature and the whole tissue weighed. During processing heart samples were kept on wet ice as much as possible. The heart was pinned onto a histology cork board and the left and right atria were removed using a dissecting scalpel, and weighed. The right ventricle wall was dissected away from the septum to open out the heart following an incision along the anterior interventricular sulcus (a 'line' formed from the left coronary artery, great cardiac vein, anterior interventricular artery towards the apex of the heart). The right and left ventricles were weighed and further dissected into three and nine strips of approximately equal proportions (0.3 – 0.45 g) in the vertical plane, respectively. Heart tissue sections were finely scissor minced and placed into 7 mL CK28 tubes containing inert ceramic beads for hard tissue homogenisation and 5x volumes of aqueous UPLC mobile phase was added. The tissue was homogenised into a liquid state using a Precellys 24 tissue lysis homogeniser (protocol two replicate bursts of 2x 20 second oscillations at 5500 rpm) maintained at +4°C via a Cryolys cooling system (Bertin Technologies, Stretton Scientific).

4.7.5.2. Cryostat Microtome Slicing for Homogenisation

Sample processing of heart tissue for sparfloxacin, moxifloxacin and verapamil was conducted using a cryostat to obtain samples suitable for homogenisation and extraction for quantitative bioanalytical analysis. In brief, harvested frozen heart tissue was 'cemented' on a pre-chilled 3cm chuck block using distilled water and placed in a cryostat microtome (Leica CM3050S) maintained between -20 and 24°C. Heart tissue was sliced (12 µm thickness), such that 50 slices of fine tissue were collected into pre-weighed tubes (7mL CK28 containing inert ceramic beads) to provide one heart tissue sample for homogenisation. This process was repeated to provide twelve replicate samples of heart tissue. Each replicate of 50x 12 µm slices was weighed and 5x volumes of aqueous UPLC mobile phase were added. The tissue was homogenised using a Precellys 24 tissue lysis and homogeniser (Bertin Technologies, Stretton Scientific). This equated to approximately half of the mounted tissue taken in slices for quantitative bioanalysis as shown in Figure 33.

Figure 4.3 Frozen Rabbit Heart Tissue for Cryostat Processing

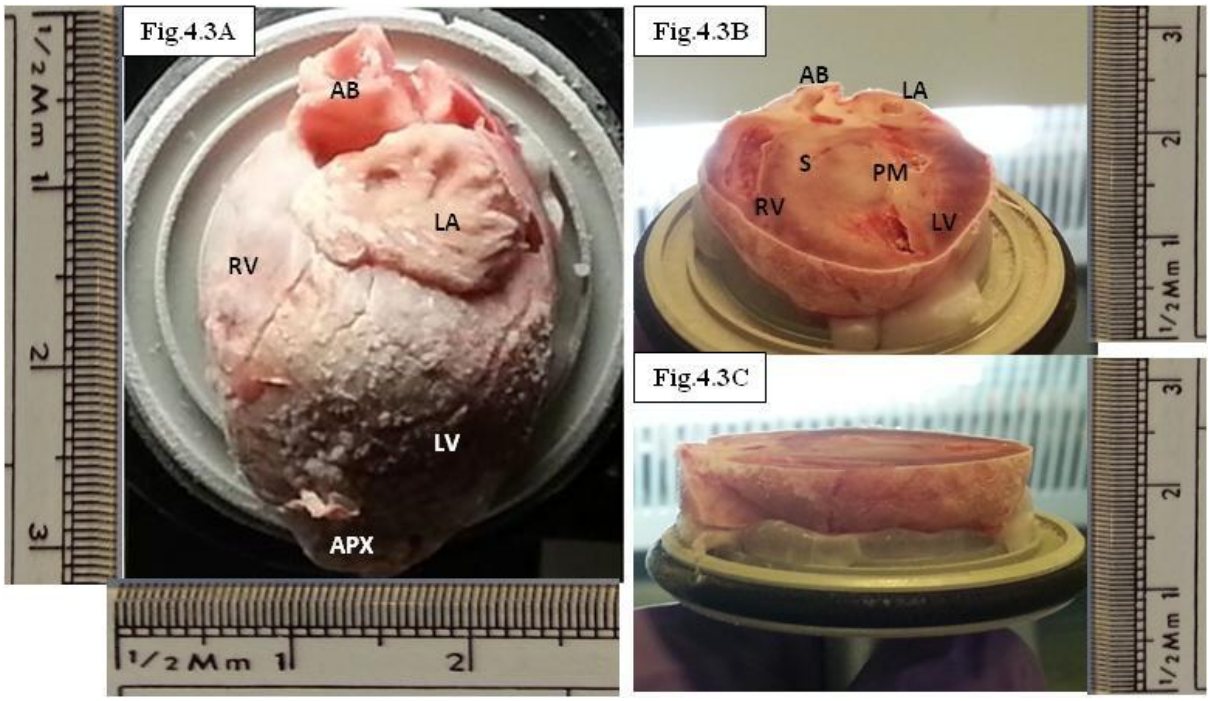

Figure 4.3A: Photographed image of a frozen rabbit heart mounted on to a 3 cm microtome chuck. Labels identify heart regions for orientation with Aortic Branch (**AB**), Left Atrium (**LA**), Right Ventricle (**RV**), Left Ventricle (**LV**) and Apex (**APX**) along with scaled ruler.

Figure 4.3B: Shows the remaining heart tissue along with identifiable labelled regions of the heart, including septum (**S**) and Papillary Muscle (**PM**) following 12x samples of 50x 12 µm slices taken for quantitative bioanalysis, which equates to approximately 600 µm of tissue per sample analysed.

Figure 4.3C: Shows a transverse section view of the remaining heart tissue mounted using distilled water to fix in position on a pre-chilled 3 cm microtome chuck. Approximately 1.2cm total in depth is taken in sliced tissue for quantitative bioanalysis which equates to approximately half of the mounted heart tissue.

4.8. Bioanalysis of Plasma and Heart

4.8.1. Anaesthetised Rabbit Plasma PK samples

Anaesthetised rabbit plasma samples were analysed to determine drug concentrations of cisapride, sparfloxacin, moxifloxacin or verapamil, as required. Each compound was analysed using an analytical method based on protein precipitation, followed by HPLC-MS/MS analysis described in Appendix 1. All samples were analysed using a 25 µL aliquot of plasma against a calibration standard curve with a range of 3 orders of magnitude. Quality Control samples (QC) were prepared at 3 different concentrations of each appropriate compound (cisapride, sparfloxacin, moxifloxacin or verapamil) and analysed with each batch of samples against separately prepared calibration standards. The applicable analytical runs for each compound met all predefined run acceptance criteria (Appendix 1). The computer system that was used to acquire and quantify data was Analyst Version 1.6.1.

4.8.2. Anaesthetised Rabbit Heart Tissue samples

Heart tissue homogenate samples were quantified as per plasma samples (Appendix 1), except using control heart tissue matrix homogenate for calibration and quality control standards. Further dilution of extracted heart tissue homogenate samples with extracted control matrix with internal standard was necessary for cisapride (1:10 dilution), sparfloxacin (1:20 dilution), moxifloxacin (1:5 dilution) and verapamil (no dilution) to be within their respective assay ranges.

4.9. Statistics for QT Response

The QTc data was analysed in SAS Proc Mixed using a repeated measures mixed model analysis approach, with fixed factors Dose and Time, random factor Animal and the initial change fitted as a covariate. As the time points were equally spaced the within-animal covariance was modelled using an autoregressive covariance structure (Bate and Clarke, 2014). The data was log transformed (with an offset) to stabilize the variance. Pair-wise planned comparisons were made between the treated groups and the vehicle group separately at each time point. Where if the *p*-value was <0.05, the difference between the treatment and the vehicle control was considered statistically significant. Blood clinical chemistry data was analysed in In Vivo Stat using a paired t-test for pre- and post-surgery, with statistical significance with *p*-values <0.05.

4.10. Anaesthetised Rabbit Results

4.10.1. Control Baseline Anaesthetised Rabbit Model Results

4.10.1.1. Control Clinical Chemistry

Pre-anaesthetic blood was compared to the post-surgery anaesthetised preparation clinical chemistry during the control preparations (n=5) and are presented in Table 4.2.

Pre-surgical induction mean readings of $paCO_2$ were at 46.7 ±5.5 mmHg and paO2 were at 259.3 ±15.1 mmHg, compared to the post-surgery anaesthetised preparation of $paCO_2$ at 38.5 ±4.1 mmHg, which had decreased but not significantly (*p*-value >0.05), and paO2 at 267.3 ±60.1 mmHg, which had increased but not significantly (*p*-value >0.05).

The blood haematocrit (Hct) did not alter pre- and post-surgery at 34.3% (*p*-value >0.05) whilst blood pH did increase slightly from 7.36 ±0.07 to 7.50 ±0.04, which was significant (*p*-value <0.05).

Blood electrolyte values obtained from arterial samples during the control model assessment prior to surgery for Na^+, Cl^-, Ca^{2+} and K^+ were 138.7 ±3.2 mmol/L, 106.3 ±3.8 mmol/L, 1.5 ±0.1 mmol/L and 4.2 ±0.4 mmol/L, respectively. Compared to post-surgery under the maintained anaesthesia, mean values of Na^+, Cl^-, Ca^{2+} and K^+ were 134.4 ±1.5 mmol/L, 103.8 ±2.4 mmol/L, 1.3 ±0.1 mmol/L, and 3.2 ±0.2 mmol/L, respectively. Sodium blood levels were unaffected (p-value >0.05), whereas chloride, calcium and potassium levels decreased (*p*-value <0.05) following surgery based on the initial pre-surgical variability.

All parameters were maintained at the post-surgery level for the experimental duration.

Table 4.2 Control Anaesthetised Rabbit: Mean Blood Clinical Chemistry Values Pre- and Post-Surgery in the Anaesthetised Rabbit

Mean ± SD	$paCO_2$ (mmHg)	paO_2 (mmHg)	Hct	pH	Na^+ (mmol/L)	Cl^- (mmol/L)	Ca^{2+} (mmol/L)	K^+ (mmol/L)
Pre-	46.7 ±5.5	259.3 ±15.1	34.3 ±2.5	7.36 ±0.07	138.7 ±3.2	106.3 ±3.8	1.5 ±0.1	4.2 ±0.4
Post	38.5 ±4.1	267.3 ±60.1	34.3 ±1.0	7.50 * ±0.04	134.4 ±1.5	103.8 * ±2.4	1.3 * ±0.1	3.2 ** ±0.2

Blood clinical chemistry parameters assessed pre- and post- surgical preparation of the anaesthetised rabbit model using a blood gas analyser, ABL77 Radiometer, UK, from control animals (n=5)
Statistical analysis conducted as a paired t-test within subject, *p*-value <0.05 denoted by * and <0.01 denoted by **

4.10.1.2. Control Blood Pressure

Following the equilibration baseline period the mean blood pressure (MBP) was between 34 and 45 mmHg with an average of 40.4 ±1.6 mmHg that was similar to the maintained blood pressure throughout the control preparation (range 31 to 47 mmHg, *p*-value>0.05), although variability did increase with time. Each individual control preparation and average MBP time-profile with S.E.M. error bars is shown in Figure 4.4.

Figure 4.4 Control Anaesthetised Rabbit: Graph of Individual Mean Blood Pressure Response in the Anaesthetised Rabbit.

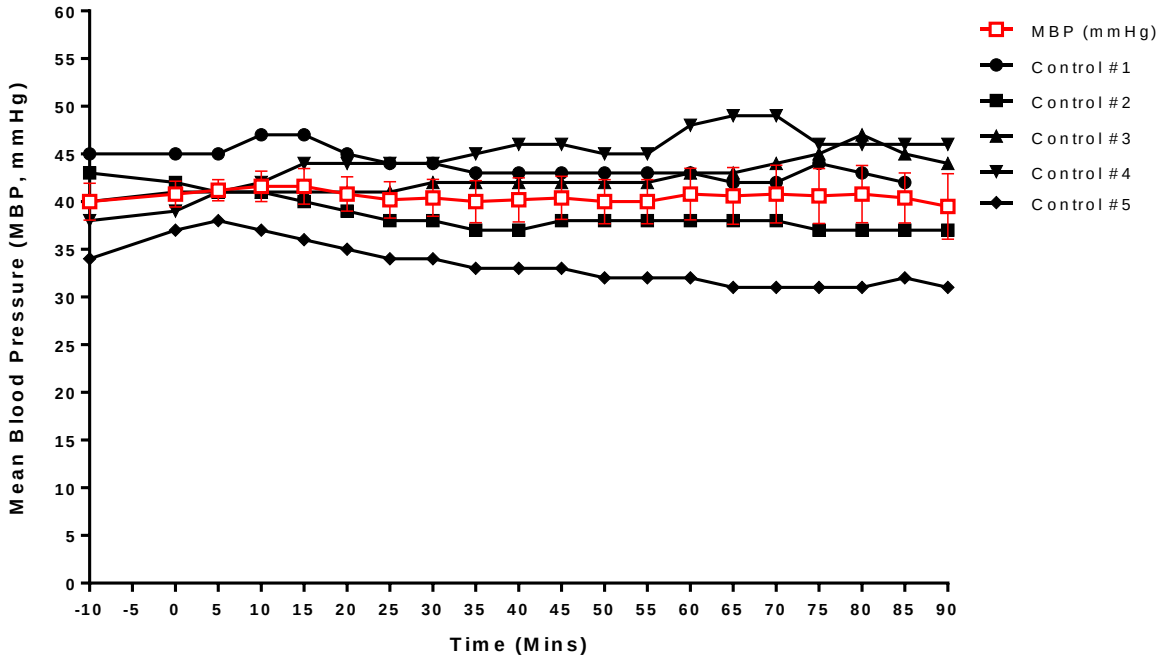

Figure 4.4: Graph of the mean blood pressure (average of systolic and diastolic) response (mmHg) data generated in a control baseline anaesthetised rabbit preparation over the experimental period. Data from n=5 control baseline preparations shown along with mean (■) and S.E.M. bars in red.

4.10.1.3. Control Heart Rate

The mean heart rate (HR) was between 174 and 224 bpm with an average of 198 ±9.2 bpm following the equilibration baseline period, which was similar to the heart rate maintained through the control preparation (range 167 to 211 bpm, *p*-value >0.05). Each individual control preparation and the average heart rate time-profile with S.E.M. error bars are shown in Figure 4.5.

Figure 4.5 Control Anaesthetised Rabbit: Graph of Individual Heart Rate Response in the Anaesthetised Rabbit.

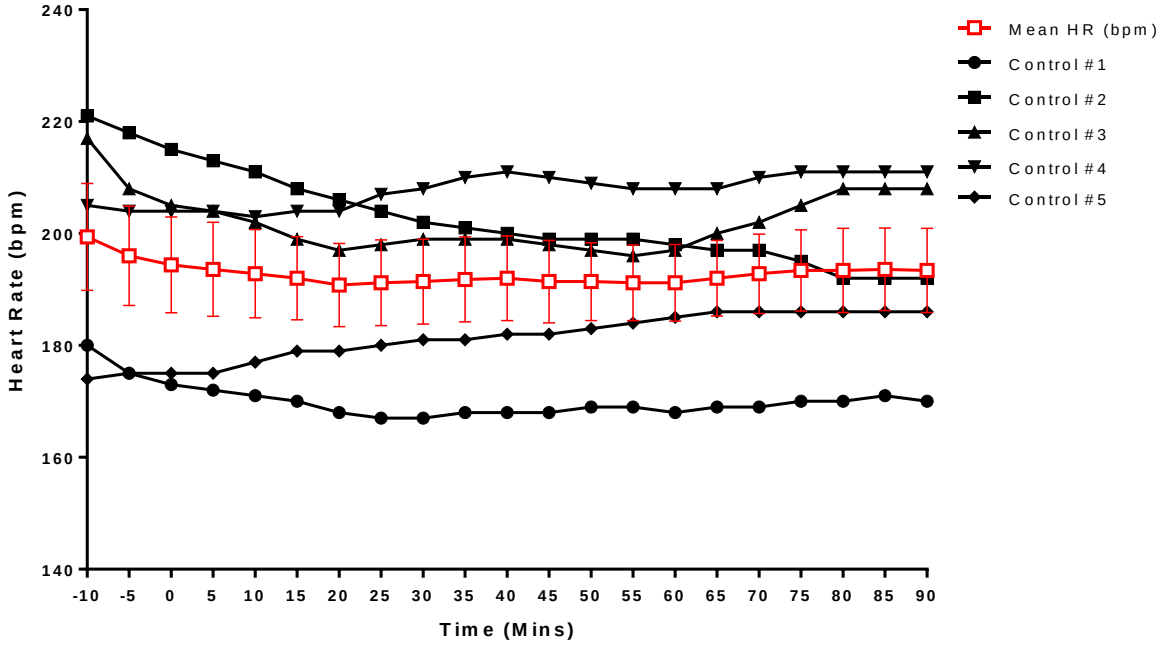

Figure 4.5: Graph of the mean heart rate response (mmHg) data generated in a control baseline anaesthetised rabbit preparation over the experimental period. Data from n=5 control baseline preparations shown along with mean (■) and S.E.M. in red.

4.10.1.4. Control Cardiovascular Parameters: QT Interval

Following the equilibration baseline period, the mean Bazett's QT corrected interval (QTc) was 270 ±2.29ms (range 261 to 273ms). During the control preparation the QTc interval was similar and maintained through the control preparation with a range between 242 to 300ms, equivalent to up to a maximum of ±10% baseline-corrected delta percentage change (ΔQTc%) (Table 4.3 and Figure 4.6). The overall mean ΔQTc% showed an overall decrease with time and increase in variability, such that after 90 minutes, the mean ΔQTc% was -2.0 ±3.2% compared to the equilibrium period (*p*-value >0.05).

Figure 4.6 Control Baseline Anaesthetised Rabbit: Graph of Individual Baseline Corrected Percentage Change in QTc (Δ%) in the Anaesthetised Rabbit.

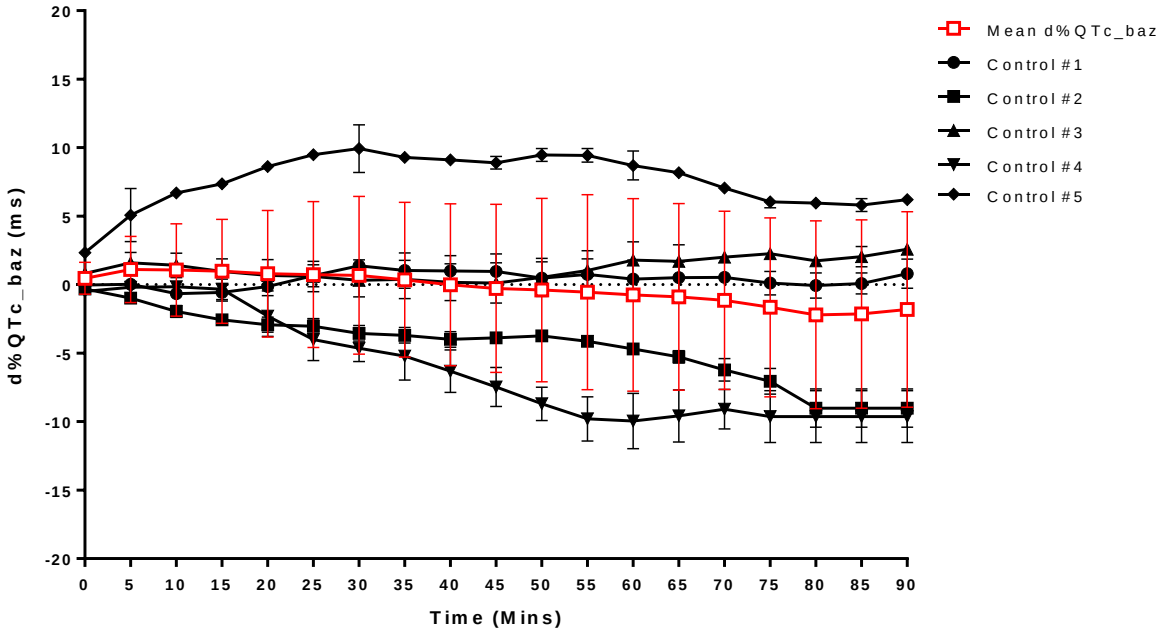

Figure 4.6: Graph of the mean change in QT interval (Δ%) data generated in a control baseline anaesthetised rabbit preparation over the experimental period. Data from n=5 control baseline preparations shown along with mean (■) and S.E.M. in red.

Figure 4.7 Control Baseline Anaesthetised Rabbit: Representative Trace of the Change in ECG in the Anaesthetised Rabbit with Time

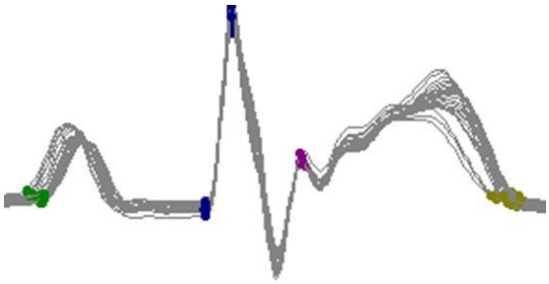

Figure 4.7: Representative overlay trace of the change in ECG waveform from each of the 5 minute time bins (n=18) generated in the anaesthetised rabbit model preparation over time under control baseline conditions with ECG waves marker points identified start of P wave (●), Q wave inflection point (●), R peak (●), S wave (●), T wave end (●).

Table 4.3 Control Anaesthetised Rabbit: Individual and Mean Baseline Corrected Percentage Change in QTc (Δ%) Response in the Anaesthetised Rabbit

Time (min)	Control #1	Control #2	Control #3	Control #4	Control #5	Mean QTc (Δ%)	S.E.M.
Predose	261 ms	273 ms	272 ms	269 ms	273 ms	**270 ms**	**2.29**
0	-0.03	-0.32	0.82	-0.49	2.34	**0.46**	**0.52**
5	0.03	-0.98	1.60	-0.19	5.08	**1.11**	**1.08**
10	-0.65	-1.95	1.41	-0.16	6.69	**1.07**	**1.51**
15	-0.56	-2.56	0.97	-0.34	7.36	**0.97**	**1.69**
20	-0.13	-2.92	0.68	-2.29	8.63	**0.79**	**2.07**
25	0.65	-3.03	0.60	-4.01	9.48	**0.74**	**2.38**
30	1.37	-3.55	0.31	-4.64	9.93	**0.69**	**2.57**
35	1.03	-3.70	0.38	-5.21	9.29	**0.36**	**2.53**
40	1.00	-4.00	0.18	-6.31	9.10	**-0.01**	**2.64**
45	0.97	-3.89	0.12	-7.47	8.90	**-0.27**	**2.74**
50	0.47	-3.73	0.53	-8.70	9.47	**-0.39**	**2.99**
55	0.74	-4.14	1.04	-9.80	9.44	**-0.54**	**3.18**
60	0.40	-4.69	1.80	-9.95	8.70	**-0.75**	**3.14**
65	0.52	-5.27	1.70	-9.58	8.18	**-0.89**	**3.05**
70	0.53	-6.22	2.01	-9.09	7.05	**-1.14**	**2.91**
75	0.11	-7.06	2.27	-9.63	6.04	**-1.65**	**2.92**
80	-0.07	-9.01	1.74	-9.63	5.95	**-2.20**	**3.07**
85	0.09	-9.01	2.05	-9.63	5.81	**-2.14**	**3.08**
90	0.80	-9.01	2.59	-9.63	6.20	**-1.81**	**3.19**

4.10.2. Cisapride Anaesthetised Rabbit Results

4.10.2.1. Cisapride Plasma Pharmacokinetics

A summary of mean pharmacokinetic parameters of cisapride, are given in Table 4.4 with mean plasma concentration-time tabulated in Table 4.5 and graphically presented in Figure 4.8, respectively.

Table 4.4 Mean Pharmacokinetics Parameters of Cisapride in Plasma Following a Single Intravenous Infusion Administration to Anaesthetised Rabbits

Dose Level (mg/kg)	T_{max} (h)	C_{max} (ng/mL)	AUC_{last} (ng*h /mL)	V_{dss} (L/kg)	CL_p (mL/min/kg)	Half-Life (hour)
0.3	20	78.5	52.2	4.07	83.0	0.57
1	25	310	127	ND	ND	ND
3	30	1120	704	3.25	60.2	0.62

Plasma concentrations of cisapride in the terminally anaesthetised rabbit following a single intravenous infusion at a nominal dose of 0.3, 1 or 3 mg/kg were each quantifiable up to 90 minutes post dose. The maximum cisapride concentrations (C_{max}) observed ranged from 78.5, 310 and 1120 ng/mL at 0.3, 1 and 3 mg/kg, respectively, occurring from 20 minutes post dose start to the end of infusion at 30 minutes indicating a near steady state infusion reached. The observed mean systemic exposure of cisapride, as determined by the area under the curve with time (AUC_{0-t}), was 52.2, 127 and 704 ng.h/mL at each increasing dose level, respectively. Parameters, C_{max} and AUC increased in an approximately dose proportional (linear) manner.

The derived pharmacokinetic parameters from the plasma concentration-time profiles at 0.3 and 3 mg/kg indicate that the volume of distribution was approximately 3.25 to 4.07 L/kg which indicates distribution through the body water and widely into tissues. The mean plasma clearance of cisapride was high at 60 to 80 ml/min/kg, approximately equivalent to liver blood flow (LBF) in the rabbit (70 mL/min/kg; Davies and Morris, 1993). The estimated half-life following an intravenous infusion administration was considered very rapid at approximately 0.6 hour. Pharmacokinetic parameters were not derived at 1 mg/kg as plasma concentration data was only collected during infusion period, as part of a ramped infusion protocol, and as a result no samples collected post dose to define the elimination.

Table 4.5 Cisapride Anaesthetised Rabbit: Mean Plasma Concentrations in the Anaesthetised Rabbit Following an Infusion of Cisapride at 0.3, 1 and 3 mg/kg

Time (min)	Mean 0.3 mg/kg Concentration (ng/mL)	±S.E.M.	Mean 1 mg/kg Concentration (ng/mL)	±S.E.M.	Mean 3 mg/kg Concentration (ng/mL)	±S.E.M.
-15	**NC**	NC	**NC**	NC	**NC**	NC
0	**NC**	NC	**NC**	NC	**NC**	NC
5	**60.7**	± 8.58	**235**	± 11.7	**778**	± 59.3
10	**64.2**	± 7.19	**263**	± 10.4	**909**	± 41.5
15	**72.5**	± 8.95	**285**	± 20.6	**990**	± 43.5
20	**78.5**	± 13.1	**282**	± 14.3	**1010**	± 57.2
25	**75.8**	± 7.54	**310**	± 26.4	**1020**	± 51.2
30	**77.1**	± 6.74	**302**	± 23.6	**1120**	± 67.9
35	**32.4**	± 3.42			**476**	± 30.3
40	**26.6**	± 3.16			**329**	± 27.3
45	**22.3**	± 2.37			**306**	± 15.1
50	**17.3**	± 1.29			**269**	± 22.4
55	**15.6**	± 1.10			**227**	± 20.1
60	**14.8**	± 1.22			**218**	± 19.5
65	**16.0**	± 1.93			**179**	± 20.1
70	**15.2**	± 2.03			**161**	± 14.2
75	**13.0**	± 1.16			**144**	± 13.5
80	**12.7**	± 2.47			**142**	± 17.4
85	**10.5**	± 0.64			**152**	± 8.89
90	**9.83**	± 0.43			**141**	± 15.9

NC Not Calculated

Figure 4.8 Cisapride Anaesthetised Rabbit: Graph of Mean Plasma Concentration-Time Profile of Cisapride in the Anaesthetised Rabbit Following an Infusion of Cisapride at 0.3, 1 and 3 mg/kg.

a) Linear plot

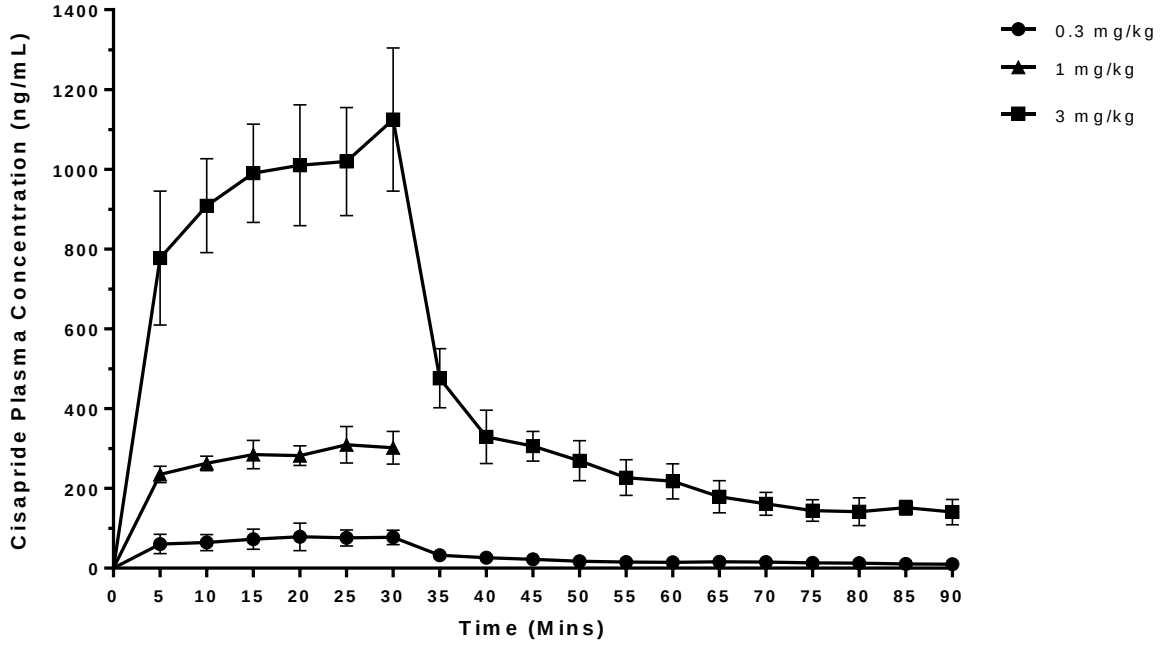

b) Log plot

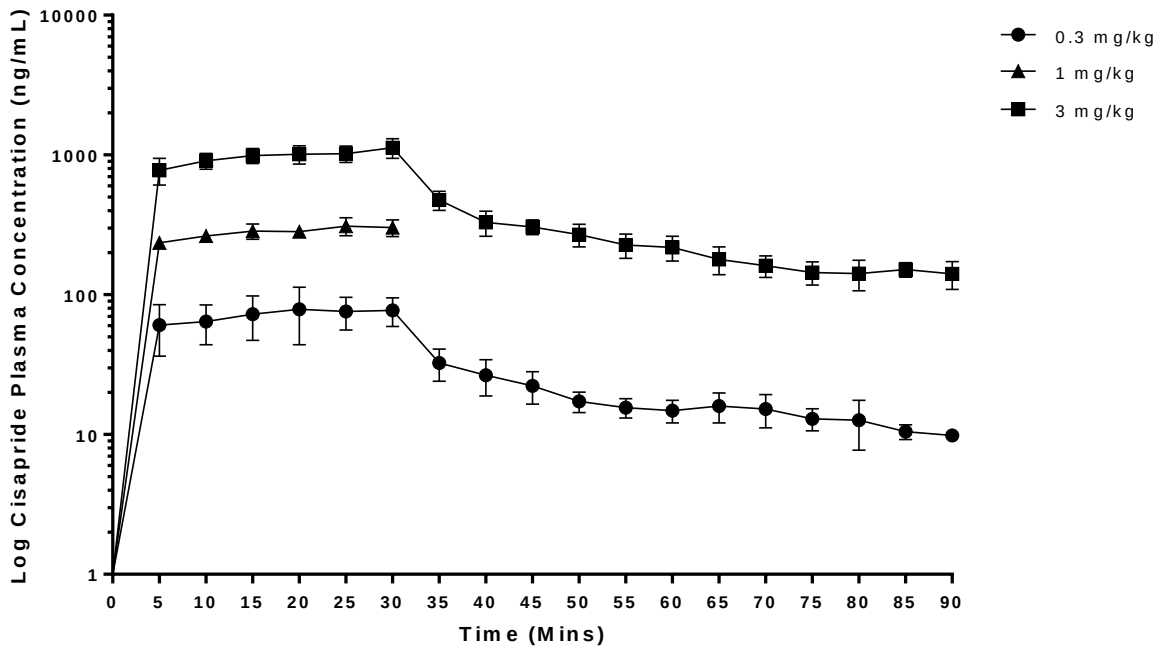

Figure 4.8: Graph of the mean and S.E.M. baseline of plasma concentration-time profile (ng/mL) generated in the anaesthetised rabbit preparation following a 30 minute intravenous infusion administration of cisapride at 0.3 mg/kg (●) (n=7), 1 mg/kg (▲) (n=3) and 3 mg/kg (■) (n=8).

4.10.2.2. Cisapride Heart Concentration Results

Heart tissue was collected and analysed by LC-MS/MS for cisapride cardiac concentrations through replicate analyses of tissue homogenates generated from dissected hearts at each time point. Rabbit hearts were collected at 15, 30, 45 and 60 minutes post start of dosing (n=1) and at 90 minutes (n=3/4) at 0.3 and 3 mg/kg. As previously described (Section 4.8), cisapride concentrations were determined for each chamber in right and left atria and ventricles. Individual replicate concentrations are given in Appendix 4. Overall mean cisapride heart tissue concentrations are summarised in Table 4.6 and Table 4.7 for 0.3 and 3 mg/kg, respectively, along with the corresponding mean plasma concentrations. Heart tissue to plasma ratio has then been derived to show the extent of tissue partitioning by cisapride at each time point.

A graphical representation of the heart tissue concentrations for each heart chamber at each dose level is shown together in Figure 4.9 as linear (a) and logarithmic (b) plots. Figure 4.10 is a further plot showing the combined concentration time profiles of cisapride in both plasma and heart.

At each dose level, 0.3 and 3 mg/kg, the overall mean cisapride heart concentrations were at their maximum at the end of the 30 minute infusion, with 521 and 11200 ng. equiv./mL, respectively. Heart tissue concentrations generally exhibited a dose proportional 10-fold increase with dose from 0.3 to 3 mg/kg and decreased with time. Similar profiles are observed for each chamber (Figure 4.9) although it can be noted that cisapride atrial (left and right) concentrations are generally lower than both the ventricle concentrations, but follow the same time course profile, with the exception of the right atria at 0.3 mg/kg which appears to be higher after the end of infusion.

The cisapride heart concentrations were greater than plasma concentrations at all time points. Heart:plasma ratios were approximately similar between the two dose levels examined. At 0.3 mg/kg, the ratio ranged from 7.0 to 21.5, and at 3 mg/kg, the ratio ranged from 4.9 to 14.0. As shown in Figure 4.10, the heart time-concentration profiles follow the same time course as plasma, with an approximate logarithmic unit (10-fold) difference.

Table 4.6 Cisapride Anaesthetised Rabbit: Mean Heart Concentrations in the Anaesthetised Rabbit Following an Infusion of Cisapride at 0.3 mg/kg

	Heart Tissue Concentration of Cisapride (ng equiv./mL)				
	Mean #1-3	**#4**	**#5**	**#6**	**#7**
Time (min)	**90**	**60**	**45**	**30**	**15**
Overall Mean Heart	**166**	277	382*	521	451
Mean Plasma	**9.8**	12.9	30.9	68.6	64.4
Heart: Plasma ratio	**16.9**	21.5	12.4	7.6	7.0

Table 4.7 Cisapride Anaesthetised Rabbit: Mean Heart Concentrations in the Anaesthetised Rabbit Following an Infusion of Cisapride at 3 mg/kg

	Heart Tissue Concentration of Cisapride (ng equiv./mL)				
	Mean #1-4	**#8**	**#7**	**#6**	**#5**
Time (min)	**90**	**60**	**45**	**30**	**15**
Overall Mean Heart	**1900**	3410	3720	11200	5050
Mean Plasma	**141**	244	288	1260	1020
Heart: Plasma ratio	**13.5**	14.0	12.9	8.9	4.9

Figure 4.9 Cisapride Anaesthetised Rabbit: Graph of Mean Heart Concentration-Time Profile of Cisapride in the Anaesthetised Rabbit Following an Infusion of Cisapride at 0.3 and 3 mg/kg.

a) Linear plot

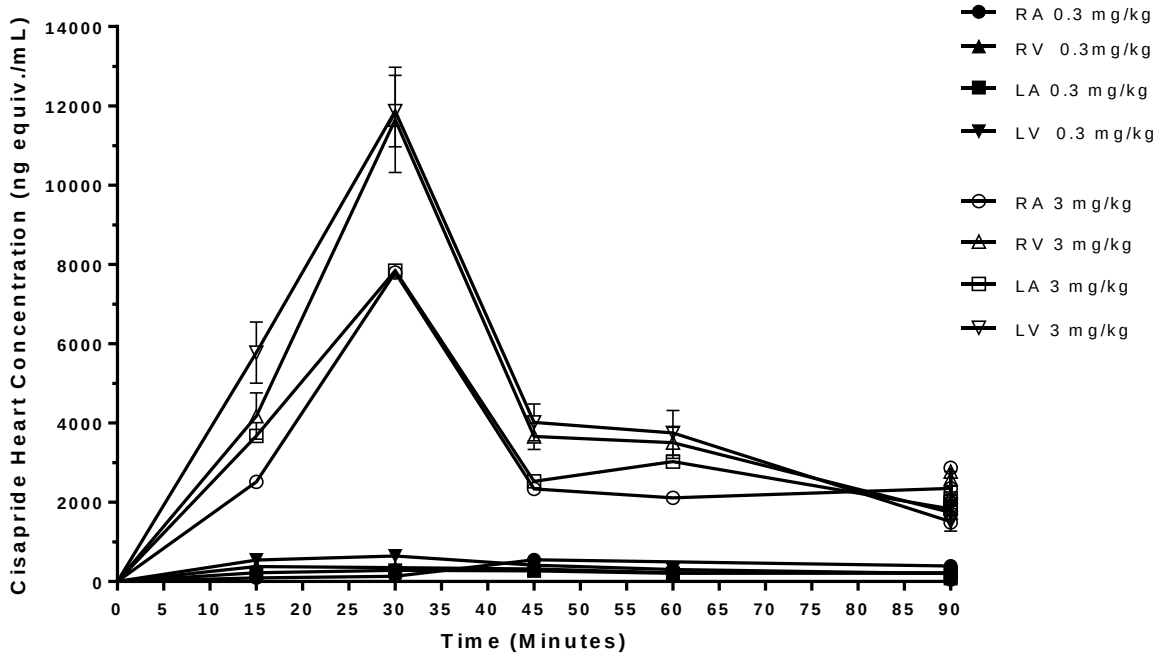

b) Log plot

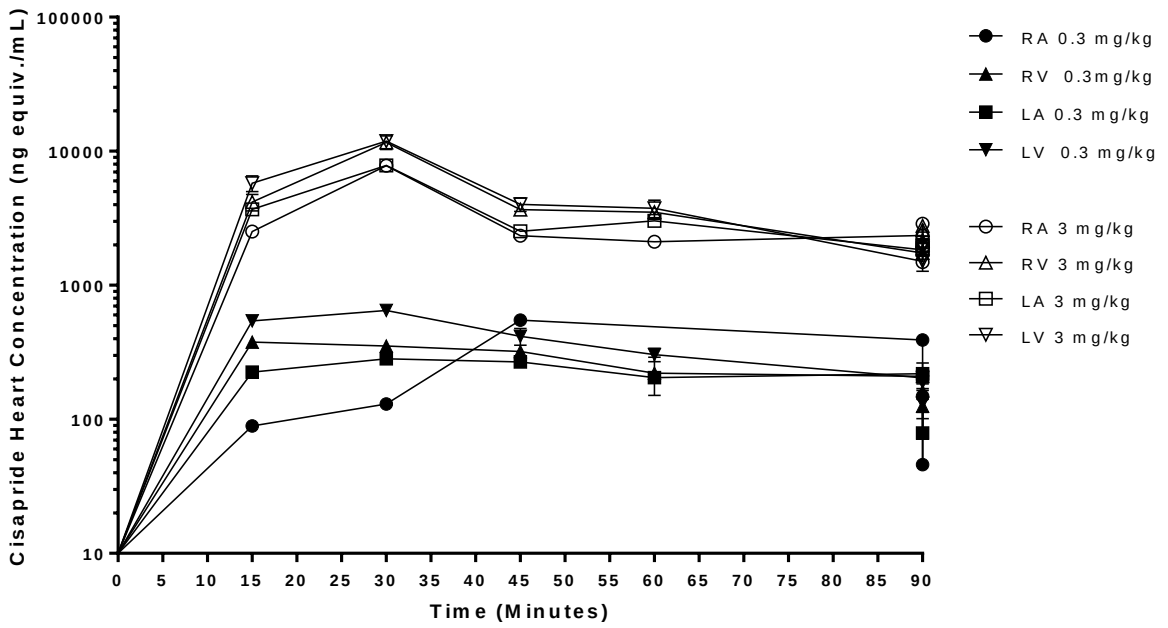

Figure 4.9: Graph of the mean and S.E.M. baseline of heart concentration-time profile (ng equivalents/mL) generated in the anaesthetised rabbit preparation following a 30 minute intravenous infusion administration of cisapride at 0.3 mg/kg (n=7) right atrium (RA●), right ventricle (RV▲), left atria (LA ■) and left ventricle (LV ▼) and 3 mg/kg (n=8) (RA ○), right ventricle (RV Δ), left atria (LA □) and left ventricle (LV ▽)

Figure 4.10 Cisapride Anaesthetised Rabbit: Comparison of Mean Plasma and Heart Concentration-Time Profile of Cisapride in the Anaesthetised Rabbit Following an Infusion of Cisapride at 0.3 and 3 mg/kg.

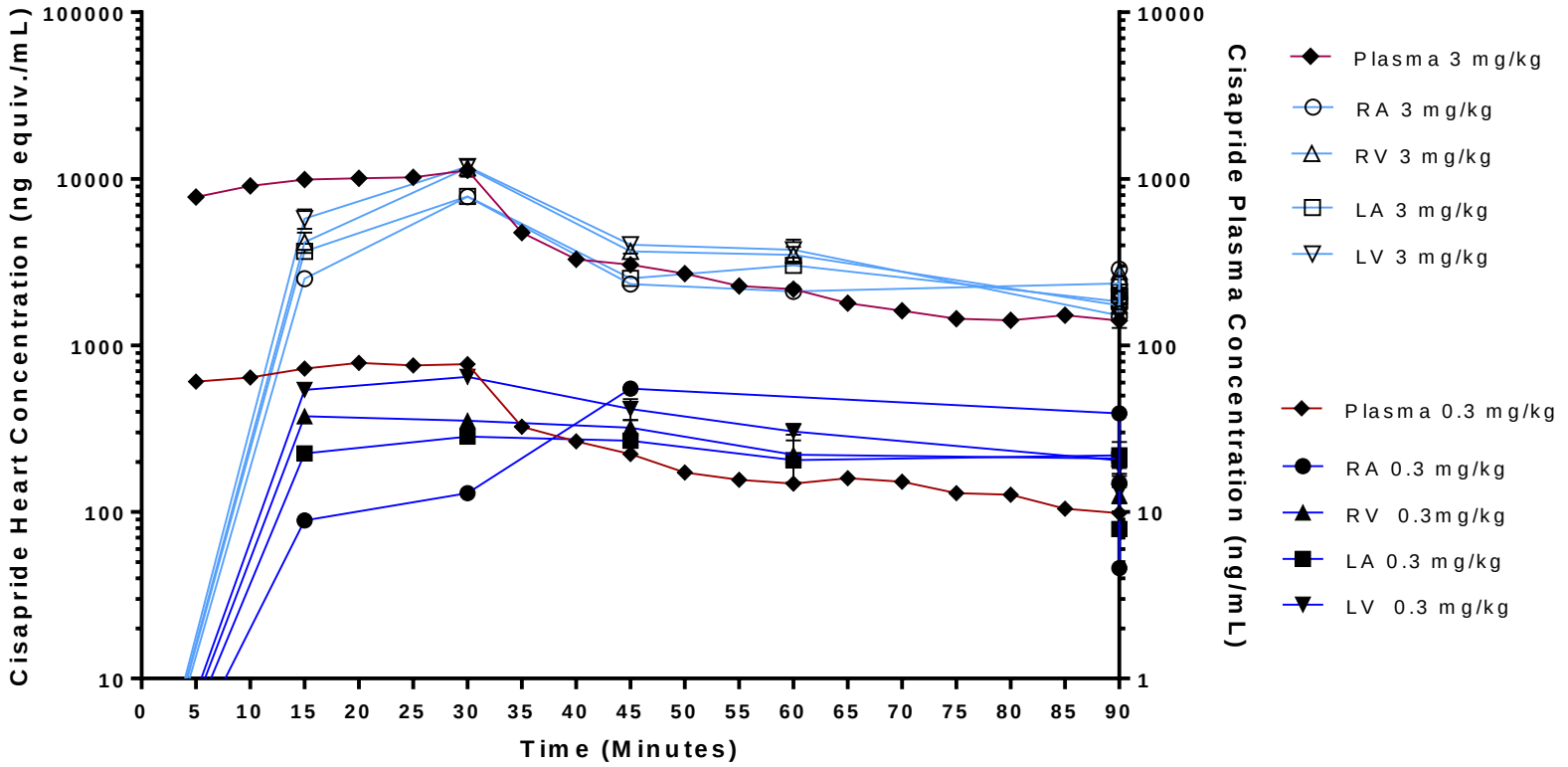

Figure 4.10 Graph of the mean and S.E.M. baseline of heart (— blue line) and plasma (— red line) concentration-time profile (ng equivalents/mL or ng/mL) generated in the anaesthetised rabbit preparation following a 30 minute intravenous infusion administration of cisapride at 0.3 mg/kg (n=7) plasma (♦) right atrium (RA●), right ventricle (RV▲), left atria (LA ■) and left ventricle (LV ▼) and 3 mg/kg (n=8) plasma (♦), (RA ○), right ventricle (RV Δ), left atria (LA □) and left ventricle (LV ∇)

4.10.2.3. Cisapride QT Prolongation

Cisapride was investigated in the anaesthetised rabbit model preparation (n=7, 3, 8) at 0.3, 1 and 0.3 mg/kg infusions over a 30 minute period. The data presented in Table 4.8 and represented graphically in Figure 4.11, shows the overall mean baseline and vehicle QTc interval corrected as a percentage change (ΔΔQTc%) with S.E.M. response following administration of cisapride with time. The full tabulated data of the individual experimental QTc intervals (ms), delta changes (ΔQTc, ms), and double delta vehicle and baseline corrected QTc intervals as percentage (ΔΔQTc%) and graphical plots at each dose range are presented in Appendix 4. Figure 4.12 shows the ECG trace at each dose level and the subsequent delay of the T wave and QT interval prolongation.

The vehicle control group equilibrium predose mean QTc interval was 275.63 ±7.49ms and at the end of a 30 minute infusion was 275.1 ±7.6ms. This represented no change in QTc interval during the infusion period, whilst the mean QTc interval was 288.2 ±12.5ms equivalent to a mean ΔQTc% increase of 4.19 ±2.36% the end of the vehicle control experiment compared to the control baseline mean ΔQTc% was -2.0 ±3.2%.

For each of the dose levels, 0.3, 1 and 3 mg/kg investigated the predose equilibration mean QTc interval was 277.42 ±9.92ms and 275.19 ±11.1ms and 274.5 ±5.60ms, respectively.

Cisapride increased the change in QTc interval with an increasing dose administration of cisapride at each dose level, 0.3, 1 and 3 mg/kg, as shown by the temporal electrocardiograph overlay in Figure 4.12A, B and C.

The mean ΔQTc interval percentage increased by 16.0 ±1.85%, 31.9 ±3.00% and 51.9 ±8.71% at the end of infusion of 0.3, 1 and 3 mg/kg, respectively, which were all statistically significant (*p*-value <0.01). At 0.3 mg/kg, the mean percentage change in ΔQTc interval was 12.7 ±5.61% at 90 minutes post-start of infusion which was not significant compared to vehicle control, whereas ΔQTc interval was 37.2 ±5.53% at 3 mg/kg at the end of experiment which was statistically significant (*p*-values <0.01) compared to vehicle control.

The double delta vehicle and baseline corrected mean QTc interval (ΔΔQTc%) increased by 17.8 ±2.17%, 32.1 ±2.17% and 52.2 ±8.71% at the end of infusion of 0.3, 1, 3 mg/kg respectively (*p*-value<0.01).

Table 4.8 Cisapride Anaesthetised Rabbit: Mean Baseline and Vehicle Corrected Percentage Change in QTc (ΔΔ%) Response in the Anaesthetised Rabbit Following an Infusion of Cisapride at 0.3, 1 and 3 mg/kg.

Time (min)	0.3 mg/kg Mean ± S.E.M. ΔΔQTc (%)	1 mg/kg Mean ± S.E.M. ΔΔQTc (%)	3mg/kg Mean ± S.E.M. ΔΔQTc (%)
Predose	277 ± 9.92	275 ± 11.1	275 ± 5.60
0	0.74 ± 0.33	0.21 ± 0.12	0.26 ± 0.14
5	7.6* ± 1.02	13.6* ± 3.31	28.4** ± 4.51
10	14.7** ± 1.66	22.8** ± 3.27	46.3** ± 7.20
15	16.0** ± 1.81	24.4** ± 2.48	53.5** ± 7.56
20	17.3** ± 2.03	26.1** ± 1.62	52.1** ± 8.46
25	17.4** ± 2.09	30.0** ± 3.16	51.9** ± 8.23
30	17.8** ± 2.17	32.1** ± 3.01	52.2** ± 8.71
35	18.5** ± 3.12		54.0** ± 10.16
40	17.4** ± 3.50		53.5** ± 8.63
45	16.5** ± 3.68		48.4** ± 7.04
50	15.8** ± 4.49		45.4** ± 7.97
55	15.8** ± 4.80		42.9** ± 8.28
60	16.5** ± 5.65		42.7** ± 8.19
65	16.9** ± 7.91		35.7** ± 5.54
70	8.94* ± 4.03		35.3** ± 5.38
75	9.04* ± 3.60		34.6** ± 5.62
80	9.54 ± 3.21		34.1** ± 5.35
85	9.36 ± 3.34		33.2** ± 5.24
90	8.89 ± 3.23		32.8** ± 5.51

Statistical difference from vehicle by repeated measure, pair-wise comparison
p-value <0.05 denoted by *; *p*-value <0.01 denoted by **

Figure 4.11 Cisapride Anaesthetised Rabbit: Graph of Mean Baseline and Vehicle Corrected Percentage Change in QTc (ΔΔ%) Response in the Anaesthetised Rabbit Following an Infusion of Cisapride at 0.3, 1 and 3 mg/kg.

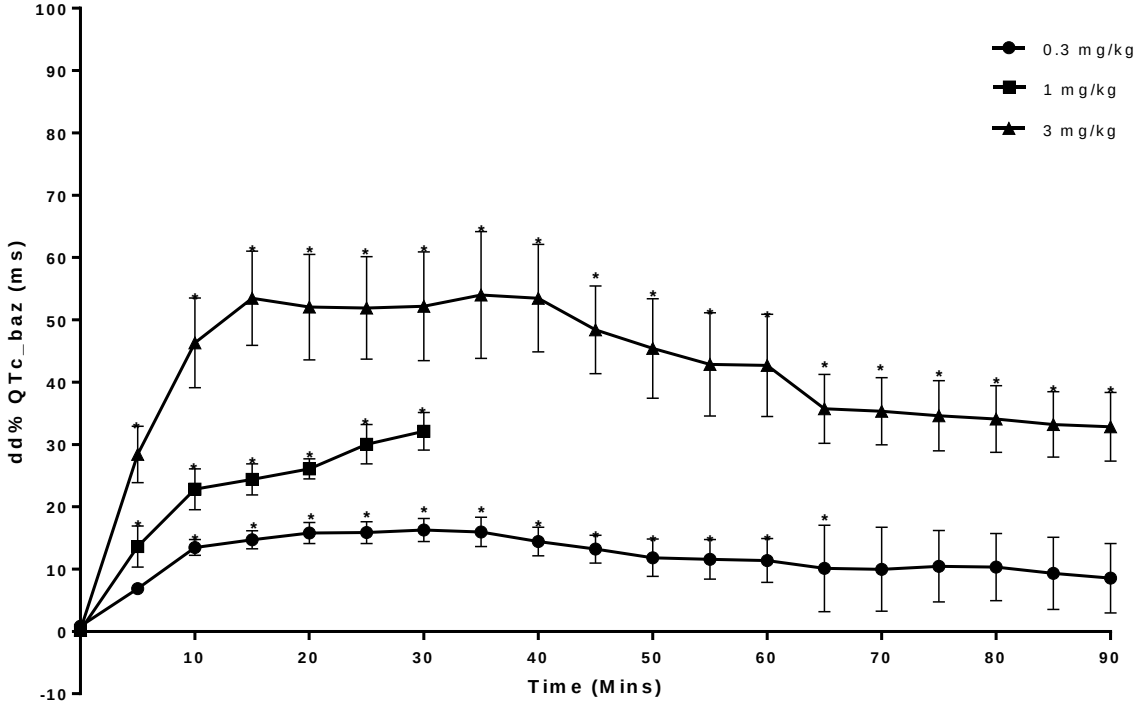

Figure 4.11: Graph of the mean and S.E.M. baseline and vehicle corrected change in QT response (ΔΔ%) generated in the anaesthetised rabbit preparation following administration of cisapride at 0.3 mg/kg (●) (n=7), 1mg/kg (■) and 3 mg/kg (▲) (n=8), where * denotes a statistical difference compared to vehicle control (*p*-value <0.05).

Figure 4.12 Cisapride Anaesthetised Rabbit: Representative Trace of the Change in ECG in the Anaesthetised Rabbit with Time and Dose Level

A: Cisapride vehicle

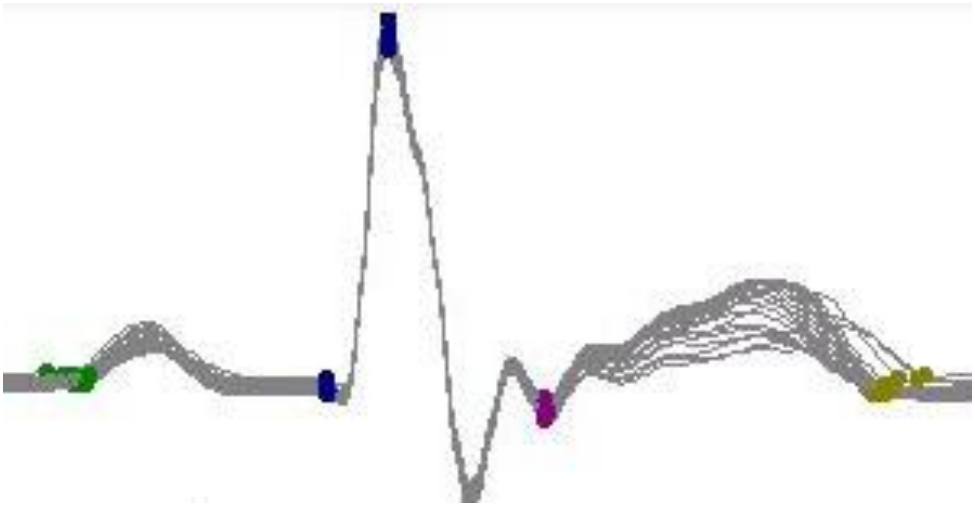

B: Cisapride 0.3 mg/kg

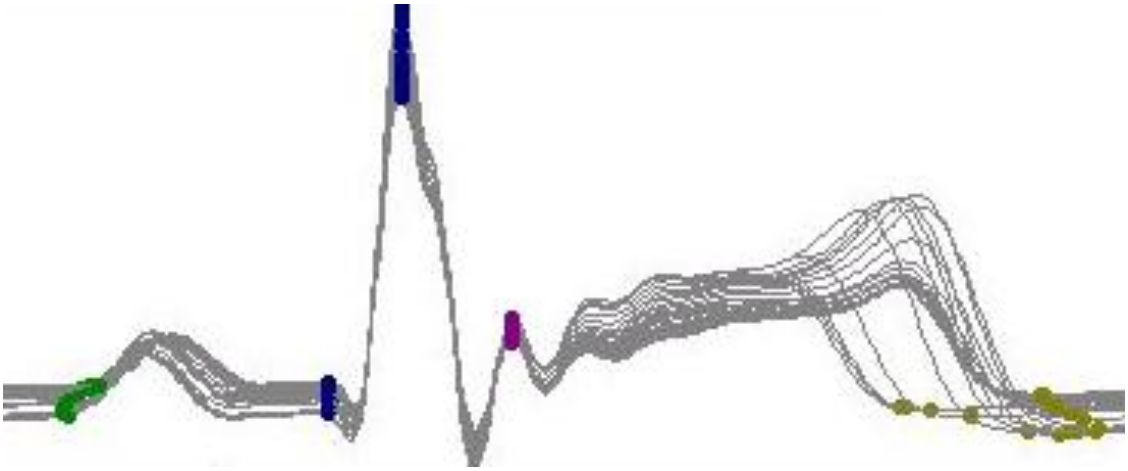

C: Cisapride 3 mg/kg

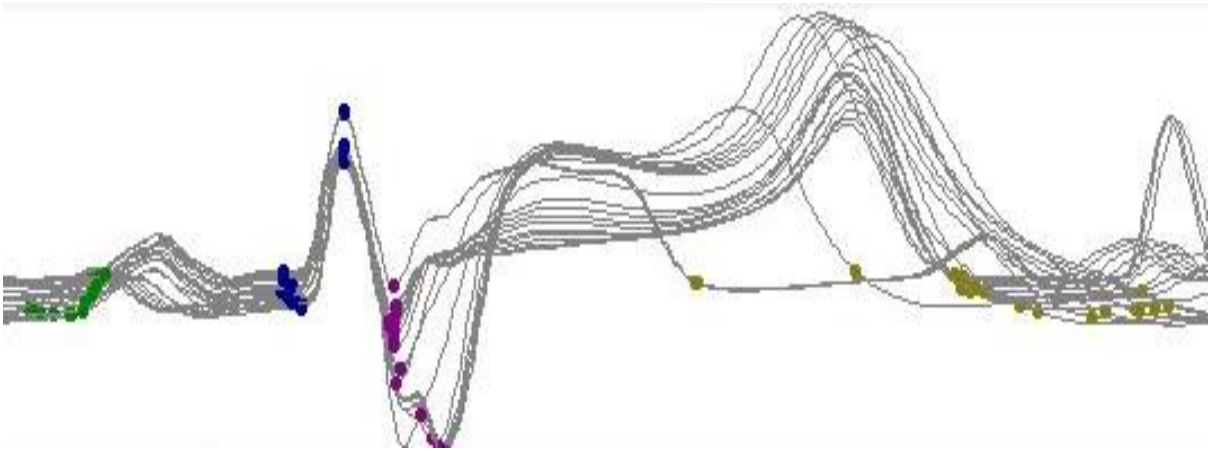

Figure 4.12: Representative overlay trace of the change in ECG waveform from each of the 5 minute time bins (n=18) generated in the anaesthetised rabbit model preparation over time following a 30 minute infusion of cisapride at 0.3 mg/kg (A), 1 mg/kg (B) and 3 mg/kg (C) with ECG waves marker points identified start of P wave (●), Q wave inflection point (●), R peak (●), S wave (●), T wave end (●).

4.10.3. Cisapride Summary Discussion

Following a single intravenous infusion of cisapride at 0.3, 1 and 3 mg/kg over 30 minutes, the resultant QT prolongation was clearly detectable and pronounced. Mean maximum plasma concentrations observed were 78.5, 310 and 1120 ng/mL that resulted in a QTc increase of 49.4 ±6.38 ms, 87.3 ±6.27 ms and 152 ±28.4 ms (equivalent to mean ΔQTc% 16.0 ±1.85%, 31.9 ±3.00% and 51.9 ±8.71%) from baseline (276 ±7.49 ms).

The baseline QTc observed in this study (276 ±7.49 ms, n=5) was comparable to Kimura et al. (2007). The vehicle used (PEG200) did not increase QT during the infusion, which was similar to that reported by Carlsson et al. (1997) that described no change in QT for its vehicle (tartaric acid, ethanol, saline (7:3:90)) (Carlsson et al., 1997). At the end of the current vehicle control experiment, QTc had increased from 276 ±7.49 ms to 288.2 ±12.5 ms equivalent to a mean ΔQTc% increase of 4.19 ±2.36%. This is less than observed by Kimura et al., whose vehicle group, 1% lactate solution, had a baseline QTc of 265 ±16 ms prolonged by a maximum of 34 ±13 ms (calculated as 13% ΔQTc).

Carlsson et al. (1997) first published effects of cisapride in the methoxamine-sensitised anaesthetised rabbit where cisapride was infused at 0.3 μmol/kg/min for 10 minutes maximum (equivalent to 1.4 mg/kg, *n*= 6), and was associated with a significant lengthening of the QTc interval from 117 ±4.2ms to 160 ±7.0 ms relative to vehicle baseline, an increase of 43 ±3.8 ms (Carlsson et al., 1997). The increase of 46 ±6.80 ms in QTc observed at 0.3 mg/kg is similar to that by Carlsson et al. (1997) at the 1.4 mg/kg cisapride dose level. Similarly, Kimura et al. (2007) administered cisapride over 10 minutes again at 1.4 mg/kg in the methoxamine-sensitised rabbit model. The baseline for the cisapride group (QTc 269 ±16 ms) was prolonged by a maximum of 86 ±27 ms, respectively (range 61-156 ms) and this is calculated to be a ΔQTc increase of 31% (Kimura et al., 2007).. The QTc change of 87 ±6.17 ms observed at 1 mg/kg is equivalent to Kimura et al. (2007). This highlights similarity to previous author's results and the potential variability in QT change as shown by the range observed by Carlsson et al and Kimura et al. Both investigators noted that mean blood pressure decreased significantly (approximately 30 mmHg) once cisapride was administered, and was coupled with the bradycardic effects (slowing HR and increasing RR interval) (Carlsson et al. 1997, Kimura et al. 2007). Changes in each of these cardiovascular parameters were similarly observed in this present study. Hypotensive effects of cisapride have been demonstrated previously in rats (Onat et al., 1994).

An adaptation of this anaesthetised model has been described to investigate the failing rabbit heart to predict torsadogenicity by prior surgical ligation of the coronary artery (Kijtawornrat et al., 2006a). Following the ligation procedure and 4-week recovery, rabbits undergo the same terminal anaesthesia process but are not sensitised with a α1-adrenoreceptor agonist. Cisapride was investigated at 0.1, 0.25 and 0.50 mg/kg in a control sham group (n = 4) and a myocardial failure group (n = 4) as a dose escalation over a period of 10 minutes, with a 20-minute interval between doses. In this model, the QTc obtained from anaesthetised rabbits before, after ligation and recovery were 262.8 ± 6.2 ms, 255.8 ± 5.2 ms and 258.4 ± 5.4 ms with corresponding heart rates of 175.0bpm ±7.0, 214.0 ± 8.0 bpm and 166.0 ± 6.0 bpm. The observed mean ΔQTc was approximately 18 ms (15-21 ms), 60 ms (35-75 ms) and 120 ms (80-160 ms). The model by Kimura et al. appears to show a greater change in QT in comparison to this study and Carlsson et al. at lower dose levels, and more so in the myocardial failure group, where a plateau-ing effect in QTc was observed in a number of the dose levels which has been reported previously (Batey and Coker, 2002; Farkas and Coker, 2002; Farkas et al., 2002). A plausible explanation may be a result of the intermittent dosing regimen and the restitution of the heart due to the sudden changes in drug-insult, reducing the extent of repolarisation. An effect which has also been observed through differing infusion rates of almokalant and in the RVW (Carlsson et al., 1993).

In this study, TdP was not observed with cisapride, a similar observation made by Kimura et al. (2007), as this model was not sensitised through a α-1 adrenoreceptor agonist such as methoxamine. In reported cases, extreme prolongation of the QT interval and ventricular repolarisation results in a 2:1 atrioventricular block, such that only every second sinoatrial beat can be conducted to the ventricles (Farkas et al., 2002). Unlike Farkas et al., the T wave did not become radically distorted and flattened, but became protracted and pronounced. This has been shown to be evident in an age-related difference in the direct effects of cisapride on the refractoriness of cardiac tissue and the His-Purkinje system in young rabbit hearts (Wu et al., 2003). There is also the potential for a sex-difference, with females more susceptible due to observed longer ventricular repolarisation (Lu et al., 2000b). Both age- and sex-related differences have been observed clinically with cisapride (Khongphatthanayothin et al., 1998; Hennessy et al., 2008).

Table 4.9 Comparison of Pharmacokinetic parameters across species following Intravenous administration of Cisapride

	Vdss (L/kg)	CL_p (ml/min/kg) (% LBF)	Half-life (hr)
Rat	4.7	91 (100%)	1-2
Dog	0.8 - 1	3 – 5.2 (10%)	4-10
Sheep	-	33-60 (~50%)	1.4 – 1.8
Human	2.4 – 4.8	5 – 6 (30%)	4.8 - 10
Rabbit	-	-	2.3
Rabbit Present study	3.3-4.1	60-83 (100%)	0.6

Combined table of parameters obtained from literature sources
blood flow (LBF, ml/min/kg) for each species rat (78), dog (56), monkey (44), human (18), rabbit (70) Davies and Morris, 1993

a. Michiels et al. 1987
b. Veereman-Wauters et al.1991
c. McCallum 1988

The pharmacokinetics of cisapride in the rabbit following infusion of 0.3 and 3 mg/kg indicate the drug distributes extensively into tissues as well as systemic circulation and extracellular water as determined by the volume of distribution (Vd_{ss} = 4.07 and 3.25 L/kg). Total plasma clearance is considered high (Cl_p = 83.0 and 60.2 mL/min/kg) as it is approximately equivalent to hepatic liver blood flow, with a relative short half-life ($t_{1/2}$ = 0.6 h) (Table 38). In context with literature information and comparison with other species the rabbit appears similar to the rat and sheep across the parameters and a comparable volume of distribution to humans (Table 4.9) (Michiels, 1987; McCallum et al., 1988; Veereman-Wauters et al., 1991); respectively). The half-life of cisapride appeared very short in the anaesthetised rabbit and may be a reflection of the short experimental duration and number of timepoints not defining the terminal elimination phase, as half-life in rabbits has been reported to be approximately 4 hours (Michiels, 1987). Clearance of cisapride in the rabbit was very high (70 ml/min/kg), unlike that observed in dog (Michiels, 1987; Webster et al., 2001) *et al.*, 2001) and humans (McCallum et al., 1988; Gladziwa et al., 1991). This may be explained by differences in metabolism across species, relative plasma protein binding and/or be the result of anaesthesia. Metabolism of cisapride is via cytochrome P450 3A4 biotransformation via the N-dealkylation and aromatic hydroxylation which is generally conserved across species (Kantharaj et al., 2003). It has been indicated that propofol

potentially inhibits 3A4 activity in human hepatocytes (Yang et al., 2003). However if the metabolism of cisapride was inhibited by the anaesthetic then the resultant clearance would be reduced and be reflected by supraproportional increases in plasma concentrations with increases in cisapride dose. Such drug-drug interactions have been highlighted clinically and indicated as a cause for concern with potential cardiovascular QT prolongation as inhibition of CYP 3A4 metabolism of cisapride has been shown by ketoconazole, cimetidine and erythromycin (Michalets and Williams, 2000; Mushiroda et al., 2000). Such increases were not observed over the dose ranges of cisapride in this study. Alternatively the increased clearance in this study may be the result of propofol on hepatic blood flow in rabbits as it has been observed to increase hepatic flow rates (Zhu et al., 2008). This would potentially increase hepatic extraction and clearance of the drug. The identified cisapride drug levels in heart were up to 10-fold greater than those circulating in the plasma which concurs with the moderate volume of distribution. This distribution must occur rapidly given the high clearance rate from the systemic circulation and that the heart tissue concentration profile follows the elimination of plasma (Figure 4.8B log plot). The range in ratios can be attributed to limited n=1 for heart tissue at selected time points against a single absolute plasma concentration, where this comparison is also between dynamic profiles and not prolonged steady state.

4.10.4. Sparfloxacin Anaesthetised Rabbit Results

4.10.4.1. Sparfloxacin Plasma Pharmacokinetics

A summary of mean pharmacokinetic parameters of sparfloxacin, are given in Table 4.10 with mean plasma concentration-time tabulated in Table 4.11 and graphically presented in Figure 4.13, respectively.

Table 4.10 Mean Pharmacokinetics Parameters of Sparfloxacin in Plasma Following a Single Intravenous Infusion Administration to Anaesthetised Rabbits

Dose Level (mg/kg)	T_{max} (h)	C_{max} (ng/mL)	AUC_{last} (ng*h /mL)	V_{dss} (L/kg)	CL_p (mL/min/kg)	Half-Life (hour)
16	60	2550	1630	ND	ND	ND
33	60	4700	3870 (6480)	6.79	21.7	3.62
100	60	16600	11800	ND	ND	ND

Area under the curve (AUC) reported for the infusion 0-60 minute period only. Value in parentheses at 33 mg/kg is the AUC determined over the 180 minute period

Plasma concentrations of sparfloxacin in the terminally anaesthetised rabbit were determined up to the end of a 60 minute single intravenous infusion at a nominal dose of 16, 33 and 100 mg/kg, and up to 180 minutes post infusion start at 33mg/kg. The maximum sparfloxacin plasma concentrations (C_{max}) at 16, 33 and 100 mg/kg observed was 2550, 4700 and 16600 ng/mL, respectively, occurring at the end of infusion at 60 minutes. The observed mean systemic exposure of sparfloxacin, for the 60-minute infusion period only, as determined by the area under the curve with time (AUC_{0-t}), was 1630, 3870 and 11800 ng.h/mL, at each increasing dose level, respectively. Parameters, C_{max} and AUC increased in an approximately dose proportional (linear) manner. The derived pharmacokinetic parameters were determined for the plasma concentration-time profiles at 33 mg/kg only. The volume of distribution was approximately 6.79 L/kg which indicates distribution through the body water and widely into tissues. The mean plasma clearance of sparfloxacin was moderate at 21.7 ml/min/kg, approximately 30% of liver blood flow (LBF) in the rabbit (70 mL/min/kg; Davies and Morris, 1993). The estimated half-life following an intravenous infusion administration was considered at approximately 3.6 hour. Pharmacokinetic parameters were not derived at 16 and 100 mg/kg as plasma concentration data was only collected up to the end of infusion.

Table 4.11 Sparfloxacin Anaesthetised Rabbit: Mean Plasma Concentrations in the Anaesthetised Rabbit Following an Infusion of Sparfloxacin at 16, 33 and 100 mg/kg

Time (min)	Mean 16 mg/kg Concentration (ng/mL)	±S.E.M.	Mean 33 mg/kg Concentration (ng/mL)	±S.E.M.	Mean 100 mg/kg Concentration (ng/mL)	±S.E.M.
-15	NQ	NC	NQ	NC	NQ	NC
0	NQ	NC	NQ	NC	NQ	NC
10	**1130**	± 35.4	**2430**	± 181	**8260**	± 565
20	**1400**	± 48.1	**3070**	± 107	**10800**	± 530
30	**1920**	± 70.4	**3500**	± 183	**12600**	± 940
40	**1920**	± 103	**3990**	± 293	**15300**	± 972
50	**2140**	± 64.0	**4320**	± 249	**15800**	± 389
60	**2550**	± 176	**4700**	± 394	**16600**	± 905
70			**2580**	± 404		
80			**1700**	± 94.5		
90			**1420**	± 119		
100			**1590**	± 252		
110			**1290**	± 24.4		
120			**1420**	± 181		
130			**1460**	± 308		
140			**1300**	± 235		
150			**1120**	± 2.30		
160			**1280**	± 99.8		
170			**1300**	± 105		
180			**1110**	± 59.8		

NC Not Caluclated

Figure 4.13 Sparfloxacin Anaesthetised Rabbit: Graph of Mean Plasma Concentration-Time Profile of Sparfloxacin in the Anaesthetised Rabbit Following an Infusion of Sparfloxacin at 16, 33 and 100 mg/kg.

a) Linear plot

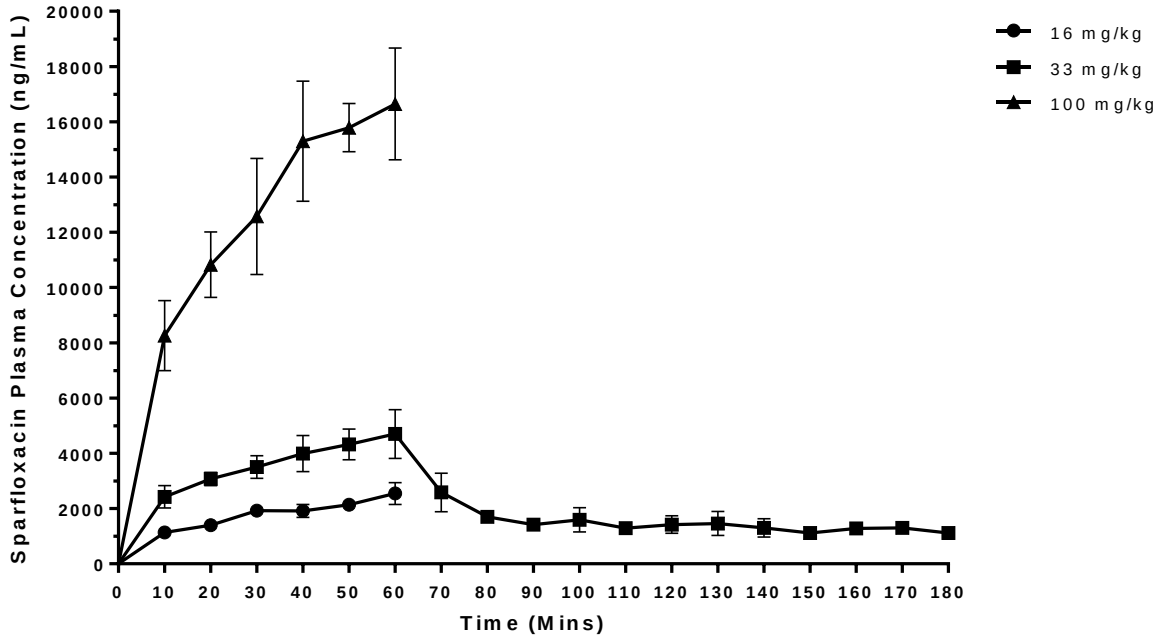

b) Log plot

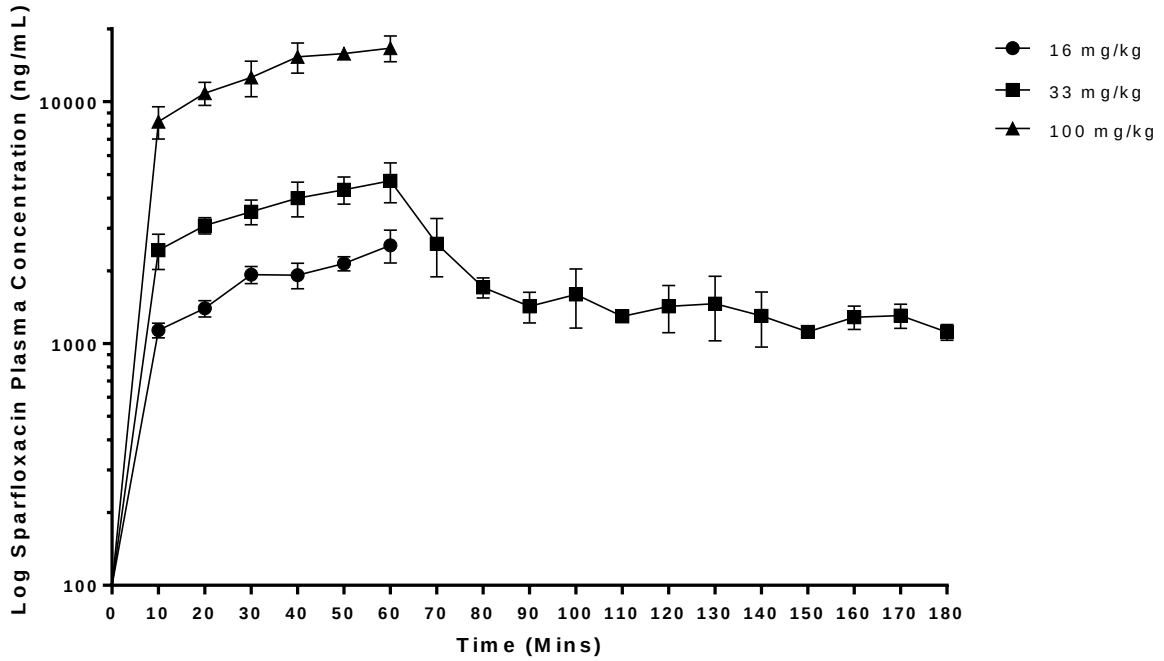

Figure 4.13: Graph of the mean and S.E.M. baseline of plasma concentration-time profile (ng/mL) generated in the anaesthetised rabbit preparation following a 30 minute intravenous infusion administration of sparfloxacin at 16 mg/kg (●) (n=5), 33mg/kg (■) (n=5) and 100 mg/kg (▲) (n=5).

4.10.4.2. Sparfloxacin Heart

Heart tissue was collected and analysed by LC-MS/MS for sparfloxacin cardiac concentrations through replicate analyses of tissue homogenates generated from heart tissue slices at each time point. Rabbit hearts were collected at the end of the 60 minutes infusion (n=5) for 16 and 100 mg/kg, and at 60 minutes (n=2), 120 minutes (n=1) and 180 minutes (n=2) at 33 mg/kg. As previously described (Section 4.8), sparfloxacin concentrations were determined for 12 replicates of heart tissue following preparation by cryostat microtome slicing. Individual replicate concentrations are given in Appendix 4. Overall mean sparfloxacin heart tissue concentrations are summarised in Table 4.12, Table 4.13 and Table 4.14 for 16, 33 and 100 mg/kg, respectively, along with the corresponding mean plasma concentrations. Heart tissue to plasma ratios have then been derived to show the extent of tissue partitioning by sparfloxacin at each time point.

A graphical representation of the heart tissue concentrations for each heart chamber at each dose level is shown together in Figure 4.14 as linear (a) and logarithmic (b) plots. Figure 4.15 is a further plot showing the combined concentration time profiles of sparfloxacin in both plasma and heart.

At each dose level, 16, 33 and 100 mg/kg, at the end of the 60 minute infusion the overall mean sparfloxacin heart concentrations were 17400, 22900 and 113000 ng equiv./mL, respectively. Heart tissue concentrations generally exhibited a dose proportional 6.5-fold increase for a 6.25-fold increase in dose from 16 to 100 mg/kg, and a 4.9-fold increase for a 3.3-fold increase in dose from 33 to 100 mg/kg. It can be seen from Figure 4.14 that there were some overlap between heart tissue concentrations at 16 mg/kg and 33 mg/kg at the end of the 60 minute infusion. The sparfloxacin heart tissue concentrations are shown to decrease with time at 33 mg/kg and with similar concentrations 6120 and 5690 ng equiv./mL at 120 and 180 minutes, respectively.

The sparfloxacin heart concentrations were greater than plasma concentrations at all time points. Heart:plasma ratios were similar between each of the three dose levels examined. At 16 mg/kg, the mean ratio was 7.29 (range 5.29 to 9.07), at 33 mg/kg, the ratio ranged from 3.95 to 5.74, and at 100 mg/kg the mean ratio was 6.73 (range 6.46 to 6.94). The plasma and heart time-concentration profiles are shown in Figure 4.15, and the 33 mg/kg heart concentrations follow the same time course as plasma.

Table 4.12 Sparfloxacin Anaesthetised Rabbit: Mean Heart Concentrations in the Anaesthetised Rabbit Following an Infusion of Sparfloxacin at 16 mg/kg

	Heart Tissue Concentration of Sparfloxacin (ng equiv./mL)					
	#1	**#2**	**#3**	**#4**	**#5**	**Mean**
Time (min)	**60**	**60**	**60**	**60**	**60**	**60**
Mean Heart	16500	14700	21900	18000	15900	**17400**
Mean Plasma	2720	1950	2420	2630	3010	**2010**
Heart: Plasma ratio	6.04	7.52	9.07	6.85	5.29	**7.08**

Table 4.13 Sparfloxacin Anaesthetised Rabbit: Mean Heart Concentrations in the Anaesthetised Rabbit Following an Infusion of Sparfloxacin at 33 mg/kg

		Heart Tissue Concentration of Sparfloxacin (ng equiv./mL)					
	#1	**#2**	**Mean**	**#3**	**#4**	**#5**	**Mean**
Time (min)	**180**	**180**	**180**	**120**	**60**	**60**	**60**
Mean Heart	5320	6050	**5690**	6120	22400	23300	**22900**
Mean Plasma	1170	1050	**1110**	1410	5670	4600	**5140**
Heart: Plasma ratio	4.53	5.74	**5.14**	4.35	3.95	5.07	**4.51**

Table 4.14 Sparfloxacin Anaesthetised Rabbit: Mean Heart Concentrations in the Anaesthetised Rabbit Following an Infusion of Sparfloxacin at 100 mg/kg

	Heart Tissue Concentration of Sparfloxacin (ng equiv./mL)					
	#1	**#2**	**#3**	**#4**	**#5**	**Mean**
Time (min)	**60**	**60**	**60**	**60**	**60**	**60**
Mean Heart	111000	99900	123000	102000	127000	**113000**
Mean Plasma	16500	14500	19100	14900	18300	**14100**
Heart: Plasma ratio	**6.75**	**6.88**	**6.46**	**6.88**	**6.94**	**6.73**

Figure 4.14 Sparfloxacin Anaesthetised Rabbit: Graph of Individual Heart Concentration-Time Profile of Sparfloxacin in the Anaesthetised Rabbit Following an Infusion of Sparfloxacin at 16, 33 and 100 mg/kg.

a) Linear

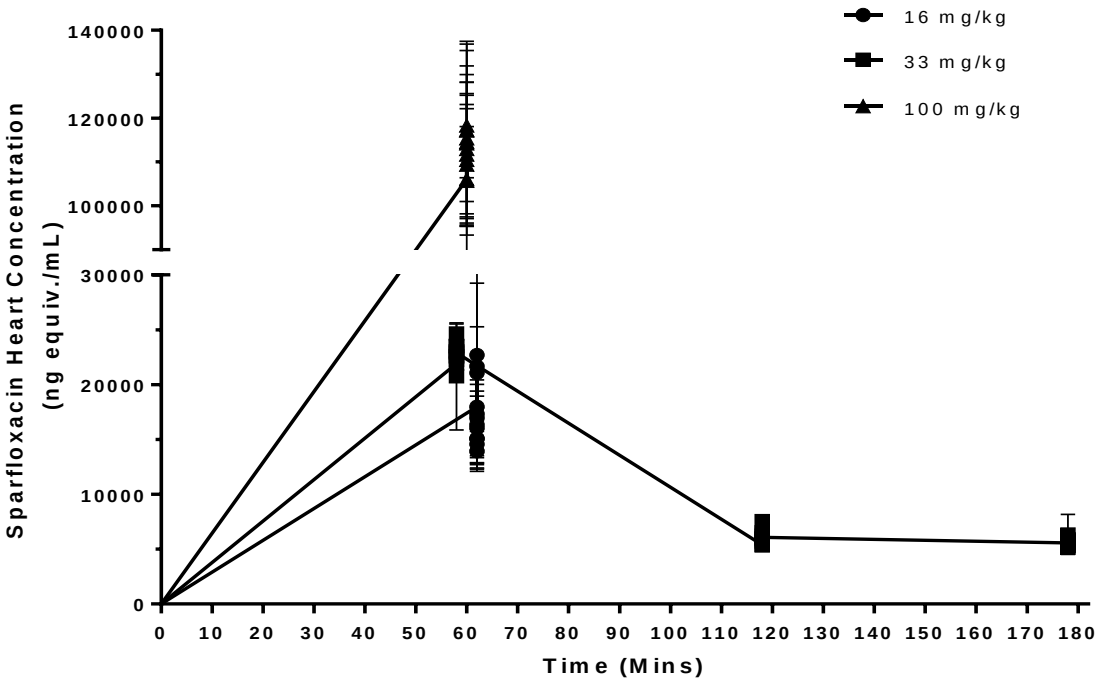

b) Log plot

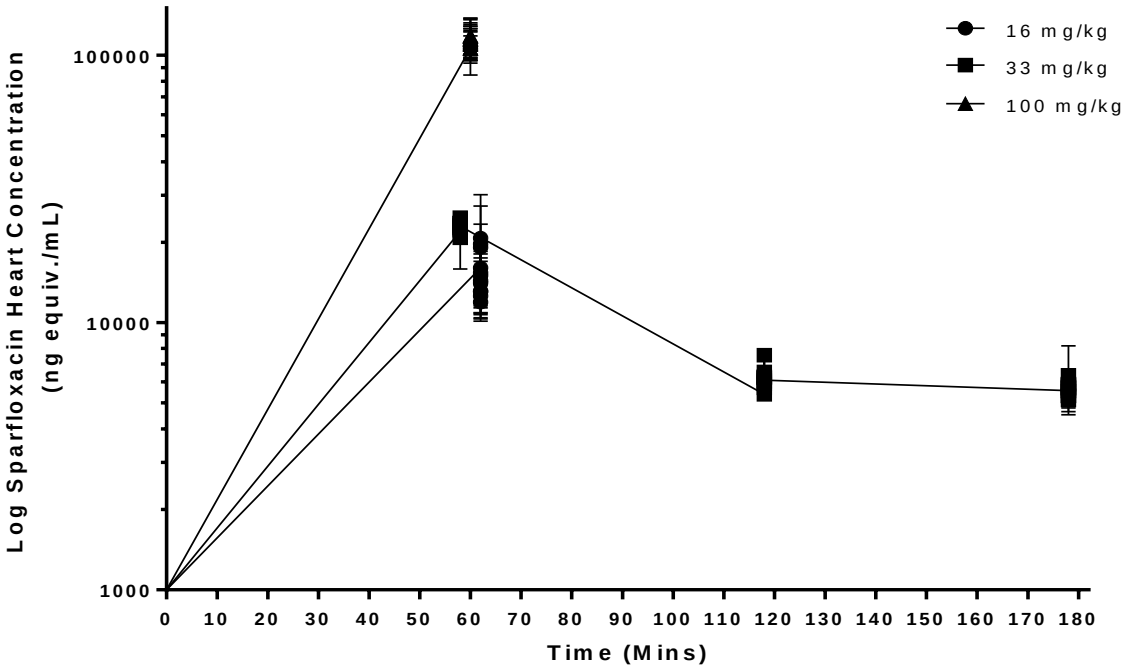

Figure 4.14: Graph of the mean and S.E.M. baseline of heart concentration-time profile (ng equivalents/mL) generated in the anaesthetised rabbit preparation following a 60 minute intravenous infusion administration of sparfloxacin at 16 mg/kg (●) (n=5), 33 mg/kg (■) (n=5) and 100mg/kg (▲) (n=5).

Figure 4.15 Sparfloxacin Anaesthetised Rabbit: Comparison of Mean Plasma and Heart Concentration-Time Profile of Sparfloxacin in the Anaesthetised Rabbit Following an Infusion of Sparfloxacin at 16, 33 and 100 mg/kg.

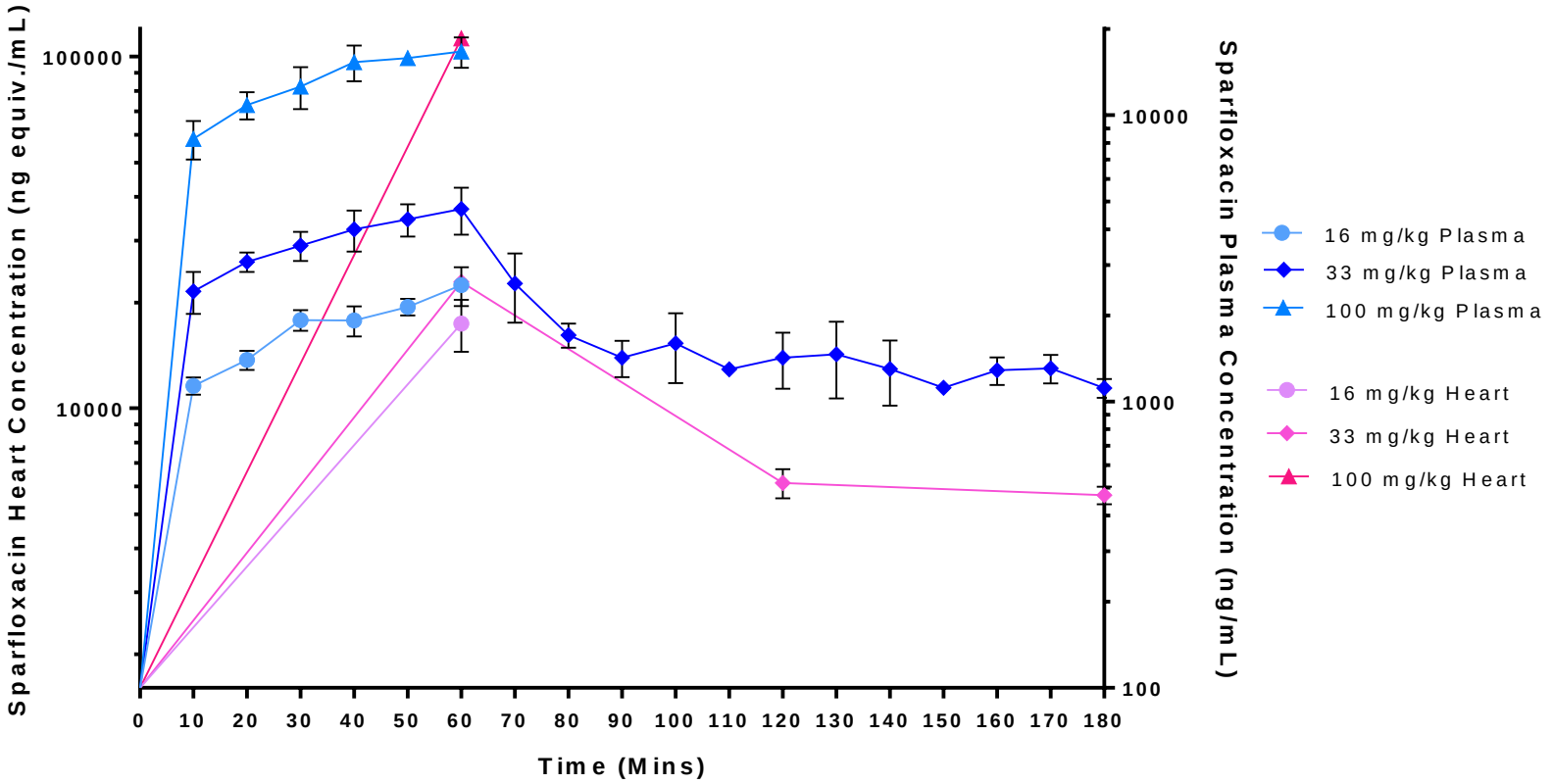

Figure 4.15: Graph of the mean and S.E.M. baseline of plasma (— blue line) and heart (— red line) concentration-time profile (ng/mL or ng equivalents/mL) generated in the anaesthetised rabbit preparation following a 60 minute intravenous infusion administration of sparfloxacin at 16 mg/kg (n=5) plasma (●) and heart (●); 33 mg/kg (n=5) plasma (♦) and heart (♦); 100 mg/kg (n=5) plasma (▲) and heart (▲)

4.10.4.3. Sparfloxacin QT Prolongation

Sparfloxacin was investigated in the anaesthetised rabbit model preparation (n=5) at 16, 33 and 100 mg/kg infusions over a 60 minute period. The data presented in Table 4.15 and represented graphically in Figure 4.16, shows the overall mean baseline and vehicle QTc interval corrected as a percentage change (ΔΔQTc%) with S.E.M. response following administration of sparfloxacin with time. The full tabulated data of the individual experimental QTc intervals (ms), delta changes (ΔQTc, ms), and double delta vehicle and baseline corrected QTc intervals as percentage (ΔΔQTc%) and graphical plots at each dose range are presented in Appendix 4. Figure 4.17 shows the ECG trace at each dose level and the subsequent delay of the T wave and QT prolongation.

The vehicle control group equilibrium predose mean QTc interval was 320 ±8.22 ms and at the end of a 60 minute infusion was 338 ±9.68 ms. This represented a small increase change in QTc interval of 4.32 ±2.13% during the infusion period, whilst the mean QTc interval was 341 ±12.2 ms equivalent to a mean ΔQTc% increase of 11.5 ±1.29% at the end of the vehicle control experiment (180 minutes). Compared to the control baseline mean ΔQTc% was -2.0 ±3.2%.

For each of the dose levels, 16, 33 and 100 mg/kg investigated the predose equilibration mean QTc interval was 309 ±4.69 ms and 306 ±4.69 ms and 301 ±8.05 ms, respectively.

Sparfloxacin increased the change in QTc interval with an increasing dose administration of sparfloxacin at each dose level, 16, 33 and 100 mg/kg, as shown by the temporal electrocardiograph overlay in Figure 4.17A, B, C and D.

The mean ΔQTc% interval increased by 30.7 ±3.19%, 35.0 ±5.67% and 72.7 ±10.6% at the end of infusion of 16, 33 and 100 mg/kg, respectively, which were all statistically significant changes (p-value <0.01). At 33 mg/kg, the mean ΔQTc% interval was not statistically different from 130 minutes post dose onwards (p-values >0.05), and was 8.90 ±7.55% at the end of 180 minutes post-start of infusion compared to control vehicle.

The double delta vehicle and baseline corrected mean QTc interval (ΔΔQTc%) increased by 24.3 ±3.22%, 28.5 ±5.67% and 66.2 ±10.2% at the end of infusion of 16, 33 and 100 mg/kg respectively.

Table 4.15 Sparfloxacin Anaesthetised Rabbit: Mean Baseline and Vehicle Corrected Percentage Change in QTc (ΔΔ%) Response in the Anaesthetised Rabbit Following an Infusion of Sparfloxacin at 0.3, 1 and 100 mg/kg.

Time (min)	16 mg/kg Mean ± S.E.M. ΔΔQTc (%)	33 mg/kg Mean ± S.E.M. ΔΔQTc (%)	100 mg/kg Mean ± S.E.M. ΔΔQTc (%)
Predose	309 ±4.69	306 ±4.69	301 ±8.05
0	-0.25 ±0.31	0.01 ±0.44	0.15 ±0.33
10	7.96** ±0.75	11.7** ±0.47	25.8** ±3.17
20	14.1** ±1.16	18.6** ±1.02	48.1** ±9.94
30	18.1** ±1.89	21.3** ±2.26	55.1** ±11.2
40	20.9** ±2.48	23.8** ±3.53	61.1** ±10.8
50	21.6** ±3.13	26.1** ±4.50	63.2** ±9.13
60	24.3** ±3.22	28.5** ±5.67	66.2** ±10.5
70		17.6** ±2.10	
80		14.3** ±1.18	
90		13.2** ±1.16	
100		12.3** ±1.81	
110		10.2* ±2.72	
120		11.1* ±4.75	
130		16.9* ±2.21	
140		14.0 ±0.98	
150		10.3 ±2.46	
160		9.22 ±3.30	
170		9.33 ±6.03	
180		8.90 ±7.55	

Statistical difference from vehicle by repeated measure, pairwise comparison
p-value <0.05 denoted by *; *p*-value <0.01 denoted by **

Figure 4.16 Sparfloxacin Anaesthetised Rabbit: Graph of Mean Baseline and Vehicle Corrected Percentage Change in QTc (ΔΔ%) Response in the Anaesthetised Rabbit Following an Infusion of Sparfloxacin at 16, 33 and 100 mg/kg.

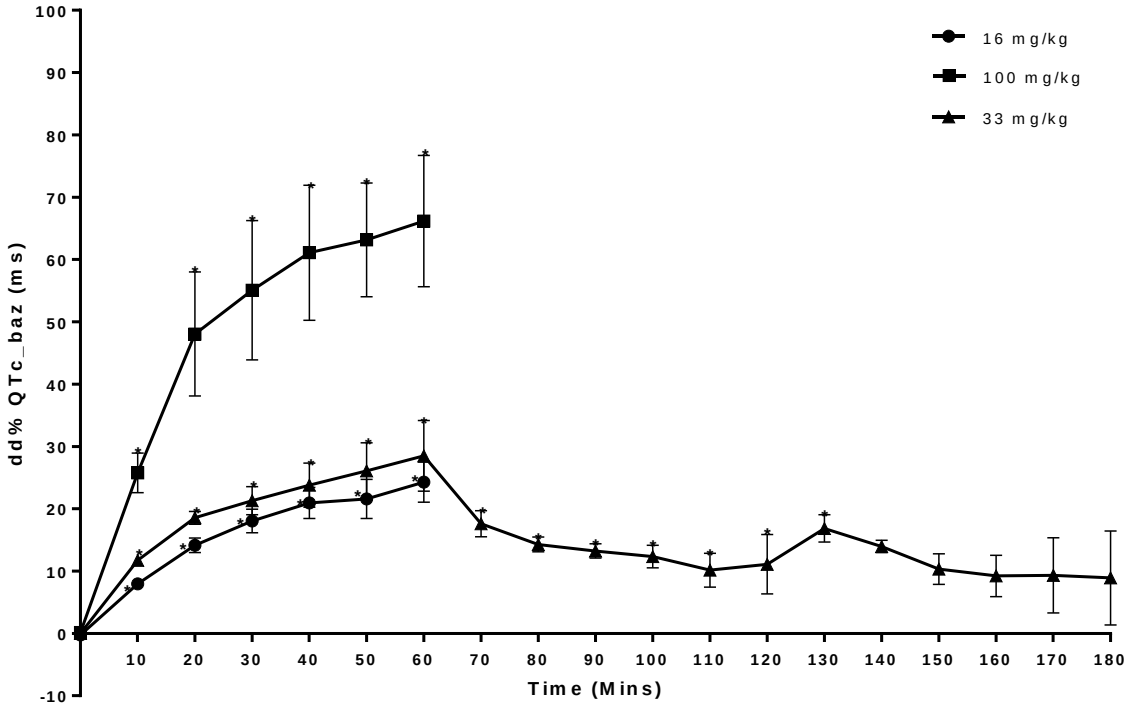

Figure 4.16: Graph of the mean and S.E.M. baseline and vehicle corrected change in QT response (ΔΔ%) generated in the anaesthetised rabbit preparation following administration of sparfloxacin at 16 mg/kg (●) (n=5), 33 mg/kg (■) (n=5) and 100 mg/kg (▲) (n=5) where * denotes a statistical difference compared to vehicle control (*p*-value <0.05).

Figure 4.17 Sparfloxacin Anaesthetised Rabbit: Representative Trace of the Change in ECG in the Anaesthetised Rabbit with Time and Dose Level

A: Sparfloxacin vehicle

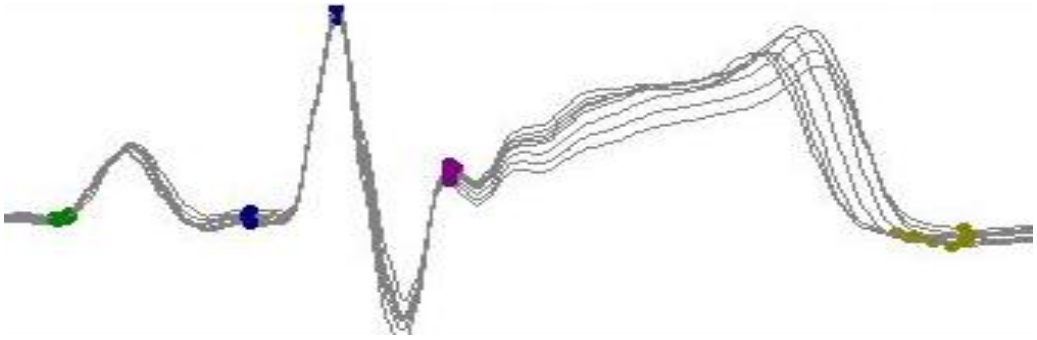

B: Sparfloxacin 16 mg/kg

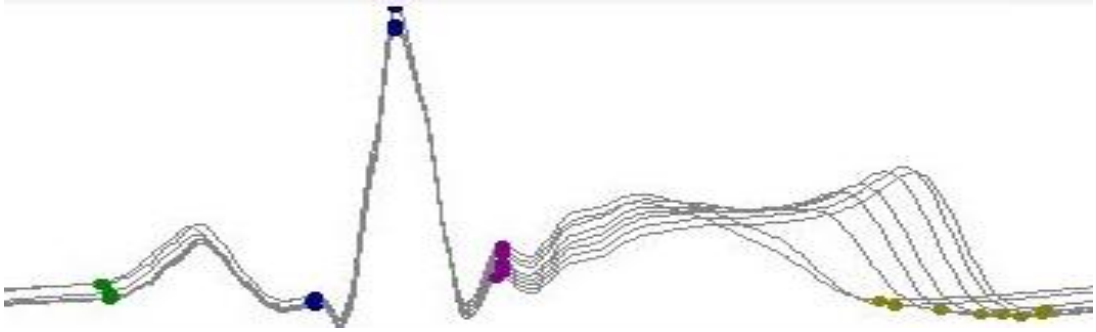

C: Sparfloxacin 33 mg/kg

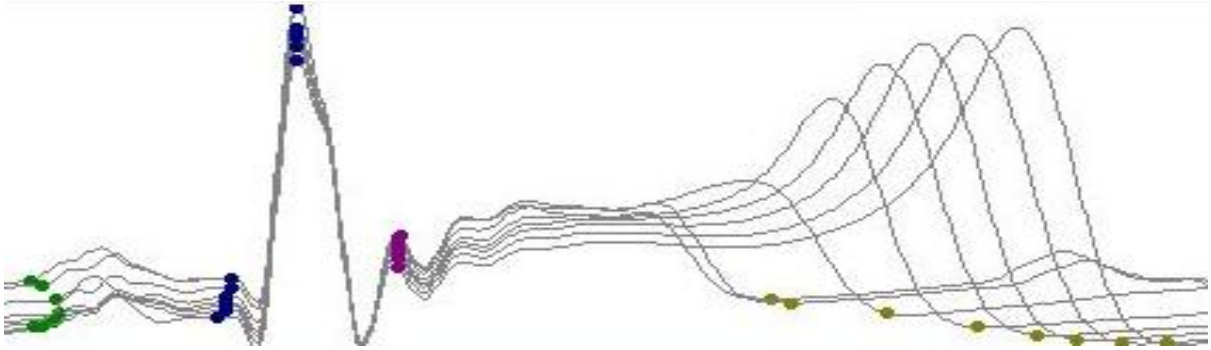

D: Sparfloxacin 100 mg/kg

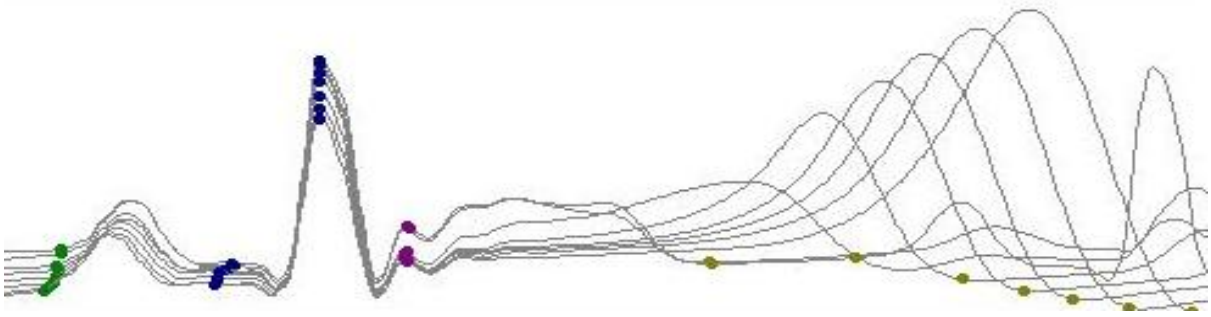

Figure 4.17: Representative overlay trace of the change in ECG waveform from each of the 5 minute time bins (n=18) generated in the anaesthetised rabbit model preparation over time under control baseline conditions with ECG waves marker points identified start of P wave (●), Q wave inflection point (●), R peak (●), S wave (●), T wave end (●).

4.10.5. Sparfloxacin Summary Discussion

Following a single intravenous infusion of sparfloxacin at 16, 33 or 100 mg/kg over 60 minutes, the resultant QT prolongation was notably pronounced. Mean maximum plasma concentrations observed were 2550, 4700 and 16600 ng/mL, and corresponding heart tissue concentrations 17400, 22900 and 113000 ng/mL, respectively, that resulted in a QTc increase of 94.8 ±10.2 ms, 107 ±17.5 ms and 218 ±27.8 ms from the baseline QTc of 306 ms (equivalent to mean ΔQTc% by 30.7 ±3.19%, 35.0 ±5.67% and 72.7 ±10.6%) from baseline (306 ±4.69 ms).

In this study, single dose infusions of sparfloxacin at 16, 33 and 100 mg/kg over 60 minutes were investigated in the anaesthetised rabbit to support a separate investigation into metabolomic biomarkers and subsequent QT prolongation. The infusion and dose levels were adapted from previous reported literature in the guinea pig (Park et al., 2013) and the rabbit (Akita et al., 2004). Park et al. investigated sparfloxacin at 33.3, 100 and 300 mg/kg in the guinea pig and Akita et al. tested 60, 90 and 120 mg/kg.

There have been other separate published articles in relation to sparfloxacin and the anaesthetised rabbit, each implementing the methoxamine-sensitised model developed by Carlsson et al. to investigate TdP liability. Anderson et al. utilised the sensitised-rabbit model with minor modifications to investigate the proarrhythmic properties of quinolone antibiotics including sparfloxacin (Anderson et al., 2001). Sparfloxacin was infused for up to 60 minutes at 2 mg/kg/min (120 mg/kg total, n=6), and of the quinolones tested, sparfloxacin caused the greatest absolute increase in both the QT and the QTc intervals. An increase from baseline (241 ±10 ms) to a maximum QTc interval 370 ±30 ms was observed; a change of 130 ms (equivalent to ΔQTc 54.2%). The increase observed by Anderson et al. is less than observed in this present study (72.7 ±10.6%) for a 100 mg/kg dose level but similarly large in magnitude. This difference may be explained due to comparing to the α1-sensitised model, the lower observed QT baseline and the method of correction used by Carlsson et al. (Carlsson et al., 1993). No adverse proarrhythmic anomalies were observed by Anderson et al. during the first 30-minutes of infusions, so to enhance the sensitivity of detecting arrhythmia induction, sparfloxacin (and moxifloxacin) infusions were continued for a total of 60 minutes in an attempt to distinguish the proarrhythmic potential of these two agents, given their more potent I_{Kr} antagonist actions. The authors suggest that there is a lack of clear

association between I_{Kr} antagonist potency and QT interval prolongation, revealing that factors independent of I_{Kr} block may also be important for QT interval prolongation.

Another group of investigators, before assessing the proarrhythmic effects of sitafloxacin, gatifloxacin and moxifloxacin, validated an α-chloralose-anesthetised rabbit model following information from Anderson et al. (2001) using sparfloxacin (*n*=5) as a positive control (Chiba et al., 2004a). No reference to QT values or changes observed were quoted after the administration of sparfloxacin by Chiba et al. but identified TdP was induced in two out of five animals. Here sparfloxacin was administered as a 60 mg/kg infusion over 20 minutes where an initial episode was observed at 14 and 15 minutes (for cumulative doses of 42 and 45 mg/kg).

In another experimental study using the methoxamine-sensitised model as part of an assessment of a different set of fluoroquinolones, sparfloxacin (n=5) was administered intravenously for 30 minutes (4 mg/kg/min) or for 60 minutes (2 or 3 mg/kg/min) (Akita et al., 2004). Sparfloxacin was dissolved in 0.2M NaOH solution as vehicle (n=6) at concentrations of 30, 45 and 60 mg/mL, and infused at a speed of 4 mL/kg/hr. The observed QT prolongations were rate corrected using both Carlsson method and Bazett's method.

The baseline QTcB interval appeared to be 300-320 ms and increased to approximately 500 ms. This change in QTcB% by sparfloxacin was significant at all timepoints, with maximum changes 57.2 ±3.0%, following 4mg/kg/min over 30 minutes. This was similar to values by Anderson et al. and in the range within this present study 72.7%. Sparfloxacin at the dose of 2mg/kg/min prolonged QT interval without inducing arrhythmia up to 60 minutes, unlike 3mg/kg/min which induced at least one type of arrhythmia in 4 out of 5 animals. The time course of the increase in the QT at 2 mg/kg/min was similar to that at 4 mg/kg/min, and indicates the effect of rate infusion on TdP as previously reported (Carlsson et al., 1993; Farkas et al., 2002)

The vehicle used in these studies, 2M NaOH, was noted to significantly prolong the RR interval, which in turn induced a less pronounced change in the QT interval, such that the vehicle effect on ΔQTc was 3.7 ±1.4% after 30 minute infusion (Akita et al., 2004). By comparison in this present study, the gluconalactone vehicle used also produced a small increase in ΔQTc interval of 4.32 ±2.13% during the infusion period (without affecting the RR interval) from baseline (306 ±4.69 ms), but at the end of the vehicle control experiment

(180 minutes) the mean QTc interval was up to 341 ±12.2 ms equivalent to a mean ΔQTc% increase of 11.5 ±1.29%. Akita et al. raise concern over electrolyte abnormalities such as hypokalaemia causing prolonged QT due to high alkalinity using 2M NaOH but indicate through vehicle control animals that the change in QT is small and only one occurrence of proarrhythmia. In this present study, NaOH was not used due to the high pH 11.0 which exceeded local formulation criteria for in vivo studies, veterinary acceptance and cause for potential vascular necrosis.

In the study by Akita et al., plasma concentrations were not measured but considered to be 15-30 times greater than the oral clinical C_{max} values (1.5 – 3 µg/mL) following 120 mg/kg. This estimated concentration range was notably greater than in this study as mean maximum circulating plasma concentrations were 2, 5 and 14 µg/mL for 16, 33 and 100 mg/kg, respectively. However heart concentrations determined at each of these dose levels (17, 23 and 113 µg/mL) were in this range.

Table 4.16 Comparison of Pharmacokinetic parameters across species following Intravenous administration of Sparfloxacin

	Vd_ss (L/kg)	CL_p (mL/min/kg) (% LBF)	Half-life (hr)
Rat	3.64 - 4.4	15.4 – 19.6 (20-25%)	2.2 – 4.1, 8
Dog	2.7 - 3.3 -	3.6 (6%)	8.7 – 10.5
Monkey	7.3	16.0 (36%)	5.3 – 11.7
Human	4.3 - 5.5	2.6 – 3.6 (15-20%)	15-20h
Rabbit	-	-	2.4 (Lui)
Present study	6.8	22 (~30%)	3.6

Combined table of parameters obtained from literature sources
Liver blood flow (LBF, ml/min/kg) for each species rat (78), dog (56), monkey (44), human (18), rabbit (70) (Davies and Morris, 1993)

a. Matsunaga: 4.4 mg/kg in rat half-life α=1.5h (0.083 to 6h interval) but also measured β= 4.6h, overall half-life = 4.1hr
b. Naora: 19.6 ml/min/kg; half-life 2.2hr, Vd = 3.64 L/kg
c. Noh: half-life of 8hr
d. Nakamura: dog
e. Yamaguchi (1990)
f. Shimada et al; Montay: half-life 15-20h in human
g. Liu 1998: in the rabbit 2.4 half-life

The pharmacokinetics of sparfloxacin in the rabbit following infusion of 33 mg/kg indicates the drug distributes extensively into tissues as well as systemic circulation and extracellular water as determined by the volume of distribution (Vd_{ss} = 6.8 L/kg) and compared to other

species it is similar to monkey (7.3 L/kg) and human (5.5 L/kg) (Yamaguchi et al., 1991; Shimada et al., 1993; Montay et al., 1994). Total plasma clearance is considered moderate (Cl_p = 22 mL/min/kg) as it is approximately a third of hepatic liver blood flow, similar to rat (20%), monkey (36%) and human (20%) (Matsunaga et al., 1991a; Matsunaga et al., 1991b; Yamaguchi et al., 1991; Naroa et al., 1992; Shimada et al., 1993; Montay et al., 1994). The observed corresponding half-life in the rabbit in this study was 3.6 hour and was comparable to a previously published value in the rabbit of 2.4 hour (Liu et al., 1998). In comparison to half-lives in other species, the rabbit was closest to the rat (2.2 - 4 hour), but less than that in the monkey (5.3 – 11.7 hour) and human (15 – 20 hour).

Some comparable pharmacokinetic parameters of sparfloxacin in the anaesthetised rabbit across species, in this instance, are reflected by the longer infusion and experimental duration (180 minutes) to better define the elimination phase. An exception is the dog, where the volume of distribution and clearance parameters were notably lower than all the species (Nakamura et al., 1990). Metabolism of sparfloxacin is via a non-cytochrome P450 dependent mechanisms, through direct glucuronidation conjugation reaction catalyzed by UDP-glucuronosyltransferase (UGT) primarily occurring in the liver, kidney and intestines. It has been reported that capacity for UGT-mediated metabolism is different and notably greater in the dog intestine and liver (Wang et al., 2006; Furukawa et al., 2014). This metabolic observation contradicts the lower dog pharmacokinetic parameters of sparfloxacin published. Previously in the rabbit it has been observed that approximately 5 % of sparfloxacin is eliminated unchanged through transepithelial processes (Rubinstein et al., 1995). It is also predominantly hepatically excreted into the bile (Matsunaga et al., 1991b).

The lower half-life for sparfloxacin in the rabbit in this study may be the result of propofol anaesthetic on hepatic blood flow in rabbits as it has been observed to increase hepatic flow rates (Zhu et al., 2008). This would potentially increase hepatic extraction and clearance of the drug. The distribution of sparfloxacin must occur rapidly given the heart tissue concentration profile identified sparfloxacin drug levels in heart were up to 7-fold greater than those circulating in the plasma which concurs with the moderate volume of distribution. This is in agreement with the rat literature parameters as sparfloxacin has been described as having high tissue penetration with up to 11-fold greater concentrations in tissues, and approximately 5-fold in heart compared to plasma (Nakamura et al., 1990).

4.10.6. Moxifloxacin Anaesthetised Rabbit Results

A summary of mean pharmacokinetic parameters of moxifloxacin, are given in Table 4.17 with mean plasma concentration-time tabulated in Table 4.18 and graphically presented in Figure 4.18, respectively.

Table 4.17 Mean Pharmacokinetics Parameters of Moxifloxacin in Plasma Following a Single Intravenous Infusion Administration to Anaesthetised Rabbits

Dose Level (mg/kg)	T_{max} (h)	C_{max} (ng/mL)	AUC_{last} (ng*h /mL)	V_{dss} (L/kg)	CL_p (mL/min/kg)	Half-Life (hour)
5	25	3680	2810	1.90	17.1	1.29
20	25	13000	10700	2.00	16.3	1.42

Plasma concentrations of moxifloxacin in the terminally anaesthetised rabbit were determined following a 30 minute single intravenous infusion at a nominal dose of 5 and 20 mg/kg, up to 90 minutes post infusion. The maximum moxifloxacin plasma concentrations (C_{max}) at 5 and 20 mg/kg observed was 3680 and 13000 ng/mL, respectively, which both occurred at 25 minutes prior to the end of infusion at 30 minutes. The observed mean systemic exposure of moxifloxacin, as determined by the area under the curve with time (AUC_{0-t}), was 2810 and 10700 ng.h/mL, at each increasing dose level, respectively. Parameters, C_{max} and AUC increased in an approximately dose proportional (linear) manner.

The derived pharmacokinetic parameters were determined for the plasma concentration-time profiles at 5 and 20 mg/kg. The volume of distribution was approximately 2.00 L/kg which indicates distribution through the body water and widely into tissues. The mean plasma clearance of moxifloxacin was moderate at 16.3 and 17.1 ml/min/kg, approximately 24% of liver blood flow (LBF) in the rabbit (70 mL/min/kg; Davies and Morris, 1993). The estimated half-life following an intravenous infusion administration was considered short at approximately 1.3 hours.

Table 4.18 Moxifloxacin Anaesthetised Rabbit: Mean Plasma Concentrations in the Anaesthetised Rabbit Following an Infusion of Moxifloxacin at 5 and 20 mg/kg

Time (min)	Mean 5 mg/kg Concentration (ng/mL)	±S.E.M.	Mean 20 mg/kg Concentration (ng/mL)	±S.E.M.
-15	**NQ**	NC	**NQ**	NC
0	**NQ**	NC	**NQ**	NC
5	**1920**	±75.0	**6750**	±220
10	**2390**	±139	**8450**	±540
15	**2920**	±150	**9670**	±500
20	**3390**	±380	**12600**	±1060
25	**3550**	±321	**13000**	±696
30	**2950**	±303	**12400**	±414
35	**2040**	±89.4	**8380**	±205
40	**1690**	±17.4	**7160**	±440
45	**1700**	±117	**6390**	±108
50	**1540**	±35.1	**6030**	±383
55	**1500**	±122	**5410**	±286
60	**1440**	±125	**5530**	±277
65	**1330**	±127	**5250**	±319
70	**1280**	±87.8	**4830**	±290
75	**1230**	±106	**5170**	±642
80	**1250**	±125	**4570**	±373
85	**1220**	±128	**4510**	±389
90	**1210**	±118	**4770**	±36.8

NC Not Calculated

Figure 4.18 Moxifloxacin Anaesthetised Rabbit: Graph of Mean Plasma Concentration-Time Profile of Moxifloxacin in the Anaesthetised Rabbit Following an Infusion of Moxifloxacin at 5 and 20 mg/kg.

a) Linear plot

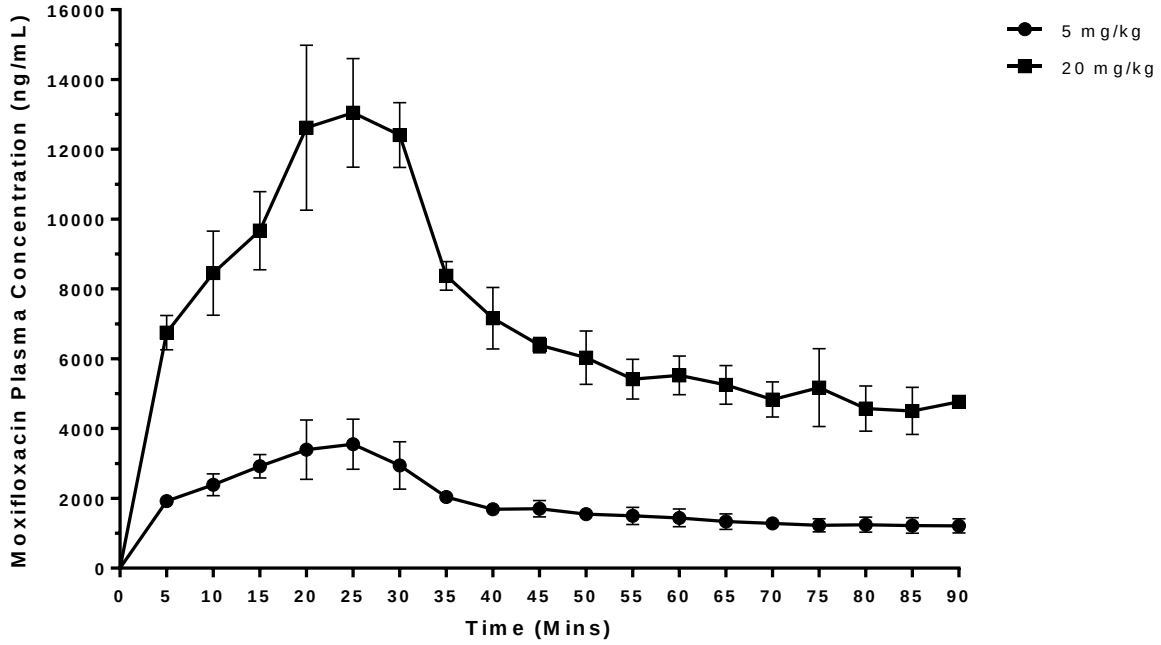

b) Log plot

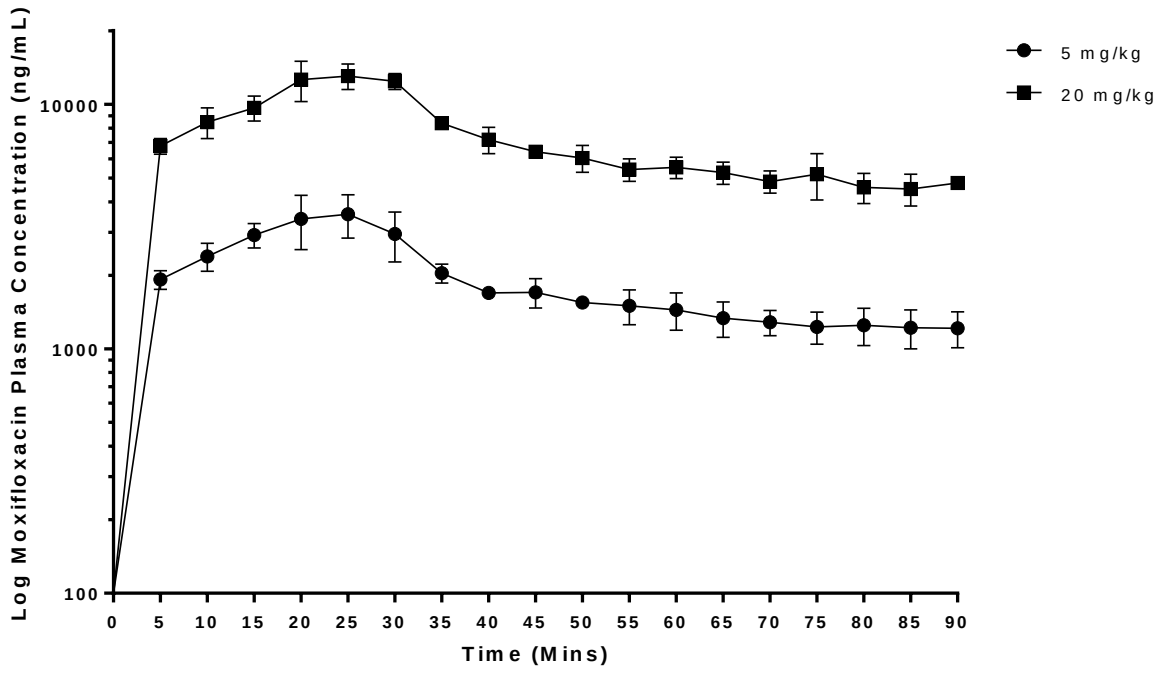

Figure 4.18: Graph of the mean and S.E.M. baseline of plasma concentration-time profile (ng/mL) generated in the anaesthetised rabbit preparation following a 30 minute intravenous infusion administration of moxifloxacin at 5 mg/kg (●) (n=5) and 20 mg/kg (■) (n=5)

4.10.6.1. Moxifloxacin Heart

Heart tissue was collected and analysed by LC-MS/MS for moxifloxacin cardiac concentrations through replicate analyses of tissue homogenates generated from heart tissue slices at each time point. Rabbit hearts were collected at the end of the 30 minutes infusion (n=1), 60 minutes (n=1) and 90 minutes (n=3) for 5 and 20 mg/kg. As previously described (Section 4.8), moxifloxacin concentrations were determined for 12 replicates of heart tissue sampled following preparation by cryostat microtome slicing. Individual replicate concentrations are given in Appendix 4. Overall mean moxifloxacin heart tissue concentrations are summarised in Table 4.19 and Table 4.20 for 5 and 20 mg/kg, respectively, along with the corresponding mean plasma concentrations. Heart tissue to plasma ratio has then been derived to show the extent of tissue partitioning by moxifloxacin at each time point.

A graphical representation of the heart tissue concentrations at each dose level is shown together in Figure 4.19 as linear (a) and logarithmic (b) plots. Figure 4.20 is a further plot showing the combined concentration time profiles of moxifloxacin in both plasma and heart.

At each dose level, 5 and 20 mg/kg, the overall mean moxifloxacin heart concentrations were at their maximum at the end of the 30 minute infusion, with 23800 and 92600 ng. equiv./mL, respectively. Heart tissue concentrations were dose proportional with a 3.9-fold increase with dose from 4 to 20 mg/kg and decreased with time at 60 and 90 minutes, except for the 90 minutes at 20 mg/kg, where the mean concentration was higher as a result of a greater *n* number.

The moxifloxacin heart concentrations were greater than plasma concentrations at all time points. Heart:plasma ratios were approximately similar between the two dose levels examined at each time point. At 4 mg/kg, the ratio ranged from 5.8 to 12.9, and at 20 mg/kg, the ratio ranged from 8.1 to 14.2. As shown in Figure 4.20, the heart time-concentration profiles follow the same time course as plasma, with an approximate logarithmic unit (10-fold) difference.

Table 4.19 Moxifloxacin Anaesthetised Rabbit: Mean Heart Concentrations in the Anaesthetised Rabbit Following an Infusion of Moxifloxacin at 5 mg/kg

	Heart Tissue Concentration of Moxifloxacin (ng equiv./mL)					
	#3	#2	#1	#4	#5	Mean
Time (min)	30	60	90	90	90	90
Mean Heart	23800	13900	11100	12900	11400	11800
Mean Plasma	4070	1700	1400	998	1240	1210
Heart: Plasma ratio	5.8	8.2	7.9	12.9	9.2	10.0

Table 4.20 Moxifloxacin Anaesthetised Rabbit: Mean Heart Concentrations in the Anaesthetised Rabbit Following an Infusion of Moxifloxacin at 20 mg/kg

	Heart Tissue Concentration of Moxifloxacin (ng equiv./mL)					
	#3	#2	#1	#4	#5	Mean
Time (min)	30	60	90	90	90	90
Mean Heart	92600	43300	48700	67200	60800	58900
Mean Plasma	11400	5140	4740	4730	4840	4770
Heart: Plasma ratio	8.1	8.4	10.3	14.2	12.6	12.4

Figure 4.19 Moxifloxacin Anaesthetised Rabbit: Graph of Individual Heart Concentration-Time Profile of Moxifloxacin in the Anaesthetised Rabbit Following an Infusion of Moxifloxacin at 5 and 20 mg/kg.

a) Linear plot

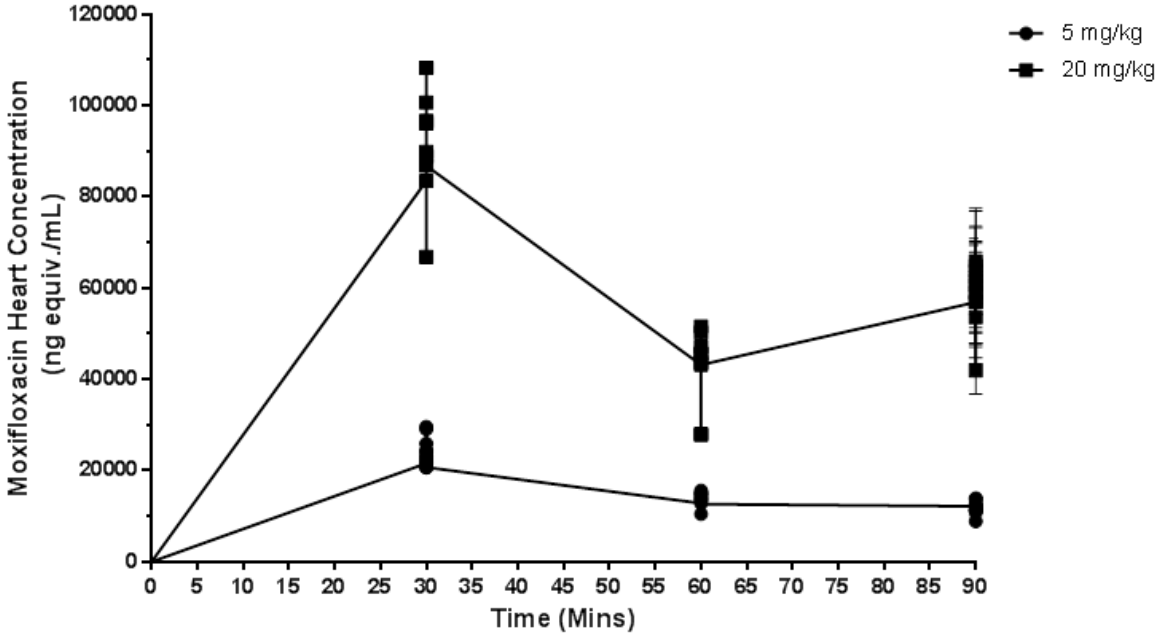

b) Log plot

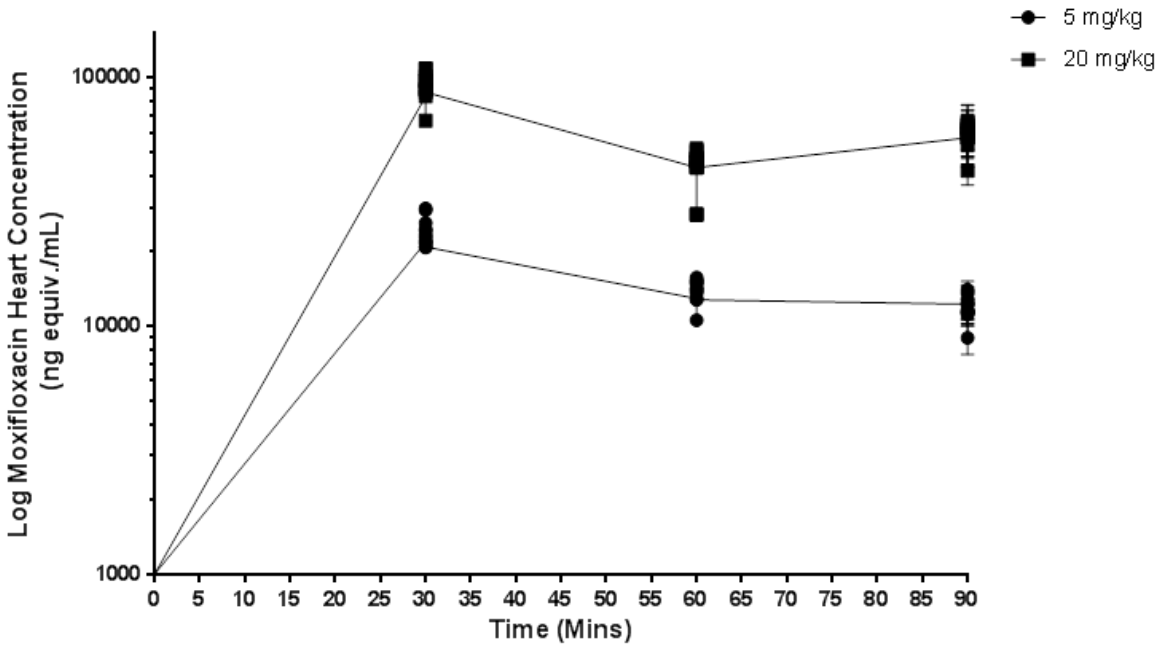

Figure 4.19: Graph of the mean and S.E.M. baseline of heart concentration-time profile (ng equivalents/mL) generated in the anaesthetised rabbit preparation following a 30 minute intravenous infusion administration of moxifloxacin at 5 mg/kg (●) (n=5), and 20 mg/kg (■) (n=5).

Figure 4.20 Moxifloxacin Anaesthetised Rabbit: Comparison of Mean Plasma and Heart Concentration-Time Profile of Moxifloxacin in the Anaesthetised Rabbit Following an Infusion of Moxifloxacin at 5 and 20 mg/kg.

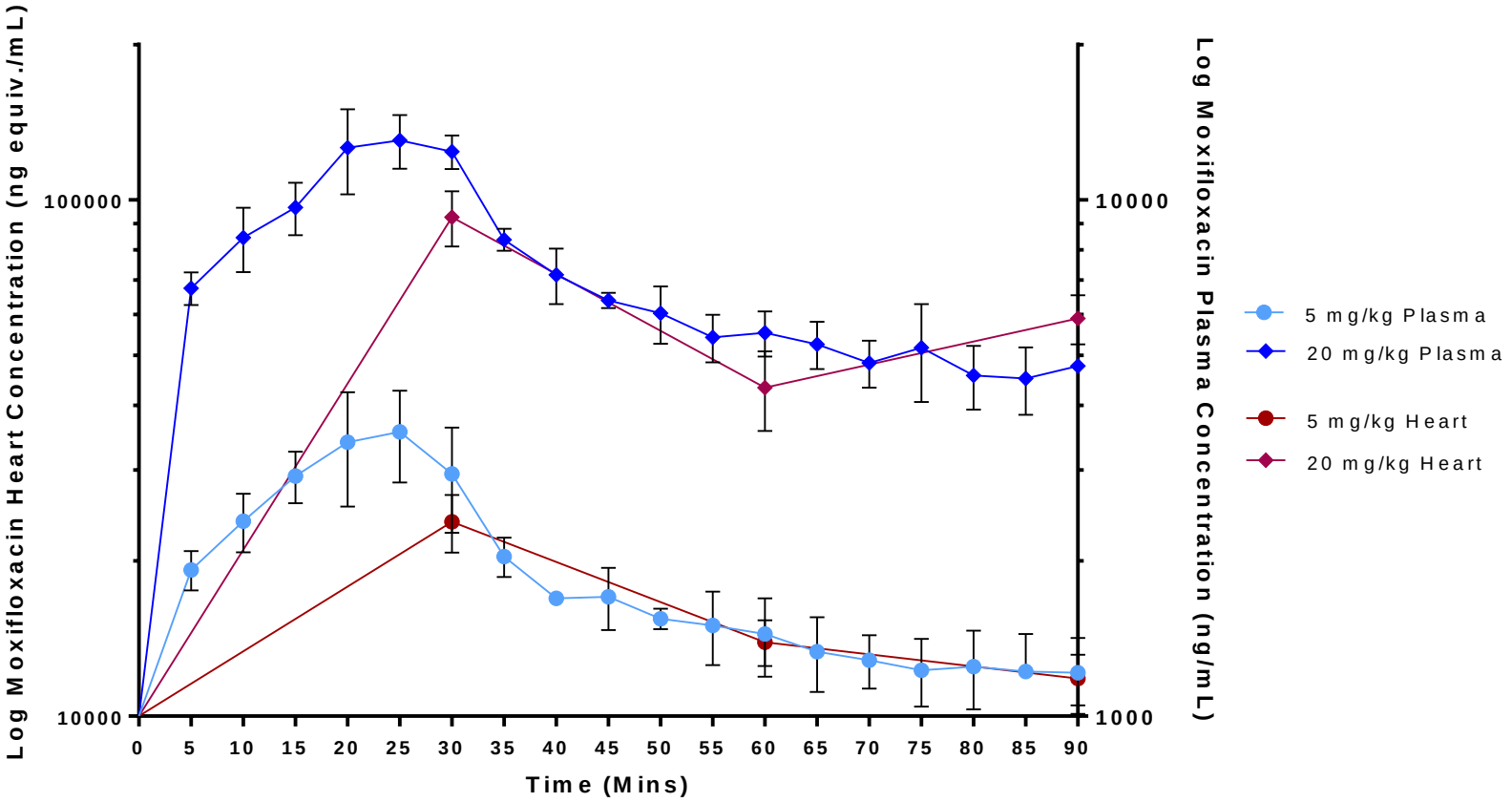

Figure 4.20: Graph of the mean and S.E.M. baseline of plasma (— blue line) and heart (— red line) concentration-time profile (ng/mL or ng equivalents/mL, respectively) generated in the anaesthetised rabbit preparation following a 60 minute intravenous infusion administration of moxifloxacin at 5 mg/kg (n=5) plasma (●) and heart (●); 20 mg/kg (n=5) plasma (♦) and heart (♦)

4.10.6.2. Moxifloxacin QT Prolongation

Moxifloxacin was investigated in the anaesthetised rabbit model preparation (n=5) at 5 and 20 mg/kg infusions over a 30 minute period. The data presented in Table 4.21 and represented graphically in Figure 4.21, shows the overall mean baseline and vehicle QTc interval corrected as a percentage change (ΔΔQTc%) with S.E.M. response following administration of moxifloxacin with time. The full tabulated data of the individual experimental QTc intervals (ms), delta changes (ΔQTc, ms), and double delta vehicle and baseline corrected QTc intervals as percentage (ΔΔQTc%) and graphical plots at each dose range are presented in Appendix 4. Figure 4.22 shows the ECG trace at each dose level and the subsequent delay of the T wave and QT prolongation.

The vehicle control group equilibrium predose mean QTc interval was 344 ±16.3 ms and at the end of a 30 minute infusion was 352 ±16.8 ms. This represented a small increase change in QTc interval of 2.36 ±0.32 % during the infusion period, whilst the mean QTc interval was 356 ±18.2 ms equivalent to a mean ΔQTc% increase of 3.52 ±1.34% the end of the vehicle control experiment (90 minutes). Compared to the control baseline mean ΔQTc% was -2.0 ±3.2%.

For each dose level, 5 and 20 mg/kg investigated, the predose equilibration mean QTc interval was 291 ±15.2 ms and 288 ±16.5 ms, respectively.

Moxifloxacin increased the change in QTc interval with an increasing dose administration of moxifloxacin at each dose level, 5 and 20 mg/kg, as shown by the temporal electrocardiograph overlay in Figure 4.22A, B and C. However the mean ΔQTc% interval increased by 7.77 ±1.90% at the end of infusion of 5 mg/kg was not different to vehicle control (p-value >0.05), whilst an increase of 11.7 ±1.49% at 20 mg/kg was statistically different (p-value <0.01). At 5 and 20 mg/kg, the mean ΔQTc% interval was 4.02 ±4.10% and 2.43 ±3.83% at 90 minutes post-start of infusion, both of which were not different compared to control vehicle(p-values >0.05). At 20 mg/kg ΔQTc% was different to vehicle control during infusion (p-value <0.05) but also between 60 to 70 minutes post infusion which reflects some variability in ΔQTc%.

The double delta vehicle and baseline corrected mean QTc interval (ΔΔQTc%) increased by 4.95 ±1.77% and 9.39 ±1.57% at the end of infusion of 5 and 20 mg/kg respectively.

Table 4.21 Moxifloxacin Anaesthetised Rabbit: Mean Baseline and Vehicle Corrected Percentage Change in QTc (ΔΔ%) Response in the Anaesthetised Rabbit Following an Infusion of Moxifloxacin at 5 and 20 mg/kg.

Time (min)	5 mg/kg Mean ± S.E.M. ΔΔQTc (%)	20 mg/kg Mean ± S.E.M. ΔΔQTc (%)
Predose	291 ms ±15.2	288 ms ±16.5
0	0.41 ±0.39	0.27 ±0.47
5	1.59 ±0.71	1.88 ±0.86
10	2.82 ±1.27	5.68* ±1.03
15	4.03 ±1.66	7.22* ±1.07
20	4.14 ±1.95	7.87* ±1.28
25	4.23 ±2.02	8.58* ±1.55
30	4.95 ±1.77	9.39** ±1.57
35	4.49 ±2.01	7.08 ±2.06
40	3.09 ±1.58	4.31 ±2.47
45	2.58 ±1.44	3.76 ±2.72
50	2.51 ±1.72	3.86 ±2.80
55	3.34 ±2.14	4.64 ±2.79
60	3.99 ±2.43	5.47* ±3.07
65	1.93 ±2.41	6.08* ±3.38
70	1.41 ±2.66	5.41* ±3.50
75	0.23 ±2.99	4.37 ±3.48
80	-0.25 ±3.34	3.38 ±3.65
85	-0.09 ±3.84	3.05 ±3.76
90	-0.39 ±4.22	2.43 ±3.83

Statistical difference from vehicle by repeated measures, pairwise comparison
p-value <0.05 denoted by *; p-value <0.01 denoted by **

Figure 4.21 Moxifloxacin Anaesthetised Rabbit: Graph of Mean Baseline and Vehicle Corrected Percentage Change in QTc (ΔΔ%) Response in the Anaesthetised Rabbit Following an Infusion of Moxifloxacin at 5 and 20 mg/kg.

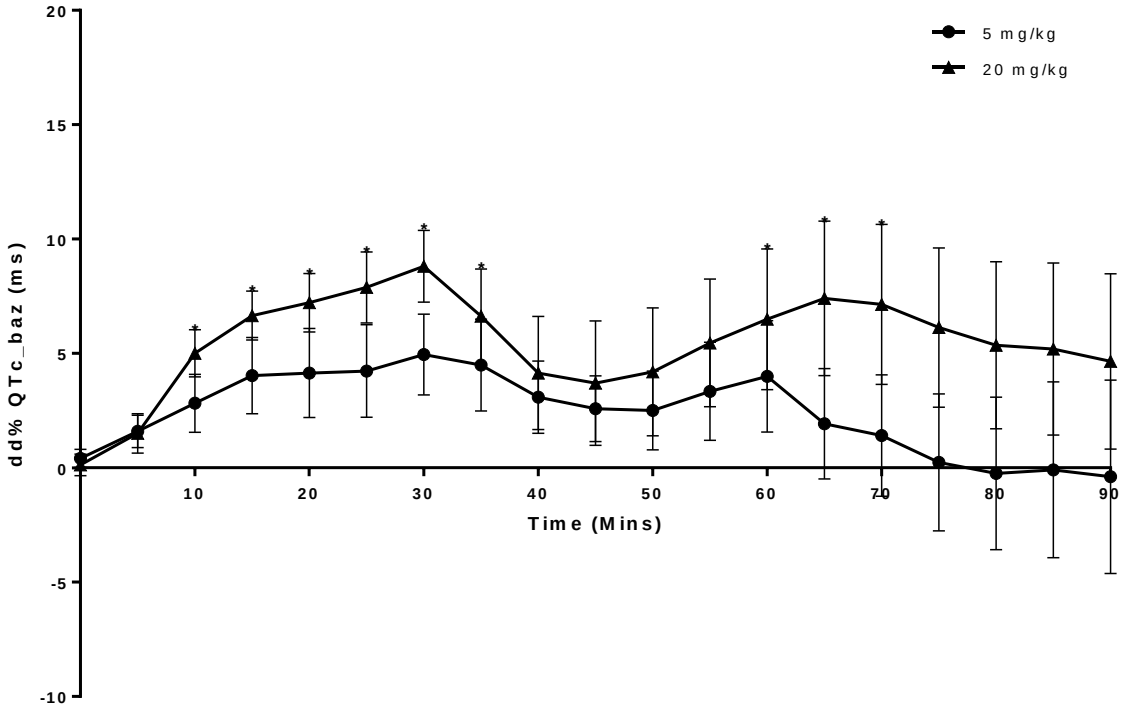

Figure 4.21: Graph of the mean and S.E.M. baseline and vehicle corrected change in QT response (ΔΔ%) generated in the anaesthetised rabbit preparation following administration of moxifloxacin at 5 mg/kg (●) (n=5) and 20 mg/kg (▲) (n=5) where * denotes a statistical difference compared to vehicle control (*p*-value <0.05).

Figure 4.22 Moxifloxacin Anaesthetised Rabbit: Representative Trace of the Change in ECG in the Anaesthetised Rabbit with Time and Dose Level

A: Moxifloxacin vehicle

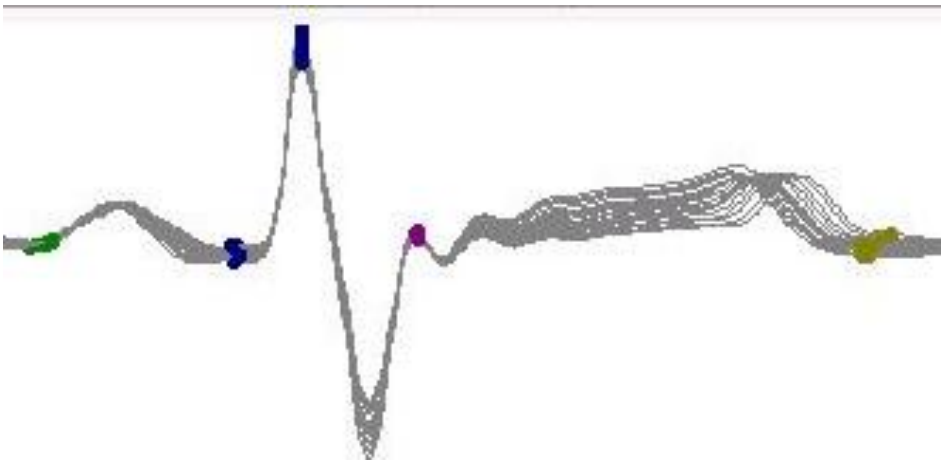

B: Moxifloxacin 5 mg/kg

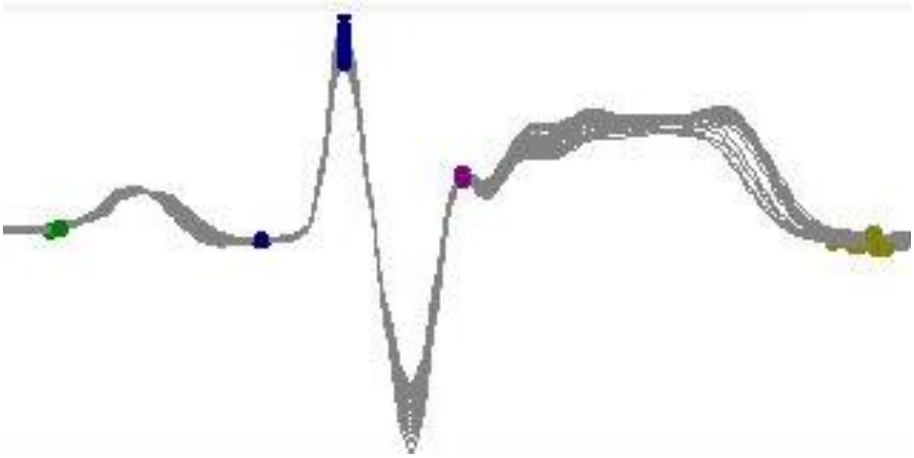

C: Moxifloxacin 20 mg/kg

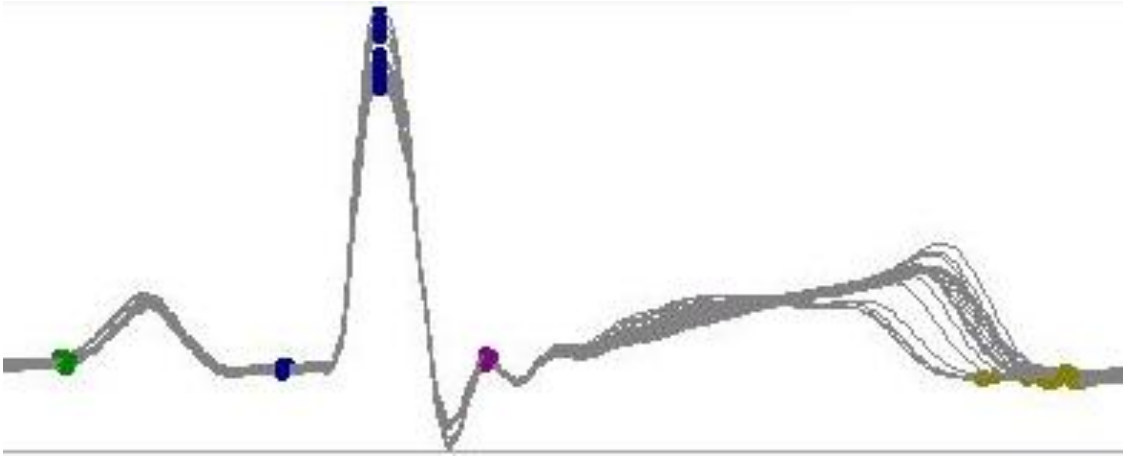

Figure 4.22: Representative overlay trace of the change in ECG waveform from each of the 5 minute time bins (n=18) generated in the anaesthetised rabbit model preparation over time under control baseline conditions with ECG waves marker points identified start of P wave (●), Q wave inflection point (●), R peak (●), S wave (●), T wave end (●).

4.10.7. Moxifloxacin Summary Discussion

Following a single intravenous infusion of moxifloxacin at 5 and 20 mg/kg over 30 minutes, the resultant QT prolongation only reached significance at 20 mg/kg. Mean maximum plasma concentrations observed were 3680 and 13000 ng/mL, and corresponding heart tissue concentrations 23800 and 92600 ng/mL, respectively, that resulted in a QTc increase of 21 ±4.10 ms and 34.0 ±5.46 ms from the baseline QTc of 291 ±15.2 ms and 288 ±16.5 ms (equivalent to mean ΔQTc% by 7.77 ±1.90% and 9.39 ±1.57%).

Anderson et al. utilised the sensitised-rabbit model with minor modifications to investigate the proarrhythmic properties of quinolone antibiotics including moxifloxacin (Anderson et al., 2001). Moxifloxacin was infused for up to 60 minutes at 2 mg/kg/min (120 mg/kg total, n=6), and of the quinolones tested, moxifloxacin did not significantly increase either the QT or the QTc intervals. The observed QTc interval increased by 31 ms from baseline (241 ±10 ms) to a maximum 270 ±30 ms (equivalent to ΔQTc 12.9%) by Anderson et al. (2001). The data presented by Anderson et al. showed that the QT response did not change after 30 minutes, with no adverse proarrhythmic anomalies observed up to 60 minutes. The increase observed following 120 mg/kg was approximate to the observed QTc change (9.39 ±1.57%) in this present study at 20 mg/kg dose levelwhich was significant (p-value <0.005). The difference observed between the studies may be explained in the absence of concentration data, due to comparing to the α1-sensitised model, the lower observed QT baseline and the method of correction used by Carlsson et al. (Carlsson et al., 1993).

Following the publication by Anderson et al. (2001) additional fluoroquinolones, sitafloxacin, gatfloxacin and moxifloxacin were investigated for proarrhythmic effects using the methoxamine sensitised-model (Chiba et al., 2004a). The QT interval and QTc (ms) at 10 minutes before the start of methoxamine infusion were 149 ±13 ms and 168 ±12 ms in the moxifloxacin-administered group, respectively, with no significant difference to the other respective control values (133 ±11 ms and 152 ±9 ms for sitafloxacin-group and 131 ±8 ms and 149 ±7 ms for gatifloxacin-group). Also, methoxamine prolonged the QT interval and QTc in each group during the initial 10 minutes of infusion, of which no significant difference was detected in the magnitude of changes among the three groups. Drugs administered were dissolved in a 1% lactate solution, and moxifloxacin was given as 60 mg/kg over 20min. Plotted data indicates the maximum QTc was approximately 200 ms, an increase of 42 ms equivalent to ΔQTc ~25%. Although there is a difference in the

baseline and corrected QT values, the percentage change is greater than this present study (9.39 ±1.57%) given the greater dose administered (20 mg/kg vs 60 mg/kg). In the Chiba et al. experimental set up, the QTc interval is similar to the QT observed; a result of lower RR interval/HR values cancelled out in the Carlsson correction method in comparison to the Bazett correction method used in this present study.

Additional reported investigations of moxifloxacin in proarrhythmia screening models, which included the sensitised-rabbit, had baseline QTc levels (n=16) at 170 ±12 ms, prior to methoxamine administration and then subsequent co-administration of a 30 minute infusion of moxifloxacin at 3 mg/kg or 90 mg/kg (Nalos et al., 2012). This resultant QTc increase to 181 ±6 ms and 223 ±37 ms, a change of 11 ms and 53 ms, was equivalent to ΔQTc ~6.5% and 31%, respectively. Changes in the QTc interval at 3 mg/kg are equivalent to the results determined in this study at 7.77 ±1.90% at 5 mg/kg. Whilst the difference observed by Nalos et al. at 90 mg/kg is similar to Chiba et al. for 60 mg/kg, both are greater than that observed by Anderson et al. at 120 mg/kg.

Although Chiba et al. did not measure the plasma drug concentrations in the anaesthetised-rabbit, the observations in their previous preclinical models together with clinical studies following single oral administration of therapeutically relevant doses of 400–500 mg of moxifloxacin, provide peak plasma concentrations (C_{max}) of 4.3 μg/ml (Lubasch et al., 2000). The author suggests that the preclinical models were supra-therapeutic based on drug induced hypotension via nonspecific mechanisms, which significantly modified the electrophysiological profile of the drugs in vivo.

Nalos et al. did take plasma samples mid- and end of infusion for both dose groups such that low-dose 3 mg/kg intravenous infusion of moxifloxacin resulted in plasma concentrations of 2800 ng/mL at 15 minutes and 3600 ng/mL after 30 minutes, and high-dose 90 mg/kg infusion resulted in 38000 ng/mL after 15 minutes and 43000 ng/mL after 30 minutes. The low-dose infusion closely corresponds to the mean maximum plasma concentrations observed in this study (3680 ng/mL at 5 mg/kg). Yet the high-dose infusion by Nalos et al. highlights a less than proportional increase, with a 12-fold increase in concentration for a 30-fold increase in dose. In contrast, the mean maximum concentration at 20 mg/kg observed in this study appear proportional, albeit only for a 4-fold increase. Maximal concentrations observed were similar to reported studies that have been conducted as part of *S. Aureus* treatment of ocular infections where concentrations at the end of a 20 mg/kg intravenous infusion over 30

minutes were 4160 ng/mL (Tzepi et al., 2009). No pharmacokinetic parameters were reported but two investigators have published information relating to moxifloxacin in the rabbit at 5 mg/kg intravenous bolus (Fernandez-Varon et al., 2005; Carceles et al., 2006). Fernandez-Varon et al. compared moxifloxacin intravenous pharmacokinetics with oral and intramuscular exposure, whilst Carceles et al. investigated the subcutaneous delivery and effect of co-administration with a polymer formulation. The concentrations at 5 minutes following 5 mg/kg intravenous bolus administration were similar to each other (4.35 µg/mL and 3.58 µg/mL) and equivalent to the concentrations observed in this present study at the end of 30 minutes infusion of 20 mg/kg.

Table 4.22 Comparison of Pharmacokinetic parameters across species following Intravenous administration of Moxifloxacin

	Vdss (L/kg)	CL_p (mL/min/kg) (% LBF)	Half-life (hr)
Rat	3.6	42.5 (54.5%)	1.2
Dog	2.7	3.7 (6.6%)	8.6
Minipig	3.8	10.8 (38.6%)	5.7
Monkey	4.9	11.5 (26.1%)	6.9
Human	2.0	2.2 (12.2%)	13
Rabbit	1.95 - 2.1	13.3 (19.0%)	1.84 – 2.2
Present study	2.0	16.7 (~24%)	1.3 – 1.4

Combined table of parameters obtained from literature sources
Liver blood flow (LBF, ml/min/kg) for each species rat (78), dog (56), minipig (28), monkey (44), human (18), rabbit (70) Davies and Morris, 1993

a. Wang (2014) rat
b. Zhu (2014)
c. Stass 2001
d. Siefert 1999 a b;
e. Fernandez-Varon 2005
f. Carceles 2006

Following intravenous infusion of 5 and 20 mg/kg over 30 minutes in the anaesthetised rabbit, parameters obtained for volume of distribution (2 L/kg), total clearance (16.7 mL/min/kg) and half-life (1.35 hour) were comparable to 1.95 - 2.1 L/kg, 13.3 mL/min/kg and 1.8 – 2.2 hour, respectively (Fernandez-Varon et al., 2005; Carceles et al., 2006). These parameters in the rabbit are similar and consistent across species for tissue

distribution and clearance (Table 4.22), with lowest values for human and dog as total body clearance decreases with size (Siefert et al., 1999a). The rat appears to have the greatest clearance and shortest half-life. Following intravenous and oral radioactive whole-body distribution studies in the rat a high level of tissue penetration relative to blood were demonstrated and parallel concentration-time courses of moxifloxacin in plasma and lung were observed (Siefert et al., 1999b). Similar parallel elimination of moxifloxacin from serum and cerebrospinal fluid (CSF) was observed following intravenous doses 10, 20 and 40 mg/kg in the rabbit, with a range of half-life from 1.1 - 1.37 (Østergaard et al., 1998).

Moxifloxacin is primarily metabolized by phase II UGT enzymes in the liver, forming a glucuronide and N-sulfate conjugate (Moise et al., 2000; Stass and Kubitza, 2001). As a result moxifloxacin metabolism is unaffected by anaesthetics shown by the clearance (Zhu et al., 2008), and is also not an inhibitor of CYP3A4 metabolism in the rabbit affecting propofol (Szałek et al., 2013). It has been reported that approximately 4.5% of moxifloxacin dose is eliminated trans-epithelially at the gut-wall, following intravenous bolus administration through the jugular vein at 15 mg/kg, over a 120 minutes anaesthetised experimental period during an investigation into the intestinal transfer (Musafija et al., 2000). Authors suggest that ~20% of moxifloxacin is eliminated in the urine as the parent compound, of which ~20% is eliminated in the urine as the glucuronidated form and 40% is eliminated in the faeces, 25% of that as unchanged moxifloxacin and the remainder as metabolites. Thus, in rabbits, the intestinal tract serves as excretory organ for moxifloxacin. Extra-biliary intestinal secretion of moxifloxacin after intravenous administration has also been demonstrated in rats (Siefert 1999). It is possible that these processes appear more prominent in rodent species albeit the same routes of metabolism observed in man (Stass and Kubitza, 1999).

4.10.8. Verapamil Anaesthetised Rabbit Results

4.10.8.1. Verapamil Plasma PK

A summary of mean pharmacokinetic parameters of verapamil, are given in Table 4.23 with mean plasma concentration-time tabulated in Table 4.24 and graphically presented in Figure 4.23, respectively.

Table 4.23 Mean Pharmacokinetics Parameters of Verapamil in Plasma Following a Single Intravenous Infusion Administration to Anaesthetised Rabbits

Dose Level (mg/kg)	T_{max} (h)	C_{max} (ng/mL)	AUC_{last} (ng*h /mL)	V_{dss} (L/kg)	CL_p (mL/min/kg)	Half-Life (hour)
0.1	30	91.9	56.0	1.59	24.6	0.75
0.3	25	247	150	1.44	28.8	0.58
1	25	1330	960	0.63	13.4	0.52

Plasma concentrations of verapamil in the terminally anaesthetised rabbit were determined following a 30 minute single intravenous infusion at a nominal dose of 0.1, 0.3 and 1 mg/kg, up to 90 minutes post infusion. The maximum verapamil plasma concentrations (C_{max}) at 0.1, 0.3 and 1 mg/kg observed was 91.9, 247, and 1330 ng/mL, respectively, which occurred between 25 minutes and the end of infusion at 30 minutes. The observed mean systemic exposure of verapamil, as determined by the area under the curve with time (AUC_{0-t}), was 56.0, 150 and 960 ng.h/mL, at each increasing dose level, respectively. Parameters, C_{max} and AUC indicate a slight increased greater than dose proportional (supra, non-linear) manner.

The derived pharmacokinetic parameters were determined for the plasma concentration-time profiles at 0.1, 0.3 and 1 mg/kg. The volume of distribution was approximately 1.59, 1.44 and 0.63 L/kg which indicates distribution primarily restricted to the central compartment. The mean plasma clearance of verapamil was moderate at 24.6, 28.8 and 13.4 ml/min/kg, approximately 35-40% of liver blood flow (LBF) in the rabbit (70 mL/min/kg; Davies and Morris, 1993) at 0.1 and 0.3 mg/kg, and a 20% LBF at 1 mg/kg. The estimated half-life following an intravenous infusion administration was rapid 0.5 to 0.75 hours.

Table 4.24 Verapamil Anaesthetised Rabbit: Mean Plasma Concentrations in the Anaesthetised Rabbit Following an Infusion of Verapamil at 0.1, 0.3, and 1 mg/kg

Time (min)	Mean 0.1 mg/kg Concentration (ng/mL)	±S.E.M.	Mean 0.3 mg/kg Concentration (ng/mL)	±S.E.M.	Mean 1 mg/kg Concentration (ng/mL)	±S.E.M.
-15	NQ	NC	NQ	NC	NQ	NC
0	NQ	NC	NQ	NC	NQ	NC
5	55.1	±2.3	139	±1.1	566	±163
10	61.0	±2.4	179	±2.8	724	±18.9
15	71.3	±3.6	199	±14.8	1020	±159
20	72.5	±3.0	239	±9.7	1160	NC
25	82.3	±2.3	247	±1.1	1330	NC
30	91.9	±12.1	238	±15.1	1250	NC
35	45.5	NC	99.1	NC	1090	NC
40	38.0	NC	74.6	NC	793	NC
45	26.0	NC	64.4	NC	562	NC
50	20.6	NC	51.9	NC	424	NC
55	19.6	NC	58.5	NC	471	NC
60	16.7	NC	40.8	NC	386	NC
65	15.4	NC	38.2	NC	446	NC
70	16.2	NC	36.7	NC	406	NC
75	13.1	NC	35.6	NC	322	NC
80	12.1	NC	30.9	NC	412	NC
85	12.6	NC	27.0	NC	323	NC
90	11.0	NC	28.4	NC	NS	NC

NC Not Calculated

Figure 4.23 Verapamil Anaesthetised Rabbit: Graph of Mean Plasma Concentration-Time Profile of Verapamil in the Anaesthetised Rabbit Following an Infusion of Verapamil at 0.1, 0.3 and 5 mg/kg.

a) Linear plot

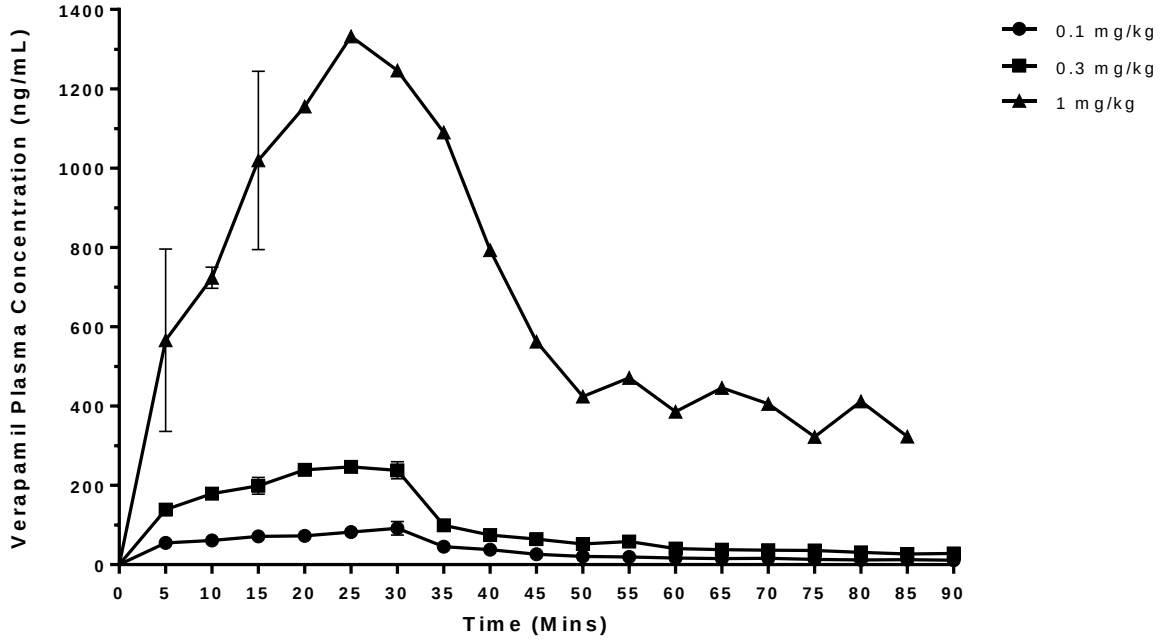

a) Log plot

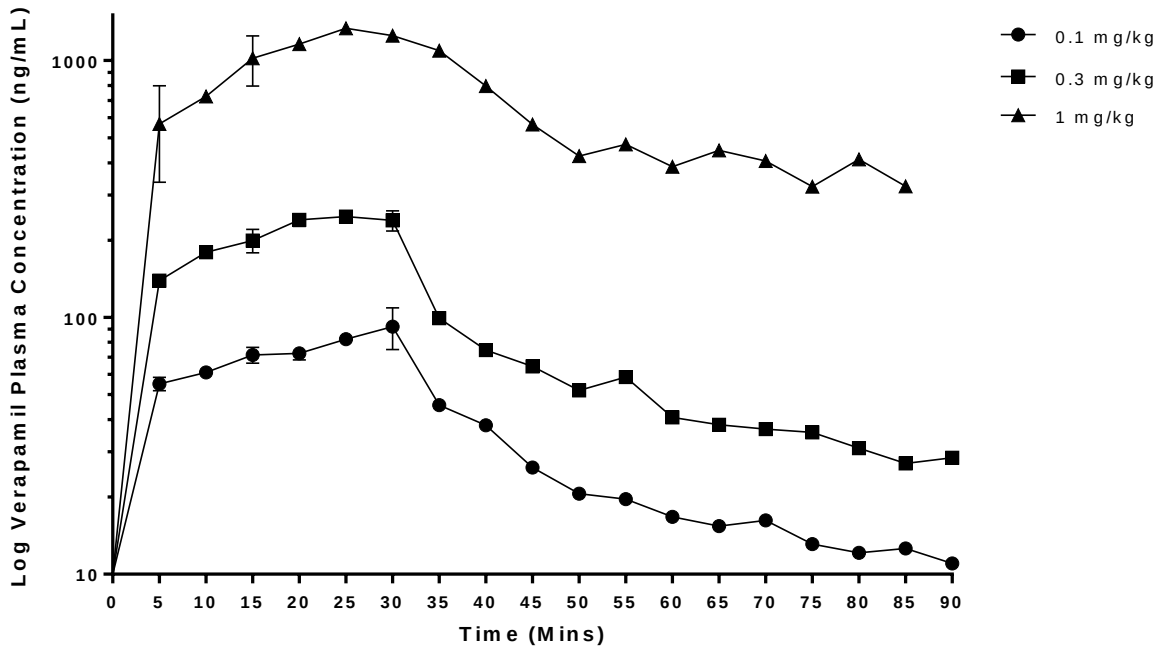

Figure 4.23: Graph of the mean and S.E.M. baseline of plasma concentration-time profile (ng/mL) generated in the anaesthetised rabbit preparation following a 30 minute intravenous infusion administration of verapamil at 0.1 mg/kg (●) (n=2), 0.3mg/kg (■) (n=2) and 1 mg/kg (▲) (n=2).

4.10.8.2. Verapamil Heart

Heart tissue was collected and analysed by LC-MS/MS for verapamil cardiac concentrations through replicate analyses of tissue homogenates generated from heart tissue slices at each time point. Rabbit hearts were collected at the end of the 30 minutes infusion (n=1) and 90 minutes (n=1) for 0.1 and 0.3 mg/kg, respectively, and at 15 and 85 minutes for the two rabbits that received 1 mg/kg. As previously described (Section 4.8), verapamil concentrations were determined for 12 replicates of heart tissue sampled following preparation by cryostat microtome slicing. Individual replicate concentrations are given in Appendix 4. Overall mean verapamil heart tissue concentrations from these sections are summarised in Table 4.25, Table 4.26 and Table 4.27 for 0.1, 0.3 and 1 mg/kg, respectively, along with the corresponding mean plasma concentrations. Heart tissue to plasma ratio has then been derived to show the extent of tissue partitioning by verapamil at each time point.

A graphical representation of the heart tissue concentrations at each dose level is shown together in Figure 4.24 as linear (a) and logarithmic (b) plots. Figure 4.25 is a further plot showing the combined concentration time profiles of verapamil in both plasma and heart.

At each dose level, 0.1 and 0.3 mg/kg, the overall mean verapamil heart concentrations were at their maximum at the end of the 30 minute infusion, with 729 ±4.96 and 1760 ±47.4 ng equiv./mL, respectively, whilst at 1 mg/kg one rabbit was terminated before the end of infusion at 15 minutes had mean heart concentration of 4260 ±153 ng equiv./mL. Heart tissue concentrations were dose proportional with a 2.6-fold increase for a 3-fold change in dose from 0.1 to 0.3 mg/kg and decreased with time at 90 minutes. At 1 mg/kg, the heart tissue at 15 minutes cannot be compared as it is midway through the infusion period, the tissue at 85 minutes shows a greater than dose proportional change of 22- and 8.2-fold increase compared to the 0.1 and 0.3 mg/kg, respectively, for 10 and 3.3 fold change in dose levels.

The verapamil heart concentrations were greater than plasma concentrations at all time points. Heart:plasma ratios were approximately similar between the dose levels examined at each time point. At 4 mg/kg, the ratio was 7.0 and 14.1 for 30 and 90 minutes; and at 0.3 mg/kg, the ratio was 7.9 and 15.1. As shown in Figure 4.25, the heart time-concentration profiles follow the same time course as plasma, with an approximate logarithmic unit (10-fold) difference.

Table 4.25 Verapamil Anaesthetised Rabbit: Mean Heart Concentrations in the Anaesthetised Rabbit Following an Infusion of Verapamil at 0.1 mg/kg

	#1	#2
Time (min)	**90**	**30**
Mean Heart ±S.E.M.	155 ±5.0	729 ±26
Plasma	11.0	104
Heart: Plasma ratio	**14.1**	**7.0**

Table 4.26 Verapamil Anaesthetised Rabbit: Mean Heart Concentrations in the Anaesthetised Rabbit Following an Infusion of Verapamil at 0.3 mg/kg

	#1	#2
Time (min)	**90**	**30**
Mean Heart ±S.E.M.	430 ±11.3	1760 ±47.4
Plasma	28.4	223
Heart: Plasma ratio	**15.1**	**7.9**

Table 4.27 Verapamil Anaesthetised Rabbit: Mean Heart Concentrations in the Anaesthetised Rabbit Following an Infusion of Verapamil at 1 mg/kg

	#1	#2
Time (min)	**85**	**15**
Mean Heart ±S.E.M.	3520 ±93.2	4260 ±153
Plasma	323	1180
Heart: Plasma ratio	**10.9**	**3.6**

Figure 4.24 Verapamil Anaesthetised Rabbit: Graph of Individual Heart Concentration-Time Profile of Verapamil in the Anaesthetised Rabbit Following an Infusion of Verapamil at 0.1, 0.3 and 1 mg/kg.

a) Linear plot

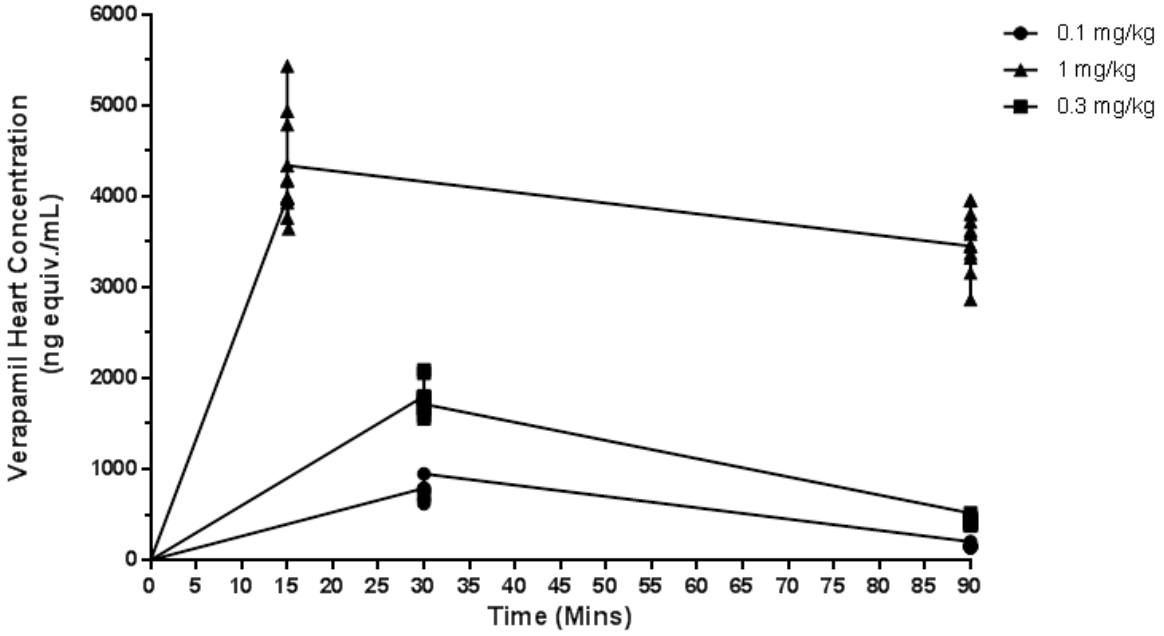

b) Log plot

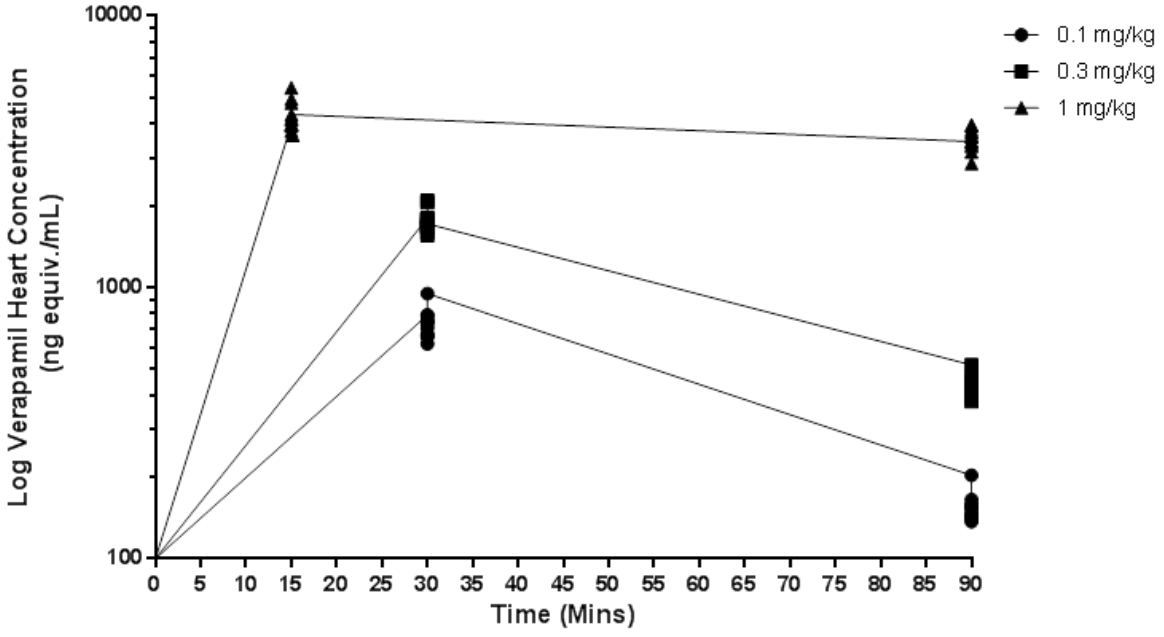

Figure 4.24: Graph of the mean and S.E.M. baseline of heart concentration-time profile (ng equivalents/mL) generated in the anaesthetised rabbit preparation following a 30 minute intravenous infusion administration of verapamil at 0.1 mg/kg (●) (n=2), 0.3 mg/kg (■) (n=2) and 1 mg/kg (▲) (n=2).

Figure 4.25 Verapamil Anaesthetised Rabbit: Comparison of Mean Plasma and Heart Concentration-Time Profile of Verapamil in the Anaesthetised Rabbit Following an Infusion of Verapamil at 0.1, 0.3 and 1 mg/kg.

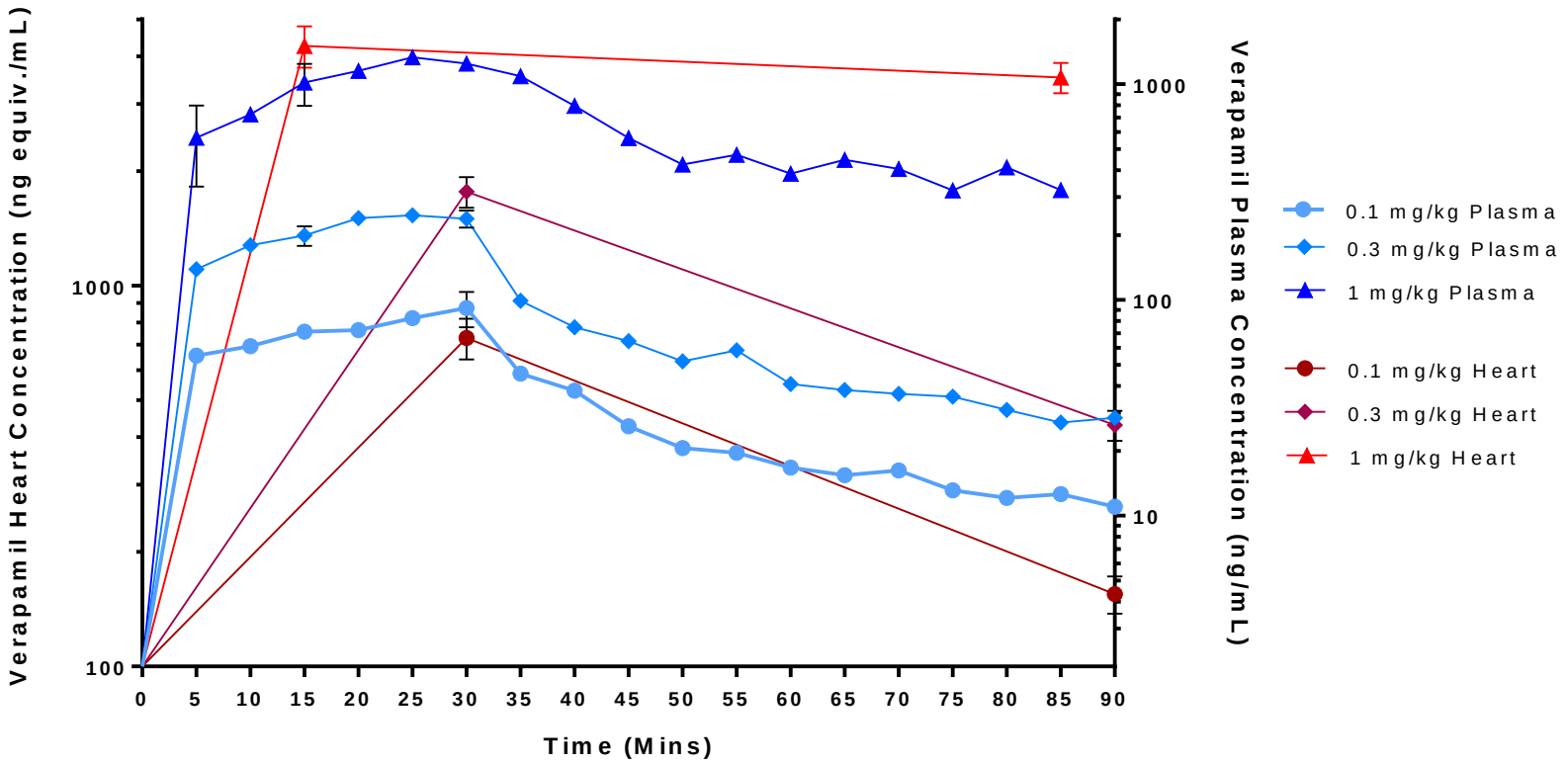

Figure 4.25: Graph of the mean and S.E.M. baseline of plasma (— blue line) and heart (— red line) concentration-time profile (ng/mL or ng equivalents/mL) generated in the anaesthetised rabbit preparation following a 30 minute intravenous infusion administration of verapamil at 0.1 mg/kg (n=2) plasma (●) and heart (●); 0.3 mg/kg plasma (♦) and heart (♦); 1 mg/kg (n=2) plasma (▲) and heart (▲)

4.10.8.3. Verapamil QT Prolongation

Verapamil was investigated in the anaesthetised rabbit model preparation (n=2) at 0.1, 0.3 and 1 mg/kg infusions over a 30 minute period. The data presented in Table 4.28 and represented graphically in Figure 4.26, shows the overall mean baseline and vehicle QTc interval corrected as a percentage change (ΔΔQTc%) with S.E.M. response following administration of verapamil with time. The full tabulated data of the individual experimental QTc intervals (ms), delta changes (ΔQTc, ms), and double delta vehicle and baseline corrected QTc intervals as percentage (ΔΔQTc%) and graphical plots at each dose range are presented in Appendix 4. Figure 4.27 shows the ECG trace at each dose level and the subsequent delay of the T wave and QT interval prolongation.

The vehicle control group equilibrium predose mean QTc interval was 266 ±3.70 ms and at the end of a 30 minute saline infusion was 290 ±6.92 ms. This represented a 24 ms change in QTc interval during the infusion period and ΔQTc% increase of 8.84 ±1.35%, by the end of the vehicle control experiment the mean QTc interval remained at 290 ±2.49 ms. This was equivalent to a mean ΔQTc% increase of 8.98 ±1.47% compared to the control baseline mean ΔQTc% was -2.0 ±3.2%. This indicates the possibility that QT and cardiac parameters may not have reached a suitable equilibrium or an effect of cold saline such that changes in QTc occurred during the infusion period only and then were maintained at a constant duration.

For each of the dose levels, 0.1, 0.3 and 1 mg/kg investigated the predose equilibration mean QTc interval was 244 ±53.1 ms and 308 ±2.80 ms and 318 ±2.02 ms, respectively.

Verapamil showed a trend for initially decreasing and subsequently increasing the change in QTc interval at each dose administration of verapamil at 0.1, 0.3 and 1 mg/kg but did reach staistical significance, only at 0.3 mg/kg at 15 and 20 minutes where ΔQTc% was –1.3% and -1.4%. The temporal electrocardiograph overlay in, as shown by Figure 4.27A, B and C.

The mean ΔQTc% interval decreased by -0.49 ±0.95% at 0.1 mg/kg, and increased 1.08 ±2.26% and 13.1% 0.3 and 1 mg/kg at the end of infusion, respectively. At 90 minutes post-start of infusion the mean percentage change in ΔQTc% interval was 5.36%, 17.9% and 10.9% at 1 mg/kg which were not statistically significant (*p*-values >0.05) compared to control vehicle.

The vehicle and baseline corrected to mean ΔΔQTc% interval decreased by -5.83 ±2.11%, -6.58 ±2.19% and -0.91 ±6.48% at the end of infusion of 0.1, 0.3, 1 mg/kg respectively.

Table 4.28 Verapamil Anaesthetised Rabbit: Mean Baseline and Vehicle Corrected Percentage Change in QTc (ΔΔ%) Response in the Anaesthetised Rabbit Following an Infusion of Verapamil at 0.1, 0.3 and 1 mg/kg.

Time (min)	0.1 mg/kg Mean ± S.E.M. ΔΔQTc (%)		0.3 mg/kg Mean ± S.E.M. ΔΔQTc (%)		1 mg/kg Mean ± S.E.M. ΔΔQTc (%)	
Predose	244	±53.1	308	±2.8	318	±2.0
0	-0.35	±0.66	-1.08	±0.15	0.12	±0.72
5	-1.59	±2.67	-3.31	±0.59	-1.49	±2.03
10	-1.93	±2.75	-5.87	±2.42	-0.32	±0.07
15	-4.00	±0.46	-6.85*	±3.21	1.44	±4.90
20	-5.14	±1.04	-7.82*	±3.70	-5.45	±0.86
25	-5.73	±1.72	-7.40	±3.08	-4.97	±1.98
30	-5.83	±2.11	-6.58	±2.19	-0.91	±6.48
35	-2.44	NC	-6.55	NC	8.00	NC
40	-1.72	NC	-4.83	NC	6.66	NC
45	-1.54	NC	-2.29	NC	5.02	NC
50	-0.99	NC	-0.50	NC	7.64	NC
55	0.23	NC	0.49	NC	6.77	NC
60	0.68	NC	0.75	NC	10.2	NC
65	1.71	NC	1.60	NC	10.8	NC
70	2.23	NC	2.44	NC	11.3	NC
75	3.29	NC	7.71	NC	10.6	NC
80	3.25	NC	10.1	NC	4.11	NC
85	2.53	NC	10.6	NC	3.70	NC
90	1.66	NC	10.2	NC	NS	NC

Statistical difference from vehicle by repeated measures, pairwise comparison
p-value <0.05 denoted by *; p-value <0.01 denoted by **
NC Not Caluclated

Figure 4.26 Verapamil Anaesthetised Rabbit: Graph of Mean Baseline and Vehicle Corrected Percentage Change in QTc (ΔΔ%) Response in the Anaesthetised Rabbit Following an Infusion of Verapamil at 0.1, 0.3 and 1 mg/kg.

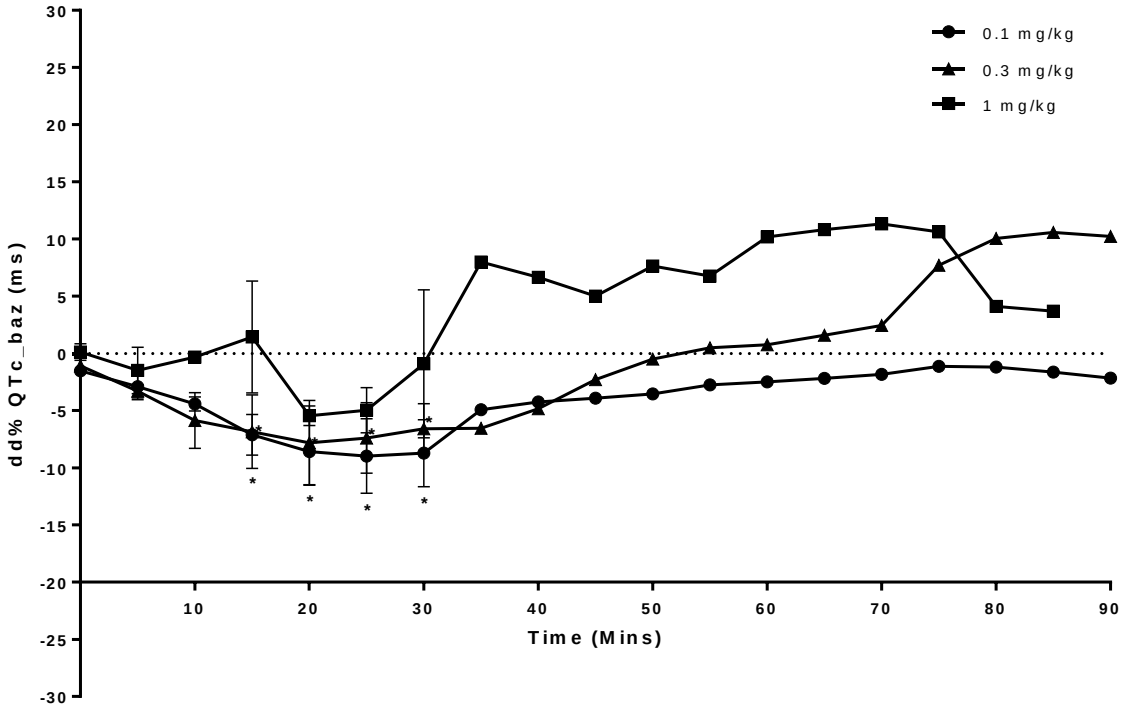

Figure 4.26: Graph of the mean and S.E.M. baseline and vehicle corrected change in QTc response (ΔΔ%) generated in the anaesthetised rabbit preparation following administration of sparfloxacin at 0.1 mg/kg (●) (n=2), 0.3 mg/kg (▲) (n=2) and 1 mg/kg (■) (n=2) where * denotes a statistical difference compared to vehicle control (*p*-value <0.05).

Figure 4.27 Verapamil Anaesthetised Rabbit: Representative Trace of the Change in ECG in the Anaesthetised Rabbit with Time and Dose Level

A: Verapamil vehicle

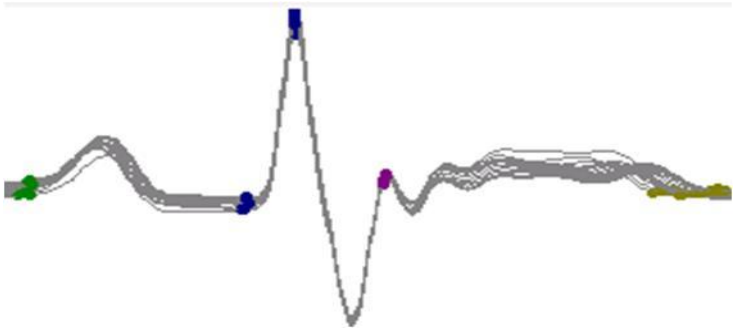

B: Verapamil 0.1 mg/kg

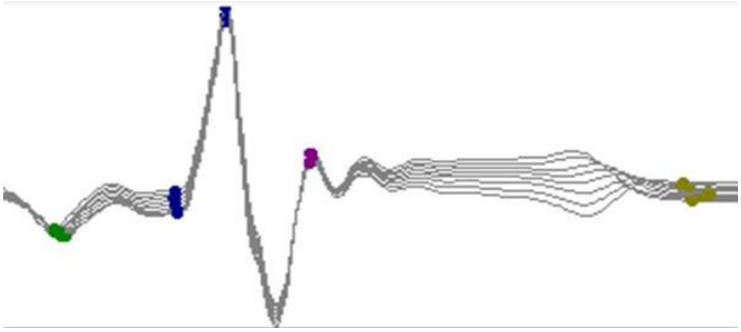

C: Verapamil 0.3 mg/kg

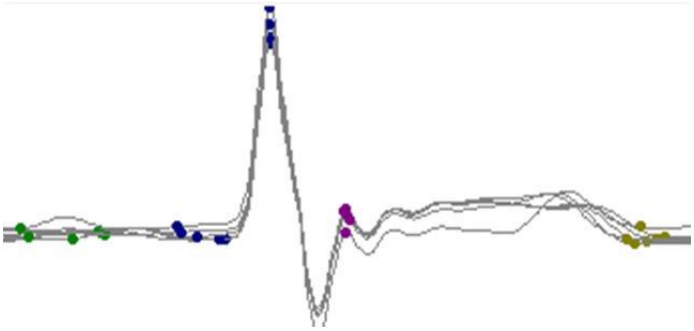

D: Verapamil 1 mg/kg

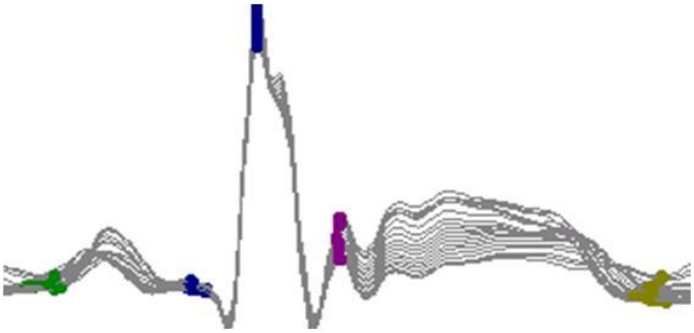

Figure 4.27: Representative overlay trace of the change in ECG waveform from each of the 5 minute time bins (n=18) generated in the anaesthetised rabbit model preparation over time under control baseline conditions with ECG waves marker points identified start of P wave (●), Q wave inflection point (●), R peak (●), S wave (●), T wave end (●).

4.10.9. Verapamil Summary Discussion

Following a single intravenous infusion of verapamil at 0.1, 0.3 and 1 mg/kg over 30 minutes, there was no significant QT prolongation (*p*-value <0.05). Mean maximum plasma concentrations observed were 91.9, 247, and 1330 ng/mL, and corresponding heart tissue concentrations 729, 1760 and 4260 ng equiv./mL, respectively. During the infusion an initial QTc decrease of -2.60 ±3.2 ms and -4.45 ±10.1 ms at 0.1 mg/kg and 0.3 mg/kg was observed, respectively, which increased to -0.71 ±2.06 ms and 3.27 ±6.93 ms by the end of infusion. At 1 mg/kg there was no initial decrease but a positive increase of up to 41.2 ms was observed. These changes were equivalent to mean ΔQTc% by -0.49 ±0.95%, 1.08 ±2.26% and 13.1% from the baseline QTc of 266 ±3.70 ms, but not statistically significant against vehicle.

It was observed that these varying changes in QT interval with increasing doses of verapamil were accompanied with decreases in heart rate and blood pressure (BP). It appears that post end of infusion of verapamil there was a trend for QT interval (including MBP and HR) to rebound in a positive manner and more so with dose, with the exception of BP at the top dose. At 1 mg/kg, one animal was terminated mid way through infusion and the other at 85 minutes due to respiratory failure as a result of low blood pressure.

The limited number of animals at each dose level, and with only one animal in each group compiling the 90 minute timecourse, makes interpretation of the data difficult with dose. Indeed there are a limited number of references in the literature that examine the effect of verapamil on QT in the rabbit, with the focus on verapamil haemodynamic perturbation, similar to that observed in this study.

Verapamil was selected as a negative control because it potently blocks I_{Kr} without an appreciable change in QT prolongation, as a result of its countering primary L-type calcium channel blocking characteristics (Redfern et al., 2003). This was a similar rationale adopted by Kijtawornrat et al., where verapamil was used as negative control in normal rabbits or in rabbits with failing hearts and prevented TdP (Kijtawornrat et al., 2006a). Here the author investigated verapamil at 0.25, 0.50, and 1.0 mg/kg (control group *n*= 6, myocardial failure group *n*= 4) in anaesthetised rabbits as part of an escalating infusion over 10 minutes with 20 minutes intervals. This observation that verapamil prevented TdP by shortening of endocardial monophasic action potential duration and reduced left ventricular transmural repolarization in the rabbit has been demonstrated clinically (Jackman et al., 1990; Milberg et al., 2005). Kijtawornrat et al. showed that verapamil continued to decrease QTc interval from

baseline after dosing to approximately 30 ms at 0.25 and 0.5 mg/kg and 45 ms at 1 mg/kg. This observation is comparable in part to the lower dose observed in this present study, and may differ as a result of the short 10 minute infusion and 20 minute recovery compared to 30 minute infusion and 60 minute recovery. In another study using failing rabbit hearts, Kijtawornrat et al. co-administered verapamil at 0.3 mg/kg as part of a pre-treatment intravenous regimen along with other test articles to determine the effect on dofetilide. Pre-treatment information showed that after a 10 minute infusion resulted in a small reduction in QTc and a significant drop in mean arterial blood pressure (Kijtawornrat et al., 2010).

In an anaesthetised model being used to test the anti-arrhythmic versus pro-arrhythmic profile of BRL-32872, a novel agent with combined potassium and calcium channel blocking activity, verapamil was examined alone and in combination with E-4031 (the class Ill anti-arrhythmic agent), in rabbits pre-treated with methoxamine. Verapamil alone (20 µg/kg/min, n = 7) caused only minor effects on the ECG variables and heart rate, but reduced the mean arterial pressure (11 ± 5% vs. pre-drug after 60 minute infusion, 1.2 mg/kg total). Verapamil alone did not induce any episodes of arrhythmia. However, verapamil reduced the incidence of TdP by E-4031, thus providing the necessary evidence that calcium channel blockade can reduce the pro-arrhythmic potential of a compound with class III anti-arrhythmic action (Bril et al., 1996). In the same investigation by Bril et al., using a dog myocardial infarction model, authors showed that verapamil (0.03, 0.1 , 0.3 mg/kg) reduced heart rate, mean arterial pressure and, to a lesser extent (+)dP/dtmax. No change in QTc interval and ventricular effective refractory periods was observed, but increased PR interval was seen. Similarly, verapamil was utilised as a negative control in the QT PRODACT assessment in the dog (Toyoshima et al., 2005).

In contrast, a review of the sensitised rabbit model discusses attempts undertaken in conscious rabbits to prevent the class III-induced pro-arrhythmia by pre-treating with drugs such as metoprolol, verapamil and diazepam. Such interventions were not successful and the only effective drug was prazosin, an antihypertensive agent that potently blocks α_1-adrenoceptors (Carlsson, 2008).

Table 4.29 Comparison of Pharmacokinetic parameters across species following Intravenous administration of Verapamil

	Vd_{ss} (L/kg)	CL_p (mL/min/kg)	Half-life (hr)
Rat	2.99 - 4.17	40 - 52.7 (51-68%)	1.5 – 2.2
Dog	5.8 – 13.2	25.8 – 106 (50 – 100%+)	2.5
Human	4.4 – 5.8	12.5 (69%)	2.7 – 4.8
Rabbit	8.1 - 9.7; 14.5 - 16.8	90, 130 – 146 (100%+)	0.9 - 1.65
Present study	0.63 – 1.59	13.4 – 28.8	0.52 - 0.75

Combined table of parameters obtained from literature sources
Liver blood flow (LBF, ml/min/kg) for each species rat (78), dog (56), minipig (28), monkey (44), human (18), rabbit (70) Davies and Morris, 1993

a. Kataoka 2016 (rat)
b. Todd & Abernethy 1987 (rat)
c. Bai 1993 (dog)
d. Chelly 1986 (dog)
e. Giacomini 1985; Mori 2001 (rabbit)
f. Hamann 1984 (human)

Following intravenous infusion of 0.1, 0.3 and 1 mg/kg over 30 minutes in the anaesthetised rabbit, parameters obtained for volume of distribution (0.63 – 1.59 L/kg), total clearance (13.4 – 28.8 mL/min/kg) and half-life (0.52 – 0.75 hour) were lower than published pharmacokinetic parameters in the rabbit (Table 4.29).

From reported literature in the rabbit, the volume of distribution and clearance is greater, 8.1 to 16.8 L/kg and 90 to 146 ml/min/kg, respectively (Giacomini et al., 1985; Mori et al., 2001). Giacomini et al. studied the PK and PD of verapamil enantiomers (d- and dl-) in conscious rabbits following a single intravenous dose of 0.8 mg/kg infused over 20 minutes. A bi-exponential decline in plasma concentration-time profile was observed similar to this study with no differences in PK properties of either enantiomers. There was a degree of inter-animal variability in the Giacomini et al publication with comparable parameters Vd_{ss} (1.49 – 2,48) and half-life (0.2 – 0.75 hour) from some animals (Giacomini et al., 1985).

A number of authors report the influence of general anaesthesia on verapamil in the rabbit and dog. The effect of anaesthetics, thiopental (10 mg/kg), ketamine (4 mg/kg) or propofol (10 mg/kg) on the verapamil (0.2 mg/kg) pharmacokinetic parameters was studied in rabbits. It was established that during thiopental or ketamine anaesthesia the concentrations of verapamil may be higher than therapeutic concentrations. An increase in systemic exposure (area under drug concentration-time curve, AUC) and the decrease of volume of distribution

of verapamil during thiopental or propofol anesthesia were noted (Orszulak-Michalak, 1996; Orszulak-Michalak et al., 2002). A similar observation was also made in the dog following isoflurane anaesthesia, with increased plasma concentrations after a single verapamil dose occurring due to decreased inter-compartmental clearance, and to a lesser extent increased initial volume of distribution and decreased apparent volume of distribution compared to conscious animals (Chelly et al., 1986). A difference in the pharmacokinetics and tissue distribution of verapamil has been studied between the non-pregnant and pregnant rabbits following verapamil intravenous bolus/infusion administration (Solans et al., 2000). The author describes that volume was significantly higher in the pregnant rabbit, whilst half-life was significantly lower in the non-pregnant rabbit. However, AUC and CL showed no significant differences between the pregnant and non-pregnant rabbit. When tissue concentrations were examined, high concentrations of verapamil were found both in the pregnant and non-pregnant rabbit. Furthermore, verapamil concentrations in the uterus, heart, spleen and kidney were significantly higher in the non-pregnant than in the pregnant rabbit, such that in the heart the tissue-to-blood ratio for non-pregnant, pregnant and foetus was 20-, 9-, and 7-fold, respectively. This finding is near to the observed tissue to plasma ratio of 7-8-fold following 0.1 and 0.3 mg/kg.

Verapamil is metabolised rapidly via CYP 3A4 to its primary N-demethylated metabolite, norverapamil, which retains some calcium channel activity approximately 20-fold less potent. It has been indicated that propofol potentially inhibits 3A4 activity in human hepatocytes (Yang et al., 2003). Verapamil itself is also a potent inhibitor of 3A4 (IC_{50} ~5µM (equivalent to ~2300 ng/mL)) and preventing its own metabolism, as well as a substrate and inhibitor of the efflux transporter P-gp (Pauli-Magnus et al., 2000; Zhou et al., 2007). However if metabolism or efflux was inhibited by the anaesthetic or verapamil then the resultant clearance would reduce, with increased plasma concentrations, as shown by studies in the rat (Kataoka et al., 2016). Limited data does not indicate any drug-drug interactions but the increased clearance in this study may be the result of propofol on hepatic blood flow in rabbits as it has been observed to increase hepatic flow rates (Zhu et al., 2008). Verapamil is subject to high first pass metabolism following oral administration, and therefore with an increased liver blood flow may increase the clearance and result in the reduced half-life observed.

It is conceivable then that the observed pharmacokinetics of verapamil in this study may have been influenced by the anaesthetic combination employed and reflects the early distributional phase and elimination half-life due to the short experimental period. The clearance is comparable to human and not too dissimilar to dog or rat, yet the volume of distribution is greatly reduced to near equivalent to the central compartment, which belies the higher heart tissue concentrations which infer greater tissue distribution. This is supported by an observation in dogs that the distribution equilibrium between myocardium and plasma was achieved rapidly following an intravenous dose of 0.5 mg/kg. The partition coefficient which describes the time averaged myocardial/plasma concentration ratio was 6.21 +/- 2.38 with a linear relationship between each other and also indicates the concentrations are in equilibrium with the hemodynamic effect (Keefe and Kates, 1982). Likewise in rats, mean arterial pressure (MAP) against verapamil concentration in plasma and cardiac muscle have been shown to be inversely correlated (Todd and Abernethy, 1987).

4.11. Anaesthetised Rabbit Model Summary Conclusion

The objectives of this study were to set-up and validate an anaesthetised rabbit model to enable analysis of QT prolongation, as the primary pharmacological endpoint and determine the PK/PD relationship through measurement of drug concentration in the plasma and heart. Further to this study it was proposed to utilise the developed model to provide a possible link to the ex vivo rabbit ventricular wedge used by Safety Pharmacology in the QT screening cascade.

4.11.1. Anaesthetised Rabbit Model

The aim of setting up the anaesthetised rabbit model in this investigation was to utilise the measurement of QT prolongation which can be stimulated by drugs under anaesthesia without incurring the detrimental effects of torsadogenicity (White *et al.*, 1999; Jacobson *et al.*, 2011). The objective was to investigate the PKPD relationship and associated distribution of drug into the cardiac tissue to relate the resulting QT effect, which was subject to a number of assumptions and/or limitations previously described (Section 4.3).

Overall use of anaesthetised preparations is generally limited in number as many anaesthetics can affect the normal function of the cardiovascular system or produce drug interactions (Mitchell et al., 2010), and the study duration is restricted. However this requires the drug of interest to be amenable to intravenous administration and have high aqueous solubility. There are accepted caveats associated with the anaesthetised model but consistency and reproducibility has been demonstrated and maintained in the control baseline group comparison, so results or changes can be measured and interpreted accordingly. Anaesthetised preparations are considered an acceptable adjunct to conscious studies, though the choice of anaesthetic is important (Hammond *et al.* 2001). There are benefits in that higher dose levels via the intravenous route can be administered in a controlled manner in an early discovery environment where drug availability may be limited.

4.11.1.1. Premedication

Many surgical models use optional premedication for sedation and analgesia which is provided by opioids (eg. oxymorphone, butorphanol) or alpha-2 agonist (e.g xylazine or medetomidine). These agents themselves may affect respiratory and cardiovascular function and need to be selected based on species and combination. Typical side effects on the

cardiovascular system of alpha-2 agonists are bradycardia, reduced cardiac output and hypertension likely due to a reflex increase in blood pressure effect on peripheral α-2 adrenoreceptors at sedative doses. However respiratory depression becomes more significant when used in combination with other sedatives, anaesthetic or injectable agents (Sinclair, 2003). Medetomidine has been shown to provide more favourable analgesia/anaesthesia and acceptable cardiovascular parameters in comparison to xylazine (Difilippo *et al.*, 2004). These cardiovascular effects counter-act those of propofol anaesthesia and as recommended a dose adjustment is required if in combination with a sedative/analgesic (Short and Bufalari 1999).

4.11.1.2. Anaesthesia Selection

The anaesthetic regimen adopted in this study; medetomidine analgesia with propofol induction and isoflurane maintenance has been reported as a successful methodology in dogs (Kuusela *et al.*, 2001) and a recommended practice in rabbits (Bourne, Twycross Zoo, 2012; Martin and Kirspipuu, IACUC, 2011).

Most anaesthetic agents in common use have inherent cardiovascular effects such as direct effects on QT, electrophysiological properties, or cardiovascular system, including autonomic tone and cardiac ion channel properties. For the anaesthesia regimen employed in this study;

- Propofol has the advantage of rapid induction and recovery, whilst a slight decrease in initial blood pressure may be observed without a compensatory increase in HR. If administered too rapidly then significant depression of respiratory function may be observed in rabbits (Short and Bufalari 1999).
- Isoflurane alone via snout/face masking is not a recommended method of induction in rabbits due to the slowness of induction and distress caused during the restraint, resulting in subsequent prolonged apnoea commonly observed (Flecknell *et al.*, 1999). A small degree of tachycardia is observed in rabbits and is similar to effects seen in man (Marano *et al.*, 1996). It is considered a suitable maintenance method with the use of suitable premedication and intubation to aid direct delivery.

The anaesthetic regimen utilised was based on the requirement of the model and the animal welfare. These considerations were made over the choice of anaesthetic used within this study and were discussed in an international survey of preclinical cardiovascular screening models (Hammond *et al.*, 2001). The method of premedication followed by anaesthesia

induction and maintenance with propofol and isoflurane was similar to more recent previous reported publications (Vincze et al., 2008; Nalos et al., 2012). In comparison other commonly used anaesthetic agents discussed that have been used in rabbit models are outlined below;

- Halothane reduces the repolarisation reserves inhibiting both I_{Ks} and I_{Kr} and attenuates the autonomic tone as has been observed in the anaesthetised dog (Takahara *et al.,* 2005). In the rabbit it has also been observed to cause a significant drop in blood pressure (Peeters *et al.*, 1988).
- Pentobarbital may reduce the AP conduction across the ventricle wall in the epicardial, endocardial and midmyocardial layers by differential prolongation of the cell repolarisation (transmural repolarisation dispersion) (Shimzu *et al.,* 1999). Many of the investigators use barbiturates as the anaesthetic agent of choice which may account for the necessity for artificial ventilation due to the extent of respiratory depression. This is not recommended as a viable method according to the International Veterinary Information Service (IVIS; Harcourt-Brown, 2005, Scivac 50th International Congress). However artificial ventilation does provide constant control over the respiratory rate, yet removes one observational parameter to assess the animal's viability.
- Ketamine/xylazine significantly displaces the relationship between QT and RR intervals. The mixture has prolonged systemic exposure and the effects are generally long-lived, so careful single dose administration is required (Hamlin *et al.*, 2003). As well as causing respiratory depression (drop in arterial BP and paO_2) the combination can produce unpredictable levels of anaesthesia (Peeters *et al.,* 1988; Wyatt *et al.,* 1989). This is in contradiction to other reports of stable anaesthesia and minimal cardiovascular effects (Difilippo *et al.,* 2004).

Many investigators describe induction with barbiturates such as methohexital or pentobarbital, whilst others have utilised ketamine/xylazine or propofol. Maintenance anaesthesia, if required, was often achieved with α-chloralose, barbiturate top ups or continuous propofol infusion, with rabbits artificially ventilated. Given the observed higher clearance in the rabbit under anaesthesia in this study it needs to be determined whether this is an effect of propofol on liver blood flow or due to the short experimental time course with plasma concentrations. Previous safety pharmacology screening studies, whether anaesthetised or not, generally relate effects to dose which limits interpretation of PK/PD.

4.11.1.3. Control Cardiovascular Endpoints in the Rabbit Model

A review of published anaesthetised rabbit model preparations demonstrates that the model developed in this study, comparing baseline assessment and pre-dose equilibrium data, is comparable regardless of the anaesthetic regimen (Table 4.30).

During initial experimental set up, heart rates and electro-cardiograms measured the normal heart rate in the anaesthetised rabbit at ~250 bpm before refinement. The heart rate in the conscious state can be highly variable (220-300+ bpm) and dependent on the animal's state of anxiety. In a stable anaesthetised state, this HR is lower (<200 bpm) if in a supine position with a higher rate (>200 bpm) indicating incomplete anaesthesia or poor venous return if the rabbit is fat or in a dorsal recumbent position (Vetronic Service Ltd). In this study, optimised limb lead placement and the adopted induction protocol described (Section 4.2), resulted in heart rates and QT intervals comparable to previously published data (Farkas et al., 2004) and presented in Table 4.30. Graphical representation of QT interval during experimental baseline and vehicle control experiments demonstrate stabile readings across the experimental period (Section 4.10.1 Figure 4.6). Other cardiovascular parameters such as heart rate, blood pressure (systolic and diastolic) and ECG intervals (data not shown) also provide additional evidence of consistent preparations.

Table 4.30 Comparison of different literature anaesthetised rabbit model preparations and summarised selective cardiovascular parameters; heart rate and QT interval.

Reference	Anaesthetic	*n*	Heart Rate (1/min)	SEM	QT interval (ms) Extrapolation method used?			
					Yes	SEM	No	SEM
Batey & Coker (2002)	Pentobarbitone	26	268	±11	161	±8	-	
Farkas & Coker (2002)	Pentobarbitone	36	265	±8	182	±8	150	±7
Farkas & Coker (2003)	Pentobarbitone	40	259	±8	184	±6	-	
Carlsson *et al.* (1997)	α-Chloralose	18	214*	±10	122	±5	-	
Farkas *et al.* (2002)	α-Chloralose	45	290	±11	157	±5	-	
Lu *et al.* (2000)	α-Chloralose	34	231	±11	-		169	±8
Lu *et al.* (2001)	α-Chloralose	34	231	±11	-		163	±7
Vincze *et al.* (2008)	α-Chloralose	10	279	±13	-		151	±4
	Propofol	10	258	±11	-		157	±5
	Pentobarbitone	30	283	±9	-		152	±4
Wang *et al.* (2008)	Ketamine/Xylazine	73	183	±11	-		156	±5
Nalos *et al.* (2012)	Ketamine/Xylazine /Isoflurane	16	188	±17	-		170	±12
Current study	**Propofol/ Isoflurane**	**77**	**197**	**±8**	**-**		**168**	**±9**

* Heart rate values obtained from Carlsson et al. (1997) were derived from estimated RR interval

In comparison to this study, the conscious state represents the normal ideal scenario, yet reported studies in conscious telemetered guinea-pigs or rabbits for screening of atrial BP, heart rate and QT interval are relatively few in number. This in part is likely due to the difficulties with anaesthesia/surgery and appropriate placement of catheters compared to other species (Shiotani et al., 2005; Hess et al., 2007). These studies in themselves possess difficulties with respect to the QT interval and correction due to elevated or variable HR rates reported (170 – 300 bpm) that can result from the stress of handling, sling restraint and dosing. The use of sling trained conscious rabbits to assess the effects of a number of drugs (cisapride, dofetilide and haloperidol) on RR and QT interval and allow repeat animal analysis has been published (Kijtawornrat et al., 2006). However, there are often ethical considerations/implications when testing drugs with potential serious cardiovascular liabilities in a conscious state in vivo model.

4.11.1.4. Clinical Chemistry

Blood clinical chemistry electrolyte values obtained from arterial samples during the control rabbit model assessment for K^+, Cl^-, Ca^{2+} before the start of surgical preparation decreased (*p*-value <0.05) by the start of equilibration and then were maintained through the proposed drug analysis period. Sodium blood levels were shown to be unaffected throughout. Physiological levels of K^+ are between 3-5 mmol/L, and the observed in this study reduced from 4.2 to 3.2 mmol/L, which indicate that the propofol induced – isoflurane/O_2 anaesthetised rabbit model is within acceptable physiological conditions (Gil et al., 2010). The reduction in blood electrolyte levels may be a result of the anaesthesia and response to surgical intervention. These blood electrolyte data are comparable to published data in the normal and anaesthetised rabbit model (Hewitt 1989; Farkas and Coker, 2002) (Table 4.2).

As a comparison to the conscious rabbit blood electrolyte levels, it is reported that methohexital/α-chloralose anaesthesia rendered the rabbits hypokalaemic (reduced K^+ blood levels), an effect also seen in pentobarbitone-anaesthetised rabbits (Carlsson et al., 1990; Farkas & Coker 2002). Carlsson suggests that normalising K^+ levels by intravenous infusion prior to administration of clofilium significantly reduces the TdP susceptibility compared to hypokalaemic rabbits. Other investigators have modified anaesthetics, ventilation, and oxygenation to correct (Farkas et al., 2004; Vincze et al., 2008). In the heart, hypokalaemia causes hyperpolarization in the myocytes' resting membrane potential. The more negative membrane potentials in the atrium (from -90mV to -110mV) may cause arrhythmias because of more complete recovery from sodium-channel inactivation, making the triggering of an action potential more likely. In addition, the reduced extracellular potassium inhibits the activity of the I_{Kr} potassium current and delays ventricular repolarisation (Sanguinetti and Jurkiewicz 1992). Data reported in this investigation from the anaesthetic regimen utilised did not adversely alter the blood potassium levels to hypokalaemic levels (Table 4.2).

Blood oxygen/carbon dioxide saturation and pH did alter between pre-anaesthetic treatment compared to equilibrium blood sampled post surgery. The paCO2 decreased and paO2 increased (both not significant *p*-value >0.05), showing higher oxygenation content, which can be a result of direct gaseous delivery of isoflurane in O_2 via the endotracheal intubation. This is linked to the observed pH, that was considered to have increased significantly (*p*-value <0.05) but not the haematocrit from pre-anaesthetic treatment compared to equilibrium blood sampled post surgery. pH will respond more rapidly to more subtle changes in biochemical alterations than the haematocrit. This has been reported as an observable change

such that a 1 mmHg change in $paCO_2$ above or below 40 mmHg results in 0.008 unit change in pH in the opposite direction in humans (Stoelting and Miller, 2007) (Table 4.2).

Through surgical model refinement, parameters from clinical chemistry (blood gases and pH, Hct), cardiovascular and haemodynamic parameters (e.g. HR, BP, QT) demonstrated the model baseline stability over the course of the experimental period under control conditions. Control baseline experiments were analysed (Section 4.10.1, Table 4.2) and shown to be within normal physiological ranges with limited deviation of any of the physiological or cardiovascular parameters recorded in accordance with previously reported studies (Hammond et al., 2001; Farkas et al., 2004; Carlsson, 2008).

A successful anaesthetised rabbit model was developed from the results obtained during the baseline control experiments to enable further evaluation of known QT prolonging drugs in the anaesthetised rabbit model, to provide a translational link to the ex vivo rabbit ventricular wedge and in vivo pharmacokinetic studies by obtaining PK/PD information in the rabbit.

Strathclyde Institute of Pharmacy and Biomedical Sciences
GlaxoSmithKline

CHAPTER 5

In Vivo PBPK/PD Modelling

5. IN VIVO MODELLING

The overall aim of this investigation was to generate a simulated pharmacokinetic-pharmacodynamic (PKPD) response profile of the changes in QT-prolongation resulting from test compounds cisapride, moxifloxacin, sparfloxacin and verapamil, known for their potential to prolong QT interval (except verapamil) in the female rabbit.

Intravenous concentration-time profiles and basic pharmacokinetic data for each compound were generated in the female rat, data which is typically available in early discovery, were then used in physiologically-based pharmacokinetic modelling (PBPK) and empirical allometric scaling from rat to rabbit, for simulation of the observed pharmacokinetic profile in the anaesthetised rabbit preparation previously described.

Simulated plasma and heart tissue concentrations from the PBPK model were combined with the concentration-response sigmoidal E_{max} model from the ex vivo rabbit ventricular wedge (RVW) preparation and the fraction unbound determined from the protein binding to predict the extent of the change in QT-interval in the anaesthetised rabbit.

5.1. Background

Basic goals of non-clinical studies in drug development are to identify a drug's pharmacological properties through mode of action (pharmacology PD), its pharmacokinetic (PK) and metabolic profile in the context of comparative physiology, in conjunction with understanding the toxicological profile to establish a safe initial dose level for the first human exposure, and subsequent safety margins (preclinical to clinical). Additionally there is the requirement to identify parameters for clinical monitoring of potential adverse effects and any special toxicity (e.g. cardiovascular, genotoxicity, carcinogenicity, reproduction toxicity) liabilities (S7A, 2000; S7B, 2005). Therefore, current drug development strategies employ approaches to predict human pharmacokinetics and estimated human starting doses using empirical allometric scaling methods and physiologically-based pharmacokinetic (PBPK) modelling of preclinical species to achieve this (Jones et al., 2013).

In terms of PK models there is a clear hierarchy of models (Aarons, 2005). The simplest empirical models are the sum of exponentials, which are purely a description of the concentration-time profile, with parameters describing the concentration coefficients and rate

constants. These models are adequate to describe data and derive primary PK parameters such as clearance (CL) and volume (V) but less so for species scaling prediction purposes.

The prediction of PK parameters, particularly clearance is central to the selection of a dose for first time in human (FTiH) studies. There are a number of techniques that can be used but the two main approaches utilising animal data are allometric scaling and the use of physiological-based PK models (PBPK) which is supported by in vitro-in vivo extrapolation (IVIVE). Allometric scaling is an empirical approach, examining the relationships between PK parameters and primarily body weight, but other empirical correction factors can be used to relate the parameters, for example mean life-span potential (MLP) and brain weight, without necessarily understanding the underlying mechanisms (Lin, 1995). In contrast, PBPK is a mechanistic approach founded on set species-specific biological and physical constraints.

Compartmental models are the most commonly used models for PK data analysis (Balant and Gex-Fabry, 2000; Rescigno, 2010). Compartmental models describe the body as a series of theoretical compartments. Although the compartments generally do not represent real spaces within the body, when a physiological parameterisation is used in a semi-physiological compartmental model, the data can be defined in terms of volumes and clearances e.g. brain volume, uptake or metabolism. These terms can be more easily related to physiological processes that affect the variability in PK and hence used for prediction of other scenarios.

Physiologically-based pharmacokinetic (PBPK) models are mechanistic and are formed by a series of compartments representative of actual tissues and organs in the body. These compartments are arranged anatomically and linked via the vascular system. The parameters that are incorporated into the model are of two types; physiological (e.g. blood flows, tissue volumes etc) and drug-specific (e.g. tissue/blood partition coefficients, intrinsic clearance, protein binding etc). A series of mass balance differential equations utilise these parameters and describe the drug concentration-time profile in blood or plasma and each tissue.

Modelling of PD data usually occurs in conjunction with PK data via an integrated PKPD model. This approach dispels the need for simultaneous concentration and effect measurements as the PK part of the model provides a continuous concentration-time profile (Holford and Sheiner, 1982). A step-wise approach to modelling PK data first (as opposed to simultaneously with PD) is most often undertaken since the PK model is often better understood and more reliable estimates of parameters can be obtained (Holford and Sheiner,

1982; Derendorf and Meibohm, 1999). The concentrations provided by the PK model then act as input to drive the PD model and describe the observed pharmacological effect. The effect can be a direct response due to drug binding at a target site such as an organ, enzyme or receptor resulting in changes in biochemical products, pathway signalling, cellular transcription levels, or physical alteration.

The concentration used in the PD models should in theory be the concentration at the effect site, however, in practice the concentration measured in blood or plasma is typically used as a surrogate due to its accessibility. Under steady-state conditions the free concentration between the blood/plasma and site of effect will be in equilibrium. In contrast under non-steady-state conditions distribution to the site of action and subsequent drug-binding to target may represent a rate-limiting step for producing the known or expected PD effect. This is typically reflected in a delay in the time-course of PD effect relative to the blood/plasma concentration and when drug-concentration is plotted against the PD effect an anti-clockwise hysteresis loop can be observed (Louizos et al., 2014). This has been described through linked effect compartment models, where a surrogate biophase 'effect' compartment represents the site of action. The concentration at the drug-binding effect site is related to the elimination rate constant, ke_0 (Danhof et al., 2007; van der Graaf and Benson, 2011). Models representing the concentration effect at the heart have been discussed (Minematsu et al., 2001; Weiss, 2011). Therefore in this investigation the observed QT prolongation effect should be directly related to heart tissue concentrations which can be derived from whole-body PBPK or semi-PBPK analysis which links the pharmacokinetics to the site of action.

5.1.1. Assumptions and Limitations of the In Vivo Modelling

The aim was to utilise simple pharmacokinetic data from the rat along with in vitro data (b:p fu_p and fu_t) in a physiologically-based model to enable translation to the rabbit and link with a pharmacodynamic concentration-effect model from the ex vivo rabbit wedge (RVW) to simulate the in vivo concentration-dQTc effect in the anaesthetised rabbit, for which there are a number of assumptions and/or limitations;

1) The single intravenous bolus dose administered to the female rat adequately describes the distribution and elimination characteristics of the test compound and only using intravenous data, many issues around absorption, solubility, permeability associated with the oral delivery remain unknown.

2) Clearance rate/routes similar between rat and rabbit and predominantly cleared by hepatic and renal processes and the test compound PK parameters can be scaled according to the single species allometric approaches in the absence of data from multiple species required for conventional allometric approaches.

3) In the rabbit, a 30 minute infusion is sufficient for tissue equilibration and elicits the pharmacological response eg. QT-prolongation equivalent to that observed in the RVW, with a limited data set of heart tissue concentration information.

4) The E_{max} model characterised from the RVW adequately describes the in vivo rabbit heart concentration-effect response under anaesthetised conditions and assumes that receptor binding is rapid and reversible.

5) A drawback of PBPK models is that they may be complex with the requirement of many species specific parameters. Potential lack of fully defined rabbit physiological components, such as tissue composition of neutral and phospholipids to adequately describe the tissue Kp and tissue distribution.

5.2. In Vivo Rat PK Study Method

An in vivo study was conducted to determine the plasma-concentration time profile and pharmacokinetics of cisapride, moxifloxacin sparfloxacin and verapamil in the female rat (n=3) following a single intravenous bolus administration at target dose levels of 1 or 10 mg/kg, as appropriate. This small in vivo study would be approximately similar to an early stage discovery study in lead optimisation to obtain basic PK information (Appendix 5).

All in vivo experiments were ethically reviewed and carried out in accordance with Animal (Scientific Procedure) Act 1986 and the GlaxoSmithKline (GSK) policy on the Care, Welfare and Treatment of laboratory animals and under the authority of Project Licence No PPL 80/2588 19b PR01 (terminally anaesthetised models). All personnel involved in the conduct of scientific procedures on animals did so under the authority of a Home Office Personal Licence issued under the Act.

5.3. Pharmacokinetic Analysis Methods

Phamacokinetic profiles of cisapride, moxifloxacin sparfloxacin and verapamil in the female rat following intravenous administration at target dose levels of 1 or 10 mg/kg, as appropriate, were determined using both compartmental and physiological modelling.

5.3.1. Non-Compartmental Analysis

Pharmacokinetic analysis of the rat data was performed using non-compartmental analysis (NCA) methods using two commercially available software packages WinNonlin™, Phoenix Version v.6.3 (Pharsight, Certara, Princeton, NJ) , and GastroPlus™, PKplus™ module, v.9 (Simulations Plus Inc, Lancaster, California). All computations utilised the actual sampling times recorded during the study. No statistical analysis of the data was carried out due to the limited number of animals (n=3) per compound.

The female rat plasma pharmacokinetics of cisapride, moxifloxacin, sparfloxacin and verapamil following intravenous bolus were determined. Parameters calculated included: C_0, C_{max}, T_{max}, $AUC_{(0-t)}$, $AUC_{(Inf)}$, CL_p, V_{dss}, $t_{1/2}$. The rat clearance (CL_p) parameter calculated was then used in the allometric scaling. Similarly, NCA of the rabbit plasma concentration-time profile from the previously described anaesthetised rabbit preparation was determined for each compound. The identified clearance parameter was used in the PBPK model as the 'observed' clearance to determine the actual simulation fit of the experimental data.

5.4. Methods for Scaling Rabbit Clearance Parameters

5.4.1. Scaling of Clearance (CL)

In the absence of any other pharmacokinetic information from other species in this study, total body clearance determined from the female rat was allometrically scaled to the rabbit. Two methods were selected to give a range of scaled clearance values from NCA analysis. Each of the derived scaled clearance values were used in the physiological-based model.

i. Single-species scaling (SS): using a method described correcting for fraction unbound in each species (Hosea et al., 2009).

$$CL_{rabbit} = CL_{rat} \times \left(\frac{WT_{rabbit}}{WT_{rat}}\right)^{0.75} \quad \text{Equation 11}$$

Where clearance (*CL*) is the pharmacokinetic parameter of interest for each species, *WT* is body weight and the physiologically relevant exponent, typically assumed to be 0.75 for clearance.

And,

ii. Using Liver Blood Flow (LBF):

An alternative is to scale based on liver blood flow (LBF or Q_H) under the assumption that the hepatic extraction (E_H) of the compound of interest is equivalent in both species. Where, *LBF* in the rat is 78 ml/min/kg and *LBF* in the rabbit is 70 ml/min/kg (Davies and Morris, 1993).

$$E_{H,rabbit} = E_{H\,rat} \quad \text{Equation 12}$$

$$CL_{rabbit} = \left(\frac{CL_{rat}}{LBF_{rat}}\right) \times LBF_{rabbit} \quad \text{Equation 13}$$

In the assessment of the clearance parameter an arbitrary classification grouping has been assigned based on approximate thirds of LBF with the low (<30%), moderate (30-70%) and high (>70%) (Pang and Rowland, 1977).

5.5. Physiological Modelling Method

A representative physiologically-based pharmacokinetic (PBPK) model is shown in Figure 5.1, formed by a series of 14 compartments representative of actual tissues and organs in the body, namely lungs, adipose tissue, muscle, liver, spleen, heart, brain, kidney, skin, reproductive organ, red marrow, yellow marrow and rest of body, arranged anatomically and linked via the vascular system (arterial and venous). In this present study GastroPlus™ v9 software was used as a commercially available platform to integrate the physico-chemical properties, species specific physiology and pharmacokinetics across tissues to simulate the whole-body drug disposition profiles for each compound. Perfusion rate-limited kinetics was assumed; each tissue was represented by a single well-stirred compartment, limited by blood flow. This assumes that the drug distributes instantaneously into the whole tissue from the incoming blood flow and that there are no concentration gradients within the tissue. The liver and kidney were considered the only sites of elimination.

Figure 5.1 General Schematic Diagram of the Whole-Body PBPK Model

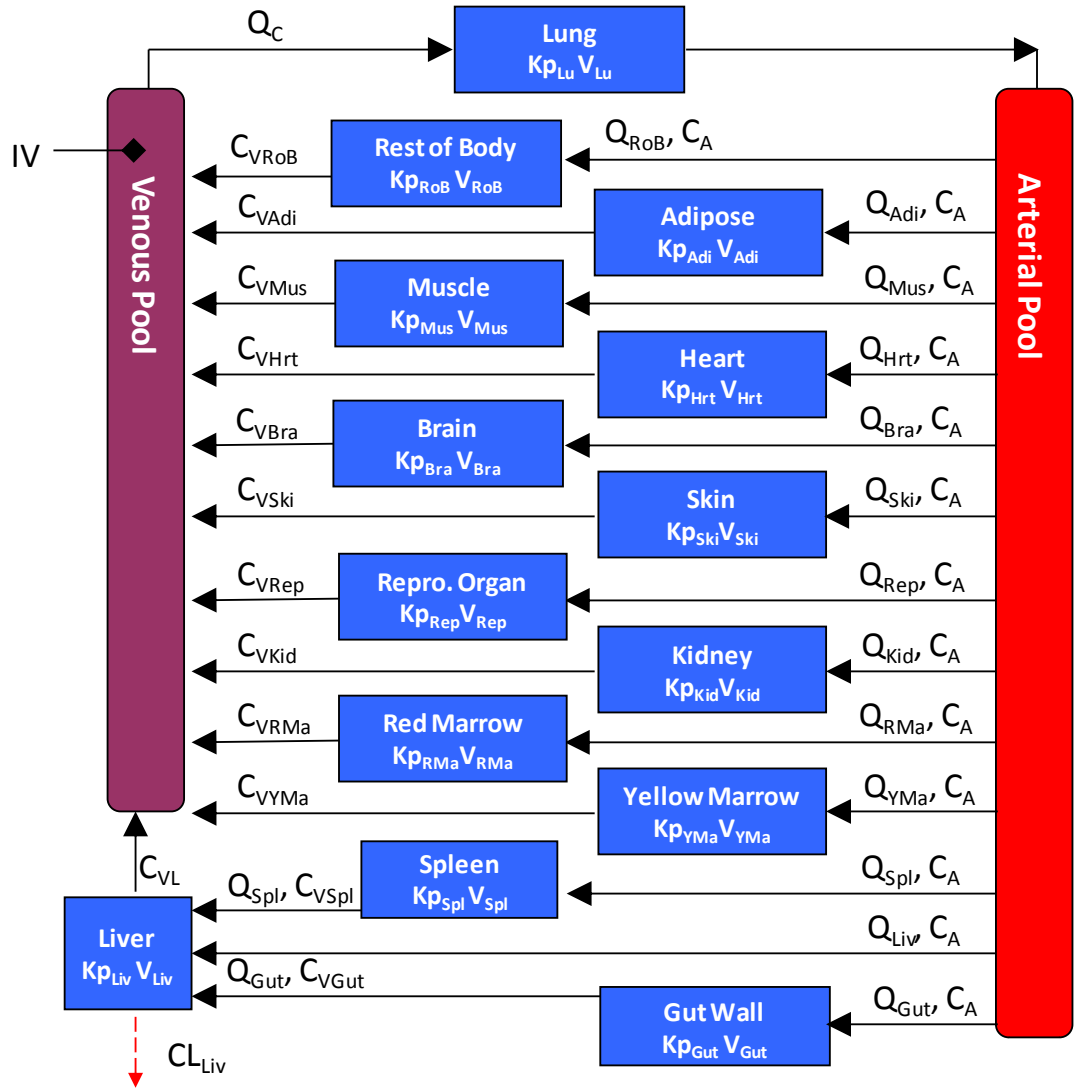

Figure 5.1: Schematic diagram of the whole body physiologically-based system anatomically arranged and described through the amount of drug in arterial (C_A) and venous (C_V) blood and organ specific blood flow (Q) and which may distribute within any given tissue according to volume (V) of that tissue and tissue partition coefficient (Kp).

A series of mass balance differential equations utilise physiological and physico-chemical parameters and describe the drug concentration-time profile in each blood/plasma/tissue compartment

Non-eliminating tissues:

$$\frac{dCt}{dt} = \left(\frac{Q_T}{V_T}\right) \times \left(C_A - \frac{C_T}{Kp_T}\right) \quad \text{Equation 14}$$

Where *dCt/dt* is the rate of change in concentration within a given tissue (*T*), Q_T and V_T are the given physiological blood flow and volume for that tissue, respectively. C_A is the amount of drug within the arterial compartment, and C_T is the amount of the drug available to leave the tissue following distribution based on the Kp_T tissue to plasma partition coefficient for the given tissue.

Eliminating tissues:

$$\frac{dCt}{dt} = \left(\frac{Q_T}{V_T}\right) \times \left(C_A - \frac{C_T}{Kp_T}\right) - \frac{fu_B \times CL_{int}}{V_T} \times \left(\frac{C_T}{Kp_T}\right) \quad \text{Equation 15}$$

Where additional terms fu_B is the fraction unbound in blood, CL_{int} is the intrinsic clearance from the tissue.

5.5.1. Physiological Properties

Physiological properties such as organ weights and blood flows within each tissue in GastroPlus™ are gathered from a wide resource of literature and were not adjusted, with the exception of the liver blood flow. Liver blood flow (LBF) was adjusted to 78 ml/min/kg and and 71 ml/min/kg in the rat and rabbit, respectively, to be in line with GSK observed values (Davies and Morris, 1993). Renal elimination was assumed to be the fraction unbound excreted at glomerular filtration rate (fu_p*GFR).

5.5.2. Physico-chemical Properties

To generate physico-chemical properties, GastroPlus™ software uses a structure-to-property algorithm (ADMET Predictor™) based on structural interpolation to give predicted parameters such as pKa's, solubility, and permeability. These parameters were maintained as predicted from structure in the absence of other experimentally derived information.

Several key properties that are also provided by ADMET Predictor™ were Log P, protein binding and blood:plasma ratio, which are important determinants in calculating tissue partition coefficients. The protein binding and blood:plasma values used for the PBPK modelling for both the rat and the rabbit were taken from the experimentally derived values previously described (Chapter 2) and summarised below.

5.5.3. Plasma Protein Binding and Blood Partitioning

A summary of the determined parameters is given in Table 5.1 below. Plasma protein binding of each compound was determined over a concentration range (n=6) using rapid equilibrium dialysis using the method described previously (Chapter 2). The distribution of compounds between plasma and whole blood was determined (1 µM, n=3) using the method described previously (Chapter 2).

Table 5.1 A Summary of Rat and Rabbit Blood:Plasma ratios and Fraction Unbound Parameters for Cisapride, Moxifloxacin, Sparfloxacin and Verapamil

	Rat		Rabbit		
	B:P	fu_p	B:P	fu_p	fu_t Heart
Cisapride	1.08	0.03	0.91	0.02	0.01
Moxifloxacin	1.45	0.574	1.22	0.562	0.12
Sparfloxacin	2.14	0.549	1.80	0.506	0.081
Verapamil	0.68	0.071	0.81	0.070	0.021

B:P Blood-to-plasma ratio
Fu_p Fraction unbound in the plasma
Fu_t Fraction unbound in the heart tissue

5.5.4. Determination of LogP

The measure of lipophilicity (LogP) used in the modelling was obtained from software databases using two in silico predicted methods and two adjusted measured values.

The two in silico methods used were ADMET Predictor™ and Biobyte™ (Biobyte Corporation, Claremont, CA), which are commercially available packages that predict from global QSAR structure models.

The two experimental methods applied used measured values from on-column chromatography hydrophobicity index (CHI) using reliable retention time values with phospholipids and C18 stationary phase that are adjusted to logP according to Valko and co-workers (Valko et al., 2000; Valko et al., 2001).

Immobilised artificial membrane chromatophaphy (IAM) is a measure of a compounds partitioning into phospholipids and can be used for modelling phospholipidotic potential, simulated intestinal fluid (SIF) enhancement, and volume of distribution. IAM is a chemically bonded phosphatidyl-choline to silica surface within commercially available HPLC columns with single fast gradient methods (Valko et al., 2000). A CHI IAM value can be converted to a membrane partition coefficient, logK(IAM)

$$logK(IAM) = 0.046 \times CHI\ IAM + 0.42 \qquad \text{Equation 16}$$

The logK(IAM) is linearised with logP values and then adjusted to the absolute values of octanol/water logP equivalent by the following equation;

$$logK(IAM)adjusted = 0.29 \times e^{logK(IAM)} + 0.70 \qquad \text{Equation 17}$$

CHI neutral (CHIN) lipophilicity is different from octanol/water lipophilicity as it is more like alkane/water partition and is conducted over different pHs much like logD. This CHI can be converted to octanol/water log scale, although the scales of CHI lipophilicity are slightly different. H-bond donor compounds partition more into octanol because the octanol OH groups can interact with the solute H-bond donor group resulting in higher logP values (i.e they look more lipophilic). The H-bond donor/acceptor groups will not interact with the C-18 hydrocarbon stationary phase in HPLC, so they will look more hydrophilic. The two scales can be aligned by introducing the H-bond acidity (Abraham's descriptor, A) that can be derived from *Smiles* (Valko et al., 2001).

$$logP = (0.054\ \times CHIN) + (1.319 \times A) - 1.877 \qquad \text{Equation 18}$$

5.5.5. Tissue Partition coefficients

The three parameters, plasma protein binding, blood:plasma ratio and log P along with pKa's are important in determining the tissue partition coefficients (Kps) needed to describe the mass balance and tissue concentration-time profiles. There are a number of methods available for the calculation of the Kps in GastroPlus™ and the default method used is the Lucakova (Rodgers-single) equation method adapted by Simulations Plus Inc derived from the two original Rodgers, equations (Rodgers et al., 2005; Rodgers and Rowland, 2006).

Lukacova equation:

$$Kpu = V_{ew} + \left(\frac{{}^{1}/_{X_{[D],iw}}}{{}^{1}/_{X_{[D],p}}}\right) \times V_{iw} + \left(\frac{P \times V_{nlt} + (0.3 \times P + 0.7) \times V_{pht}}{{}^{1}/_{X_{[D],p}}}\right) + (F_n + F_a) \times \left[\frac{1}{f_{up}} - 1 - \left(\frac{P \times V_{nlp} + (0.3 \times P + 0.7) \times V_{php}}{{}^{1}/_{X_{[D],p}}}\right)\right] \times RA_{tp} + (F_c)\left(\frac{K \times [AP]_t \times \left(\left({}^{1}/_{X_{[D],iw}}\right) - 1\right)}{{}^{1}/_{X_{[D],p}}}\right)$$

Equation 19

where:

V_{nlt}, V_{pht}, V_{ewt}, V_{iwt} = volume fraction of neutral lipids, phospholipids, intracellular and extracellular water in tissues.
V_{nlp}, V_{php} = volume fraction of neutral lipids and phospholipds in plasma.
$(Fn+Fa)$ is the fraction of drug without positive charge in plasma (the zwitterions with total charge = 0 are not included in this fraction since they contain positive charge that would be associating with the acidic phospholipids)
Fc is the fraction of drug with positive charge in plasma (cations or zwitterions with at least one positive charge on the molecule regardless of the total charge of the molecule)
RA_t = the ratio of albumin (for ionizable compounds) or lipoprotein (for non-ionizable compounds) concentration found in tissue over plasma.
$X_{[D],IW}$, $X_{[D],P}$ = fraction of neutral drug species in intracellular space (pH=7) and plasma (pH=7.4).
P = solvent/water partition coefficient for the drug (vegetable oil/water partition coefficient for adipose and yellow marrow; 1-octanol/water partition coefficient for all other tissues).
K = association constant of basic compound with acidic phospholipids.
$[AP]_t$ = concentration of acidic phospholipids in tissue.
fu_p = fraction unbound in plasma

Tissue partition coefficients are calculated based on the tissue composition and fraction unbound in plasma, taking into account drug ionization and specific interactions of bases with acidic tissue phospholipids. This equation provides a continuous shift from neutrals and acids binding almost exclusively to albumin towards strong bases binding almost exclusively to acidic phospholipids (GastroPlus™ v9 Manual p.198). For all types of compounds, the final *Kp* is calculated as:

$$Kp = Kpu \times fup$$

Equation 20

Where *Kpu* is the unbound tissue:plasma partition coefficient and fu_p is the fraction unbound in plasma.

5.5.6. GastroPlus PBPK Model Generation

i. For the rat PBPK:

Applying the four different values of logP obtained, rat PBPK models were built in GastroPlus™ using the experimentally derived rat B:P and fu_p to obtain a set of tissue Kp's and the observed NCA derived clearance applied to the liver. This was carried out to give a range of simulated concentration-time profiles in plasma against the observed experimental rat intravenous bolus data.

ii. For the rabbit:

The upper and lower log P values derived were used along with the two scaled rabbit clearance values (single species, SS and liver blood flow, LBF) obtained from the rat. Simulated rabbit concentration-time profiles in plasma were obtained to give a predicted profile range against the observed experimental anaesthetised rabbit intravenous infusion data. Heart tissue concentration-time profiles from the rabbit PBPK model were also extracted and plotted against the measured experimental heart tissue concentrations.

GastroPlus™ PBPK simulations were re-processed using the upper and lower observed calculated NCA clearance from the experimental rabbit data at the different dose levels along with the upper and lower heart:plasma ratio observed substituted as the heart tissue Kp.

Therefore each PBPK simulation consisted of four concentration-time data sets that were exported to Graphpad PRISM™ for plotting mean and SD with 95% confidence intervals.

5.6. Semi-Compartmental PBPK Model Analysis

Compartmental analysis was conducted on the rat to assess the number of compartments and rate constants (inter-compartment distribution rate constants, k12 and k21, and elimination rate constants, k10) that adequately described the pharmacokinetic profile of each compound (Figure 5.2). This was performed using simultaneous analysis in GastroPlus™, PKplus™ module, v.9 and confirmed by manual interrogation using WinNonlin™, Phoenix v.6.3.

Figure 5.2 Schematic of a Two Compartmental PK Model

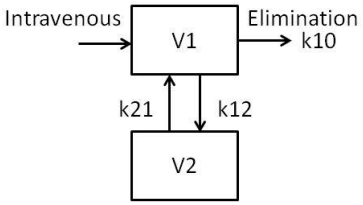

Figure 5.2: Schematic diagram of an empirical two compartmental PK model to describe intravenous drug administration into a central compartment (V1), which may distribute to a peripheral compartment (V2) via distributional rate constants (k12 and k21), and eliminated from the central compartment by the elimination rate constant (k10).

This compartmental analysis assisted in development of a semi-compartmental physiological model (semi-PBPK) approach to integrate the compartmental PK analysis undertaken in the rat and extrapolate the pharmacokinetic parameters as described for the distributional rate constants, clearance, volume and the elimination rate constant to give the compartmental rabbit PK plasma-concentration time profile. This was combined with tissue specific physiological parameters for the rabbit heart (e.g. rabbit heart volume, blood flow and tissue partitioning) where concentrations received into the tissue were directly related to the central plasma compartment. This analysis was conducted in SAAMII software package (Simulation Analysis and Modeling for Kinetic Analysis, version 2.0, University of Washington) and the model structure given in Figure 5.3.

Figure 5.3 Schematic of a Semi-PBPK Model of the Heart linked to a Two Compartmental PK Model

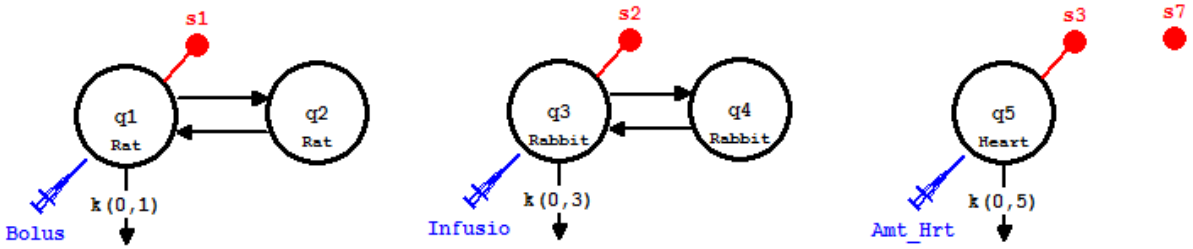

Figure 5.3: Schematic diagram of an empirical two compartmental PK model to describe intravenous drug administration into a central compartment

Figure 5.3 shows the two compartment model for rat (q1 and q2) and rabbit (q3 and q4), with distributional rate constants between the compartments (shown by arrows →). The elimination rate constant, kel, is given for the rat (k0,1) and rabbit (k0,3). The amount of drug administered (ng) was determined for the bolus dose in the rat and constant rate infusion over the specific time for the rabbit. The measured plasma concentrations for rat (s1) and

rabbit (s2) were determined by the volume of the central compartment (Vc_{rat} or Vc_{rab}) and linked to the observed plasma concentration data.

For the tissue compartment designated as the rabbit heart, the amount of drug 'administered' over time was derived from the central plasma compartment (C_A) which was corrected for blood:plasma (B:P) ratio and multiplied by the heart blood flow (Q_{hrt}). Whilst the amount of drug out (k0,5) from the heart tissue is related to the organ blood flow (Q_{hrt}), volume (V_{hrt}) and tissue partition coefficient (Kp_{hrt}).

Heart tissue compartment:

$$\frac{dC_{hrt}}{dt} = \left(\frac{Q_{hrt}}{V_{hrt}}\right) \times \left(C_A - \frac{C_T}{Kp_{hrt}}\right) \qquad \text{Equation 21}$$

The change in the amount of drug in the heart tissue (dC_{hrt}/dt) was derived from Equation 21, as it is a non-eliminating organ. The simulated heart concentrations were obtained from the amount of drug in the heart and corrected for tissue volume (V_{hrt}), and this was linked with observed heart tissue concentration data (s3). The resultant heart tissue concentrations were then used to simulate dQTc as determined by the re-arranged E_{max} below (Equation 22) and the associated observed dQTc data (s7).

The semi-PBPK model used the PK compartmental parameters following fitting of simultaneous dose groups based from GastroPlus™ PKPlus™ analysis (Hook & Jeeves Pattern search; weighting $1/Yhat^2$). The fitted compartmental PK was to demonstrate that the physiological description of the heart with the literature blood flow and volume with the measured tissue partition coefficient could simulate the heart concentration profile in isolation.

5.7. In Vivo PD Modelling

In terms of the PD model, the previously described non-linear concentration-effect relationship of the sigmoidal E_{max} model from the RVW was applied to the heart (Chapter 3, Section 3.5.2 Equation 9).

$$E = E_0 + \frac{E_{max} \times {C_{Hrt}}^n}{{EC_{50}}^n + {C_{Hrt}}^n} \qquad \text{Equation 9}$$

Where E is effect as a function of E_{max}, which is the maximum effect, C_{Hrt} is the free drug concentration in the heart, EC_{50} is the concentration of drug producing half maximal effect and n is the Hill coefficient referred to as the shape factor. The E_{max} model is based on receptor theory, therefore the E_{max} reflects the efficacy of the drug and EC_{50} the potency. The parameter n can be thought of as the number of molecules binding but in practice it is simply used to give a better fit to the data (Derendorf and Meibohm, 1999). Since drug responses are often measured as a change from a baseline state (E_0) which may be incorporated and allow for potential variability to be included.

The simulated heart tissue concentrations from the GastroPlus™ whole-body PBPK model or the SAAMII semi-PBPK model were then corrected for fraction unbound in the tissue using the previously experimentally derived heart fu_t (Chapter 2), converted to molar concentrations and log transformed and used in the rearranged RVW sigmoidal E_{max} model to predict the dQTc.

$$E = E_0 + \frac{(E_{max} - E_0)}{(1+10^{(LogEC_{50} - C_{Hrt}) \times Hillslope})} \qquad \text{Equation 22}$$

5.8. Cisapride In Vivo Modelling Results and Discussion

5.8.1. Cisapride: Rat

Following a single intravenous dose at a nominal dose of 1 mg/kg of cisapride to female rats the mean volume of distribution was approximately 17 L/kg which indicates distribution through the body water and widely into tissues, is considered high (>10 L/kg), and is notably greater than the literature 4.7 L/kg, (Michiels, 1987) (Table 5.14). The mean plasma clearance of cisapride was 0.715 L/h which is approximately 70% liver blood flow (LBF) in the rat and considered high (>70% LBF), yet lower than published 1.37 L/h equivalent to LBF (Michiels, 1987) (Table 5.14). The terminal half-life following an intravenous bolus administration was considered moderate in this study at 3.6 hour and comparable to that reported 1-2 hours.

5.8.2. Cisapride: Rabbit

The pharmacokinetics of cisapride in the rabbit following infusion of 0.3 and 3 mg/kg indicate the drug distributes into tissues as well as systemic circulation and extracellular water as determined by the volume of distribution (Vd_{ss} = 1.6 and 2.6 L/kg). Total plasma clearance (Cl_p = 13.5 and 8.18 L/h) was approximately equivalent to hepatic liver blood flow which is considered high, with a short half-life ($t_{1/2}$ = 0.6 h). In context with literature information and comparison with other species the rabbit appears similar to the rat and sheep across the parameters and has a comparable volume of distribution to dog and human (Table 78) (Michiels, 1987; McCallum et al., 1988; Veereman-Wauters et al., 1991); respectively). The half-life of cisapride appeared very short in the anaesthetised rabbit and may be a reflection of the short experimental duration not fully defining the terminal elimination phase, as half-life in rabbits has been reported to be approximately 4 hours (Michiels, 1987). Clearance of cisapride in the rabbit was high, unlike that observed in dog (Michiels, 1987; Webster et al., 2001) and humans (McCallum et al., 1988; Gladziwa et al., 1991) (Table 5.14).

5.8.3. Cisapride: Scaling

Cisapride CL_p was high in the rat (70% LBF) and compared favourably to the 100% published (Michiels, 1987). The resulting scaled clearance value from rat was low using single-species (SS = 2.66 L/h, 25%) and moderate using liver blood flow (LBF = 4.25 L/h, 40%). Both were less than the observed rabbit clearances determined from 0.3 and 3 mg/kg

dose level, which were approximately equivalent to LBF in rabbit (8.18 and 13.53 L/h, respectively). This difference in scaled clearance from high in the rat to low/moderate in the rabbit grouping may be the result of a lower blood:plasma ratio in the rabbit which was less than 1, and a lower fraction unbound, as the observed measured clearance is high in both species.

5.8.4. Cisapride Rat Physiological PBPK

Tissue partition coefficients (Kps) were generated within GastroPlus™ based upon the single-Rodgers method described by Lucakova. Four different logP values obtained from in silico (ADMET and Biobyte) and measured CHI (logK(IAM) and log(CHIN)) were used with experimental blood:plasma ratio (B:P) value 1.1 and fraction unbound in the plasma (fu_p) 0.03 in the rat.

The range of logP values from 3.51 log(CHIN), 3.61 ADMET, and 3.74 logK(IAM) to 3.81 Biobyte provided a limited difference of tissue coefficients. However the goodness of fit provided by R-squared values (0.924 – 0.926) indicates a close simulation of the predicted rat PBPK as shown in Figure 5.4 and Table 5.2. The simulated predictions with each logP value were plotted together as a mean and 95% confidence interval band. Due to the similarity of predictions, the confidence band cannot be observed.

The NCA derived clearance of 0.715 L/h was used in the rat PBPK model and it was also used for single-species and liver blood flow scaling to the rabbit.

Figure 5.4 Cisapride Rat PBPK: Simulated Plasma Concentration-Time Profile of Cisapride in Female Rats Following a Single Intravenous Administration of Cisapride at 1 mg/kg

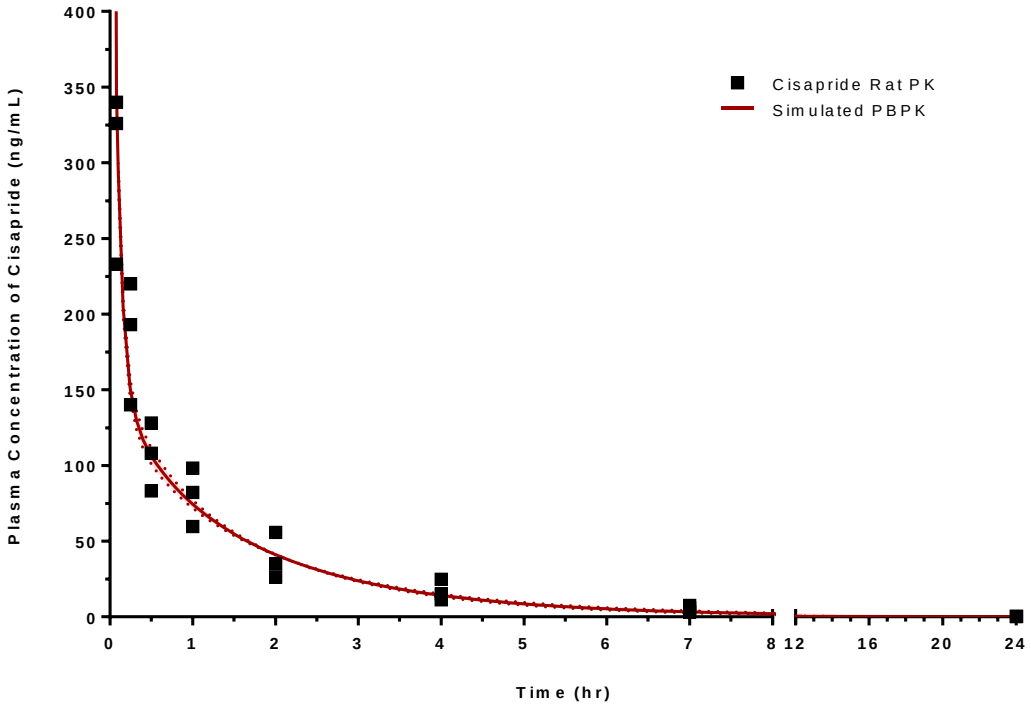

Figure 5.4: Graph of the individual plasma concentration-time profile data points (■) following a single intravenous bolus administration of cisapride at 1 mg/kg to three female rats and the simulated concentration-time using PBPK (—)

Table 5.2 Cisapride Rat PBPK: In Silico Determination of Tissue Partition Coefficients (Kp) in the Rat using different Log P values

LogP	ADMET™	Biobyte™	logK(IAM)	Adj. log(CHIN)
	3.61	3.81	3.74	3.51
Tissue				
Lung	7.59	7.71	7.90	8.02
Adipose	5.29	6.45	8.35	9.57
Muscle	3.10	3.17	3.29	3.36
Liver	8.40	8.46	8.56	8.62
Spleen	5.69	5.69	5.68	5.68
Heart	4.52	4.61	4.76	4.86
Brain	17.93	18.13	18.46	18.67
Kidney	9.07	9.09	9.12	9.15
Skin	3.66	3.91	4.32	4.57
Repro Org	9.08	9.10	9.13	9.15
Red Marrow	2.50	2.78	3.20	3.47
Yellow Marrow	5.29	6.45	8.35	9.57
Rest of Body	5.70	5.70	5.69	5.69
R-squared (R^2)	0.924	0.926	0.925	0.926

Table 5.2: Tissue partition coefficients (Kps) in the rat using different logP values derived from ADMET, Biobyte, logK(IAM) and adjusted log(CHIN) with experimental value for rat B:P value 1.1 used and Fup = 0.03; and NCA derived clearance of 0.715L/h

5.8.5. Cisapride Rabbit Physiological PBPK – using Scaled Clearance and logP range

Scaled clearance values were determined from the rat observed 0.715 L/h non-compartmental analysis (NCA) data using single-species (SS = 2.66 L/h) and liver blood flow (LBF = 4.25 L/h) scaling methods previously described (Table 5.3).

Tissue partition coefficients (Kps) were generated within GastroPlus™ using the upper and lower logP values (3.81 and 3.51 obtained from Biobyte and log(CHIN) with experimental blood:plasma ratio (B:P) value 0.91 and fraction unbound in the plasma (fu_p) 0.02 in the rabbit. The PBPK simulations were carried out for doses of cisapride at 0.3 and 3 mg/kg following 30 minute intravenous infusion, with regression analysis of fit given for each. Simulations were not conducted for 1 mg/kg infusion as only plasma-dQTc data were available up to the end of infusion and there were no heart concentration data to compare with the simulations. The R-squared values indicate a relatively moderate fit using both logP values and scaled clearance methods (0.564 to 0.780), with LBF scaled clearance simulation fitting best, and also 3 mg/kg fitting better than 0.3 mg/kg using both clearance values and the Biobyte logP.

The simulated scaled clearance predictions with each logP value were plotted together as a mean and 95% confidence interval band in Figures 5.5 and Figure 5.6 (plasma and heart at 0.3 mg/kg and 3 mg/kg). It can be seen from these graphical representations against the actual observed plasma concentration-time data that the plasma profile over-predicts during the infusion period (within a 2-fold, which is considered to be adequate) and the overall shape of the elimination curve is correct (observed vs predicted slope estimate best for LBF CL of 4.25 L/h and LogP 3.81).

The subsequent derived simulated mean and 95% confidence heart concentration-time profile were plotted against the range of tissue concentration data from the replicate analysis with error bars. The simulated heart concentrations from scaled clearance with the heart Kp value (3.12 – 3.52) slightly under predicts the overall profile but is approximately similar to the observed (within 2-fold) Figures 5.5 and Figure 5.6.

Table 5.3 Cisapride Rabbit PBPK: In Silico Determination of Tissue Partition Coefficients (Kp) using different Log P values in the Rabbit, with Scaled Clearance and Predicted Regression Analysis of Fit against Observed

Log P		Biobyte		Adj. log(CHIN)	
		3.81		3.51	
Clearance		SS CL	LBF CL	SS CL	LBF CL
		2.66 L/h	4.25 L/h	2.66 L/h	4.25 L/h
Tissue Kp					
Lung		4.08		3.89	
Adipose		3.06		5.23	
Muscle		2.31		2.72	
Liver		5.75		6.27	
Spleen		3.93		4.22	
Heart		3.12		3.53	
Brain		2.44		3.80	
Kidney		5.73		5.87	
Skin		2.37		2.91	
ReproOrg		5.73		5.87	
Red Marrow		2.94		4.40	
Yellow Marrow		3.06		5.23	
Rest of Body		3.94		4.23	
		Regression Analysis of Fit			
0.3 mg/kg	R^2	0.571	0.606	0.564	0.598
	SSE	5.83E+05	3.34E+05	6.86E+05	3.85E+05
	RMSE	8.65E+01	6.54E+01	9.38E+01	7.03E+01
	MAE	7.47E+01	5.20E+01	8.17E+01	5.64E+01
	Slope est.	0.4082	0.4368	0.3925	0.4233
	95CI - Low	0.3821	0.4181	0.3638	0.4054
	95CI - Upp	0.4344	0.4555	0.4211	0.4413
	Slope StdErr	0.01234	0.008808	0.0135	0.008463
3 mg/kg	R^2	0.678	0.780	0.656	0.756
	SSE	2.66E+07	1.06E+07	3.39E+07	1.36E+07
	RMSE	5.11E+02	3.23E+02	5.76E+02	3.64E+02
	MAE	4.47E+02	2.48E+02	5.09E+02	2.88E+02
	Slope est.	0.6319	0.6797	0.6074	0.656
	95CI - Low	0.5933	0.6593	0.5643	0.6368
	95CI - Upp	0.6706	0.7	0.6506	0.6751
	Slope StdErr	0.01822	0.009608	0.02037	0.009022

Experimental value for rabbit B:P value 0.91 and Fup = 0.02 used;

SS CL Single-species scaled Clearance
LBF CL Liver Blood Flow Clearance
R^2 R-squared
SSE Sum of the squared error
RMSE Residual mean sum of errors
MAE Mean average error
95%CI 95% Confidence Interval (upper and lower)

5.8.6. Cisapride Rabbit Physiological PBPK – using Observed Clearance and Measured Heart Kp

The process of PBPK simulations was repeated using the two observed rabbit NCA clearances values (GastroPlus™, PKPlus™) from 0.3 and 3 mg/kg dose level, determined as 8.18 and 13.53 L/h.

A fixed logP value of 3.81 from Biobyte with experimental blood:plasma ratio (B:P) value 0.91 and fraction unbound in the plasma (fu_p) 0.02 were used to generate the tissue partition coefficients (Kps) in the rabbit (values as presented in previous Table 5.3). In this instance the observed upper and lower mean measured heart tissue:plasma ratios were used as the heart partition coefficient values of 13.08 and 10.84 (compared to in silico determined 3.12 to 3.53), with the regression analysis of fit given for each PBPK simulation (Table 5.4). The R-squared values indicated an improved fit using observed clearance and measured heart Kp (0.702 to 0.919), with the upper clearance (13.53 L/h) and upper Kp (13.08) slope of observed vs predicted approaching unity.

The simulated scaled clearance predictions were plotted together as a mean and 95% confidence interval band in Figures 5.5 and Figure 5.6 (plasma and heart at 0.3 mg/kg and 3 mg/kg). It can be seen from these graphical representations against the actual observed plasma concentration-time data that the plasma profile provides a better prediction during the infusion period and maintains the overall shape of the elimination curve, as determined by the slope estimate of the observed vs predicted. The subsequent derived simulated mean and 95% confidence heart concentration-time profile were plotted against the range of tissue concentration data from the replicate analysis with error bars. The simulated heart concentrations from observed clearance with the heart Kp value (10.84 – 13.08) provides a good approximation of the tissue profile, with only the end of infusion tissue concentration being over-predicted at 0.3 mg/kg (within 2-fold) Figures 5.5 and Figure 5.6.

Table 5.4 Cisapride Rabbit PBPK: Regression Analysis of Fit Determined using Observed Rabbit Clearance and Heart Tissue Partition Coefficient (Kp)

Observed Clearance in Rabbit (L/h)		Upper Clearance (L/h)		Lower Clearance (L/h)	
		13.53		8.18	
Measured Observed Heart : Plasma Kp		Upper Heart Kp	Lower Heart Kp	Upper Heart Kp	Lower Heart Kp
		13.08	10.84	13.08	10.84
Dose		**Regression Analysis of Fit**			
0.3 mg/kg	R^2	0.763	0.762	0.702	0.702
	SSE	4.77E+04	4.81E+04	9.47E+04	9.56E+04
	RMSE	2.47E+01	2.48E+01	3.48E+01	3.50E+01
	MAE	1.91E+01	1.92E+01	2.36E+01	2.37E+01
	Slope est.	0.6264	0.6248	0.5559	0.5535
	95CI - Low	0.5584	0.5565	0.5112	0.5083
	95CI - Upp	0.6943	0.6932	0.6005	0.5987
	Slope StdErr	0.03205	0.03224	0.02108	0.02133
3 mg/kg	R^2	0.831	0.831	0.919	0.92
	SSE	3.53E+06	3.53E+06	1.73E+06	1.76E+06
	RMSE	1.86E+02	1.86E+02	1.30E+02	1.31E+02
	MAE	1.59E+02	1.59E+02	1.09E+02	1.10E+02
	Slope est.	0.9711	0.9688	0.8609	0.8579
	95CI - Low	0.8717	0.8687	0.7975	0.7938
	95CI - Upp	1.0706	1.0689	0.9243	0.922
	Slope StdErr	0.04693	0.04722	0.02991	0.03024

Experimental value for rabbit B:P value 0.91 and Fup = 0.02 used;
SS CL Single-species scaled Clearance
LBF CL Liver Blood Flow Clearance
R2 R-squared
SSE Sum of the squared error
RMSE Residual mean sum of errors
MAE Mean average error
95%CI 95% Confidence Interval (upper and lower)

Figure 5.5 Cisapride Rabbit PBPK: Simulated Plasma and Heart Concentration-Time Profile of Cisapride in the Rabbit Following a 30 Minute Intravenous Infusion Administration of Cisapride at 0.3 mg/kg

a) Plasma

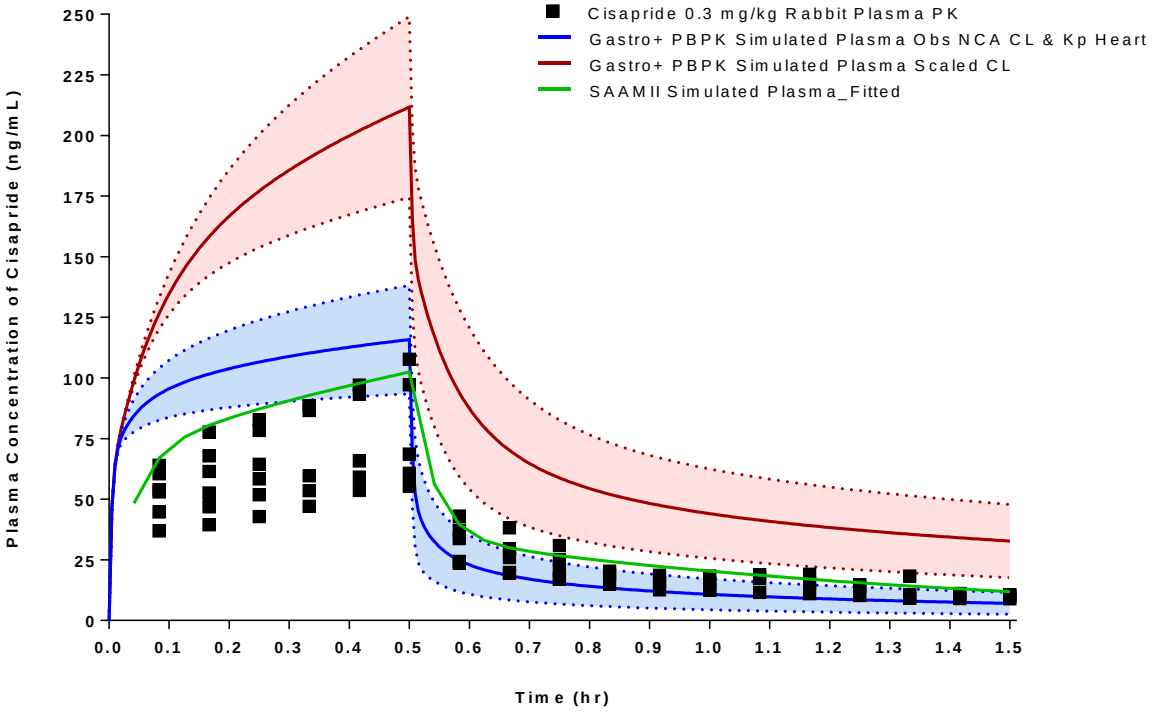

b) Heart

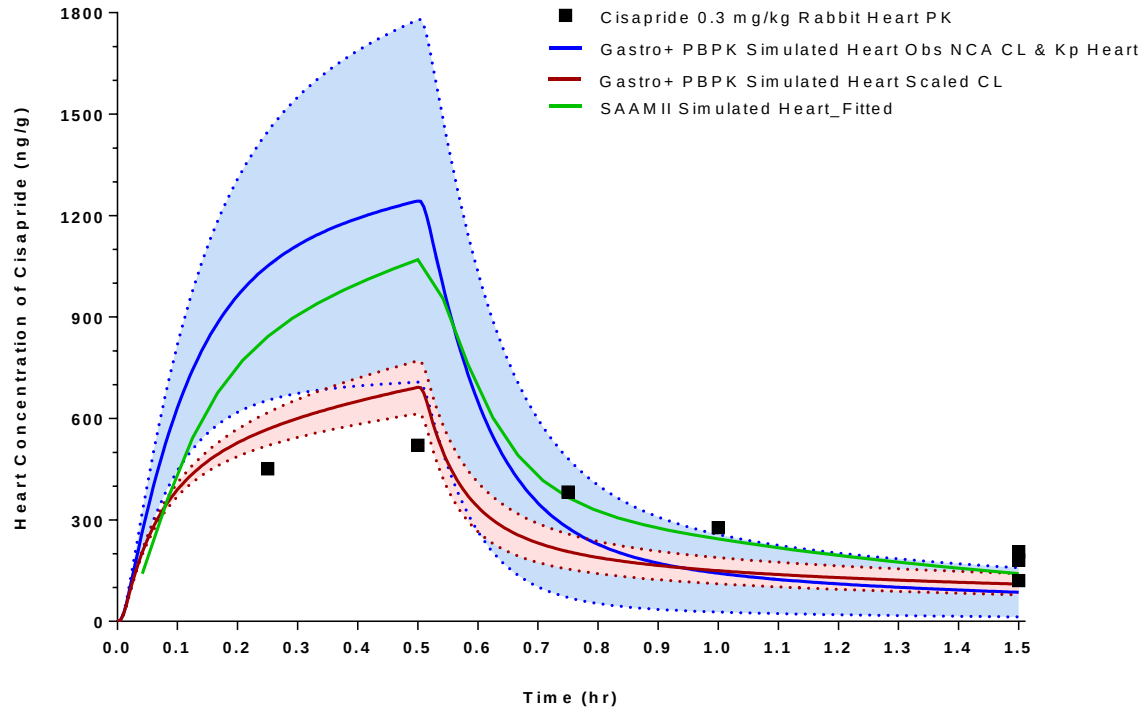

Figure 5.5: Graph of the individual plasma (a) and heart (b) concentration-time profile with observed data points (■) following a single intravenous infusion administration of cisapride at 0.3 mg/kg to female rabbits and the predicted concentration-time using GastroPlus PBPK model with Scaled Clearance and LogP (—) or Observed Clearance and measured Heart Kp (—) with 95% confidence interval in shaded area and SAAMII semi-PBPK model (—) fitted compartmental analysis.

Figure 5.6 Cisapride Rabbit PBPK: Simulated Plasma and Heart Concentration-Time Profile of Cisapride in the Rabbit Following a 30 Minute Intravenous Infusion Administration of Cisapride at 3 mg/kg

a) Plasma

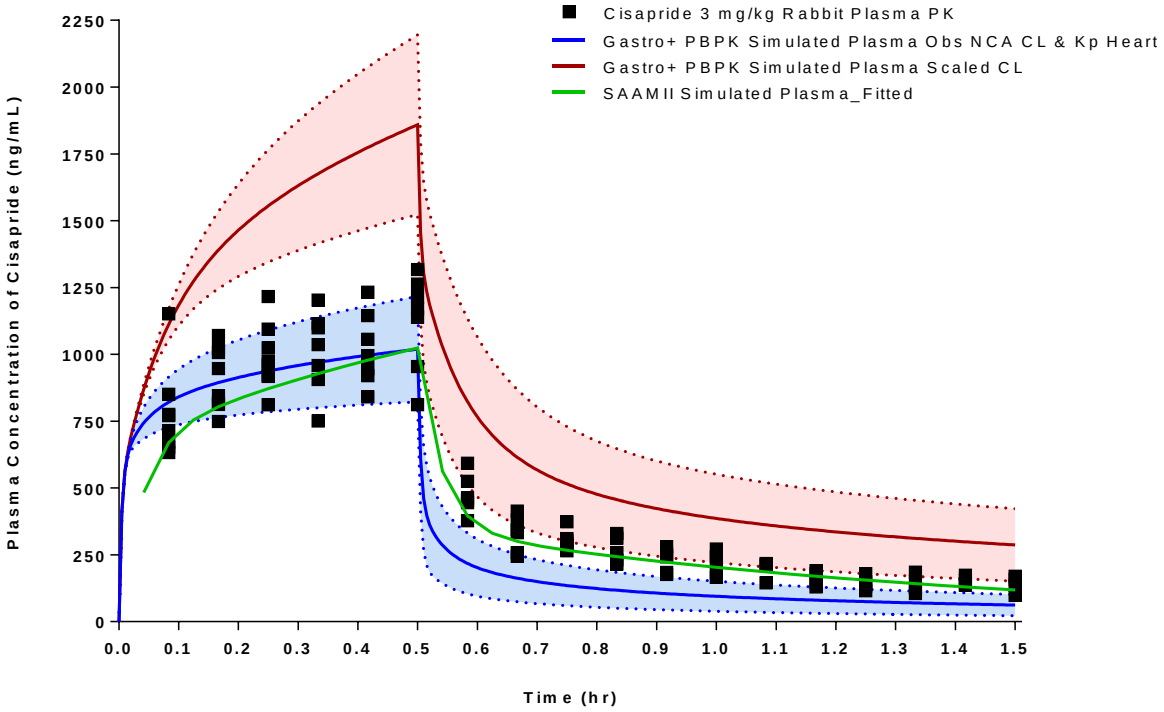

b) Heart

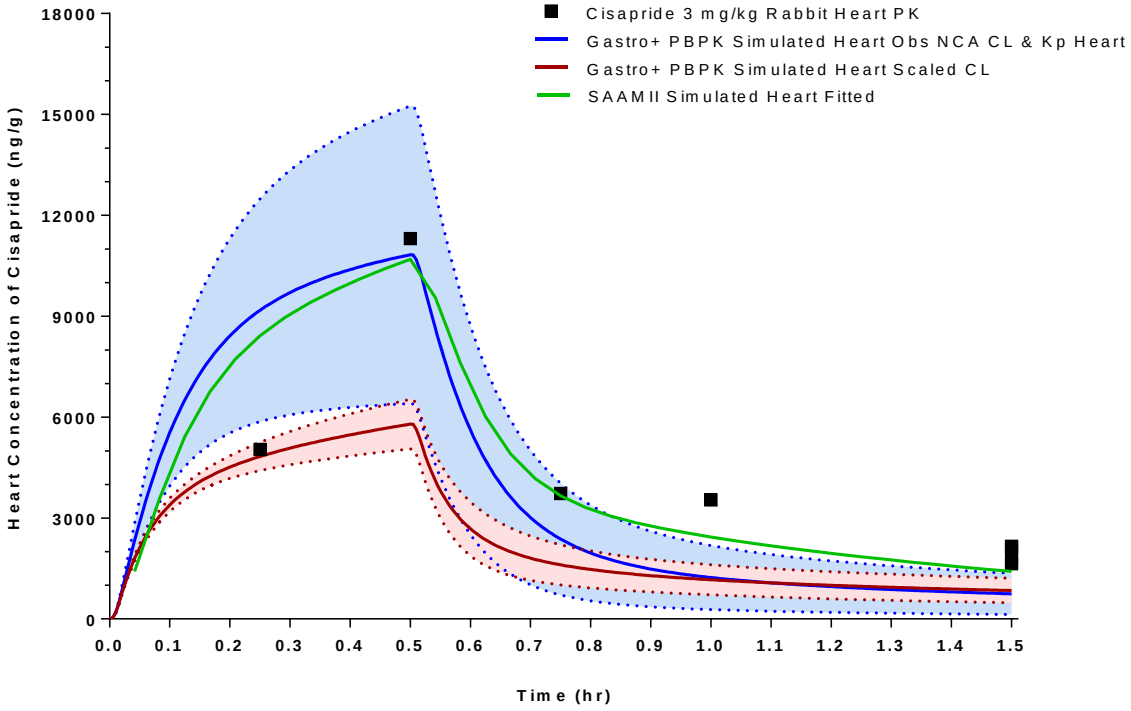

Figure 5.6: Graph of the individual plasma (a) and heart (b) concentration-time profile with observed data points (■) following a single intravenous infusion administration of cisapride at 3 mg/kg to female rabbits and the predicted concentration-time using GastroPlus PBPK model with Scaled Clearance and LogP (—) or Observed Clearance and measured Heart Kp (—) with 95% confidence interval in shaded area and SAAMII semi-PBPK model (—) fitted compartmental analysis.

5.8.7. Cisapride Rabbit PBPK/PD

The simulated rabbit heart concentrations were corrected to free concentrations using the experimental fraction unbound in heart tissue (fu_t = 0.01) and converted to µM to predict the associated change in QTc prolongation from the E_{max} equation (Figure 5.7). This plot shows that each of the methods employed using the simulated PBPK/PD provide a reasonable approximation of the observed vehicle-baseline corrected QTc (ddQTc) in the anaesthetised rabbit. The scaled clearance does not give a similar maximal change in QTc for the observed due to the under predicted heart tissue concentration compared to the using the observed clearance. The error bars are less for the scaled clearance and remain within the bounds of the observed clearance predicted concentration-dQTc. The PBPK/PD predicted dQTc response is similar to the fitted semi-PBPK model where the plasma PK is fitted to a 2-compartmental model that then describes the heart concentration-time profile.

Figure 5.7 Cisapride Rabbit PBPK/PD: Simulated Free Heart Concentration-dQTc Response Profile of Cisapride in the Rabbit

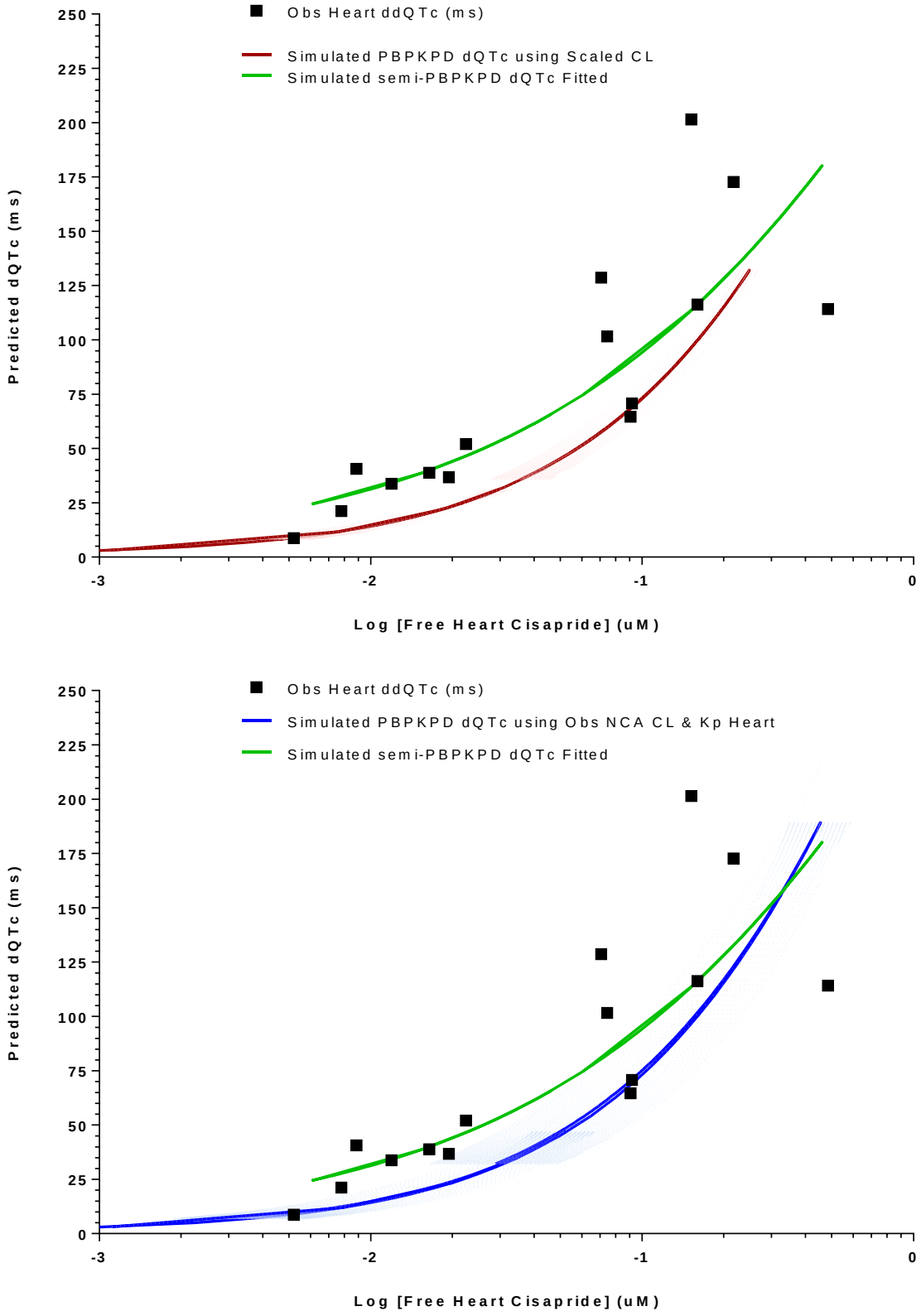

Figure 5.7: Graph of the individual heart concentration-dQTc response profile with observed data points (■) following a single intravenous infusion administration of cisapride to female rabbits and the predicted concentration-dQTc response using GastroPlus PBPK/PD model with Scaled Clearance and LogP (—) or Observed Clearance and measured Heart Kp (—) with ±SD error bars in shaded area and SAAMII semi-PBPK model (—) fitted compartmental analysis

5.9. Sparfloxacin Modelling Results and Discussion

5.9.1. Sparfloxacin: Rat

Following a single intravenous dose at a nominal dose of 10 mg/kg of sparfloxacin to female rats the mean volume of distribution was approximately 16 L/kg which indicates distribution through total body water and widely into tissues, and is considered high (>10 L/kg). The mean plasma clearance of sparfloxacin was 0.585 L/h, approximately 50% liver blood flow (LBF) in the rat and is considered moderate (30-70% LBF) (Table 5.14). The terminal half-life following an intravenous bolus administration was also moderate at 4.7 hour (1-10 h). In contrast both clearance and volume have been reported to be lower in the scientific literature (Matsunaga et al., 1991a; Matsunaga et al., 1991b; Naroa et al., 1992; Noh et al., 2010) (Table 5.14).

5.9.2. Sparfloxacin: Rabbit

The pharmacokinetics of sparfloxacin in the rabbit following infusion of 33 mg/kg indicates the drug distributes extensively into tissues as well as systemic circulation and extracellular water as determined by the volume of distribution (Vd_{ss} = 8.4 L/kg) and compared to other species it is similar to monkey (7.3 L/kg) and human (5.5 L/kg) (Yamaguchi et al., 1991; Shimada et al., 1993; Montay et al., 1994) (Table 5.14). Total clearance (8.25 L/h) is approximately 75% of hepatic liver blood flow and considered high (50-100% LBF), which was considerably greater than all other species such as rat (20%), monkey (36%) and human (20%) (Matsunaga et al., 1991a; Matsunaga et al., 1991b; Yamaguchi et al., 1991; Naroa et al., 1992; Shimada et al., 1993; Montay et al., 1994) (Table 5.14). The observed corresponding half-life in the rabbit in this study was moderate at 2.4 hour and the same as published (Liu et al., 1998). In comparison to half-lives in other species, the rabbit was closest to the rat (2.2 - 4 hour), but less than that in the monkey (5.3 – 11.7 hour) and human (15 – 20 hour). Some comparable pharmacokinetic parameters in the anaesthetised rabbit across species, in this instance, are reflected by the longer infusion and experimental duration (180 minutes) to better define the elimination phase. An exception is the dog, where the volume of distribution and clearance parameters are notably lower than all the other species (Nakamura et al., 1990) (Table 5.14).

5.9.3. Sparfloxacin: Scaling

Sparfloxacin CL_p was moderate in the rat (50% LBF) compared to the low range in literature (20-25%). The resulting scaled clearance from rat was low using single-species (SS = 2.74 L/h, 26%) and moderate using liver blood flow (LBF = 4.37 L/h, 42%). Both scaled clearance values were less than the observed rabbit clearances, at just over 2-fold, as determined from 33 mg/kg, which was classified as high, approximately 75% LBF (6.06 and 10.72 L/h).

5.9.4. Sparfloxacin Rat Physiological PBPK

Tissue partition coefficients (Kps) were generated within GastroPlus™ based upon the Lucakova method described. For sparfloxacin, three different logP values obtained from in silico (ADMET and Biobyte) and measured CHI log(CHIN)) were used with experimental blood:plasma ratio (B:P) value 2.14 and fraction unbound in the plasma (fu_p) 0.549 in the rat. Chromatographic measured logK(IAM) was not available for sparfloxacin.

The wide range of logP values from the in silico -0.55 ADMET and -0.605 Biobyte to the measured 1.258 log(CHIN), provided very little difference in tissue coefficients. This is a result of sparfloxacin being a zwitterion and its interaction with acidic phospholipids the single-Rodgers equation by Lukacova in GastroPlus™ (equation 19). Each respective log P simulation provided similar R-squared goodness of fit values (0.58) that indicated a relatively poor simulation of the predicted rat PBPK as shown in Figure 5.8 and Table 5.5. The simulated predictions with each logP value were plotted together as a mean and 95% confidence interval band. Due to the similarity of predictions, the confidence band cannot be observed. The graphical representation demonstrates that the simulated fit describes the initial time-course and terminal phase of the rat intravenous profile and under predicts the distributional phase, with a more pronounced bi-phasic profile.

The NCA derived clearance of 0.528 L/h was used in the rat PBPK model and it was also used for single-species and liver blood flow scaling to the rabbit.

Figure 5.8 Sparfloxacin Rat PK: Simulated Plasma Concentration-Time Profile of Sparfloxacin in Female Rats Following a Single Intravenous Administration of Sparfloxacin at 10 mg/kg

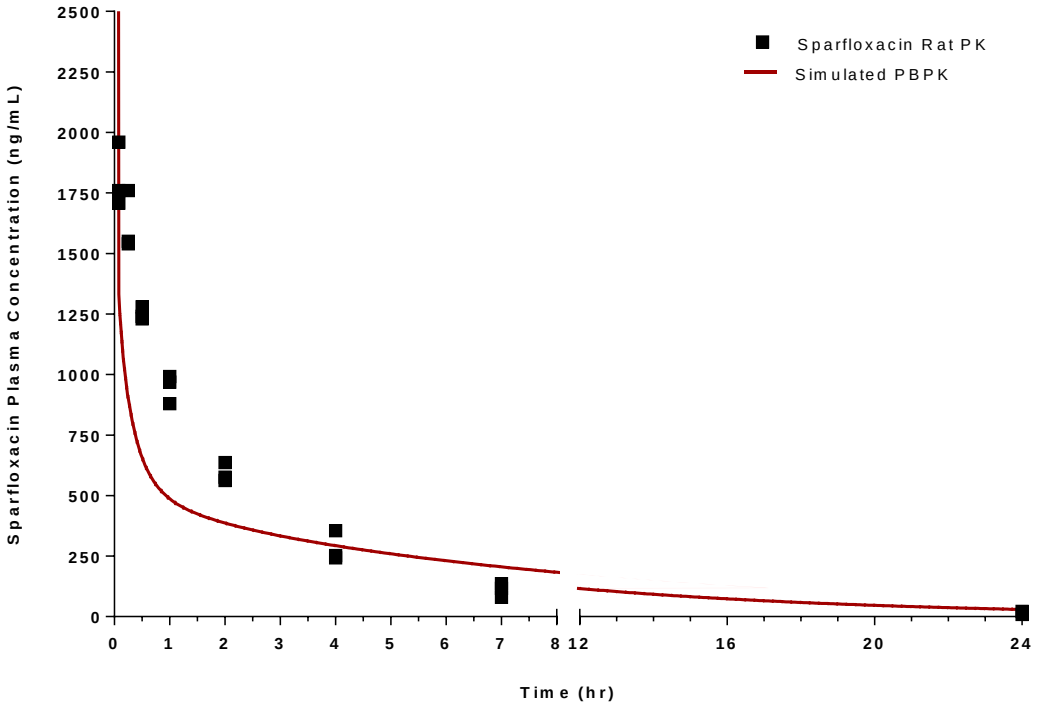

Figure 5.8: Graph of the individual plasma concentration-time profile data points (■) following a single intravenous bolus administration of sparfloxacin at 10 mg/kg to three female rats and the simulated concentration-time using PBPK (—)

Table 5.5 Sparfloxacin Rat PBPK: In Silico Determination of Tissue Partition Coefficients (Kp) in the Rat using different Log P values

LogP	ADMET™	Biobyte™	logK(IAM)	Adj. log(CHIN)
	-0.55	-0.605	ND	1.258
Tissue				
Lung	36.92	36.92	ND	36.97
Adipose	3.80	3.80	ND	4.26
Muscle	14.71	14.71	ND	14.74
Liver	42.94	42.94	ND	42.93
Spleen	30.10	30.10	ND	30.06
Heart	21.43	21.43	ND	21.48
Brain	90.00	90.00	ND	90.05
Kidney	47.36	47.36	ND	47.31
Skin	12.69	12.69	ND	12.88
ReproOrg	47.36	47.36	ND	47.31
Red Marrow	6.51	6.51	ND	6.72
Yellow Marrow	3.80	3.80	ND	4.26
Rest of Body	30.10	30.10	ND	30.06
R-squared (R^2)	0.58	0.58	-	0.578

Table 5.5: Tissue partition coefficients (Kps) in the rat using different logP values derived from ADMET, Biobyte and adjusted log(CHIN). logK(IAM) was not available and Kps not determined (ND) with experimental value for rat B:P value 2.14 used and Fup = 0.549; and NCA derived clearance of 0.528 L/h

5.9.5. Sparfloxacin Rabbit Physiological PBPK – using Scaled Clearance and logP range

Scaled clearance values were determined from the rat observed 0.528 L/h non-compartmental analysis (NCA) data using single-species (SS = 2.74 L/h) and liver blood flow (LBF = 4.73 L/h) scaling methods previously described (Table 5.6).

Tissue partition coefficients (Kps) were generated within GastroPlus™ using the upper and lower logP values (-0.0605 and 1.258 obtained from Biobyte and log(CHIN) with experimental blood:plasma ratio (B:P) value 1.80 and fraction unbound in the plasma (fu_p) 0.506 in the rabbit. The PBPK simulations were carried out for doses of cisapride at 16, 33 and 100 mg/kg following 60 minute intravenous infusion, with regression analysis of fit given for each. The R-squared values indicate a reasonable fit using both logP values and scaled clearance methods (0.587 to 0.747), with LBF scaled clearance simulation fitting better than single-species scaling, but no difference regarding the logP value. The 33 mg/kg profile fitted better than 16 and 100 mg/kg, in part due to the number of data points, using either clearance value, although the slope estimate for observed vs predicted was nearer unity for 16 and 100 mg/kg.

The simulated scaled clearance predictions with each logP value were plotted together as a mean and 95% confidence interval band in Figures 5.9 to Figure 5.11 (plasma and heart at each dose level). It can be seen from these graphical representations against the actual observed plasma concentration-time data that the plasma profile predicts the infusion period relatively well with greater plasma concentrations (within a 2-fold). For 33 mg/kg, the simulated plasma curve over predicts the early elimination phase whilst the overall shape of the elimination curve is correct (within a 2-fold). The simulated mean heart concentration-time profile and 95% confidence interval were plotted against the tissue concentration data from the replicate analysis with error bars. The simulated heart concentrations over predicted by approximately 4-fold based from end of infusion heart data for each of the doses from scaled clearance with the predicted heart Kp value (21.04 – 21.43) Figures 5.9 to Figure 5.11. Limited data points make understanding of the tissue distribution difficult.

Table 5.6 Sparfloxacin Rabbit PBPK: In Silico Determination of Tissue Partition Coefficients (Kp) using different Log P values in the Rabbit, with Scaled Clearance and Predicted Regression Analysis of Fit against Observed

LogP		Biobyte		Adj. log(CHIN)	
		-0.605		1.258	
Clearance		SS CL	LBF CL	SS CL	LBF CL
		CL=2.74 L/h	CL=4.37 L/h	CL=2.74 L/h	CL=4.37 L/h
Tissue Kp					
Lung		36.92		35.91	
Adipose		3.80		4.11	
Muscle		14.71		14.47	
Liver		42.94		42.09	
Spleen		30.10		29.45	
Heart		21.43		21.04	
Brain		90.00		4.58	
Kidney		47.36		46.22	
Skin		12.69		12.59	
ReproOrg		47.36		46.22	
Red Marrow		6.51		6.90	
Yellow Marrow		3.80		4.11	
Rest of Body		30.10		29.46	
Dose		Regression Analysis of Fit			
16 mg/kg	R^2	0.589	0.595	0.589	0.595
	SSE	2.20E+07	1.47E+07	2.20E+07	1.47E+07
	RMSE	8.56E+02	7.00E+02	8.56E+02	7.00E+02
	MAE	8.08E+02	6.59E+02	8.08E+02	6.59E+02
	Slope est.	0.7123	0.8356	0.7186	0.8421
	95CI - Low	0.4761	0.5427	0.4806	0.5475
	95CI - Upp	0.9486	1.1285	0.9566	1.1366
	Slope StdErr	0.08509	0.1055	0.08573	0.1061
33 mg/kg	R^2	0.677	0.743	0.679	0.747
	SSE	1.57E+08	9.38E+07	1.51E+08	9.03E+07
	RMSE	1.62E+03	1.25E+03	1.59E+03	1.23E+03
	MAE	1.41E+03	1.01E+03	1.38E+03	9.88E+02
	Slope est.	0.6387	0.6329	0.6441	0.6379
	95CI - Low	0.5694	0.5808	0.5745	0.5854
	95CI - Upp	0.708	0.6849	0.7137	0.6903
	Slope StdErr	0.03267	0.02456	0.03285	0.02474
100 mg/kg	R^2	0.643	0.666	0.647	0.671
	SSE	4.59E+08	2.65E+08	4.34E+03	2.49E+08
	RMSE	3.91E+03	2.97E+03	3.81E+03	2.88E+03
	MAE	3.47E+03	2.63E+03	3.36E+03	2.55E+03
	Slope est.	0.7462	0.8785	0.7526	0.8852
	95CI - Low	0.6148	0.7296	0.6199	0.7351
	95CI - Upp	0.8775	1.0275	0.8854	1.0354
	Slope StdErr	0.04731	0.05366	0.04782	0.05409

Experimental value for rabbit B:P value 0.91 and Fup = 0.02 used;

SS CL Single-species scaled Clearance
LBF CL Liver Blood Flow Clearance
R2 R-squared
SSE Sum of the squared error
RMSE Residual mean sum of errors
MAE Mean average error
95%CI 95% Confidence Interval (upper and lower)

5.9.6. Sparfloxacin Rabbit Physiological PBPK – using Observed Clearance and Measured Heart Kp

The process of PBPK simulations was repeated using the upper and lower observed rabbit NCA clearances values (GastroPlus™, PKPlus™) determined as 10.7 L/h from 33 mg/kg and from the 2-compartmental fit 6.06 L/h from 33 mg/kg. Clearance was not calculated from 16 and 100 mg/kg due to just the infusion profile and estimated value of 24.5 and 21.1 L/h, which are greater than twice LBF and not physiologically plausible. The observed clearance from 33 mg/kg was used as the full plasma-concentration time course describes the drug clearance.

A fixed logP value of -0.0605 from Biobyte with experimental blood:plasma ratio (B:P) value 1.80 and fraction unbound in the plasma (fu_p) 0.506 were used to generate the tissue partition coefficients (Kps) in the rabbit (values as presented in previous Table 5.6). In this instance the observed upper and lower mean measured heart tissue:plasma ratios were used as the heart partition coefficient values of 6.95 and 4.73 (compared to in silico determined 21), with the regression analysis of fit given for each PBPK simulation (Table 5.7). According to the R-squared values the goodness of fit reduced for 16 and 100 mg/kg (0.359 – 0.430) and improved for 33 mg/kg (0.644 – 0.837), yet visually the 95% confidence interval band encompasses the observed plasma profile (Figures 5.9 to Figure 5.11).

The subsequent simulated mean heart concentration-time profile and 95% confidence were plotted against the range of tissue concentration data from the replicate analysis with error bars. It can be seen from these graphical representations against the actual observed plasma and heart concentration-time data that the 95% confidence interval of the predicted plasma profile encompasses all of the observed data points albeit with limited actual heart concentration data Figures 5.9 to Figure 5.11. From the regression analysis the lower observed clearance value (6.06 L/h) provides a better fit based on the slope estimate for observed vs predicted at or near unity, yet there is no distinction between the observed measured heart Kp values.

Table 5.7 Sparfloxacin Rabbit PBPK: Regression Analysis of Fit Determined using Observed Rabbit Clearance and Heart Tissue Partition Coefficients (Kp)

Observed Clearance in Rabbit (L/h)		Upper Clearance (L/h)		Lower Clearance (L/h)	
		10.72		6.06	
Measured Observed Heart : Plasma Kp		Upper Heart Kp	Lower Heart Kp	Upper Heart Kp	Lower Heart Kp
		6.95	4.73	6.95	4.73
Dose		**Regression Analysis of Fit**			
16 mg/kg	R^2	0.43	0.428	0.59	0.589
	SSE	3.42E+06	3.44E+06	1.02E+07	1.03E+07
	RMSE	3.38E+02	3.39E+02	5.83E+02	5.85E+02
	MAE	2.93E+02	2.94E+02	5.44E+02	5.46E+02
	Slope est.	1.7491	1.7544	1.005	1.0063
	95CI - Low	0.9732	0.9765	0.6272	0.6279
	95CI - Upp	2.525	2.5323	1.3829	1.3847
	Slope StdErr	0.2795	0.2802	0.1361	0.1363
33 mg/kg	R^2	0.837	0.836	0.798	0.798
	SSE	3.59E+07	3.61E+07	6.02E+07	6.05E+07
	RMSE	7.74E+02	7.75E+02	1.00E+03	1.00E+03
	MAE	6.94E+02	6.95E+02	7.94E+02	7.96E+02
	Slope est.	0.6817	0.681	0.6327	0.6319
	95CI - Low	0.5905	0.5895	0.5817	0.5809
	95CI - Upp	0.7729	0.7724	0.6837	0.6829
	Slope StdErr	0.04303	0.04314	0.02406	0.02407
100 mg/kg	R^2	0.385	0.383	0.671	0.67
	SSE	1.50E+08	1.50E+08	1.54E+08	1.56E+03
	RMSE	2.24E+03	2.24E+03	2.27E+03	2.28E+03
	MAE	1.80E+03	1.80E+03	2.00E+03	2.01E+03
	Slope est.	1.8567	1.8623	1.0605	1.0619
	95CI - Low	1.3993	1.4037	0.8701	0.8712
	95CI - Upp	2.3142	2.321	1.2508	1.2526
	Slope StdErr	0.1648	0.1652	0.06857	0.06868

Experimental value for rabbit B:P value 0.91 and Fup = 0.02 used;
SS CL Single-species scaled Clearance
LBF CL Liver Blood Flow Clearance
R2 R-squared
SSE Sum of the squared error
RMSE Residual mean sum of errors
MAE Mean average error
95%CI 95% Confidence Interval (upper and lower)

Figure 5.9 Sparfloxacin Rabbit PBPK: Simulated Plasma and Heart Concentration-Time Profile of Sparfloxacin in the Rabbit Following a 60 Minute Intravenous Infusion Administration of Sparfloxacin at 16 mg/kg

a) Plasma

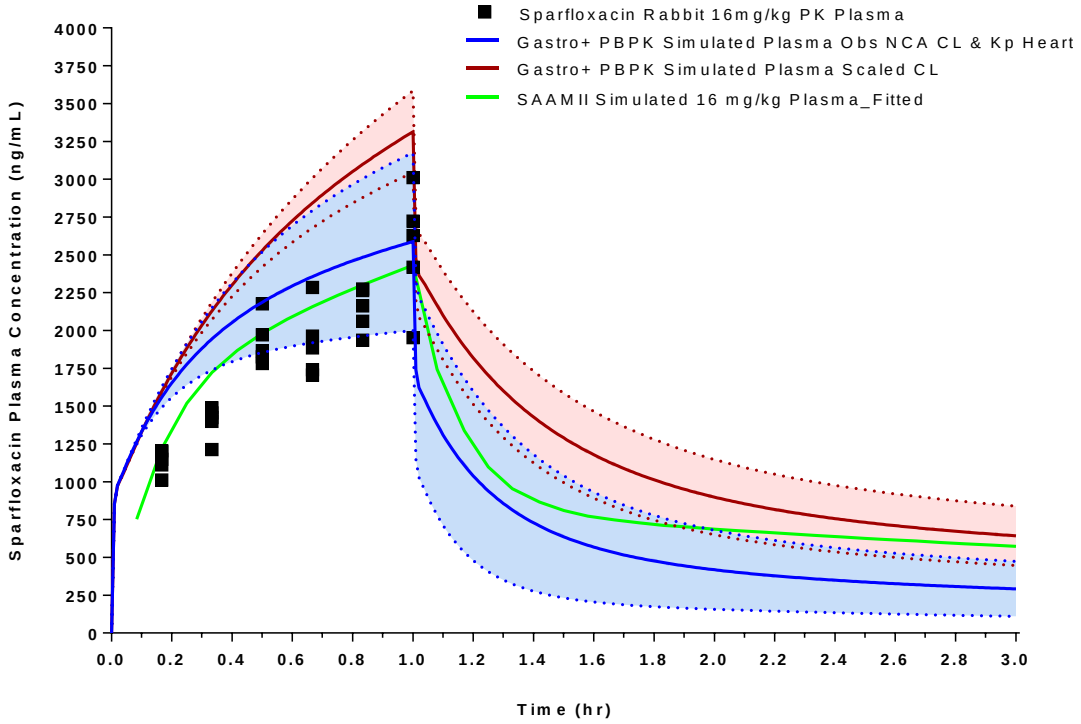

b) Heart

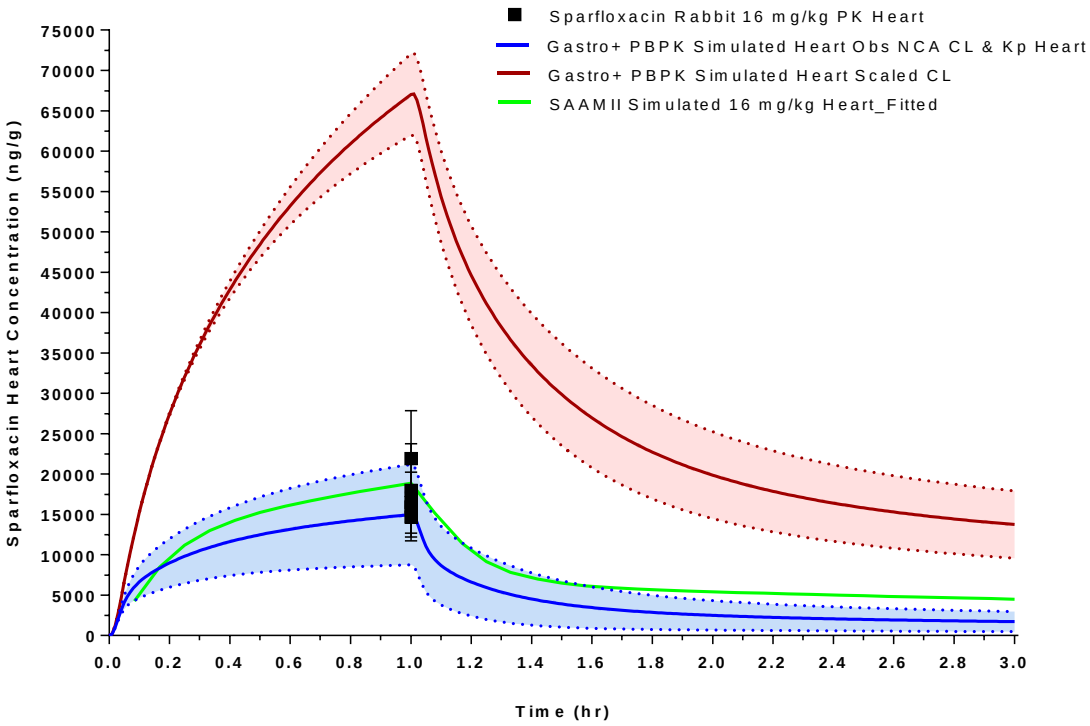

Figure 5.9: Graph of the individual plasma (a) and heart (b) concentration-time profile with observed data points (■) following a single intravenous infusion administration of sparfloxacin at 16 mg/kg to female rabbits and the predicted concentration-time using GastroPlus PBPK model with Scaled Clearance and LogP (—) or Observed Clearance and measured Heart Kp (—) with 95% confidence interval in shaded area and SAAMII semi-PBPK model (—) fitted compartmental analysis

Figure 5.10 Sparfloxacin Rabbit PBPK: Simulated Plasma and Heart Concentration-Time Profile of Sparfloxacin in the Rabbit Following a 60 Minute Intravenous Infusion Administration of Sparfloxacin at 33 mg/kg

a) Plasma

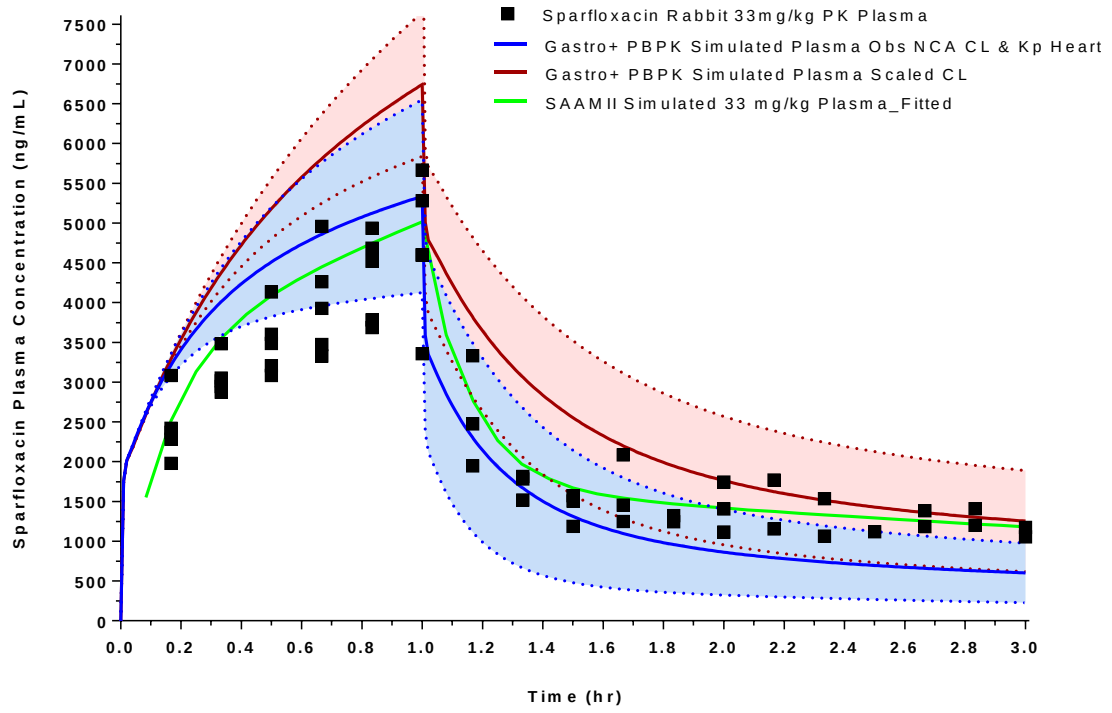

b) Heart

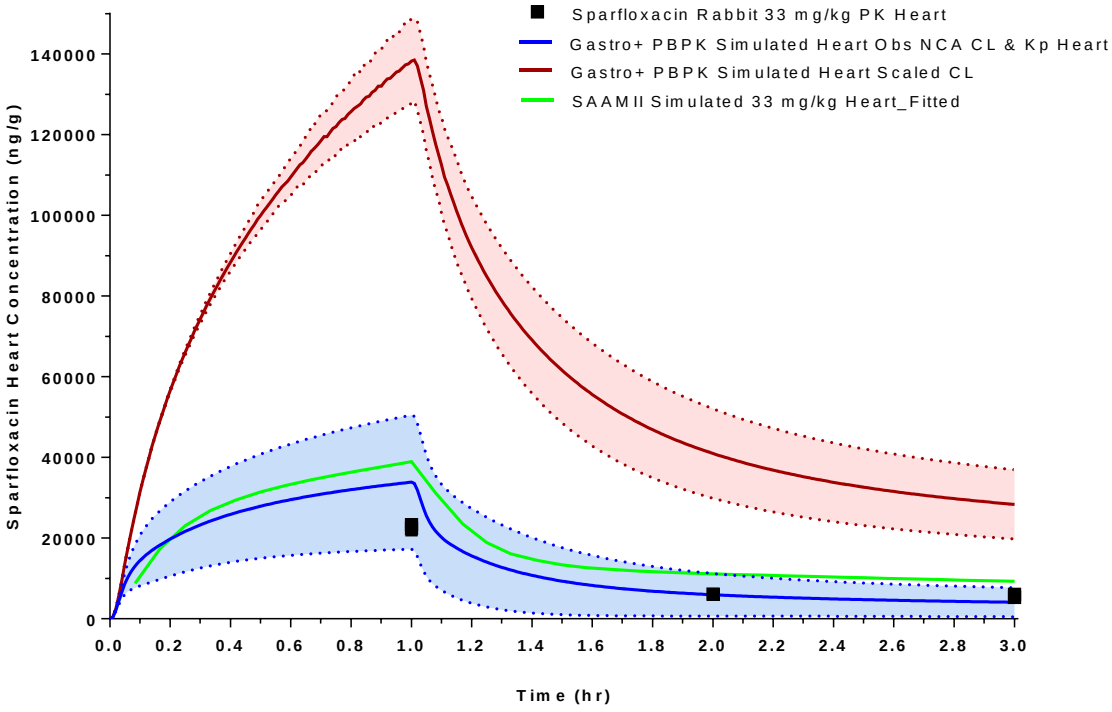

Figure 5.10: Graph of the individual plasma (a) and heart (b) concentration-time profile with observed data points (■) following a single intravenous infusion administration of sparfloxacin at 33 mg/kg to female rabbits and the predicted concentration-time using GastroPlus PBPK model with Scaled Clearance and LogP (—) or Observed Clearance and measured Heart Kp (—) with 95% confidence interval in shaded area and SAAMII semi-PBPK model (—) fitted compartmental analysis

Figure 5.11 Sparfloxacin Rabbit PBPK: Simulated Plasma and Heart Concentration-Time Profile of Sparfloxacin in the Rabbit Following a 60 Minute Intravenous Infusion Administration of Sparfloxacin at 100 mg/kg

a) Plasma

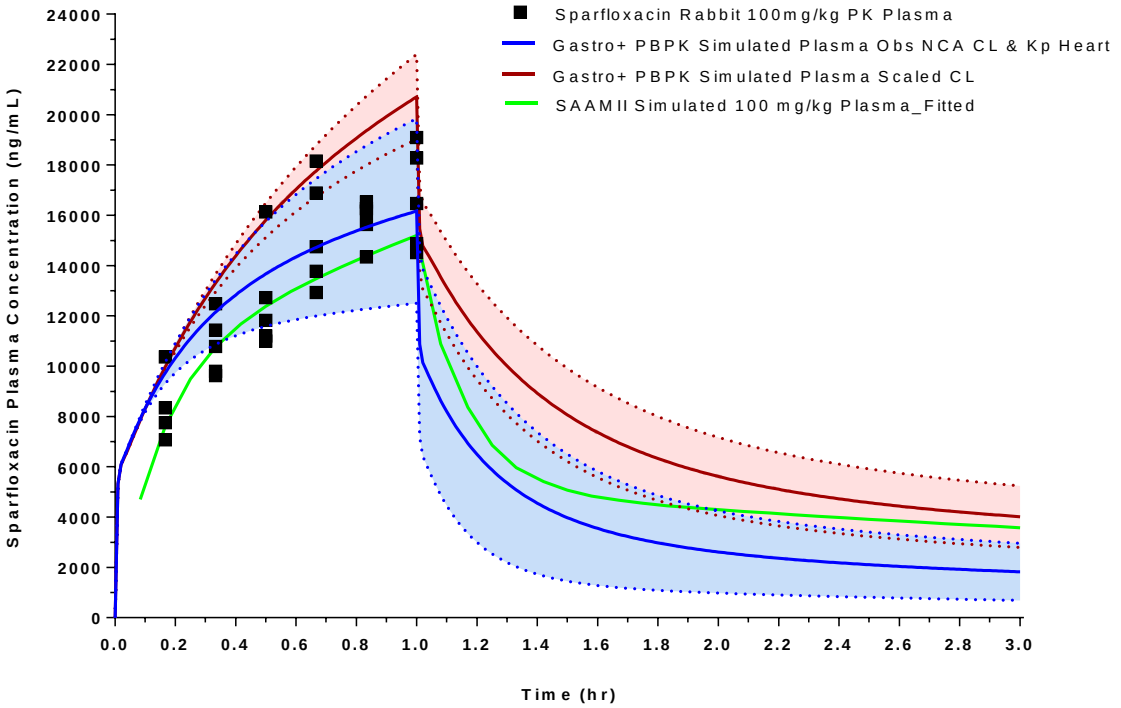

b) Heart

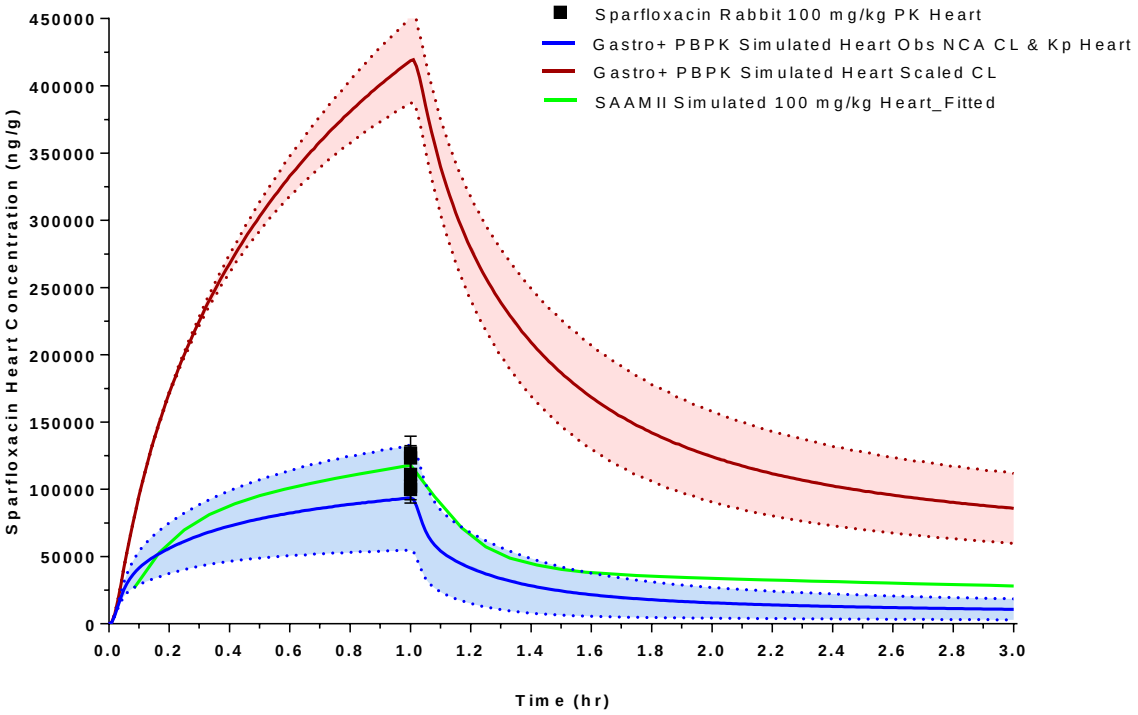

Figure 5.11: Graph of the individual plasma (a) and heart (b) concentration-time profile with observed data points (■) following a single intravenous infusion administration of sparfloxacin at 100 mg/kg to female rabbits and the predicted concentration-time using GastroPlus PBPK model with Scaled Clearance and LogP (—) or Observed Clearance and measured Heart Kp (—) with 95% confidence interval in shaded area and SAAMII semi-PBPK model (—) fitted compartmental analysis

5.9.7. Sparfloxacin Rabbit PBPK/PD

These simulated rabbit heart concentrations were corrected to free concentrations using the experimental fraction unbound in heart tissue (fu_t = 0.081) and converted to µM to predict the associated change in QTc prolongation from the E_{max} equation 22 (Figure 5.12). This figure shows that the simulated PBPK/PD using the scaled clearance over predicted maximal change in dQTc due to over prediction of the heart concentrations compared to using the observed clearance. The predicted concentration-dQTc using the observed clearance in the PBPK/PD model provides a reasonable approximation of the observed vehicle-baseline corrected QTc (ddQTc) in the anaesthetised rabbit and similar to the fitted semi-PBPK compartmental model.

Figure 5.12 Sparfloxacin Rabbit PBPK/PD: Simulated Free Heart Concentration-dQTc Profile of Sparfloxacin in the Rabbit

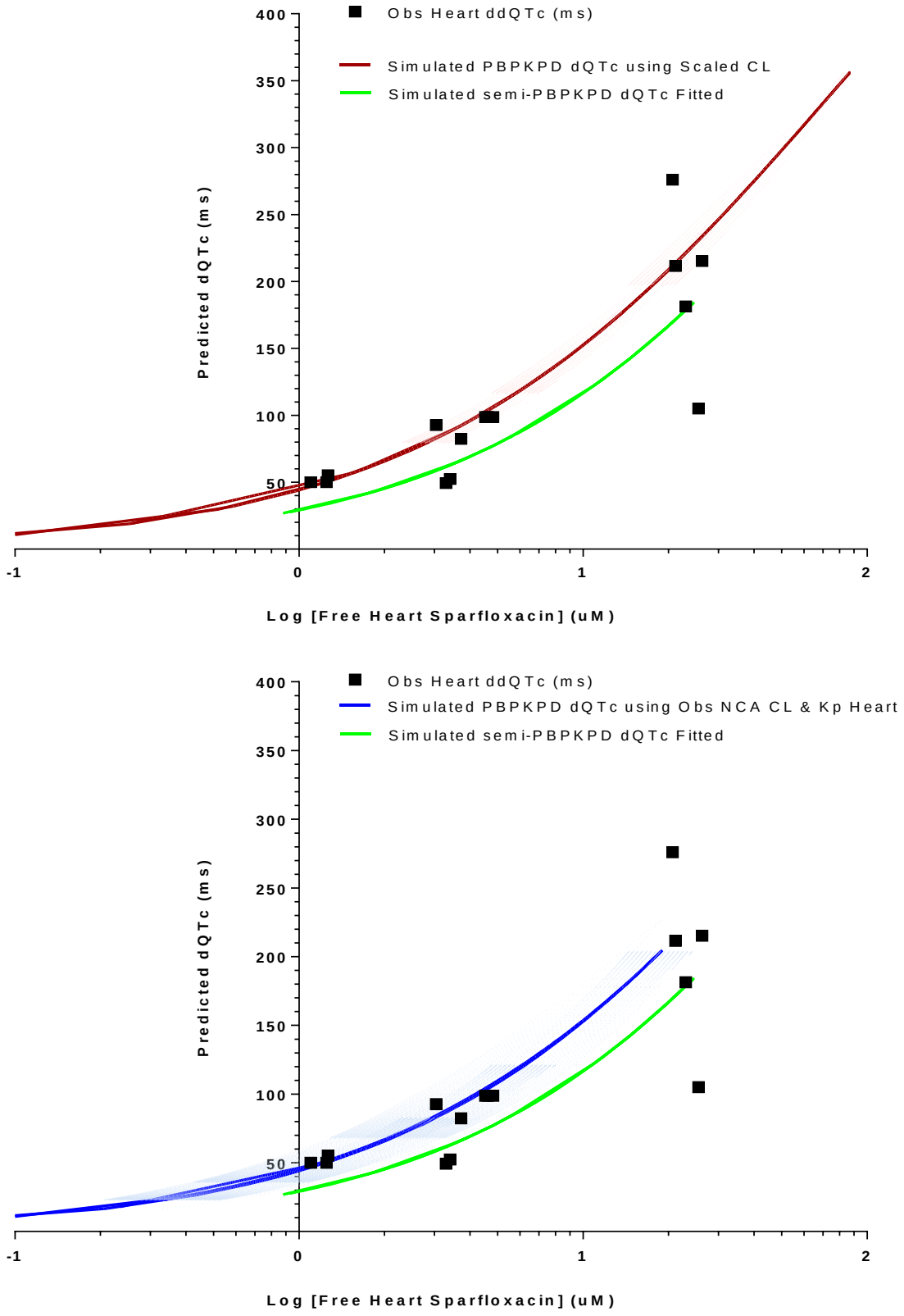

Figure 5.12: Graph of the individual heart concentration-dQTc response profile with observed data points (■) following a single intravenous infusion administration of sparfloxacin to female rabbits and the predicted concentration-dQTc response using GastroPlus PBPK/PD model with Scaled Clearance and LogP (—) or Observed Clearance and measured Heart Kp (—) with ±SD error bars in shaded area (pink and blue) and SAAMII semi-PBPK model (—) fitted compartmental analysis

5.10. Moxifloxacin In Vivo Modelling Results

5.10.1. Moxifloxacin: Rat

Following a single intravenous dose at a nominal dose of 10 mg/kg of moxifloxacin to female rats the mean volume of distribution was approximately 5.6 L/kg which indicates distribution through total body water and into tissues, and is considered moderate (1-10 L/kg) (Table 78). The mean plasma clearance of moxifloxacin was 1.2 L/h, which is approximately 100% liver blood flow (LBF) in the rat compared to the moderate 55% published value (Siefert et al., 1999b; Wang et al., 2014) (Table 5.14). The terminal half-life following an intravenous bolus administration was also short at less than 1 hour and in agreement with the 1.2 hour published. Following intravenous and oral radioactive whole-body distribution studies in the rat high levels of tissue penetration relative to blood were demonstrated and parallel concentration-time courses of moxifloxacin in plasma and lung were observed (Siefert et al., 1999b).

5.10.2. Moxifloxacin : Rabbit

Following intravenous infusion of 5 and 20 mg/kg over 30 minutes in the anaesthetised rabbit, parameters were obtained for volume of distribution (1.6 - 2.6 L/kg), total clearance (0.62 – 1.3 L/h) and half-life (1 hour) that were comparable to 1.95 - 2.1 L/kg and 1.8 – 2.2 hour, respectively (Fernandez-Varon et al., 2005; Carceles et al., 2006). These parameters in the rabbit are similar and consistent across species for tissue distribution and clearance (Table 5.14), with lowest values for human and dog, as total body clearance decreases with size (Siefert et al., 1999a). A study into the treatment of meningitis gave 10, 20 and 40 mg/kg intravenously in the rabbit, and identified parallel elimination of moxifloxacin from serum and cerebrospinal fluid (CSF), with half-life quoted as 1.1, 1.37 and 1.35 hours, at each dose respectively (Østergaard et al., 1998).

5.10.3. Moxifloxacin: Scaling

Moxifloxacin CL_p was high in the rat (100% LBF) compared to the moderate reported value (55%). The resulting scaled clearance from rat was classified as high using both single-species (SS = 7.66 L/h, 73%) and liver blood flow (LBF = 12.23 L/h, 100%). Both scaled clearance values were notably (5 to 10-fold) greater than the observed rabbit clearances determined from 5 and 20 mg/kg, which was considered low, approximately 10% LBF (1.287 and 0.618 L/h) and comparable to published data.

5.10.4. Moxifloxacin Rat Physiological PBPK

Tissue partition coefficients (Kps) were generated within GastroPlus™ based upon the Lucakova method described. Four different logP values obtained from in silico (ADMET and Biobyte) and measured CHI (logK(IAM) and log(CHIN)) were used with experimental blood:plasma ratio (B:P) value 1.45 and fraction unbound in the plasma (fu_p) 0.574 in the rat.

The range of logP values from 0.0932 ADMET, -0.082 Biobyte and 5.421 logK(IAM) and 0.873 log(CHIN), provided different tissue coefficients (primary difference due to the larger logP value from logK(IAM). However each of the goodness of fit provided by R-squared values (0.488 – 0.548) indicates a poor simulation of the predicted rat PBPK as shown in Figure 5.13 and Table 5.8. The simulated predictions with each logP value were plotted together as a mean and 95% confidence interval band. The graphical representation demonstrates that the simulated fit describes the initial time-course and terminal phase of the rat intravenous profile and under predicts the distributional phase, where the 95% confidence interval is greatest, a result of the differing logP values.

The NCA derived clearance of 1.392 L/h was used in the rat PBPK model and it was also used for single-species and liver blood flow scaling to the rabbit.

Figure 5.13 Moxifloxacin Rat PBPK: Simulated Plasma Concentration-Time Profile of Moxifloxacin in Female Rats Following a Single Intravenous Administration of Moxifloxacin at 10 mg/kg

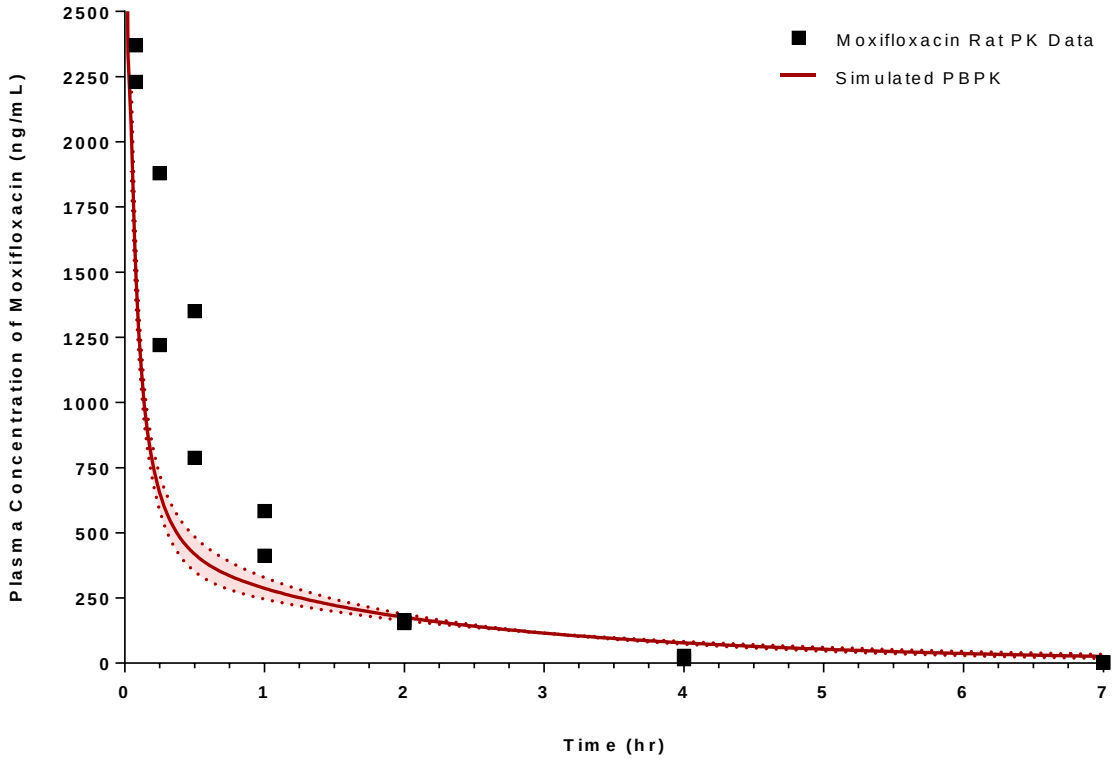

Figure 5.13: Graph of the individual plasma concentration-time profile data points (■) following a single intravenous bolus administration of moxifloxacin at 10 mg/kg to three female rats and the simulated concentration-time using PBPK (—)

Table 5.8 Moxifloxacin Rat PBPK: In Silico Determination of Tissue Partition Coefficients (Kp) in the Rat using different Log P values

LogP	ADMET™	Biobyte™	logK(IAM)	Adj. log(CHIN)
	0.0932	-0.082	5.421	0.873
Tissue				
Lung	19.46	19.46	21.57	19.48
Adipose	2.04	2.03	67.70	2.20
Muscle	7.89	7.88	9.47	7.90
Liver	22.57	22.57	22.03	22.56
Spleen	15.90	15.90	13.62	15.88
Heart	11.39	11.39	13.46	11.41
Brain	47.10	47.10	49.27	47.12
Kidney	24.88	24.89	22.46	24.86
Skin	6.81	6.81	15.79	6.89
ReproOrg	24.88	24.89	22.46	24.86
Red Marrow	3.54	2.53	13.51	3.62
Yellow Marrow	2.04	2.03	67.60	2.20
Rest of Body	15.90	15.90	13.62	15.88
R-squared (R^2)	0.548	0.548	0.488	0.547

Table 5.8: Tissue partition coefficients (Kps) in the rat using different logP values derived from ADMET, Biobyte, logK(IAM) and adjusted log(CHIN) with experimental value for rat B:P value 1.45 used and Fup = 0.574; and NCA derived clearance of 1.392 L/h

5.10.5. Moxifloxacin Rabbit Physiological PBPK – using Scaled Clearance and logP range

Scaled clearance values were determined from the rat observed 1.392 L/h non-compartmental analysis (NCA) data using single-species (SS = 7.66 L/h) and liver blood flow (LBF = 12.23 L/h) scaling methods previously described (Table 5.9).

Tissue partition coefficients (Kps) were generated within GastroPlus™ using the upper and lower logP values (-0.082 and 5.421 obtained from Biobyte and logK(IAM) with experimental blood:plasma ratio (B:P) value 1.22 and fraction unbound in the plasma (fu_p) 0.562 in the rabbit. The PBPK simulations were carried out for doses of moxifloxacin at 5 and 20 mg/kg following 30 minute intravenous infusion, with the regression analysis of fit given for each. The R-squared values indicate a relatively poor fit using both logP values and scaled clearance methods (0.504 to 0.565), however based on the slope estimate of observed vs predicted being closer to unity single-species scaled clearance simulation fitted better with the Biobyte LopP, than LBF scaled, whilst 5 mg/kg fitted better than 20 mg/kg using either clearance value. The simulated scaled clearance predictions with each logP value were plotted together as a mean and 95% confidence interval band in Figures 5.14 and Figure 5.15 (plasma and heart at 5 mg/kg and 20 mg/kg). It can be seen from these graphical representations against the actual observed plasma concentration-time data that the simulated plasma profile under-predicts during the infusion period (within a 2-fold) and the whole profile but with a correct overall shape (observed vs predicted). The subsequent derived simulated mean and 95% confidence heart concentration-time profile was plotted against the range of tissue concentration data from the replicate analysis with error bars. The simulated heart concentrations from scaled clearance with the heart Kp value (9.23 – 12.91) under predicts the overall profile but is approximately similar to the observed (within 2-fold) Figures 5.14 and Figure 5.15.

Table 5.9 Moxifloxacin Rabbit PBPK: In Silico Determination of Tissue Partition Coefficients (Kp) using different Log P values in the Rabbit, with Scaled Clearance and Predicted Regression Analysis of Fit against Observed

Log P		Biobyte		Adj. logK(IAM)	
		-0.082		5.421	
Clearance		SS CL	LBF CL	SS CL	LBF CL
		CL=7.66 L/h	CL=12.23 L/h	CL=7.66 L/h	CL=12.23 L/h
Tissue					
Lung		15.69		15.23	
Adipose		1.67		25.76	
Muscle		6.41		9.86	
Liver		18.21		23.67	
Spleen		12.85		15.93	
Heart		9.23		12.91	
Brain		2.06		12.59	
Kidney		20.04		22.64	
Skin		5.57		10.04	
ReproOrg		20.04		22.64	
Red Marrow		2.90		14.63	
Yellow Marrow		1.67		25.76	
Rest of Body		12.85		15.93	
Dose		Regression Analysis of Fit			
5 mg/kg	R^2	0.545	0.513	0.525	0.504
	SSE	1.13E+08	1.60E+08	1.33E+08	1.74E+08
	RMSE	1.25E+03	1.49E+03	1.36E+03	1.55E+03
	MAE	1.18E+03	1.41E+03	1.28E+03	1.47E+03
	Slope est.	1.0686	1.2356	1.1884	1.3406
	95CI - Low	0.8958	0.9708	0.9805	1.0367
	95CI - Upp	1.2414	1.5003	1.3963	1.6445
	Slope StdErr	0.08153	0.1249	0.09806	0.1433
20 mg/kg	R^2	0.564	0.523	0.54	0.513
	SSE	1.45E+09	2.13E+09	1.72E+09	2.31E+09
	RMSE	4.48E+03	5.44E+03	4.88E+03	5.67E+03
	MAE	4.25E+03	5.18E+03	4.65E+03	5.40E+03
	Slope est.	0.9599	1.0914	0.9578	1.091
	95CI - Low	0.7643	0.7945	0.7627	0.7942
	95CI - Upp	1.1554	1.3882	1.1529	1.3878
	Slope StdErr	0.09224	0.14	0.09204	0.14

Experimental value for rabbit B:P value 1.22 and Fup = 0.562 used;
SS CL Single-species scaled Clearance
LBF CL Liver Blood Flow Clearance
R2 R-squared
SSE Sum of the squared error
RMSE Residual mean sum of errors
MAE Mean average error
95%CI 95% Confidence Interval (upper and lower)

5.10.6. Moxifloxacin Rabbit Physiological PBPK – using Observed Clearance and Measured Heart Kp

The process of PBPK simulations was repeated using the two observed rabbit NCA clearances values (GastroPlus™, PKPlus™) from 5 and 20 mg/kg dose level determined as 0.681 and 1.287 L/h.

A fixed logP value of -0.082 from Biobyte with experimental blood:plasma ratio (B:P) value 1.22 and fraction unbound in the plasma (fu_p) 0.562 were used to generate the tissue partition coefficients (Kps) in the rabbit (values as presented in previous Table 5.9). In this instance the observed upper and lower mean measured heart tissue:plasma ratios were used as the heart partition coefficient values of 10.72 and 8.80 (compared to in silico determined 9.23 – 12.91), with the regression analysis of fit given for each PBPK simulation (Table 5.10). The R-squared values indicated an improved fit using observed clearance and measured heart Kp (0.622 to 0.783). The simulated scaled clearance predictions were plotted together as a mean and 95% confidence interval band in Figures 5.14 and Figure 5.15 (plasma and heart at 5 mg/kg and 20 mg/kg). It can be seen from these graphical representations against the actual observed plasma concentration-time data that the plasma profile provides a better prediction during the infusion period and maintains the overall shape of the elimination curve with a narrow confidence interval. The slope of observed vs predicted was close to unity for all clearance and Kp combinations, with the upper clearance (1.287 L/h) and lower Kp (8.80) analysis parameters indicating the best fit. The resultant simulated mean heart concentration-time profile and 95% confidence were plotted against the range of tissue concentration data from the replicate analysis with error bars. The simulated heart concentrations from observed clearance with the measured heart Kp value (8.80 – 10.72) provides a good approximation of the tissue profile, with a slight under prediction of tissue concentration at the end Figures 5.14 and Figure 5.15.

Table 5.10 Moxifloxacin Rabbit PBPK: Regression Analysis of Fit Determined using Observed Rabbit Clearance and Heart Tissue Partition Coefficients (Kp)

Observed Clearance in Rabbit (L/h)		Upper Clearance (L/h)		Lower Clearance (L/h)	
		1.287		0.618	
Measured Observed Heart : Plasma Kp		Upper Heart Kp	Lower Heart Kp	Upper Heart Kp	Lower Heart Kp
		10.72	8.80	10.72	8.80
Dose		**Regression Analysis of Fit**			
5 mg/kg	R^2	**10.72**	**8.8**	**10.72**	**8.8**
	SSE	0.627	0.629	0.622	0.625
	RMSE	3.01E+07	2.99E+07	2.46E+07	2.44E+07
	MAE	6.47E+02	6.45E+02	5.85E+02	5.82E+02
	Slope est.	1.0776	1.0741	1.1093	1.1056
	95CI - Low	0.8932	0.8911	0.8853	0.8835
	95CI - Upp	1.2621	1.257	1.3333	1.3278
	Slope StdErr	0.08701	0.08632	0.1057	0.1048
20 mg/kg	R^2	0.75	0.753	0.781	0.783
	SSE	2.32E+08	2.30E+08	1.60E+08	1.58E+08
	RMSE	1.79E+03	1.79E+03	1.49E+03	1.48E+03
	MAE	1.46E+03	1.45E+03	1.06E+03	1.06E+03
	Slope est.	1.0238	1.0201	1.0653	1.0616
	95CI - Low	0.92	0.9172	0.9368	0.9343
	95CI - Upp	1.1276	1.123	1.1939	1.1888
	Slope StdErr	0.04895	0.04855	0.06063	0.06003

Experimental value for rabbit B:P value 1.22 and Fup = 0.562 used;

SS CL Single-species scaled Clearance
LBF CL Liver Blood Flow Clearance
R2 R-squared
SSE Sum of the squared error
RMSE Residual mean sum of errors
MAE Mean average error
95%CI 95% Confidence Interval (upper and lower)

Figure 5.14 Moxifloxacin Rabbit PBPK: Simulated Plasma and Heart Concentration-Time Profile of Moxifloxacin in the Rabbit Following a 30 Minute Intravenous Infusion Administration of Moxifloxacin at 5 mg/kg

a) Plasma

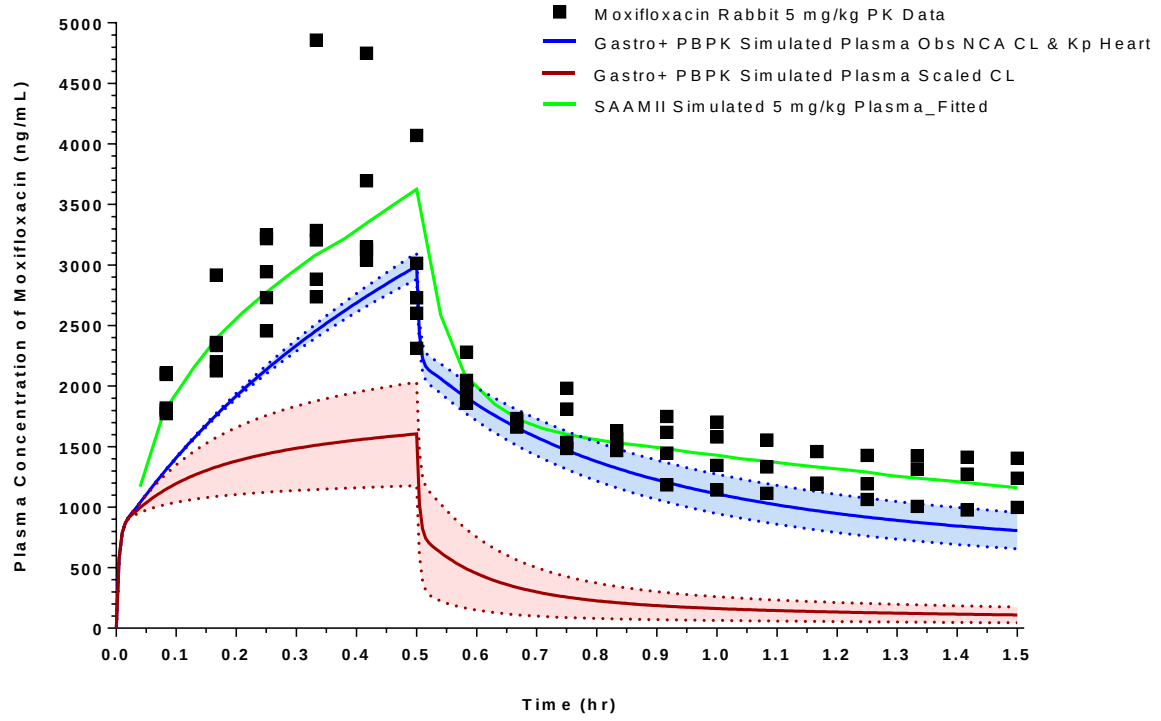

b) Heart

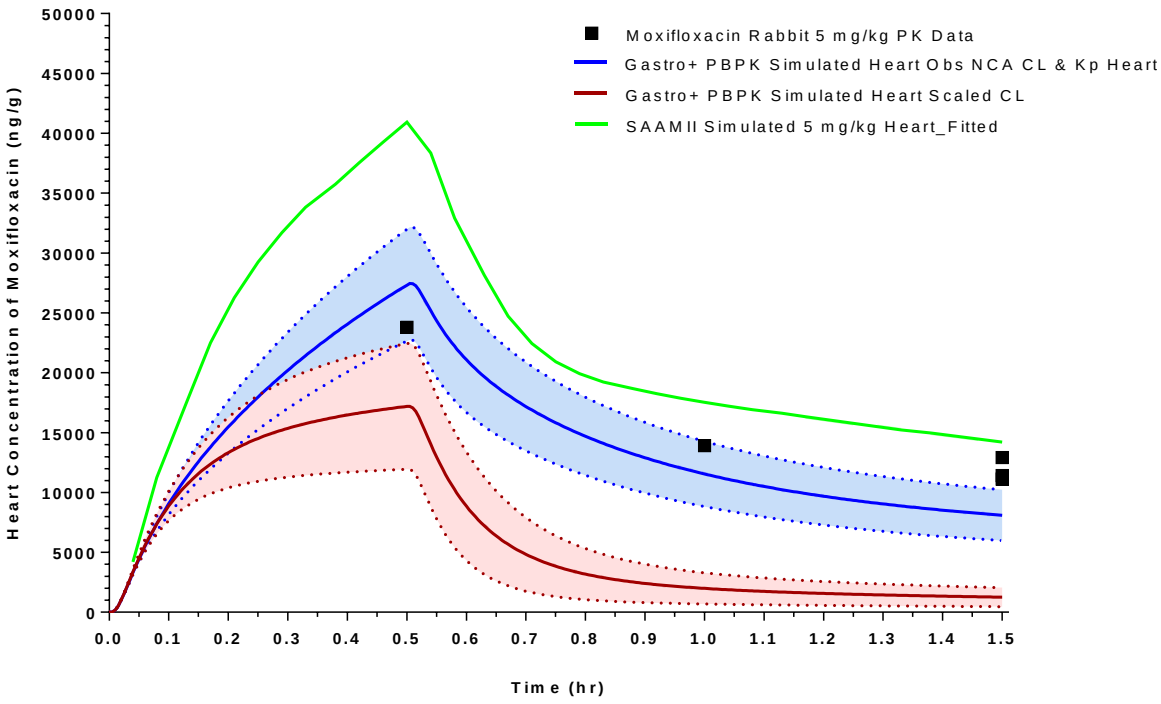

Figure 5.14: Graph of the individual plasma (a) and heart (b) concentration-time profile with observed data points (■) following a single intravenous bolus administration of moxifloxacin at 5 mg/kg to female rabbits and the predicted concentration-time using GastroPlus PBPK model with Scaled Clearance and LogP (—) or Observed Clearance and measured Heart Kp (—) with 95% confidence interval in shaded area and SAAMII semi-PBPK model (—) fitted compartmental analysis

Figure 5.15 Moxifloxacin Rabbit PBPK: Simulated Plasma and Heart Concentration-Time Profile of Moxifloxacin in the Rabbit Following a 30 Minute Intravenous Infusion Administration of Moxifloxacin at 20 mg/kg

a) Plasma

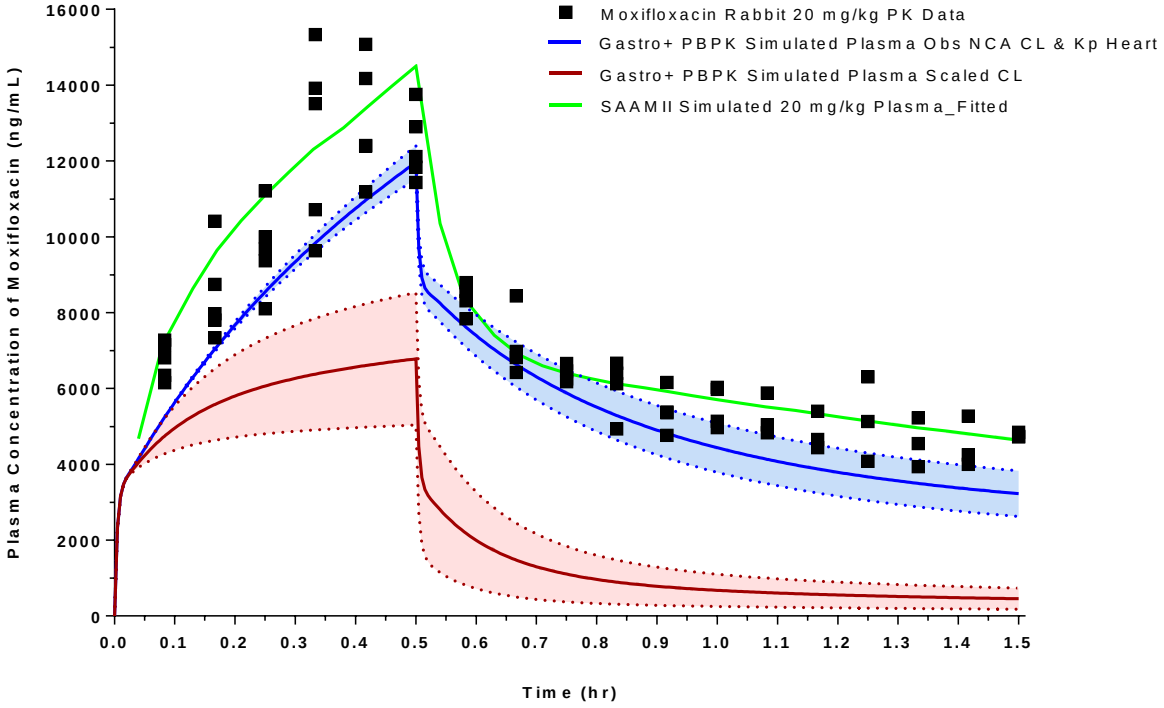

b) Heart

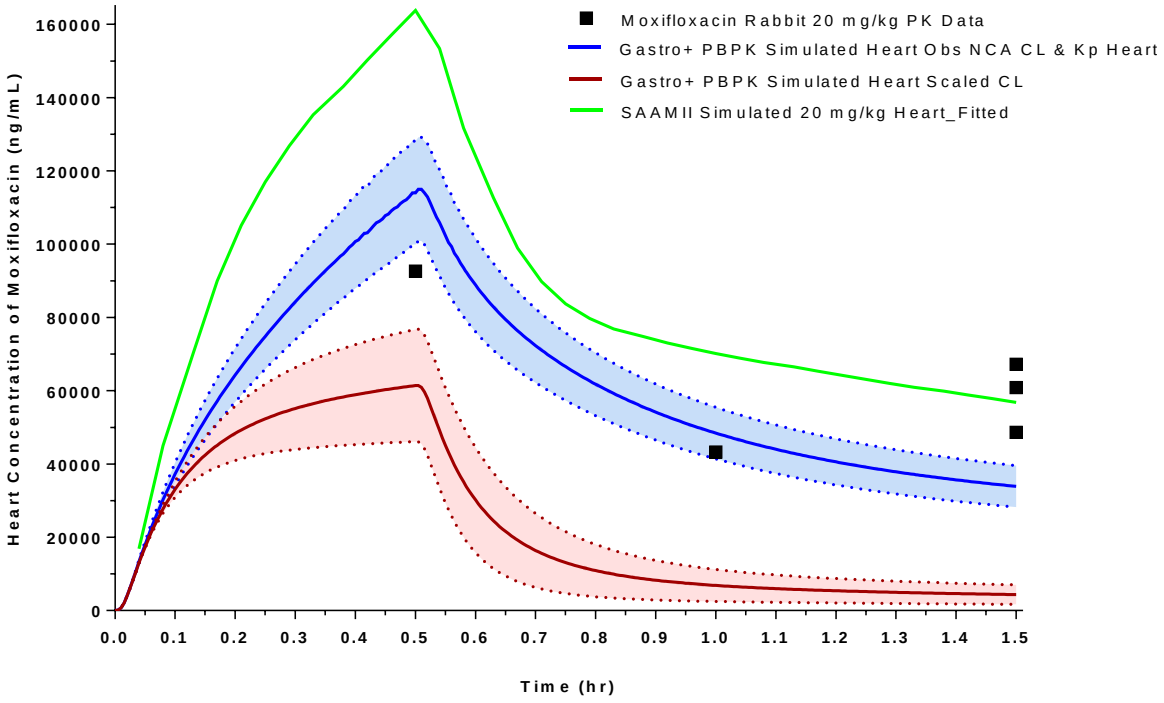

Figure 5.15: Graph of the individual plasma (a) and heart (b) concentration-time profile with observed data points (■) following a single intravenous bolus administration of moxifloxacin at 20 mg/kg to female rabbits and the predicted concentration-time using GastroPlus PBPK model with Scaled Clearance and LogP (—) or Observed Clearance and measured Heart Kp (—) with 95% confidence interval in shaded area and SAAMII semi-PBPK model (—) fitted compartmental analysis

5.10.7. Moxifloxacin Rabbit PBPK/PD

The simulated heart concentrations were again corrected to free concentrations using the experimental fraction unbound in heart tissue (fu_t = 0.12) and converted to µM to predict the associated change in QTc prolongation from the E_{max} equation (Figure 5.16). This plot shows that the simulated PBPK/PD provides an over-prediction of the predicted dQTc for heart tissue concentrations using both the scaled clearance and more so for the observed clearance against the observed vehicle-baseline corrected QTc (ddQTc) in the anaesthetised rabbit. This is a result of variability from the observed in vivo data compared to the ex vivo E_{max} response model generated and reflects the different concentration-response given using the fitted semi-PBPK compartmental model. The observed in vivo ddQTc values are variable in response for any similar tissue concentration. Also the E_{max} model employed will not predict a decrease in dQTc given that it is a function between a baseline and a maximum. The negative values are a result of the vehicle-baseline correction.

Figure 5.16 Moxifloxacin Rabbit PBPK/PD: Simulated Free Heart Concentration-dQTc Profile of Moxifloxacin in the Rabbit

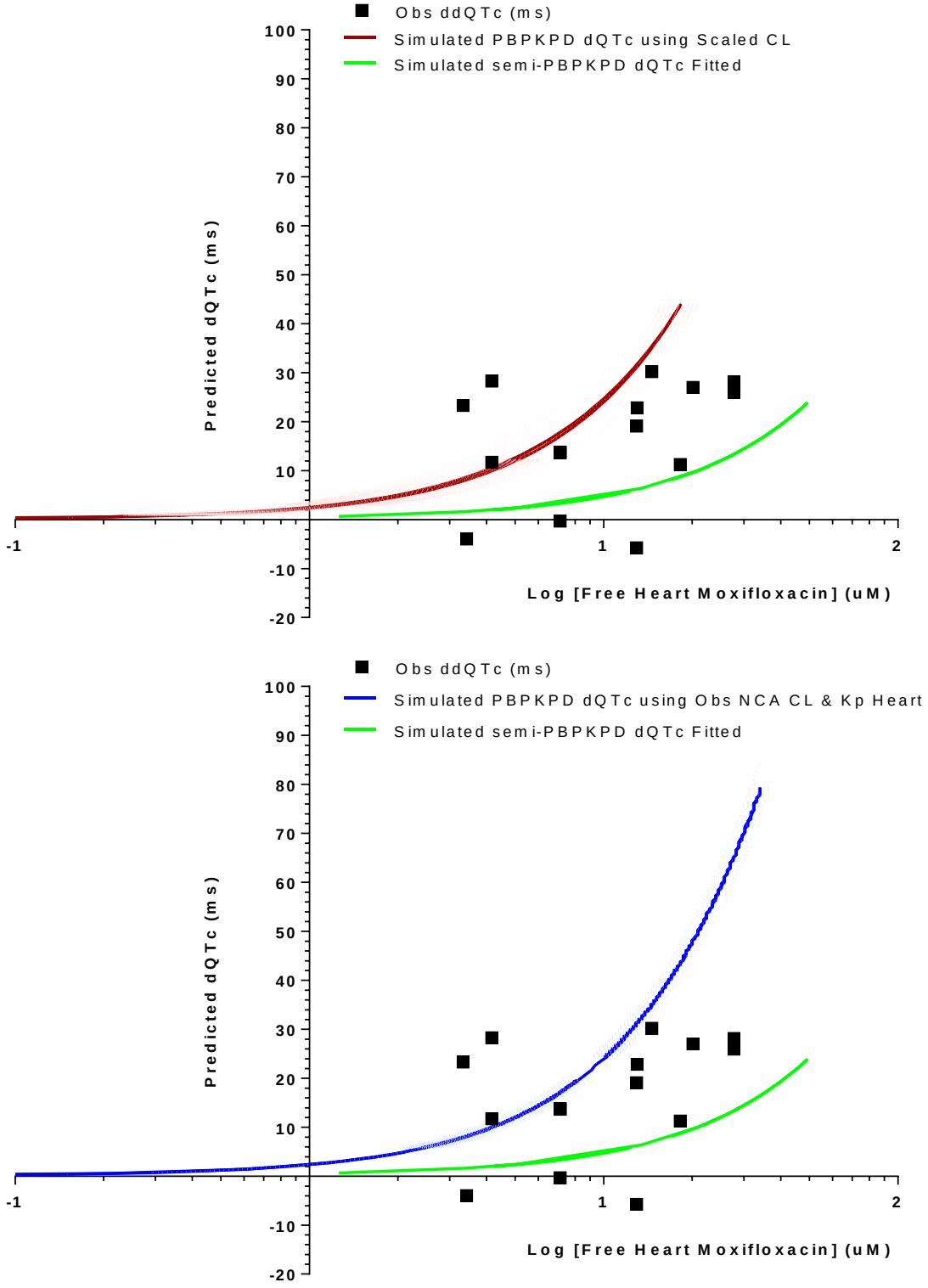

Figure 5.16: Graph of the individual heart concentration-dQTc response profile with observed data points (■) following a single intravenous infusion administration of moxifloxacin to female rabbits and the predicted concentration-dQTc response using GastroPlus PBPK/PD model with Scaled Clearance and LogP (—) or Observed Clearance and measured Heart Kp (—) with ±SD error bars in shaded area (pink or blue) and SAAMII semi-PBPK model (—) fitted compartmental analysis

5.11. Verapamil In Vivo Modelling Results and Discussion

5.11.1. Verapamil: Rat

Following a single intravenous dose at a nominal dose of 1 mg/kg of verapamil to female rats the mean volume of distribution was approximately 4 L/kg, which indicates distribution approximate to total body water and considered moderate (1-10 L/kg) (Table 5.14). The mean plasma clearance of verapamil was moderate at 0.6 L/h, approximately 50% liver blood flow (LBF) in the rat, a result similar to that published (0.6 – 0.8 L/kg) (Todd and Abernethy, 1987; Kataoka et al., 2016) (Table 5.14). The terminal half-life following an intravenous bolus administration was short at 1 hour.

5.11.2. Verapamil: Rabbit

Following intravenous infusion of 0.1, 0.3 and 1 mg/kg over 30 minutes in the anaesthetised rabbit, parameters were obtained for volume of distribution (0.7 L/kg), total clearance (3.5 L/h) and half-life (0.5 hour) were lower than published pharmacokinetic parameters in the rabbit (Table 5.14). From reported literature in the rabbit, the volume of distribution is greater, 8.1 to 16.8 L/kg, and clearance is at or above liver blood flow 13.5 to 21.9 L/hr (Giacomini et al., 1985; Mori et al., 2001). Giacomini et al. studied the PK and PD of verapamil enantiomers (d- and dl-) in conscious rabbits following a single intravenous dose of 0.8 mg/kg infused over 20 minutes. There was a bi-exponential decline in plasma concentrations with time and no differences observed in PK properties of either enantiomer; a profile similar to this study. There was a degree of inter-animal variability in the Giacomini et al. publication, such as one animal with Vd_{ss} (1.49 – 2.48) and half-life (0.2 – 0.75 hour) (Giacomini et al., 1985).

A difference in the pharmacokinetics and tissue distribution of verapamil has been studied between the non-pregnant and pregnant rabbits following verapamil intravenous bolus/infusion administration (Solans et al., 2000). The author describes that volume was significantly higher in the pregnant than in the non-pregnant rabbit, whilst half-life was significantly lower in the non-pregnant than in the pregnant rabbit. However, AUC and CL showed no significant differences between the pregnant and non-pregnant rabbit. When tissue concentrations were examined, it was found that in most of the tissues studied high concentrations of verapamil were found both in the pregnant and non-pregnant rabbit. Furthermore, verapamil concentrations in the uterus, heart, spleen and kidney were significantly higher in the non-pregnant than in the pregnant rabbit, such that in the heart the

tissue-to-blood ratio for non-pregnant, pregnant and foetus was 20-, 9-, and 7-fold, respectively. This finding is near to the observed tissue to plasma ratio of 7-8-fold following 0.1 and 0.3 mg/kg.

5.11.3. Verapamil: Scaling

Verapamil CL_p was moderate in the rat (50% LBF) and was comparable to the published range observed. The resulting scaled clearance from rat was moderate using both single-species (SS = 3.14 L/h, 30%) and liver blood flow (LBF = 5.00 L/h, 48%). Both scaled clearance values were approximate to the observed rabbit clearance as determined from 0.1, 0.2 and 1 mg/kg, which was also moderate at 20-33% LBF (2.34 and 4.45 L/h). However the scaled and observed clearances were less than the reported clearance in the rabbit which was equivalent to LBF.

5.11.4. Verapamil Rat Physiological PBPK

Tissue partition coefficients (Kps) were generated within GastroPlus™ based upon the Lucakova method described. For verapamil, four different logP values obtained from in silico (ADMET and Biobyte) and measured CHI (logK(IAM) and log(CHIN)) were used with experimental blood:plasma ratio (B:P) value 0.68 and fraction unbound in the plasma (fu_p) 0.071 in the rat.

The range of logP values from the in silico 4.45 ADMET and 4.47 Biobyte to the measured 3.59 logK(IAM) and3.69 log(CHIN), provided little difference in tissue coefficients, with the exception of adipose and yellow marrow. This is a result of verapamil being basic and its interaction with the tissue phospholipids as defined by the single-Rodgers equation by Lukacova in GastroPlus™ (Equation 19). Each respective log P simulation provided similar R-squared goodness of fit values (0.865 – 0.935) that indicated a good simulation of the predicted rat PBPK as shown in Figure 5.17 and Table 5.11. The simulated predictions with each logP value were plotted together as a mean and 95% confidence interval band. The graphical representation demonstrates that the simulated fit describes the rat intravenous profile.

The NCA derived clearance of 0.565 L/h was used in the rat PBPK model and it was also used for single-species and liver blood flow scaling to the rabbit.

Figure 5.17 Verapamil Rat PK: Simulated Plasma Concentration-Time Profile of Verapamil in Female Rats Following a Single Intravenous Administration of Verapamil at 1 mg/kg

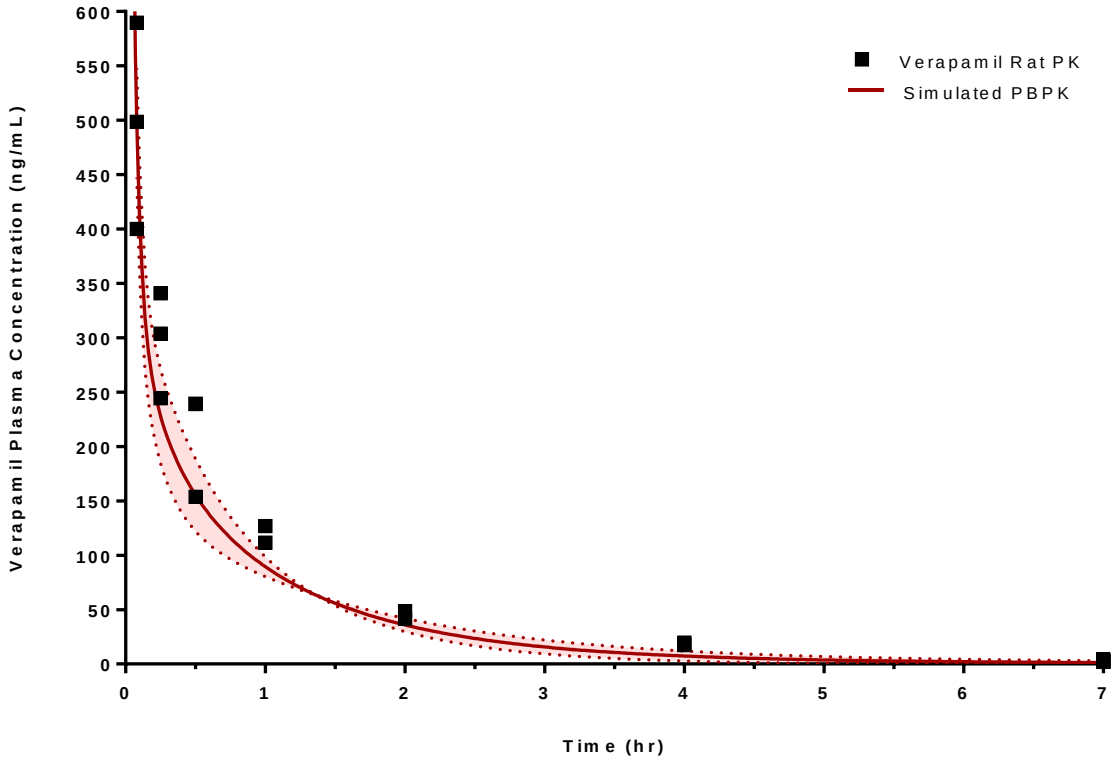

Figure 5.17: Graph of the individual plasma concentration-time profile data points (■) following a single intravenous bolus administration of verapamil at 1 mg/kg to three female rats and the simulated concentration-time using PBPK (—)

Table 5.11 Verapamil Rat PBPK: In Silico Determination of Tissue Partition Coefficients (Kp) in the Rat using different Log P values

LogP	ADMET™	Biobyte™	logK(IAM)	Adj. log(CHIN)
	4.45	4.47	3.59	3.69
Tissue				
Lung	3.12	3.22	2.75	2.73
Adipose	14.4	14.96	2.30	2.86
Muscle	1.56	1.61	1.20	1.20
Liver	2.74	2.83	3.02	2.96
Spleen	1.45	1.50	2.06	1.99
Heart	2.12	2.19	1.68	1.68
Brain	6.50	6.71	6.40	6.31
Kidney	2.50	2.58	3.23	3.14
Skin	3.47	3.59	1.41	1.51
ReproOrg	2.50	2.58	3.23	3.14
Red Marrow	3.32	3.43	1.02	1.14
Yellow Marrow	14.40	14.96	2.30	2.86
Rest of Body	1.46	1.50	2.06	2.00
R-squared (R^2)	0.871	0.865	0.935	0.933

Table 5.11 Tissue partition coefficients (Kps) in the rat using different logP values derived from ADMET, Biobyte, logK(IAM) and adjusted log(CHIN) with experimental value for rat B:P value 0.68 used and Fup = 0.071; and NCA derived clearance of 0.565L/h

5.11.5. Verapamil Rabbit Physiological PBPK – using Scaled Clearance and logP range

Scaled clearance values were determined from the rat observed 0.565 L/h non-compartmental analysis (NCA) data using single-species (SS = 3.14 L/h) and liver blood flow (LBF = 5.00 L/h) scaling methods previously described (Table 5.12).

Tissue partition coefficients (Kps) were generated within GastroPlus™ using the upper and lower logP values (4.47 and 3.59) obtained from Biobyte and logK(IAM) with experimental blood:plasma ratio (B:P) value 0.81 and fraction unbound in the plasma (fu_p) 0.07 in the rabbit. The PBPK simulations were carried out for doses of verapamil at 0.1, 0.3 and 1 mg/kg following 30 minute intravenous infusion, with the regression analysis of fit given for each. The R-squared values indicate a good fit using both logP values and scaled clearance methods for 0.1 and 0.3mg/kg (0.673 to 0.979), with SS scaled clearance simulation fitting better than LBF scaling, compared to 1mg/kg, as shown by the estimate slope of the observed vs predicted being closer to unity.

The simulated scaled clearance predictions with each logP value were plotted together as a mean and 95% confidence interval band in Figure 5.18 to Figure 5.20 (plasma & heart at each dose level). It can be seen from these graphical representations the simulated plasma profile under predicts against the actual observed plasma concentration-time data (within a 2-fold).

The subsequent simulated mean heart concentration-time profile and 95% confidence interval was plotted against the tissue concentration data from the replicate analysis with error bars. The simulated heart concentrations under predicted by approximately 4-fold based from end of infusion heart data for each of the doses from scaled clearance with the predicted heart Kp value (3.05 – 4.50) Figure 5.18 to Figure 5.20. Limited data points make understanding of the tissue distribution difficult.

Table 5.12 Verapamil Rabbit PBPK: In Silico Determination of Tissue Partition Coefficients (Kp) using different Log P values in the Rabbit, with Scaled Clearance and Predicted Regression Analysis of Fit against Observed

LogP		Biobyte		logK(IAM)	
		4.47		3.59	
Clearance		SS CL	LBF CL	SS CL	LBF CL
		CL=3.14 L/h	CL=5.00 L/h	CL=3.14 L/h	CL=5.00 L/h
Tissue Kp					
Lung		0.89		0.67	
Adipose		17.62		9.51	
Muscle		3.99		2.74	
Liver		6.52		4.50	
Spleen		4.05		2.83	
Heart		4.40		3.05	
Brain		10.38		7.08	
Kidney		3.95		2.74	
Skin		4.88		3.36	
ReproOrg		4.00		2.81	
Red Marrow		11.40		7.80	
Yellow Marrow		17.62		9.51	
Rest of Body		4.02		2.79	
Dose		Regression Analysis of Fit			
0.3 mg/kg	R^2	0.845	0.674	0.939	0.750
	SSE	2.94E+03	8.60E+03	1.10E+03	5.85E+03
	RMSE	1.11E+01	1.89E+01	6.76E+00	1.56E+01
	MAE	8.54E+00	1.63E+01	4.30E+00	1.33E+01
	Slope est.	1.1513	1.2638	1.0702	1.1816
	95CI - Low	1.0426	1.0885	0.993	1.0442
	95CI - Upp	1.26	1.439	1.1474	1.319
	Slope StdErr	0.05126	0.08266	0.03642	0.06481
3 mg/kg	R^2	0.922	0.735	0.979	0.826
	SSE	1.13E+04	4.90E+04	3.16E+03	2.93E+04
	RMSE	2.17E+01	4.52E+01	1.15E+01	3.49E+01
	MAE	1.47E+01	3.74E+01	9.29E+00	2.86E+01
	Slope est.	1.1541	1.2719	1.0673	1.186
	95CI - Low	1.0892	1.1454	1.0204	1.0924
	95CI - Upp	1.219	1.3983	1.1141	1.2795
	Slope StdErr	0.03062	0.05967	0.0221	0.04411
3 mg/kg	R^2	0.520	0.494	0.550	0.508
	SSE	3.24E+06	4.57E+06	2.53E+06	4.03E+06
	RMSE	4.03E+02	4.78E+02	3.56E+02	4.49E+02
	MAE	3.57E+02	4.26E+02	3.15E+02	4.01E+02
	Slope est.	1.2741	1.334	1.2165	1.2742
	95CI - Low	0.8672	0.807	0.8797	0.8178
	95CI - Upp	1.6811	1.8611	1.5534	1.7306
	Slope StdErr	0.1909	0.2473	0.158	0.2141

Experimental value for rabbit B:P value 0.81 and fu_p = 0.07 used;
SS CL Single-species scaled Clearance
LBF CL Liver Blood Flow Clearance
R2 R-squared
SSE Sum of the squared error
RMSE Residual mean sum of errors
MAE Mean average error
95%CI 95% Confidence Interval (upper and lower)

5.11.6. Verapamil Rabbit Physiological PBPK – using Observed Clearance and Measured Heart Kp

The process of PBPK simulations was repeated using the upper and lower observed rabbit NCA clearances values (GastroPlus™, PKPlus™) from 0.1, 0.3 and 1 mg/kg dose level determined as 4.45 L/h from 0.3 mg/kg and 2.34 L/h from 1 mg/kg (observed clearance at 0.1 mg/kg was 3.97 L/h).

A fixed logP value of 4.47 from Biobyte with experimental blood:plasma ratio (B:P) value 0.81 and fraction unbound in the plasma (fu_p) 0.07 were used to generate the tissue partition coefficients (Kps) in the rabbit (values as presented in previous Table 5.12). In this instance the observed upper and lower mean measured heart tissue:plasma ratios were used as the heart partition coefficient values of 11.5 and 7.25 (compared to in silico determined 4.40), with the regression analysis of fit given for each PBPK simulation (Table 5.13). According to the R-squared values the goodness of fit were no different for 0.1 mg/kg (0.708 – 0.921) and 0.3 mg/kg (0.778 – 0.967), and visually the 95% confidence interval band encompasses the observed plasma profile (Figures 5.18 to Figure 5.20). The simulated plasma profile for 1 mg/kg (0.499 – 0.538) was now within two-fold. On each simulation occasion the lower clearance value 2.35 L/h provided a better fit irrespective of the heart Kp used, as shown by the regression slope and standard error of the observed vs predicted. The subsequent simulated mean heart concentration-time profile and 95% confidence was plotted against the range of tissue concentration data from the replicate analysis with error bars. The simulated heart concentrations from observed clearance with the heart Kp value (7.25 – 11.5) provided tissue concentrations generally within the confidence interval (within 2-fold) Figures 5.18 to Figure 5.20.

Table 5.13 Verapamil Rabbit PBPK: Regression Analysis of Fit Determined using Observed Rabbit Clearance and Heart Tissue Partition Coefficients (Kp)

Observed Clearance in Rabbit (L/h)		Upper Clearance (L/h)		Lower Clearance (L/h)	
		4.45		2.34	
Measured Observed Heart : Plasma Kp		Upper Heart Kp	Lower Heart Kp	Upper Heart Kp	Lower Heart Kp
		11.5	7.25	11.5	7.25
Dose		**Regression Analysis of Fit**			
0.1 mg/kg	R^2	0.708	0.712	0.916	0.921
	SSE	6.96E+03	6.88E+03	1.38E+03	1.32E+03
	RMSE	1.70E+01	1.69E+01	7.59E+00	7.40E+00
	MAE	1.45E+01	1.44E+01	5.03E+00	4.86E+00
	Slope est.	1.2498	1.2372	1.1435	1.13
	95CI - Low	1.1002	1.0852	1.0635	1.0486
	95CI - Upp	1.3993	1.3892	1.2235	1.2114
	Slope StdErr	0.07054	0.07171	0.03775	0.0384
0.3 mg/kg	R^2	0.778	0.783	0.963	0.967
	SSE	3.75E+04	3.67E+04	5.09E+03	4.65E+03
	RMSE	3.95E+01	3.91E+01	1.46E+01	1.39E+01
	MAE	3.21E+01	3.18E+01	1.20E+01	1.14E+01
	Slope est.	1.2553	1.2434	1.1401	1.1273
	95CI - Low	1.1529	1.1387	1.091	1.0786
	95CI - Upp	1.3577	1.3481	1.1893	1.1759
	Slope StdErr	0.04829	0.04938	0.0232	0.02294
1 mg/kg	R^2	0.499	0.500	0.536	0.538
	SSE	4.23E+06	4.22E+06	2.59E+06	2.57E+06
	RMSE	4.60E+02	4.59E+02	3.60E+02	3.59E+02
	MAE	4.10E+02	4.09E+02	3.17E+02	3.16E+02
	Slope est.	1.3424	1.3256	1.306	1.2881
	95CI - Low	0.8531	0.8369	0.9533	0.9364
	95CI - Upp	1.8317	1.8144	1.6587	1.6398
	Slope StdErr	0.2296	0.2293	0.1655	0.165

Experimental value for rabbit B:P value 0.81 and fup = 0.07 used;

SS CL Single-species scaled Clearance
LBF CL Liver Blood Flow Clearance
R2 R-squared
SSE Sum of the squared error
RMSE Residual mean sum of errors
MAE Mean average error
95%CI 95% Confidence Interval (upper and lower)

Figure 5.18 Verapamil Rabbit PBPK: Simulated Plasma and Heart Concentration-Time Profile of Verapamil in the Rabbit Following a 30 Minute Intravenous Infusion Administration of Verapamil at 0.1 mg/kg

a) Plasma

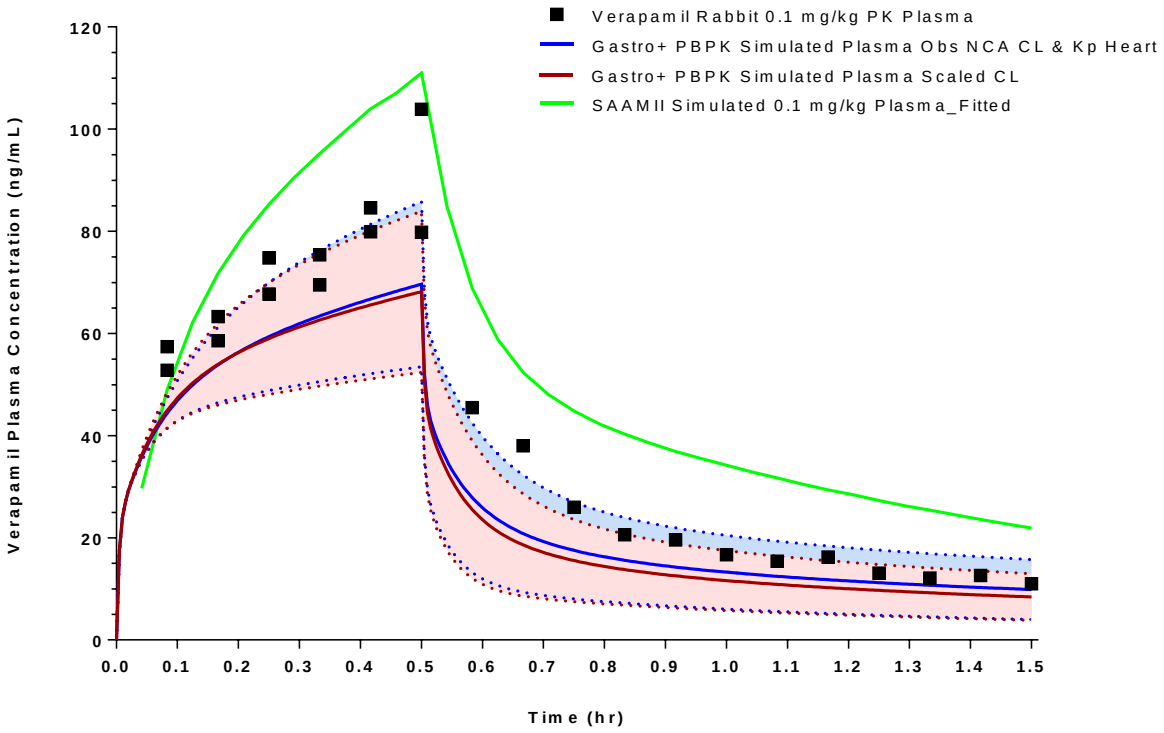

b) Heart

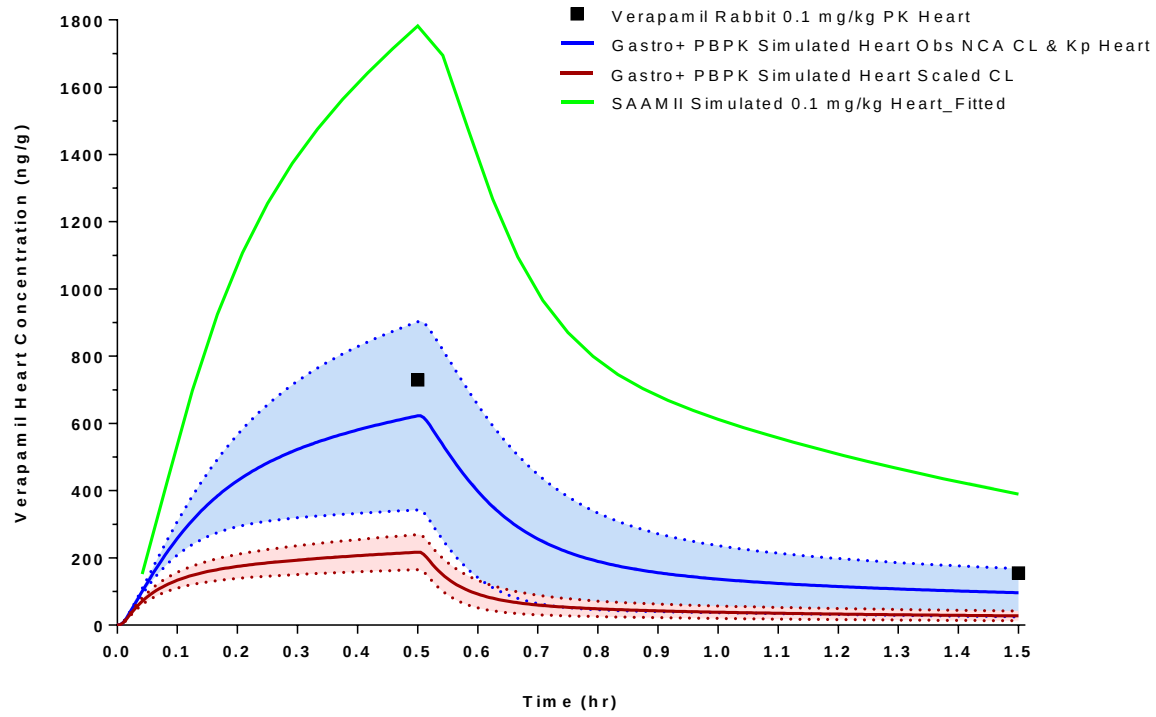

Figure 5.18: Graph of the individual plasma (a) and heart (b) concentration-time profile with observed data points (■) following a single intravenous bolus administration of verapamil at 0.1 mg/kg to female rabbits and the predicted concentration-time using GastroPlus PBPK model with Scaled Clearance and LogP (—) or Observed Clearance and measured Heart Kp (—) with 95% confidence interval in shaded area and SAAMII semi-PBPK model (—) fitted compartmental analysis.

Figure 5.19 Verapamil Rabbit PBPK: Simulated Plasma and Heart Concentration-Time Profile of Verapamil in the Rabbit Following a 30 Minute Intravenous Infusion Administration of Verapamil at 0.3 mg/kg

a) Plasma

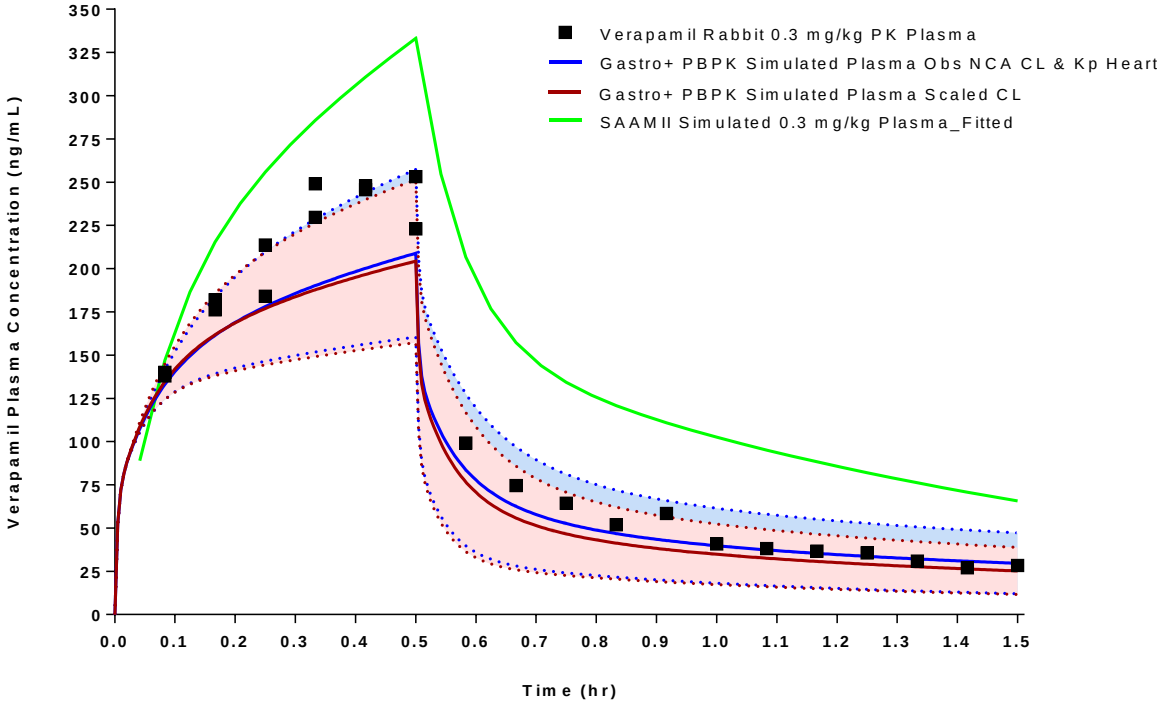

b) Heart

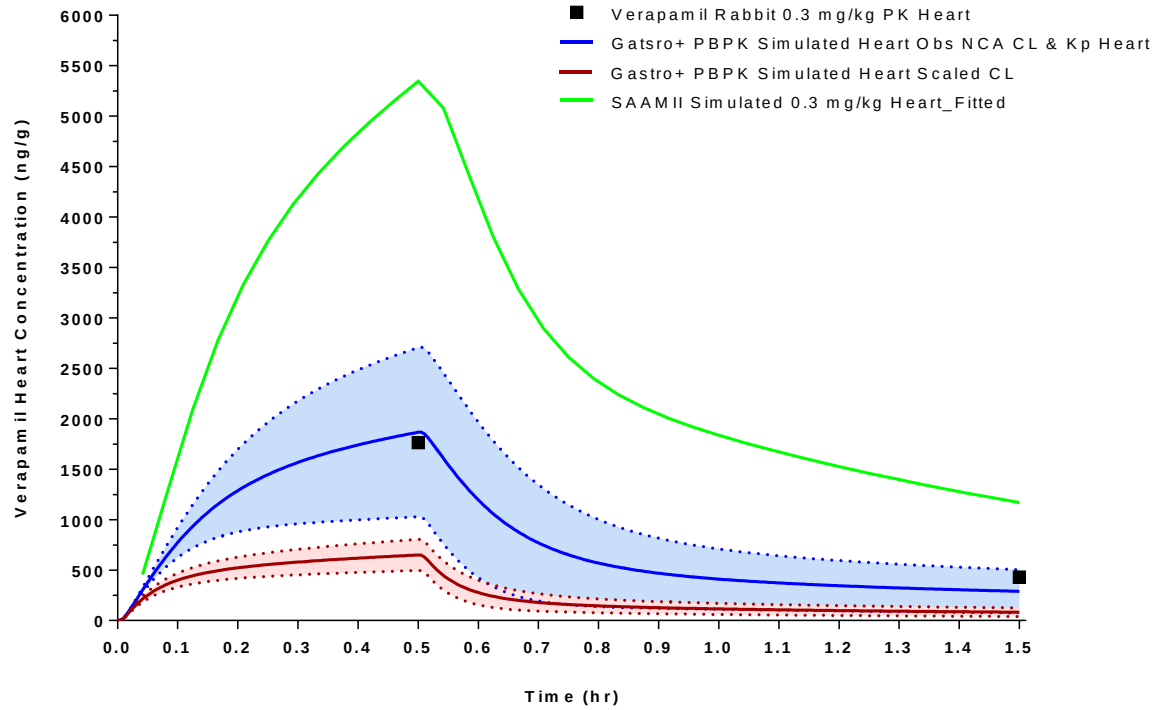

Figure 5.19: Graph of the individual plasma (a) and heart (b) concentration-time profile with observed data points (■) following a single intravenous bolus administration of verapamil at 0.3 mg/kg to female rabbits and the predicted concentration-time using GastroPlus PBPK model with Scaled Clearance and LogP (—) or Observed Clearance and measured Heart Kp (—) with 95% confidence interval in shaded area and SAAMII semi-PBPK model (—) fitted compartmental analysis.

Figure 5.20 Verapamil Rabbit PBPK: Simulated Plasma and Heart Concentration-Time Profile of Verapamil in the Rabbit Following a 30 Minute Intravenous Infusion Administration of Verapamil at 1 mg/kg

a) Plasma

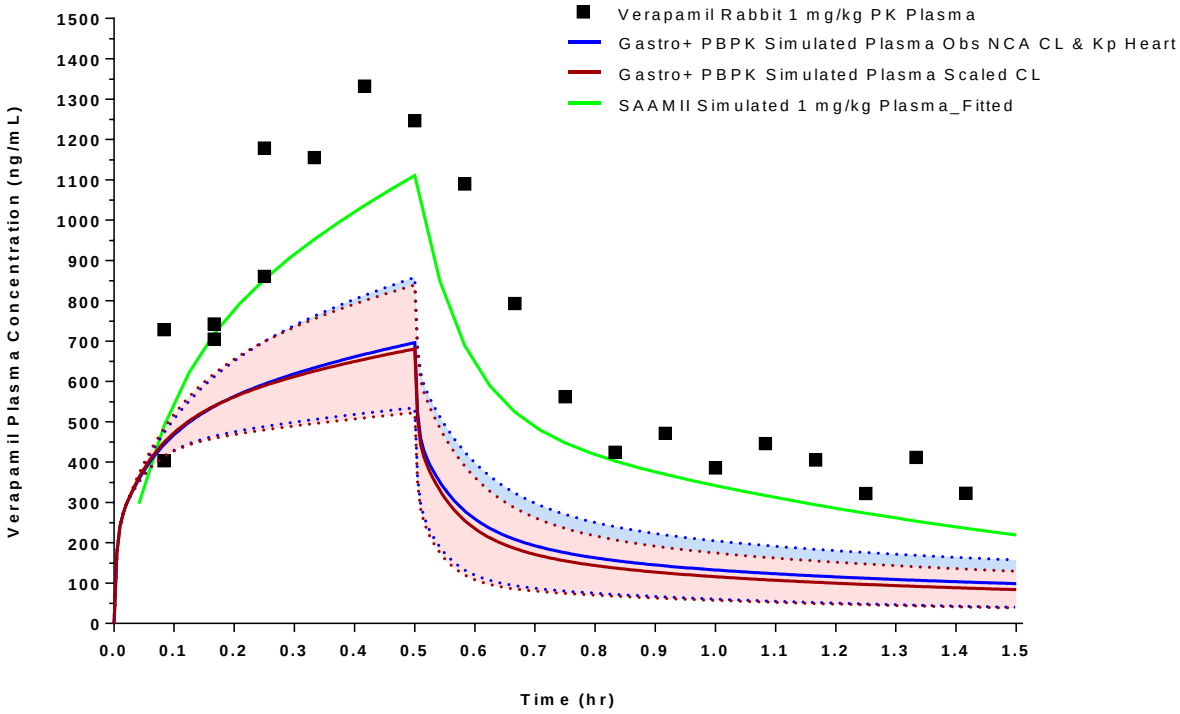

b) Heart

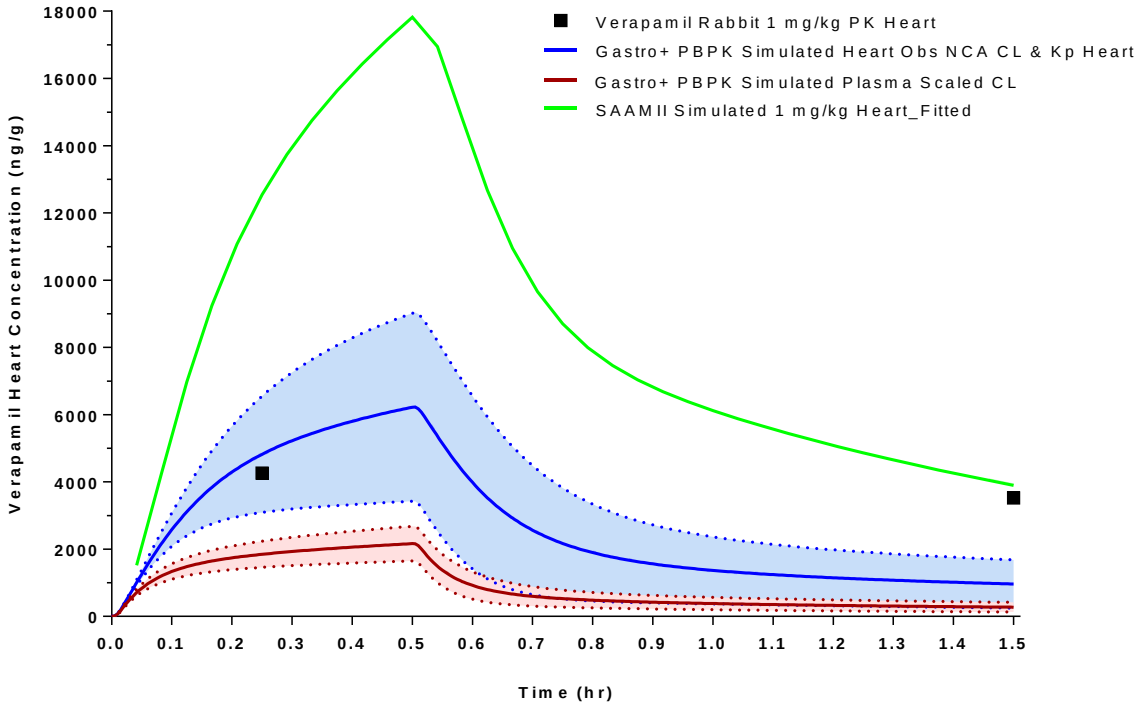

Figure 5.20: Graph of the individual plasma (a) and heart (b) concentration-time profile with observed data points (■) following a single intravenous bolus administration of verapamil at 1 mg/kg to female rabbits and the predicted concentration-time using GastroPlus PBPK model with Scaled Clearance and LogP (—) or Observed Clearance and measured Heart Kp (—) with 95% confidence interval in shaded area and SAAMII semi-PBPK model (—) fitted compartmental analysis.

Table 5.14 Comparison with Literature of the Pharmacokinetic Parameters Across Species Following Intravenous Administration of Cisapride, Sparfloxacin, Moxifloxacin and Verapamil

Parameter	Vd (L/kg)				CL_p (L/h) (% LBF)				Half-life (h)			
Species / Reference	Cisapride	Sparfloxacin	Moxifloxacin	Verapamil	Cisapride	Sparfloxacin	Moxifloxacin	Verapamil	Cisapride	Sparfloxacin	Moxifloxacin	Verapamil
Rat (present study)	17.1	15.7	5.6	3.9	0.83 (70%)	0.59 (50%)	1.2 (100%)	0.60 (50%)	3.6	4.7	0.8	1.1
Rat a, d, e, f, h, l,o, r, s	4.7	3.6 - 4.4	3.6	3.0 - 4.2	1.37 (100%)	0.23 – 0.30 (20-25%)	0.64 (54.5%)	0.60 – 0.79 (51-68%)	1 - 2	2.2 – 4.1, 8	1.2	1.5 – 2.2
Dog a, g, h, o, t, u	0.8 - 1	2.7 - 3.3 -	2.7	5.8 – 13.2	1.8 – 3.1 (10%)	2.2 (6%)	2.2 (6.6%)	15.5 – 63.6 (50 – 100%)	4-10	8.7 – 10.5	8.6	2.5
Sheep* b /Mini-pig**o	-	-	3.9 **	-	19.8 - 36 * (~50%)	-	6.5 ** (38.6%)	-	1.4 – 1.8*	-	5.7 **	-
Monkey h, o	-	7.3	4.9	-		2.88 (36%)	2.07 (26.1%)	-	-	5.3 – 11.7	6.9	-
Human c, l, j, m, n, o, x	2.4 – 4.8	4.3 - 5.5	2.0	4.4 – 5.8	21 – 25.2 (30%)	10.9 – 15.1 (15-20%)	9.2 (12.2%)	52.5 (69%)	4.8 - 10	15-20	13	2.7 – 4.8
Rabbit a, g, k, p, q, v, w	-	-	1.95 - 2.1	8.1 - 9.7; 15 - 17	-	-	2.0 (19.0%)	13.5 – 22 (100%+)	2.3	2.4	1.84 – 2.2	0.9 - 1.65
Rat CL scaled SS to Rabbit					2.66 25%	2.74 26%	7.66 73%	3.14 30%				
Rat CL scaled LBF to Rabbit					4.25 40%	4.37 42%	12.23 100%	5.00 48%				
Rabbit (present study)	1.6 – 2.6	8.4	1.4	0.56 – 0.83	9.75-13.2 (100%)	8.25 (~75%)	0.6 - 1.3 (10%)	3.47 (20-33%)	0.5	2.4	0.8 – 1.1	0.5

Combined table of parameters obtained from literature sources and present study data generated using PKPlus module component of GastroPlus

Liver blood flow (LBF, ml/min/kg) for each species rat (78), dog (56), monkey (44), human (18), rabbit (70) Davies and Morris, 1993

Animal bodyweights (Bwt, kg) for each species; rat (0.25), dog (10), sheep (10), mini-pig (10), monkey (3), human (70), rabbit (2.5) Davies and Morris 1993

Parameters categorised into broad groups: low (green): volume <1 L/kg; clearance <30% LBF , half-life <1 hr

moderate (yellow): volume 1-10 L/kg; clearance 30-70% LBF; half-life 1-10 h

high (red): volume >10 L/kg; clearance >70% LBF; half-life >10 h

Cisapride reference sources:

a. Michiels et al. 1987
b. Veereman-Wauters et al.1991
c. McCallum et al. 1988

Sparfloxacin reference sources:

d. Matsunaga et al. 1991
e. Naroa et al. 1992
f. Noh et al. 2010
g. Nakamura et al. 1990
h. Yamaguchi et al. 1991
i. Shimada et al. 1993
j. Montay et al. 1994
k. Liu et al 1998

Moxifloxacin reference sources:

l. Wang et al. 2014
m. Zhu et al. 2014
n. Stass and Dalhof 1997
o. Siefert et al. 1999a 1999b;
p. Fernandez-Varon et al.2005
q. Carceles et al. 2006

Verapamil reference sources:

r. Kataoka et al. 2016)
s. Todd and Abernethy 1987
t. Bai et al.1993
u. Chelly et al. 1986
v. Giacomini et al 1985;
w. Mori et al. 2001
x. Hamann et al. 1984

5.12. In Vivo Modelling Summary Conclusion

This work describes development towards an integrated prospective approach to modelling the in vivo rabbit QTc by utilising simple pharmacokinetic data from the female rat in a physiologically-based PK model (PBPK) to enable a scaled translation to the female rabbit PBPK model, and link with in vitro data and a pharmacodynamic concentration-effect model from the ex vivo rabbit wedge (RVW) model to simulate the in vivo concentration-dQTc effect in the anaesthetised rabbit.

5.12.1. Scaled Clearance

The female rat clearance was scaled to the female rabbit using two approaches, single-species (SS) and liver blood flow (LBF), that were corrected for fraction unbound and bodyweight . An assumption is that the process of clearance rates/routes is the same between rat and rabbit and predominantly cleared by hepatic and renal processes. It can be seen from the cross-species pharmacokinetic parameters Table 5.14 summarising literature and work conducted in this thesis that there are differences between the rat and rabbit in this study and compared to literature. Each of the compounds used were moderate (30-70% LBF) to highly cleared (>70% LBF) in the rat and did not scale in the same manner. The method of scaling by physiological LBF was better than using single species allometry method as determined by regression analysis comparing observed data to predicted data. This is in agreement with a comparison where mechanistic (physiological) allometry has been shown to be superior to empirical scaling approaches following a Pharmaceutical Research and Manufacturers of America (PhRMA) initiative (Poulin et al., 2011a; Poulin et al., 2011b).

It has been shown that physiological parameters, such as glomerular filtration and hepatic blood flow, and anatomical parameters such as liver and kidney size, can be allometrically scaled. Since these parameters can be directly related to drug disposition, the belief is that PK parameters can be scaled in the same way (Ings, 1990; Huang et al., 2015). In general those drugs that successfully scale are where PK parameters are directly related to physiological and anatomical parameters i.e. primarily renally cleared or have a high hepatic extraction where clearance approximates liver blood flow, which the compounds investigated were. Those drugs that fail are often a direct result of biochemical parameters or physiological processes, such as protein binding or transporter trafficking which do not express a direct allometric relationship (Lin, 1995; Mahmood, 1999; Mahmood, 2007; Huang et al., 2015) or low hepatic extraction (Riviere et al., 1997).

In this study the protein binding was used to correct parameters for species differences, which should have improved the scaling correlation (Bregante et al., 1999; Mahmood, 2007). However in this instance there may also be a species difference in route or rate of clearance between rat and rabbit, as shown by sparfloxacin (low-moderate clearance in rat compared to high in rabbit) and moxifloxacin (moderate-high clearance in rat yet low in rabbit). There is also the consideration that the anaesthetised state has also affected the clearance between the species. Further improvement of the scaling approach in this study can be conducted and supported through additional species to plot the clearance parameter against bodyweights for each compound in traditional allometric scaling. However this approach can also add variability on the regression line, so an improvement here can be made by taking each individual species measured and conducting multiple single-species scaling that would provide a range of scaled clearance values, rather than just one.

The traditional allometric relationship for a PK parameter is derived via linear regression of a log-log plot of the kinetic parameter against body weight of various non-clinical species (Lin, 1995). The exponents of CL_p, Vd_{ss}, t1/2 are often found close to 0.75, 1 and 0.25 respectively (Ings, 1990; Mahmood, 2007). An example of this was a retrospective allometric scaling analysis of several fluoroquinolones, which included moxifloxacin, conducted by Cox et al. Pharmacokinetic parameters (CL_p, Vd_{ss} and t1/2,) were collected from mouse, rat, monkey, dog, minipig, human and rabbit. The analysis identified the allometric equations $18.77W^{0.54}$ and $3.25W^{0.91}$ for CL (ml/min) and Vd_{ss} (L), so for a 2.5kg rabbit, this gives a predicted clearance of 1.8 L/h (Cox, 2007). Siefert et al. had previously carried out a similar allometric scaling across species for moxifloxacin and proposed $1.185W^{0.529}$ for CL (L/h) which equates to 1.9 L/h (Siefert et al., 1999a) which is less than observed in this present study. Fluoroquinolones undergo both renal elimination and hepatic metabolism. The differences between exponents could suggest that when the total clearance value is used as the sum of hepatic and renal clearances, prediction may be difficult because the rate of the two elimination processes could be different in different species. Differences in metabolism among the mammalian species could also explain the values for the allometric exponents of half-life in the study (Table 5.14). Application of a simple PBPK model consisting of two compartments describing slowly and rapidly perfused tissues and a hepatic compartment have been used to enable allometric scaling principles to simultaneously describe moxifloxacin PK in five species that were fitted with common K_p values and using fractional cardiac output associated with each compartment and species (Cao and Jusko,

2012). There were no other examples of cross-species allometric scaling for cisparide, sparfloxacin or verapamil. As part of this work, pharmacokinetic parameters were collected across a number of species and a retrospective analysis could be conducted for these compounds for future improvement and investigation of scaling.

5.12.2. PBPK Modelling

PBPK models are mechanistic, where by the parameters are divided into physiological and drug-specific terms. In addition, the structure is common to all animals and therefore these models are ideal for cross-species scaling (Rowland et al., 2004). PBPK is becoming an integral part of drug discovery and development to the extent that it is replacing in vivo studies and being used as supportive evidence in clinical submissions (Thomas, 2010; Smith, 2012; Jones et al., 2015). For example; pharmaceutical industry leader Pfizer describe the application of PBPK modelling to aid their drug development (Jones et al., 2012); or the regulatory acceptance of SimCyp for drug-drug interactions and growing use as a model-based drug development platform for study design (Jamei et al., 2013). In this approach, the model is validated in non-clinical species using data relevant to that species including in vitro data and if the model can successfully predict the outcome then there is confidence in predictions of human PK (using relevant human data) to be sufficiently accurate. This approach was undertaken in this study by firstly conducting the modelling in rat and then rabbit.

5.12.2.1. PBPK Rat

For each of the compounds the whole-body PBPK models in GastroPlus™ provided a good description of the plasma concentration time profile, and confidence that PBPK analysis would be suitable for the rabbit. The different logP values used from in silico (Biobyte and ADMET) and experimental (logK(IAM) and logCHIN) methods did not give a large range in the tissue specific Kp values for the compounds investigated in this work.

The rat plasma-concentration time profiles generated from the simple intravenous study were simulated in a whole-body PBPK model using different logP values (two in silico and two chromatographic) with measured in vitro data (B:P and fu_p) as input parameters to derive tissue partition coefficients (Kp). The clearance parameter obtained from the female rat using non-compartmental analysis was used as the hepatic clearance with the in silico Kp values to determine the appropriate fit of the distribution in the rat on the simulated profile.

Early preclinical PK screening studies are often only conducted as one dose level per species initially for intravenous administration. These would be conducted at a low dose primarily to obtain kinetic and bioavailability information, along with possible pharmacological response data. The single intravenous bolus doses administered to the female rat in this investigation were at sufficient dose levels to quantify plasma concentration-time course to describe the distribution and elimination characteristics of cisapride, sparfloxacin, moxifloxacin and verapamil compounds. The female rat was used to maintain consistency in the sex of the animals used. An alternative would have been to conduct multiple intravenous doses to inform whether there was any rate limiting clearance processes. A more complex approach would have been to use dual cannulated animals (jugular and bile duct) and collect urine. Surgically prepared animals would enable analysis of routes and rates of elimination by collection of bile and urine, and provide study design options for dose administration and sampling. A steady state infusion (or 5x half-lives) with tissue collection would have provided information around distribution and Kp partition coefficients in the rat to support the PBPK model. By only having intravenous rat data, many issues around absorption, solubility, permeability associated with the oral delivery would remain unknown but could be addressed through a series of oral doses at or around the intravenous dose level. In this current study, oral data was not required as it was the intravenous pharmacokinetics and disposition that was being investigated, and overcome those issues to focus on concentration-effect only in the rabbit.

5.12.2.2. PBPK Rabbit

The lowest and highest logP values were used to determine a range of rabbit Kp values in combination with the two clearance scaling method values, and thus simulate the rabbit plasma concentration-time profile against the observed anaesthetised data. From the regression analysis the in silico Biobyte™ logP values generally supported a better fit for each compound. Further work using different compound structures and from different classes may indicate how sensitive logP is as one of the parameters used for the tissue Kp calculation and whether the Biobyte software algorithm consistently provides a better simulation of plasma and tissue distribution profiles.

Rabbit PBPK profiles were re-simulated in GastroPlus™ using the in silico Biobyte™ logP value, with the observed non-compartmental (NCA) clearance value and measured heart:plasma ratio as a surrogate for the heart Kp. This was conducted to demonstrate an

expected improved goodness of fit as identified by comparing the R-squared values between scaled and observed clearances used in the rabbit PBPK. The improved simulation using the observed clearance and measured heart Kp demonstrates the functional use of the whole-body PBPK model.

A drawback of PBPK models is that they may be complex with the requirement of many species specific parameters. The rabbit is also not the most common pharmacological /toxicological species and as a result there is a potential lack of fully defined rabbit physiological components, such as tissue composition of neutral and phospholipids to adequately describe the tissue Kp and tissue distribution. GastroPlus™ has used referenced physiological parameters for organ volumes and tissue blood flows, whereas the tissue composition is a hybrid of rat and human. However, there are many different levels of complexity to PBPK models, from a simplified model where organs are "lumped" together, to a full whole-body model or combined with empirical compartment descriptors in a semi-physiological model (Rowland et al., 2004). In addition, advances have been made in methods for the prediction of input parameters, such as scaling distributional rate constants (Jones et al., 2006). The separation of physiological parameters from drug effect allows both the mechanistic insight into the properties of a compound and prediction of PK in a number of different circumstances such as disease states (Jones et al., 2015).

5.12.2.3. Semi-Compartmental PBPK/PD

For each of the compounds, a 2-compartmental PK model was adequate to describe both the rat and rabbit plasma concentration-time profiles, using a simultaneous fit of plasma data from all dose levels in PKPlus module of GastroPlus™ (and also in SAAMII).

The two compartmental fixed PK model was combined with the semi-PBPK component of a separate biophase effect compartment representing the rabbit heart, in SAAMII software. The heart compartment was defined mechanistically using physiological parameters such as heart blood flow and volume, and the observed partitioning and fraction unbound in the cardiac tissue.

For each compound at each dose level in the rabbit, the simulated heart concentration time profile fitted the limited measured heart tissue concentrations demonstrating that the concentrations were perfusion-driven and directly related to the plasma concentrations. From the heart tissue concentrations, free tissue levels of the drug were determined as input into the

E_{max} QT response model. The resulting fit of the PKPD becomes limited by the input parameters of the E_{max} model and the observed inter-animal variability for changes in QTc.

Whilst the semi-compartmental PBPK/PD approach provides a good description of the tissue concentration-QT response, a limitation is that it required a "top-down" retrospective fitting of existing data. This semi-PBPK model approach would be improved with greater tissue concentration data around the E_{max} model.

5.12.2.4. PBPK/PD models

The general expectation for PD parameters is that the rates of biological turnover processes should be predictable between species based on allometry, whereas intrinsic capacity (E_{max}) and sensitivity (EC_{50}) tend to be similar across species (Mager and Jusko, 2008). Some studies investigating animal to human PD translation have only looked at receptor occupancy aspects (Bourdet et al., 2012) and others require adjustment of pharmacological values by differences in in vitro binding (Chang et al., 2011). It appears that with enough knowledge about the mechanism of action, cross-species translation is possible (Kenyon, 2012). Therefore from this thesis, if the pharmacological effect is sufficiently separated from the physiological processes and accurately described, successful translation of animal to animal and to human is possible. Therefore it would be a worthy further investigation to translate the PBPK plasma/heart concentration profile into the dog or human and prospectively predict the dQTc using the E_{max} model from the rabbit.

An alternative to the PBPK model here, is the empirical compartmental PKPD model using a "biophase" effect compartment which has been used to describe the kinetics at a target effect site (Csajka and Verotta, 2006; Danhof et al., 2007; van der Graaf and Benson, 2011). An example of this was applied to the cardiac tissue concentrations determined in the anaesthetised guinea-pig by Minematsu et al. with tacrolimus and quinidine (Minematsu et al., 1999; Minematsu et al., 2001). Extensive heart tissue concentration and plasma concentration-time profiles were generated in the anaesthetised model for tacrolimus, an immune-suppressant FK506, and also quinidine, the type I Na-channel inhibitor. The PKPD models used either a two or three compartmental PK model to describe the plasma profile, linked to the ventricle compartment. Using associated ventricle weights to determine the heart ventricle compartment volume and fitted distributional rate constants (k10, k12, k21, k1vent and kvent1) as well as the central compartment volume to describe the relationship with QTc prolongation. The authors concluded that an E_{max} model adequately described

tacrolimus, yet a direct linear model fitted quinidine. It is possible that Minematsu et al. did not investigate high enough concentrations of quinidine to define the E_{max} slope and provide a sigmoidal model.

Other simpler PD models are related to the sigmoidal E_{max} model, such as the simple E_{max} model (where n=1), the linear model, log-linear model and the fixed-effect model (Holford and Sheiner, 1982). However these models are less commonly used as they are generally only valid over a limited concentration range (Csajka and Verotta, 2006). The E_{max} model assumes that receptor binding is rapid and reversible, as in the case of ion channels. In some instances binding may occur more slowly and becomes a rate limiting step for drug effect. In these cases the binding kinetics are required such as drug-receptor complex or turnover (Dayneka et al., 1993). These models can be used to account for delays in response due to transduction processes and the rate constants are considered system specific but in the case of cardiac electrical conduction these are not often required because the response is rapid and QTc prolongation can often be directly related to plasma concentrations. A number of different PD models have been used to describe compounds with QTc prolongation using indirect and threshold PD models to account for lag/distributional delay as presented by anti-clockwise hysteresis in relation to plasma concentration-effects (Caruso et al., 2014). This highlights that when using empirical PKPD approaches that different PD models need to be employed for the same PD endpoint, yet PBPK modelling enables the physico-chemical distribution of compounds and thus a consistent single PD model can be used, as in this thesis. More mechanistic PD approaches have been described for QTc modelling to incorporate the circadian and sinus rhythm, yet these approaches again require extended ECG recordings coupled with PK data for retrospective fitting (Dubois et al., 2015; Huh and Hutmacher, 2015).

In both instances of the preclinical models by Minematsu et al. and Weiss et al., the traditional PKPD modelling approach was used, where the plasma concentration was fitted and linked to the time course of the pharmacological effect, $E(t)$, via a first order delay determining a hypothetical concentration-time curve at the effect site, and the pharmacodynamic response was related to myocardial concentration by a sigmoidal E_{max} model (Hill equation). A limitation of these models is that they are not truly mechanistic. While it may work for drugs that distribute to their site of action by passive diffusion, factors such as physico-chemical properties, binding and functionality of transporter proteins may restrict a drug's distribution to the biophase (tissue/site of action). At present there are a

number of semi-parametric and non-parametric approaches used for modelling effect compartment kinetics, however the only mechanistic alternative is to use a PBPK model in conjunction with a mechanistic PKPD model (Danhof et al., 2008; Chetty et al., 2014). The approaches by Minematsu et al., Weiss et al. and Mirams et al. support the PBPK/PD approach taken to link the QTc interval prolongation to the heart concentration-time profile in this thesis (Minematsu et al., 2001; Weiss, 2011; Mirams et al., 2014).

More specifically heart tissue concentrations have also been described using uptake, metabolism and interstitial diffusion using compartmental models (Weiss, 2011). Weiss et al. describes the fitting of the isolated animal heart (Langendorff preparation) in-flow and out-flow of the tissue with distribution into the myocardium, or by a process into the interstitial space. This separation of the heart tissue into the extravascular and intracellular space enables differentiation between site of action and the receptor location, for instance cell surface ion channels to sarcolemmal membrane (Weiss, 2011). A further example of a human heart PBPK model has been applied for amitriptyline which consisted of four heart compartments (epicardium, midmyocardium, endocardium and pericardial fluid) using SimCyp Heart Simulator. The Kp distribution between each of the heart compartments were in a fixed ratio based on cardiotoxic shellfish poisoning data and fitted the pericardial blood flow. In addition the authors also took into account cardiac metabolism through CYP450 as an eliminating tissue accounting for mean microsomal fractions in human cardiovascular tissue. Human whole-body PBPK simulations then matched plasma profiles and the sparse data points for human heart tissue concentrations of amitriptyline (Tylutki and Polak, 2017). The authors obtained data from human cardiac surgery and post-mortem in attempts to inform the drug distribution into the human heart but did not expand this model to incorporate the observed adverse QT prolongation known to occur with amitriptyline (Zemrak and Kenna, 2008).

In summary, the PBPK/PD modelling described in this work demonstrates that PBPK translation to the rabbit is feasible from the rat and that the scaling method for clearance using liver blood flow was better than single-species allometry for this limited compound set. The simulations adequately described the heart tissue concentration-time profile within 2-fold, the industry standard for adequate predictions. From the predicted heart tissue concentration over time, the resultant change in QTc was simulated through the linked E_{max}

model generated from the RVW and incorporated the in vitro protein binding data. Greater tissue concentration data over a longer experimental period for each compound would provide more confidence in the predicted tissue concentrations and the simulated dQTc. However, the advantage of PBPK is a reduction of animal numbers by allowing integration of multiple data sets that can be incorporated into one in silico model.

Strathclyde Institute of Pharmacy and Biomedical Sciences
GlaxoSmithKline

CHAPTER 6

Summary

6. SUMMARY OVERVIEW

This thesis was able to integrate in vitro, with ex vivo and in vivo data, incorporating cross-species translation through physiologically-based PK (PBPK) modelling to provide and generate predicted plasma and heart tissue concentration-time profiles in the rabbit and the resultant changes in QTc prolongation following administration of test compounds cisapride, sparfloxacin, moxifloxacin and verapamil. Work described in this thesis is a first example of using a PBPK model of a rabbit combined with the cardiovascular QT-interval endpoint.

Protein binding for the fraction unbound in plasma and heart tissue, and the blood-to-plasma ratio were generated across species using rapid equilibrium dialysis (RED) device as a standard approach. Albeit a small compound data set this assessment highlighted that there were some differences between the rabbit and other species, adding value to the importance of collecting data in the species of interest. The species specific data was used to inform the PBPK modelling for both the rat and the rabbit, and to understand the free concentration-response curve from the RVW and in the linked PBPK/PD model.

QT prolongation data was generated in the rabbit ventricular wedge (RVW) cardiovascular screening model, and this was a first example of interpretation of the concentration-QTc response using the E_{max} sigmoidal response in the ex vivo model. During this work a similar approach has been applied to in vitro ion channel screening to predict the MEA hiPSC cardiomyocytes assay. This PD model was then applied to the prospective in vivo PBPK model through an anaesthetised rabbit preparation.

The in vivo anaesthetised rabbit model was adapted and developed to provide serial plasma concentration-time profiles and heart tissue concentration data at selected timepoints over different dose levels for cisapride, sparfloxacin, moxifloxacin and verapamil to aid the simulation of the heart-concentration time profile and subsequent hERG inhibition to affect the QT interval. This was the first example of using the anaesthetised rabbit model in GSK worldwide and also using rabbit for PBPK/PD modelling.

This thesis has demonstrated that through the generation of different data sets readily available in early discovery phase, that integration using PBPK can be utilised. This is a development towards prospective in vivo modelling of QTc response in the in vivo rabbit.

6.1. Application of PBPK

The application of PBPK modelling within the pharmaceutical industry has been limited and is now increasing due to the availability of in silico and in vitro systems, which act as surrogates for in vivo absorption, distribution, metabolism, and excretion (ADME) processes and the advancement in the in vitro-in vivo correlation of these data. The growing use of PBPK is reflected by the increasing number of publications on this topic, with nearly 1000 articles associated with PBPK over the last 5 years, which is more than the total reported prior to this date (Smith, 2012; Jones et al., 2015; Zhuang and Lu, 2016). PBPK approaches have transitioned from academic curiosity and sceptical use in the pharmaceutical industry to increasingly being included in regulatory submissions, for example; the prediction of drug–drug interactions (DDI), drug-exposure predictions in special populations to impact drug labels. Applications of PBPK specific to industry that support decision making now include lead optimisation, prediction of first-in-human PK and continue to later phases with DDI (Rowland et al., 2015; Wagner et al., 2015; Jamei, 2016; Wiśniowska and Polak, 2016). More mechanistic models provide a quantitative framework for prediction of systemic and tissue exposures with the distinct separation of physiology and drug-dependent information to enable the extrapolation from in vitro to in vivo (Poulin et al., 2012) and from animal to human (Poulin et al., 2011c) (Zhuang and Lu, 2016).

6.1.1. QTc In Vivo Modelling in Safety Pharmacology

Predominantly many of the modelling applications in safety pharmacology regarding QT prolongation focus around the translation from the dog to man and have used the conventional "top-down" approach modelling existing data sets with empirical methods (Parkinson et al., 2013; Dubois et al., 2015). It has been identified that a lack of adverse PD clinical data is limited to the few compounds studied (moxifloxacin, sotalol, cisapride and dofetilide) and the prospective approach leaves a translational gap (Chain et al., 2013; Marostica et al., 2015). The translational gap is being bridged through understanding of the species differences in systems pharmacology, such as hERG receptor density and differences in in vitro to in vivo response to improve the sensitivity (Gotta et al., 2015b; Gotta et al., 2016). Furthermore, given that many QT-prolongation cardiovascular PKPD models exist in the dog to translate to human, it would be feasible to conduct a retrospective analysis applying PBPK modelling with these examples for dog and human. An opportunity exists in the dog as one of the primary species with historical physiological information and

background data that may incorporate the tissue and cellular pharmacology (Knight-Schrijver et al., 2016).

Other species such as the guinea-pig and rabbit contribute towards the cardiovascular screening and in vivo data from these models would aid retrospective modelling towards a prospective translation across species and to man (Marks et al., 2012; Kang et al., 2016). Mini-pigs are also being adopted as an approach in cardiovascular safety due to the number of whole body structural similarities to human and ethical use over dogs, and the need to increase characterisation going forward (Authier et al., 2011).

Examples of rabbit PBPK models are limited in the literature, 20 in total to date, and applications are restricted to methyl-iodide disposition, impact of gestational pharmacokinetics and brain development/exposure (Kim et al., 2001; Thrall et al., 2009; Pilari et al., 2011). For the guinea-pig there is even greater porosity of literature, with one translation reference model for soman intoxication in the rat, marmoset, guinea pig and pig, where actual tissue:blood partition coefficients were determined for guinea-pig and assumed identical across species (Chen and Seng, 2012). In the instance of the mini-pig, albeit limited references, many physiological parameters have been documented through the breeding of the Gottingen species (Suenderhauf and Parrott, 2013; Van Peer et al., 2016).

The implementation of PBPK and in silico modelling into drug safety evaluation increases as computing capability, systems pharmacology and understanding of physiological processes increases along with external pressures for reduction and refinement of animal studies through 3R's (Reduction, Refinement and Replacement). PBPK modelling allows for predictive and prospective modelling to optimise study designs (d'Yvoire et al., 2007; Doke and Dhawale, 2015). In safety pharmacology studies, PBPK is currently only beginning to be applied to the gastrointestinal system as part of the core battery, primarily around the gut models available such as ADAM and ACAT which interrogate the physical properties, process and physiological interactions involved in absorption (Hamdam et al., 2013). For CNS liability, there is an increasing approach of using in vitro-in vivo extrapolation (IVIVE) to generate PBPK models as a more mechanistic strategy for the interspecies translation of preclinical models of the CNS and blood-brain barrier (BBB) penetration. However, a major hurdle exists in verifying these predictions with observed data, since human brain concentrations cannot be directly measured (Ball et al., 2013). Future progress would be the implementation of PBPK for more cardiovascular species where the power of PBPK

translation can be applied in a “bottom-up” approach, as shown by a recent review of an oral Biopharmaceutics project by Innovative Medicines Initiative (IMI) (Darwich et al., 2017).

Industry barriers have been highlighted regarding PBPK modelling, in part due to the diverse application, role and span across the whole drug discovery paradigm, and the need for industry consortia and perspectives required (Smith, 2012), as well as consistent model approaches, validation and evaluation (Davies et al., 2016; Kuepfer et al., 2016). Recent progress through a number of industry consortia are looking to advance the in silico modelling capability, such as the Comprehensive in vitro Proarrhythmia Assay (CiPA), virtual heart and Cardiac Safety Simulator. The CiPA initiative is intended to replace the ICH S7B guidance and has recently conducted an industry survey on current practices (Authier et al., 2017). This demonstrates the in silico shift in cardiovascular efforts in the Safety Pharmacology Society review in 2001 and 2011 compared to 2016 (Cavero and Kaplan, 2008; Pollard et al., 2010; Cavero, 2011; Cavero et al., 2016). CiPA is evaluating drug effects on key cardiac ion channel screening, to simulate in a computational human ventricular cardiomyocyte action potential model and then relevance in induced-pluripotent human stem cell (iPhSC) derived cardiomyocytes to clinical TQT (Cavero et al., 2016). Whilst the virtual heart offers a complete computer generated 3-D functioning heart model and the SimCyp Cardiac Simulator™ offers an in silico population PKPD prediction, both approaches incorporate multiple ion channel interactions (Yuan et al., 2015; Wiśniowska and Polak, 2016).

In this study the PD model employed was the E_{max} response model based on the tissue response in the RVW. Ion channel inhibition curves affect the action potential duration in the same manner. The CiPA prediction of the thorough QT interval is being conducted based on simulations of ion channel screens and although these are complex computer simulations (using mathematical models such as ten Tusscher, Gandi and O’Hara-Rudy); the fundamental principles are based on the compound induced current inhibition characterised using concentration–effect curves, namely the E_{max} and Hill function (Mirams et al., 2014). Therefore it may be feasible to link PBPK models of concentration-time profiles to these in silico action potential ventricular models to obtain a mechanistic whole-body simulation.

6.1.2. Heart Tissue Distribution

In this study heart tissue concentrations and tissue:plasma ratios (Kps) were obtained from in vivo studies and simulation of the tissue concentrations from predicted tissue Kps (Lukacova) allowed comparison to in vivo values. As part of PBPK modelling the tissue partition coefficients form a key determinant of the plasma PK profile and tissue PK distribution profile, especially when examining concentration-exposure at target tissue sites, based on the compound ionisation and interaction with acidic and neutral phospholipids (tissue-composition based) (Rodgers et al., 2005; Rodgers and Rowland, 2006). Alternatively a number of empirical partition coefficient correlation-based methods available improved correlation between muscle and other tissues compared to measured values were achieved based on their volume of distribution and lipophilicity (Jansson et al., 2008). The most recent of methods utilises a hybrid approach which accounts for the transition through ionisation interactions and tissue composition (Poulin et al., 2011a).

A practical approach to obtain accurate Kp values is the collection and analysis of blood/plasma against a number of tissues for each compound following a steady state infusion. At steady state, equilibrium is constant between plasma and tissue compartments and even then there may be a tissue lag, compared to the dynamic equilibrium during the distribution and elimination phases of an oral or intravenous bolus PK profile (Berezhkovskiy, 2007). However tissue collection would require labour intensive animal studies and large animal numbers, along with challenges of different tissue analysis, yet historical reviews of tissue-to-blood AUC ratios from quantitative whole-autoradiography (QWBA) have been shown to provide good correlation for tissue distribution based on physico-chemical properties (Harrell et al., 2015). Recently a decision tree approach for which method-based algorithm for predicting Kps has been proposed in light of the fact that no standard approach has been agreed within the modelling community and no single Kp prediction is applicable to all compounds in all tissues (Yun et al., 2014). Accuracy of Kp prediction is a limitation for PBPK modelling and one that could be explored regarding the best practice and applicability towards heart tissue distribution as the measured tissue data remain of the greatest value (Jones et al., 2013).

There are studies reporting the correlation between tissue-to-blood partition coefficients in rats obtained in vitro and in vivo. However, different results and conclusions were reached by the authors; Paixao et al. observed significant differences between these Kp values (Paixão et

al., 2013), whereas Lin et al. and Harashima et al. found a good correlation between the in vivo and in vitro Kp (Lin et al., 1982; Harashima et al., 1984). The latter author described a number of methods to compare tissue binding for quinidine from in vitro equilibrium dialysis to in vivo following intravenous administration using quinidine (Harashima et al., 1984). In this study a similar approach could be adapted to calculate the in vitro heart tissue partitioning using the distribution between the plasma and tissue dialysate.

Understanding the true drug tissue concentration in the heart would give a better correlation with a change in QT prolongation, as demonstrated in guinea-pig (Minematsu et al., 2001; Katagi et al., 2016), dog (Kates and Jaillon, 1980; Keefe and Kates, 1982; Webster et al., 2001) and humans (Debbas et al., 1984; Gillis et al., 1993; Ritchie et al., 1998). A comprehensive literature data review conducted recently by Tylutki and Polak investigated human blood and heart tissue drug concentrations for over 200 drugs from human cardiac surgery and post-mortem samples in an attempt to inform the drug distribution into the human heart. The author's focus was on whether a drug penetrates into heart tissue at a therapeutic level from a range of common antibiotics, antifungals and anticancer drugs. Drugs that directly affect cardiomyocyte electrophysiology were another group of interest, and levels were measured in different sites in human cardiac tissue to give an insight into any differential distribution in the heart (Tylutki and Polak, 2015). This appears to be a novel approach to obtaining what would be otherwise be restricted human sampling data to aid model development.

6.2. Future Experiments

The first approach would be to build on the existing component data sets to strengthen and support the hypotheses and modelling approaches already undertaken in this thesis.

6.2.1. Protein Binding

The successful implementation of the protein binding determination using the RED device enabled in vitro free fraction data to be incorporated into the PBPK modelling and also be applied to the free heart tissue concentration profile for the resultant effect on QT prolongation. The common and robust technique allowed for cross-species comparison and different matrices to be analysed, which had been limited to date and presumptuous that all species were similar. To identify if the rabbit or any of the other species (rat, dog, guinea pig and man, but also mini-pig and monkey) were consistently different with their respective protein binding, greater compound numbers need to be investigated with not only a range of expected binding but also physicochemical properties (acids, bases and zwitterions) and cover a range of drug classifications both cardiovascular and non-cardiovascular.

6.2.2. Rabbit Ventricular Wedge

The data set obtained for cisapride, sparfloxacin and moxifloxacin using the RVW matched that reported in literature from a number of different authors. The sigmoidal concentration-effect curves generated from this ex vivo tissue model was used to link with the in vivo anaesthetised rabbit model regarding QTc prolongation. To improve the E_{max} PD model the data could be combined with the literature output. A staggered dosing regimen could be conducted which is not fixed on the log or ½ log increments, such that RVW dose preps overlap and allow for a wider concentration range to be investigated to define the sigmoidal curve with more data points. Additional compounds that are known to affect the hERG channel and prolong QT could be investigated, such as those in the blinded validation study reported (Chen et al., 2006; Liu et al., 2006). The sigmoidal E_{max} model could be applied to to compounds utilised by these authors to further interrogate the assumptions and limitations of this approach. Currently in silico work is being conducted with the ion channel screening to predict the hiPSC-cardiomyocytes (CM) and CM prediction of the rabbit ventricular wedge which could be utilised i.e. an alternative in vitro/in silico PD input into the PBPK modelling (Beattie et al., 2013; Mirams et al., 2014) (Harris et al., 2013; Harris, 2015).

6.2.3. Anaesthetised Rabbit

The anaesthetised rabbit QTc model offers continuous PKPD data over the experimental time course. In this study a number of replicate terminal heart tissue samples were obtained at the end of the experimental period (e.g. 90 minutes), however the tissue concentration-time profile were often limited to one sample per preparation during the time course. Therefore further studies would need to be conducted to obtain heart tissue concentration-effect data at the dose-levels that have also been investigated but also further dose levels. The intravenous infusions to date in the rabbit have been conducted in this study over 30 and 60 minutes. During the infusion period the greatest changes in QTc are observed as the plasma and tissue concentrations are increasing rapidly and the QTc significantly. Therefore collecting heart concentration data throughout the infusion period would provide a greater range of tissue concentrations. It may also be possible to conduct extended infusion periods to reduce the rate of QTc change. Previously many authors conducted the drug infusions over 10 minutes in the anaesthetised rabbit whilst differences in effects due to infusion rates have been noted (Carlsson, 2008). Additional heart concentration data would allow further determination of the tissue distribution of each of the compounds and interrogation of the in vivo E_{max} model related to QTc changes.

6.2.4. Free and Total Heart Tissue Concentration

As discussed above, in vivo experiments to derive tissue concentrations and partition coefficients are destructive methods that result in high *n* numbers, inter-animal and time-course variability, which can be overcome through repeated measured experiments.

6.2.4.1. Tissue Microdialysis

Tissue microdialysis (MD) experiments would provide an in vivo sampling alternative to give continuous measurement of free unbound drug in the extracellular fluid (ECF) space. The MD probe would be able to sample in situ free drug in approximate equilibrium with the tissue of interest and add further information in this investigational thesis. There are a number of literature reports of peripheral soft tissues where this technique has been applied, liver, lung, brain and skin (de la Peña et al., 2000). MD would provide continuous drug concentration data at specific tissue locations and target site that can inform the PKPD model (Brunner et al., 2005; Müller, 2009). An example of where MD has been applied to practical

preclinical-to-clinical translation was the prediction of human brain extracellular fluid (ECF) concentrations. Preclinical rat brain MD data was generated and used in a translational PBPK model to fit the surrogate cerebrospinal fluid (CSF) data available from human CSF which may be beneficial for brain penetrant drugs (Ball et al., 2014).

Heart MD to date has largely been around myocardial biochemical metabolism (lactate/pyruvate) and the effects of open-chested surgery, such as coronary-pulmonary bypass and ischemia in patients and porcine models (Pöling et al., 2007; Abrahamsson et al., 2011). MD can be directly linked to online analytical systems for real time data analysis, biochemical effects and response (Nandi and Lunte, 2009). Subtle biochemical changes can be detected by combining MD with metabolomics to obtain information around the perturbation of pathways as a result of drug administration comparing blood, brain and heart (Price et al., 2005; Price et al., 2008). The caveat around MD data accuracy is the technical challenge of placement, tissue damage (e.g. bleeding or probe contamination), dialysate flow and the probe recovery that has to be factored into consideration.

MD is yet to be directly applied to free drug concentrations in the heart with only in situ aortic MD of diltiazem and metoprolol used as a cardiac surrogate to create a PKPD model in hypertensive rats (Höcht et al., 2006; Bertera et al., 2007). Application of reverse MD would enable direct delivery of the cardiovascular agent to the extracellular space, similar to a dermal implantation (Höcht et al., 2007). This information would help describe the perfusion-limited and permeability-limited models and support better model description of compounds, such as in the heart (Weiss, 2011). The GastroPlus PBPK modelling software used in this thesis can differentiate between tissue extracellular fluid/water and intracellular concentrations to use such free concentration data.

6.2.4.2. Use of SPME

A discontinuous method of obtaining free drug concentrations would be via solid-phase microextraction (SPME) sampling. This technique utilises a microfiber tip that extends from a hypodermic needle which is coated with a biocompatible inert surface that when placed in a blood vessel or tissue adsorbs only free drug. These new devices permit application of in vivo SPME to a variety of analyses, including pharmacokinetics, bioaccumulation and metabolomics studies, providing fast and quantitative results without the need to achieve equilibrium (Vuckovic et al., 2010). The utility of SPME is highlighted by the small 'bloodless' sample volume that can be applied to multiple analyte pharmacokinetic studies

for example the analysis of carbamazepine and its active metabolite carbamazepine-10,11-epoxide in mice (Vuckovic et al., 2011). Examples of direct sampling of tissue is more limited, skin and fish muscle, but is a viable method as described in a review by Cudjoe et al. (Cudjoe et al 2012). Potential limitations of SPME are the related physical 'needle-stick' component which may result in tissue damage (e.g. bleeding) and prohibit its application to highly perfused organs as well as the limited SPME fibre coatings to work with a wide range of chemicals.

The extent of drug protein binding can also be determined when free drug concentrations are measured using SPME against total drug concentrations (Musteata et al., 2006). SPME provides clean samples (devoid of interfering matrix proteins) that aids sensitive analytical accurate methods for drugs that are highly protein bound and offers a dynamic in vivo protein binding assessment (Lambrinidis et al., 2015; Peltenburg et al., 2015). A further extension of this technique can be applied to protein binding/free concentrations in different tissue matrices to derive partition coefficients (PC). SPME has been applied largely in organic pesticides and herbicides to generate in vitro PCs to support PBPK modelling (Vaes et al., 1997; Artola-Garicano et al., 2000; Tremblay et al., 2012).

The SPME remains a largely unrecognised strategy waiting to be employed to more common preclinical and clinical studies across drug discovery improving 3R's, animal welfare, sample stability and versatility of application, even though it is an established technique (Bojko and Pawliszyn, 2014; Goryński et al., 2016). In this thesis SPME (or MD) would offer a versatile range of applications from the in vitro protein binding and PC determination, ex vivo and in vivo free drug concentrations for blood, plasma and heart tissue in the RVW preparation, Langendorff Screenit heart model, or an adapted in vivo preparation.

6.2.5. Cardiomyocyte Uptake, Efflux and Metabolism

An extension to further this investigational study would be to clarify the role of cardiac transporters and metabolising enzymes such as P-gp efflux transport and its potential importance for drug-drug interactions; quantify cardiac drug uptake mediated by transporters in order to reveal their kinetic importance and the abundant capacity for heart tissue to metabolise drugs. It is also possible that drugs can exert their effects by inhibiting the uptake (or metabolism) of endogenous substrates of transporters (or enzymes) and thus altering the

tissue concentration and pharmacological effects (Weiss, 2011). In vitro studies would provide information around the cardiomyocyte intrinsic clearance or uptake of a drug, much like that conducted in hepatocytes, to enable scaling to the tissue level and incorporation into the PK model (Tylutki and Polak, 2017).

The process of uptake/efflux of cardioactive drugs into the myocardium is a major determinant of the efficacy and potential toxicity of such agents (Horowitz and Powell, 1986). Myocardial drug content may not be readily predictable on the basis of estimation of plasma drug concentrations alone, methodology for direct assessment of myocardial drug content has remained limited as described above using MD or SPME. From this current investigation it may aid understanding of the effects on the drug clearance and tissue concentrations from in vitro cardiomyocytes, tissue drug levels in the ex vivo RVW and distributional and PKPD effects in the anaesthetised rabbit, which can be integrated into a PBPK model.

6.2.5.1. Cardiac Efflux Transporters

The role of efflux transporters, such as ATP-binding cassette (ABC) proteins of which P-glycoprotein (P-gp) is the most predominant family, having two isoforms in rodents encoded by *mdr1a* and *mdr1b* which fulfill the same function as the single *ABCB1* gene (also called *MDR1*) in humans (Schinkel, 1997). The impact and role in cardiac drug disposition was discussed by Couture et al. as P-gp exports endogenous and exogenous molecules out of the cell (Couture et al., 2006). Because the expression of P-gp in cells of human heart vessels is similar to that of P-gp in brain, it was proposed that P-gp serves as a functional barrier between blood and cardiac myocytes (Meissner et al., 2002). The I_{Kr} binding site for many drugs is believed to be on the intracellular site of the channel embedded in the plasma membrane (Sanguinetti and Tristani-Firouzi, 2006). Consequently, factors such as ABC transporters that regulate intracellular concentrations of I_{Kr} binding drugs could modulate risk of cardiac toxicity. A number of in vitro and in vivo studies have already demonstrated drug-drug interactions (DDIs) from several cardiovascular ion channel inhibitors with human P-gp and its animal analogs, including verapamil, digoxin, and amiodarone that have been associated with adverse QT prolongation (Wiśniowska and Polak, 2016; Ledwitch and Roberts, 2017).

6.2.5.2. Cardiac Uptake Transporters

Conversely, uptake transporter proteins increase intracellular concentrations of substrates to meet the requirement of cellular pathways or metabolism. Co-expression of the organic cation transporter, OCTN1, expressed in human cardiac myocytes, has been shown to intensify quinidine-induced hERG block likely as a result of increasing intracellular concentrations (McBride et al., 2009). The neurotransmitter norepinephrine (NE) in the heart is cleared by neuronal uptake-1 and extraneuronal uptake-2 transporters. Cardiac uptake-1 and -2 expression varies among species, but uptake-1 is the primary transporter in humans. It has been shown that a NE analog labeled with ^{18}F for PET was retained in the heart of rabbits and NHPs primarily via the neuronal uptake-1 with high selectivity, similar to human, but not in rats (Yu et al., 2013).

Other transporters responsible for the maintenance of the biochemical energy pathways in the cardiomyocyte play a vital role, such as the cellular uptake of both long-chain fatty acids (LCFA) and glucose which is regulated by the sarcolemmal transport proteins, fatty acid translocase (FAT)/CD36 and GLUT4, respectively. These transport proteins are not only present at the sarcolemma, but also in intracellular storage compartments. Both an increased workload and the hormone insulin induce translocation of FAT/CD36 and GLUT4 to the sarcolemma. Therefore alterations in substrate uptake and utilization may play a pathological role in the progression towards type-2 diabetes mellitus (Coort et al., 2007).

6.2.5.3. Cardiac Metabolism

Cytochrome P450 enzymes (CYP450), are the most predominant exogenous metabolising enzymes in mammalian cells, with 3A4 isoform the most commonly involved across many cell tissue types and greatest abundance in the liver (Zhou et al., 2007). Many CYP enzymes have been identified in the heart and their expression levels have been reported to be different to other tissues and altered during cardiac hypertrophy and heart failure. Cardiac CYP1B and CYP2A, CYP2B, CYP2E, CYP2J, CYP4A and CYP11 mRNA levels and related enzyme activities are usually increased due to heart failure. On the other hand, concurrent down-regulation of hepatic CYP involved in drug metabolism through several mechanisms which include hepatocellular damage, hypoxia, and elevated levels of pro-inflammatory cytokines is observed (Ayman 2008). Many extrahepatic tissues, like heart, contain active CYP450 but there is a lack of information regarding their role in cellular injury or homeostasis. Much of our current knowledge about cardiac CYP450 enzymes has been limited to studies

investigating the role of fatty acid metabolites in heart linked to diabetes, smoking, and hypertension (Chaudhary et al., 2009).

In contrast to hepatocytes and enterocytes, CYP3A activity is lacking in human cardiomyocytes as shown by midazolam not being metabolised, but instead CYP2J2 is the dominant isozyme with minor contributions from CYP2D6 and CYP2E1 (Evangelista et al., 2013). CYP2J2 primarily metabolizes polyunsaturated fatty acids such as arachidonic acid to cardioactive epoxyeicosatrienoic acids. Additionally, CYP2J2 metabolizes a number of xenobiotics such as the antihistamines, astemizole and terfenadine, and is potently inhibited by danazol and telmisartan (Xu et al., 2013). In recent years CYP2J2 has been actively studied with the focus on its biological functions in cardiac pathophysiology and subsequent impact of induction or inhibition, including expression in tumour cells (Evangelista et al., 2013; Karkhanis et al., 2017).

An in vitro cellular investigation using both hepatocytes and cardiomyocytes in a comparative manner would enable in vitro-in vivo extrapolation (IVIVE) as an alternative by using intrinsic scaling of clearance, metabolism information, without the need for multiple species or retrospective allometry (Shiran et al., 2006; Rostami-Hodjegan, 2012). Heart-tissue specific information around the potential drug uptake, metabolism, tissue partitioning, extracellular vs. intracellular free drug concentrations and ion channel interactions resulting in QT prolongation can only improve the understanding of the drug dispositional effects by way of PBPK/PD modelling, as described by Weiss et al. and by Tylutki and Polak (Weiss, 2011; Tylutki and Polak, 2017)

Strathclyde Institute of Pharmacy and Biomedical Sciences
GlaxoSmithKline

REFERENCES

REFERENCES

Aarons L (2005) Physiologically based pharmacokinetic modelling: a sound mechanistic basis is needed. *British Journal of Clinical Pharmacology* **60**:581-583.

Abernethy D, Todd E and Mitchell J (1984) Verapamil and norverapamil determination in human plasma by gas-liquid chromatography using nitrogen-phosphorus detection: application to single-dose pharmacokinetic studies. *Pharmacology* **29**:264-268.

Abrahamsson P, Aberg AM, Johansson G, Winso O, Waldenstrom A and Haney M (2011) Detection of myocardial ischaemia using surface microdialysis on the beating heart. *Clinical Physiology and Functional Imaging* **31**:175-181.

Adamantidis MM, Dumotier BM, Caron JF and Bordet R (1998) Sparfloxacin but not levofloxacin or ofloxacin prolongs cardiac repolarization in rabbit Purkinje fibers. *Fundamental & Clinical Pharmacology* **12**:70-76.

Adeyemi O, Roberts S, Harris J, West H, Shome S and Dewhurst M (2009) QA interval as an indirect measure of cardiac contractility in the conscious telemeterised rat: Model optimisation and evaluation. *Journal of Pharmacological and Toxicological Methods* **60**:159-166.

Akita M, Shibazaki Y, Izumi M, Hiratsuka K, Sakai T, Kurosawa T and Shindo Y (2004) Comparative Assessment of Prufloxacin, Sparfoxacin, Gatifloxacin and Levofloxacin in the Rabbit Model of Proarrhythmia. *The Journal of Toxicological Sciences* **29**:63-71.

Al-Wabel N (2002) Electrocardiographic and Hemodynamic effects of Cisapride alone and combined with Erythromycin in Anaesthetized Dogs, in *Cardiovasc Toxicol* pp 195-207.

Anderson ME, Mazur A, Yang T and Roden DM (2001) Potassium Current Antagonist Properties and Proarrhythmic Consequences of Quinolone Antibiotics. *Journal of Pharmacology and Experimental Therapeutics* **296**:806-810.

Andersson MI and MacGowan AP (2003) Development of the quinolones. *Journal of Antimicrobial Chemotherapy* **51**:1-11.

Ando K, Hombo T, Kanno A, Ikeda H, Imaizumi M, Shimizu N, Sakamoto K, Kitani S, Yamamoto Y, Hizume S, Nakai K, Kitayama T and Yamamoto K (2005) QT PRODACT: In Vivo QT Assay With a Conscious Monkey for Assessment of the Potential for Drug-Induced QT Interval Prolongation. *J Pharm Sci* **99**:487-500.

Anttila M, Arstila M, Pfeffer M, Tikkanen R, Vallinkoski V and Sundquist H (1976) Human Pharmacokinetics of Sotalol. *Acta Pharmacologica et Toxicologica* **39**:118-128.

Argekar AP and Sawant JG (1999) Determination of cisapride in pharmaceutical dosage forms by reversed-phase liquid chromatography. *Journal of Pharmaceutical and Biomedical Analysis* **21**:221-226.

Artola-Garicano E, Vaes WHJ and Hermens JLM (2000) Validation of Negligible Depletion Solid-Phase Microextraction as a Tool to Determine Tissue/Blood Partition Coefficients for Semivolatile and Nonvolatile Organic Chemicals. *Toxicology and Applied Pharmacology* **166**:138-144.

Ashour S and Bayram R (2015) Development and validation of sensitive kinetic spectrophotometric method for the determination of moxifloxacin antibiotic in pure and commercial tablets. *Spectrochimica Acta Part A: Molecular and Biomolecular Spectroscopy* **140**:216-222.

Authier S, Gervais J, Fournier S, Gauvin D, Maghezzi S and Troncy E (2011) Cardiovascular and respiratory safety pharmacology in G+Âttingen minipigs: Pharmacological characterization. *Journal of Pharmacological and Toxicological Methods* **64**:53-59.

Authier S, Pugsley MK, Koerner JE, Fermini B, Redfern WS, Valentin J-P, Vargas HM, Leishman DJ, Correll K and Curtis MJ (2017) Proarrhythmia liability assessment and the Comprehensive In Vitro Proarrhythmia Assay (CiPA): An Industry Survey on Current Practice. *Journal of Pharmacological and Toxicological Methods*.

Authier S, Tanguay JF, Gauvin D, Fruscia RD and Troncy E (2007) A cardiovascular monitoring system used in conscious cynomolgus monkeys for regulatory safety pharmacology: Part 2: Pharmacological validation. *Journal of Pharmacological and Toxicological Methods* **56**:122-130.

Bai S, Lankford S and Johnson L (1993) Pharmacokinetics of the Enantiomers of Verapamil in the Dog. *Chirality* **5**:436-442.

Balant LP and Gex-Fabry M (2000) Modelling during drug development. *European Journal of Pharmaceutics and Biopharmaceutics* **50**:13-26.

Ball K, Bouzom F, Scherrmann J-M, Walther B and Declèves X (2013) Physiologically Based Pharmacokinetic Modelling of Drug Penetration Across the Blood–Brain Barrier—Towards a Mechanistic IVIVE-Based Approach. *The AAPS Journal* **15**:913-932.

Ball K, Bouzom F, Scherrmann J-M, Walther B and Declèves X (2014) Comparing translational population-PBPK modelling of brain microdialysis with bottom-up prediction of brain-to-plasma distribution in rat and human. *Biopharmaceutics & Drug Disposition* **35**:485-499.

Ballow C, Lettieri J, Agarwal V, Liu P, Stass H and Sullivan JT (1999) Absolute bioavailability of moxifloxacin. *Clinical Therapeutics* **21**:513-522.

Banker MJ and Clark TH (2008) Plasma / Serum Protein Binding Determinations. *Current Drug Metabolism* **9**:854-859.

Banker MJ, Clark TH and Williams JA (2003) Development and validation of a 96-well equilibrium dialysis apparatus for measuring plasma protein binding. *Journal of Pharmaceutical Sciences* **92**:967-974.

Bart J, Willemsen ATM, Groen HJM, van der Graaf WTA, Wegman TD, Vaalburg W, de Vries EGE and Hendrikse NH (2003) Quantitative assessment of P-glycoprotein function in the rat blood–brain barrier by distribution volume of [11C]verapamil measured with PET. *NeuroImage* **20**:1775-1782.

Basile J (2004) The Role of Existing and Newer Calcium Channel Blockers in the Treatment of Hypertension. *The Journal of Clinical Hypertension* **6**:621-629.

Bass A, Kinter L and Williams P (2004) Origins, practices and future of safety pharmacology. *Journal of Pharmacological and Toxicological Methods* **49**:145-151.

Bass AS, Vargas HM, Valentin JP, Kinter LB, Hammond T, Wallis R, Siegl PKS and Yamamoto K (2011) Safety pharmacology in 2010 and beyond: Survey of significant events of the past 10 years and a roadmap to the immediate-, intermediate- and long-term future in recognition of the tenth anniversary of the Safety Pharmacology Society. *Journal of Pharmacological and Toxicological Methods* **64**:7-15.

Bate ST and Clarke RA (2014) *The Design and Statistical Analysis of Animal Experiments*. Cambridge University Press.

Batey AJ and Coker SJ (2002) Proarrhythmic potential of halofantrine, terfenadine and clofilium in a modified in vivo model of torsade de pointes. *British Journal of Pharmacology* **135**:1003-1012.

Beattie KA, Luscombe C, Williams G, Munoz-Muriedas J, Gavaghan DJ, Cui Y and Mirams GR (2013) Evaluation of an in silico cardiac safety assay: Using ion channel screening data to predict QT interval changes in the rabbit ventricular wedge. *Journal of Pharmacological and Toxicological Methods* **68**:88-96.

Beckmann J, Kees F, Schaumburger J, Kalteis T, Lehn N, Grifka J and Lerch K (2007) Tissue concentrations of vancomycin and Moxifloxacin in periprosthetic infection in rats. *Acta Orthopaedica* **78**:766-773.

Bedford T and Rowbotham D (1996) Cisapride: Drug Interactions of Clinical Significance, in *Drug Saf* pp 167-175, Department of Anaesthesia, Leicester Royal Infirmary NHS Trust, Leicester, England.

Belpaire FM, Bogaert MG and Rosseneu M (1982) Binding of+¦-adrenoceptor blocking drugs to human serum albumin, to +¦1-acid glycoprotein and to human serum. *European Journal of Clinical Pharmacology* **22**:253-256.

Benet LZ and Hoener BA (2002) Changes in plasma protein binding have little clinical relevance. *Clinical Pharmacology & Therapeutics* **71**:115-121.

Berezhkovskiy LM (2007) On the determination of the time delay in reaching the steady state drug concentration in the organ compared to plasma. *Journal of Pharmaceutical Sciences* **96**:3432-3443.

Berezhkovskiy LM (2010) On the influence of protein binding on pharmacological activity of drugs. *Journal of Pharmaceutical Sciences* **99**:2153-2165.

Berridge BR, Hoffmann P, Turk JR, Sellke F, Gintant G, Hirkaler G, Dreher K, Schultze AE, Walker D, Edmunds N, Halpern W, Falls J, Sanders M and Pettit SD (2013) Integrated and translational nonclinical in vivo cardiovascular risk assessment: Gaps and opportunities. *Regulatory Toxicology and Pharmacology* **65**:38-46.

Bertera FM, Mayer MA, Opezzo JAW, Taira CA, Bramuglia GF and Höcht C (2007) Pharmacokinetic–pharmacodynamic modeling of diltiazem in spontaneously hypertensive rats: A microdialysis study. *Journal of Pharmacological and Toxicological Methods* **56**:290-299.

Birtwistle MR, Mager DE and Gallo JM (2013) Mechanistic Vs. Empirical Network Models of Drug Action. *CPT: Pharmacometrics & Systems Pharmacology* **2**:1-3.

Boffito M, Back DJ, Hoggard PG, Caci A, Bonora S, Raiteri R, Sinicco A, Reynolds HE, Khoo S and Di Perri G (2003) Intra-individual variability in lopinavir plasma trough concentrations supports therapeutic drug monitoring. *AIDS* **17**.

Bohnert T and Gan LS (2013) Plasma protein binding: From discovery to development. *Journal of Pharmaceutical Sciences* **102**:2953-2994.

Bojko B and Pawliszyn J (2014) In vivo and ex vivo SPME: a low invasive sampling and sample preparation tool in clinical bioanalysis. *Bioanalysis* **6**:1227-1239.

Borner E, Borner K and Lode H (1992) Determination of sparfloxacin in serum and urine by high-performance liquid chromatography. *J Chromatogr* **579**:285-289.

Bourdet DL, Tsuruda PR, Obedencio GP and Smith JAM (2012) Prediction of Human Serotonin and Norepinephrine Transporter Occupancy of Duloxetine by Pharmacokinetic/Pharmacodynamic Modeling in the Rat. *Journal of Pharmacology and Experimental Therapeutics* **341**:137-145.

Bregante MA, Saez P, Aramayona JJ, Fraile LJ, Garcia MA and Solans C (1999) Comparative pharmacokinetics of enrofloxacin in mice, rats, rabbits, sheep, and cows. *Am J Vet Res* **60**:1111-1116.

Briasoulis A, Agarwal V and Pierce WJ (2011) QT Prolongation and Torsade de Pointes Induced by Fluoroquinolones: Infrequent Side Effects from Commonly Used Medications. *Cardiology* **120**:103-110.

Bril A, Gout B, Bonhomme M, Landais L, Faivre JF, Linee P, Poyser RH and Ruffolo RR (1996) Combined potassium and calcium channel blocking activities as a basis for antiarrhythmic efficacy with low proarrhythmic risk: experimental profile of BRL-32872. *Journal of Pharmacology and Experimental Therapeutics* **276**:637-646.

Brown HS, Griffin M and Houston JB (2007) Evaluation of Cryopreserved Human Hepatocytes as an Alternative in Vitro System to Microsomes for the Prediction of Metabolic Clearance. *Drug Metabolism and Disposition* **35**:293-301.

Brunner M, Derendorf H and Müller M (2005) Microdialysis for in vivo pharmacokinetic/pharmacodynamic characterization of anti-infective drugs. *Current Opinion in Pharmacology* **5**:495-499.

Burman WJ, Goldberg S, Johnson JL, Muzanye G, Engle M, Mosher AW, Choudhri S, Daley CL, Munsiff SS, Zhao Z, Vernon A and Chaisson RE (2006) Moxifloxacin versus Ethambutol in the First 2 Months of Treatment for Pulmonary Tuberculosis. *American Journal of Respiratory and Critical Care Medicine* **174**:331-338.

Campanero MA, Calahorra B, García-Quetglás E, Honorato J and Carballal JJ (1998) Determination of cisapride in human plasma by high-performance liquid chromatography. *Chromatographia* **47**:9-10.

Campbell TJ and Williams KM (1998) Therapeutic drug monitoring: antiarrhythmic drugs. *British Journal of Clinical Pharmacology* **46**:307-319.

Cao Y and Jusko W (2012) Applications of minimal physiologically-based pharmacokinetic models. *J Pharmacokinet Pharmacodyn* **39**:711-723.

Carceles CM, Serrano JM, Marin P, ESCUDERO E and Fernandez-Varon E (2006) Pharmacokinetics of Moxifloxacin in Rabbits After Intravenous, Subcutaneous and a Long-acting Poloxamer 407 Gel Formulation Administration. *Journal of Veterinary Medicine Series A* **53**:300-304.

Carlsson L (2008) The anaesthetised methoxamine-sensitised rabbit model of torsades de pointes. *Pharmacology & Therapeutics* **119**:160-167.

Carlsson L, Abrahamsson C, Andersson B, Duker G and Schiller-Linhardt G (1993) Proarrhythmic effects of the class III agent almokalant: importance of infusion rate, QT dispersion, and early afterdepolarisations. *Cardiovascular Research* **27**:2186-2193.

Carlsson L, Almgren O and Duker G (1990) QTU-Prolongation and Torsades de Pointes Induced by Putative Class III Antiarrhythmic Agents in the Rabbit: Etiology and Interventions, in *J Cardiovasc Pharmacol* pp 276-285, Department of Cardiovascular Pharmacology, Hassle Research Laboratories, Molndal, Sweden.

Carlsson L, Amos GJ, Andersson B, Drews L, Duker G and Wadstedt G (1997) Electrophysiological Characterization of the Prokinetic Agents Cisapride and Mosapride in Vivo and in Vitro: Implications for Proarrhythmic Potential? *Journal of Pharmacology and Experimental Therapeutics* **282**:220-227.

Carlsson L, Drews L and Duker G (1996) Rhythm anomalies related to delayed repolarization in vivo: influence of sarcolemmal Ca++ entry and intracellular Ca++ overload. *Journal of Pharmacology and Experimental Therapeutics* **279**:231-239.

Carmeliet E (2006) Action Potential Duration, Rate of Stimulation, and Intracellular Sodium. *Journal of Cardiovascular Electrophysiology* **17**:S2-S7.

Carr RA, Pasutto FM, Lewanczuk RZ and Foster RT (1995) Protein binding of sotalol enantiomers in young and elderly human and rat serum using ultrafiltration. *Biopharmaceutics & Drug Disposition* **16**:705-712.

Caruso A, Frances N, Meille C, Greiter-Wilke A, Hillebrecht A and Lav+® T (2014) Translational PK/PD modeling for cardiovascular safety assessment of drug candidates: Methods and examples in drug development. *Journal of Pharmacological and Toxicological Methods* **70**:73-85.

Cavero I (2007) Using pharmacokinetic/pharmacodynamic modelling in safety pharmacology to better define safety margins: a regional workshop of the Safety Pharmacology Society. *Expert Opinion on Drug Safety* **6**:465-471.

Cavero I (2011) 10th annual meeting of the Safety Pharmacology Society: an overview. *Expert Opinion on Drug Safety* **10**:319-333.

Cavero I, Guillon J-M, Ballet V, Clements M, Gerbeau J-F and Holzgrefe H (2016) Comprehensive in vitro Proarrhythmia Assay (CiPA): Pending issues for successful validation and implementation. *Journal of Pharmacological and Toxicological Methods* **81**:21-36.

Cavero I and Kaplan HR (2008) Drug discovery paradigms: past, present, future ΓÇô a centennial symposium of the American Society for Pharmacology and Experimental Therapeutics. *Expert Opinion on Drug Discovery* **3**:1145-1154.

Chain ASY, Dubois VFS, Danhof M, Sturkenboom MCJM, Della Pasqua O and Team CSP (2013) Identifying the translational gap in the evaluation of drug-induced QTc interval prolongation. *British Journal of Clinical Pharmacology* **76**:708-724.

Chan KP, Chu KO, Lai WW-K, Choy KW, Wang CC, Lam DS-C and Pang CP (2006) Determination of ofloxacin and moxifloxacin and their penetration in human aqueous and vitreous humor by using high-performance liquid chromatography fluorescence detection. *Analytical Biochemistry* **353**:30-36.

Chang C, Byon W, Lu Y, Jacobsen L, Badura L, Sawant-Basak A, Miller E, Liu J, Grimwood S, Wang E and Maurer T (2011) Quantitative PKΓÇôPD Model-Based Translational Pharmacology of a Novel Kappa Opioid Receptor Antagonist Between Rats and Humans. *AAPS J* **13**:565-575.

Chaudhary KR, Batchu SN and Seubert JM (2009) Cytochrome P450 enzymes and the heart. *IUBMB Life* **61**:954-960.

Chelly JE, Hysing ES, Abernethy DR, Doursout MF and Merin RG (1986) Effects of inhalational anesthetics on verapamil pharmacokinetics in dogs. *ANESTHESIOLOGY* **65**:266-271.

Chen K and Seng K-Y (2012) Calibration and validation of a physiologically based model for soman intoxication in the rat, marmoset, guinea pig and pig. *Journal of Applied Toxicology* **32**:673-686.

Chen X, Cass JD, Bradley JA, Dahm CM, Sun Z, Kadyszewski E, Engwall MJ and Zhou J (2005) QT prolongation and proarrhythmia by moxifloxacin: concordance of preclinical models in relation to clinical outcome. *British Journal of Pharmacology* **146**:792-799.

Chen X, Cordes JS, Bradley JA, Sun Z and Zhou J (2006) Use of arterially perfused rabbit ventricular wedge in predicting arrhythmogenic potentials of drugs. *Journal of Pharmacological and Toxicological Methods* **54**:261-272.

Cherry EM, Fenton FH and Gilmour RF, Jr. (2012) Mechanisms of ventricular arrhythmias: a dynamical systems-based perspective. *Am J Physiol Heart Circ Physiol* **302**:H2451-H2463.

Chesnut SM and Salisbury JJ (2007) The role of UHPLC in pharmaceutical development. *Journal of Separation Science* **30**:1183-1190.

Chetty M, Rose R, Abduljalil K, Patel N, Lu G, Cain T, Jamei M and Rostami-Hodjegan A (2014) Applications of linking PBPK and PD models to predict the impact of genotypic variability, formulation differences, differences in target binding capacity and target site drug concentrations on drug responses and variability. *Frontiers in Pharmacology* **5**.

Chiba K, Sugiyama A, Hagiwara T, Takahashi Si, Takasuna K and Hashimoto K (2004a) In vivo experimental approach for the risk assessment of fluoroquinolone antibacterial agents-induced long QT syndrome. *European Journal of Pharmacology* **486**:189-200.

Chiba K, Sugiyama A, Takasuna K and Hashimoto K (2004b) Comparison of sensitivity of surrogate markers of drug-induced torsades de pointes in canine hearts. *European Journal of Pharmacology* **502**:117-122.

Cho HY, Park SA and Lee YB (2006) Improvement and validation of an HPLC method for examining the effects of the MDR1 gene polymorphism on sparfloxacin pharmacokinetics. *Journal of Chromatography B* **834**:84-92.

Chytil L, Štrauch B, Cvačka J, Marešová V, Widimský Jr J, Holaj R and Slanař O (2010) Determination of doxazosin and verapamil in human serum by fast LC–MS/MS: Application to document non-compliance of patients. *Journal of Chromatography B* **878**:3167-3173.

Cisternino S, Schlatter J and Saulnier JL (1998) Determination of cisapride and norcisapride in human plasma using high-performance liquid chromatography with ultraviolet detection. *Journal of Chromatography B: Biomedical Sciences and Applications* **714**:395-398.

Colburn W and Lee J (2003) Biomarkers, Validation and Pharmacokinetic-Pharmacodynamic Modelling. *Clin Pharmacokinet* **42**:997-1022.

Cole SCJ, Flanagan RJ, Johnston A and Holt DW (1981) Rapid high-performance liquid Chromatographie method for the measurement of verapamil and norverapamil in blood, plasma or serum. *Journal of Chromatography* **218**:621-629.

Coort SLM, Bonen A, van der Vusse GJ, Glatz JFC and Luiken JJFP (2007) Cardiac substrate uptake and metabolism in obesity and type-2 diabetes: Role of sarcolemmal substrate transporters. *Molecular and Cellular Biochemistry* **299**:5-18.

Couture L, Nash JA and Turgeon J (2006) The ATP-Binding Cassette Transporters and Their Implication in Drug Disposition: A Special Look at the Heart. *Pharmacological Reviews* **58**:244-258.

Cox SK (2007) Allometric scaling of marbofloxacin, moxifloxacin, danofloxacin and difloxacin pharmacokinetics: a retrospective analysis. *Journal of Veterinary Pharmacology and Therapeutics* **30**:381-386.

CPMP and EMEA (1997) *Points to Consider: The Assessment of the Potential for QT Interval Prolongation by Non-Cardiovascular Medicinal Products (CPMP/986/96)*.

Csajka C and Verotta D (2006) PharmacokineticΓÇôPharmacodynamic Modelling: History and Perspectives. *J Pharmacokinet Pharmacodyn* **33**:227-279.

d'Yvoire B, Prieto P, Blaauboer B, Bois F, Boobis A, Brochet C, Coecke S, Freidig A, Gundert-Remy U, Hartung T, Jacobs M, Lave T, Leahy D, Lennernas H, Loizou G, Meek B, Pease C, Rowland M, Spendiff M, Yang J and Zeilmaker M (2007) Physiologically-based Kinetic Modelling (PBK Modelling): meeting the 3Rs agenda. The report and recommendations of ECVAM Workshop 63. *ATLA* **35**:661-671.

Danhof M, de Jongh J, de Lange ECM, Della Pasqua O, Ploeger BA and Voskuyl RA (2007) Mechanism-Based Pharmacokinetic-Pharmacodynamic Modeling: Biophase Distribution, Receptor Theory, and Dynamical Systems Analysis. *Annual Review of Pharmacology and Toxicology* **47**:357-400.

Danhof M, de Lange ECM, Della Pasqua OE, Ploeger BA and Voskuyl RA (2008) Mechanism-based pharmacokinetic-pharmacodynamic (PK-PD) modeling in translational drug research. *Trends in Pharmacological Sciences* **29**:186-191.

Darwich AS, Margolskee A, Pepin X, Aarons L, Galetin A, Rostami-Hodjegan A, Carlert S, Hammarberg M, Hilgendorf C, Johansson P, Karlsson E, Murphy D, Tannergren C, Thörn H, Yasin M, Mazuir F, Nicolas O, Ramusovic S, Xu C, Pathak SM, Korjamo T, Laru J, Malkki J, Pappinen S, Tuunainen J, Dressman J, Hansmann S, Kostewicz E, He H, Heimbach T, Wu F, Hoft C, Pang Y, Bolger MB, Huehn E, Lukacova V, Mullin JM, Szeto KX, Costales C, Lin J, McAllister M, Modi S, Rotter C, Varma M, Wong M, Mitra A, Bevernage J, Biewenga J, Van Peer A, Lloyd R, Shardlow C, Langguth P, Mishenzon I, Nguyen MA, Brown J, Lennernäs H and Abrahamsson B (2017) IMI – Oral biopharmaceutics tools project – Evaluation of bottom-up PBPK prediction success part 3: Identifying gaps in system parameters by analysing In Silico performance across different compound classes. *European Journal of Pharmaceutical Sciences* **96**:626-642.

Davies B and Morris T (1993) Physiological Parameters in Laboratory Animals and Humans. *Pharm Res* **10**:1093-1095.

Davies MR, Wang K, Mirams GR, Caruso A, Noble D, Walz A, Lavé T, Schuler F, Singer T and Polonchuk L (2016) Recent developments in using mechanistic cardiac modelling for drug safety evaluation. *Drug Discovery Today* **21**:924-938.

Dayneka N, Garg V and Jusko W (1993) Comparison of Four Basic Models of Indirect Pharmacodynamic Responses. *J Pharmacokinet Biopharm* **21**:457-478.

De Buck SS, Sinha VK, Fenu LA, Gilissen RA, Mackie CE and Nijsen MJ (2007a) The Prediction of Drug Metabolism, Tissue Distribution, and Bioavailability of 50 Structurally Diverse Compounds in Rat Using Mechanism-Based Absorption, Distribution, and Metabolism Prediction Tools. *Drug Metabolism and Disposition* **35**:649-659.

De Buck SS, Sinha VK, Fenu LA, Nijsen MJ, Mackie CE and Gilissen RAHJ (2007b) Prediction of Human Pharmacokinetics Using Physiologically Based Modeling: A Retrospective Analysis of 26 Clinically Tested Drugs. *Drug Metabolism and Disposition* **35**:1766-1780.

De Clerck F, Van de Water A, D'Aubioul J, Lu HR, Van Rossem K, Hermans A and Van Ammel K (2002) In vivo measurement of QT prolongation, dispersion and arrhythmogenesis: application to the preclinical cardiovascular safety pharmacology of a new chemical entity. *Fundamental & Clinical Pharmacology* **16**:125-140.

de la Peña A, Liu P and Derendorf H (2000) Microdialysis in peripheral tissues. *Advanced Drug Delivery Reviews* **45**:189-216.

Debbas NM, du Cailar C, Bexton RS, Demaille JG, Camm AJ and Puech P (1984) The QT interval: a predictor of the plasma and myocardial concentrations of amiodarone. *British Heart Journal* **51**:316-320.

Dejaegher B, Pieters S and Vander Heyden Y (2010) Emerging Analytical Separation Techniques with High Throughput Potential for Pharmaceutical Analysis, Part II: Novel Chromatographic Modes. *Combinatorial Chemistry & High Throughput Screening* **13**:530-547.

Derendorf H, Lesko LJ, Chaikin P, Colburn WA, Lee P, Miller R, Powell R, Rhodes G, Stanski D and Venitz J (2000) Pharmacokinetic/Pharmacodynamic Modeling in Drug Research and Development. *The Journal of Clinical Pharmacology* **40**:1399-1418.

Derendorf H and Meibohm B (1999) Modeling of Pharmacokinetic/Pharmacodynamic (PK/PD) Relationships: Concepts and Perspectives. *Pharm Res* **16**:176-185.

Di Diego JM, Sicouri S, Myles RC, Burton FL, Smith GL and Antzelevitch C (2013) Optical and electrical recordings from isolated coronary-perfused ventricular wedge preparations. *Journal of Molecular and Cellular Cardiology* **54**:53-64.

Ding X, Ghobarah H, Zhang X, Jaochico A, Liu X, Deshmukh G, Liederer BM, Hop CECA and Dean B (2013) High-throughput liquid chromatography/mass spectrometry method for the quantitation of small molecules using accurate mass technologies in supporting discovery drug screening. *Rapid Communications in Mass Spectrometry* **27**:401-408.

Doke SK and Dhawale SC (2015) Alternatives to animal testing: A review. *Saudi Pharmaceutical Journal* **23**:223-229.

Döppenschmitt S, Langguth P, Regårdh CG, Andersson TB, Hilgendorf C and Spahn-Langguth H (1999) Characterization of Binding Properties to Human P-Glycoprotein: Development of a [³H]Verapamil Radioligand-Binding Assay. *Journal of Pharmacology and Experimental Therapeutics* **288**:348-357.

Drayer DE (1984) Clinical Consequences of the Lipophilicity and Plasma Protein Binding of Antiarrhythmic Drugs and Active Metabolites in Man. *Annals of the New York Academy of Sciences* **432**:45-56.

Dubois VFS, Yu H, Danhof M, Della Pasqua O and Platform CSPTaTPP (2015) Model-based evaluation of drug-induced QTc prolongation for compounds in early development. *British Journal of Clinical Pharmacology* **79**:148-161.

Dumotier BM, Bastide M and Adamantidis MM (2001) Use-dependent effects of cisapride on postrest action potentials in rabbit ventricular myocardium. *European Journal of Pharmacology* **422**:137-148.

Dunlop J, Bowlby M, Peri R, Vasilyev D and Arias R (2008) High-throughput electrophysiology: an emerging paradigm for ion-channel screening and physiology. *Nat Rev Drug Discov* **7**:358-368.

E14 I (2005) ICH E14: The Clinical Evaluation of QT/QTc Interval Prolongation and Proarrhythmic Potential for Non-Antiarrhythmic Drugs, in (Harmonisation ICf ed).

Eichelbaum M, Birket P, Grube E, Gutgemann U and Somogyi A (1980) Effects of verapamil on P-R intervals in relation to verapamil plasma levels following single i.v. and oral administration and during chronic treatment. *Central European Journal of Medicine* **58**:919-925.

Eichelbaum M, Ende M, Remberg G, Schomerus M and Dengler HJ (1979) The metabolism of DL-[14C]verapamil in man. *Drug Metabolism and Disposition* **7**:145-148.

Eichelbaum M, Mikus G and Vogelgesang B (1984) Pharmacokinetics of (+)-, (-)- and (+/-)-verapamil after intravenous administration. *British Journal of Clinical Pharmacology* **17**:453-458.

Eichenbaum G, Pugsley MK, Gallacher DJ, Towart R, McIntyre G, Shukla U, Davenport JM, Lu HR, Rohrbacher J and Hillsamer V (2012) Role of mixed ion channel effects in the cardiovascular safety assessment of the novel anti-MRSA fluoroquinolone JNJ-Q2. *British Journal of Pharmacology* **166**:1694-1707.

Eissing T, Kuepfer L, Becker C, Block M, Coboeken K, Gaub T, Goerlitz L, Jaeger J, Loosen R, Ludewig B, Meyer M, Niederalt C, Sevestre M, Siegmund HU, Solodenko J, Thelen K, Telle U, Weiss W, Wendl T, Willmann S and Lippert J (2011) A computational systems biology software platform for multiscale modeling and simulation: Integrating whole-body physiology, disease biology, and molecular reaction networks. *Frontiers in Physiology* **2**.

Emoto C, Murayama N, Rostami-Hodjegan A and Yamazaki H (2009) Utilization of estimated physicochemical properties as an integrated part of predicting hepatic clearance in the early drug-discovery stage: Impact of plasma and microsomal binding. *Xenobiotica* **39**:227-235.

Esteves da Silva JCG, Leitão JMM, Costa FS and Ribeiro JLA (2002) Detection of verapamil drug by fluorescence and trilinear decomposition techniques. *Analytica Chimica Acta* **453**:105-115.

Evangelista EA, Kaspera R, Mokadam NA, Jones JP and Totah RA (2013) Activity, Inhibition, and Induction of Cytochrome P450 2J2 in Adult Human Primary Cardiomyocytes. *Drug Metabolism and Disposition* **41**:2087-2094.

Farkas Aí, Batey AJ and Coker SJ (2004) How to measure electrocardiographic QT interval in the anaesthetized rabbit. *Journal of Pharmacological and Toxicological Methods* **50**:175-185.

Farkas Aí and Coker SJ (2002) Limited induction of torsade de pointes by terikalant and erythromycin in an in vivo model. *European Journal of Pharmacology* **449**:143-153.

Farkas Aí, Lepr+ín Ií and Papp JG (2002) Proarrhythmic Effects of Intravenous Quinidine, Amiodarone, d -Sotalol, and Almokalant in the Anesthetized Rabbit Model of Torsade de Pointes. *Journal of Cardiovascular Pharmacology* **39**.

Farkas AS, Makra P, Csík N, Orosz S, Shattock MJ, Fülöp F, Forster T, Csanády M, Papp JG, Varró A and Farkas A (2009) The role of the Na+/Ca2+ exchanger, INa and ICaL in the genesis of dofetilide-induced torsades de pointes in isolated, AV-blocked rabbit hearts. *British Journal of Pharmacology* **156**:920-932.

Farkas AS, Rudas L, Makra P, Cs+¡k N, Lepr+ín Ií, Forster Tí, Csan+ídy Ms, Papp JG, Varr+¦ Aí and Farkas Aí (2010) Biomarkers and endogenous determinants of dofetilide-induced torsades de pointes in +¦1-adrenoceptor-stimulated, anaesthetized rabbits. *British Journal of Pharmacology* **161**:1477-1495.

FDA U (1999) Draft Guidance for Industry: Bioanalytical Method Validation, in.

FDA U (2001) *Guidance for Industry: Bioanalytical method Validation*. US Department of Health and Human Services FDA, Center for Drug Evaluation and Research.

Fernandez-Varon E, BOVAIRA MJ, ESPUNY A, ESCUDERO E, VANCRAEYNEST D and Carceles CM (2005) Pharmacokinetic-pharmacodynamic integration of moxifloxacin in rabbits after intravenous, intramuscular and oral administration. *Journal of Veterinary Pharmacology and Therapeutics* **28**:343-348.

Ferri N, Siegl P, Corsini A, Herrmann J, Lerman A and Benghozi R (2013) Drug attrition during pre-clinical and clinical development: Understanding and managing drug-induced cardiotoxicity. *Pharmacology & Therapeutics* **138**:470-484.

Fiset C, Philippon F, Gilbert M and Turgeon J (1993) Stereoselective disposition of (+/-)-sotalol at steady-state conditions. *British Journal of Clinical Pharmacology* **36**:75-77.

Florian JA, Torn+©e CW, Brundage R, Parekh A and Garnett CE (2011) Population Pharmacokinetic and ConcentrationΓÇöQTc Models for Moxifloxacin: Pooled Analysis of 20 Thorough QT Studies. *The Journal of Clinical Pharmacology* **51**:1152-1162.

Fluhler E, Hayes R, Garofolo F, Dumont I, Blaye OL, Arnold M, Bansal S, Verhaeghe T, Wilson A, Stevenson L, Myler H, Bauer R, Bergeron A, Bustard M, Cai XY, Carbone M, Cojocaru L, Desai-Krieger D, Duggan J, Haidar S, Ho S, Ingelse B, Katori N, L+®vesque A, Lowes S, Ma M, Mettke K, Michon Je, Musuku A, Olah T, Patel S, Rose M, Schultz G, Smeraglia J, Spooner N, Stouffer B, Vazvaei F, Wakelin-Smith J, Wang J, Welink J, Whale E, Woolf E, Xue L and Yang TY (2014) 2014 White Paper on recent issues in bioanalysis: a full immersion in bioanalysis (Part 1 ΓÇô small molecules by LCMS). *Bioanalysis* **6**:3039-3049.

Fryer RM, Harrison PC, Muthukumarana A, Nodop Mazurek SG, Ng KJ, Chen RR, Harrington KE, Dinallo RM, Chi L and Reinhart GA (2012) Strategic Integration of In Vivo Cardiovascular Models During Lead Optimization: Predictive Value of 4 Models Independent of Species, Route of Administration, and Influence of Anesthesia. *Journal of Cardiovascular Pharmacology* **59**.

Furukawa T, Naritomi Y, Tetsuka K, Nakamori F, Moriguchi H, Yamano K, Terashita S, Tabata K and Teramura T (2014) Species differences in intestinal glucuronidation activities between humans, rats, dogs and monkeys. *Xenobiotica* **44**:205-216.

Gaborit N, Le Bouter S, Szuts V, Varro A, Escande D, Nattel S and Demolombe S (2007) Regional and tissue specific transcript signatures of ion channel genes in the non-diseased human heart. *The Journal of Physiology* **582**:675-693.

Georgiadis T, Markantonis-Kyroudis S and Triantafillidis J (2000) Prokinetic agents: current aspects with focus on cisapride. *Annals of Gastroenterology* **13**:269-289.

Gertz M, Harrison A, Houston JB and Galetin A (2010) Prediction of Human Intestinal First-Pass Metabolism of 25 CYP3A Substrates from In Vitro Clearance and Permeability Data. *Drug Metabolism and Disposition* **38**:1147-1158.

Ghafourian T and Amin Z (2013) QSAR Models for the Prediction of Plasma Protein Binding. *Bioimpacts* **3**:21-27.

Giacomini JC, Nelson WL, Theodore L, Mi Wong F, Rood D and Giacomini KM (1985) The Pharmacokinetics and Pharmacodynamics of d- and dl-Verapamil in Rabbits. *Journal of Cardiovascular Pharmacology* **7**.

Gibbs CL and Johnson EA (1961) Effect of Changes in Frequency of Stimulation Upon Rabbit Ventricular Action Potential. *Circulation Research* **9**:165-170.

Gillis AM, Duff HJ, Mitchell LB and Wyse DG (1993) Myocardial uptake and pharmacodynamics of procainamide in patients with coronary heart disease and sustained ventricular tachyarrhythmias. *Journal of Pharmacology and Experimental Therapeutics* **266**:1001-1006.

Giudicelli J-F, Tillement J-P and Boissier J (1973) Activite 1Badrenolytique comparee in vitro et in vivo et fixation proteique. *J Pharmac* **4**:129-136.

Gladziwa U, Bares R, Klotz U, Dakshinamurty KV, Ittel TH, Seiler KU and Sieberth Hg (1991) Pharmacokinetics and pharmacodynamics of cisapride in patients undergoing hemodialysis. *Clin Pharm Ther* **50**:673-681.

Gomoll AWA (1990) Comparability of the electrophysiologic responses and plasma and myocardial tissue concentrations of sotalol and its d stereoisomer in the dog. *Journal of Cardiovascular Pharmacology* **16**:204-211.

Gonzalez R, Gomis-Tena J, Corrias A, Ferrero JM, Rodriguez B and Saiz J (2010) Sex and age related differences in drug induced QT prolongation by dofetilide under reduced repolarization reserve in simulated ventricular cells, in *Engineering in Medicine and Biology Society (EMBC), 2010 Annual International Conference of the IEEE* pp 3245-3248.

Goryński K, Goryńska P, Górska A, Harężlak T, Jaroch A, Jaroch K, Lendor S, Skobowiat C and Bojko B (2016) SPME as a promising tool in translational medicine and drug discovery: From bench to bedside. *Journal of Pharmaceutical and Biomedical Analysis* **130**:55-67.

Gosetti F, Mazzucco E, Gennaro MC and Marengo E (2013) Ultra high performance liquid chromatography tandem mass spectrometry determination and profiling of prohibited steroids in human biological matrices. A review. *Journal of Chromatography B* **927**:22-36.

Gotta V, Cools F, van Ammel K, Gallacher DJ, Visser SAG, Sannajust F, Morissette P, Danhof M and van der Graaf PH (2015a) Inter-study variability of preclinical in vivo safety studies and translational exposureΓÇôQTc relationships ΓÇô a PKPD meta-analysis. *British Journal of Pharmacology* **172**:4364-4379.

Gotta V, Cools F, Van Ammel K, Gallacher DJ, Visser SAG, Sannajust F, Morissette P, Danhof M and Van der Graaf PH (2015b) Sensitivity of pharmacokineticΓÇôpharmacodynamic analysis for detecting small magnitudes of QTc prolongation in preclinical safety testing. *Journal of Pharmacological and Toxicological Methods* **72**:1-10.

Gotta V, Yu Z, Cools F, van Ammel K, Gallacher DJ, Visser SAG, Sannajust F, Morissette P, Danhof M and van der Graaf PH (2016) Application of a systems pharmacology model for translational prediction of hERG-mediated QTc prolongation. *Pharmacology Research & Perspectives* **4**:e00270-n/a.

Greene HL, Roden DM, Katz RJ, Woosley RL, Salerno DM and Henthorn RW (1992) The cardiac arrhythmia suppression trial: First CAST ΓÇª then CAST-II. *Journal of the American College of Cardiology* **19**:894-898.

Guentert TW, Huang JD and ie S (1982) Disposition of Quinidine in the Rabbit. *Journal of Pharmaceutical Sciences* **71**:812-815.

Guentert TW and Oie S (1980) Effect of plasma protein binding on quinidine kinetics in the rabbit. *Journal of Pharmacology and Experimental Therapeutics* **215**:165-171.

Guentert TW and Oie S (1982) Factors Influencing the Apparent Protein Binding of Quinidine. *Journal of Pharmaceutical Sciences* **71**:325-328.

Guo J, Massaeli H, Xu J, Jia Z, Wigle JT, Mesaeli N and Zhang S (2009a) Extracellular K(+) concentration controls cell surface density of I(Kr) in rabbit hearts and of the HERG channel in human cell lines. *J Clin Invest* **119**:2745-2757.

Guo L, Dong Z and Guthrie H (2009b) Validation of a guinea pig Langendorff heart model for assessing potential cardiovascular liability of drug candidates. *Journal of Pharmacological and Toxicological Methods* **60**:130-151.

Guth BD, Germeyer S, Kolb W and Markert M (2004) Developing a strategy for the nonclinical assessment of proarrhythmic risk of pharmaceuticals due to prolonged ventricular repolarization. *Journal of Pharmacological and Toxicological Methods* **49**:159-169.

Guth BD and Rast G (2010) Dealing with hERG liabilities early: diverse approaches to an important goal in drug development. *British Journal of Pharmacology* **159**:22-24.

Hamann S, Blouin R and McAllister RG, Jr. (1984) Clinical Pharmacokinetics of Verapamil. *Clin Pharmacokinet* **9**:26-41.

Hamdam J, Sethu S, Smith T, Alfirevic A, Alhaidari M, Atkinson J, Ayala M, Box H, Cross M, Delaunois A, Dermody A, Govindappa K, Guillon J-M, Jenkins R, Kenna G, Lemmer B, Meecham K, Olayanju A, Pestel S, Rothfuss A, Sidaway J, Sison-Young R, Smith E, Stebbings R, Tingle Y, Valentin J-P, Williams A, Williams D, Park K and Goldring C (2013)

Safety pharmacology — Current and emerging concepts. *Toxicology and Applied Pharmacology* **273**:229-241.

Hammond TG, Carlsson L, Davis AS, Lynch WG, MacKenzie I, Redfern WS, Sullivan AT and Camm AJ (2001) Methods of collecting and evaluating non-clinical cardiac electrophysiology data in the pharmaceutical industry: results of an international survey. *Cardiovascular Research* **49**:741-750.

Hamon J, Whitebread S, Techer-Etienne V, Coq HL, Azzaoui K and Urban L (2009) In vitro safety pharmacology profiling: what else beyond hERG? *Future Medicinal Chemistry* **1**:645-665.

Hanada K, Akimoto S, Mitsui K, Hashiguchi M and Ogata H (1998) Quantitative determination of disopyramide, verapamil and flecainide enantiomers in rat plasma and tissues by high-performance liquid chromatography. *J Chromatogr B Biomed Sci Appl* **710**:129-135.

Harashima H, Sugiyama Y, Sawada Y, IGA T and Hanano M (1984) Comparison between in-vivo and in-vitro tissue-to-plasma unbound concentration ratios (Kp,f) of quinidine in rats. *Journal of Pharmacy and Pharmacology* **36**:340-342.

Hardman and Limbird (2011) *The Pharmacological Basis of Therapeutics*. MacGraw-Hill Medical, New York : Macmillan.

Hare LG, Mitchel DS, Millership JS, Collier PS, McElnay JC, Shields MD, Carson DJ and Fair R (2004) Liquid chromatographic determination including simultaneous ΓÇ£on-cartridgeΓÇØ separation of ranitidine cisapride drug combinations from paediatric plasma samples using an automated solid-phase extraction procedure. *Journal of Chromatography B* **806**:263-269.

Harrell AW, Sychterz C, Ho MY, Weber A, Valko K and Negash K (2015) Interrogating the relationship between rat in-ávivo tissue distribution and drug property data for >200 structurally unrelated molecules. *Pharmacology Research & Perspectives* **3**:n/a-n/a.

Harris K (2015) A Human Induced Pluripotent Stem Cell–Derived Cardiomyocyte (hiPSC-CM) Multielectrode Array Assay for Preclinical Cardiac Electrophysiology Safety Screening, in *Current Protocols in Pharmacology* p Supplement 71, John Wiley & Sons, Inc.

Harris K, Aylott M, Cui Y, Louttit JB, McMahon NC and Sridhar A (2013) Comparison of Electrophysiological Data From Human-Induced Pluripotent Stem CellΓÇôDerived Cardiomyocytes to Functional Preclinical Safety Assays. *Toxicological Sciences* **134**:412-426.

Hashimoto K (2008) Torsades de pointes liability inter-model comparisons: The experience of the QT PRODACT initiative. *Pharmacology & Therapeutics* **119**:195-198.

Hassan EM, Hagga MEM and Al Johar HI (2001) Determination of cisapride in pharmaceutical preparations using derivative spectrophotometry. *Journal of Pharmaceutical and Biomedical Analysis* **24**:659-665.

Hauser DS, Stade M, Schmidt A and Hanauer G (2005) Cardiovascular parameters in anaesthetized guinea pigs: A safety pharmacology screening model. *Journal of Pharmacological and Toxicological Methods* **52**:106-114.

Hedeland M, Fredriksson E, Lennernäs H and Bondesson U (2004) Simultaneous quantification of the enantiomers of verapamil and its N-demethylated metabolite in human plasma using liquid chromatography–tandem mass spectrometry. *Journal of Chromatography B* **804**:303-311.

Hege H (1979) Gas chromatographic determination of verapamil in plasma and urine. *Arzneimittelforschung* **29**:1681-1684.

Henderson KA, Borders RB, Ross JB, Huwar TB, Travis CO, Wood BJ, Ma ZJ, Hong SP, Vinci TM and Roche BM (2013) Effects of tyrosine kinase inhibitors on rat isolated heart function and protein biomarkers indicative of toxicity. *Journal of Pharmacological and Toxicological Methods* **68**:150-159.

Hennessy S, Leonard CE, Newcomb C, Kimmel SE and Bilker WB (2008) Cisapride and ventricular arrhythmia. *British Journal of Clinical Pharmacology* **66**:375-385.

Hess P, Rey M, Wanner D, Steiner B and Clozel M (2007) Measurements of blood pressure and electrocardiogram in conscious freely moving guineapigs: a model for screening QT interval prolongation effects. *Laboratory Animals* **41**:470-480.

Higton DM (2001) A rapid, automated approach to optimisation of multiple reaction monitoring conditions for quantitative bioanalytical mass spectrometry. *Rapid Communications in Mass Spectrometry* **15**:1922-1930.

Ho S (2014) Best practices for discovery bioanalysis: balancing data quality and productivity. *Bioanalysis* **6**:2705-2708.

Höcht C, Di Verniero C, Opezzo JAW, Bramuglia GF and Taira CA (2006) Pharmacokinetic-pharmacodynamic (PK-PD) modeling of cardiovascular effects of metoprolol in spontaneously hypertensive rats: a microdialysis study. *Naunyn-Schmiedeberg's Archives of Pharmacology* **373**:310-318.

Höcht C, Opezzo JAW and Taira CA (2007) Applicability of reverse microdialysis in pharmacological and toxicological studies. *Journal of Pharmacological and Toxicological Methods* **55**:3-15.

Holford NHG and Sheiner LB (1982) Kinetics of pharmacologic response. *Pharmacology & Therapeutics* **16**:143-166.

Holzgrefe H, Ferber G, Champeroux P, Gill M, Honda M, Greiter-Wilke A, Baird T, Meyer O and Saulnier M (2014) Preclinical QT safety assessment: Cross-species comparisons and human translation from an industry consortium. *Journal of Pharmacological and Toxicological Methods* **69**:61-101.

Hondeghem L (1994) Computer Aided Development of Antiarrhythmic Agents with Class IIIa Properties. *Journal of Cardiovascular Electrophysiology* **5**:711-721.

Hondeghem L, Lu HR, ROSSEM Kv and De Clerck F (2003) Detection of Proarrhythmia in the Female Rabbit Heart:. *Journal of Cardiovascular Electrophysiology* **14**:287-294.

Hopkins AL (2008) Network pharmacology: the next paradigm in drug discovery. *Nat Chem Biol* **4**:682-690.

Horowitz JD and Powell AC (1986) Myocardial Uptake of Drugs and Clinical Effects. *Clinical Pharmacokinetics* **11**:354-371.

Hosea NA, Collard WT, Cole S, Maurer TS, Fang RX, Jones H, Kakar SM, Nakai Y, Smith BJ, Webster R and Beaumont K (2009) Prediction of Human Pharmacokinetics From Preclinical Information: Comparative Accuracy of Quantitative Prediction Approaches. *The Journal of Clinical Pharmacology* **49**:513-533.

Huang Q, Gehring R, Tell LA, Li M and Riviere JE (2015) Interspecies allometric meta-analysis of the comparative pharmacokinetics of 85 drugs across veterinary and laboratory animal species. *Journal of Veterinary Pharmacology and Therapeutics* **38**:214-226.

Huang Q and Riviere JE (2014) The application of allometric scaling principles to predict pharmacokinetic parameters across species. *Expert Opinion on Drug Metabolism & Toxicology* **10**:1241-1253.

Huang Y, Shi R, Gee W and Bonderud R (2012) Regulated drug bioanalysis for human pharmacokinetic studies and therapeutic drug management. *Bioanalysis* **4**:1919-1931.

Huang Z and Ung T (2013) Effect of Alpha-1-Acid Glycoprotein Binding on Pharmacokinetics and Pharmacodynamics. *Current Drug Metabolism* **14**:226-238.

Huh Y and Hutmacher MM (2015) Evaluating the Use of Linear Mixed-Effect Models for Inference of the Concentration-QTc Slope Estimate as a Surrogate for a Biological QTc Model. *CPT: Pharmacometrics & Systems Pharmacology* **4**:1-9.

Hynning PA, Anderson P, Bondesson U and Boréus LO (1988) Liquid-chromatographic quantification compared with gas-chromatographic-mass-spectrometric determination of verapamil and norverapamil in plasma. *Clinical Chemistry* **34**:2502-2503.

Ikenoue N, Saitsu Y, Shimoda M and Kokue E (2000) DiseaseΓÇÉinduced alterations in plasma drugΓÇÉbinding proteins and their influence on drug binding percentages in dogs. *Veterinary Quarterly* **22**:43-49.

Imazato M (2013) Conference Report: International harmonization of bioanalysis regulation: discussion in Global Bioanalysis Consortium harmonization teams. *Bioanalysis* **5**:281-283.

Ingram-Ross JL, Curran AK, Miyamoto M, Sheehan J, Thomas G, Verbeeck J, de Waal EJ, Verstynen B and Pugsley MK (2012) Cardiorespiratory safety evaluation in non-human primates. *Journal of Pharmacological and Toxicological Methods* **66**:114-124.

Ings RMJ (1990) Interspecies scaling and comparisons in drug development and toxicokinetics. *Xenobiotica* **20**:1201-1231.

Jackman WM, Szabo B, Friday KJ, Margolis PD, Moulton K, Wang X, Patterson E and Lazzara R (1990) Ventricular Tachyarrhythmias Related to Early Afterdepolarizations and Triggered Firing: Relationship to QT Interval Prolongation and Potential Therapeutic Role for Calcium Channel Blocking Agents. *Journal of Cardiovascular Electrophysiology* **1**:170-195.

Jacobson I, Carlsson L and Duker G (2011) Beat-by-beat QT interval variability, but not QT prolongation per se, predicts drug-induced torsades de pointes in the anaesthetised methoxamine-sensitized rabbit. *Journal of Pharmacological and Toxicological Methods* **63**:40-46.

Jaillon P, Morganroth J, Brumpt I, Talbot G and Group TSS (1996) Overview of electrocardiographic and cardiovascular safety data for sparfloxacin. *Journal of Antimicrobial Chemotherapy* **37**:161-167.

Jamei M (2016) Recent Advances in Development and Application of Physiologically-Based Pharmacokinetic (PBPK) Models: a Transition from Academic Curiosity to Regulatory Acceptance. *Current Pharmacology Reports* **2**:161-169.

Jamei M, Marciniak S, Edwards D, Wragg K, Feng K, Barnett A and Rostami-Hodjegan A (2013) The Simcyp Population Based Simulator: Architecture, Implementation, and Quality Assurance. *In Silico Pharmacology* **1**:9.

Jansson R, Bredberg U and Ashton M (2008) Prediction of drug tissue to plasma concentration ratios using a measured volume of distribution in combination with lipophilicity. *Journal of Pharmaceutical Sciences* **97**:2324-2339.

Ji HY, Park EJ, Lee KC and Lee HS (2008) Quantification of doxazosin in human plasma using hydrophilic interaction liquid chromatography with tandem mass spectrometry. *Journal of Separation Science* **31**:1628-1633.

Jones H, Mayawala K and Poulin P (2013) Dose Selection Based on Physiologically Based Pharmacokinetic (PBPK) Approaches. *AAPS J* **15**:377-387.

Jones H, Parrott N, Jorga K and Lav+® T (2006) A Novel Strategy for Physiologically Based Predictions of Human Pharmacokinetics. *Clin Pharmacokinet* **45**:511-542.

Jones HM, Chen Y, Gibson C, Heimbach T, Parrott N, Peters SA, Snoeys J, Upreti VV, Zheng M and Hall SD (2015) Physiologically based pharmacokinetic modeling in drug discovery and development: A pharmaceutical industry perspective. *Clinical Pharmacology & Therapeutics* **97**:247-262.

Jones HM, Dickins M, Youdim K, Gosset JR, Attkins NJ, Hay TL, Gurrell IK, Logan YR, Bungay PJ, Jones BC and Gardner IB (2012) Application of PBPK modelling in drug discovery and development at Pfizer. *Xenobiotica* **42**:94-106.

Joshi A, Dimino T, Vohra Y, Cui C and Yan GX (2004) Preclinical strategies to assess QT liability and torsadogenic potential of new drugs: The role of experimental models. *Journal of Electrocardiology* **37, Supplement**:7-14.

Jost N, Virág L, Comtois P, Ördög B, Szuts V, Seprényi G, Bitay M, Kohajda Z, Koncz I, Nagy N, Szél T, Magyar J, Kovács M, Puskás LG, Lengyel C, Wettwer E, Ravens U, Nánási PP, Papp JG, Varró A and Nattel S (2013) Ionic mechanisms limiting cardiac repolarization reserve in humans compared to dogs. *The Journal of Physiology* **591**:4189-4206.

Kalvass JC and Maurer TS (2002) Influence of nonspecific brain and plasma binding on CNS exposure: implications for rational drug discovery. *Biopharmaceutics & Drug Disposition* **23**:327-338.

Kalvass JC, Maurer TS and Pollack GM (2007) Use of Plasma and Brain Unbound Fractions to Assess the Extent of Brain Distribution of 34 Drugs: Comparison of Unbound Concentration Ratios to in Vivo P-Glycoprotein Efflux Ratios. *Drug Metabolism and Disposition* **35**:660-666.

Kamberi M, Kamberi P, Hajime N, Uemura N, Nakamura K and Nakano S (1999) Determination of Sparfloxacin in Plasma and Urine by a Simple and Rapid Liquid Chromatographic Method. *Therapeutic Drug Monitoring* **21**.

Kamiya K, Niwa R, Morishima M, Honjo H and C.Sanguinetti M (2015) Molecular Determinants of hERG Channel Block by Terfenadine and Cisapride. *J Pharm Sci* **108**:301-307.

Kang C, Brennan JA, Kuzmiak-Glancy S, Garrott KE, Kay MW and Efimov IR (2016) Technical advances in studying cardiac electrophysiology – Role of rabbit models. *Progress in Biophysics and Molecular Biology* **121**:97-109.

Kang J, Wang L, Chen XL, Triggle DJ and Rampe D (2001) Interactions of a Series of Fluoroquinolone Antibacterial Drugs with the Human Cardiac K+ Channel HERG. *Molecular Pharmacology* **59**:122-126.

Kantharaj E, Tuytelaars A, Proost PEA, Ongel Z, van Assouw HP and Gilissen RAHJ (2003) Simultaneous measurement of drug metabolic stability and identification of metabolites using ion-trap mass spectrometry. *Rapid Communications in Mass Spectrometry* **17**:2661-2668.

Kariv I, Cao H and Oldenburg KR (2001) Development of a High Throughput Equilibrium Dialysis Method. *Journal of Pharmaceutical Sciences* **90**:580-587.

Karkhanis A, Hong Y and Chan ECY (2017) Inhibition and inactivation of human CYP2J2: Implications in cardiac pathophysiology and opportunities in cancer therapy. *Biochemical Pharmacology*.

Katagi J, Nakamura Y, Cao X, Ohara H, Honda A, Izumi-Nakaseko H, Ando K and Sugiyama A (2016) Why Can dl-Sotalol Prolong the QT Interval In Vivo Despite Its Weak Inhibitory Effect on hERG K+ Channels In Vitro? Electrophysiological and Pharmacokinetic Analysis with the Halothane-Anesthetized Guinea Pig Model. *Cardiovascular Toxicology* **16**:138-146.

Kataoka M, Kojima C, Ueda K, Minami K, Higashino H, Sakuma S, Togashi K, Mutaguchi K and Yamashita S (2016) Quantitative analysis of pharmacokinetic profiles of verapamil and drug–drug interactions induced by a CYP inhibitor using a stable isotope-labeled compound. *Drug Metabolism and Pharmacokinetics* **31**:405-410.

Kates RE and Jaillon P (1980) A model to describe myocardial drug disposition in the dog. *Journal of Pharmacology and Experimental Therapeutics* **214**:31-36.

Katoh H and Kaneko A (1991) Distribution of Sparfloxacin (AT-4140) into Serum and Oral Tissues. *Oral Ther & Pharmacol* **10**:81-84.

Keating G and Scott L (2004) Moxifloxacin. *Drugs* **64**:2347-2377.

Keefe DL and Kates RE (1982) Myocardial disposition and cardiac pharmacodynamics of verapamil in the dog. *Journal of Pharmacology and Experimental Therapeutics* **220**:91-96.

Kenyon E (2012) Interspecies Extrapolation, in *Computational Toxicology* (Reisfeld B and Mayeno AN eds) pp 501-520, Humana Press.

Kerns EH and Di L (2006) Utility of Mass Spectrometry for Pharmaceutical Profiling Applications. *Current Drug Metabolism* **7**:457-466.

Khongphatthanayothin A, Lane J, Thomas D, Yen L, Chang D and Bubolz B (1998) Effects of cisapride on QT interval in children. *The Journal of Pediatrics* **133**:51-56.

Kii Y, Nakatsuji K, Nose I, Yabuuchi M, Mizuki Y and Ito T (2001) Effects of 5-HT4 Receptor Agonists, Cisapride and Mosapride Citrate on Electrocardiogram in Anaesthetized Rats and Guinea-Pigs and Conscious Cats. *Pharmacology & Toxicology* **89**:96-103.

Kijtawornrat A, Nishijima Y, Roche BM, Keene BW and Hamlin RL (2006a) Use of a Failing Rabbit Heart as a Model to Predict Torsadogenicity. *Toxicological Sciences* **93**:205-212.

Kijtawornrat A, Ozkanlar Y, Keene BW, Roche BM, Hamlin DM and Hamlin RL (2006b) Assessment of drug-induced QT interval prolongation in conscious rabbits. *Journal of Pharmacological and Toxicological Methods* **53**:168-173.

Kijtawornrat A, Ziolo MT, Nishijima Y, Roche BM and Hamlin RL (2010) Effects of Sarcolemmal Ca²⁺ Entry, Ryanodine Function, and Kinase Inhibitors on a Rabbit Model of Heart Failure. *International Heart Journal* **51**:285-290.

Kim CS, Sandberg JA, Slikker Jr W, Binienda Z, Schlosser PM and Patterson TA (2001) Quantitative exposure assessment: application of physiologically-based pharmacokinetic (PBPK) modeling of low-dose, long-term exposures of organic acid toxicant in the brain. *Environmental Toxicology and Pharmacology* **9**:153-160.

Kimura K, Tabo M, Itoh M, Mizoguchi K, Kato A, Suzuki M, Itoh Z, Omura S and Takanashi H (2007) PRECLINICAL ELECTROPHYSIOLOGY ASSAYS OF MITEMCINAL (GM-611), A NOVEL PROKINETIC AGENT DERIVED FROM ERYTHROMYCIN. *The Journal of Toxicological Sciences* **32**:217-230.

King L, Kotian A and Jairaj M (2014) Introduction of a routine quan/qual approach into research DMPK: experiences and evolving strategies. *Bioanalysis* **6**:3337-3348.
Kinter LB and Valentin JP (2002) Safety pharmacology and risk assessment. *Fundamental & Clinical Pharmacology* **16**:175-182.
Kiss BD, Nemes KB and Klebovich I (2003) Determination of cisapride in human plasma by high-performance liquid chromatography with fluorescence detection. *Chromatographia* **57**:47-50.
Klein SK and Redfern WS (2015) Cardiovascular safety risk assessment for new candidate drugs from functional and pathological data: Conference report. *Journal of Pharmacological and Toxicological Methods* **76**:1-6.
Kleinstreuer NC, Yang J, Berg EL, Knudsen TB, Richard AM, Martin MT, Reif DM, Judson RS, Polokoff M, Dix DJ, Kavlock RJ and Houck KA (2014) Phenotypic screening of the ToxCast chemical library to classify toxic and therapeutic mechanisms. *Nat Biotech* **32**:583-591.
Klotz IM and Urquhart JM (1949) The Binding of Organic Ions by Proteins. Effect of Temperature. *Journal of the American Chemical Society* **71**:847-851.
Klotz IM and Walker FM (1947) The Binding of Organic Ions by Proteins. Charge and pH Effects. *Journal of the American Chemical Society* **69**:1609-1612.
Knight-Schrijver VR, Chelliah V, Cucurull-Sanchez L and Le Novère N (2016) The promises of quantitative systems pharmacology modelling for drug development. *Computational and Structural Biotechnology Journal* **14**:363-370.
Kojima T, Inoue M and Mitsuhashi S (1989) In vitro activity of AT-4140 against clinical bacterial isolates. *Antimicrobial Agents and Chemotherapy* **33**:1980-1988.
Kola I (2008) The State of Innovation in Drug Development. *Clin Pharmacol Ther* **83**:227-230.
Kratochwil NA, Huber W, M++ller F, Kansy M and Gerber PR (2002) Predicting plasma protein binding of drugs: a new approach. *Biochemical Pharmacology* **64**:1355-1374.
Krisko RM, McLaughlin K, Koenigbauer MJ and Lunte CE (2006) Application of a column selection system and DryLab software for high-performance liquid chromatography method development. *Journal of Chromatography A* **1122**:186-193.
KS P and M R (1977a) Hepatic clearance of drugs. I. Theoretical considerations of a "well-stirred" model and a "parallel tube" model. Influence of hepatic blood flow, plasma and blood cell binding, and the hepatocellular enzymatic activity on hepatic drug clearance. *J Pharmacokinet Biopharm* **5**:625-653.
KS P and M R (1977b) Hepatic clearance of drugs. II. Experimental evidence for acceptance of the "well-stirred" model over the "parallel tube" model using lidocaine in the perfused rat liver in situ preparation. *J Pharmacokinet Biopharm* **5**:655-680.
Kuepfer L, Niederalt C, Wendl T, Schlender JF, Willmann S, Lippert J, Block M, Eissing T and Teutonico D (2016) Applied Concepts in PBPK Modeling: How to Build a PBPK/PD Model. *CPT: Pharmacometrics & Systems Pharmacology* **5**:516-531.
Kuroha M, Son DS and Shimoda M (2001) Effects of altered plasma +¦-1-acid glycoprotein levels on pharmacokinetics of some basic antibiotics in pigs: simulation analysis. *Journal of Veterinary Pharmacology and Therapeutics* **24**:423-431.
Laban-Djurdjeviç A, Jelikiç-Stankov M and Djurdjeviç P (2006) Optimization and validation of the direct HPLC method for the determination of moxifloxacin in plasma. *Journal of Chromatography B* **844**:104-111.
Lambrinidis G, Vallianatou T and Tsantili-Kakoulidou A (2015) In vitro, in silico and integrated strategies for the estimation of plasma protein binding. A review. *Advanced Drug Delivery Reviews* **86**:27-45.
Laverty HG, Benson C, Cartwright EJ, Cross MJ, Garland C, Hammond T, Holloway C, McMahon N, Milligan J, Park BK, Pirmohamed M, Pollard C, Radford J, Roome N, Sager P, Singh S, Suter T, Suter W, Trafford A, Volders PGA, Wallis R, Weaver R, York M and Valentin JP (2011) How can we improve our understanding of cardiovascular safety liabilities to develop safer medicines? *British Journal of Pharmacology* **163**:675-693.
Lawrence CL, Pollard CE, Hammond TG and Valentin JP (2005) Nonclinical proarrhythmia models: Predicting Torsades de Pointes. *Journal of Pharmacological and Toxicological Methods* **52**:46-59.

Lawrence CL, Pollard CE, Hammond TG and Valentin JP (2008) In vitro models of proarrhythmia. *British Journal of Pharmacology* **154**:1516-1522.

Ledwitch KV and Roberts AG (2017) Cardiovascular Ion Channel Inhibitor Drug-Drug Interactions with P-glycoprotein. *The AAPS Journal* **19**:409-420.

Lee HM, Choi SJ, Jeong CK, Kim YS, Lee KC and Lee HS (1999) Microbore high-performance liquid chromatographic determination of cisapride in rat serum samples using column switching. *Journal of Chromatography B: Biomedical Sciences and Applications* **727**:213-217.

Lee HW, Ji HY, Kim HH, Cho HY, Lee YB and Lee HS (2003) Determination of tiropramide in human plasma by liquid chromatographyΓÇôtandem mass spectrometry. *Journal of Chromatography B* **796**:395-400.

Lee MJ, Lee HW, Kang JM, Seo JH, Tak SK, Shim W, Yim SV, Hong SJ and Lee KT (2010) Application of a rapid and selective method for the simultaneous determination of carebastine and pseudoephedrine in human plasma by liquid chromatographyΓÇôelectrospray mass spectrometry for bioequivalence study in Korean subjects. *Biomedical Chromatography* **24**:1031-1037.

Leishman DJ, Beck TW, Dybdal N, Gallacher DJ, Guth BD, Holbrook M, Roche B and Wallis RM (2012) Best practice in the conduct of key nonclinical cardiovascular assessments in drug development: Current recommendations from the Safety Pharmacology Society. *Journal of Pharmacological and Toxicological Methods* **65**:93-101.

Lesko LJ and Atkinson AJ (2001) USE OF BIOMARKERS AND SURROGATE ENDPOINTS IN DRUG DEVELOPMENT AND REGULATORY DECISION MAKING: Criteria, Validation, Strategies. *Annual Review of Pharmacology and Toxicology* **41**:347-366.

Li J, Yuan Y, Fan R, Su Q, Wang S, Zhou T and Lu W (2015) A Simple LC/MS/MS Method for the Determination of Moxifloxacin N-Sulfate in Rat Plasma and Its Application in a Pharmacokinetic Study. *Journal of AOAC International* **98**:921-926.

Limberis JT, McDermott JS, Salmen HJ, Su Z, Mikhail A, Green JR, Cox BF, Gintant GA and Martin RL (2007) The effects of plasma proteins on delayed repolarization in vitro with cisapride, risperidone, and d, l-sotalol. *Journal of Pharmacological and Toxicological Methods* **56**:11-17.

Lin JH (1995) Species similarities and differences in pharmacokinetics. *Drug Metabolism and Disposition* **23**:1008-1021.

Lin JH, Sugiyama Y, Awazu S and Hanano M (1982) In vitro and in vivo evaluation of the tissue-to-blood partition coefficient for physiological pharmacokinetic models. *J Pharmacokinet Biopharm* **10**:637-647.

Lindgren S, Bass AS, Briscoe R, Bruse K, Friedrichs GS, Kallman MJ, Markgraf C, Patmore L and Pugsley MK (2008) Benchmarking Safety Pharmacology regulatory packages and best practice. *Journal of Pharmacological and Toxicological Methods* **58**:99-109.

Lipsky BA, Dorr MB, Magner DJ and Talbot GH (1999) Safety profile of sparfloxacin, a new fluoroquinolone antibiotic. *Clinical Therapeutics* **21**:148-159.

Liu T, Brown BS, Wu Y, Antzelevitch C, Kowey PR and Yan GX (2006) Blinded validation of the isolated arterially perfused rabbit ventricular wedge in preclinical assessment of drug-induced proarrhythmias. *Heart Rhythm* **3**:948-956.

Liu W, Liu QF, Perkins R, Drusano G, Louie A, Madu A, Mian U, Mayers M and Miller MH (1998) Pharmacokinetics of Sparfloxacin in the Serum and Vitreous Humor of Rabbits: Physicochemical Properties That Regulate Penetration of Quinolone Antimicrobials. *Antimicrobial Agents and Chemotherapy* **42**:1417-1423.

Liu X, Wright M and Hop CECA (2014) Rational Use of Plasma Protein and Tissue Binding Data in Drug Design. *Journal of Medicinal Chemistry* **57**:8238-8248.

Lode HM and Schmidt-Ioanas M (2008) Moxifloxacin: update and perspectives after 8 years of usage. *Expert Review of Respiratory Medicine* **2**:443-453.

Louizos C, Yáñez JA, Forrest L and Davies NM (2014) Understanding the Hysteresis Loop Conundrum in Pharmacokinetic / Pharmacodynamic Relationships. *Journal of pharmacy & pharmaceutical sciences : a publication of the Canadian Society for Pharmaceutical Sciences, Societe canadienne des sciences pharmaceutiques* **17**:34-91.

Lu HR, Mari+½n R, Saels A and De Clerck F (2000) Are There Sex-Specific Differences in Ventricular Repolarization or in Drug-Induced Early Afterdepolarizations in Isolated Rabbit Purkinje Fibers? *Journal of Cardiovascular Pharmacology* **36**.

Lu HR, Vlaminckx E, Van de Water A, Rohrbacher J, Hermans A and Gallacher DJ (2006) In-vitro experimental models for the risk assessment of antibiotic-induced QT prolongation. *European Journal of Pharmacology* **553**:229-239.

Lu HR, Yan GX and Gallacher DJ (2013) A new biomarker – index of Cardiac Electrophysiological Balance (iCEB) – plays an important role in drug-induced cardiac arrhythmias: beyond QT-prolongation and Torsades de Pointes (TdPs). *Journal of Pharmacological and Toxicological Methods* **68**:250-259.

Lubasch A, Keller I, Borner K, Koeppe P and Lode H (2000) Comparative pharmacokinetics of ciprofloxacin, gatifloxacin, grepafloxacin, levofloxacin, trovafloxacin, and moxifloxacin after single oral administration in healthy volunteers. *Antimicrobial Agents and Chemotherapy* **44**:2600-2603.

Machado SG, Miller R and Hu C (1999) A regulatory perspective on pharmacokinetic/pharmacodynamic modelling. *Statistical Methods in Medical Research* **8**:217-245.

Mager DE and Jusko WJ (2008) Development of Translational PharmacokineticΓÇôPharmacodynamic Models. *Clinical Pharmacology & Therapeutics* **83**:909-912.

Mahmood I (1999) Allometric issues in drug development. *Journal of Pharmaceutical Sciences* **88**:1101-1106.

Mahmood I (2007) Application of allometric principles for the prediction of pharmacokinetics in human and veterinary drug development. *Advanced Drug Delivery Reviews* **59**:1177-1192.

Manitpisitkul P and Chiou WL (1993) Intravenous verapamil kinetics in rats: Marked arteriovenous concentration difference and comparison with humans. *Biopharmaceutics & Drug Disposition* **14**:555-566.

Mariappan T, Mandlekar S and Marathe P (2013) Insight into Tissue Unbound Concentration: Utility in Drug Discovery and Development. *Current Drug Metabolism* **14**:324-340.

Marks L, Borland S, Philp K, Ewart L, Lain+®e P, Skinner M, Kirk S and Valentin JP (2012) The role of the anaesthetised guinea-pig in the preclinical cardiac safety evaluation of drug candidate compounds. *Toxicology and Applied Pharmacology* **263**:171-183.

Marostica E, Van Ammel K, Teisman A, Boussery K, Van Bocxlaer J, De Ridder F, Gallacher D and Vermeulen A (2015) Modelling of drug-induced QT-interval prolongation: estimation approaches and translational opportunities. *Journal of Pharmacokinetics and Pharmacodynamics* **42**:659-679.

Martin MIG, Perez CG and Lopez MAB (1994) Fluorimetric Determination of Cisapride. *Analytical Letters* **27**:1713-1718.

Matsunaga Y, Miyazaki H, Nomura N and Hashimoto M (1991a) Disposition and metabolism of [14C]sparfloxacin after repeated administration in the rat. *Arzneimittelforschung* **41**:760-763.

Matsunaga Y, Miyazaki H, Oh-e Y, Nambu K, Furukawa H, Yoshida K and Hashimoto M (1991b) Disposition and metabolism of [14C]sparfloxacin in the rat. *Arzneimittelforschung* **41**:747-759.

Mayeux R (2004) Biomarkers: Potential uses and limitations. *Neurotherapeutics* **1**:182-188.

McAllister RG and Howell SM (1976) Fluorometric Assay of Verapamil in Biological Fluids and Tissues. *Journal of Pharmaceutical Sciences* **65**:431-432.

McBride BF, Yang T, Liu K, Urban TJ, Giacomini KM, Kim RB and Roden DM (2009) The Organic Cation Transporter, OCTN1, Expressed in the Human Heart, Potentiates Antagonism of the HERG Potassium Channel. *Journal of cardiovascular pharmacology* **54**:63-71.

McCallum R, Prakash C, Campoli-Richards D and Goa K (1988) Cisapride. A preliminary review of its pharmacodynamic and pharmacokinetic properties, and therapeutic use as a prokinetic agent in gastrointestinal motility disorders. *Drugs* **36**:652-681.

McGowan FX, Reiter MJ, Pritchett ELC and Shand DG (1983) Verapamil plasma binding: Relationship to +¦1-acid glycoprotein and drug efficacy. *Clinical Pharmacology & Therapeutics* **33**:485-490.

McIlhenny H (1971) Metabolism of [14C]verapamil. *J Med Chem* **14**:1178-1184.

Meibohm B and Derendorf H (1997) Basic concepts of pharmacokinetic/pharmacodynamic (PK/PD) modelling. *Int J Clin Pharmacol Ther Toxicol* **35**:401-413.

Meissner K, Sperker B, Karsten C, Meyer zu Schwabedissen H, Seeland U, Böhm M, Bien S, Dazert P, Kunert-Keil C, Vogelgesang S, Warzok R, Siegmund W, Cascorbi I, Wendt M and Kroemer HK (2002) Expression and Localization of P-glycoprotein in Human Heart. Effects of Cardiomyopathy. *J Histochem Cytochem* **50**:1351-1356.

MHW-Japan (1975) *Notes on Application for Approval to Manufacture (Import) New Drugs*.

MHW-Japan (1995) *Japanese Guidelines for Non-Clinical Studies of Drugs Manual*. Yakuji Nippo, Tokyo.

Michalets EL and Williams CR (2000) Drug interactions with cisapride: clinical implications. *Clin Pharmacokinetics* **39**:49-75.

Michiels M (1987) Pharmacokinetics and Tissue Distribution of the new Gastroprokinetic agent Cisapride in rat, Rabbit and Dog, in *Drug Res* pp 1159-1167.

Mihaly GW, Ching MS, Klejn MB, Paull J and Smallwood RA (1987) Differences in the binding of quinine and quinidine to plasma proteins. *British Journal of Clinical Pharmacology* **24**:769-774.

Milberg P, Reinsch N, Osada N, Wasmer K, Mönnig G, Stypmann J, Breithardt G, Haverkamp W and Eckardt L (2005) Verapamil prevents torsade de pointes by reduction of transmural dispersion of repolarization and suppression of early afterdepolarizations in an intact heart model of LQT3. *Basic Research in Cardiology* **100**:365-371.

Milnes JT, Witchel HJ, Leaney JL, Leishman DJ and Hancox JC (2010) Investigating dynamic protocol-dependence of hERG potassium channel inhibition at 37 -¦C: Cisapride versus dofetilide. *Journal of Pharmacological and Toxicological Methods* **61**:178-191.

Minematsu T, Ohtani H, Sato H and Iga T (1999) Pharmacokinetic/Pharmacodynamic Analysis of Tacrolimus-Induced QT Prolongation in Guinea Pigs. *Biological & Pharmaceutical Bulletin* **22**:1341-1346.

Minematsu T, Ohtani H, Yamada Y, Sawada Y, Sato H and Iga T (2001) Quantitative Relationship Between Myocardial Concentration of Tacrolimus and QT Prolongation in Guinea Pigs: Pharmacokinetic/Pharmacodynamic Model Incorporating a Site of Adverse Effect. *J Pharmacokinet Pharmacodyn* **28**:533-554.

Mirams GR, Davies MR, Brough SJ, Bridgland-Taylor MH, Cui Y, Gavaghan DJ and Abi-Gerges N (2014) Prediction of Thorough QT study results using action potential simulations based on ion channel screens. *Journal of Pharmacological and Toxicological Methods* **70**:246-254.

Mitchell AZ, McMahon C, Beck TW and Sarazan RD (2010) Sensitivity of two noninvasive blood pressure measurement techniques compared to telemetry in cynomolgus monkeys and beagle dogs. *Journal of Pharmacological and Toxicological Methods* **62**:54-63.

Mizuki Y, Fujiwara I and Yamaguchi T (1996) Pharmacokinetic interactions related to the chemical structures of fluoroquinolones. *Journal of Antimicrobial Chemotherapy* **37**:41-55.

ML H, JJ H, GR G and MA M (2010) Plasma Protein Binding in Drug Discovery and Development. *Combinatorial Chemistry & High Throughput Screening* **13**:170-187.

Mody VD, Pandya KK, Satia MC, Modi IA, Modi RI and Gandhi TP (1998) High performance thin-layer chromatographic method for the determination of sparfloxacin in human plasma and its use in pharmacokinetic studies. *Journal of Pharmaceutical and Biomedical Analysis* **16**:1289-1294.

Mohammad S, Zhou Z, Gong Q and January C (1997) Blockage of the HERG human cardiac K^+ channel by the gastrointestinal prokinetic agent cisapride. *American Journal of Physiology - Heart and Circulatory Physiology* **273**:H2534-H2538

Moise PA, Birmingham MC and Schentag JJ (2000) PHARMACOKINETICS AND METABOLISM OF MOXIFLOXACIN. *Drugs of Today* **36**:229-244.

Molla A, Vasavanonda S, Kumar G, Sham HL, Johnson M, Grabowski B, Denissen JF, Kohlbrenner W, Plattner JJ, Leonard JM, Norbeck DW and Kempf DJ (1998) Human Serum Attenuates

the Activity of Protease Inhibitors toward Wild-Type and Mutant Human Immunodeficiency Virus. *Virology* **250**:255-262.

Molnar I (2002) Computerized design of separation strategies by reversed-phase liquid chromatography: development of DryLab software. *Journal of Chromatography A* **965**:175-194.

Montay G, Bruno R, Vergniol JC, Ebmeier M, Roux YL, Guimart C, Frydman A, Chassard D and Thebault JJ (1994) Pharmacokinetics of Sparfloxacin in Humans After Single Oral Administration at Doses of 200, 400, 600, and 800 mg. *The Journal of Clinical Pharmacology* **34**:1071-1076.

Morganroth J, Talbot GH, Dorr MB, Johnson RD, Geary W and Magner D (1999) Effect of single ascending, supratherapeutic doses of sparfloxacin on cardiac repolarization (QTc interval). *Clinical Therapeutics* **21**:818-828.

Mori Y, Hanada K, Mori T, Tsukahara Y, Hashiguchi M and Ogata H (2001) Stereoselective Pharmacokinetics and Pharmacodynamics of Verapamil and Norverapamil in Rabbits. *Biological and Pharmaceutical Bulletin* **24**:806-810.

Morse DS, Abernethy DR and Greenblatt DJ (1985) Methodologic factors influencing plasma binding of alpha-1-acid glycoprotein-bound and albumin-bound drugs. *International journal of clinical pharmacology, therapy, and toxicology* **23**:535-539.

Moscardo E, Fasdelli N, Giarola A, Tontodonati M and Dorigatti R (2009) An optimised neurobehavioural observation battery integrated with the assessment of cardiovascular function in the beagle dog. *Journal of Pharmacological and Toxicological Methods* **60**:198-209.

MS R and M R (1986) A dispersion model of hepatic elimination: 2. Steady-state considerations--influence of hepatic blood flow, binding within blood, and hepatocellular enzyme activity. *J Pharmacokinet Biopharm* **14**:261-288.

Mukherjee A, Haghani J, Brady L, Bush W, McBride L, Buja L and Willerson J (1983) Differences in myocardial alpha- and beta-adrenergic receptor numbers in different species. *American Journal of Physiology - Heart and Circulatory Physiology* **245**:H957-H961.

Müller M (2009) Monitoring tissue drug levels by clinical microdialysis. *Altern Lab Anim* **37**:57-59.

Musafija A, Ramon J, Shtelman Y, Yoseph G, Rubinovitz B, Segev S and Rubinstein E (2000) Trans-epithelial intestinal elimination of moxifloxacin in rabbits. *Journal of Antimicrobial Chemotherapy* **45**:803-805.

Mushiroda T, Douya R, Takahara E and Nagata O (2000) The Involvement of Flavin-Containing Monooxygenase but Not CYP3A4 in Metabolism of Itopride Hydrochloride, a Gastroprokinetic Agent: Comparison with Cisapride and Mosapride Citrate. *Drug Metabolism and Disposition* **28**:1231-1237.

Musteata FM, Pawliszyn J, Qian MG, Wu J-T and Miwa GT (2006) Determination of drug plasma protein binding by solid phase microextraction. *Journal of Pharmaceutical Sciences* **95**:1712-1722.

Nadai M, Lan Zhao Y, Wang L, Nishio Y, Takagi K, Kitaichi K, Takagi K, Yoshizumi H and Hasegawa T (2001) Endotoxin impairs biliary transport of sparfloxacin and its glucuronide in rats. *European Journal of Pharmacology* **432**:99-105.

Nakamura S, Kurobe N, Ohue T, Hashimoto K and Shimizu N (1990) Pharmacokinetics of a novel quinolone, AT-4140, in animals. *Antimicrobial Agents and Chemotherapy* **34**:89-93.

Nakamura S, Minami A, Nakata K, Kurobe N, Kouno K, Sakaguchi Y, Kashimoto S, Yoshida H, Kojima T and Ohue T (1989) In vitro and in vivo antibacterial activities of AT-4140, a new broad-spectrum quinolone. *ANTIMICROB AGENTS CHEMOTHER* **33**:1167-1173.

Nalos L, Varkevisser R, Jonsson MKB, Houtman MJC, Beekman JD, van der Nagel R, Thomsen MB, Duker G, Sartipy P, de Boer TP, Peschar M, Rook MB, van Veen TAB, van der Heyden MAG and Vos MA (2012) Comparison of the IKr blockers moxifloxacin, dofetilide and E-4031 in five screening models of pro-arrhythmia reveals lack of specificity of isolated cardiomyocytes. *British Journal of Pharmacology* **165**:467-478.

Nandi P and Lunte SM (2009) Recent trends in microdialysis sampling integrated with conventional and microanalytical systems for monitoring biological events: A review. *Analytica Chimica Acta* **651**:1-14.

Naroa K, Iwamoto Y, Tanaka K, Yamaguchi T and Sekine Y (1992) Effects of fenbufen on teh pharmacokinetics of sparfloxacinin rats. *Journal of Antimicrobial Chemotherapy* **30**:673-683.

Naylor S (2003) Biomarkers: current perspectives and future prospects. *Expert Review of Molecular Diagnostics* **3**:525-529.

Nguyen HA, Grellet J, Ba BB, Quentin C and Saux MC (2004) Simultaneous determination of levofloxacin, gatifloxacin and moxifloxacin in serum by liquid chromatography with column switching. *Journal of Chromatography B* **810**:77-83.

Nilsen OG, Leren P, Aakesson I and Jacobsen S (1978) Binding of quinidine in sera with different levels of triglycerides, cholesterol, and orosomucoid protein. *Biochemical Pharmacology* **27**:871-876.

Nilsson LB (2013) The bioanalytical challenge of determining unbound concentration and protein binding for drugs. *Bioanalysis* **5**:3033-3050.

Noh K, Kwon Ki, Jeong TC and Kang W (2010) Quantitative determination of sparfloxacin in rat plasma by liquid chromatography/tandem mass spectrometry. *Biomedical Chromatography* **24**:1199-1202.

Odening KE and Kohl P (2016) Follow the white rabbit: Experimental and computational models of the rabbit heart provide insights into cardiac (patho-) physiology. *Progress in Biophysics and Molecular Biology* **121**:75-76.

Ollerstam A, Visser SAG, Duker G, Forsberg T, Persson AH, Nilsson LB, Bj+Ârkman JA, Gabrielsson J and Al-Saffar A (2007) Comparison of the QT interval response during sinus and paced rhythm in conscious and anesthetized beagle dogs. *Journal of Pharmacological and Toxicological Methods* **56**:131-144.

Onat F, Yegen B, Berkman K and Oktay S (1994) The hypotensive effect of cisapride in rat. *Gen Pharmacol* **25**:1253-1256.

Opie LH, Yusuf S and Kübler W (2000) Current status of safety and efficacy of calcium channel blockers in cardiovascular diseases: A critical analysis based on 100 studies. *Progress in Cardiovascular Diseases* **43**:171-196.

Orszulak-Michalak D (1996) The influence of selected general anesthetics on pharmacokinetic parameters of some antiarrhythmic drugs in rabbits. Part V. Verapamil. *Acta Pol Pharm* **53**:57-61.

Orszulak-Michalak D, Owczarek J and Wiktorowska-Owczarek A (2002) INFLUENCE OF MIDAZOLAM ON PHARMACOKINETICS OF VERAPAMIL IN RABBITS. *Polish Journal of Pharmacology* **54**:501-506.

Østergaard C, Klitmøller Sørensen T, Dahl Knudsen J and Frimodt-Møller N (1998) Evaluation of Moxifloxacin, a New 8-Methoxyquinolone, for Treatment of Meningitis Caused by a PenicillinResistant Pneumococcus in Rabbits. *Antimicrobial Agents and Chemotherapy* **42**:1706-1712.

Osuna MC and unit GND (2006) Sotalol protein binding value in guinea-pig blood using the RED device, in.

Pacifici GM and Viani A (1992) Methods of Determining Plasma and Tissue Binding of Drugs. *Clinical Pharmacokinetics* **23**:449-468.

Paixão P, Aniceto N, Gouveia LF and Morais JAG (2013) Tissue-to-blood distribution coefficients in the rat: Utility for estimation of the volume of distribution in man. *European Journal of Pharmaceutical Sciences* **50**:526-543.

Park ES, Hahn M, Rhee YS and Chi SC (2001) HIGH PERFORMANCE LIQUID CHROMATOGRAPHIC ANALYSIS OF CISAPRIDE IN HUMAN PLASMA. *Analytical Letters* **34**:1285-1294.

Park J, Noh K, Lee HW, Lim MS, Seong SJ, Seo JJ, Kim EJ, Kang W and Yoon YR (2013) Pharmacometabolomic approach to predict QT prolongation in guinea pigs. *PLoS One* **8**:e60556.

Parkinson J, Visser SAG, Jarvis P, Pollard C, Valentin JP, Yates JWT and Ewart L (2013) Translational pharmacokineticΓÇôpharmacodynamic modeling of QTc effects in dog and human. *Journal of Pharmacological and Toxicological Methods* **68**:357-366.

Pauli-Magnus C, von Richter O, Burk O, Ziegler A, Mettang T, Eichelbaum M and Fromm MF (2000) Characterization of the Major Metabolites of Verapamil as Substrates and Inhibitors of P-glycoprotein. *Journal of Pharmacology and Experimental Therapeutics* **293**:376-382.

Pedersen OD, Bagger H, Keller N, Marchant B, K+©ber L, Torp-Pedersen C and Group ftDIoAaMODS (2001) Efficacy of Dofetilide in the Treatment of Atrial Fibrillation-Flutter in Patients With Reduced Left Ventricular Function: A Danish Investigations of Arrhythmia and Mortality ON Dofetilide (DIAMOND) Substudy. *Circulation* **104**:292-296.

Pedraglio S, Rozio MG, Misiano P, Reali V, Dondio G and Bigogno C (2007) New perspectives in bio-analytical techniques for preclinical characterization of a drug candidate: UPLC-MS/MS in in vitro metabolism and pharmacokinetic studies. *Journal of Pharmaceutical and Biomedical Analysis* **44**:665-673.

Peltenburg H, Bosman IJ and Hermens JLM (2015) Sensitive determination of plasma protein binding of cationic drugs using mixed-mode solid-phase microextraction. *Journal of Pharmaceutical and Biomedical Analysis* **115**:534-542.

Perkins RJ, Liu W, Drusano G, Madu A, Mayers M, Madu C and Miller MH (1995) Pharmacokinetics of ofloxacin in serum and vitreous humor of albino and pigmented rabbits. *Antimicrobial Agents and Chemotherapy* **39**:1493-1498.

Perry M, Sanguinetti M and Mitcheson J (2010) SYMPOSIUM REVIEW: Revealing the structural basis of action of hERG potassium channel activators and blockers. *The Journal of Physiology* **588**:3157-3167.

Pettit SD, Berridge B and Sarazan RD (2010) A call for more integrated cardiovascular safety assessment. *Journal of Pharmacological and Toxicological Methods* **61**:1-2.

Pfefferkorn JA, Litchfield J, Hutchings R, Cheng XM, Larsen SD, Auerbach B, Bush MR, Lee C, Erasga N, Bowles DM, Boyles DC, Lu G, Sekerke C, Askew V, Hanselman JC, Dillon L, Lin Z, Robertson A, Olsen K, Boustany C, Atkinson K, Goosen TC, Sahasrabudhe V, Chupka J, Duignan DB, Feng B, Scialis R, Kimoto E, Bi YA, Lai Y, El-Kattan A, Bakker-Arkema R, Barclay P, Kindt E, Le V, Mandema JW, Milad M, Tait BD, Kennedy R, Trivedi BK and Kowala M (2011) Discovery of novel hepatoselective HMG-CoA reductase inhibitors for treating hypercholesterolemia: A bench-to-bedside case study on tissue selective drug distribution. *Bioorganic & Medicinal Chemistry Letters* **21**:2725-2731.

Picard S, Goineau S, Guillaume P, Henry Jl, Hanouz JL and Rouet R (2011) Supplemental Studies for Cardiovascular Risk Assessment in Safety Pharmacology: A Critical Overview. *Cardiovasc Toxicol* **11**:285-307.

Pieters S, Dejaegher B and Vander Heyden Y (2010) Emerging Analytical Separation Techniques with High Throughput Potential for Pharmaceutical Analysis, Part I: Stationary Phase and Instrumental Developments in LC. *Combinatorial Chemistry & High Throughput Screening,* **13**:510-529.

Pilari S, Preuße C and Huisinga W (2011) Gestational influences on the pharmacokinetics of gestagenic drugs: A combined in silico, in vitro and in vivo analysis. *European Journal of Pharmaceutical Sciences* **42**:318-331.

Piotrovsky V (2005) Pharmacokinetic-pharmacodynamic modeling in the data analysis and interpretation of drug-induced QT/QTc prolongation. *AAPS J* **7**:E609-E624.

Plumb RS (2008) Addressing the analytical throughput challenges in ADME screening using rapid ultraperformance liquid chromatography/tandem mass spectrometry methodologies. *Rapid Communications in Mass Spectrometry* **22**:2139-2152.

Polak S, Wisniowska B and Brandys J (2009) Collation, assessment and analysis of literature in vitro data on hERG receptor blocking potency for subsequent modeling of drugs' cardiotoxic properties. *Journal of Applied Toxicology* **29**:183-206.

Pöling J, Rees W, Klaus S, Bahlmann L, Hübner N, Mantovani V and Warnecke H (2007) Myocardial metabolic monitoring with the microdialysis technique during and after open heart surgery. *Acta Anaesthesiologica Scandinavica* **51**:341-346.

Pollard CE, bi Gerges N, Bridgland-Taylor MH, Easter A, Hammond TG and Valentin JP (2010) An introduction to QT interval prolongation and non-clinical approaches to assessing and reducing risk. *British Journal of Pharmacology* **159**:12-21.

Pollard CE, Valentin JP and Hammond TG (2008) Strategies to reduce the risk of drug-induced QT interval prolongation: a pharmaceutical company perspective. *British Journal of Pharmacology* **154**:1538-1543.

Poulin P, Ekins S and Theil F-P (2011a) A hybrid approach to advancing quantitative prediction of tissue distribution of basic drugs in human. *Toxicology and Applied Pharmacology* **250**:194-212.

Poulin P, Hop CECA, Ho Q, Halladay JS, Haddad S and Kenny JR (2012) Comparative Assessment of In Vitro–In Vivo Extrapolation Methods used for Predicting Hepatic Metabolic Clearance of Drugs. *Journal of Pharmaceutical Sciences* **101**:4308-4326.

Poulin P, Jones HM, Jones RD, Yates JWT, Gibson CR, Chien JY, Ring BJ, Adkison KK, He H, Vuppugalla R, Marathe P, Fischer V, Dutta S, Sinha VK, Bj+Ârnsson T, Lav+® T and Ku MS (2011b) PhRMA CPCDC initiative on predictive models of human pharmacokinetics, part 1: Goals, properties of the PhRMA dataset, and comparison with literature datasets. *Journal of Pharmaceutical Sciences* **100**:4050-4073.

Poulin P, Jones RDO, Jones HM, Gibson CR, Rowland M, Chien JY, Ring BJ, Adkison KK, Ku MS, He H, Vuppugalla R, Marathe P, Fischer V, Dutta S, Sinha VK, Bj+Ârnsson T, Lav+® T and Yates JWT (2011c) PHRMA CPCDC initiative on predictive models of human pharmacokinetics, part 5: Prediction of plasma concentrationΓÇôtime profiles in human by using the physiologically-based pharmacokinetic modeling approach. *Journal of Pharmaceutical Sciences* **100**:4127-4157.

Pratt MD CM, Camm MD AJ, Cooper MS W, Friedman MD P, MacNeil MD DJ, Moulton RN KM, Pitt MD B, Schwartz MD PJ, Veltri MD EP and Waldo MD AL (1998) Mortality in the Survival With ORal D-Sotalol (SWORD) Trial: Why Did Patients Die? 1. *The American Journal of Cardiology* **81**:869-876.

Preechagoon Y and Charles BG (1995) Analysis of cisapride in neonatal plasma using high-performance liquid chromatography with a base-stable column and fluorescence detection. *Journal of Chromatography B: Biomedical Sciences and Applications* **670**:139-143.

Price KE, Lunte CE and Larive CK (2008) Development of tissue-targeted metabonomics. Part 1. Analytical considerations. *Journal of Pharmaceutical and Biomedical Analysis* **46**:737-747.

Price KE, Vandaveer SS, Lunte CE and Larive CK (2005) Tissue targeted metabonomics: Metabolic profiling by microdialysis sampling and microcoil NMR. *Journal of Pharmaceutical and Biomedical Analysis* **38**:904-909.

Prior H, McMahon N, Schofield J and Valentin JP (2009) Non-invasive telemetric electrocardiogram assessment in conscious beagle dogs. *Journal of Pharmacological and Toxicological Methods* **60**:167-173.

Pueyo E, Husti Z, Hornyik T, Baczko I, Laguna P, Varro A and Rodriguez B (2010) Mechanisms of ventricular rate adaptation as a predictor of arrhythmic risk. *American Journal of Physiology - Heart and Circulatory Physiology* **298**:H1577-H1587.

Pugsley MK, Authier S and Curtis MJ (2008) Principles of Safety Pharmacology. *British Journal of Pharmacology* **154**:1382-1399.

Pugsley MK, Authier S and Curtis MJ (2014) Back to the future: Safety pharmacology methods and models in 2013. *Journal of Pharmacological and Toxicological Methods*.

Pugsley MK, Authier S, Stonerook M and Curtis MJ (2015) The shifting landscape of safety pharmacology in 2015. *Journal of Pharmacological and Toxicological Methods* **75**:5-9.

Rajman I (2008) PK/PD modelling and simulations: utility in drug development. *Drug Discovery Today* **13**:341-346.

Raju B, Ramesh M, Borkar RM, Padiya R, Banerjee SK and Srinivas R (2012) Development and validation of liquid chromatographyΓÇômass spectrometric method for simultaneous determination of moxifloxacin and ketorolac in rat plasma: application to pharmacokinetic study. *Biomedical Chromatography* **26**:1341-1347.

Rakhit A, Holford NHG, Effeney DJ and Riegelman S (1984) Induction of quinidine metabolism and plasma protein binding by phenobarbital in dogs. *Journal of Pharmacokinetics and Biopharmaceutics* **12**:495-515.

Ramanathan R, Jemal M, Ramaqiri S, Xia Y, Humpreys W, Olah T and Korfmacher W (2011) It is time for a paradigm shift in drug discovery bioanalysis: from SRM to HRMS. *J Mass Spectrom* **46**:595-601.

Rampe D and Brown AM (2013) A history of the role of the hERG channel in cardiac risk assessment. *Journal of Pharmacological and Toxicological Methods* **68**:13-22.

Redfern WS, Carlsson L, Davis AS, Lynch WG, MacKenzie I, Palethorpe S, Siegl PKS, Strang I, Sullivan AT, Wallis R, Camm AJ and Hammond TG (2003) Relationships between preclinical cardiac electrophysiology, clinical QT interval prolongation and torsade de pointes for a broad range of drugs: evidence for a provisional safety margin in drug development. *Cardiovascular Research* **58**:32-45.

Redfern WS and Valentin JP (2011) Trends in safety pharmacology: Posters presented at the annual meetings of the Safety Pharmacology Society 2001ΓÇô2010. *Journal of Pharmacological and Toxicological Methods* **64**:102-110.

Rescigno A (2010) Compartmental Analysis and its Manifold Applications to Pharmacokinetics. *AAPS J* **12**:61-72.

Ritchie RH, Morgan DJ and Horowitz JD (1998) Myocardial effect compartment modeling of metoprolol and sotalol: Importance of myocardial subsite drug concentration. *Journal of Pharmaceutical Sciences* **87**:177-182.

Riviere JE, Martin-Jimenez T, Sundlof SF and Craigmill AL (1997) Interspecies allometric analysis of the comparative pharmacokinetics of 44 drugs across veterinary and laboratory animal species. *Journal of Veterinary Pharmacology and Therapeutics* **20**:453-463.

Rodgers T, Leahy D and Rowland M (2005) Physiologically Based Pharmacokinetic Modeling 1: Predicting the Tissue Distribution of Moderate-to-Strong Bases. *Journal of Pharmaceutical Sciences* **94**:1259-1276.

Rodgers T and Rowland M (2006) Physiologically based pharmacokinetic modelling 2: Predicting the tissue distribution of acids, very weak bases, neutrals and zwitterions. *Journal of Pharmaceutical Sciences* **95**:1238-1257.

Rostami-Hodjegan A (2012) Physiologically Based Pharmacokinetics Joined With In Vitro–In Vivo Extrapolation of ADME: A Marriage Under the Arch of Systems Pharmacology. *Clinical Pharmacology & Therapeutics* **92**:50-61.

Routledge PA (1986) The plasma protein binding of basic drugs. *British Journal of Clinical Pharmacology* **22**:499-506.

Rowland M (1980) Plasma Protein Binding and Therapeutic Drug Monitoring. *Therapeutic Drug Monitoring* **2**.

Rowland M, Balant LP and Peck C (2004) Physiologically based pharmacokinetics in Drug Development and Regulatory Science: A workshop report (Georgetown University, Washington, DC, May 29–30, 2002). *AAPS PharmSci* **6**:56-67.

Rowland M, Lesko LJ and Rostami-Hodjegan A (2015) Physiologically Based Pharmacokinetics Is Impacting Drug Development and Regulatory Decision Making. *CPT: Pharmacometrics & Systems Pharmacology* **4**:313-315.

Rubinstein E, Dautrey S, Farinoti R, St Julien L, Ramon J and Carbon C (1995) Intestinal elimination of sparfloxacin, fleroxacin, and ciprofloxacin in rats. *Antimicrobial Agents and Chemotherapy* **39**:99-102.

S7A I (2000) ICH S7A: Safety Pharmacology studies for Human Pharmaceuticals, in (Harmonisation ICf ed).

S7B I (2005) ICH S7B: The Non-Clinical Evaluation of the Potential for Delayed Ventricular Repolarisation (QT Interval Prolongation) by Human Pharmaceuticals, in (Harmonisation ICf ed).

Sanguinetti MC and Jurkiewicz NK (1990) Two components of cardiac delayed rectifier K+ current. Differential sensitivity to block by class III antiarrhythmic agents. *The Journal of General Physiology* **96**:195-215.

Sanguinetti MC and Tristani-Firouzi M (2006) hERG potassium channels and cardiac arrhythmia. *Nature* **440**:463-469.

Sastry CSP, Srinivas Y and Rao PVS (1997) Assay of cisapride in pharmaceutical formulations by extraction spectrophotometry. *Talanta* **44**:517-526.

Sattari S, Dryden WF, Eliot LA and Jamali F (2003) Despite increased plasma concentration, inflammation reduces potency of calcium channel antagonists due to lower binding to the rat heart. *British Journal of Pharmacology* **139**:945-954.

Savoie N, Garofolo F, van Amsterdam P, Bansal S, Beaver C, Bedford P, Booth BP, Evans C, Jemal M, Lefebvre M, Lopes de Silva AL, Lowes S, Marini JC, Mass+® R, Mawer L, Ormsby E, Rocci Jr ML, Viswanathan CT, Wakelin-Smith J, Welink J, White JT and Woolf E (2010) 2010 White Paper on Recent Issues in Regulated Bioanalysis & Global Harmonization of Bioanalytical Guidance. *Bioanalysis* **2**:1945-1960.

Savoie N, Garofolo F, van Amsterdam P, Booth BP, Fast DM, Lindsay M, Lowes S, Masse R, Mawer L, Ormsby E, Phull R, Rocci ML, Vallano PT and Yin X (2009) 2009 White Paper on Recent Issues in Regulated Bioanalysis from The 3rd Calibration and Validation Group Workshop. *Bioanalysis* **2**:53-68.

Sawada Y, Hanano M, Sugiyama Y, Harashima H and Iga T (1984) Prediction of the volumes of distribution of basic drugs in humans based on data from animals. *Journal of Pharmacokinetics and Biopharmaceutics* **12**:587-596.

Schentag JJ (2000) Sparfloxacin: A review. *Clinical Therapeutics* **22**:372-387.

Schillinger W, Christians C, Sossalla S, Teucher N, Nguyen Van P, Kögler H, Zeitz O and Hasenfuss G (2007) α1-adrenergic stress induces downregulation of Na+/Ca2+ exchanger in myocardial preparations from rabbits at physiological preload. *European Journal of Heart Failure* **9**:329-335.

Schinkel AH (1997) The physiological function of drug-transporting P-glycoproteins. *Seminars in Cancer Biology* **8**:161-170.

Schirle M and Jenkins JL (2015) Identifying compound efficacy targets in phenotypic drug discovery. *Drug Discovery Today*.

Schmidt S, Gonzalez D and Derendorf H (2010) Significance of protein binding in pharmacokinetics and pharmacodynamics. *Journal of Pharmaceutical Sciences* **99**:1107-1122.

Schnelle K and Garrett ER (1973) Pharmacokinetics of the +¦-adrenergic blocker sotalol in dogs. *Journal of Pharmaceutical Sciences* **62**:362-375.

Shafi MM (2011) A simple spectrophotometric determination of cisapride in pharmaceutical preparations. *International Journal of Chemical Sciences* **9**:1349-1352.

Shah V, Midha K and Dighe S (1992) Analytical methods validation: bioavailability, bioequivalence and pharmacokinetic studies. *Pharm Res* **9**:588-592.

Shah VP and Bansal S (2011) Historical perspective on the development and evolution of bioanalytical guidance and technology. *Bioanalysis* **3**:823-827.

Shimada J, Nogita T and Ishibashi Y (1993) Clinical Pharmacokinetics of Sparfloxacin. *Clin Pharmacokinet* **25**:358-369.

Shiotani M, Harada T, Abe J, Sawada Y, Hashimoto K, Hamada Y and Horii I (2005) Practical Application of Guinea Pig Telemtry System for QT Evaluation. *The Journal of Toxicological Sciences* **30**:239-247.

Shiran MR, Proctor NJ, Howgate EM, Rowland-Yeo K, Tucker GT and Rostami-Hodjegan A (2006) Prediction of metabolic drug clearance in humans: In vitro–in vivo extrapolation vs allometric scaling. *Xenobiotica* **36**:567-580.

Siefert HM, Domdey-Bette A, Henninger K, Hucke F, Kohlsdorfer C and Stass HH (1999a) Pharmacokinetics of the 8-methoxyquinolone, moxifloxacin: a comparison in humans and other mammalian species. *Journal of Antimicrobial Chemotherapy* **43**:69-76.

Siefert HM, Kohlsdorfer C, Steinke W and Witt A (1999b) Pharmacokinetics of the 8-methoxyquinolone, moxifloxacin: tissue distribution in male rats. *Journal of Antimicrobial Chemotherapy* **43**:61-67.

Simpson M, Lappin G and Keely BJ (2010) Development of 2D chiral chromatography with accelerator mass spectrometry for quantification of 14C-labeled R- and S-verapamil in plasma. *Bioanalysis* **2**:397-405.

Sims C, Reisenweber S, Viswanathan PC, Choi BR, Walker WH and Salama G (2008) Sex, Age, and Regional Differences in L-Type Calcium Current Are Important Determinants of Arrhythmia Phenotype in Rabbit Hearts With Drug-Induced Long QT Type 2. *Circulation Research* **102**:e86-e100.

Singhal P, Yadav M, Winter S, Guttikar S, Patel D, Mills M and Shrivastav PS (2012) Enantiomeric Separation of Verapamil and its Active Metabolite, Norverapamil, and Simultaneous Quantification in Human Plasma by LC–ESI-MS-MS. *Journal of Chromatographic Science* **50**:839-848.

Sivarajah A, Collins S, Sutton MR, Regan N, West H, Holbrook M and Edmunds N (2010) Cardiovascular safety assessments in the conscious telemetered dog: Utilisation of super-intervals to enhance statistical power. *Journal of Pharmacological and Toxicological Methods* **62**:12-19.

Smith BJ (2012) An industrial perspective on contemporary applications of PBPK models in drug discovery and development. *Biopharmaceutics & Drug Disposition* **33**:53-54.

Smith DA, Di L and Kerns EH (2010) The effect of plasma protein binding on in vivo efficacy: misconceptions in drug discovery. *Nat Rev Drug Discov* **9**:929-939.

Smith G (2010) Bioanalytical method validation: notable points in the 2009 draft EMA Guideline and differences with the 2001 FDA Guidance. *Bioanalysis* **2**:929-935.

Solans C, Bregante MA, Aramayona JJ, Fraile LJ and Garcia MA (2000) Comparison of the pharmacokinetics of verapamil in the pregnant and non-pregnant rabbit: study of maternal and foetal tissue levels. *Xenobiotica* **30**:93-102.

Srinivas N, Narasu L, Shankar BP and Mullangi R (2008) Development and validation of a HPLC method for simultaneous quantitation of gatifloxacin, sparfloxacin and moxifloxacin using levofloxacin as internal standard in human plasma: application to a clinical pharmacokinetic study. *Biomedical Chromatography* **22**:1288-1295.

Stass H and Dalhoff A (1997) Determination of BAY 12-8039, a new 8-methoxyquinolone, in human body fluids by high-performance liquid chromatography with fluorescence detection using on-column focusing. *Journal of Chromatography B: Biomedical Sciences and Applications* **702**:163-174.

Stass H and Kubitza D (1999) Pharmacokinetics and elimination of moxifloxacin after oral and intravenous administration in man. *Journal of Antimicrobial Chemotherapy* **43**:83-90.

Stass H and Kubitza D (2001) Profile of Moxifloxacin Drug Interactions. *Clinical Infectious Diseases* **32**:S47-S50.

Steidl-Nichols JV, Hanton G, Leaney J, Liu RC, Leishman D, McHarg A and Wallis R (2008) Impact of study design on proarrhythmia prediction in the SCREENIT rabbit isolated heart model. *Journal of Pharmacological and Toxicological Methods* **57**:9-22.

Stevens JL and Baker TK (2009) The future of drug safety testing: expanding the view and narrowing the focus. *Drug Discovery Today* **14**:162-167.

Stoelting RK and Miller RD (2007) *Basics of Anaesthesia*. Churchill Livingstone Elsevier.

Suenderhauf C and Parrott N (2013) A Physiologically Based Pharmacokinetic Model of the Minipig: Data Compilation and Model Implementation. *Pharmaceutical Research* **30**:1-15.

Sugiyama A (2008) Sensitive and reliable proarrhythmia in vivo animal models for predicting drug-induced torsades de pointes in patients with remodelled hearts. *British Journal of Pharmacology* **154**:1528-1537.

Suh YS, Kamruzzaman M, Alam AM, Lee SH, Kim YH, Kim GM and Dang TD (2014) Chemiluminescence determination of moxifloxacin in pharmaceutical and biological samples based on its enhancing effect of the luminolΓÇôferricyanide system using a microfluidic chip. *Luminescence* **29**:248-253.

Summerfield SG, Lucas AJ, Porter RA, Jeffrey P, Gunn RN, Read KR, Stevens AJ, Metcalf AC, Osuna MC, Kilford PJ, Passchier J and Ruffo AD (2008) Toward an improved prediction of human in vivo brain penetration. *Xenobiotica* **38**:1518-1535.

Summerfield SG, Stevens AJ, Cutler L, del Carmen Osuna M, Hammond B, Tang SP, Hersey A, Spalding DJ and Jeffrey P (2006) Improving the in Vitro Prediction of in Vivo Central Nervous System Penetration: Integrating Permeability, P-glycoprotein Efflux, and Free Fractions in Blood and Brain. *Journal of Pharmacology and Experimental Therapeutics* **316**:1282-1290.

Sundquist H (1980) Basic review and comparison of beta-blocker pharmacokinetics. *Current Therapeutic Research* **28**:388-448.

Szabo G, Szentandrassy N, Biro T, Toth BI, Czifra G, Magyar J, Banyasz T, Varro A, Kovacs L and Nanasi PP (2005) Asymmetrical distribution of ion channels in canine and human left-ventricular wall: epicardium versus midmyocardium. *Pflugers Arch* **450**:307-316.

Szałek E, Karbownik A, Grabowski T, Sobańska K, Wolc A and Grześkowiak E (2013) Pharmacokinetics of sunitinib in combination with fluoroquinolones in rabbit model. *Pharmacology Reports* **65**:1383-1390.

Tack J, Camilleri M, Chang L, Chey WD, Galligan JJ, Lacy BE, M++ller-Lissner S, Quigley EMM, Schuurkes J, De Maeyer JH and Stanghellini V (2012) Systematic review: cardiovascular safety profile of 5-HT4 agonists developed for gastrointestinal disorders. *Alimentary Pharmacology & Therapeutics* **35**:745-767.

Tashibu H, Miyazaki H, Aoki K, Akie Y and Yamamoto K (2005) QT PRODACT: In Vivo QT Assay in Anesthetized Dog for Detecting the Potential for QT Interval Prolongation by Human Pharmaceuticals. *Journal of Pharmacological Sciences* **99**:473-486.

Testai L, Breschi MC, Martinotti E and Calderone V (2007) QT prolongation in guinea pigs for preliminary screening of torsadogenicity of drugs and drug-candidates. II. *Journal of Applied Toxicology* **27**:270-275.

Testai L, Calderone V, Salvadori A, Breschi MC, Nieri P and Martinotti E (2004) QT prolongation in anaesthetized guinea-pigs: an experimental approach for preliminary screening of torsadogenicity of drugs and drug candidates. *Journal of Applied Toxicology* **24**:217-222.

Thomas S (2010) Physiologically-based pharmacokinetic modelling for the reduction of animal use in the discovery of novel pharmaceuticals. *Altern Lab Anim* **38**:81-85.

Thrall KD, Sasser LB, Creim JA, Gargas ML, Kinzell JH and Corley RA (2009) Studies supporting the development of a physiologically based pharmacokinetic (PBPK) model for methyl iodide: pharmacokinetics of sodium iodide (NaI) in pregnant rabbits. *Inhalation Toxicology* **21**:519-523.

Timmerman P, White S, McDougall S, Kall MA, Smeraglia J, Fjording MS and Knutsson M (2015) Tiered approach into practice: scientific validation for chromatography-based assays in early development ΓÇô a recommendation from the European Bioanalysis Forum. *Bioanalysis* **7**:2387-2398.

Todd EL and Abernethy DR (1987) Physiological pharmacokinetics and pharmacodynamics of (±)-verapamil in female rats. *Biopharmaceutics & Drug Disposition* **8**:285-297.

Tontodonati M, Fasdelli N and Dorigatti R (2011) An improved method of electrode placement in configuration Lead II for the reliable ECG recording by telemetry in the conscious rat. *Journal of Pharmacological and Toxicological Methods* **63**:1-6.

Toyoshima S, Kanno A, Kitayama T, Sekiya K, Nakai K, Haruna M, Mino T, Miyazaki H, Yano K and Yamamoto K (2005) QT PRODACT: In Vivo QT Assay in the Conscious Dog for Assessing the Potential for QT Interval Prolongation by Human Pharmaceuticals. *Journal of Pharmacological Sciences* **99**:459-471.

Tozer TN, Gambertoglio JG, Furst DE, Avery DS and Holford NHG (1983) Volume Shifts and Protein Binding Estimates using Equilibrium Dialysis: Application to Prednisolone Binding in Humans. *Journal of Pharmaceutical Sciences* **72**:1442-1446.

Tremblay RT, Kim D and Fisher JW (2012) Determination of Tissue to Blood Partition Coefficients for Nonvolatile Herbicides, Insecticides, and Fungicides Using Negligible Depletion Solid-Phase Microextraction (nd-SPME) and Ultrafiltration. *Journal of Toxicology and Environmental Health, Part A* **75**:288-298.

Tylutki Z and Polak S (2015) Plasma vs heart tissue concentration in humans ΓÇô literature data analysis of drugs distribution. *Biopharmaceutics & Drug Disposition* **36**:337-351.

Tylutki Z and Polak S (2017) A four-compartment PBPK heart model accounting for cardiac metabolism - model development and application. *Scientific Reports* **7**:39494.

Tzepi I, Vergados I, Kanellakopoulou K, Papathanassiou M, Kranidioti H, Tsaganos T, Liarakos V, Giamarellos-Bourboulis EJ and Theodossiadis P (2009) Pharmacokinetics of intravenously administered moxifloxacin in eye compartments: an experimental study. *International Journal of Antimicrobial Agents* **33**:160-162.

US 21 Code of Federal Regulations FaD (2002) 320.29 Analytical methods for an in vivo bioavailability study. 42 FR 1648, 7 January 1977, as amended at 67 FR 77674, in.

Vaes WHJ, Urrestarazu Ramos E, Hamwijk C, van Holsteijn I, Blaauboer BJ, Seinen W, Verhaar HJM and Hermens JLM (1997) Solid Phase Microextraction as a Tool To Determine Membrane/Water Partition Coefficients and Bioavailable Concentrations in in Vitro Systems. *Chemical Research in Toxicology* **10**:1067-1072.

Valentin JP (2010) Reducing QT liability and proarrhythmic risk in drug discovery and development. *British Journal of Pharmacology* **159**:5-11.

Valentin JP and Hammond T (2008) Safety and secondary pharmacology: Successes, threats, challenges and opportunities. *Journal of Pharmacological and Toxicological Methods* **58**:77-87.

Valentin JP, Hoffmann P, De Clerck F, Hammond TG and Hondeghem L (2004) Review of the predictive value of the Langendorff heart model (Screenit system) in assessing the proarrhythmic potential of drugs. *Journal of Pharmacological and Toxicological Methods* **49**:171-181.

Valentin JP, Pollard C, Lainee P and Hammond T (2010) Value of non-clinical cardiac repolarization assays in supporting the discovery and development of safer medicines. *British Journal of Pharmacology* **159**:25-33.

Valko K, Du CM, Bevan C, Reynolds D, P. and Abraham M, H. (2001) Rapid Method for the Estimation of Octanol / Water Partition Coefficient (Log Poct) from Gradient RP-HPLC Retention and a Hydrogen Bond Acidity Term (Sigma alpha2H). *Current Medicinal Chemistry* **8**:1137-1146.

Valko K, Du CM, Bevan CD, Reynolds DP and Abraham MH (2000) Rapid-Gradient HPLC Method for Measuring Drug Interactions with Immobilized Artificial Membrane: Comparison with Other Lipophilicity Measures. *Journal of Pharmaceutical Sciences* **89**:1085-1096.

van Amsterdam P, Arnold M, Bansal S, Fast D, Garofolo F, Lowes S, Timmerman P and Woolf E (2010) Building the Global Bioanalysis Consortium ΓÇô working towards a functional globally acceptable and harmonized guideline on bioanalytical method validation. *Bioanalysis* **2**:1801-1803.

van der Graaf P and Benson N (2011) Systems Pharmacology: Bridging Systems Biology and Pharmacokinetics-Pharmacodynamics (PKPD) in Drug Discovery and Development. *Pharm Res* **28**:1460-1464.

Van Peer E, Downes N, Casteleyn C, Van Ginneken C, Weeren A and Van Cruchten S (2016) Organ data from the developing Göttingen minipig: first steps towards a juvenile PBPK model. *Journal of Pharmacokinetics and Pharmacodynamics* **43**:179-190.

Varro A and Baczko I (2011) Cardiac ventricular repolarization reserve: a principle for understanding drug-related proarrhythmic risk. *British Journal of Pharmacology* **164**:14-36.

Veereman-Wauters G, Monbaliu J, Meuldermans W, Woestenborghs R, Verlinden M, Heykants J and Rudolph CD (1991) Study of the placental transfer of cisapride in sheep. Plasma levels in the pregnant ewe, the fetus, and the lamb. *Drug Metabolism and Disposition* **19**:168-172.

Vicente J, Johannesen L, Galeotti L and Strauss DG (2014) Mechanisms of sex and age differences in ventricular repolarization in humans. *American Heart Journal* **168**:749-756.

Vincze D, Farkas AS, Rudas L, Makra P, Cs+¡k N, Lepr+ín I, Forster T, Csan+ídy M, Papp JG, Varr+¦ A and Farkas A (2008) Relevance of anaesthesia for dofetilide-induced torsades de pointes in +¦1-adrenoceptor-stimulated rabbits. *British Journal of Pharmacology* **153**:75-89.

Virag L, Acsai K, Hala O, Zaza A, Bitay M, Bogats G, Papp JG and Varro A (2009) Self-augmentation of the lengthening of repolarization is related to the shape of the cardiac action potential: implications for reverse rate dependency. *Br J Pharmacol* **156**:1076-1084.

Vishwanathan K, Bartlett MG and Stewart JT (2002) Determination of moxifloxacin in human plasma by liquid chromatography electrospray ionization tandem mass spectrometry. *Journal of Pharmaceutical and Biomedical Analysis* **30**:961-968.

von Keutz E and Schluter G (1999) Preclinical safety evaluation of moxifloxacin, a novel fluoroquinolone. *Journal of Antimicrobial Chemotherapy* **43**:91-100.

von Richter O, Eichelbaum M, Schönberger F and Hofmann U (2000) Rapid and highly sensitive method for the determination of verapamil, [2H7]verapamil and metabolites in biological fluids by liquid chromatography-mass spectrometry. *J Chromatogr B Biomed Sci Appl* **738**:137-147.

Vozeh S, Bindschedler M, Ha HRm, Kaufmann G, Guentert TW and Follath F (1987) Pharmacodynamics of 3-hydroxyquinidine alone and in combination with quinidine in healthy persons. *The American Journal of Cardiology* **59**:681-684.

Vozeh S, Schmidlin O and Taeschner W (1988) Pharmacokinetic Drug Data. *Clin-Pharmacokinet* **15**:254-282.

Vuckovic D, de Lannoy I, Gien B, Yang Y, Musteata FM, Shirey R, Sidisky L and Pawliszyn J (2011) In vivo solid-phase microextraction for single rodent pharmacokinetics studies of carbamazepine and carbamazepine-10,11-epoxide in mice. *Journal of Chromatography A* **1218**:3367-3375.

Vuckovic D, Zhang X, Cudjoe E and Pawliszyn J (2010) Solid-phase microextraction in bioanalysis: New devices and directions. *Journal of Chromatography A* **1217**:4041-4060.

W M (1988) Excretion and biotransformation of Cisapride in Dogs and Humans after Oral Administration, in *DMD* pp 403-409.

Wagner C, Zhao P, Pan Y, Hsu V, Grillo J, Huang SM and Sinha V (2015) Application of Physiologically Based Pharmacokinetic (PBPK) Modeling to Support Dose Selection: Report of an FDA Public Workshop on PBPK. *CPT: Pharmacometrics & Systems Pharmacology* **4**:226-230.

Wan H and Rehngren M (2006) High-throughput screening of protein binding by equilibrium dialysis combined with liquid chromatography and mass spectrometry. *Journal of Chromatography A* **1102**:125-134.

Wang D, Patel C, Cui C and Yan GX (2008) Preclinical assessment of drug-induced proarrhythmias: Role of the arterially perfused rabbit left ventricular wedge preparation. *Pharmacology & Therapeutics* **119**:141-151.

Wang J, Della Penna K, Wang H, Karczewski J, Connolly TM, Koblan K, Bennett PB and Salata J (2003) Functional and pharmacological properties of canine ERG potassium channels. *American Physiological Society* **284**:H256-H267.

Wang J, Yoo HS, Obrochta KM, Huang P and Napoli JL (2015a) Quantitation of retinaldehyde in small biological samples using ultrahigh-performance liquid chromatography tandem mass spectrometry. *Analytical Biochemistry* **484**:162-168.

Wang L, Xu Y, Liang L, Diao C, Liu X, Zhang J and Zhang S (2014) LCΓÇôMS/MS method for the simultaneous determination of PA-824, moxifloxacin and pyrazinamide in rat plasma and its application to pharmacokinetic study. *Journal of Pharmaceutical and Biomedical Analysis* **97**:1-8.

Wang Q, YE C, Jia R, Owen AJ, Hidalgo IJ and Li J (2006) Inter-species comparison of 7-hydroxycoumarin glucuronidation and sulfation in liver S9 fractions. *In Vitro Cellular & Developmental Biology - Animal* **42**:8-12.

Wang Y, Xing J, Xu Y, Zhou N, Peng J, Xiong Z, Liu X, Luo X, Luo C, Chen K, Zheng M and Jiang H (2015b) In silico ADME/T modelling for rational drug design. *Quarterly Reviews of Biophysics* **FirstView**:1-28.

Watari N, Wakamatsu A and Kaneniwa N (1989) Comparison of Disposition Parameters of Quinidine and Quinine in the Rat. *Journal of Pharmacobio-Dynamics* **12**:608-615.

Waters NJ, Jones R, Williams G and Sohal B (2008) Validation of a Rapid Equilibrium Dialysis Approach for the Measurement of Plasma Protein Binding. *Journal of Pharmaceutical Sciences* **97**:4586-4595.

Watson E and Kapur P (1981) High-performance liquid chromatographic determination of verapamil in plasma by fluorescence detection. *J Pharm Sci* **70**:800-801.

Watson KJ, Gorczyca WP, Umland J, Zhang Y, Chen X, Sun SZ, Fermini B, Holbrook M and Van der Graaf PH (2011) PharmacokineticΓÇôpharmacodynamic modelling of the effect of Moxifloxacin on QTc prolongation in telemetered cynomolgus monkeys. *Journal of Pharmacological and Toxicological Methods* **63**:304-313.

Webster R, Allan G, Anto-Awuakye K, Harrison A, Kidd T, Leishman D, Phipps J and Walker D (2001) Pharmacokinetic/pharmacodynamic assessment of the effects of E4031, cisapride, terfenadine and terodiline on monophasic action potential duration in dog. *Xenobiotica* **31**:633-650.

Weiss M (2011) Functional characterization of drug uptake and metabolism in the heart. *Expert Opinion on Drug Metabolism & Toxicology* **7**:1295-1306.

White CM, Xie J, Chow MSS and Kluger J (1999) Prophylactic Magnesium to Decrease the Arrhythmogenic Potential of Class III Antiarrhythmic Agents in a Rabbit Model. *Pharmacotherapy: The Journal of Human Pharmacology and Drug Therapy* **19**:635-640.

Williams G and Mirams GR (2015) A web portal for in-silico action potential predictions. *Journal of Pharmacological and Toxicological Methods* **75**:10-16.

Wishart D (2007) Improving Early Drug Discovery through ADME Modelling. *Drugs R D* **8**:349-362.

Wisniowska B, Mendyk A, Fijorek K, Glinka A and Polak S (2012) Predictive model for L-type channel inhibition: multichannel block in QT prolongation risk assessment. *Journal of Applied Toxicology* **32**:858-866.

Wiśniowska B and Polak S (2016) The Role of Interaction Model in Simulation of Drug Interactions and QT Prolongation. *Current Pharmacology Reports* **2**:339-344.

Woestenborghs R, Lorreyne W, Van Rompaey F and Heykants J (1988) Determination of cisapride in plasma and animal tissues by high-performance liquid chromatography. *J Chromatogr* **424**:195-200.

Wu MH, Su MJ and Siu-Man Sun S (2003) Age-Related Differences in the Direct Cardiac Effects of Cisapride: Narrower Safety Range in the Hearts of Young Rabbits. *Pediatr Res* **53**:493-499.

Wu Y, Carlsson L, Liu T, Kowey PR and Yan GX (2005) Assessment of the Proarrhythmic Potential of the Novel Antiarrhythmic Agent AZD7009 and Dofetilide in Experimental Models of Torsades De Pointes. *Journal of Cardiovascular Electrophysiology* **16**:898-904.

Wysowski DK, Corken A, Gallo-Torres H, Talarico L and Rodriguez EM (2001) Postmarketing reports of QT prolongation and ventricular arrhythmia in association with cisapride and food and drug administration regulatory actions. *Am J Gastroenterol* **96**:1698-1703.

Xia C, Qian M, Chen S, Lee F and Huang T-N (2009) **In-vitro Tissue Protein Binding in rat, dog, monkey and human**, in *16th N American ISSX meeting poster presentation*.

Xiong Z and Sperelakis N (1995) Regulation of L-type calcium channels of vascular smooth muscle cells. *Journal of Molecular and Cellular Cardiology* **27**:75-91.

Xu M, Ju W, Hao H, Wang G and Li P (2013) Cytochrome P450 2J2: distribution, function, regulation, genetic polymorphisms and clinical significance. *Drug Metabolism Reviews* **45**:311-352.

Xu X, Salata J, Wang J, Wu Y, Yan GX, Liu T, Marinchak RA and Kowey PR (2002) Increasing I_{Ks} corrects abnormal repolarization in rabbit models of acquired LQT2 and ventricular hypertrophy. *American Journal of Physiology - Heart and Circulatory Physiology* **283**:H664-H670.

Xu YH, Li D, Liu XY, Li YZ and Lu J (2010) High performance liquid chromatography assay with ultraviolet detection for moxifloxacin: Validation and application to a pharmacokinetic study in Chinese volunteers. *Journal of Chromatography B* **878**:3437-3441.

Yamaguchi I, Obayashi K and Mandel W (1978) Electrophysiological effects of verapamil. *Cardiovascular Research* **12**:597-608.

Yamaguchi T, Yokogawa M, Hashizume T, Baba M, Higuchi Y, Matsuoka N and Sekine Y (1991) Pharmacokinetics of Sparfloxacin in Rats, Dogs and Monkeys. *Drug Metabolism and Pharmacokinetics* **6**:33-41.

Yan GX and Antzelevitch C (1996) Cellular Basis for the Electrocardiographic J Wave. *Circulation* **93**:372-379.

Yan GX, Wu Y, Liu T, Wang J, Marinchak RA and Kowey PR (2001) Phase 2 early afterdepolarization as a trigger of polymorphic ventricular tachycardia in acquired long-QT syndrome : direct evidence from intracellular recordings in the intact left ventricular wall. *Circulation* **103**:2851-2856.

Yang L-Q, Yu W-F, Cao Y-F, Gong B, Chang Q and Yang G-S (2003) Potential inhibition of cytochrome P450 3A4 by propofol in human primary hepatocytes. *World Journal of Gastroenterology* **9**:1959-1962.

Yao X, Anderson DL, Ross SA, Lang DG, Desai BZ, Cooper DC, Wheelan P, McIntyre MS, Bergquist ML, MacKenzie KI, Becherer JD and Hashim MA (2008) Predicting QT

prolongation in humans during early drug development using hERG inhibition and an anaesthetized guinea-pig model. *British Journal of Pharmacology* **154**:1446-1456.

Yu M, Bozek J, Kagan M, Guaraldi M, Silva P, Azure M, Onthank D and Robinson SP (2013) Cardiac retention of PET neuronal imaging agent LMI1195 in different species: Impact of norepinephrine uptake-1 and -2 transporters. *Nuclear Medicine and Biology* **40**:682-688.

Yuan Y, Bai X, Luo C, Wang K and Zhang H (2015) The virtual heart as a platform for screening drug cardiotoxicity. *British Journal of Pharmacology* **172**:5531-5547.

Yue Z, Lin X, Tang S, Chen X, Ji C, Hua H and Liu Y (2007) Determination of 16 quinolone residues in animal tissues using high performance liquid chromatography coupled with electrospray ionization tandem mass spectrometry. *Se Pu* **25**:491-495.

Yun YE, Cotton CA and Edginton AN (2014) Development of a decision tree to classify the most accurate tissue-specific tissue to plasma partition coefficient algorithm for a given compound. *Journal of Pharmacokinetics and Pharmacodynamics* **41**:1-14.

Zemrak WR and Kenna GA (2008) Association of antipsychotic and antidepressant drugs with Q-T interval prolongation. *American Journal of Health-System Pharmacy* **65**:1029-1038.

Zhang F, Xue J, Shao J and Jia L (2012) Compilation of 222 drugsΓÇÖ plasma protein binding data and guidance for study designs. *Drug Discovery Today* **17**:475-485.

Zhang J, Vath M, Ferraro C, Li Y, Murphy K, Zvyaga T, Weller H and Shou W (2013) A high-speed liquid chromatography/tandem mass spectrometry platform using multiplexed multiple-injection chromatography controlled by single software and its application in discovery ADME screening. *Rapid Communications in Mass Spectrometry* **27**:731-737.

Zhou S-F, Xue CC, Yu X-Q, Li C and Wang G (2007) Clinically Important Drug Interactions Potentially Involving Mechanism-based Inhibition of Cytochrome P450 3A4 and the Role of Therapeutic Drug Monitoring. *Therapeutic Drug Monitoring* **29**:687-710.

Zhu L, Yang J, Zhang Y, Wang Y, Zhang J, Zhao Y and Dong W (2015) Prediction of Pharmacokinetics and Penetration of Moxifloxacin in Human with Intra-Abdominal Infection Based on Extrapolated PBPK Model. *Korean J Physiol Pharmacol* **19**:99-104.

Zhu T, Pang Q, McCluskey SA and Luo C (2008) Effect of propofol on hepatic blood flow and oxygen balance in rabbits. *Canadian Journal of Anesthesia* **55**:364.

Zhuang X and Lu C (2016) PBPK modeling and simulation in drug research and development. *Acta Pharmaceutica Sinica B* **6**:430-440.

Zicha S, Moss I, Allen B, Varro A, Papp J, Dumaine R, Antzelevich C and Nattel S (2003) Molecular basis of species-specific expression of repolarizing K⁺ currents in the heart. *American Journal of Physiology - Heart and Circulatory Physiology* **285**:H1641-H1649.

Zlotos G, Bucker A, Kinzig-Schippers M, Sorgel F and Holzgrabe U (1998a) Plasma Protein Binding of Gyrase Inhibitors. *Journal of Pharmaceutical Sciences* **87**:215-220.

Zlotos G, Oehlmann M, Nickel P and Holzgrabe U (1998b) Determination of protein binding of gyrase inhibitors by means of continuous ultrafiltration. *Journal of Pharmaceutical and Biomedical Analysis* **18**:847-858.

Strathclyde Institute of Pharmacy and Biomedical Sciences
GlaxoSmithKline

APPENDICES

APPENDICES

1. APPENDIX 1: BIOANALYTICAL METHODS

1.1. Bioanalytical Assay Development

The primary aims of the bioanalytical assays were to demonstrate linearity of the standard line, acceptable accuracy and precision across the calibration range or peak-area response, using quality control (QC) samples and internal standards, to generate data for this investigative project.

Methods utilised within this investigative project were either based upon existing validated assays that have been adapted from regulated studies or from literature to be fit for purpose. Bioanalytical assays used were 'qualified' and a full validation was not deemed appropriate.

Bioanalytical assay qualification was achieved by mass spectrometry optimization and analysis of single and double blanks, standard curves, and quality controls (QCs) for each compound were performed before analysing study samples. This verified the chromatography on the system and the suitability (accuracy and precision, selectivity, carryover, linearity, etc) were acceptable as qualified assay.

Following optimisation of the UHPLC and MS conditions samples were analysed using an analytical method based on protein precipitation, followed by UHPLC-MS/MS analysis. Each assay has a defined assay range from a lower limit of quantification (LLQ) and a higher limit of quantification (HLQ) using a specified amount of sample for a particular matrix.

1.1.1. Chemicals and Reagents

All chemicals, solvents and reagents, unless stated, were of analytical or HPLC grade or equivalent suitable for research use and purchased from Sigma Aldrich (St Louis, MO) or Fisher Scientific.

1.1.2. Sample Receipt/Storage

Samples were analysed as soon as practically possible after receipt, either fresh or following defrosting. Samples were stored frozen at an -20°C or below, pre- and/or post- analysis. Prior to analysis, frozen study samples were removed from storage and thawed at room temperature.

For PK study samples, QCs were prepared in the same matrix as the samples, and were stored with the study samples as soon as is practicable, and analysed with samples.

For protein binding, an appropriate positive control compound was not selected as each tool compound utilised in this project was a marketed compound with literature reference.

1.1.3. Sample Protein Precipitation

Experimental samples collected for each compound from each investigational technique were subjected to appropriate sample preparation in order to be analysed by LC-MS/MS as described below, respectively.

Samples were prepared by protein precipitation using at least 3:1 (v/v) ratio of organic solvent (acetonitrile) to sample; for example 50 µL of sample precipitated with 150 µL of acetontrile. The final composition of the matrix calibration standards and QCs contained no more than 5% (v/v) of non-matrix solvent from the spiking stocks used. Following centrifugation the subsequent supernatant extract was then injected onto UPLC-MS/MS system for analysis. Where more sensitivity was required, an aliquot of the solvent from the extracted sample may be evaporated to dryness and reconstituted prior to injection.

1.1.4. Standards

Two sets of analytical solutions (A/B) of each compound from independent weighings were dissolved in the required volume of solvent as appropriate to give stock solutions of the free compound; one for calibration standards (A) and one for quality control samples (B).

1.1.4.1. Calibration Standards

For pharmacokinetic studies or where a concentration of any given analyte was required, a minimum of 6-8 standard concentrations were included. There were a minimum of 3 standards within each order of magnitude of the concentration range of the line, i.e. for a 10 to 10,000 ng/mL range, there would be 3 standards in the range 10 to 100ng/mL, 3 standards in the range 100 to 1000 ng/ml and 3 in the range 1000 to 10,000ng/ml. It is recommended as good bioanlytical practice that the full calibration range should not exceed more than 3 orders of magnitude (Ho, 2014).

1.1.4.2. Quality Control Standards

For pharmacokinetic studies or where a concentration of any given analyte was required, quality control (QC) standards were prepared for data integrity. QC's were prepared typically at 3-4x times the LLQ, a mid-calibration range and at approximately 80% of the HLQ concentration.

1.1.5. Internal Standard

Where possible, the internal standard used had similar physicochemical properties to that of the analyte of interest and a similar retention time or be a closely related analogue. Ideally, a stable isotopicically labelled (SIL) analogue was used if available. A generic IS (e.g., [$^{2}H_{3}$ ^{13}C]-SB243213 (GSK internal)) was used if considered appropriate. A suitable concentration of internal standard (I.S.) working solution was prepared in the extraction solvent (eg. acetonitrile). For the sample analysis, various analytical reference materials were used as internal standards (IS) for each compound of interest. [$^{2}H_{3}{}^{13}C$]SB243213 was used for verapamil and cisapride; for moxifloxacin a stable isotopic label [$^{2}H_{9}{}^{15}N$]GW646803 was available; and sotalol was used for sparfloxacin. The internal standard response reflected the middle region of the anticipated calibration curve (usually 30-70 % of the expected HLQ), where applicable.

1.2. Sample Analysis

All samples generated were analysed using Liquid Chromatography–Mass Spectrometry (LC-MS/MS) and undertaken in accordance to guidelines within the Bioanalytical Sample Management and Toxicokinetics, DMPK (GlaxoSmithKline).

Prepared extracted samples collected or calibration standards, quality controls and blanks were injected onto a LC-MS/MS system consisting of an auto sampler, a high pressure gradient binary solvent system (Acquity Waters UPLC, Model 1200) and a mass spectrometer (Applied Biosystems/MDS Sciex, Model API4000). Injected samples were separated under appropriate UPLC conditions for each compound such as reverse phase or isocratic gradient described.

Following LC separation, column eluent was diverted to the mass spectrometer for MS/MS analysis using a heat assisted electrospray interface in positive ion mode. The UPLC system was controlled by MassLynx companion software (Waters) and mass spectrometer was

controlled by Analyst software (Applied Biosystems, version 1.4.2), using an optimised multiple reaction monitoring (MRM) for data acquisition. The MRM transitions selected for analysis of each compound and its respective internal standard are described.

1.2.1. Sample Run Analysis

All samples were either allowed to defrost at room temperature or analysed fresh which were prepared along with appropriate matrix standards, quality control, blanks, as required. All samples within a given analytical run were extracted at the same time.

For assaying blood:plasma ratio and protein binding study samples, no calibration standard line or QCs were necessary as part of the analysis. Only Total Blank (blank matrix extracted with organic solvent) and Blank +I.S. (blank matrix extracted with organic solvent containing I.S.) were required as well as including appropriate Blank + I.S. as the 'wash' between sets of samples to act as negative controls. Calibration standards were not required for protein binding work, as peak area ratios were used for comparative determination.

For assaying pharmacokinetic study samples, each analytical run included:

- A Total Blank and Blank+IS, at the beginning and end of the run (Negative Controls).
- Calibration standards, prepared on the day of sample preparation, at the beginning and end of the run. Calibration standards were injected from low to high concentrations.
- QCs at 3 levels at the beginning and end of the run sandwiching the study samples, and also interspersed throughout the analytical run where there were excessive study sample numbers. The total number of QC's (when run) in a worklist was at least 5% of the total number of samples in the analytical run (minimum of 6 required which allowed up to 120 samples in a run).
- At least 1 wash sample after the highest standard and high QC's, and between QC's and study samples.

Worklist sequences were created for all sample analytical runs in MS Excel, uploaded into Notepad for import into the MS software program Analyst™ (Version 1.6.1, Applied Biosystems/MDS Sciex, Canada).

1.2.1.1. Sample Dilution

If sample concentrations exceeded the HLQ by 20%, they were either diluted with blank matrix and extracted for re-analysis, or the original sample extract was diluted with extract taken from wash samples (Blank + IS) extracted from the same run as the original study samples, for results to be within the range of the calibration line. If sample concentrations were above the HLQ but <20% and linear regression used for the calibration standard line then results were deemed acceptable.

1.3. Bionalytical Data Review

Samples from protein binding and blood:plasma ratio experiments were analysed qualitatively by peak:area ratio of each compound with an internal reference standard. Pharmacokinetic experimental samples were analysed quantitatively in plasma (and heart tissue) across species using linear regression against a calibration curve.

1.3.1. Chromatograms and Integration

All chromatograms were reviewed to verify that the appropriate analyte peaks were correctly identified and integrated consistently across the run. A minimum level of smoothing (usually 1 or 2) and bunching factor (usually 1-3) was applied consistently across all chromatograms in the run. Other parameters (e.g. background noise, peak retention window) were optimised for all chromatograms to achieve accurate and consistent data integration.

If a particular chromatogram could not be integrated according to the settings achieved, it was integrated separately and the reasoning stated in the raw data/study file (indicated in as 'Record Modified').

If any analyte peak area in the Total Blank and Blank + IS sample(s) exceeded 20% of the LLQ, the LLQ standard was rejected and the next calibration standard level set as the LLQ.

If samples had been diluted for analysis the number of fold diluted was applied to raise the LLQ e.g. if the assay had an LLQ of 1 ng/mL and samples were diluted 5-fold, then the new LLQ would 5 ng/mL.

1.3.2. Acceptance Criteria Calibration Standards and QC's

A calibration standard or QC was rejected if its back-calculated concentration differed from its nominal concentration by more than ±20%. Up to ±30% was considered for tissue work.

Calibration standards were also rejected for valid analytical reasons (e.g. poor chromatography). The higher limit of quantification (HLQ) of the run was defined as the highest standard, which meets the acceptance criteria. The lower limit of quantification (LLQ) of the run is defined as the lowest concentration calibration standard, which meets the acceptance criterion. The optimal signal to noise ratio should be greater than 5:1. If the signal to noise ratio of the lowest standards on a particular run fell below 5:1 then these standards were rejected and the LLQ quoted as a the next highest set of standards with a signal to noise ratio exceeding 5:1.

At least two thirds of the calibration standards of any analyte were needed to be acceptable for the analytical run to be valid, including if both standards of a particular concentration were removed. If this caused a line to be truncated (eg LLQ or HLS standards), two thirds of the remaining standards were needed to be acceptable.

Quality Control samples (QC), prepared at least 3 different concentrations were analyzed with each batch of samples against separately prepared calibration standards. For the analysis to be acceptable, generally no more than one-third of the total QC results and no more than one-half of the results from each concentration level were to deviate from the nominal concentration by more than ±20% (unless specified). One QC level was allowed to be lost if the line was truncated, such that 3 out of 4 remaining QC's needed to be acceptable.

All details of the regression used to fit the calibration line, rejection of any standards along with a statement of applicable analytical runs meeting predefined run acceptance criteria were documented.

1.3.2.1. Specificity and Carry-Over blanks

The response in the Total Blank was required to be less than 20% of the LLQ. If greater than this, the response in Blank + IS sample was assessed and the impact on the data determined.

To assess carry-over, matrix blank+IS (or washes) were run immediately after the HLQ standard to show <0.1% of peak area carry-over. If carry-over was greater than this from

initial analysis then chromatography or needle wash cycles were checked to reduce column carryover. Otherwise an increased number of washes between smaller sample numbers were conducted and the impact on data was assessed as a final option.

1.3.2.2. Internal Standard

The internal standard area in calibration samples was required to be no more than 25% different from the area in adjacent study samples. Internal standard response across an analytical run was used to determine patterns, such as matrix ionisation effects or mis-injection response and required investigation before rejecting the batch. For the occasional sample/calibration standard out of range, but within the quantification limit, it was accepted.

1.3.2.3. Samples

Sample concentration results were only reported if they were within the assay range as defined between the LLQ and the HLQ.

Sample concentration results that fall within 20% above HLQ were accepted only with a linear regression function where the calibration line showed no indication of significant curvature (two highest standards within +/-10%). To avoid this, the best practice of dilution of samples/sample extract was conducted to maintain unknown samples within the calibration range.

1.3.3. Data Acquisition and Processing

UHPLC-MS/MS data were acquired and processed (integrated) using the proprietary software application Analyst™ (Version 1.6.1, Applied Biosystems/MDS Sciex, Canada).

The regression function and weighting that best fit the data, as measured by the difference between nominal and back-calculated concentration, was used. Where possible, weighted linear (1/x*x) regression was used as the preferred method of integration. However, if significant evidence of curvature existed quadratic regression was considered as a viable option, but with no extrapolation beyond the HLQ as this would be inaccurate.

Calibration plots of analyte/internal standard peak area ratio versus drug concentration were constructed and a linear - weighted 1/(x*x) regression applied to the data. Concentrations of drug in QC validation samples were determined from the appropriate calibration line, and used to calculate the bias and precision of the method. The numerical bioanalytical

concentration data presented in this report are computer generated; because of rounding, recalculation of derived values from individual data presented in this report will, in some instances, yield minor variation. Nominal plasma sampling data time points have been used.

1.4. Cisapride Bioanalysis Method

Cisapride monohydrate (Batch no. C4740, Lot. No. 080m4751) with an assigned purity of 99%, weighing factor 1.05 g contains 1.00 g of cisapride free base.

1.4.1. Cisapride IS

An internal stable-label isotopic standard of a chemically unrelated compound, denoted [$^{2}H_{3}{}^{13}C$]-SB243213, was accurately weighed at an appropriate amount and dissolved in the required volume of dimethyl formamide (DMF) to give a 1 mg/mL stock solution (C). This was diluted in acetonitrile to a final working solution concentration of 50 ng/mL (C1).

Working Solution	Final Concentration (ng/mL)	Volume of Spiking Solution	Total Volume in Acetonitrile (mL)
C1	50	12.5 μL of solution C	250

Store solutions at room temperature. Use solutions as long as they are shown to be fit for purpose during the analysis of a matrix blank sample.

1.4.2. Cisapride Working Stock Solutions

Stocks (A/B) were subsequently diluted with 50:50 acetonitrile:water to provide the working stock solutions at 10, 1, 0.1 and 0.01 μg/mL (A1-4; B1-4) for the preparation of species matrix calibration standards (0.5, 1, 2, 5, 20, 50, 400, 500 ng/mL) and quality control standards (0.5, 1.5, 20, 400 and 500 ng/mL) from diluted stocks A and B, respectively. All stocks are prepared fresh for analysis and thoroughly mixed.

Working Solution	Final Concentration (μg/mL)	Volume of Spiking Solution	Volume of 50/50 Acetonitrile/Water (v/v) (μL)
A1/B1	10	10 μL of solution A/B	990
A2/B2	1	100 μL of solution A1/B1	900
A3/B3	0.1	100 μL of solution A2/B2	900
A4/B4	0.01	100 μL of solution A3/B3	900

Stock solutions may be stored for at least 28 days at 4°C. Working solutions are made fresh on the day of analysis.

1.4.3. Cisapride Calibration Standard Solutions

Calibration standards were prepared fresh as follows and thoroughly mixed.

Standard Concentration (ng/mL)	Volume of Working Solution (μL)				Volume of Control Blank Matrix (μL)
	A4 0.01 μg/mL	A3 0.1 μg/mL	A2 1 μg/mL	A1 10μg/mL	
0.5	25	-	-	-	475
1	-	5	-	-	495
2	-	10	-	-	490
5	-	25	-	-	475
20	-	-	10	-	490
50	-	-	25	-	475
400	-	-	-	20	480
500	-	-	-	25	475

The total volumes prepared may be scaled up or down as required

1.4.4. Cisapride Quality Control Standard Solutions

Quality controls (QC) were prepared as follows and thoroughly mixed. Replicate aliquots, where necessary, were transferred to appropriate assay tubes for storage at -20°C.

QC Concentration (ng/mL)	Volume of Spiking Solution (μL)				Volume of Control Blank Matrix (μL)
	B4 0.01 μg/mL	B3 0.1 μg/mL	B2 1 μg/mL	B1 10 μg/mL	
0.5 [1]	50	-	-	-	950
1.5	-	15	-	-	985
20	-	-	20	-	980
400	-	-	-	40	960
500 [1]	-	-	-	50	950

1. Prepared for validation only

The total volumes prepared may be scaled up or down as required

1.4.5. Cisapride Sample Preparation

An aliquot (50 μL) of blank matrix, sample (i.e. plasma), standard or QC were transferred to individual polypropylene tubes in a 96-well block (Micronix) to which I.S. (150 μL) working solution (C1; 50 ng/mL) was added for protein precipitation. Double blank samples were generated in the same way using acetonitrile only. Tubes were capped with pierceable lids and vortex mix thoroughly and placed on a bed-shaker for 5 minutes before centrifugation for at least 10 minutes at approximately 3000 g. The subsequent plasma extract was then injected onto UPLC-MS/MS system for analysis.

Step	Process
1	Aliquot 50 μL of sample, standard or QC into tube
2	Add 150 μL acetonitrile to double blank
3	Add 150 μL internal standard working solution (C1; 50 ng/mL) to all other tubes
4	Cap tubes and vortex mix thoroughly, place on a bed-shaker for 5 minutes
5	Centrifuge the tubes for at least 10 minutes at approximately 3000 g
6	Inject onto HPLC-MS/MS system for analysis (typically 3 μL)

1.4.6. Cisapride Method

1.4.6.1. Cisapride UPLC Conditions

Autosampler	Waters Acquity
Weak Wash Solvent	0.1% Formic Acid (aq)
Strong Wash Solvent	40/30/30/0.01 ACN/Water/IPA/Formic Acid (v/v/v/v)
Injection Mode	Partial Loop With Needle Overfill
Typical Injection Volume	3 μL
Chromatography System	Waters Acquity UPLC
Flow Rate	1 mL/min
Analytical Column	50 x 2.0 mm i.d. Gemini NX 3 μm, Phenomenex
Column Temperature	50°C
Column Divert	Column effluent diverted to the MS between 0.7 and 1.4 min
Run Time	1.5 minutes
Mobile Phase A	10 mM ammonium formate containing 0.1% (v/v) formic acid
Mobile Phase B	Acetonitrile

1.4.6.2. Cisapride UPLC Gradient

Time (mins)	%A	%B
0	85	15
0.7	85	15
1.0	20	80
1.2	20	80
1.21	85	15
1.5	85	15

1.4.6.3. Cisapride MS/MS Conditions

Mass Spectrometer	Applied Biosystems/MDS Sciex API-4000
Ionisation Interface and Temperature	TurboIonSpray™ at 600°C (3500V)
Pause Time	5 msec
Gas 1 Setting(Nitrogen)	50 psi
Gas 2 Setting (Nitrogen)	50 psi
Curtain Gas Setting (Nitrogen)	25
Collision Gas Setting (Nitrogen)	8
DP Value	80 (IS = 80)
CE Value	45 (IS = 39)
EP Value	10 (IS = 10)
CXP Value	18 (IS = 16)

1.4.6.4. Cisapride MRM Transitions

Analyte	Precursor Ion (m/z)	Product Ion (m/z)	Dwell Time (msec)	Polarity	Typical R.T. (min)
Cisapride	466	184	150	Positive	1.0
[$^{2}H_{3}{}^{13}C$]-SB243213 (I.S.)	433	228	150	Positive	1.2

Masses for Precursor/Product ions are nominal

1.4.6.5. Representative Cisapride MS/MS Chromatogram

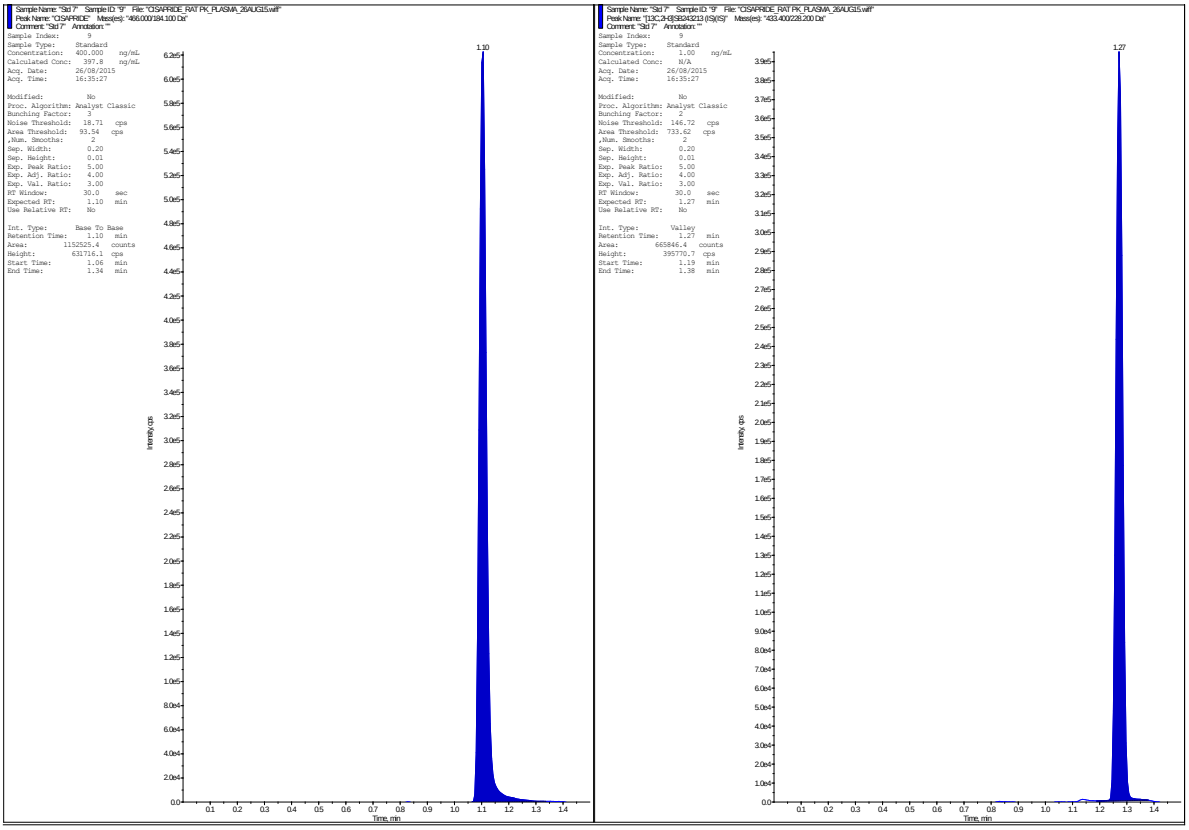

1.4.6.6. Representative Cisapride Calibration Standard Curve

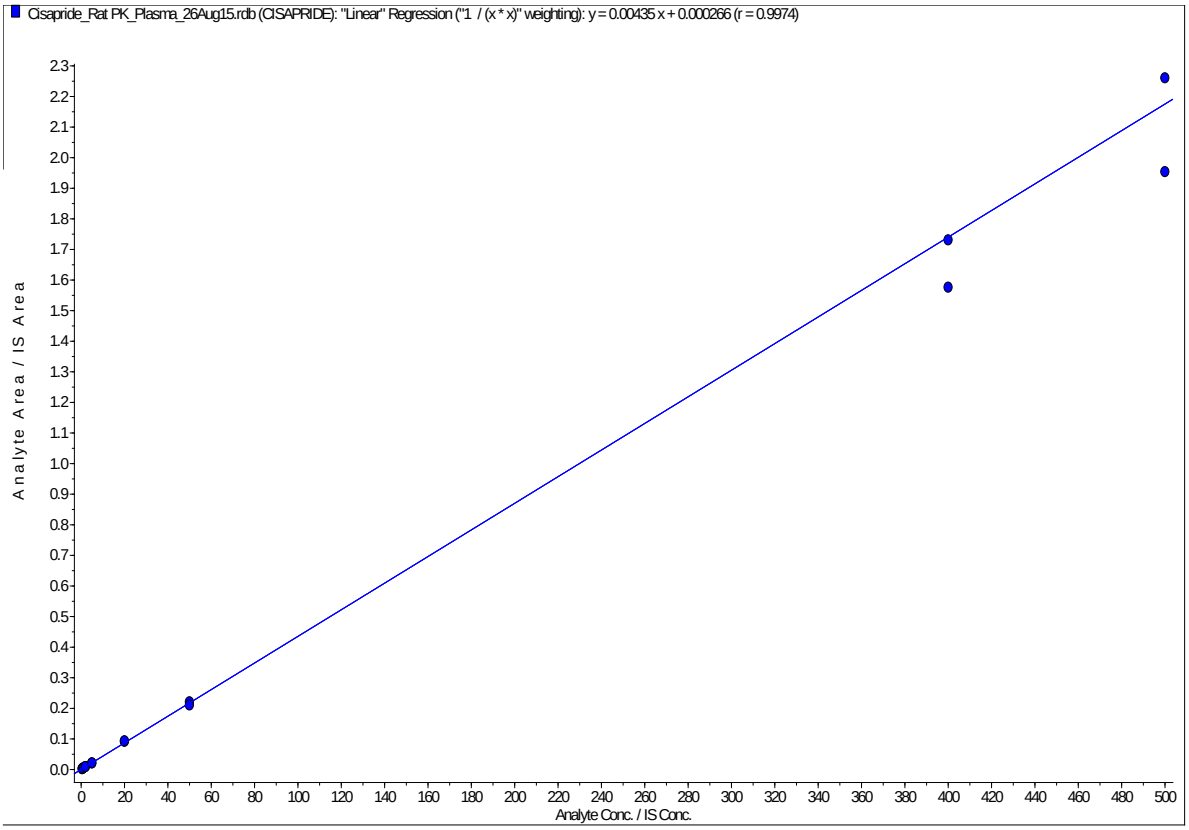

1.5. Moxifloxacin Bioanalysis Method

Moxifloxacin hydrochloride (also referred to as GW646803A) (Batch no.VBOG/5504/8/4) with an assigned chemical purity 98%, weighing factor 1.11 g contains 1.00 g of moxifloxacin free base) was obtained from within , UK.

1.5.1. Moxifloxacin IS

An internal stable-label isotopic standard of Moxifloxacin, denoted [$^{2}H_{9}$ ^{15}N]-GW646803 was accurately weighed at an appropriate amount and dissolved in the required volume of DMF to give a 1 mg/mL stock solution (C). This was diluted in acetonitrile to a final working solution concentration of 2500 ng/mL (C1).

Working Solution	Final Concentration (ng/mL)	Volume of Spiking Solution	Total Volume in Acetonitrile (mL)
C1	2500	500 μL of solution C	200

Stock solutions may be stored for at least 28 days at 4°C. Working solutions are made fresh on the day of analysis.

1.5.2. Moxifloxacin Working Stock Solutions

Stocks (A/B) were subsequently diluted with 50:50 acetonitrile:water to provide the working stock solutions at 100 μg/mL (A1; B1) for the preparation of species matrix calibration standards (5, 25, 50, 100, 250, 500, 1000, 4000 and 5000 ng/mL) and quality control standards (25, 100, 800, 4000 and 5000 ng/mL) from diluted stocks A and B, respectively. All stocks are prepared fresh for analysis and thoroughly mixed.

Working solutions for standards

Working Solution	Final Concentration (μg/mL)	Volume of Spiking Solution	Volume of 50:50 Milli-Q Water: acetonitrile (μL)
A1	100	50 μL of solution A	450

Stock solutions may be stored for at least 28 days at 4°C. Working solutions are made fresh on the day of analysis.

1.5.3. Moxifloxacin Calibration Standard Solutions

Calibration samples are prepared as follows:

Calibration Stds	Final Concentration (ng/mL)	Volume of Spiking Solution	Volume of Control Blank Matrix (μL)
STD 9	5000	20 μL of solution A1	380
STD 8	4000	20 μL of solution A1	480
STD 7	1000	100 μL of Std8	300
STD 6	500	200 μL of Std7	200
STD 5	250	200 μL of Std6	200
STD 4	100	200 μL of Std5	300
STD 3	50	200 μL of Std4	200
STD 2	25	200 μL of Std3	200
STD 1	5	100 μL of Std2	400

1.5.4. Moxifloxacin Quality Control Solutions

Quality controls (QC) were prepared as follows and thoroughly mixed. Replicate 50 μL aliquots, where appropriate, were transferred to appropriate assay tubes for storage at -20°C.

QC samples	Final Concentration (ng/mL)	Volume of Spiking Solution	Volume of Control Blank Matrix (μL)
QC5	5000	5 μL of solution B	995
QC4	4000	5 μL of solution B	1245
QC3	800	200 μL of solution QC4	800
QC2	100	100 μL of solution QC3	700
QC1[1]	25	200 μL of solution QC2	600

1. Prepared for validation only

The total volumes prepared may be scaled up or down as required

1.5.5. Moxifloxacin Sample Preparation

An aliquot (50 μL) of blank matrix, sample (i.e. plasma sample), standard or QC were transferred to individual polypropylene tubes in a 96-well block (Micronix) to which I.S. (200 μL) working solution (C1: 2500 ng/mL) was added for protein precipitation. Double blank samples were generated in the same way using acetonitrile only. Tubes were capped with pierceable lids and vortex mix thoroughly and placed on a bed-shaker for 5 minutes before centrifugation for at least 10 minutes at approximately 3000 g. The subsequent plasma extract was then transferred into clean vials to be dried down under nitrogen and reconstituted in 20/80 acetonitrile:0.5% formic in water. Tubes were capped with pierceable lids and vortex mixed thoroughly and ready to be injected onto UPLC-MS/MS system for analysis.

Step	Process
1	Aliquot 50 μL of sample, standard or QC into vial
2	Add 200 μL acetonitrile to double blank
3	Add 200 μL internal standard working solution (C1: 2500 ng/mL) to all other vials
4	Cap vials and vortex mix thoroughly, place on a bed-shaker for 5 minutes
5	Centrifuge the vials for approximately 10 minutes at approximately 3000 g
6	Transfer the supernatant to clean vials and blow dry under the nitrogen at 40°C.
7	Reconstitute the dried samples with 100 μL 20/80 acetonitrile/0.5% formic acid aqueous
8	Cap vials and vortex mix briefly
9	Inject onto HPLC-MS/MS system for analysis (typically 3 μL)

1.5.6. Moxifloxacin Method

1.5.6.1. Moxifloxacin UPLC Conditions

Autosampler	Waters Acquity
Weak Wash Solvent	0.1% Formic Acid (aq)
Strong Wash Solvent	40/30/30/0.01 ACN/Water/IPA/Formic Acid (v/v/v/v)
Injection Mode	Partial Loop With Needle Overfill
Typical Injection Volume	3 μL
Chromatography System	Waters Acquity UPLC
Flow Rate	0.4 mL/min
Analytical Column	50 x 2.1 mm i.d. BEH C18, 1.7 μm, Acquity
Column Temperature	50°C
Column Divert	Column effluent diverted to the MS between 0.4 and 1.2 min
Run Time	1.8 minutes
Mobile Phase A	Water containing 0.5% (v/v) formic acid
Mobile Phase B	Acetonitrile

1.5.6.2. Moxifloxacin UPLC Gradient

Time (mins)	%A	%B
0	80	20
0.4	80	20
0.8	5	95
1.3	5	95
1.31	80	20
1.8	80	20

1.5.6.3. Moxifloxacin MS/MS Conditions

Mass Spectrometer	Applied Biosystems/MDS Sciex API-4000
Ionisation Interface and Temperature	TurboIonSpray™ at 450°C (4500V)
Pause Time	5 msec
Gas 1 Setting(Nitrogen)	50 psi
Gas 2 Setting (Nitrogen)	50 psi
Curtain Gas Setting (Nitrogen)	10
Collision Gas Setting (Nitrogen)	8
DP Value	80 (= IS)
CE Value	26 (= IS)
EP Value	8 (= IS)
CXP Value	19 (= IS)

1.5.6.4. Moxifloxacin MRM Transitions

Analyte	Precursor Ion (m/z)	Product Ion (m/z)	Dwell Time (msec)	Polarity	Typical R.T (mins)
Moxifloxacin	402	358	150	Positive	0.67
[$^{2}H_{9}{}^{15}N$]-GW646803 (I.S.)	412	368	150	Positive	0.66

1.5.6.5. Representative Moxifloxacin MS/MS Chromatogram

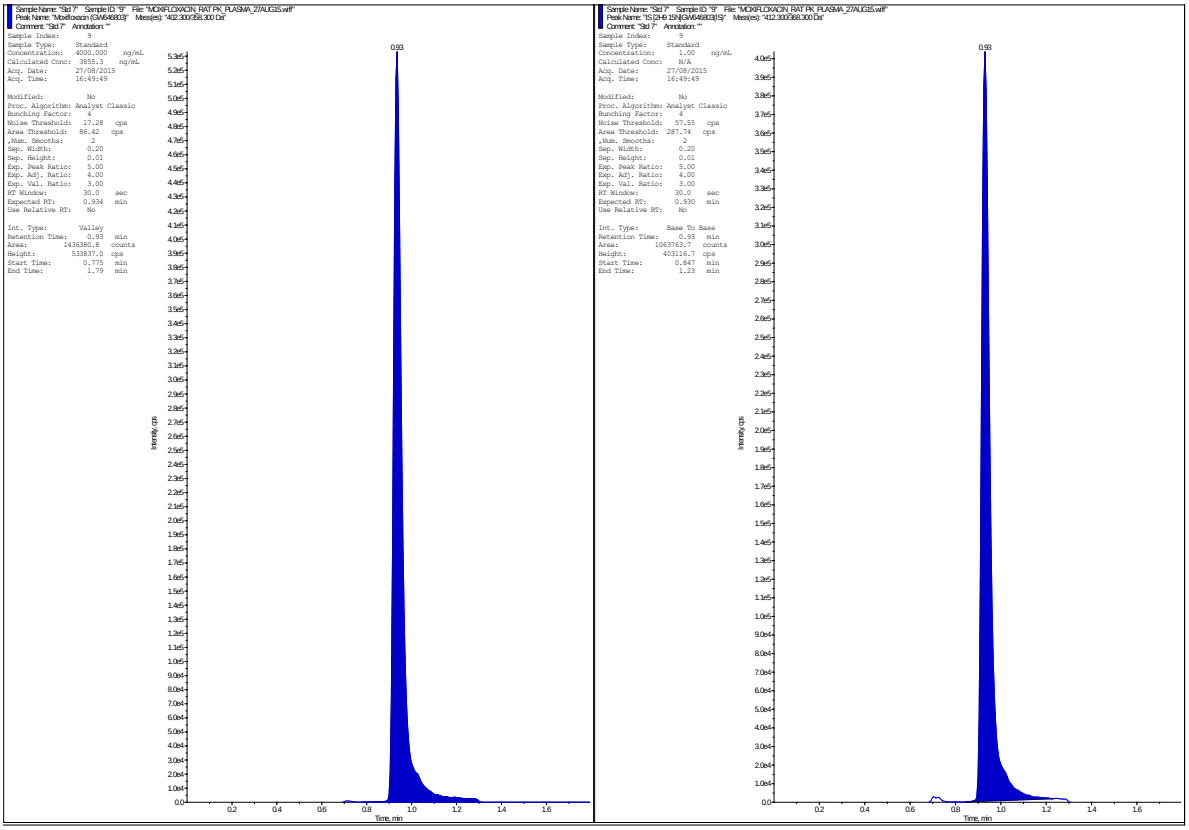

1.5.6.6. Representative Moxifloxacin Calibration Standard Curve

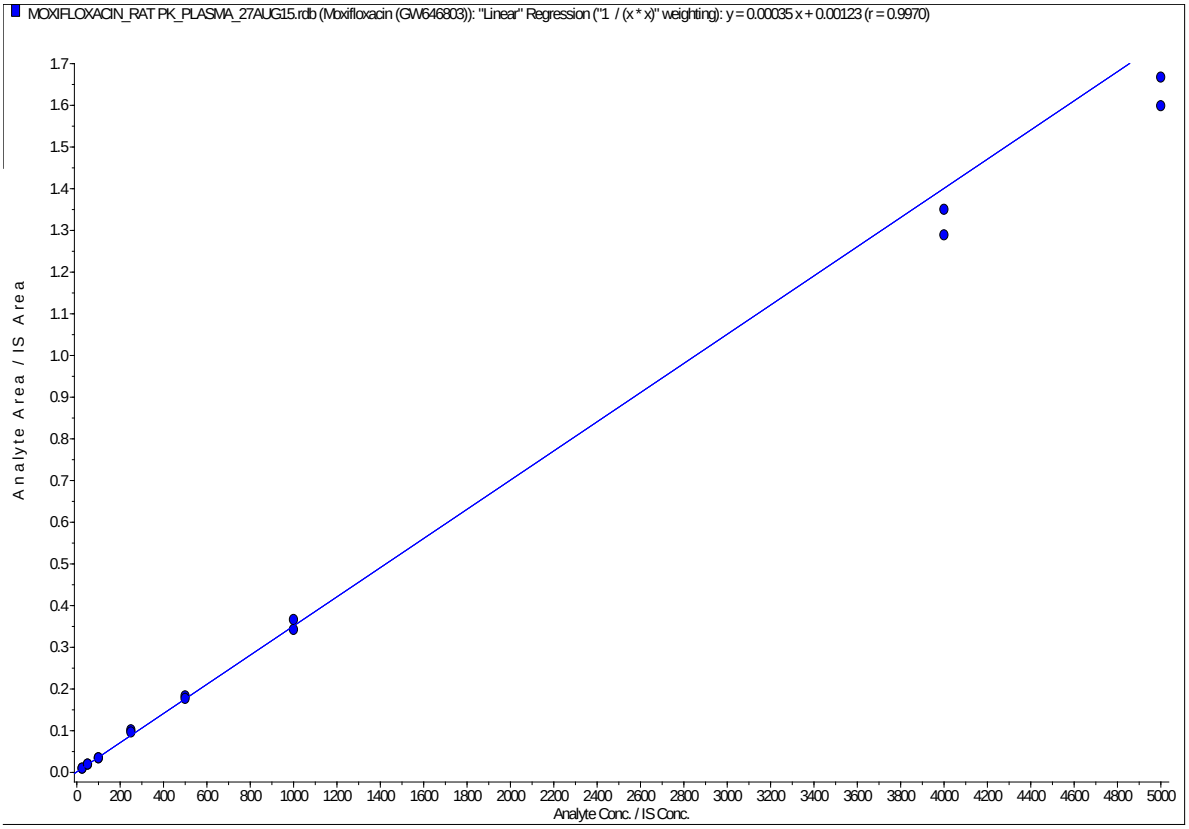

1.6. Sparfloxacin Bioanalysis Method

Sparfloxacin (Batch no. BCBF4939) with an assigned chemical purity 98%, weighing factor 1.02 g contains 1.00 g of sparfloxacin free base.

1.6.1. Sparfloxacin IS

Used as an internal standard of sparfloxacin, sotalol was accurately weighed at an appropriate amount and dissolved in the required volume of dimethyl formamide to give a 1 mg/mL stock solution (C). This was diluted in acetonitrile to a final working solution concentration of 50 ng/mL (C1).

Working Solution	Final Concentration (ng/mL)	Volume of Spiking Solution	Total Volume in Acetonitrile (mL)
C1	50	12.5 μL of solution C	250

Stock solutions may be stored for at least 28 days at 4°C. Working solutions are made fresh on the day of analysis.

1.6.2. Sparfloxacin Working Stock Solutions

Stocks (A/B) were subsequently diluted with 50:50 acetonitrile:water to provide the working stock solutions at 100, 10, 1 and 0.1 μg/mL (A1-4; B1-4) for the preparation of species matrix calibration standards (1, 2, 5, 20, 50, 100, 500 and 1000 ng/mL) and quality control standards (1, 4, 80, 800 and 100 ng/mL) from diluted stocks A and B, respectively. All stocks are prepared fresh for analysis and thoroughly mixed.

Working Solution	Final Concentration (μg/mL)	Volume of Spiking Solution	Volume of 50/50 Acetonitrile/Water (v/v) (μL)
A1/B1	100	100 μL of solution A/B	900
A2/B2	10	100 μL of solution A1/B1	900
A3/B3	1	100 μL of solution A2/B2	900
A4/B4	0.1	100 μL of solution A3/B3	900

Stock solutions may be stored for at least 28 days at 4°C. Working solutions are made fresh on the day of analysis.

1.6.3. Sparfloxacin Calibration Standard Solutions

Calibration standards are prepared fresh as follows and thoroughly mixed.

Standard Concentration (ng/mL)	Volume of Working Solution (μL)				Volume of Control Blank Matrix (μL)
	A4 0.1 μg/mL	A3 1 μg/mL	A2 10 μg/mL	A1 100μg/mL	
1	5	-	-	-	495
2	10	-	-	-	490
5	25	-	-	-	475
20	-	10	-	-	490
50	-	25	-	-	475
100	-	-	5	-	495
500	-	-	25	-	475
1000	-	-	-	5	495

The total volumes prepared may be scaled up or down as required

1.6.4. Sparfloxacin Quality Control Solutions

Quality controls (QC) are prepared as follows and thoroughly mixed. Replicate aliquots should be transferred to appropriate assay tubes for storage at -20°C.

QC Concentration (ng/mL)	Volume of Spiking Solution (μL)				Volume of Control Blank Matrix (μL)
	B4 0.1 μg/mL	B3 1 μg/mL	B2 10 μg/mL	B1 100 μg/mL	
1 [1]	10	-	-	-	990
4	-	4	-	-	996
80	-	-	8	-	992
800	-	-	-	8	992
1000 [1]	-	-	-	10	990

1. Prepared for validation only

The total volumes prepared may be scaled up or down as required

1.6.5. Sparfloxacin Sample Preparation

An aliquot (50 μL) of blank matrix, sample (i.e. plasma), standard or QC were transferred to individual polypropylene tubes in a 96-well block (Micronix) to which I.S. (150 μL) working solution (C1; 50 ng/mL) was added for protein precipitation. Double blank samples were generated in the same way using acetonitrile only. Tubes were capped with pierceable lids and vortex mix thoroughly and placed on a bed-shaker for 5 minutes before centrifugation for at least 10 minutes at approximately 3000 g. The subsequent plasma extract was then injected onto UPLC-MS/MS system for analysis.

Step	Process
1	Aliquot 50 μL of sample, standard or QC into tube
2	Add 150 μL acetonitrile to double blank
3	Add 150 μL internal standard working solution (C1; 50 ng/mL) to all other tubes
4	Cap tubes and vortex mix thoroughly, place on a bed-shaker for 5 minutes
5	Centrifuge the tubes for at least 10 minutes at approximately 3000 g
6	Inject onto HPLC-MS/MS system for analysis (typically 3 μL)

1.6.6. Sparfloxacin Method

1.6.6.1. Sparfloxacin UPLC Conditions

Mass Spectrometer	Applied Biosystems/MDS Sciex API-4000
Ionisation Interface and Temperature	TurboIonSpray™ (IS: 5000V) at 650°C
Autosampler	Waters Acquity
Weak Wash Solvent	Acetontrile:Water (20:80) (aq)
Strong Wash Solvent	40/30/30/0.01 ACN/Water/IPA/Formic Acid (v/v/v/v)
Injection Mode	Partial Loop With Needle Overfill
Typical Injection Volume	3 μL
Chromatography System	Waters Acquity UPLC
Flow Rate	0.5 mL/min
Analytical Column	50 x 2.0 mm i.d. dC18 Atlantis 3 μm,
Column Temperature	50°C
Column Divert	Column effluent diverted to the MS between 0.1 and 0.9 min
Run Time	1.5 minutes
Mobile Phase A	20 mM Ammonium Acetate, pH 3.5 with acetic acid
Mobile Phase B	Acetonitrile containing 0.1% formic acid

1.6.6.2. Sparfloxacin UPLC Gradient

Time (mins)	%A	%B
0	50	50
1.5	50	50

1.6.6.3. Sparfloxacin MS/MS Conditions

Mass Spectrometer	Applied Biosystems/MDS Sciex API-4000
Ionisation Interface and Temperature	TurboIonSpray™ at 650°C (5000V)
Pause Time	5 msec
Gas 1 Setting(Nitrogen)	50 psi
Gas 2 Setting (Nitrogen)	60 psi
Curtain Gas Setting (Nitrogen)	25
Collision Gas Setting (Nitrogen)	10
DP Value	70 (IS = 45)
CE Value	28 (IS = 16)
EP Value	10 (IS = 10)
CXP Value	20 (IS = 15)

1.6.6.4. Sparfloxacin MRM Transitions

Analyte	Precursor Ion (m/z)	Product Ion (m/z)	Dwell Time (msec)	Polarity	Typical R.T (mins)
Sparfloxacin	393	349	150	Positive	0.4
Sotalol (I.S.)	273	255	150	Positive	0.4

1.6.6.5. Representative Sparfloxacin MS/MS Chromatogram

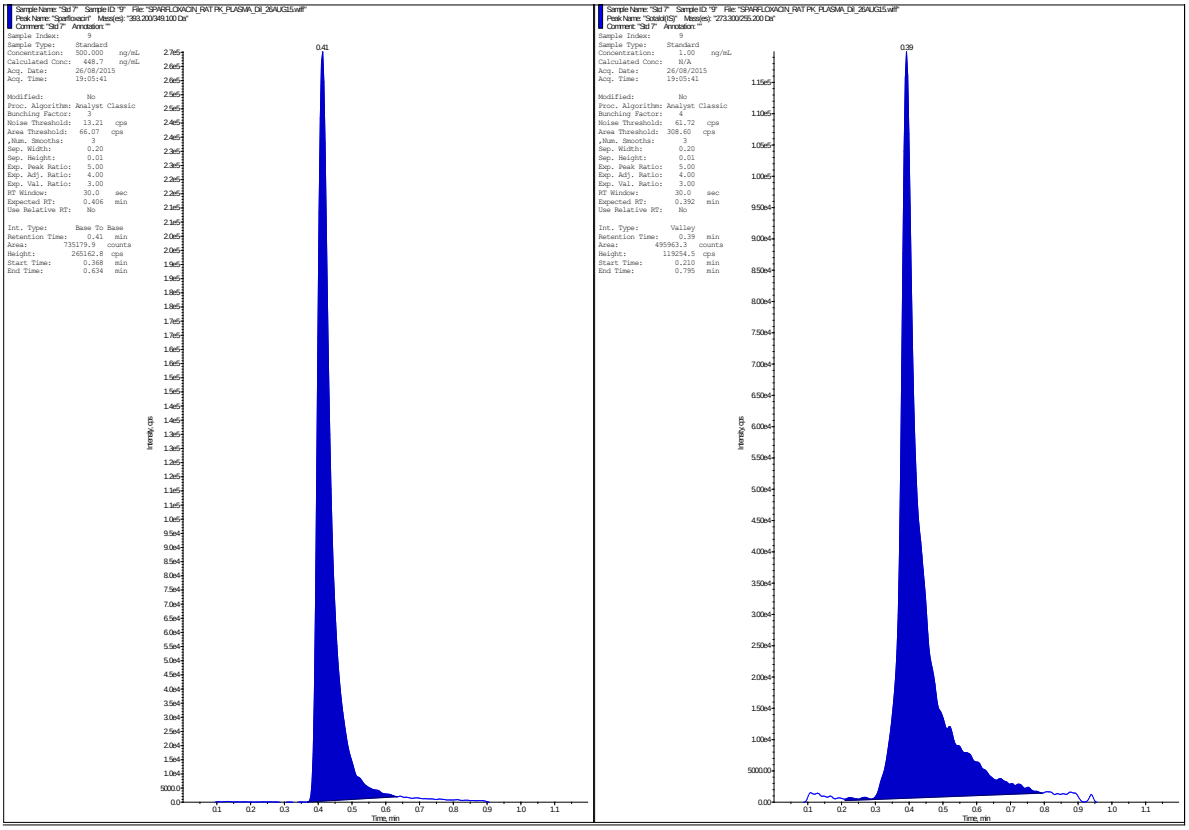

1.6.6.6. Representative Sparfloxacin Calibration Standard Curve

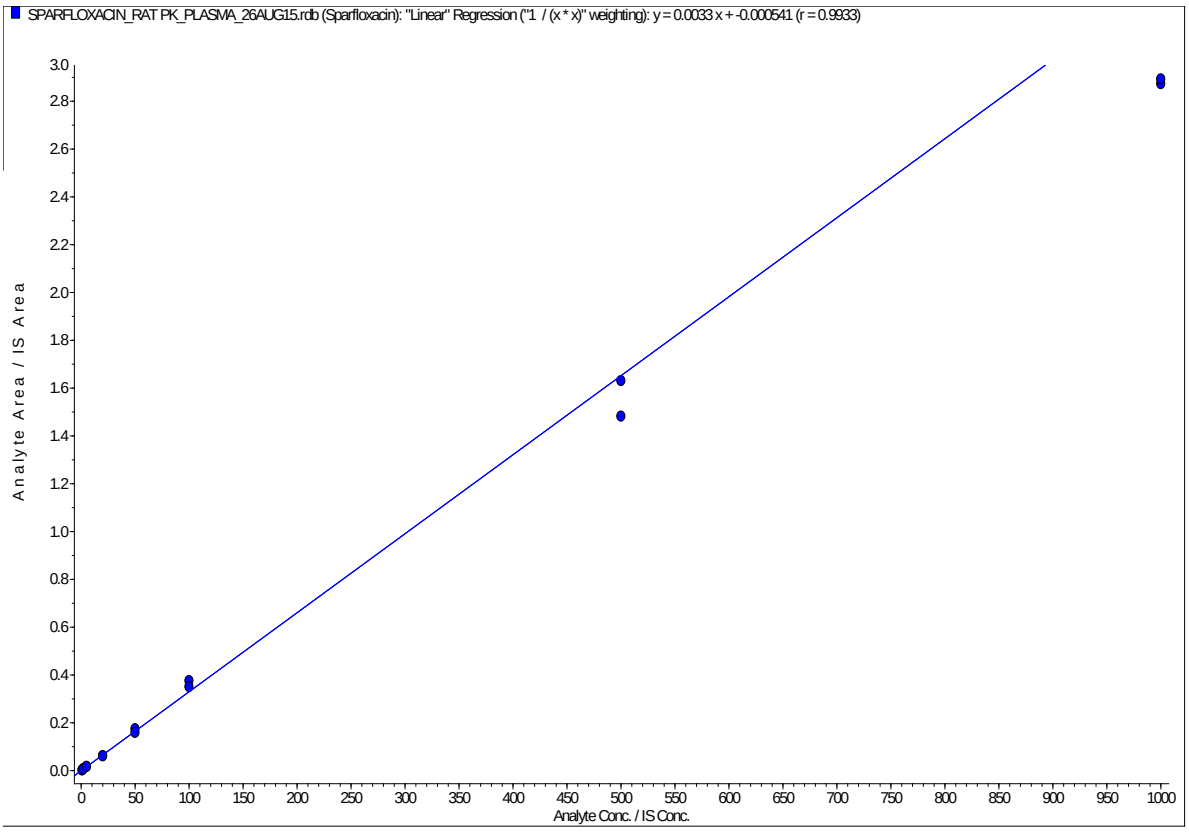

1.7. Verapamil Bioanalysis Method

Verapamil hydrochloride (Batch no. 047206, Lot no. L75939) with an assigned chemical purity 100%, weighing factor for salt 1.08 g contains 1.00 g of verapamil free base.

1.7.1. Verapamil IS

An internal stable-label isotopic standard of a chemically unrelated compound, denoted [$^{2}H_{3}{}^{13}C$]-SB243213, was accurately weighed at an appropriate amount and dissolved in the required volume of dimethyl formamide (DMF) to give a 1 mg/mL stock solution (C). This was diluted in acetonitrile to a final working solution concentration of 50 ng/mL (C1).

Working Solution	Final Concentration (ng/mL)	Volume of Spiking Solution	Total Volume in Acetonitrile (mL)
C1	50	12.5 μL of solution C	250

Stock solutions may be stored for at least 28 days at 4°C. Working solutions are made fresh on the day of analysis.

1.7.2. Verapamil Working Stock Solutions

Stocks (A/B) were subsequently diluted with 50:50 acetonitrile:water to provide the working stock solutions at 50, 5, 0.5 and 0.05 μg/mL (A1-4; B1-4) for the preparation of species matrix calibration standards (1, 2, 4, 10, 50, 100, 500, 1000 and 2000 ng/mL) and quality control standards (1, 4, 100, 1600 and 2000 ng/mL) from diluted stocks A and B, respectively. All stocks are prepared fresh for analysis and thoroughly mixed.

Working Solution	Final Concentration (μg/mL)	Volume of Spiking Solution	Volume of 50/50 Acetonitrile/Water (v/v) (μL)
A1/B1	50	50 μL of solution A/B	950
A2/B2	5	100 μL of solution A1/B1	900
A3/B3	0.5	100 μL of solution A2/B2	900
A4/B4	0.05	100 μL of solution A3/B3	900

Stock solutions may be stored for at least 28 days at 4°C. Working solutions are made fresh on the day of analysis.

1.7.3. Verapamil Calibration Standard Solutions

Calibration standards are prepared fresh as follows and thoroughly mixed.

Standard Concentration (ng/mL)	Volume of Working Solution (μL)				Volume of Control Blank Matrix (μL)
	A4 0.05 μg/mL	A3 0.5 μg/mL	A2 5 μg/mL	A1 50μg/mL	
1	10	-	-	-	490
2	20	-	-	-	480
4	40	-	-	-	460
10	-	10	-	-	490
50	-	50	-	-	450
100	-	-	10	-	490
500	-	-	50	-	450
1000	-	-	-	10	490
2000	-	-	-	20	480

The total volumes prepared may be scaled up or down as required

1.7.4. Verapamil Quality Control Standard Solutions

Quality controls (QC) are prepared as follows and thoroughly mixed. Replicate aliquots should be transferred to appropriate assay tubes for storage at -20°C.

QC Concentration (ng/mL)	Volume of Spiking Solution (μL)				Volume of Control Blank Matrix (μL)
	B4 0.05 μg/mL	B3 0.5 μg/mL	B2 5 μg/mL	B1 50 μg/mL	
1 [1]	10	-	-	-	490
4	40	-	-	-	460
100	-	-	10	-	490
1600	-	-	-	16	484
2000 [1]	-	-	-	20	480

1. Prepared for validation only

The total volumes prepared may be scaled up or down as required

1.7.5. Verapamil Sample Preparation

An aliquot (50 μL) of blank matrix, sample (i.e. plasma), standard or QC were transferred to individual polypropylene tubes in a 96-well block (Micronix) to which I.S. (150 μL) working solution (C1; 50 ng/mL) was added for protein precipitation. Double blank samples were generated in the same way using acetonitrile only. Tubes were capped with pierceable lids and vortex mix thoroughly and placed on a bed-shaker for 5 minutes before centrifugation for at least 10 minutes at approximately 3000 g. The subsequent plasma extract was then injected onto UPLC-MS/MS system for analysis.

Step	Process
1	Aliquot 50 μL of sample, standard or QC into tube
2	Add 150 μL acetonitrile to double blank
3	Add 150 μL internal standard working solution (C1; 50 ng/mL) to all other tubes
4	Cap tubes and vortex mix thoroughly, place on a bed-shaker for 5 minutes
5	Centrifuge the tubes for at least 10 minutes at approximately 3000 g
6	Inject onto HPLC-MS/MS system for analysis (typically 10 μL)

1.7.6. Verapamil Method

1.7.6.1. Verapamil UPLC Conditions

Autosampler	Waters Acquity
Weak Wash Solvent	50/50 (v/v) Acetonitrile/Water
Strong Wash Solvent	40/30/30/0.01 Acetontrile/Water/IPA/Formic Acid (v/v/v/v)
Injection Mode	Partial Loop With Needle Overfill
Typical Injection Volume	1 μL
Chromatography System	Waters Acquity UPLC
Flow Rate	1 mL/min
Analytical Column	50 x 4.6 mm i.d. Hypersil Gold C18, 5 μm, Thermo
Column Temperature	60°C
Column Divert	Column effluent diverted to the MS between 0.4 and 1.4 min
Run Time	2.0 minutes
Mobile Phase A	10 mM ammonium acetate containing 0.1% (v/v) ammonia
Mobile Phase B	Methanol

1.7.6.2. Verapamil UPLC Gradient

Time (mins)	%A	%B
0	60	40
0.4	5	95
1.4	5	95
1.5	60	40
2.0	60	40

1.7.6.3. Verapamil MS/MS Conditions

Mass Spectrometer	Applied Biosystems/MDS Sciex API-4000
Ionisation Interface and Temperature	TurboIonSpray™ at 450°C (4000V)
Pause Time	5 msec
Gas 1 Setting(Nitrogen)	50 psi
Gas 2 Setting (Nitrogen)	50 psi
Curtain Gas Setting (Nitrogen)	40
Collision Gas Setting (Nitrogen)	4
DP Value	80 (IS = 67)
CE Value	38 (IS = 39)
EP Value	10 (IS = 10)
CXP Value	15 (IS = 16)

1.7.6.4. Verapamil MRM Transitions

Analyte	Precursor Ion (m/z)	Product Ion (m/z)	Dwell Time (msec)	Polarity	Typical R.T (mins)
Verapamil	455	165	150	Positive	1.4
[$^{2}H_{3}{}^{13}C$]-SB243213 (I.S.)	433	228	150	Positive	1.4

1.7.6.5. Representative Verapamil MS/MS Chromatogram

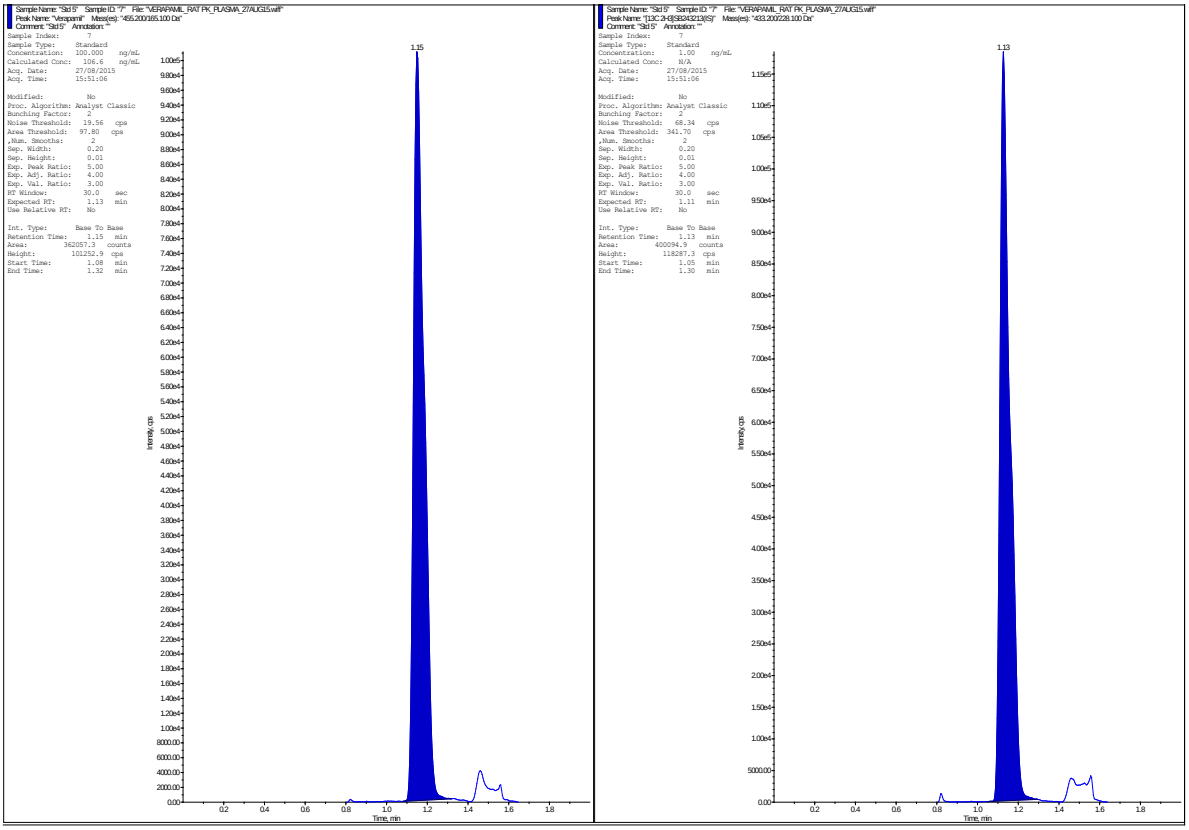

1.7.6.6. Representative Verapamil Calibration Standard Curve (Example)

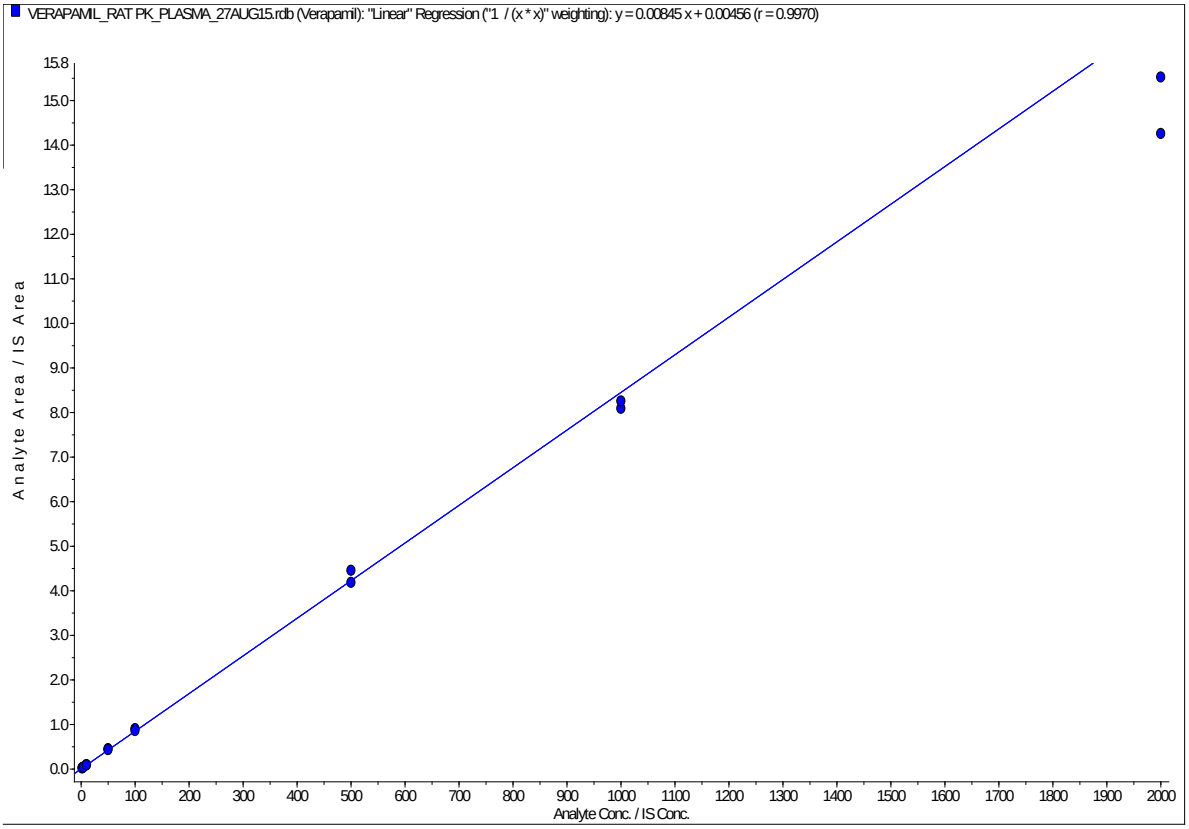

1.8. Sotalol Bioanalysis Method

Sotalol (Batch no. S0278-100MG, Lot 063M4028V) with an assigned chemical purity of 99%, weighing factor of 1.01 g contains 1.00 g of sotalol fees base

1.8.1. Sotalol IS

Used as an internal standard of sotalol, sparfloxacin was accurately weighed at an appropriate amount and dissolved in the required volume of dimethyl formamide to give a 1 mg/mL stock solution (C). This was diluted in acetonitrile to a final working solution concentration of 100 ng/mL (C1).

Working Solution	Final Concentration (ng/mL)	Volume of Spiking Solution	Total Volume in Acetonitrile (mL)
C1	100	25 μL of solution C	250

Stock solutions may be stored for at least 28 days at 4°C. Working solutions are made fresh on the day of analysis.

1.8.2. Sotalol Working Stock Solutions

Stocks (A/B) were subsequently diluted with 50:50 acetonitrile:water to provide the working stock solutions at 100, 10, 1 and 0.1 μg/mL (A1-4; B1-4) for the preparation of species matrix calibration standards (1, 2, 5, 20, 50, 100, 500 and 1000 ng/mL) and quality control standards (1, 4, 80, 800 and 100 ng/mL) from diluted stocks A and B, respectively. All stocks are prepared fresh for analysis and thoroughly mixed.

Working Solution	Final Concentration (μg/mL)	Volume of Spiking Solution	Volume of 50/50 Acetonitrile/Water (v/v) (μL)
A1/B1	100	100 μL of solution A/B	900
A2/B2	10	100 μL of solution A1/B1	900
A3/B3	1	100 μL of solution A2/B2	900
A4/B4	0.1	100 μL of solution A3/B3	900

Stock solutions may be stored for at least 28 days at 4°C. Working solutions are made fresh on the day of analysis.

1.8.3. Sotalol Calibration Standard Solutions

Calibration standards are prepared fresh as follows and thoroughly mixed.

Standard Concentration (ng/mL)	Volume of Working Solution (μL)				Volume of Control Blank Matrix (μL)
	A4 0.1 μg/mL	A3 1 μg/mL	A2 10 μg/mL	A1 100μg/mL	
1	5	-	-	-	495
2	10	-	-	-	490
5	25	-	-	-	475
20	-	10	-	-	490
50	-	25	-	-	475
100	-	-	5	-	495
500	-	-	25	-	475
1000	-	-	-	5	495

The total volumes prepared may be scaled up or down as required

1.8.4. Sotalol Quality Control Solutions

Quality controls (QC) are prepared as follows and thoroughly mixed. Replicate aliquots should be transferred to appropriate assay tubes for storage at -20°C.

QC Concentration (ng/mL)	Volume of Spiking Solution (μL)				Volume of Control Blank Matrix (μL)
	B4 0.1 μg/mL	B3 1 μg/mL	B2 10 μg/mL	B1 100 μg/mL	
1 [1]	10	-	-	-	990
4	-	4	-	-	996
80	-	-	8	-	992
800	-	-	-	8	992
1000 [1]	-	-	-	10	990

1. Prepared for validation only

The total volumes prepared may be scaled up or down as required

1.8.5. Sotalol Sample Preparation

An aliquot (50 μL) of blank matrix, sample (i.e. plasma), standard or QC were transferred to individual polypropylene tubes in a 96-well block (Micronix) to which I.S. (150 μL) working solution (C1; 100 ng/mL) was added for protein precipitation. Double blank samples were generated in the same way using acetonitrile only. Tubes were capped with pierceable lids and vortex mix thoroughly and placed on a bed-shaker for 5 minutes before centrifugation for at least 10 minutes at approximately 3000 g. The subsequent plasma extract was then injected onto UPLC-MS/MS system for analysis.

Step	Process
1	Aliquot 50 μL of sample, standard or QC into tube
2	Add 150 μL acetonitrile to double blank
3	Add 150 μL internal standard working solution (C1; 100 ng/mL) to all other tubes
4	Cap tubes and vortex mix thoroughly, place on a bed-shaker for 5 minutes
5	Centrifuge the tubes for at least 10 minutes at approximately 3000 g
6	Inject onto HPLC-MS/MS system for analysis (typically 3 μL)

1.8.6. Sotalol Method

1.8.6.1. Sotalol UPLC Conditions

Mass Spectrometer	Applied Biosystems/MDS Sciex API-4000
Ionisation Interface and Temperature	TurboIonSpray™ (IS: 5000V) at 650°C
Autosampler	Waters Acquity
Weak Wash Solvent	Acetontrile:Water (20:80) (aq)
Strong Wash Solvent	40/30/30/0.01 ACN/Water/IPA/Formic Acid (v/v/v/v)
Injection Mode	Partial Loop With Needle Overfill
Typical Injection Volume	3 μL
Chromatography System	Waters Acquity UPLC
Flow Rate	0.5 mL/min
Analytical Column	50 x 2.0 mm i.d. dC18 Atlantis 3 μm,
Column Temperature	50°C
Column Divert	Column effluent diverted to the MS between 0.1 and 0.9 min
Run Time	1.5 minutes
Mobile Phase A	20 mM Ammonium Acetate, pH 3.5 with acetic acid
Mobile Phase B	Acetonitrile containing 0.1% formic acid

1.8.6.2. Sotalol UPLC Gradient

Time (mins)	%A	%B
0	50	50
1.5	50	50

1.8.6.3. Sotalol MS/MS Conditions

Mass Spectrometer	Applied Biosystems/MDS Sciex API-4000
Ionisation Interface and Temperature	TurboIonSpray™ at 650°C (5000V)
Pause Time	5 msec
Gas 1 Setting(Nitrogen)	50 psi
Gas 2 Setting (Nitrogen)	60 psi
Curtain Gas Setting (Nitrogen)	25
Collision Gas Setting (Nitrogen)	10
DP Value	70 (IS = 45)
CE Value	28 (IS = 16)
EP Value	10 (IS = 10)
CXP Value	20 (IS = 15)

1.8.6.4. Sotalol MRM Transitions

Analyte	Precursor Ion (m/z)	Product Ion (m/z)	Dwell Time (msec)	Polarity	Typical R.T (mins)
Sotalol	273	255	150	Positive	0.4
Sparfloxacin (I.S.)	393	349	150	Positive	0.4

1.8.6.5. Representative Sotalol MS/MS Chromatogram

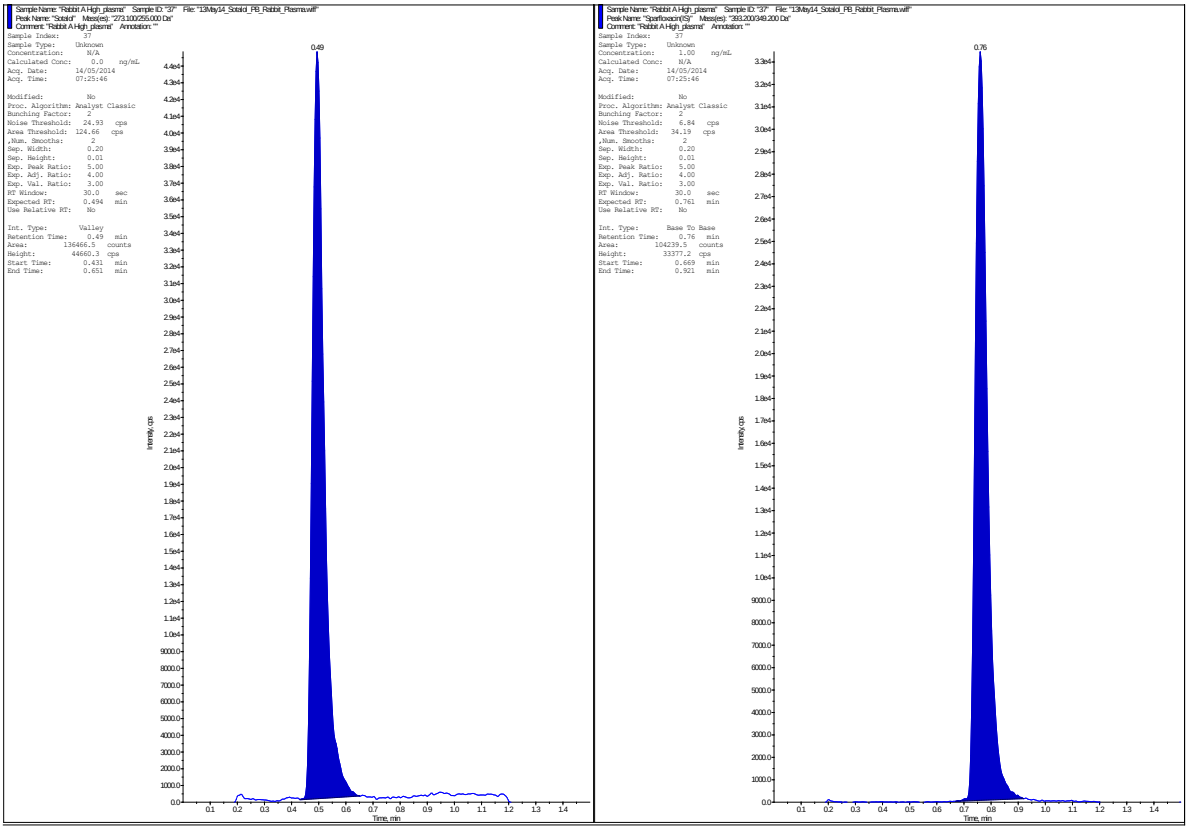

1.8.6.6. Representative Sotalol Calibration Standard Curve

Not applicable, as no calibration was conducted for quantitative determination.

1.9. Quinidine Bioanalysis Method

Quinidine hydrochloride monohydrate (Batch Q0750 Lot 047K1475) with an assigned chemical purity of 88%, weighing factor for salt 1.32 g contains 1.00 g of quinidine free base.

1.9.1. Quinidine IS

An internal stable-label isotopic standard of quinidine, denoted [$^{2}H_{3}$]-Quinidine, was accurately weighed at an appropriate amount and dissolved in the required volume of DMF to give a 1 mg/mL stock solution (C). This was diluted in acetonitrile to a final working solution concentration of 0.5 µg/mL (C1).

Working Solution	Final Concentration (µg/mL)	Volume of Spiking Solution	Total volume of Acetonitrile (mL)
C1	0.5	100 µL of solution C	200

Stock solutions may be stored for at least 28 days at 4°C. Working solutions are made fresh on the day of analysis.

1.9.2. Quinidine Working Stock Solutions

Stocks (A/B) were subsequently diluted with 50:50 acetonitrile:water to provide the working stock solutions at 10, 1, 0.1 and 0.01 µg/mL (A1-4; B1-4) for the preparation of species matrix calibration standards (0.5, 1, 2, 5, 20, 50, 400, 500 ng/mL) and quality control standards (0.5, 1.5, 20, 400 and 500 ng/mL) from diluted stocks A and B, respectively. All stocks are prepared fresh for analysis and thoroughly mixed.

Working Solution	Final Concentration (µg/mL)	Volume of Spiking Solution	Volume of Acetonitrile:water (50:50) (µL)
A1/B1	10000	100 µL of solution A/B	900
A2/B2	1000	100 µL of solution A1/B1	900
A3/B3	100	100 µL of solution A2/B2	900

Stock solutions may be stored for at least 28 days at 4°C. Working solutions are made fresh on the day of analysis.

1.9.3. Quinidine Calibration Standard Solutions

Calibration standards are prepared fresh as follows and thoroughly mixed.

Standard Concentration (μg/mL)	Volume of Working Solution (μL)				Volume of Control Blank Matrix (μL)
	A3 10 μg/mL	A2 100 μg/mL	A1 1000 μg/mL	A 10000 μg/mL	
0.5	50	-	-	-	950
1	-	10	-	-	990
2	-	20	-	-	980
5	-	50	-	-	950
10	-	-	10	-	990
20	-	-	20	-	980
40	-	-	40	-	960
50	-	-	50	-	950

The total volumes prepared may be scaled up or down as required

1.9.4. Quinidine Quality Control Solutions

Quality controls (QC) and validation samples (VS) are prepared as follows and thoroughly mixed.

QC/VS Concentration μg/mL)	Volume of Spiking Solution (μL)				Volume of Control Blank Matrix (μL)
	B4 10 μg/mL	B3 100 μg/mL	B2 1000 μg/mL	B1 10000 μg/mL	
0.5 [1]	50	-	-	-	950
2	-	20	-	-	980
10	-	-	10	-	990
40	-	-	40	-	960
50 [1]	-	-	50	-	950

1. Prepared for validation only

The total volumes prepared may be scaled up or down as required

1.9.5. Quinidine Sample Preparation

An aliquot (50 μL) of blank matrix, sample (i.e. plasma), standard or QC were transferred to individual polypropylene tubes in a 96-well block (Micronix) to which I.S. (300 μL) working solution (C1; 0.5 μg/mL) was added for protein precipitation. Double blank samples were generated in the same way using acetonitrile only. Tubes were capped with pierceable lids and vortex mix thoroughly and placed on a bed-shaker for 5 minutes before centrifugation for at least 10 minutes at approximately 3000 g. The subsequent plasma extract was then injected onto UPLC-MS/MS system for analysis.

Step	Process
1	Aliquot 50 μL of standard or QC into tube
2	Add 50 μL water into all tubes
3	Add 300 μL acetonitrile to double blank
4	Add 300 μL internal standard working solution (C1; 0.5 μg/mL) to all other tubes
5	Cap tubes and vortex mix briefly, place on a bed-shaker for 5 minutes
6	Centrifuge the tubes for approximately 10 minutes at approximately 3000 g
7	Inject onto HPLC-MS/MS system for analysis (typically 5 μL)

1.9.6. Quinidine Method

1.9.6.1. Quinidine UPLC Conditions

Autosampler	Waters Acquity
Weak Wash Solvent	70/30, v/v, acetonitrile/UPW,
Strong Wash Solvent	4:3:3:0.1, acetonitrile:propan-2-ol:UPW:formic acid
Injection Mode	Partial Loop With Needle Overfill
Typical Injection Volume	3 μL
Chromatography System	Waters Acquity UPLC
Flow Rate	1 mL/min
Analytical Column	50 x 4.6 mm i.d. Hypersil Gold, 5 μm, (Thermo)
Column Temperature	40°C
Column Divert	Column effluent diverted to the MS between 0.7 and 1.4 min
Run Time	1.5 minutes
Mobile Phase A	20 mM ammonium acetate containing 0.1% acetic acid
Mobile Phase B	Acetonitrile

1.9.6.2. Quinidine UPLC Gradient

Time (mins)	%A	%B
0	62	38
1.5	62	38

1.9.6.3. Quinidine MS/MS Conditions

Mass Spectrometer	Applied Biosystems/MDS Sciex API-4000
Ionisation Interface and Temperature	TurboIonSpray™ at 450°C (4500V)
Pause Time	5 msec
Gas 1 Setting(Nitrogen)	50 psi
Gas 2 Setting (Nitrogen)	50 psi
Curtain Gas Setting (Nitrogen)	25
Collision Gas Setting (Nitrogen)	4
DP Value	78 (= IS)
CE Value	80 (= IS)
EP Value	10 (= IS)
CXP Value	15 (IS = 16)

1.9.6.4. Quinidine MRM Transitions

Analyte	Precursor Ion (m/z)	Product Ion (m/z)	Dwell Time (msec)	Polarity	Typical R.T (mins)
Quinidine	325	172	150	Positive	1.0
[$^2H_3$]-Quinidine (I.S.)	328	175	150	Positive	1.0

1.9.6.5. Representative Quinidine MS/MS Chromatogram

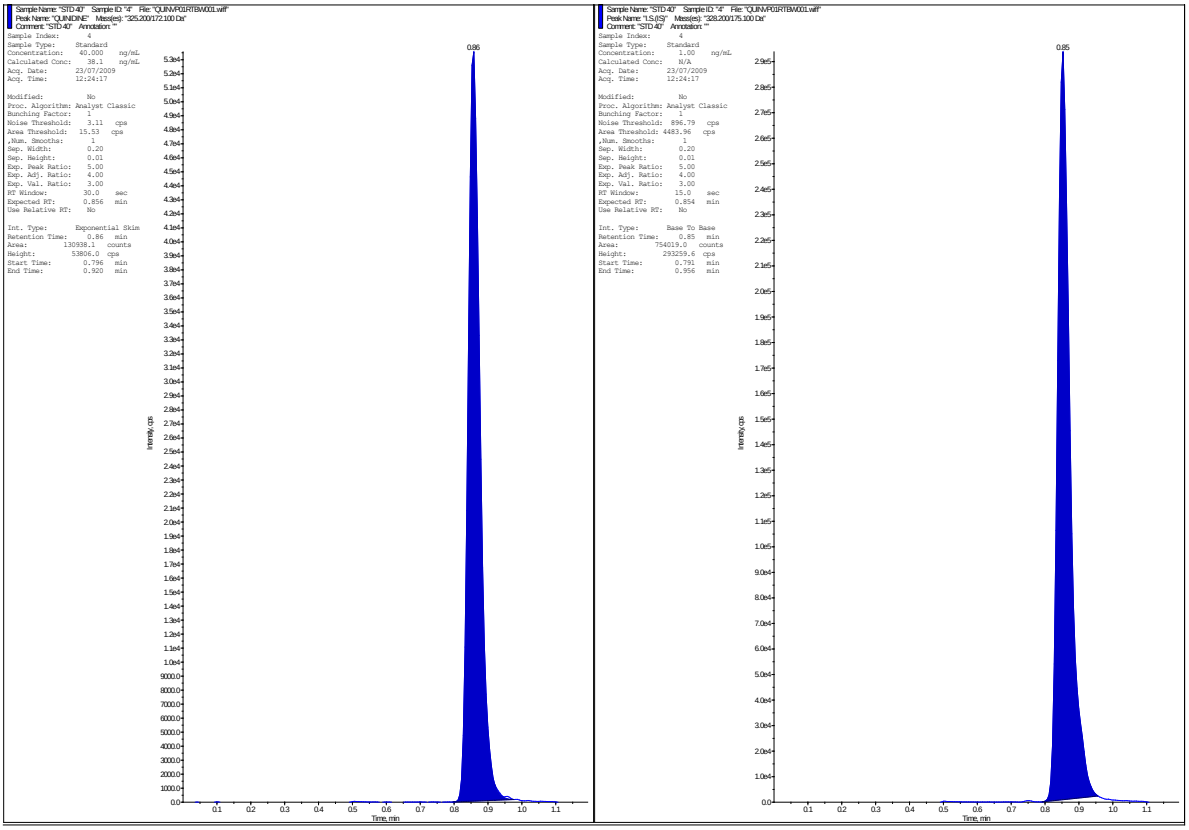

1.9.6.6. Representative Quinidine Calibration Standard Curve

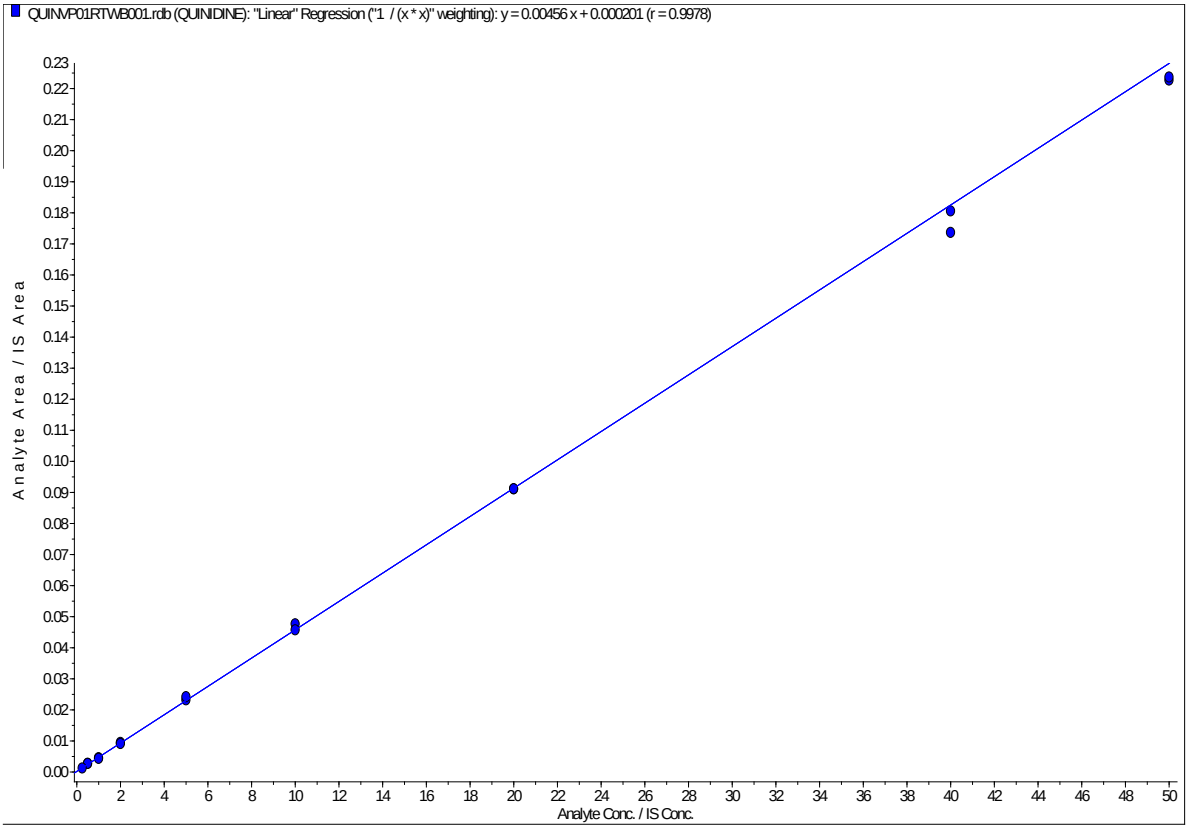

2. APPENDIX 2 PROTEIN BINDING

2.1. Cisapride Protein Binding Data

2.1.1. Individual and Mean Protein Binding in Rat Plasma

Compound	Replicate							
Cisapride	1	2	3	4	5	6	Mean	S.E.M.
Low [a]	96.3	96.6	96.0	95.6	95.7	96.8	96.2	0.198
Medium [b]	96.7	96.3	96.3	96.9	96.3	96.7	96.5	0.109
High [c]	97.1	96.7	96.4	97.6	97.1	96.9	97.0	0.167

2.1.2. Individual and Mean Protein Binding in Dog Plasma

Compound	Replicate							
Cisapride	1	2	3	4	5	6	Mean	S.E.M.
Low [a]	87.3	91.2	93.2	94.3	87.4	88.2	90.3	1.25
Medium [b]	98.7	98.3	97.6	98.4	98.2	98.4	98.3	0.150
High [c]	97.4	98.8	96.4	98.2	96.3	98.6	97.7	0.446

2.1.3. Individual and Mean Protein Binding in Rabbit Plasma

Compound	Replicate							
Cisapride	1	2	3	4	5	6	Mean	S.E.M.
Low [a]	97.8	98.1	98.2	99.1	98.7	97.9	98.3	0.205
Medium [b]	97.6	98.0	97.9	98.9	98.1	98.1	98.1	0.177
High [c]	96.6	96.7	71.0*	NS	98.2	98.4	97.5	0.478

2.1.4. Individual and Mean Protein Binding in Guinea Pig Plasma

Compound	Replicate							
Cisapride	1	2	3	4	5	6	Mean	S.E.M.
Low [a]	98.2	98.4	97.6	98.1	97.4	98.4	98.0	0.172
Medium [b]	98.0	98.2	98.7	98.4	97.4	98.4	98.2	0.183
High [c]	98.0	97.8	97.8	97.5	98.4	98.2	98.0	0.131

2.1.5. Individual and Mean Protein Binding in Human Plasma

Compound	Replicate							
Cisapride	1	2	3	4	5	6	Mean	S.E.M.
Low [a]	97.7	97.8	98.9	96.0	97.7	98.7	97.8	0.420
Medium [b]	99.1	99.1	99.0	99.0	99.4	99.4	99.2	0.0760
High [c]	98.5	98.5	99.0	98.7	99.2	98.8	98.8	0.114

2.1.6. Individual and Mean Protein Binding in Rat Blood

Compound	Replicate							
Cisapride	1	2	3	4	5	6	Mean	S.E.M.
Low [a]	91.2	100*	93.1	93.3	89.8	88.0	91.1	1.00
Medium [b]	91.7	91.8	92.1	91.9	90.4	93.4	91.9	0.391
High [c]	92.9	93.3	90.3	93.8	92.4	92.4	92.5	0.495

2.1.7. Individual and Mean Protein Binding in Dog Blood

Compound	Replicate							
Cisapride	1	2	3	4	5	6	Mean	S.E.M.
Low [a]	97.3	97.2	96.8	97.0	98.3	95.9	97.1	0.318
Medium [b]	96.2	95.9	80.7*	96.8	97.1	96.6	96.5	0.213
High [c]	95.8	95.5	95.8	95.7	95.2	95.6	95.6	0.0931

2.1.8. Individual and Mean Protein Binding in Rabbit Blood

Compound	Replicate							
Cisapride	1	2	3	4	5	6	**Mean**	**SEM**
Low [a]	91.2	90.6	94.4	92.4	91.2	89.5	91.6	0.688
Medium [b]	90.5	89.9	88.9	89.5	90.4	88.7	89.7	0.307
High [c]	87.8	87.2	88.2	88.5	87.2	87.3	87.7	0.228

2.1.9. Individual and Mean Protein Binding in Guinea Pig Blood

Compound	Replicate							
Cisapride	1	2	3	4	5	6	Mean	S.E.M.
Low [a]	87.1	89.9	88.9	89.4	88.8	90.5	89.1	0.477
Medium [b]	86.8	88.9	88.5	86.9	86.4	87.0	87.4	0.417
High [c]	83.0	82.3	82.8	81.9	81.5	78.3	81.6	0.704

2.1.10. Individual and Mean Protein Binding in Human Blood

Compound	Replicate							
Cisapride	1	2	3	4	5	6	Mean	S.E.M.
Low [a]	94.6	96.5	95.8	98.1	97.0	95.8	96.3	0.489
Medium [b]	92.3	95.8	96.0	95.8	95.7	94.9	95.1	0.578
High [c]	94.3	94.5	94.6	94.4	92.5	93.1	93.9	0.358

2.1.11. Individual and Mean Protein Binding in Rat Heart Tissue

Compound	Replicate							
Cisapride	1	2	3	4	5	6	Mean	S.E.M.
Low [a]	98.3	97.5	97.7	99.0	98.4	99.2	98.4	0.277
Medium [b]	99.0	99.1	98.6	98.9	99.0	98.3	98.8	0.125
High [c]	98.5	99.0	98.7	98.7	98.9	98.2	98.7	0.117

2.1.12. Individual and Mean Protein Binding in Dog Heart Tissue

Compound	Replicate							
Cisapride	1	2	3	4	5	6	Mean	S.E.M.
Low [a]	98.3	98.8	98.5	98.8	98.8	98.7	98.7	0.0847
Medium [b]	98.4	98.8	98.7	98.6	98.9	98.5	98.7	0.0764
High [c]	97.8	97.7	98.0	98.3	98.5	97.7	98.0	0.137

2.1.13. Individual and Mean Protein Binding in Rabbit Heart Tissue

Compound	Replicate							
Cisapride	1	2	3	4	5	6	Mean	S.E.M.
Low [a]	98.4	98.1	98.6	98.7	98.8	99.2	98.6	0.152
Medium [b]	99.4	99.7	99.2	99.0	99.1	98.0	99.1	0.236
High [c]	98.2	99.3	98.7	98.1	98.7	99.2	98.7	0.202

Concentrations of cisapride investigated representing parity, 10x and 100x approximate clinical therapeutic concentration with respect to plasma were:

a. 100 ng/mL (low),
b. 1,000 ng/mL (medium) and
c. 10,000 ng/mL (high),

2.2. Moxifloxacin Protein Binding Data

2.2.1. Individual and Mean Protein Binding in Rat Plasma

Compound	Replicate							
Moxifloxacin	1	2	3	4	5	6	Mean	S.E.M.
Low [a]	45.4	52.0	22.1	31.5	34.1	28.5	35.6	4.53
Medium [b]	44.6	45.8	44.9	46.7	51.7	37.6	45.2	1.85
High [c]	54.3	44.7	46.2	52.0	47.5	38.0	47.1	2.35

2.2.2. Individual and Mean Protein Binding in Dog Plasma

Compound	Replicate							
Moxifloxacin	1	2	3	4	5	6	Mean	S.E.M.
Low [a]	43.2	36.3	35.1	35.1	39.9	32.5	37.0	1.57
Medium [b]	42.0	37.6	35.8	45.2	32.8	38.8	38.7	1.81
High [c]	44.9	38.9	40.1	29.4	10.8*	32.3	37.1	2.78

2.2.3. Individual and Mean Protein Binding in Rabbit Plasma

Compound	Replicate							
Moxifloxacin	1	2	3	4	5	6	**Mean**	**SEM**
Low [a]	-325*	51.2	70.3	39.5	34.8	54.2	50.0	6.22
Medium [b]	43.9	49.1	44.1	46.2	41.9	36.2	43.5	1.78
High [c]	47.1	48.5	41.8	44.9	48.5	47.5	46.4	1.06

2.2.4. Individual and Mean Protein Binding in Guinea Pig Plasma

Compound	Replicate							
Moxifloxacin	1	2	3	4	5	6	Mean	S.E.M.
Low [a]	36.3	36.7	45.5	42.3	38.5	50.2	41.6	2.26
Medium [b]	45.1	36.5	43.0	41.1	39.4	35.0	40.0	1.57
High [c]	59.6	48.4	46.5	45.8	48.6	27.7	46.1	4.22

2.2.5. Individual and Mean Protein Binding in Human Plasma

Compound	Replicate							
Moxifloxacin	1	2	3	4	5	6	Mean	S.E.M.
Low [a]	37.0	23.6	24.9	7.93*	26.1	28.5	28.0	2.38
Medium [b]	44.0	47.5	47.0	45.2	28.5	24.8	39.5	4.13
High [c]	49.9	51.5	50.4	47.2	47.7	29.7	46.1	3.33

2.2.6. Individual and Mean Protein Binding in Rat Blood

Compound	Replicate							
Moxifloxacin	1	2	3	4	5	6	Mean	S.E.M.
Low [a]	68.4	69.9	67.6	68.7	69.0	65.5	68.2	0.616
Medium [b]	67.7	70.8	68.7	72.1	72.8	69.1	70.2	0.817
High [c]	64.8	67.0	70.6	69.7	66.3	66.6	67.5	0.903

2.2.7. Individual and Mean Protein Binding in Dog Blood

Compound	Replicate							
Moxifloxacin	1	2	3	4	5	6	Mean	S.E.M.
Low [a]	75.1	72.8	82.2	80.5	83.4	85.1	79.8	1.98
Medium [b]	71.8	69.0	68.4	73.7	73.7	69.8	71.1	0.956
High [c]	73.9	72.8	76.8	71.7	75.9	72.2	73.9	0.837

2.2.8. Individual and Mean Protein Binding in Rabbit Blood

Compound	Replicate							
Moxifloxacin	1	2	3	4	5	6	Mean	S.E.M.
Low [a]	57.3	63.9	69.4	43.2	60.4	53.7	58.0	3.69
Medium [b]	81.3	83.1	78.8	76.6	77.6	76.2	78.9	1.13
High [c]	68.9	66.3	68.3	65.1	60.8	62.0	65.2	1.34

2.2.9. Individual and Mean Protein Binding in Guinea Pig Blood

Compound	Replicate							
Moxifloxacin	1	2	3	4	5	6	Mean	S.E.M.
Low [a]	54.2	59.0	56.9	48.7	59.7	54.1	55.4	1.65
Medium [b]	67.8	63.0	65.4	61.6	63.4	68.1	64.9	1.08
High [c]	66.4	65.4	65.0	64.4	68.3	65.4	65.8	0.570

2.2.10. Individual and Mean Protein Binding in Human Blood

Compound	Replicate							
Moxifloxacin	1	2	3	4	5	6	Mean	S.E.M.
Low [a]	65.4	71.5	75.7	74.8	77.2	72.0	72.8	1.72
Medium [b]	72.6	73.5	75.0	78.2	78.4	73.4	75.2	1.03
High [c]	70.0	73.2	74.7	75.3	75.5	76.1	74.1	0.918

2.2.11. Individual and Mean Protein Binding in Rat Heart Tissue

Compound	Replicate							
Moxifloxacin	1	2	3	4	5	6	Mean	S.E.M.
Low [a]	86.3	86.7	88.5	88.4	87.9	85.3	87.2	0.530
Medium [b]	80.1	78.9	83.6	82.8	86.6	85.0	82.8	1.19
High [c]	84.5	82.4	84.4	82.1	81.0	79.6	82.3	0.780

2.2.12. Individual and Mean Protein Binding in Dog Heart Tissue

Compound	Replicate							
Moxifloxacin	1	2	3	4	5	6	Mean	S.E.M.
Low [a]	90.8	93.6	93.8	93.6	93.6	89.3	92.4	0.787
Medium [b]	92.5	93.9	95.0	93.5	92.4	89.5	92.8	0.765
High [c]	86.7	90.4	91.9	89.2	89.7	88.2	89.4	0.741

2.2.13. Individual and Mean Protein Binding in Rabbit Heart Tissue

Compound	Replicate							
Moxifloxacin	1	2	3	4	5	6	Mean	S.E.M.
Low [a]	69.8	89.5	88.5	87.4	88.4	79.4	83.8	3.19
Medium [b]	87.0	88.1	88.4	89.7	88.9	81.2	87.2	1.26
High [c]	84.3	85.3	85.1	85.1	84.9	78.0	83.8	1.17

Concentrations of moxifloxacin investigated representing 10x below, parity and 10x above approximate clinical therapeutic concentration with respect to plasma were:

a. 500 ng/mL (low),
b. 5,000 ng/mL (medium) and
c. 50,000 ng/mL (high),

2.3. Sparfloxacin Protein Binding Data

2.3.1. Individual and Mean Protein Binding in Rat Plasma

Compound	Replicate							
Sparfloxacin	1	2	3	4	5	6	Mean	S.E.M.
Low [a]	NR	NR	NR	NR	NR	NR	NC	NC
Medium [b]	64.5	43.4	44.4	50.7	50.6	55.7	51.6	3.19
High [c]	50.3	45.4	42.5	48.2	45.9	41.7	45.6	1.35

2.3.2. Individual and Mean Protein Binding in Dog Plasma

Compound	Replicate							
Sparfloxacin	1	2	3	4	5	6	Mean	S.E.M.
Low [a]	NR	NR	NR	NR	NR	NR	NC	NC
Medium [b]	51.3	21.0	35.2	39.8	49.8	47.9	40.8	4.70
High [c]	45.4	45.1	39.1	38.9	45.0	37.6	41.9	1.49

2.3.3. Individual and Mean Protein Binding in Rabbit Plasma

Compound	Replicate							
Sparfloxacin	1	2	3	4	5	6	Mean	S.E.M.
Low [a]	NR	NR	NR	NR	NR	NR	NC	NC
Medium [b]	54.7	48.2	46.0	54.3	52.6	41.6	49.6	2.13
High [c]	46.4	43.2	48.1	52.7	52.7	44.6	47.9	1.64

2.3.4. Individual and Mean Protein Binding in Guinea Pig Plasma

Compound	Replicate							
Sparfloxacin	1	2	3	4	5	6	Mean	S.E.M.
Low [a]	NR	NR	NR	NR	NR	NR	NC	NC
Medium [b]	74.8	74.7	74.7	73.9	76.1	68.3	73.8	1.13
High [c]	75.5	73.7	64.9	77.4	77.2	72.4	73.5	1.90

2.3.5. Individual and Mean Protein Binding in Human Plasma

Compound	Replicate							
Sparfloxacin	1	2	3	4	5	6	Mean	S.E.M.
Low [a]	NR	NR	NR	NR	NR	NR	NC	NC
Medium [b]	54.6	54.4	58.8	58.2	52.1	51.4	54.9	1.24
High [c]	59.1	55.4	56.0	60.9	61.1	56.2	58.1	1.05

NR Not Reported
NC Not Calculated

2.3.6. Individual and Mean Protein Binding in Rat Blood

Compound	Replicate							
Sparfloxacin	1	2	3	4	5	6	Mean	S.E.M.
Low [a]	NR	NR	NR	NR	NR	NR	NC	NC
Medium [b]	73.9	75.6	92.5	81.4	77.6	71.0	78.7	3.10
High [c]	75.3	74.0	72.3	75.0	73.1	73.4	73.9	0.477

2.3.7. Individual and Mean Protein Binding in Dog Blood

Compound	Replicate							
Sparfloxacin	1	2	3	4	5	6	Mean	S.E.M.
Low [a]	NR	NR	NR	NR	NR	NR	NC	NC
Medium [b]	62.3	85.1	40.7	63.3	67.7	57.1	62.7	5.89
High [c]	60.3	59.9	61.6	58.6	56.2	59.1	59.3	0.749

2.3.8. Individual and Mean Protein Binding in Rabbit Blood

Compound	Replicate							
Sparfloxacin	1	2	3	4	5	6	Mean	S.E.M.
Low [a]	NR	NR	NR	NR	NR	NR	NC	NC
Medium [b]	71.6	74.2	75.7	69.5	66.8	78.2	72.7	1.72
High [c]	72.4	73.6	73.7	72.0	72.4	70.6	72.4	0.463

2.3.9. Individual and Mean Protein Binding in Guinea Pig Blood

Compound	Replicate							
Sparfloxacin	1	2	3	4	5	6	Mean	S.E.M.
Low [a]	NR	NR	NR	NR	NR	NR	NC	NC
Medium [b]	67.6	66.1	68.4	60.3	70.6	61.7	65.8	1.64
High [c]	67.4	67.6	63.4	62.8	63.6	62.7	64.6	0.930

2.3.10. Individual and Mean Protein Binding in Human Blood

Compound	Replicate							
Sparfloxacin	1	2	3	4	5	6	Mean	S.E.M.
Low [a]	NR	NR	NR	NR	NR	NR	NC	NC
Medium [b]	75.4	82.1	81.2	79.3	77.8	79.6	79.2	0.985
High [c]	80.2	80.8	84.0	83.7	81.9	76.5	81.2	1.13

NR Not Reported
NC Not Calculated

2.3.11. Individual and Mean Protein Binding in Rat Heart Tissue

Compound	Replicate							
Sparfloxacin	1	2	3	4	5	6	Mean	S.E.M.
Low [a]	37.5*	55.2	56.8	86.5	75.2	62.0	67.1	5.98
Medium [b]	80.3	81.0	77.1	82.8	78.6	67.8	77.9	2.19
High [c]	83.2	84.4	81.8	79.2	79.2	78.0	81.0	1.05

2.3.12. Individual and Mean Protein Binding in Dog Heart Tissue

Compound	Replicate							
Sparfloxacin	1	2	3	4	5	6	Mean	S.E.M.
Low [a]	90.3	92.2	93.3	91.5	94.3	93.9	92.6	0.633
Medium [b]	92.9	94.1	94.1	93.3	93.5	92.2	93.3	0.301
High [c]	91.6	92.6	93.8	92.7	91.2	90.7	92.1	0.465

2.3.13. Individual and Mean Protein Binding in Rabbit Heart Tissue

Compound	Replicate							
Sparfloxacin	1	2	3	4	5	6	Mean	S.E.M.
Low [a]	94.5	95.8	96.3	97.8	95.0	93.6	95.5	0.608
Medium [b]	96.5	95.8	97.3	97.3	95.7	88.2	95.1	1.42
High [c]	93.7	94.5	95.3	94.7	96.6	91.9	94.4	0.647

Concentrations of sparfloxacin investigated representing 10x below, parity and 10x above approximate clinical therapeutic concentration with respect to plasma were:

a. 100 ng/mL (low),
b. 1,000 ng/mL (medium) and
c. 10,000 ng/mL (high),

2.4. Sotalol Protein Binding Data

2.4.1. Individual and Mean Protein Binding in Rat Plasma

Compound	Replicate							
Sotalol	1	2	3	4	5	6	Mean	S.E.M.
Low [a]	29.9	26.6	16.7	44.9	48.4	42.4	34.8	5.05
Medium [b]	30.2	34.1	20.9	38.2	20.6	23.2	27.9	3.02
High [c]	40.5	34.5	34.5	34.6	32.8	28.0	34.2	1.63

2.4.2. Individual and Mean Protein Binding in Dog Plasma

Compound	Replicate							
Sotalol	1	2	3	4	5	6	Mean	S.E.M.
Low [a]	NR	19.9	24.4	29.9	NR	2.16	19.1	6.01
Medium [b]	33.4	12.2	26.8	7.16	27.2	7.94	19.1	4.63
High [c]	32.6	31.2	29.4	32.2	29.5	15.7	28.4	2.61

NR Not Reported

2.4.3. Individual and Mean Protein Binding in Rabbit Plasma

Compound	Replicate							
Sotalol	1	2	3	4	5	6	Mean	S.E.M.
Low [a]	33.4	12.6	5.53	13.3	6.73	6.89	13.1	4.27
Medium [b]	21.3	13.7	17.7	27.1	18.5	17.5	19.3	1.85
High [c]	25.5	25.0	16.3	25.7	19.8	17.8	21.7	1.73

2.4.4. Individual and Mean Protein Binding in Guinea Pig Plasma

Compound	Replicate							
Sotalol	1	2	3	4	5	6	Mean	S.E.M.
Low [a]	3.70	7.21	0.51	15.5	4.75	2.27	5.65	2.17
Medium [b]	30.0	29.1	30.8	25.0	20.8	7.08	23.8	3.68
High [c]	29.6	29.4	35.4	32.5	28.7	13.4	28.1	3.12

2.4.5. Individual and Mean Protein Binding in Human Plasma

Compound	Replicate							
Sotalol	1	2	3	4	5	6	Mean	S.E.M.
Low [a]	3.46	7.79	6.94	11.0	10.2	8.84	8.04	1.10
Medium [b]	16.1	21.1	24.6	23.7	36.5	26.1	24.7	2.76
High [c]	31.8	36.3	30.4	30.2	26.7	20.6	29.3	2.16

2.4.6. Individual and Mean Protein Binding in Rat Blood

Compound	Replicate							
Sotalol	1	2	3	4	5	6	Mean	S.E.M.
Low [a]	19.7	8.90	18.7	1.62	16.1	19.4	14.1	2.98
Medium [b]	29.9	36.9	25.2	33.0	37.3	20.9	30.5	2.67
High [c]	27.6	33.8	35.9	42.3	32.6	31.6	33.9	2.02

2.4.7. Individual and Mean Protein Binding in Dog Blood

Compound	Replicate							
Sotalol	1	2	3	4	5	6	Mean	S.E.M.
Low [a]	6.26	9.37	4.24	5.78	2.40	24.6	8.78	3.30
Medium [b]	33.9	36.1	34.5	25.6	37.7	26.1	32.3	2.12
High [c]	50.6	49.1	47.7	47.1	46.1	40.4	46.9	1.47

2.4.8. Individual and Mean Protein Binding in Rabbit Blood

Compound	Replicate							
Sotalol	1	2	3	4	5	6	Mean	S.E.M.
Low [a]	12.2	18.8	26.8	11.6	24.8	14.3	18.1	2.66
Medium [b]	27.8	27.6	34.1	34.7	43.1	23.9	31.9	2.81
High [c]	41.7	48.5	40.5	48.0	43.0	39.8	43.6	1.53

2.4.9. Individual and Mean Protein Binding in Guinea Pig Blood

Compound	Replicate							
Sotalol	1	2	3	4	5	6	Mean	S.E.M.
Low [a]	26.6	5.99	21.2	11.6	8.59	15.1	14.8	3.20
Medium [b]	41.4	37.0	36.7	23.7	45.0	33.3	36.1	3.00
High [c]	45.4	43.1	47.8	45.1	48.0	33.5	43.8	2.20

2.4.10. Individual and Mean Protein Binding in Human Blood

Compound	Replicate							
Sotalol	1	2	3	4	5	6	Mean	S.E.M.
Low [a]	2.66	4.63	17.8	27.4	7.89	3.92	10.7	4.01
Medium [b]	42.2	55.0	50.7	48.8	60.7	48.5	51.0	2.57
High [c]	58.5	60.7	61.8	61.8	60.9	50.1	59.0	1.84

2.4.11. Individual and Mean Protein Binding in Rat Heart Tissue

Compound	Replicate							
Sotalol	1	2	3	4	5	6	Mean	S.E.M.
Low [a]	16.3	79.4	66.2	18.3	62.0	197*	48.4	13.0
Medium [b]	64.8	64.3	50.1	46.8	36.0	38.5	50.1	5.04
High [c]	59.9	65.4	64.9	58.7	44.6	40.4	55.6	4.34

2.4.12. Individual and Mean Protein Binding in Dog Heart Tissue

Compound	Replicate							
Sotalol	1	2	3	4	5	6	Mean	S.E.M.
Low [a]	81.7	87.4	89.0	83.9	80.9	77.1	83.3	1.79
Medium [b]	83.9	87.0	89.0	86.1	85.2	79.6	85.1	1.31
High [c]	78.9	83.5	84.9	84.3	83.6	73.6	81.5	1.79

2.4.13. Individual and Mean Protein Binding in Rabbit Heart Tissue

Compound	Replicate							
Sotalol	1	2	3	4	5	6	Mean	S.E.M.
Low [a]	69.4	70.2	68.2	72.5	57.3	64.4	67.0	2.22
Medium [b]	81.3	74.1	90.3	75.4	75.8	74.2	78.5	2.60
High [c]	68.4	75.9	87.2	81.5	71.7	45.0	71.6	6.00

Concentrations of sotalol investigated representing 10x below, parity and 10x above approximate clinical therapeutic concentration with respect to plasma were:

a. 100 ng/mL (low),
b. 1000 ng/mL (medium) and
c. 10,000 ng/mL (high),

2.5. Verapamil Protein Binding Data

2.5.1. Individual and Mean Protein Binding in Rat Plasma

Compound	Replicate							
Verapamil	1	2	3	4	5	6	Mean	S.E.M.
Low [a]	93.5	93.0	93.0	93.0	93.5	92.9	93.1	0.119
Medium [b]	94.7	93.7	93.7	93.4	94.1	92.2	93.6	0.341
High [c]	93.1	91.4	91.2	91.9	91.3	90.6	91.6	0.339

2.5.2. Individual and Mean Protein Binding in Dog Plasma

Compound	Replicate							
Verapamil	1	2	3	4	5	6	Mean	S.E.M.
Low [a]	94.6	93.6	93.7	93.8	94.8	93.0	93.9	0.278
Medium [b]	94.3	94.6	95.4	93.8	94.6	93.5	94.4	0.271
High [c]	93.6	94.0	94.0	94.0	94.2	93.6	93.9	0.0975

2.5.3. Individual and Mean Protein Binding in Rabbit Plasma

Compound	Replicate							
Verapamil	1	2	3	4	5	6	Mean	S.E.M.
Low [a]	95.9	95.2	94.4	94.9	95.2	94.9	93.6	0.482
	92.8	92.4	92.9	92.8	92.2	90.2		
Medium [b]	96.0	95.4	95.1	95.5	94.7	94.9	93.9	0.460
	93.3	93.3	92.3	92.5	92.6	91.0		
High [c]	95.2	94.6	94.9	94.6	94.2	94.2	93.2	0.464
	93.5	91.9	92.1	92.3	91.0	90.5		

2.5.4. Individual and Mean Protein Binding in Guinea Pig Plasma

Compound	Replicate							
Verapamil	1	2	3	4	5	6	Mean	S.E.M.
Low [a]	99.4	99.6	99.2	99.2	99.5	99.6	99.4	0.0736
Medium [b]	99.4	99.4	99.5	99.4	99.5	99.4	99.4	0.0235
High [c]	99.3	99.3	99.3	99.3	99.4	99.3	99.3	0.0220

2.5.5. Individual and Mean Protein Binding in Human Plasma

Compound	Replicate							
Verapamil	1	2	3	4	5	6	**Mean**	**SEM**
Low [a]	81.4	80.9	80.0	81.7	84.6	81.8	81.7	0.641
Medium [b]	80.9	79.4	81.0	84.5	84.1	82.9	82.1	0.819
High [c]	79.1	80.2	77.9	84.6	85.0	83.5	81.7	1.24

2.5.6. Individual and Mean Protein Binding in Rat Blood

Compound	Replicate							
Verapamil	1	2	3	4	5	6	Mean	S.E.M.
Low [a]	83.8	86.0	85.2	84.6	84.5	83.0	84.5	0.417
Medium [b]	86.7	85.7	87.3	85.7	82.7	83.4	85.2	0.742
High [c]	84.4	85.6	87.1	85.3	82.7	80.9	84.3	0.901

2.5.7. Individual and Mean Protein Binding in Dog Blood

Compound	Replicate							
Verapamil	1	2	3	4	5	6	Mean	S.E.M.
Low [a]	85.7	87.7	87.2	84.0	85.8	84.3	85.8	0.604
Medium [b]	86.9	87.2	86.7	87.2	88.8	86.9	87.3	0.303
High [c]	86.4	86.7	85.6	86.5	88.4	84.7	86.4	0.495

2.5.8. Individual and Mean Protein Binding in Rabbit Blood

Compound	Replicate							
Verapamil	1	2	3	4	5	6	Mean	S.E.M.
Low [a]	78.8	82.4	80.5	83.1	84.7	84.0	82.2	0.904
Medium [b]	84.3	84.5	84.0	83.6	80.6	85.9	83.8	0.720
High [c]	84.4	83.7	83.0	85.1	80.6	85.3	83.7	0.716

2.5.9. Individual and Mean Protein Binding in Guinea Pig Blood

Compound	Replicate							
Verapamil	1	2	3	4	5	6	Mean	S.E.M.
Low [a]	96.4	96.8	96.7	96.5	97.0	96.6	96.7	0.0885
Medium [b]	97.3	97.2	97.3	97.0	97.4	96.6	97.1	0.120
High [c]	96.1	96.2	95.8	96.1	96.1	95.5	96.0	0.110

2.5.10. Individual and Mean Protein Binding in Human Blood

Compound	Replicate							
Verapamil	1	2	3	4	5	6	Mean	S.E.M.
Low [a]	89.8	88.3	91.3	89.8	85.9	86.1	88.5	0.902
Medium [b]	88.9	93.3	91.5	90.5	89.9	90.0	90.7	0.617
High [c]	89.6	90.2	90.7	91.6	93.0	87.1	90.3	0.807

2.5.11. Individual and Mean Protein Binding in Rat Heart Tissue

Compound	Replicate							
Verapamil	1	2	3	4	5	6	Mean	S.E.M.
Low [a]	97.7	97.9	98.4	98.1	98.3	98.3	98.1	0.109
Medium [b]	94.5	98.0	94.0	97.4	97.4	97.8	96.5	0.734
High [c]	96.2	95.3	96.8	97.3	97.1	96.2	96.5	0.304

2.5.12. Individual and Mean Protein Binding in Dog Heart Tissue

Compound	Replicate							
Verapamil	1	2	3	4	5	6	Mean	S.E.M.
Low [a]	98.5	98.8	98.7	98.9	98.8	97.9	98.6	0.156
Medium [b]	98.5	98.5	99.0	98.8	98.4	97.5	98.4	0.208
High [c]	97.8	97.8	97.5	97.9	97.2	95.5	97.3	0.372

2.5.13. Individual and Mean Protein Binding in Rabbit Heart Tissue

Compound	Replicate							
Verapamil	1	2	3	4	5	6	Mean	S.E.M.
Low [a]	98.3	98.6	98.4	98.0	97.5	97.6	98.0	0.182
Medium [b]	97.3	98.6	98.2	98.4	97.5	97.1	97.8	0.269
High [c]	97.5	97.4	96.9	97.6	97.0	95.3	96.9	0.353

Concentrations of verapamil investigated representing parity, 10x and 100x above approximate clinical therapeutic concentration with respect to plasma were:

a. 100 ng/mL (low),
b. 1,000 ng/mL (medium) and
c. 10,000 ng/mL (high)

2.6. Quinidine Protein Binding Data

2.6.1. Individual and Mean Protein Binding in Rat Plasma

Compound	Replicate							
Quinidine	1	2	3	4	5	6	Mean	S.E.M.
Low [a]	78.8	80.1	77.4	79.2	77.9	78.2	78.6	0.396
Medium [b]	75.8	71.0	75.7	73.9	72.5	70.4	73.2	0.945
High [c]	69.0	68.9	66.4	70.3	69.7	62.7	67.8	1.17

2.6.2. Individual and Mean Protein Binding in Dog Plasma

Compound	Replicate							
Quinidine	1	2	3	4	5	6	Mean	S.E.M.
Low [a]	98.7	98.7	98.7	98.1	98.6	99.0	98.7	0.116
Medium [b]	90.5	90.3	88.8	89.5	90.8	90.7	90.1	0.312
High [c]	69.4	69.4	70.3	66.6	63.5	61.9	66.8	1.43

2.6.3. Individual and Mean Protein Binding in Rabbit Plasma

Compound	Replicate							
Quinidine	1	2	3	4	5	6	Mean	S.E.M.
Low [a]	89.1	90.7	88.1	89.3	88.5	86.9	88.8	0.522
Medium [b]	90.9	90.9	89.0	89.5	90.2	89.1	89.9	0.357
High [c]	86.4	86.2	83.9	86.0	85.8	86.4	85.8	0.379

2.6.4. Individual and Mean Protein Binding in Guinea Pig Plasma

Compound	Replicate							
Quinidine	1	2	3	4	5	6	Mean	S.E.M.
Low [a]	99.1	98.8	99.3	99.0	98.4	99.2	98.9	0.126
Medium [b]	92.4	92.1	92.1	92.7	92.8	92.3	92.4	0.127
High [c]	82.0	82.9	79.5	83.0	84.0	80.6	82.0	0.673

2.6.5. Individual and Mean Protein Binding in Human Plasma

Compound	Replicate							
Quinidine	1	2	3	4	5	6	Mean	S.E.M.
Low [a]	91.9	91.1	91.4	90.4	91.1	91.2	91.2	0.203
Medium [b]	86.9	86.8	86.5	87.3	87.6	88.3	87.2	0.266
High [c]	74.1	74.1	74.1	73.3	74.4	73.2	73.9	0.200

2.6.6. Individual and Mean Protein Binding in Rat Blood

Compound	Replicate							
Quinidine	1	2	3	4	5	6	Mean	S.E.M.
Low [a]	89.5	86.4	87.7	84.4	89.9	89.8	87.9	0.907
Medium [b]	84.2	85.6	87.3	83.1	84.9	82.3	84.6	0.734
High [c]	75.7	76.6	76.5	75.1	71.8	69.5	74.2	1.18

2.6.7. Individual and Mean Protein Binding in Dog Blood

Compound	Replicate							
Quinidine	1	2	3	4	5	6	Mean	S.E.M.
Low [a]	98.4	96.5	98.8	97.7	98.6	98.6	98.1	0.355
Medium [b]	91.2	90.8	91.3	93.0	93.0	87.9	91.2	0.768
High [c]	84.3	84.9	82.9	81.8	82.6	81.8	83.0	0.524

2.6.8. Individual and Mean Protein Binding in Rabbit Blood

Compound	Replicate							
Quinidine	1	2	3	4	5	6	Mean	S.E.M.
Low [a]	87.8	88.5	87.5	86.9	84.8	83.9	86.6	0.732
Medium [b]	82.1	85.0	82.6	81.4	81.4	80.4	82.2	0.653
High [c]	78.5	80.0	79.2	79.8	80.1	77.5	79.2	0.408

2.6.9. Individual and Mean Protein Binding in Guinea Pig Blood

Compound	Replicate							
Quinidine	1	2	3	4	5	6	Mean	S.E.M.
Low [a]	89.5	90.7	90.1	89.7	91.4	91.1	90.4	0.323
Medium [b]	74.0	77.2	72.7	75.6	78.9	74.8	75.5	0.915
High [c]	69.2	75.1	71.2	67.0	74.4	69.9	71.1	1.27

2.6.10. Individual and Mean Protein Binding in Human Blood

Compound	Replicate							
Quinidine	1	2	3	4	5	6	Mean	S.E.M.
Low [a]	86.5	87.6	88.5	88.5	90.3	88.6	88.3	0.513
Medium [b]	84.6	84.4	84.4	86.9	81.9	84.5	84.5	0.641
High [c]	79.4	82.6	82.3	83.1	85.0	79.6	82.0	0.877

2.6.11. Individual and Mean Protein Binding in Rat Heart Tissue

Compound	Replicate							
Quinidine	1	2	3	4	5	6	Mean	S.E.M.
Low [a]	99.5	98.5	98.0	97.3	98.0	98.2	98.3	0.302
Medium [b]	97.6	97.8	98.8	97.2	98.5	94.1	97.3	0.695
High [c]	97.2	94.9	96.4	95.6	94.4	97.9	96.1	0.549

2.6.12. Individual and Mean Protein Binding in Dog Heart Tissue

Compound	Replicate							
Quinidine	1	2	3	4	5	6	Mean	S.E.M.
Low [a]	96.8	97.5	97.8	96.8	97.9	96.3	97.2	0.267
Medium [b]	96.9	97.7	97.7	97.4	97.5	96.8	97.3	0.172
High [c]	96.4	96.9	96.8	97.2	96.7	95.2	96.5	0.291

2.6.13. Individual and Mean Protein Binding in Rabbit Heart Tissue

Compound	Replicate							
Quinidine	1	2	3	4	5	6	Mean	S.E.M.
Low [a]	98.6	99.0	98.6	98.9	98.7	98.6	98.7	0.0734
Medium [b]	97.7	98.6	98.2	98.2	98.4	98.4	98.3	0.130
High [c]	98.1	98.4	NS	98.3	98.0	97.5	98.0	0.161

Concentrations of quinidine investigated representing 10x below, parity and 10x above approximate clinical therapeutic concentration with respect to plasma were:

a. 1,000 ng/mL (low),
b. 10,000 ng/mL (medium) and
c. 100,000 ng/mL (high)

3. APPENDIX 3: RABBIT VENTRICULAR WEDGE DATA

3.1. Cisapride: Individual Experimental RVW Data at GSK

Expt.	Concentration (μM)	QRS (ms)	QT (ms)	Tp-e (ms)	Ratio Tp-e/QT	Contraction (ICF) %
A	Vehicle Control	36.8	326.5	70.0	0.21	1.1
	0.01	3.8	10.0	15.0	0.0	0.7
	0.10	0.3	31.0	10.3	0.0	1.0
	1.00	ND	ND	ND	ND	ND
	10.00[a]	-0.8	128.5	32.3	0.0	0.1
B	Vehicle Control	36.0	323.5	58.5	0.2	1.3
	0.01	1.5	32.8	7.3	0.0	-0.2
	0.10	1.0	147.3	77.0	0.1	-0.5
	1.00	2.3	321.5	213.3	0.2	-0.9
	10.00[a]	4.8	144.3	38.8	0.0	-0.9
C	Vehicle Control	34.0	310.0	72.8	0.23	1.4
	0.01	-0.3	0.5	-1.0	0.0	-0.1
	0.10	0.0	61.8	23.0	0.0	0.2
	1.00	-0.3	226.8	119.8	0.1	0.3
	10.00[a]	0.0	163.3	82.5	0.1	-0.2
D	Vehicle Control	44.0	257.5	50.5	0.2	4.8
	0.01	0.5	4.5	0.0	0.0	0.5
	0.10	0.0	40.0	13.0	0.0	1.7
	1.00	1.0	93.5	25.5	0.0	1.6
	10.00[a]	3.0	73.5	5.0	0.0	-1.7
E	Vehicle Control	41.0	344.3	74.0	0.2	1.0
	0.01	0.0	50.8	16.3	0.0	-0.2
	0.10	4.0	259.0	81.0	0.0	0.0
	1.00	5.3	297.8	116.5	0.1	-0.4
	10.00[a]	9.0	167.8	13.8	0.0	-0.8
GSK (US)	Vehicle Control	37.0 ±1.4	336.9 ±28	70.1 ±7	0.2	1.0
	0.01	-0.1 ±1.5	36.8 ±39	7.4 ±12	0.21	0.2 ±5.8
	0.10	-0.2 ±1.3	123.0 ±59	38.9 ±13	0.24	0.4 ±8.0
	1.00	0.8 ±1.3	217.7 ±59	88.9 ±30	0.29	-10.7 ±1.9
	10.00[a]	2.6 ±1.3	119.9 ±36	30.9 ±10	0.22	-38.0 ±1.6

Tabulated data obtained from RVW preparations following 0.5Hz stimulation

Vehicle control data represents the vehicle baseline values to which subsequent doses were corrected and delta change given

a. Values at 10 μM have been excluded for QT modelling purposes due to Na+ channel involvement

ND Not Determined

3.2. Moxifloxacin: Individual Experimental RVW Data at GSK

Expt.	Concentration (μM)	QRS (ms)	QT (ms)	Tp-e (ms)	Ratio Tp-e/QT	Contraction (ICF) %
A	Vehicle Control	42.5	331.8	69.0	0.21	1.3
	3	-6.5	-8.0	3.3	7.2	15.6
	10	-4.8	33.0	19.3	16.3	-12.9
	30	-4.5	60.3	23.5	13.6	-19.3
	100	-6.5	233.3	105.3	48.3	-21.7
B	Vehicle Control	47.8	303.8	53.5	0.18	2.0
	3	-2.5	13.0	12.0	17.5	-15.2
	10	-5.5	15.8	15.3	22.3	-16.1
	30	-8.5	84.3	61.0	67.5	-2.4
	100	-6.3	188.8	94.5	70.7	36.5
C	Vehicle Control	38.0	313.0	54.5	0.17	2.2
	3	3.0	5.0	0.8	-0.3	4.0
	10	ND	ND	ND	ND	ND
	30	4.0	48.8	16.5	12.6	-14.3
	100	4.0	184.8	74.3	48.5	-4.8
D	Vehicle Control	34.0	327.5	62.3	0.19	2.9
	3	-1.5	14.5	2.5	-0.3	7.0
	10	-2.0	35.3	8.0	2.0	14.3
	30	-1.0	79.3	30.0	19.5	18.7
	100	2.8	178.5	68.5	35.9	73.2

Tabulated data obtained from RVW preparations following 0.5Hz stimulation
Vehicle control data represents the vehicle baseline values to which subsequent doses were corrected and delta change given
ND Not Determined

3.3. Sparfloxacin: Individual Experimental RVW Data at GSK

Expt.	Concentration (µM)	QRS (ms)	QT (ms)	Tp-e (ms)	Ratio Tp-e/QT (%)	Contraction (ICF) %
A	Vehicle Control	42.0	335.5	78.5	0.2	0.5
	1.00	-0.5	3.0	-2.5	-4.0	-39.9
	10.00	2.5	112.0	50.0	22.7	2.7
	100.00	5.0	397.5	150.0	33.2	124.1
	333.00	9.5	505.0	92.0	-13.3	300.8
B	Vehicle Control	44.0	365.5	81.5	0.2	0.2
	1.00	0.0	11.0	-0.5	-3.5	-18.2
	10.00	0.5	98.5	32.0	9.7	29.0
	100.00	4.0	369.0	132.0	30.4	202.7
	333.00	7.0	448.0	140.5	22.4	435.2
C	Vehicle Control	50.5	340.5	56.5	0.2	0.2
	1.00	1.0	37.0	11.0	7.8	-30.3
	10.00	1.0	174.5	36.5	8.8	-16.7
	100.00	3.5	389.0	53.0	-9.5	128.0
	333.00	12.5	443.0	50.0	-18.1	150.8
D	Vehicle Control	41.5	358.5	67.5	0.2	0.1
	1.00	0.0	40.0	15.0	10.0	-35.4
	10.00	0.0	223.5	91.5	45.1	77.7
	100.00	2.5	431.5	142.0	40.8	436.2
	333.00	8.0	468.5	203.5	74.0	662.6

Tabulated data obtained from RVW preparations following 0.5Hz stimulation
Vehicle control data represents the vehicle baseline values to which subsequent doses were corrected and delta change given

3.4. Verapamil: Individual Experimental RVW Data at GSK

Expt.	Concentration (µM)	QRS (ms)	QT (ms)	Tp-e (ms)	Ratio Tp-e/QT (%)	Contraction (ICF) %
GSK (US) Mean (n=4)	Vehicle Control	34.6 ±2	327.4±35	75.4±8	0.230	0
	0.01	0.2 ±1.9	23.2 ±27	3.5 ±5	0.225	-9.9±1.9*
	0.10	-0.3 ±2.2	13.5 ±31	-4.9 ±9	0.207	-26.2±3.7*
	1.00	0.3 ±2.4	14.0 ±18	-20.0 ±5	0.162	-71.4±1.8*
	10.00	2.0 ±2.5*	-12.6 ±13	-30.6 ±7*	0.142	-92.6±1.7*

Tabulated data obtained from RVW preparations following 0.5Hz stimulation
Vehicle control data represents the vehicle baseline values to which subsequent doses were corrected and delta change given
* denotes mean difference statistically significant (p-value<0.05) as determined by 2-way ANOVA and Dunnett's test

4. APPENDIX 4 ANAESTHETISED RABBIT QTC MODEL

4.1. Control Anaesthetised Rabbit Data

4.1.1. Individual QTc Response in the Anaesthetised Rabbit

Time (min)	Control #1	Control #2	Control #3	Control #4	Control #5	Mean QTc (ms)	S.E.M.
-10	260.70	273.53	269.86	270.49	267.85	**268.49**	**2.15**
-5	260.87	272.75	271.75	268.93	271.90	**269.24**	**2.19**
0	259.08	271.83	274.15	267.73	279.47	**270.45**	**3.42**
5	259.32	270.02	276.27	268.55	286.94	**272.22**	**4.57**
10	260.45	267.38	275.75	268.63	291.35	**272.71**	**5.25**
15	262.48	265.73	274.55	268.13	293.16	**272.81**	**5.46**
20	264.37	264.75	273.77	262.88	296.63	**272.48**	**6.33**
25	263.48	264.44	273.56	258.27	298.96	**271.74**	**7.24**
30	263.39	263.03	272.76	256.57	300.20	**271.19**	**7.70**
35	263.32	262.60	272.95	255.03	298.45	**270.47**	**7.55**
40	262.00	261.79	272.40	252.07	297.91	**269.23**	**7.86**
45	262.71	262.10	272.25	248.96	297.37	**268.68**	**8.07**
50	261.83	262.54	273.35	245.64	298.94	**268.46**	**8.81**
55	262.13	261.41	274.76	242.69	298.85	**267.97**	**9.26**
60	262.18	259.91	276.82	242.27	296.84	**267.60**	**9.14**
65	261.07	258.32	276.55	243.28	295.41	**266.93**	**8.86**
70	260.59	255.73	277.39	244.59	292.33	**266.13**	**8.41**
75	261.03	253.46	278.08	243.13	289.57	**265.05**	**8.37**
80	262.88	248.14	276.66	243.13	289.33	**264.03**	**8.63**
85	262.83	248.14	277.49	243.13	288.95	**264.11**	**8.64**
90	DM	248.14	278.97	243.13	290.01	**265.06**	**11.49**

4.2. Cisapride Anaesthetised Rabbit Data

4.2.1. Individual Plasma Concentrations in the Anaesthetised Rabbit Following an Infusion of Cisapride at 0.3 mg/kg

Time (min)	0.3 mg/kg #1	0.3 mg/kg #2	0.3 mg/kg #3	0.3 mg/kg #4	0.3 mg/kg #5	0.3 mg/kg #6	0.3 mg/kg #7	Mean Concentration (ng/mL)	S.E.M.
-15	NQ	NQ	NQ	NQ	NQ	NQ	NQ	**NC**	NC
0	NQ	NQ	NQ	NQ	NQ	NQ	NQ	**NC**	NC
5	44.8	64.0	112	36.9	53.0	53.9	60.5	**60.7**	8.58
10	46.9	88.6	92.8	39.5	67.9	52.6	61.4	**64.2**	7.19
15	51.8	108	104	42.8	78.4	58.4	64.4	**72.5**	8.95
20	53.5	82.7	141	47.1	86.6	59.6		**78.5**	13.1
25	59.1	77.7	102	53.6	97.0	65.8		**75.8**	7.54
30	60.7	93.2	87.7	55.3	97.2	68.6		**77.1**	6.74
35	24.4	33.8	37.2	23.6	43.1			**32.4**	3.42
40	19.5	25.9	29.5	19.8	38.2			**26.6**	3.16
45	17.4	21.1	25.1	17.0	30.9			**22.3**	2.37
50	15.0	19.10	20.3	14.6				**17.3**	1.29
55	12.6	15.8	18.6	15.3				**15.6**	1.10
60	12.4	15.7	18.3	12.9				**14.8**	1.22
65	11.6	18.9	17.4					**16.0**	1.93
70	11.0	19.1	15.5					**15.2**	2.03
75	10.3	14.0	14.6					**13.0**	1.16
80	9.1	18.3	10.6					**12.7**	2.47
85	9.00	11.2	11.2					**10.5**	0.64
90	8.90	10.0	10.6					**9.83**	0.43

NQ Not Quantifiable below assay limit of quantification (LOQ = 0.5 ng/mL).
NC Not Calculated

4.2.2. Individual Plasma Concentrations in the Anaesthetised Rabbit Following an Infusion of Cisapride at 1 mg/kg

Time (min)	1 mg/kg #1	1 mg/kg #2	1 mg/kg #3	Mean Concentration (ng/mL)	S.E.M.
-15	NQ	NQ	NQ	**NC**	NC
0	NQ	NQ	NQ	**NC**	NC
5	238	254	213	**235**	11.7
10	277	269	243	**263**	10.4
15	318	290	247	**285**	20.6
20	288	303	255	**282**	14.3
25	362	284	282	**310**	26.4
30	343	301	262	**302**	23.6

NQ Not Quantifiable below assay limit of quantification (LOQ = 0.5 ng/mL).
NC Not Calculated

4.2.3. Individual Plasma Concentrations in the Anaesthetised Rabbit Following an Infusion of Cisapride at 3 mg/kg

Time (min)	3 mg/kg #1	3 mg/kg #2	3 mg/kg #3	3 mg/kg #4	3 mg/kg #5	3 mg/kg #6	3 mg/kg #7	3 mg/kg #8	Mean Concentration (ng/mL)	S.E.M.
-15	NQ	NQ	NQ	NQ	NQ	NQ	NQ	NQ	**NC**	NC
0	NQ	NQ	NQ	NQ	NQ	NQ	NQ	NQ	**NC**	NC
5	851	1150	775	672	771	633	653	715	**778**	59.3
10	1020	1070	947	819	812	749	845	1010	**909**	41.5
15	1090	1220	924	812	1020	918	974	960	**990**	43.5
20	1200	958	1110	751		906	1040	1100	**1010**	57.2
25	1230	995	946	841		921	1150	1060	**1020**	51.20
30	1318	1140	1210	812		1260	955	1170	**1120**	67.9
35	453	464	445	377			525	593	**476**	30.3
40	333	244	381	259			344	414	**329**	27.3
45	304	292	374	266			288	311	**306**	15.1
50	259	231	330	216				313	**269**	22.4
55	252	177	280	184				242	**227**	20.1
60	181	225	272	167				244	**218**	19.5
65	217	145	211	144					**179**	20.1
70	191	130	179	145					**161**	14.2
75	149	116	179	139					**144**	13.5
80	152	125	185	105					**142**	17.4
85	138	157	174	136					**152**	8.89
90	136	159	170	98.1					**141**	15.9

NQ Not Quantifiable below assay limit of quantification (LOQ = 0.5 ng/mL).
NC Not Calculated

4.2.4. Individual Heart Concentrations in the Anaesthetised Rabbit Following an Infusion of Cisapride at 0.3 mg/kg

	0.3 mg/kg #1	0.3 mg/kg #2	0.3 mg/kg #3	Mean (ng/mL)	0.3 mg/kg #4	0.3 mg/kg #5	0.3 mg/kg #6	0.3 mg/kg #7
Time (min)	90	90	90	**90**	**60**	**45**	**30**	**15**
RA	391 [a]	46	149	**195**	NR	550 [a]	130	89
LA	219	79	208	**169**	205	268	283	225
RV1	193	140	142	**158**	140	280	371	364
RV2	215	119	160	**164**	263	347	378	364
RV3	220	117	185	**174**	259	334	309	401
Mean RV	**209**	**125**	**162**	**166**	**221**	**320**	**353**	**376**
LV1	211	149	209	**190**	273	436	650	567
LV2	245	164	187	**199**	290	428	548	541
LV3	213	171	209	**198**	326	544	694	560
LV4	334 [a]	139	149	**207**	376	395	623	530
LV5	130	122	177	**143**	317	368	631	512
LV6	170	64.8	179	**138**	276	452	633	529
LV7	157	128	192	**159**	263	367	617	572
LV8	201	112	197	**170**	316	346	782	515
LV9	173	143	196	**171**	296	407	650	544
Mean LV	**204**	**133**	**188**	**175**	**304**	**416**	**648**	**541**
Overall Mean Heart	**196**	**121**	**181**	**166**	**277**	**382**	**521**	**451**
Plasma Concen-tration	8.9	10.0	10.6	**9.8**	**12.9**	**30.9**	**68.6**	**64.4**
Heart: Plasma ratio	22.1	12.1	17.1	16.9	21.5	12.4	7.6	7.0

a. Value omitted from mean calculations as an outlier without an analytical repeat.
NR No Result reported

4.2.5. Individual Heart Concentrations in the Anaesthetised Rabbit Following an Infusion of Cisapride at 3 mg/kg

	3 mg/kg #1	3 mg/kg #2	3 mg/kg #3	3 mg/kg #4	Mean (ng/mL)	3 mg/kg #8	3 mg/kg #7	3 mg/kg #6	3 mg/kg #5
Time (min)	90	90	90	90	**90**	**60**	**45**	**30**	**15**
RA	2350	1490	2870	1905	**2160**	2110	2340	7790	2510
LA	1830	2000	1860	2096	**1950**	3030	2530	7840	3680
RV1	1700	2230	2410	2672	**2250**	3230	3300	10700	3500
RV2	1730	2060	2780	2948	**2380**	3330	3750	13200	4530
RV3	1800	2150	2570	2703	**2310**	3950	3940	11100	4490
Mean RV	**1740**	**2150**	**2590**	**2774**	**2310**	**3500**	**3660**	**11600**	**4170**
LV1	1260	1740	1900	2194	**1780**	3400	4730	12900	4770
LV2	1630	2290	2070	1716	**1930**	3880	4220	13300	5370
LV3	1730	1820	1890	1691	**1780**	5090	4600	12300	6140
LV4	1540	1470	1770	2233	**1750**	3750	3430	10500	5890
LV5	1470	1390	1740	2234	**1710**	3810	4230	11300	5240
LV6	1600	1440	1920	1627	**1650**	3810	3450	11100	7490
LV7	1450	1320	1940	1931	**1660**	3190	3870	11700	5450
LV8	1460	1470	1920	1778	**1660**	3570	3710	11700	5590
LV9	1430	1350	1860	2111	**1690**	3250	3930	12100	6020
Mean LV	**1510**	**1590**	**1890**	**1946**	**1730**	**3750**	**4020**	**11900**	**5770**
Overall Mean Heart	**1640**	**1730**	**2110**	**2131**	**1900**	**3410**	**3720**	**11200**	**5050**
Plasma Concen-tration	136	159	170	136 [a] (98.1)	**141**	**244**	**288**	**1260**	**1020**
Heart: Plasma ratio	12.1	10.9	12.4	15.6 (21.7)	13.5	14.0	12.9	8.9	4.9

a. Plasma value for animal #4, given for 85 minutes and in parentheses at 90 minutes for calculation of heart;plasma ratio

4.2.6. Individual QTc Response (ms) in the Anaesthetised Rabbit Following an Infusion of Cisapride Vehicle

Time (min)	Vehicle #1	Vehicle #2	Vehicle #3	Vehicle #4	Vehicle #5	Vehicle #6	Vehicle #7	Mean QTc (ms)	S.E.M.
-10	293	266	295	286	251	254	286	**276**	**7.05**
-5	293	260	297	288	251	253	289	**276**	**7.61**
0	293	259	298	289	249	252	289	**276**	**7.98**
5	293	259	298	289	239	251	289	**274**	**8.92**
10	294	259	294	289	236	250	289	**273**	**9.08**
15	297	264	293	291	235	249	291	**274**	**9.40**
20	300	262	292	291	233	249	293	**274**	**9.88**
25	301	260	293	295	234	249	296	**275**	**10.3**
30	302	255	293	296	234	249	297	**275**	**10.6**
35	302	254	294	297	237	249	302	**276**	**10.8**
40	302	252	297	300	239	249	305	**278**	**11.1**
45	301	252	298	303	240	250	308	**279**	**11.3**
50	301	251	299	303	241	250	310	**279**	**11.5**
55	301	250	300	303	240	250	313	**280**	**11.8**
60	301	249	301	302	238	251	316	**280**	**12.2**
65	301	252	305	302	242	252	319	**282**	**12.1**
70	300	251	307	302	243	252	323	**283**	**12.4**
75	300	248	309	306	243	254	324	**283**	**12.8**
80	302	250	311	304	242	257	326	**284**	**12.7**
85	303	251	312	303	241	266	325	**286**	**12.4**
90	303	255	314	304	240	272	329	**288**	**12.5**

4.2.7. Individual QTc Response (ms) in the Anaesthetised Rabbit Following an Infusion of Cisapride at 0.3 mg/kg

Time (min)	0.3 mg/kg #1	0.3 mg/kg #2	0.3 mg/kg #3	0.3 mg/kg #4	0.3 mg/kg #5	0.3 mg/kg #6	0.3 mg/kg #7	Mean QTc (ms)	S.E.M.
-10	283	293	225	269	278	290	295	**285**	**4.19**
-5	285	294	217	279	277	291	296	**287**	**3.24**
0	295	295	221	274	278	294	298	**289**	**4.21**
5	313	304	246	291	294	314	313	**305**	**4.19**
10	335	318	268	309	320	330	328	**323**	**3.94**
15	344	322	273	310	324	338	332	**328**	**4.99**
20	344	323	275	311	324	341		**329**	**6.16**
25	346	324	276	311	325	342		**330**	**6.46**
30	350	326	277	311	322	343		**331**	**7.09**
35	352	328	285	312	323			**329**	**8.47**
40	348	324	288	311	319			**326**	**8.04**
45	344	320	289	310	319			**323**	**7.27**
50	340	317	285	309				**322**	**9.12**
55	339	315	288	311				**322**	**8.83**
60	340	313	295	311				**321**	**9.46**
65	342	309	294					**325**	**16.6**
70	342	310	242					**326**	**16.0**
75	341	315	242					**328**	**13.0**
80	341	317	247					**329**	**12.0**
85	341	314	252					**328**	**13.2**
90	340	315	254					**328**	**12.6**

4.2.8. Individual QTc Response (ms) in the Anaesthetised Rabbit Following an Infusion of Cisapride at 1 mg/kg

Time (min)	1 mg/kg #1	1 mg/kg #2	1 mg/kg #3	Mean QTc (ms)	S.E.M.
-10	280	291	253	**275**	**11.2**
-5	280	292	254	**275**	**11.2**
0	280	292	255	**275**	**11.0**
5	300	345	289	**311**	**17.2**
10	327	374	307	**336**	**19.6**
15	337	375	314	**342**	**17.9**
20	344	374	320	**346**	**15.5**
25	349	378	344	**357**	**10.5**
30	355	384	348	**362**	**11.1**

4.2.9. Individual QTc Response (ms) in the Anaesthetised Rabbit Following an Infusion of Cisapride at 3 mg/kg

Time (min)	3 mg/kg #1	3 mg/kg #2	3 mg/kg #3	3 mg/kg #4	3 mg/kg #5	3 mg/kg #6	3 mg/kg #7	3 mg/kg #8	Mean QTc (ms)	S.E.M.
-10	276	276	273	293	237	278	279	281	**274**	**5.71**
-5	275	277	274	290	238	282	280	281	**275**	**5.53**
0	275	279	274	289	237	281	282	282	**275**	**5.59**
5	346	336	338	346	359	402	320	347	**349**	**8.51**
10	414	377	356	371	428	482	364	387	**397**	**14.9**
15	437	472	349	403	409	519	371	395	**419**	**19.5**
20	445	477	346	411		525	377	388	**424**	**23.5**
25	451	455	343	415		530	395	382	**425**	**23.0**
30	458	450	341	420		537	394	375	**425**	**24.4**
35	444	453	344	429		546		372	**431**	**28.7**
40	453	448	350	421		523		389	**431**	**24.2**
45	450	411	353	400		492		400	**417**	**19.5**
50	423	396	355	387		487			**409**	**22.2**
55	404	393	354	374		488			**403**	**23.0**
60	406	395	351	375		486			**402**	**22.8**
65	418	391	350	377					**384**	**14.2**
70	415	392	349	378					**384**	**13.9**
75	417	390	346	378					**383**	**14.8**
80	417	386	349	378					**382**	**13.9**
85	415	384	351	376					**382**	**13.4**
90	416	391	350	373					**383**	**13.9**

4.3. Moxifloxacin Anaesthetised Rabbit Data

4.3.1. Individual Plasma Concentrations in the Anaesthetised Rabbit Following an Infusion of Moxifloxacin at 5 mg/kg

Time (min)	5 mg/kg #1	5 mg/kg #2	5 mg/kg #3	5 mg/kg #4	5 mg/kg #5	Mean Concentration (ng/mL)	S.E.M.
-15	NQ	NQ	NQ	NQ	NQ	**NQ**	**NQ**
0	NQ	NQ	NQ	NQ	NQ	**NQ**	**NQ**
5	1770	1820	2100	1800	2110	**1920**	**75.0**
10	2200	2360	2920	2340	2130	**2390**	**139**
15	2460	2940	3250	2730	3220	**2920**	**150**
20	2740	3290	4860	2880	3210	**3390**	**380**
25	3040	3690	4750	3150	3130	**3550**	**321**
30	2310	3020	4070	2730	2600	**2950**	**303**
35	1860	2280		2050	1970	**2040**	**89.4**
40	1730	1710		1660	1660	**1690**	**17.4**
45	1810	1540		1480	1980	**1700**	**117**
50	1570	1630		1470	1520	**1540**	**35.1**
55	1620	1750		1180	1450	**1500**	**122**
60	1580	1700		1140	1350	**1440**	**125**
65	1550			1110	1330	**1330**	**127**
70	1460			1190	1200	**1280**	**87.8**
75	1190			1060	1430	**1230**	**106**
80	1420			1010	1310	**1250**	**125**
85	1410			978	1270	**1220**	**128**
90	1400			998	1240	**1210**	**118**

NQ Not Quantifiable below assay limit of quantification (LOQ = 5 ng/mL).
NC Not Calculated

4.3.2. Individual Plasma Concentrations in the Anaesthetised Rabbit Following an Infusion of Moxifloxacin at 20 mg/kg

Time (min)	20 mg/kg #1	20 mg/kg #2	20 mg/kg #3	20 mg/kg #4	20 mg/kg #5	Mean Concentration (ng/mL)	S.E.M.
-15	NQ	NQ	NQ	NQ	NQ	**NC**	**NC**
0	NQ	NQ	NQ	NQ	NQ	**NC**	**NC**
5	7160	6340	6150	6810	7270	**6750**	**220**
10	8750	7800	7340	7980	10400	**8450**	**540**
15	11200	10000	8100	9370	9680	**9670**	**502**
20	13900	13500	9630	10700	15300	**12600**	**1060**
25	15100	12400	11200	12400	14200	**13000**	**696**
30	11800	12100	11400	12900	13800	**12400**	**414**
35	7840	8310		8560	8790	**8380**	**205**
40	6420	6810		6980	8440	**7160**	**440**
45	6180	6260		6660	6470	**6390**	**108**
50	4930	6130		6660	6400	**6030**	**383**
55	4770	5380		5360	6160	**5410**	**286**
60	4960	5140		5970	6030	**5530**	**277**
65	4830			5040	5880	**5250**	**319**
70	4440			4660	5400	**4830**	**290**
75	4080			5130	6310	**5170**	**642**
80	3940			4550	5230	**4570**	**373**
85	4000			4250	5270	**4510**	**389**
90	4740			4730	4840	**4770**	**36.8**

NQ Not Quantifiable below assay limit of quantification (LOQ = 5 ng/mL).
NC Not Calculated

4.3.3. Individual Heart Concentrations in the Anaesthetised Rabbit Following an Infusion of Moxifloxacin at 5 mg/kg

Replicate	5 mg/kg #1	5 mg/kg #2	5 mg/kg #3	5 mg/kg #4	5 mg/kg #5
1	10100	15600	20700	14200	12400
2	7640	10500	21600	10200	8940
3	13200	15100	29600	15200	13400
4	13600	14900	29100	14600	12700
5	12100	14100	25900	13600	12600
6	11900	14700	24000	13400	11800
7	11500	15200	24500	12200	11200
8	10800	13700	23200	12300	11100
9	10800	14100	22700	12200	10900
10	10800	13500	22000	12200	11200
11	10300	12700	21400	12300	10600
12	10700	12800	20600	12600	10300
Time (min)	**90**	**60**	**30**	**90**	**90**
Overall Mean Heart	**11100**	**13900**	**23800**	**12900**	**11400**
Plasma Concentration	1400	1700	4070	998	1240
Heart: Plasma ratio	7.9	8.2	5.8	12.9	9.2

Assay limit of quantification raised 20-fold due to samples diluted into range (LOQ = 100 ng/mL).

4.3.4. Individual Heart Concentrations in the Anaesthetised Rabbit Following an Infusion of Moxifloxacin at 20 mg/kg

Replicate	20 mg/kg #1	20 mg/kg #2	20 mg/kg #3	20 mg/kg #4	20 mg/kg #5
1	50700	28100	83500	61700	58400
2	36500	27800	66800	46800	42500
3	53100	51600	108000	75700	68800
4	63000	50300	108000	71000	60800
5	55700	47200	96700	68100	67600
6	49500	45700	101000	66200	61800
7	48900	45700	96400	71500	64600
8	46200	43700	96000	70600	65300
9	47900	47200	89900	76900	62300
10	47000	45600	88800	68700	60900
11	43500	43200	89000	67500	60200
12	42100	43200	86800	61700	57000
Time (min)	**90**	**60**	**30**	**90**	**90**
Overall Mean Heart	**48700**	**43300**	**92600**	**67200**	**60800**
Plasma Concentration	4740	5140	11400	4730	4840
Heart: Plasma ratio	10.3	8.4	8.1	14.2	12.6

Assay limit of quantification raised 20-fold due to samples diluted into range (LOQ = 100 ng/mL).

4.3.5. Individual QTc Response (ms) in the Anaesthetised Rabbit Following an Infusion of Moxifloxacin Vehicle

Time (min)	Vehicle #1	Vehicle #2	Vehicle #3	Mean QTc (ms)	S.E.M.
-10	371	341	317	**343**	**15.8**
-5	373	342	317	**344**	**16.4**
0	373	344	315	**344**	**16.8**
5	377	347	314	**346**	**18.1**
10	380	347	318	**349**	**18.0**
15	382	349	321	**350**	**17.7**
20	386	350	322	**353**	**18.4**
25	388	350	323	**354**	**18.7**
30	383	348	325	**352**	**16.8**
35	384	348	325	**352**	**17.0**
40	389	346	326	**354**	**18.7**
45	393	345	324	**354**	**20.2**
50	390	344	324	**353**	**19.5**
55	387	342	321	**350**	**19.4**
60	386	343	315	**348**	**20.7**
65	385	344	315	**348**	**20.4**
70	383	345	318	**349**	**18.9**
75	387	346	321	**352**	**19.4**
80	394	346	323	**354**	**20.9**
85	392	345	327	**355**	**19.4**
90	392	346	330	**356**	**18.2**

4.3.6. Individual QTc Response (ms) in the Anaesthetised Rabbit Following an Infusion of Moxifloxacin at 5 mg/kg

Time (min)	5mg/kg #1	5 mg/kg #2	5 mg/kg #3	5 mg/kg #4	5 mg/kg #5	Mean QTc (ms)	S.E.M.
-10	310	288	326	292	237	**290**	**15.1**
-5	311	291	327	289	236	**291**	**15.3**
0	314	297	328	287	239	**293**	**15.2**
5	314	303	331	293	248	**298**	**14.0**
10	318	307	339	296	260	**304**	**13.1**
15	326	309	343	299	269	**309**	**12.6**
20	327	311	348	298	273	**311**	**12.7**
25	327	314	349	298	275	**313**	**12.5**
30	328	317	349	300	272	**313**	**13.0**
35	327	318		299	268	**303**	**13.1**
40	328	319		297	260	**301**	**15.1**
45	330	320		297	254	**300**	**16.9**
50	330	322		295	250	**299**	**17.9**
55	330	323		291	248	**298**	**18.8**
60	334	325		290	246	**299**	**20.0**
65	335			288	245	**289**	**26.0**
70	336			286	245	**289**	**26.2**
75	337			284	244	**288**	**26.9**
80	340			284	245	**290**	**27.6**
85	344			283	246	**291**	**28.8**
90	346			282	245	**291**	**29.7**

4.3.7. Individual QTc Response (ms) in the Anaesthetised Rabbit Following an Infusion of Moxifloxacin at 20 mg/kg

Time (min)	20 mg/kg #1	20 mg/kg #2	20 mg/kg #3	20 mg/kg #4	20 mg/kg #5	Mean QTc (ms)	S.E.M.
-10	290	268	309	239	328	**287**	**15.7**
-5	286	267	318	239	332	**288**	**16.8**
0	283	270	321	238	334	**289**	**17.3**
5	286	275	330	241	343	**295**	**18.6**
10	300	287	345	249	359	**308**	**19.9**
15	305	293	354	256	364	**314**	**19.9**
20	307	298	359	258	368	**318**	**20.3**
25	307	303	365	261	371	**321**	**20.6**
30	306	304	365	263	374	**322**	**20.7**
35	299		359	260	369	**322**	**25.7**
40	290		357	257	358	**316**	**25.1**
45	288		358	257	356	**315**	**25.1**
50	287		358	261	355	**315**	**24.5**
55	286		356	264	355	**315**	**23.7**
60	285		359	266	357	**317**	**24.0**
65			363	270	357	**330**	**30.0**
70			360	273	357	**330**	**28.5**
75			359	274	356	**330**	**28.0**
80			359	276	357	**331**	**27.2**
85			359	277	355	**331**	**26.5**
90			358	278	355	**330**	**26.2**

4.4. Verapamil Anaesthetised Rabbit Data

4.4.1. Individual Plasma Concentrations in the Anaesthetised Rabbit Following an Infusion of Verapamil at 0.1 mg/kg

Time (min)	0.1 mg/kg #1	0.1 mg/kg #2	Mean Concentration (ng/mL)	S.E.M.
-15	NQ	NQ	**NQ**	**NC**
0	NQ	NQ	**NQ**	**NC**
5	52.8	57.4	**55.1**	**2.3**
10	58.6	63.3	**61.0**	**2.4**
15	74.8	67.7	**71.3**	**3.6**
20	75.4	69.5	**72.5**	**3.0**
25	84.6	79.9	**82.3**	**2.3**
30	79.8	104	**91.9**	**12.1**
35	45.5		**45.5**	**NC**
40	38.0		**38.0**	**NC**
45	26.0		**26.0**	**NC**
50	20.6		**20.6**	**NC**
55	19.6		**19.6**	**NC**
60	16.7		**16.7**	**NC**
65	15.4		**15.4**	**NC**
70	16.2		**16.2**	**NC**
75	13.1		**13.1**	**NC**
80	12.1		**12.1**	**NC**
85	12.6		**12.6**	**NC**
90	11.0		**11.0**	**NC**

NQ Not Quantifiable below assay limit of quantification (LOQ = 2 ng/mL).
NC Not Calculated

4.4.2. Individual Plasma Concentrations in the Anaesthetised Rabbit Following an Infusion of Verapamil at 0.3 mg/kg

Time (min)	0.3 mg/kg #1	0.3 mg/kg #2	Mean Concentration (ng/mL)	S.E.M.
-15	NQ	NQ	**NQ**	**NQ**
0	NQ	NQ	**NQ**	**NQ**
5	138	140	**139**	**1.1**
10	182	176	**179**	**2.8**
15	184	214	**199**	**14.8**
20	249	230	**239**	**9.7**
25	248	246	**247**	**1.1**
30	253	223	**238**	**15.1**
35	99.1		**99.1**	**NC**
40	74.6		**74.6**	**NC**
45	64.4		**64.4**	**NC**
50	51.9		**51.9**	**NC**
55	58.5		**58.5**	**NC**
60	40.8		**40.8**	**NC**
65	38.2		**38.2**	**NC**
70	36.7		**36.7**	**NC**
75	35.6		**35.6**	**NC**
80	30.9		**30.9**	**NC**
85	27.0		**27.0**	**NC**
90	28.4		**28.4**	**NC**

NQ Not Quantifiable below assay limit of quantification (LQQ = 2 ng/mL).
NC Not Calculated

4.4.3. Individual Plasma Concentrations in the Anaesthetised Rabbit Following an Infusion of Verapamil at 1 mg/kg

Time (min)	1 mg/kg #1	1 mg/kg #2	Mean Concentration (ng/mL)	S.E.M.
-15	NQ	NQ	**NQ**	**NQ**
0	NQ	NQ	**NQ**	**NQ**
5	403	728	**566**	**163**
10	743	705	**724**	**18.9**
15	860	1180	**1020**	**159**
20	1160	NS	**1160**	**NC**
25	1330	NS	**1330**	**NC**
30	1250	NS	**1250**	**NC**
35	1090		**1090**	**NC**
40	793		**793**	**NC**
45	562		**562**	**NC**
50	424		**424**	**NC**
55	471		**471**	**NC**
60	386		**386**	**NC**
65	446		**446**	**NC**
70	406		**406**	**NC**
75	322		**322**	**NC**
80	412		**412**	**NC**
85	323		**323**	**NC**
90	NS		NS	NC

NQ Not Quantifiable below assay limit of quantification (LOQ = 2 ng/mL).
NC Not Calculated
NS No Sample, animal terminated early due to respiratory failure

4.4.4. Individual Heart Concentrations in the Anaesthetised Rabbit Following an Infusion of Verapamil at 0.1, 0.3 and 1 mg/kg

Replicate	0.1 mg/kg #1	0.1 mg/kg #2	0.3 mg/kg #1	0.3 mg/kg #2	1 mg/kg #1	1 mg/kg #2
1	203	949	517	2050	3800	5430
2	165	791	443	2090	3450	4940
3	157	757	470	1760	3620	4790
4	157	748	439	1790	3160	4340
5	145	787	439	1790	3370	4180
6	153	708	455	1680	3950	3930
7	158	665	417	1550	3320	3970
8	142	670	393	1660	3450	4170
9	155	659	388	1590	3720	3990
10	137	620	380	1680	2860	3640
11	140	737	413	1720	3580	3760
12	147	656	407	1800	3950	3990
Time (min)	**90**	**30**	**90**	**30**	**85**	**15**
Mean Heart ±S.E.M	155 ±4.96	729 ±25.6	430 ±11.3	1760 ±47.4	3520 ±93.2	4260 ±153
Plasma Concentration	11.0	104	28.4	223	323	1180
Heart: Plasma ratio	**14.1**	**7.0**	**15.1**	**7.9**	**10.9**	**3.6**

Assay limit of quantification (LQQ = 2 ng/mL).

4.4.5. Individual QTc Response (ms) in the Anaesthetised Rabbit Following an Infusion of Verapamil Vehicle

Time (min)	Vehicle #1	Vehicle #2	Vehicle #3	Mean QTc (ms)	S.E.M.
-10	258	259	268	**262**	**3.11**
-5	261	265	272	**266**	**3.30**
0	263	270	279	**271**	**4.82**
5	265	276	287	**276**	**6.27**
10	268	281	291	**280**	**6.64**
15	270	285	293	**283**	**6.73**
20	273	289	297	**286**	**6.99**
25	275	290	299	**288**	**6.92**
30	277	292	300	**290**	**6.92**
35	277	292	298	**289**	**6.51**
40	276	293	298	**289**	**6.56**
45	275	293	297	**289**	**6.70**
50	274	293	299	**289**	**7.44**
55	268	293	299	**287**	**9.34**
60	275	293	297	**288**	**6.82**
65	282	293	295	**290**	**4.00**
70	282	293	292	**289**	**3.56**
75	280	293	290	**288**	**3.83**
80	280	294	289	**288**	**4.2**
85	284	293	289	**289**	**2.74**
90	285	294	290	**290**	**2.47**

4.4.6. Individual QTc Response (ms) in the Anaesthetised Rabbit Following an Infusion of Verapamil at 0.1 mg/kg

Time (min)	0.1 mg/kg #1	0.1 mg/kg #2	Mean QTc (ms)	S.E.M.
-10	506	332	**419**	**86.8**
-5	507	329	**418**	**89.0**
0	504	329	**416**	**87.2**
5	495	334	**415**	**80.3**
10	494	332	**413**	**81.2**
15	495	318	**406**	**88.8**
20	497	312	**405**	**92.2**
25	499	312	**405**	**93.4**
30	500	315	**408**	**92.2**
35	504		**504**	**NC**
40	507		**507**	**NC**
45	508		**508**	**NC**
50	510		**510**	**NC**
55	512		**512**	**NC**
60	515		**515**	**NC**
65	519		**519**	**NC**
70	519		**519**	**NC**
75	521		**521**	**NC**
80	521		**521**	**NC**
85	520		**520**	**NC**
90	518		**518**	**NC**

NC Not Calculated

4.4.7. Individual QTc Response (ms) in the Anaesthetised Rabbit Following an Infusion of Verapamil at 0.3 mg/kg

Time (min)	0.3 mg/kg #1	0.3 mg/kg #2	Mean QTc (ms)	S.E.M.
-10	309	304	**307**	**2.56**
-5	310	305	**308**	**2.57**
0	312	306	**309**	**3.22**
5	309	307	**308**	**0.87**
10	299	309	**304**	**4.85**
15	296	311	**303**	**7.29**
20	295	313	**304**	**8.85**
25	300	314	**307**	**6.91**
30	307	315	**311**	**4.15**
35	313		**313**	**NC**
40	319		**319**	**NC**
45	326		**326**	**NC**
50	332		**332**	**NC**
55	333		**333**	**NC**
60	335		**335**	**NC**
65	340		**340**	**NC**
70	341		**341**	**NC**
75	356		**356**	**NC**
80	364		**364**	**NC**
85	366		**366**	**NC**
90	366		**366**	**NC**

NC Not Calculated

4.4.8. Individual QTc Response (ms) in the Anaesthetised Rabbit Following an Infusion of Verapamil at 1 mg/kg

Time (min)	1 mg/kg #1	1 mg/kg #2	Mean QTc (ms)	S.E.M.
-10	314	314	**314**	**0.29**
-5	310	322	**316**	**6.03**
0	323	322	**323**	**0.26**
5	315	331	**323**	**8.43**
10	329	333	**331**	**1.80**
15	321	357	**339**	**17.6**
20	321		**321**	**NC**
25	328		**328**	**NC**
30	357		**357**	**NC**
35	364		**364**	**NC**
40	360		**360**	**NC**
45	354		**354**	**NC**
50	362		**362**	**NC**
55	358		**358**	**NC**
60	370		**370**	**NC**
65	374		**374**	**NC**
70	374		**375**	**NC**
75	371		**371**	**NC**
80	350		**350**	**NC**
85	350		**350**	**NC**
90	NS		**NS**	**NC**

NC Not Calculated
NS No Sample

5. APPENDIX 5: IN VIVO MODELLING

5.1. In Vivo Rat PK Study Method

Pharmacokinetic assessment of each compound was determined in 3 female Han Wistar (Crl:WI(Han)) rats per compound, supplied by Charles River, UK. The rats were approximately 10 weeks old and weighed approximately 231-296 g at the time of dosing. Animals were identified by tail marking and cage labels. All animals were subject to a pre-study visual health check and had free access to standard recommended diet and water from the domestic supply.

During the study the rats were individually housed and offered a complete dry diet (details held by LAS, GlaxoSmithKline, Ware) throughout the study and domestic mains quality water *ad libitum*. The diet and water supplied to the animal is routinely analysed for quality and there were no contaminants in the diet or water that were considered to have affected the integrity or outcome of the study. Environmental controls were maintained at 21 ± 2°C (temperature) and 55 ± 10% (humidity).

5.1.1. Compound Formulation and Administration

Doses of cisapride, moxifloxacin sparfloxacin and verapamil were prepared by the Safety Assessment Dispensary unit, Ware as above and all i*n vivo* aspects (housing, welfare, dosing and sampling) were conducted by Laboratory Animal Sciences (LAS) at Ware. Groups of 3 female rats each received a single intravenous administration of cisapride, moxifloxacin sparfloxacin or verapamil via the tail vein as a bolus injection at a target dose volume of 1 mL/kg, as shown in the table below. Doses were selected based on previous doses identified in literature.

Compound	Dose (mg/kg)	M. Wt	Compound Form	Salt M. Wt	Chemical Purity (%)	Adjusted Purity (%)	Formulation
Cisapride	1	483.9	Cisapride Monohydrate (Batch 080M4751V)	465.9	99	95.3	15% HP-b-cyclodextrin in 25 mM methanesulphonic acid
Moxifloxacin	10	401.4	Moxifloxacin Hydrochloride (Batch VBOG/5504/8/4)	437.9	98	89.8	5% DMSO–10% SBE–cyclodextrin in 5 mM methanesulphonic acid
Sparfloxacin	10	392.4	Sparfloxacin (Batch BCBF4939)	n/a	98	98	10 mg/mL lactic acid in 5% dextrose in water
Verapamil	1	454.6	Verapamil Hydrochloride (Batch 047206 L75939)	454.6	100	92.6	0.9% (w/v) aqueous sodium chloride

5.1.2. Rat Blood Sample Collection, Preparation and Storage

Serial blood samples (0.25 mL) were collected into tubes with EDTA as anti-coagulant from all animals at each of the following times after dose administration: 0.08, 0.25, 0.5, 1, 2, 4, 7 and 24 hours from the jugular and tail vein. Blood samples were mixed and placed on crushed ice immediately after collection. All samples were centrifuged for 10 minutes at 1800 g to yield plasma and stored at approximately -80°C.

5.1.3. Bioanalysis of Rat Plasma Samples

Rat plasma samples were analysed by quantitative bioanalysis with an appropriate LC-MS/MS method to determine plasma concentrations of cisapride, moxifloxacin, sparfloxacin or verapamil, respectively, using qualified analytical methods developed, adapted or based on existing methodology as described in Appendix 1Bioanalytical Methods.

5.1.4. Individual Plasma Concentrations in the Female Rat Following a Single Intravenous Administration of Cisapride at 1 mg/kg

Time (h)	Cisapride Plasma Concentration (ng/mL)		
	Rat 4	Rat 5	Rat 6
0.08	340	326	233
0.25	193	220	140
0.5	108	128	83.2
1	82.1	98.3	59.6
2	35.0	55.7	26.4
4	15.2	24.8	11.2
7	5.70	7.5	3.10
24	*0.3* [a]	*0.3* [a]	*0.2* [a]

a. Concentration data point reviewed & deemed acceptable for investigative purposes based on background signal:noise >5:1 and calibration linearity. (LLQ 0.5 ng/mL)

5.1.5. Statistical Parameters of Analysis of Fit for Compartmental Models of Cisapride in the Female Rat Following a Single Intravenous Administration of Cisapride at 1 mg/kg

Analysis of Fit	**1-comp**	**2-comp**	**3-comp**
R^2	0.5673	0.8847	0.9479
AIC	-24.2118	-50.9886	-56.6099
SC	-21.8557	-46.2764	-49.5416
WSSE	3.0867E-1	8.5618E-2	5.7341E-2

Data presented from GastroPlus v.9, PKPlus for the pharmacokinetic compartmental analysis assessment for goodness of fit using the R-squared value, Akaike Information Criterion (AIC), Schwarz Criterion (SC) and the Weighted Sum of Squared Error (WSSE)

5.1.6. Individual Plasma Concentrations in the Female Rat Following a Single Intravenous Administration of Sparfloxacin at 10 mg/kg

Time (h)	Sparfloxacin Plasma Concentration (ng/mL) [a]		
	Rat 10	Rat 11	Rat 12
0.08	1708	1760	1960
0.25	1550	1540	1760
0.5	1240	1230	1280
1	992	880	969
2	576	562	636
4	243	252	355
7	79.8	117	136
24	9.00	8.60	21.2

a. Assay LLQ raised from 1 ng/mL to 5 ng/mL, as samples diluted 5-fold to be within assay range

5.1.7. Statistical Parameters of Analysis of Fit for Compartmental Models of Sparfloxacin in the Female Rat Following a Single Intravenous Administration of Sparfloxacin at 10 mg/kg

Analysis of Fit	**1-comp**	**2-comp**	**3-comp**
R squared	0.7242	0.9798	0.9900
AIC	-39.1044	-71.9159	-70.3463
SC	-36.7483	-67.2037	-63.278
WSSE	1.6596E-1	3.5799E-2	3.2351E-2

Data presented from GastroPlus v.9, PKPlus for the pharmacokinetic compartmental analysis assessment for goodness of fit using the R-squared value, Akaike Information Criterion (AIC), Schwarz Criterion (SC) and the Weighted Sum of Squared Error (WSSE)

5.1.8. Individual Plasma Concentrations in the Female Rat Following a Single Intravenous Administration of Moxifloxacin at 10 mg/kg

Time (h)	Moxifloxacin Plasma Concentration (ng/mL)		
	Rat 7	Rat 8	Rat 9
0.08	2230	2070	2370
0.25	1220	1334	1880
0.5	788	3680 [b]	1350
1	412	2060	584
2	154	682	165
4	15.4	72.7	27.6
7	*2.10* [a]	7.40	*3.90* [a]
24	NQ	NQ	NQ

a. Concentration data point reviewed & deemed acceptable for investigative purposes based on background signal:noise and calibration linearity. (assay LLQ 5 ng/mL)
b. Potential partial subcutaneous dose administration with delayed C_{max}
NQ Not Quantifiable; below assay LLQ (5 ng/mL)

5.1.9. Statistical Parameters of Analysis of Fit for Compartmental Models of Moxifloxacin in the Female Rat Following a Single Intravenous Administration of Moxifloxacin at 10 mg/kg

Analysis of Fit	**1-comp**	**2-comp**	**3-comp**
R^2	0.8368	0.9502	0.9564
AIC	-23.9371	-35.6898	-32.1372
SC	-22.659	-33.1336	-28.3028
WSSE	1.3594E-1	4.4126E-2	4.2739E-2

Data presented from GastroPlus v.9, PKPlus for the pharmacokinetic compartmental analysis assessment for goodness of fit using the R-squared value, Akaike Information Criterion (AIC), Schwarz Criterion (SC) and the Weighted Sum of Squared Error (WSSE)

5.1.10. Individual Plasma Concentrations in the Female Rat Following a Single Intravenous Administration of Verapamil at 1 mg/kg

Time (h)	Verapamil Plasma Concentration (ng/mL)		
	Rat 1	Rat 2	Rat 3 [a]
0.08	400	499	590
0.25	244	304	341
0.5	154	239	239
1	112	127	128
2	41.5	48.5	48.1
4	NS	19.7	17.3
7	4.30	2.30	1.80 [a]
24	NQ	NQ	NQ

a. Concentration data point reviewed & deemed acceptable for investigative purposes based on background signal:noise >5:1 and calibration linearity (LLQ 2 ng/mL).

NS No Sample

NQ Not Quantifiable; below assay LLQ (2 ng/mL)

5.1.11. Statistical Parameters of Analysis of Fit for Compartmental Models of Verapamil in the Female Rat Following a Single Intravenous Administration of Verapamil at 1 mg/kg

Goodness of Fit	1-comp	2-comp	3-comp
R squared	0.7453	0.9402	0.9527
AIC	-37.4392	-56.9361	-54.2301
SC	-35.4477	-52.9532	-48.2557
WSSE	1.2594E-1	3.8898E-2	3.6461E-2

Data presented from GastroPlus v.9, PKPlus for the pharmacokinetic compartmental analysis assessment for goodness of fit using the R-squared value, Akaike Information Criterion (AIC), Schwarz Criterion (SC) and the Weighted Sum of Squared Error (WSSE)